

Lecture Notes in Civil Engineering

Krishna R. Reddy
Arvind K. Agnihotri
Yeliz Yukselen-Aksoy
Brajesh K. Dubey
Ajay Bansal *Editors*

Sustainable Environmental Geotechnics

Proceedings of EGRWSE 2019

 Springer

Lecture Notes in Civil Engineering

Volume 89

Series Editors

Marco di Prisco, Politecnico di Milano, Milano, Italy

Sheng-Hong Chen, School of Water Resources and Hydropower Engineering,
Wuhan University, Wuhan, China

Ioannis Vayas, Institute of Steel Structures, National Technical University of
Athens, Athens, Greece

Sanjay Kumar Shukla, School of Engineering, Edith Cowan University, Joondalup,
WA, Australia

Anuj Sharma, Iowa State University, Ames, IA, USA

Nagesh Kumar, Department of Civil Engineering, Indian Institute of Science
Bangalore, Bengaluru, Karnataka, India

Chien Ming Wang, School of Civil Engineering, The University of Queensland,
Brisbane, QLD, Australia

Lecture Notes in Civil Engineering (LNCE) publishes the latest developments in Civil Engineering - quickly, informally and in top quality. Though original research reported in proceedings and post-proceedings represents the core of LNCE, edited volumes of exceptionally high quality and interest may also be considered for publication. Volumes published in LNCE embrace all aspects and subfields of, as well as new challenges in, Civil Engineering. Topics in the series include:

- Construction and Structural Mechanics
- Building Materials
- Concrete, Steel and Timber Structures
- Geotechnical Engineering
- Earthquake Engineering
- Coastal Engineering
- Ocean and Offshore Engineering; Ships and Floating Structures
- Hydraulics, Hydrology and Water Resources Engineering
- Environmental Engineering and Sustainability
- Structural Health and Monitoring
- Surveying and Geographical Information Systems
- Indoor Environments
- Transportation and Traffic
- Risk Analysis
- Safety and Security

To submit a proposal or request further information, please contact the appropriate Springer Editor:

- Mr. Pierpaolo Riva at pierpaolo.riva@springer.com (Europe and Americas);
- Ms. Swati Meherishi at swati.meherishi@springer.com (Asia - except China, and Australia, New Zealand);
- Dr. Mengchu Huang at mengchu.huang@springer.com (China).

All books in the series now indexed by Scopus and EI Compendex database!

More information about this series at <http://www.springer.com/series/15087>

Krishna R. Reddy · Arvind K. Agnihotri ·
Yeliz Yukselen-Aksoy · Brajesh K. Dubey ·
Ajay Bansal
Editors

Sustainable Environmental Geotechnics

Proceedings of EGRWSE 2019

 Springer

Editors

Krishna R. Reddy
Department of Civil, Materials, and
Environmental Engineering
University of Illinois
Chicago, IL, USA

Yeliz Yukselen-Aksoy
Department of Civil Engineering
Dokuz Eylül University
İzmir, Turkey

Ajay Bansal
Dr. B. R. Ambedkar National Institute of
Technology
Jalandhar, Punjab, India

Arvind K. Agnihotri
Dr. B. R. Ambedkar National Institute of
Technology
Jalandhar, Punjab, India

Brajesh K. Dubey
Department of Civil Engineering
Indian Institute of Technology Kharagpur
Kharagpur, West Bengal, India

ISSN 2366-2557

ISSN 2366-2565 (electronic)

Lecture Notes in Civil Engineering

ISBN 978-3-030-51349-8

ISBN 978-3-030-51350-4 (eBook)

<https://doi.org/10.1007/978-3-030-51350-4>

© Springer Nature Switzerland AG 2020

This work is subject to copyright. All rights are reserved by the Publisher, whether the whole or part of the material is concerned, specifically the rights of translation, reprinting, reuse of illustrations, recitation, broadcasting, reproduction on microfilms or in any other physical way, and transmission or information storage and retrieval, electronic adaptation, computer software, or by similar or dissimilar methodology now known or hereafter developed.

The use of general descriptive names, registered names, trademarks, service marks, etc. in this publication does not imply, even in the absence of a specific statement, that such names are exempt from the relevant protective laws and regulations and therefore free for general use.

The publisher, the authors and the editors are safe to assume that the advice and information in this book are believed to be true and accurate at the date of publication. Neither the publisher nor the authors or the editors give a warranty, expressed or implied, with respect to the material contained herein or for any errors or omissions that may have been made. The publisher remains neutral with regard to jurisdictional claims in published maps and institutional affiliations.

This Springer imprint is published by the registered company Springer Nature Switzerland AG
The registered company address is: Gewerbestrasse 11, 6330 Cham, Switzerland

Preface

Geoenvironmental engineering has evolved from being a mere combination of geotechnical engineering and environmental engineering into a highly interdisciplinary field which demands contributions from many professionals including geotechnical engineers, environmental engineers, hydrogeologists, earth scientists, geochemists, water engineers, biologists, and ecologists, among others to solve engineering problems involving waste management, waste disposal, environmental risk assessment, soil, sediments and groundwater remediation, ecosystem services protection, and environmental rehabilitation.

As the nature of the problems addressed in geoenvironmental engineering is diverse, the solutions to these problems typically require the expertise of a variety of professionals, who possess a similar diversity in terms of educational background and training. It is, therefore, always imperative for the teaching and practicing professionals to have a breadth of knowledge in a variety of disciplines associated with geoenvironmental problems in order to facilitate the professional interaction needed for the successful completion of geoenvironmental projects within a multidisciplinary setting. Geoenvironmental engineering is still a new and emerging field that offers numerous technical challenges, which are great opportunities to understand multidisciplinary problems and develop solutions to protect public health and the environment.

In the current world scenario, population growth, rapid urbanization along with global climate change at unprecedented rates are some of the grand challenges faced by engineers across all disciplines. Civil and environmental engineers are among the people at the front end of facing the immediate impacts and are posed with pressing needs to solve these burning problems. With the exploding population growth, more land is needed; many soil deposits previously claimed to be unfit for residential housing and other construction projects are now being used. Moreover, in a progressive society, rising living standards indicate an increase in industrial growth. As a result, increase in the greenhouse gas emissions and pollution of air, water pollution and land degradation, industrial waste, and urban refuse production have become inevitable, thus endangering the global environment. To cope with these problematic soil deposits and adverse environmental conditions, the present

conventional construction technology must take, by necessity, a new direction toward sustainable environmental geotechnics. Problematic soil deposits, ground-water pollution problems have challenged the current soil mechanics concepts and methods of analyzing soil's geochemical behavior under varied environmental conditions. In addition, the environmental aspects of geotechnology have been expanded and have paved the way for the emergence of sustainable solutions to geoenvironmental problems. This book covers a variety of articles focused on such multidisciplinary topics, which will be useful for students, working professionals, practitioners, and academic researchers. Each article was peer-reviewed by two professionals with relevant technical background. We are grateful to all of the authors and the reviewers without their contribution this book would not have been a reality.

Chicago, USA
Jalandhar, India
İzmir, Turkey
Kharagpur, India
Jalandhar, India

Editors
Krishna R. Reddy
Arvind K. Agnihotri
Yeliz Yukselen-Aksoy
Brajesh K. Dubey
Ajay Bansal

Contents

Electrokinetic Reactivation of Activated Carbon: Possibilities for the Treatment of the End-Waste Effluents	1
Claudio Cameselle and Susana Gouveia	
Estimating Municipal Solid Waste Generation: From Traditional Methods to Artificial Neural Networks	11
Katerina Donevska	
Bioremediation: Recent Advancements and Limitations	21
Ming Zhang and Miho Yoshikawa	
Consolidation and Hydraulic Conductivity of Soil-Bentonite Backfill Containing SHMP-Amended Ca-Bentonite in CCR-Impacted Groundwater	31
Yan-Jun Du, Krishna R. Reddy, Yu-Ling Yang, and Ri-Dong Fan	
Engineered Water Repellency for Applications in Environmental Geotechnology	39
John L. Daniels	
Integrated Bioprocessing of Urban Organic Wastes by Anaerobic Digestion Coupled with Hydrothermal Carbonization for Value Added Bio-Carbon and Bio-Product Recovery: A Concept of Circular Economy	47
Sagarika Panigrahi, Hari Bhakta Sharma, and Brajesh K. Dubey	
Geoenvironmental Investigation Methods Used for Landfills and Contaminated Sites Management	55
Eugeniusz Koda, Piotr Osiński, Anna Podlasek, and Magdalena D. Vaverková	
Minimizing the Impact of Groundwater Pumping on the Environment: Optimization Strategies	69
S. Mohan	

Numerical Modeling of Landfill Processes: Complexity Versus Practicality	85
Girish Kumar and Krishna R. Reddy	
Status of C&D Waste Recycling in India	95
Mohan Ramanathan and V. G. Ram	
An Ontological Analysis of Challenges Involved in Urban Solid Waste Management	107
Shwetmala Kashyap, Arkalgud Ramaprasad, and Chetan Singai	
Development of New Precursors for One-Part Alkali-Activated Geopolymer Using Industrial Wastes	115
Monower Sadique, Abdullah Kadhim, William Atherton, and Patryk Kot	
Waste Management in Textile Industry—A Novel Application of Carbon Footprint Analysis	125
S. Mohan and Ninad Oke	
New Ternary Blend Limestone Calcined Clay Cement for Solidification/Stabilization of Pb²⁺ Contaminated Soil	131
Anand V. Reddy, Chandresh H. Solanki, Shailendra Kumar, and Krishna R. Reddy	
A Study on Evaluating the Usefulness and Applicability of Additives for Neutralizing Extremely Alkaline Red Mud Waste	139
Manas Chandan Mishra, N. Gangadhara Reddy, B. Hanumantha Rao, and Sarat Kumar Das	
Contribution to the Remediation of Saline Soils by Electrokinetic Process: Experimental Study	151
Faiza Klouche, Karim Bendani, Ahmed Benamar, Hanifi Missoum, Mustapha Maliki, and Laila Mesrar	
A Case Study Sequel: Sustainable Remediation Using Succession Crops for PAH Impacted Soil	161
Linda C. Yang, Matt Catlin, and Michael Jordan	
Characterization and Ecotoxicological Evaluation of Nanostructured Chitosan Particles	173
Fabiana Pereira Coelho, Thaynara Santana Rabelo, Louise da Cruz Felix, Daniele Maia Bila, and Elisabeth Ritter	
Clean Hydraulic Reclamation Technology and Clean Foundation Treatment Technology—Countermeasures to Contaminated Fills	185
Jianxiu Wang, Linbo Wu, Xuexin Yan, Zhao Wu, Guanhong Long, Hanmei Wang, and Na Xu	

Nanobioremediation of Soils Contaminated with Lindane: Overview and Research Challenges	195
Liang Zhao, Jyoti K. Chetri, and Krishna R. Reddy	
<i>Spirodela Polyrhiza</i>: An Efficient Hyperaccumulator of Nickel at Low Concentration	207
Chandrima Goswami, Kaushik Bandyopadhyay, and Arunabha Majumder	
Enhancement of Water Reuse by Treating Wastewater in Constructed Wetlands: Minimization of Nutrients and Fecal Coliform	213
B. Lekshmi, Rahul S. Sutar, Dilip R. Ranade, Yogen J. Parikh, and Shyam R. Asolekar	
Evaluation of Sodium Adsorption in Clay Soil in the Presence of Crude Oil	225
Thaynara Santana Rabelo, Stella Melgaço, Fabiana Pereira Coelho, Daniele Maia Bila, and Elisabeth Ritter	
Photochemical Oxidation of Complex Organic Contaminants in Water	235
Santiago Urréjola, Claudio Cameselle, Susana Gouveia, and Mercedes Pardo	
A Zero Emissions Landfill: Turning Myth to Reality	243
Jyoti K. Chetri and Krishna R. Reddy	
Treatment of Diethyl Phthalate from Municipal Solidwaste Open Dumpsite Through Ozone-Based Advanced Oxidation Process	253
S. Mohan and D. Gokul	
Static and Dynamic Leaching Studies on Coal Gangue	261
Mohammed Ashfaq, M. Heera Lal, and Arif Ali Baig Moghal	
Sustainability of Vertical Barriers for Environmental Containment	271
Jeffrey C. Evans, Daniel G. Ruffing, Krishna R. Reddy, Girish Kumar, and Jyoti K. Chetri	
A Study on the Behavior of Pond Ash in Unsaturated Conditions Through WRCC	285
Sanjay Kumar Singh and Janmeet Singh	
Utilization of Bagasse Ash in the Compacted Clay Liner	297
Dharmil Baldev, Apurv Kumar, Sutesh Tiwari, M. Muthukumar, and Sanjay Kumar Shukla	
Shear Behaviour of Geosynthetic Clay Liner (GCL) Interfacing with Manufactured Sand	303
Anjali G. Pillai and Gali Madhavi Latha	

Impact on Bentonite Due to the Presence of Various Concentrations of Lead and Copper Solutions	323
Saswati Ray, Anil Kumar Mishra, and Ajay S. Kalamdhad	
Seismic Response of Bentonite Enhanced Soils to be Used as Fabricated Liner in Engineered Landfills	333
Jaskiran Sobti and Sanjay Kumar Singh	
Interpretation of Hydraulic Conductivity of Bentonites Based on Sedimentation Characteristics	345
Esra Dikişçi, El Hassen Abd Moulana, and A. Hakan Ören	
Effect of Organic Matter on Index Swell Properties of a Conventional and Bentonite–Polymer GCL	353
Christian Wireko and Tarek Abichou	
Chemical Compatibility of Slurry Trench Cutoff Wall Backfills Comprised of SHMP-Amended Ca-Bentonites in Lead-Contaminated Solutions: Hydraulic Conductivity Assessment	365
Yu-Ling Yang, Yan-Jun Du, Krishna R. Reddy, and Ri-Dong Fan	
Mechanical, Hydraulic, and Chemical Behavior of Steel Slag-Amended Loessical Silt–Bentonite Liners	373
Franco M. Francisca, Clara A. Mozejko, and Daniel A. Glatstein	
Finite Element Analysis and Simulation Test Research of Deformation of Anti-Seepage Wall in Landfill	383
Guozhong Dai, Jia Zhu, Guicai Shi, and Shujin Li	
Predicting Gaseous Emissions and Leachate Production in Landfills Using Neural Model	391
Sunayana and Arvind Kumar	

About the Editors

Dr. Krishna R. Reddy is a Professor of Civil and Environmental Engineering, Director of Sustainable Engineering Research Laboratory, and also the Director of the Geotechnical and Geoenvironmental Engineering Laboratory at the University of Illinois at Chicago. He received his Ph.D. in Civil Engineering from the Illinois Institute of Technology, Chicago. He received gold medals for being first in his class of B.E. (Civil Engineering) at Osmania University and M.E. (Civil Engineering) at the Indian Institute of Technology, Roorkee. Dr. Reddy has over 25 years of teaching, consulting and research experience within the fields of civil engineering, geotechnical engineering, environmental engineering, and sustainable engineering.

Dr. Arvind K. Agnihotri is a Professor in the Department of Civil Engineering NIT Jalandhar. He completed his Ph.D. from IIT Roorkee, M.Tech. from NIT Kurukshetra and B.E. from Panjab University Chandigarh. He has over 29 years' experience in research, teaching and academic administration, with several years spent holding key leadership positions. His areas of interest are Geotechnical and Geoenvironmental Engineering, Reinforced Earth (Geosynthetics and Geofibers), Ground Improvement and Soil-Structure-interaction. He has supervised 9 Ph.D. theses and 40 M.Tech. dissertations. He has 50 publications in international refereed journals, 10 publications in national refereed journals and 34 publications in various national and international conferences/symposia.

Dr. Yeliz Yukselen-Aksoy is a Professor in the Geotechnical Engineering Division of Department of Civil Engineering of Dokuz Eylul University. She received a B.S. from Dokuz Eylül University, and an M.S. from the Dokuz Eylül University. She received her Ph.D. in Geotechnical Engineering from the University of Dokuz Eylül. She was also at the University of Illinois at Chicago in the Department of Civil and Materials Engineering for one year as a visiting professor. Her research efforts have focused on environmental geotechnics, ground improvement, surface properties of clay minerals, and remediation of contaminated soils. Dr. Yukselen-Aksoy has published

over 40 journal papers, 1 book chapter, and 25 conference papers. She was the recipient of the Turkish National and Scientific Research Council Scholarship.

Dr. Brajesh K. Dubey is an Associate Professor in Environmental Engineering at the Department of Civil Engineering at Indian Institute of Technology, Kharagpur, India. Dr. Dubey received his Ph.D. from the University of Florida, USA. He obtained his B. Tech. (Hons.) in Civil Engineering from IIT Kharagpur. He has more than 17 years of research, teaching, training and industrial outreach experience in areas of integrated solid and hazardous waste management, sustainable engineering and application of life cycle assessment techniques, environmental risk assessment, circular economy and environmental nanotechnology. He has published 62 journal papers, 26 conference papers, and 6 book chapters. He has received awards from Government of Australia, International Research Group on Wood Protection–Sweden, Hinkley Center for Solid, and Hazardous Waste Management, Florida. He has also worked as a Waste Management Expert for UN agencies and World Bank.

Dr. Ajay Bansal is a Professor of Chemical Engineering at Dr B R Ambedkar National Institute of Technology, Jalandhar, India. Dr Bansal received his Ph.D. in Chemical Engineering from Panjab University, Chandigarh, M.Tech. from Indian Institute of Technology, Delhi, and B.E. from Government Engineering College, Raipur (now NIT Raipur). Dr. Bansal has over 24 years of teaching, consulting and research experience within the fields of chemical and environmental engineering. His research expertise includes Nano-photocatalysis, Advanced Oxidation Processes, Waste Water Treatment, Solid Waste Management, Multiphase Reactors, and Rheologically complex fluids. He has supervised 8 Ph.D. dissertations, published 3 books, 3 book chapters, 40 journal papers, and 60 conference papers. He has been an active member of various professional societies and is Fellow of Institution of Engineers (India), Fellow of Indian Institute of Chemical Engineers (IICChE), Kolkata.

Electrokinetic Reactivation of Activated Carbon: Possibilities for the Treatment of the End-Waste Effluents



Claudio Cameselle and Susana Gouveia

Abstract Activated carbon is a common adsorbent material for the retention of organic and inorganic contaminants. The spent activated carbon is usually regenerated with a thermal process. The electrochemical regeneration of the activated carbon has been proposed as an efficient and sustainable alternative to the classical reactivation methods. The electrochemical treatment consumes less energy and produces less CO₂ than the traditional thermal activation. The electrochemical regeneration uses a DC electric current directly applied to the carbon specimen. The electric current desorbs and mobilizes the contaminants retained in the activated carbon. At the end of the regeneration process, the contaminants released from the carbon remain in the electrode solutions (anolyte and catholyte). Such end-waste effluents require treatment before their final disposal. This work analyzed the chemical composition of the end-waste effluents and proposed and tested various technologies for the separation/degradation of organic and inorganic contaminants. Furthermore, the end-waste effluents may contain valuable materials: metals, phosphorus, specific organics, etc., that can be recovered using various selective separation processes.

Keywords Activated carbon · Electrochemical regeneration · End-waste effluent

1 Introduction

Activated carbon (AC) is a common adsorbent used in various industrial sectors, including pharmaceutical and chemical industries. It is also used in the treatment of water/wastewater and in the purification of drinking water. The saturated AC can be reactivated or disposed of in a landfill. The reactivation is a practice much more sustainable than final disposal in a landfill, but the classical reactivation methods also show several drawbacks. The most common technology for the reactivation of AC is thermal treatment. The main limitations of the thermal reactivation are energy consumption, CO₂ emissions, and the loss of carbon and activity in the reactivation

C. Cameselle (✉) · S. Gouveia
BiotechIA, Chemical Engineering, University of Vigo Rua Maxwell S/N. Building Fundicion,
36310 Vigo, Spain
e-mail: claudio@uvigo.es

process. As an alternative, the electrochemical reactivation [1] of the carbon has been proposed as an effective and more sustainable method.

The electrochemical regeneration of the AC uses a direct electric current to induce the mobilization of the contaminants adsorbed in the carbon, and their transportation toward the electrodes (anode and cathode). The contaminants are concentrated in the electrode solutions: anolyte and catholyte. The treatment of the end-waste solutions from the electrochemical reactivation of the AC is one of the key stages for the development of a reliable and sustainable alternative technology to the classical reactivation methods [2].

2 Materials and Methods

2.1 *Regeneration of the Activated Carbon*

The electrochemical reactivation tests of the AC were done by the University of Alicante (Alicante, Spain) using the spent (saturated) carbon supplied by Emivasa, a company that uses large carbon filters in the purification of drinking water in Valencia region (Spain). The end-waste effluents used in this study were supplied by Univ. of Alicante. The effluents come from the electrode solutions using a pilot AC regeneration cell developed in the University of Alicante (PortableCRAC Project, ref.: 768905, funded by the European Union through the program H2020-SPIRE-2017). The pilot cell uses 15 kg of activated carbon and 100 L of electrolyte solutions. Sulfuric acid 0.50 mol/L was used as electrolyte in both, the catholyte and anolyte. In previous studies, it has been demonstrated that the use of sulfuric acid favored the removal of organic contaminants, but especially inorganic cations such as Ca^{2+} ; improving the adsorption capacity of the reactivated carbon [3].

2.2 *Analysis of the End-Waste Effluents*

Tables 1 and 2 summarize the parameters measured in the end-waste effluents and the concentrations of organic and inorganic components that can be found in the natural water treated with the activated carbon, and therefore they may appear in the reactivation effluents. Table 2 includes various pesticides and organic contaminants of concern in drinking water as per the Spanish regulation Royal Decree RD 902/2018 about drinking water quality.

Table 1 Parameters and analysis of end-waste effluents

Parameters	Solid content	Organic content
pH	Total solids	COD
Electric	Volatile solids	TOC
Conductivity	Fixed solids	TN
Total Acidity	Suspended solids	Phenol
Density	Volatile suspended solids	Hydrocarbon
	Fixed suspended solids	Surfactants
Inorganic compounds	Chemical elements (ICP-OES) ^a	
NH ₄ ⁺ , F ⁻ , Cl ⁻ , Br ⁻ , NO ₃ ⁻ , NO ₂ ⁻ , PO ₄ ³⁻ , CN ⁻ , SiO ₂	Ag, Al, As, B, Ba, Be, Bi, Ca, Cd, Co, Cr, Cu, Fe, Ga, K, Li, Mg, Mn, Mo, Na, Ni, P, Pb, Rb, S, Se, Si, Sr, Te, Tl, V, Zn	

^a(ICP-OES: Inductively Coupled Plasma Optical Emission Spectrometry)

Table 2 Organic compounds of concern in drinking water

Pesticides
Aldrin, Dieldrin, Heptachlor, Heptachlor epoxide
Organohalogenated COVs
1,2-dichloroethane
Tetrachloroethene (PCE) + Trichloroethylene (TCE)
BTEX
Benzene
PAHs
PAH-Benzo [a] pyrene
PAH-Benzo [b] flourene
PAH-Benzo [g,h,l] perylene
PAH-Benzo [k] fluorantene
PAH-Fluorantene
PAH-Indene [1,2,3-c,d] pyrene

3 Results and Discussion

3.1 Characterization of the End-Waste Effluents

The results of the analysis of the end-waste effluent are listed in Table 3. The electrochemical regeneration of the activated carbon uses 0.5 mol/L sulfuric acid, and therefore the main characteristics of the end-waste effluents are related to the original electrolyte solutions. Thus, the pH of the effluents is below pH 1; the electric conductivity ranges from 131 to 187 ms/cm, and the total acidity is very close to the

Table 3 Analysis of end-waste effluents: anolyte and catholyte

Parameter	Units	Anolyte	Catholyte
pH		0.13	0.34
EC	(ms/cm)	187.1	131.3
Total Acidity	(mM H ⁺)	1045 ± 2.2	759 ± 1.8
Density	(kg/dm ³)	1.033 ± 0.002	1.026 ± 0.005
<i>Solid content</i>			
TS	(g/L)	65.20 ± 0.39	52.70 ± 0.17
VS	(g/L)	62.49 ± 0.32	42.12 ± 0.27
FS	(g/L)	2.71 ± 0.05	10.58 ± 0.07
SS	(mg/L)	17.47	130.04
VSS	(mg/L)	1.23	120.87
FSS	(mg/L)	16.24	9.17
<i>Organic content</i>			
COD	(mg/L)	5.8 ± 2.2	43.7 ± 3.2
TOC	(mg/L)	1.54	8.32
TN	(mg/L)	1.09	13.31
<i>Inorganic ions</i>			
NH ₄ ⁺	(mg/L)	0.77	3.05
F ⁻	(mg/L)	0.61	0.16
Cl ⁻	(mg/L)	240.44	268.93
Br ⁻	(mg/L)	0.50	25.58
NO ₃ ⁻	(mg/L)	0.19	12.99
PO ₄ ³⁻	(mg/L)	1.41	1.89
SiO ₂	(mg/L)	59.37	19.50
<i>Elemental Analysis (ICP-OES)</i>			
Ca	(mg/L)	182.2	695.8
Al	(mg/L)	67.00	484.6
Fe	(mg/L)	113.8	324.2
Mg	(mg/L)	89.50	437.0
Si	(mg/L)	40.38	231.2
Na	(mg/L)	91.5	129.7
Sr	(mg/L)	3.90	11.42
P	(mg/L)	3.52	18.10
Mn	(mg/L)	1.24	6.50
K	(mg/L)	9.70	18.50
Zn	(mg/L)	0.68	2.80
Ni	(mg/L)	0.38	2.28
B	(mg/L)	1.08	4.86

(continued)

Table 3 (continued)

Parameter	Units	Anolyte	Catholyte
As	(mg/L)	<1	<1
Cr	(mg/L)	0.30	1.74
Cu	(mg/L)	0.66	0.78

initial concentration of the sulfuric acid. The electrolysis of water during the electrochemical regeneration of the carbon slightly modified those parameters by the production of H^+ ion in the anode and the consumption of H^+ in the cathode. Thus, for instance, the pH is lower, and the acidity and the EC are higher in the anolyte than in the catholyte.

The solid content in the effluents is related to the initial concentration of sulfuric acid with the subsequent accumulation in the electrode solutions of the extracted contaminants and suspended particles from the carbon. Suspended solids are mainly present in the catholyte. They are small particles of carbon released from the mass of carbon during the reactivation process. These suspended particles can be easily removed by filtration with a regular glass fiber filter, although the use of a 0.45 μm membrane filter assures the total removal of those suspended particles. The volatile solids (VS) are more than 80% of the total solids in both effluents. The ratio VSS/FSS (volatile/fixed suspended solids) is higher in the catholyte than anolyte because of the higher organic contaminant concentration in the catholyte.

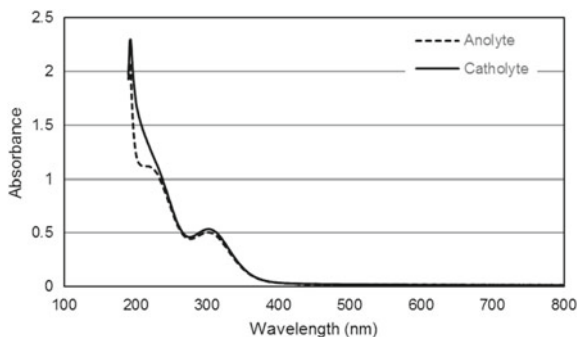
The end-waste effluents contain sulfate ions in a concentration that corresponds to the initial sulfuric acid concentration. Other substances present in the effluents are chloride and bromide ions, silicates, nitrates, phosphates, and ammonium. In general, the concentrations are higher in the catholyte than in the anolyte.

The organic content is relatively low in both effluents (anolyte and catholyte) but the catholyte shows higher concentrations confirming that the contaminants are accumulated in the catholyte where the electrochemical regeneration of the carbon takes place. No specific organic contaminants were detected in the end-waste effluent (phenols, surfactants, etc.). The chromatography analyses of organic contaminants of special concern for drinking water (as per RD 902/2018) resulted in no detection of any of the tested analytes (Table 2).

The determination of more than 30 elements in the end-waste effluents proved that the main components of the catholyte are Ca, Al, Fe, Mg, Si, and Na, with concentrations higher than 100 mg/L. Other elements (Sr, P, Mn, K, Zn, Ni, B, Cr) were found in concentrations between 1 and 20 mg/L. The concentration of elements in the catholyte was much higher than in the anolyte. Other analyzed elements were present only as traces or below the detection limit.

Figure 1 shows the UV-Vis spectra of the end-waste effluents. There is no absorbance in the visible spectrum, and the absorbance is concentrated only in the UV range 190–300 nm. The absorbance in the UV range is supposed to be due to the organic matter content, especially the peak at 200 nm. The peak at 300 nm is mainly

Fig. 1 UV-Vis spectra of the end-waste effluents



associated to inorganic elements or anions. The UV spectrum can be used to evaluate and monitor the removal of contaminants during the treatment of those effluents.

3.2 Neutralization and Precipitation

Selected chemicals have been used for the neutralization of the effluent and precipitation of soluble components. The neutralizing/precipitation chemicals are: Sodium Hydroxide, Sodium Carbonate, Calcium Carbonate, Calcium Oxide/Calcium Hydroxide, and Sodium Sulfide.

The treatment of the effluents with these chemicals resulted in the neutralization of the effluent and the precipitation of the elements in solution forming insoluble salts: metal hydroxides and carbonates. The precipitation with sodium carbonate is more effective than NaOH because carbonate forms insoluble salts with most of the metals. However, sulfur (present in the effluents as sulfate ions) is not removed with the treatment with sodium carbonate. Besides, there is a clear increment of sodium concentration in the final effluent, after the treatment. These limitations can be overcome using calcium carbonate or calcium oxide (or calcium hydroxide). Ca forms an insoluble salt with sulfate. Thus, the best removal results were achieved with calcium carbonate or calcium oxide for both samples (Table 4).

The study also considers the use of sodium sulfide for the precipitation of ions in the effluents. Sulfide forms insoluble salts with all the metals but Na and K. Sodium sulfide was used alone or in combination with calcium carbonate or calcium oxide. The results show that metal removal is equivalent to the treatment with calcium compounds alone. Considering the cost of sulfide and the possible exposition to toxic H_2S , this reagent was discarded for further tests or studies.

Figure 2 shows the UV-Vis spectra of the catholyte after the neutralization/precipitation treatment. The peak at 300 nm, associated to the presence of various inorganic components in solution disappeared after the treatment, and only the peak at 200 nm, associated to the organic compounds, remains. The organic content in the effluents is not affected by the neutralization/precipitation treatment, except for the

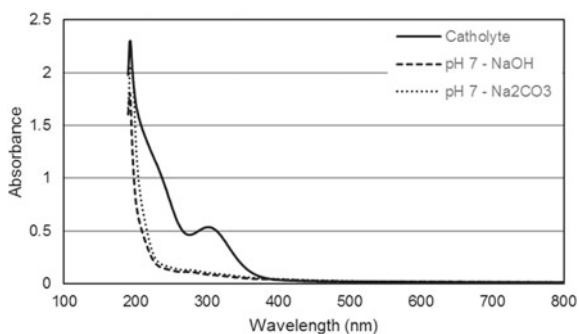
Table 4 Analysis of end-waste effluents: anolyte and catholyte

	NaOH	Na ₂ CO ₃	CaCO ₃	CaO	NaOH/Na ₂ S ^a	CaO/Na ₂ S ^b	Na ₂ S
S	–	–	94%	82%	–	–	–
Ca	31%	92%	13%	29%	21%	51%	34%
Al	>99%	>99%	>99%	>99%	95%	>99%	86%
Fe	97%	99%	92%	>99%	>99%	>99%	>99%
Mg	14%	28%	–	–	99%	–	99%
Si	99%	99%	91%	99%	>99%	99%	>99%
Na	–	–	15%	44%	–	–	–
Sr	16%	91%	91%	88%	25%	93%	31%
P	>94%	>94%	>94%	>94%	>94%	>94%	>94%
Mn	28%	98%	–	99%	>99%	>99%	>99%
K	–	–	–	6%	–	–	–
Zn	86%	89%	76%	88%	90%	89%	87%
Ni	88%	>91%	14%	>91%	>91%	>91%	>91%
B	–	3%	–	56%	14%	67%	11%
As	–	–	–	–	–	–	–
Cr	>89%	>89%	>89%	>89%	>89%	>89%	>89%
Cu	>74%	>74%	>74%	>74%	>74%	>74%	>74%

– No removal observed or accumulation due to reactant addition

^a0.35 g Na₂S/100 mL. ^b0.50 g Na₂S/100 mL

Fig. 2 UV-Vis spectra of catholyte after the neutralization with NaOH or Na₂CO₃



treatment with carbonates where TOC (Total organic carbon) was below the detection limit. TN (Total nitrogen) was reduced by 90% and COD was reduced by 35%. These results suggest that calcium carbonate could be the best candidate for the rapid treatment of the end-waste effluents. Furthermore, the concentration of any element or organic compound in the treated effluent with calcium carbonate is so low, that the treated effluent can be considered for the preparation of new anolyte or catholyte

solutions for new AC regeneration batches. Thus, the final treated aqueous effluent will not be discharged (zero liquid discharge technology.)

3.3 Recovery of Valuable Inorganics

The presence of metals and other valuable inorganics in the regeneration effluents suggest the development of treatment processes designed for the selective recovery of such elements. The recovery of metals and phosphate can be achieved by selective precipitation. Fe and Al are the most abundant metals in the regeneration effluent. The recovery and separation of Fe and Al can be achieved with the controlled neutralization of the effluent to pH 3.5 with NaOH to precipitate Fe as ferric hydroxide. The supernatant is then neutralized with NaOH up to pH 10. All the remaining metals are precipitated but Al, that is then easily recovered from the solution.

The proposed method for the recovery of phosphate as struvite ($\text{NH}_4\text{MgPO}_4 \cdot 6\text{H}_2\text{O}$) involves the partial neutralization of the effluent up to pH 5.5 using NaOH. Then, the effluent is neutralized with ammonia up to pH 8 with agitation. Struvite is formed in these conditions and it is separated from the solution by centrifugation or filtration.

3.4 Recovery of Valuable Organics

The origin of the activated carbon (purification water plant) as well as the conditions of the carbon regeneration process (the electrochemical process) resulted in a very low organic content of the end-waste effluents. These conditions make it difficult to identify any interesting organic compound to be recovered. Even with other sources of carbon used for the adsorption of valuable organics, the recovery of those compounds from the end-waste effluents is also limited by the electrochemical transformations that the organics may undergo during the electrochemical regeneration of the carbon. Anyway, the recovery of selected organics from the end-waste effluent is possible using extraction with selective solvents.

Selective extraction with deep eutectic solvents (DES) is the most attractive technology for the recovery of organics from the end-waste effluents. These solvents, sometimes considered a specific group of ionic liquids, show several advantages over other solvents: they are stable, easy to prepare, inexpensive, durable, and show high solubility for organic compounds. They can be designed to be hydrophilic or hydrophobic. In this study, two hydrophobic DES were prepared mixing an organic acid (octanoic acid or dodecanoic acid) and an organic base (menthol). Both components have to be hydrophobic to get a DES immiscible with water. DES were tested for the recovery of thiamethoxam, nitenpyram, and phosmet (20 mg/L); three pesticides with different solubility in water. In this study, the extraction efficiency seems to be highly dependent on the solubility in water of the organic compound

Table 5 Extraction efficiency of selected pesticides with deep eutectic solvents (DES)

DES	Recovery (%)		
	Thiamethoxam	Nitenpyram	Phosmet
MOA (Menthol-Octanoic Acid)	45.24 ± 0.04	23.17 ± 0.53	95.95 ± 1.4
MDA (Menthol-Dodecanoic Acid)	25.24 ± 0.30	7.84 ± 0.62	>99%
Solubility in water (mg/L)	4100	590000	20

(Table 5). Phosmet was completely recovered with both DES. Nitenpyram, the most soluble compound in water, also showed a relatively high extraction in just one step. Comparing the two DES, MOA is more efficient with the soluble organics in water whereas MDA is more effective with the hydrophobic compounds (e.g., phosmet). These results suggest that the longer the aliphatic chain in the organic acid, the more hydrophobic the DES. Thus, the DES can be tailored for the specific organic compounds to be recovered in each application.

4 Conclusions

The end-waste effluents show a low concentration of contaminants. The catholyte is more contaminated than the anolyte. This is because the electrochemical regeneration of AC takes place in the cathode compartment immersed in the catholyte. The low concentration of contaminants in the end-waste effluents suggests their direct reuse in the regeneration of the carbon, especially the anolyte that shows a very low concentration of inorganic and organic contaminants. The treatment of the end-waste effluent is possible by neutralization and precipitation with hydroxides or carbonates of sodium and calcium, or sodium sulfide. The resulting effluent meets the legal limits to be discharged in the municipal sewage system. The neutralization and precipitation with carbonates remove also the organic matter. The neutralization and precipitation with calcium carbonate is able to remove inorganic and organic contaminants in the effluents. Thus, the resulting aqueous stream can be considered for the preparation of new electrolyte solutions (anolyte and catholyte). This can be considered a zero liquid discharge (ZLD) treatment. The selective recovery of inorganic and organic valuable components in the end-waste effluent is possible during the treatment of the effluent. Metals and phosphate can be separated by selective precipitation. Deep eutectic solvents are innovative solvents with interesting properties for the recovery of organics.

References

1. McQuillan RV, Stevens GW, Mumford KA (2018) The electrochemical regeneration of granular activated carbons: a review. *J Hazard Mater* 355:34–49
2. García-Otón M, Montilla F, Lillo-Ródenas MA, Morallon E, Vázquez JL (2005) Electrochemical regeneration of activated carbon saturated with toluene. *J Appl Electrochem* 35(3):319–325
3. Cameselle C, Gouveia S (2018) Treatment of end-waste effluent from the electrokinetic reactivation of activated carbon. In: *Book of abstracts of the XVI international symposium on electrokinetic remediation*. Çanakkale, Turkey, p 13

Estimating Municipal Solid Waste Generation: From Traditional Methods to Artificial Neural Networks



Katerina Donevska

Abstract Accurate quantification and prediction of municipal solid waste generation is a prerequisite for establishing an integrated municipal solid waste (MSW) system. Data about both quantity and quality of generated wastes as well as their temporal distribution are essential for planning the MSW system and capacities of the required facilities and equipment. Effective MSW system planning relies both on data availability and reliability and selection of the most appropriate data-driven method for estimating MSW generation. Traditional methods for estimating the amount of generated solid waste are established mostly on the basis of some elements such as number of population, waste generation coefficient per capita, and social-economic development of the region. Conventional methods for predicting MSW generation: weight volume analysis, material balance analysis, and load count analyses are basic methods for estimating the generated waste. Classical statistical models including regression analyses were mainly developed over the last three decades of the twentieth century to estimate MSW generation for specific region/city. Lately, time series models were developed and considered to be more appropriate for predicting waste generation for up to several decades. Artificial Neural Networks (ANNs), relatively new modeling concepts and tools, were successfully used in waste management problems and MSW generation due to their potential to capture temporal effects from data series and reliable predicting of future MSW generation. This paper presents a brief overview on the methods for estimating MSW generation and demonstrates implementation of ANNs to model and predict monthly waste generation for the City of Skopje.

Keywords Municipal solid waste generation · Artificial neural networks · Modeling

K. Donevska (✉)

Faculty of Civil Engineering, University Ss Cyril and Methodius, Partizanski odredi 24, Skopje, Republic of North Macedonia

e-mail: donevska@gf.ukim.edu.mk

© Springer Nature Switzerland AG 2020

K. R. Reddy et al. (eds.), *Sustainable Environmental Geotechnics*, Lecture Notes in Civil Engineering 89, https://doi.org/10.1007/978-3-030-51350-4_2

1 Introduction

Planning of effective integrated waste management system design relies on accurate prediction of municipal solid waste generation data in terms of their generation rates and waste composition. However, the data should be assessed with considerable care and should not be taken as certain information since they are highly subjective [17]. These data are heterogeneous and depend on many global and regional factors like various rates of increase of population, changing lifestyles, and consumption pattern, economic development, number of population, etc.

Many different methods are available to estimate waste generation rates. Traditional methods for estimating the amount of generated solid waste are established mostly on the basis of some elements such as number of population, waste generation coefficient per capita, and social-economic development of the region as well. Different empirical models for number of population projection are presented by Patel and Srinivasarao [15]. Conventional methods for predicting MSW generation: weight volume analysis, material balance analysis, and load count analyses are basic for estimating the generated waste [18]. In load count analysis, the rate of waste collection is determined by recording the estimated volume and general composition of each load of waste for a specified period of time. The total mass is estimated using data on average density for each waste category. Weight and volume analysis is based on the weight of each load in order to provide better information about the density of the various types of solid wastes for a particular site. Load count analysis and weight volume analysis are based on the waste collection and cannot determine the rate of waste generation. Successful implementation of materials balance analysis requires accurate records of all activities that affect the waste generation rate and the associated rate of generation and well-defined boundary around the studied unit. Although materials balance analysis is a reliable way to determine generation rates, for developing countries it is a very complex task.

Classical statistical models including regression analyses were mainly developed over the last three decades of the twentieth century to estimate MSW generation for specific region/city [13]. Time series models were developed and considered to be more appropriate for predicting waste generation for up to several decades [4, 5]. Kolekar et al. [11] in their review on prediction of municipal solid waste generation models conclude that entire published models are diverse in nature for application. Most of them are based on correlation and regression analysis and few researches have been made on artificial intelligent systems like fuzzy logic.

Recently, Artificial Neural Network (ANN) has been found to provide more accurate results for MSW generation compared to conventional regression analysis and traditional time series analysis [9, 3]. Artificial Neural Network models are replicating the functioning of the human brain where a single computing node is called a neuron. ANNs were first introduced by McCulloch and Pitts [14], but started to draw a lot of attention in the scientific world since the 1980s. Since that time many different ANN types have evolved. If provided with sufficient data, ANNs can be

trained to model any relationship between the series of independent and dependent variables [10]. Flexibility and adaptability of ANNs enable them to model any nonlinear function to the required degree of accuracy. Therefore, ANNs are extensively implemented as powerful predictors in many engineering problems, economy, medicine, etc.

ANNs are successfully used in waste management problems and MSW generation due to their potential to capture temporal effects from data series and reliable prediction of future MSW generation. Several authors predict the weight of generated waste using time series of weekly data. Shahabi et al. [16] propose a model based on feed-forward artificial neural network, while Jalili and Noori [10] research different structures of artificial neural networks and then select the best model for predicting the City of Mashhad's waste generation. Abdoli et al. [1] introduce new approach series in ANNs application for long-term prediction of solid waste generation including preprocessing for reaching the stationary chain in time. Antanasi-jevic et al. [2] develop ANN models for predicting MSW generation on a national scale to overcome the frequent problem of discontinuity of time series in developing countries.

In the present study, the focus is on the estimation of MSW generation for the City of Skopje, the capital of the Republic of North Macedonia using the traditional method and ANN. The traditional method is based on number of population and waste generation coefficient per capita estimated in compliance with available data about MSW quantities disposed on the landfill for Skopje Region. ANN containing one hidden layer was trained and tested to model monthly waste generation. Input data for both methods consist of the number of waste collection vehicles and associated quantities of MSW received at the regional landfill. Data were provided by Public-Private Partnership—Drisla, the legal entity that operates the regional landfill.

2 Materials and Methods

2.1 Background and Study Area

The Skopje Region is located in the northernmost part of the country, covering 7.3% of the total land area of the country (Fig. 1). The region consists of 17 municipalities and 142 settlements. The City of Skopje, the capital of the country is located in the region, and presents administrative, cultural, economic, and academic center of the country. The total number of residents in all municipalities within the region is 578,144 according to the last population census in 2002.

The waste management system is based mainly on waste collection and disposal on a regional landfill. The waste collection and transportation is provided by Public Utility Enterprise and several private entities. Collection coverage in the region is variable and incomplete, especially in the rural areas where most of the population doesn't receive any collection service. According to the waste quantitative survey

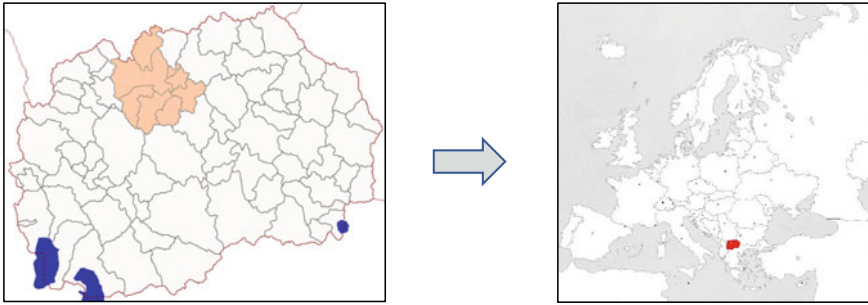


Fig. 1 Location of the study area

within the project for Establishing Regional Waste Management Plan for Skopje Region [7], the total collected waste was assessed on 150,621 tons in the year 2016 and the total generated waste was calculated to 162,883 tons. The collection coverage has been calculated to 92% showing an increasing trend compared to the previously estimated value of 88.5% [12]. The waste generation coefficient per capita in 2016 has been assessed on 262 kg/ca/year [7]. Due to the low percentage of recycling in the past, nearly the total quantity of collected MSW was disposed on the landfill. Drisla landfill operates as regional landfill for the Skopje Region, providing services for the City of Skopje and suburban areas for permanent disposal of MSW. The landfill is located southeast of the City of Skopje, at about 14 km from the City center. Designed volume of Drisla landfill is 26 million m³, i.e., total capacity of 16,9 million tons of municipal solid waste [8]. The landfill operation started in 1995 and is operated by Public–Private Partnership—Drisla. Monthly reports about the number of waste collection vehicles and associated monthly quantities of MSW from the City of Skopje received at the landfill for the period 2000–2017 were provided by Public–Private Partnership—Drisla. Taking into consideration that no reuse or recycling of MSW was practiced in the past, for estimation purposes it was assumed that nearly all generated waste was received and disposed at the landfill. Therefore, data about received/disposed MSW were used for modeling and predicting solid waste generation. According to the data, the amount of received/disposed waste on the landfill is between 119,000 tons/year to 168,000 tons/year. Average monthly received/disposed MSW is 12,060 tons/month. Statistical analyses of MSW during the different seasons in the period 2000–2017 are presented in Fig. 2.

Seasonal variations are presented by higher values of average monthly MSW generation that appear during the warmer part of the year. Seasonal variations are mainly due to larger quantities of biodegradable waste during vegetation season and people's habits. Biodegradable waste has the biggest share of the housing sector waste composition.

Statistical analyses of the autocorrelation coefficient of the data are presented in Fig. 3. The autocorrelation plot indicates monthly oscillations of data and verifies

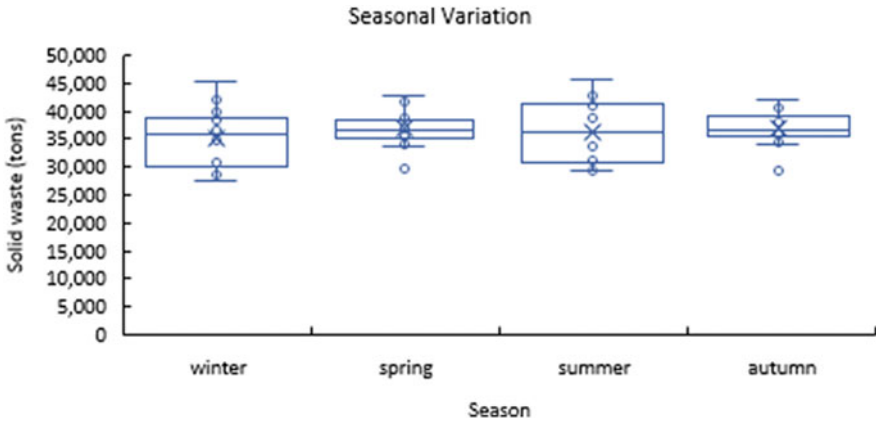


Fig. 2 Seasonal variation of disposed municipal solid waste

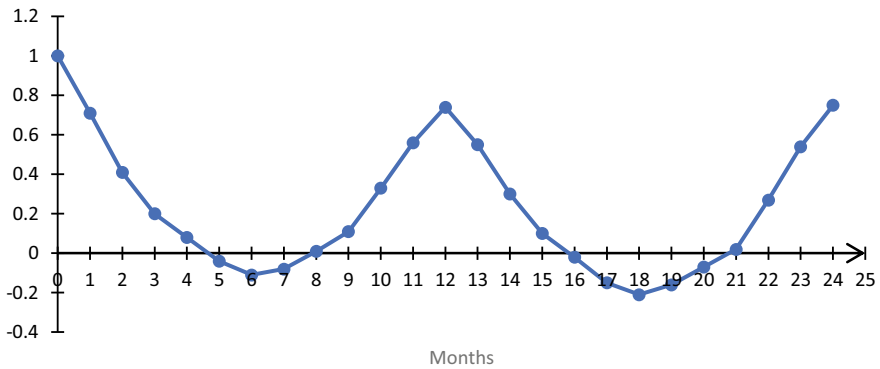


Fig. 3 Autocorrelation of monthly data of disposed MSW

the presence of periodicity with twelve months duration of each cycle. The autocorrelation plot is a sinusoidal model, confirming that data come from an underlying sinusoidal model.

2.2 Methodology

The principle behind ANNs is that a neuron, a mathematical logistic regression, can pass already processed information as abstractions down the rest of the ANN. This is very powerful when extracting seemingly uncorrelated features. ANNs can also be regarded as weighted and directed graph structures with the neurons as nodes and the weighted links between them edges. The weight of each edge has a real number

assigned showing the importance of the connection between the neurons. As directed graphs, ANNs are created as feed forward. This means, the selected features on input only propagates through the neurons toward the output and is not recurrent. Opposed to this, networks that have recurrent neurons are called Recurrent Neural Networks (RNNs) and are overly complex for the desired estimation in this work.

The paper focused on estimating the future values by exploiting ANNs trained in a supervised manner. In detail, supervised learning of Machine Learning (ML) models is performed by achieving the desired output of the model by adjusting its internal weights to meet the actual output value. The phase when ML algorithms are adjusted to fit a desired objective is called training.

To adjust the internals of the ANN model a cost function is used for calculating the difference between the actual value and the real output of the network, which for our implementation is the Mean Square Error (MSE). Once calculated, the actual values for modifying the internal weights is done through Gradient Descent. As feed forward, ANNs are split into layers. Here, back-propagation is used for the internal weights adjustment which calculates the gradient descent one layer at a time from the output toward the input [6].

The size of the input layer depends on the number of features required by the network to perform proper estimation. To choose better features, we need to analyze the autocorrelation of the data and choose features that are useful. As in Fig. 3, we can see that there is a strict periodicity within the data with a period of 12 months.

This means that the most useful data to estimate a value for month t are the values of $t-1$, $t-2$, $t-12$, and $t-13$. This means that the last useful data that we can use without shrinking the training set too much is the $t-13$ value. As such, we use all the months until the $t-13$ value that might be useful resulting in an input layer of size 12. The size of the middle layer is chosen arbitrarily to 32. And finally, as our goal is to estimate the value for month t , we have one output neuron.

3 Results

Having introduced the ANN structure, we will explain the final model and its conception. To achieve good results several measures were taken to avoid overfitting and achieve good estimator. The first mandatory step is to split the data into two different groups one used solely for training and the other for testing. In our case the data is split in roughly one quarter for testing and three quarters for training. The purpose of this is to make sure that the model does not become overfit. In more detail, overfitting is the phenomenon of having a model that near perfectly estimates the data that it is trained for while being unable to perform well when faced with new data. Therefore, the testing dataset is always new for the model and is used to control the real performance of the algorithm. A good model is chosen during training when the MSE calculated for the testing and the training datasets do not diverge. Monthly distribution of observed MSW and estimated values using the ANN model for the period of observation (2000–2017) is presented in Fig. 4. Consequently, the ANN

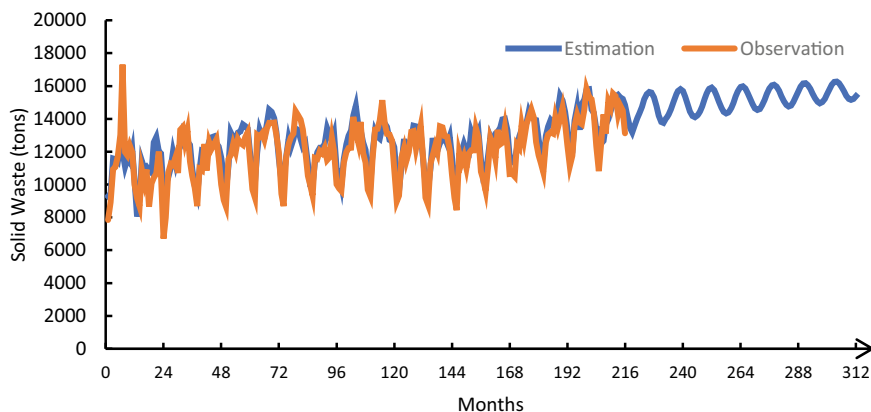


Fig. 4 Monthly distribution of predicted quantities of disposed municipal solid waste using ANN

model was used to predict monthly values of generated MSW for the next 8 years (Fig. 4).

For comparison purposes, the traditional method based on number of population and waste generation coefficient per capita was used to predict solid waste quantities for the same period of 8 years. The number of population was estimated according to the data published data within Census 2002, assuming a rate of population increase of 0.24% per year for urban part and -0.38% for the rural part of the region. The average rate of daily waste production per capita was estimated on the bases of the data about MSW quantities disposed on the landfill. The average rate of daily waste production per capita for 2018 is estimated at 0.92 kg/capita/day with 1.0% of annual increase in waste production per capita per year. Efficiency of collecting waste of 92% is assumed for the whole period of 8 years. Results of the annual generation of MSW estimated using the traditional method are compared to the predicted values using the ANN method. Estimated values using traditional methods are in general greater than the predicted values using ANN by maximal difference of 5.5%:

4 Conclusions

In this study, ANN was used for modeling and short-term prediction of monthly MSW generation for the City of Skopje. For the purpose of modeling MSW generation simple ANN containing one hidden layer was trained and tested. For the adopted ANN model, during training of the model, the values for MSE calculated for the testing and the training datasets do not diverge. The ANN model was used to predict monthly values of generated MSW for the next 8 years. For comparison purposes, the traditional method based on number of population and waste generation coefficient per capita was used to estimate MSW generation for the same time frame. Comparing

results of annual generation of MSW estimated using the traditional method to the results obtained by the ANN method, it can be concluded that estimated values using traditional methods are in general greater than the predicted values using ANN by maximal difference of 5.5%.

In summary, the present study shows the application of the traditional method and ANNs for municipal waste generation. It presents the capability of the ANNs modeling to generate accurate data about MSW generation that will support the planners in solving the complex MSW generation problem.

Acknowledgments The author gratefully acknowledges the support from the waste managers from the Public–Private Partnership—Drisla for providing the necessary data to conduct this research.

References

1. Abdoli MA, Nezhad MF, Sede RS, Behboudian S (2012) Long term forecasting of solid waste generation by the artificial neural networks. *Environ Progress Sustain Energy* 31(4):628–636
2. Antanasijevic D, Pocajt V, Popovic I, Redzic N, Ristic M (2013) The forecasting of municipal waste generation using artificial neural networks and sustainability indicators. *Sustain Sci* 8:37–46
3. Batinic B, Vukmirovic S, Vujic G, Stanisavljevic N, Ubavin D, Vukmirovic (2011) Using ANN model to determine future waste characteristics in order to achieve specific waste management targets-case study of Serbia. *J Sci Ind Res* 70:513–518
4. Bridgwater AV (1986) Refuse compositions projections and recycling technology. *Resour Conserv* 12:159–174
5. Chang N-B, Lin YT (1997) An analysis of recycling impacts on solid waste generation by time series intervention modeling. *Resour Conserv Recycl* 19:165–186
6. Donevski I (2018) Energy saving in cellular base stations under the control of supervised neural networks, MSc Thesis, Politecnico di Torino, Torino
7. Enviroplan SA (2016) Preparation of necessary documents for establishing of an integrated and financially self-sustainable waste management system in Pelagonija, Southwest, Vardar and Skopje Regions, Skopje Region–Regional Waste Management Plan, Skopje
8. IFC by Mott MacDonald Ltd (2011) Drisla landfill feasibility study, Volume 1–Main findings–Final report
9. Intharathirat R, Salam PA, Kumar S, Untong A (2015) Forecasting of municipal solid waste quantity in a developing country using multivariate grey models. *Waste Manag* 39:3–14
10. Jalili GZM, Noori R (2008) Prediction of municipal solid waste generation by use of artificial neural network: a case study of Mashhad. *Int J Environ Res* 2(1):13–22
11. Kolekar KA, Hazra T, Chakrabarty SN (2016) A review on prediction of municipal solid waste generation models. In: International conference on solid waste management, 5IconSWM 2015, Procedia environmental sciences, vol 35. Elsevier, pp 238–244
12. Local Environmental Action Plan for the City of Skopje (LEAP) (2011) City of Skopje, Republic of Macedonia
13. McBean E, Fortin M (1993) A forecast model of refuse tonnage with recapture and uncertainty bounds. *Waste Manage Res* 11:373–385
14. McCulloch WS, Pitts W (1943) A logical calculus of the ideas imminent in nervous activity. *Mater Process Technol* 5:115–133
15. Patel V, Srinivasarao M (2013) Forecasting of municipal solid waste generation for medium scale towns located in the State of Gujarat, India. *Int J Innov Res Sci Eng Technol* 2(9):4707–4717

16. Shahabi H, Khezri S, Ahmad BB, Zabihi H (2012) Application of artificial neural network in prediction of municipal solid waste generation (Case Study: Saqqez City in Kurdistan Province). *World Appl Sci J* 20(2):336–343
17. Sharma HD, Reddy KR (2004) *Geoenvironmental engineering: site remediation, waste containment, and emerging waste management technologies*. Wiley, New Jersey. (ISBN: 0-471-21599-6)
18. Tchobanoglous G, Theisen H, Vigil SA (1993) *Integrated solid waste management: engineering principles and management issues*. McGraw-Hill, Singapore

Bioremediation: Recent Advancements and Limitations



Ming Zhang and Miho Yoshikawa

Abstract Bioremediation is a process that uses living organisms, mostly naturally occurring microorganisms, to degrade, detoxify, and/or transform contaminants from wastewater and contaminated soils. The technology is considered as a cost-effective and environmentally friendly approach, and has been used to decontaminate different kinds of contaminants, such as toxic heavy metals and organic compounds. With emphasis on biodegradation of volatile organic compounds (VOCs), one of the most common contaminants that occur both in developed and developing countries, this paper overviews some recent advancements and limitations associated with biodegradation. The most significant advancements include biodegradation of multiple contaminants and understanding of microbial process including the use of next-generation sequencing (NGS), and stable-isotope probing (SIP) techniques to identify functional microbial species. The limitations and future challenges include, but not limited to selecting and supplying stimulating materials, and promoting contact between contaminants, microorganisms, and stimulating materials in engineering practice.

Keywords Bioremediation · Recent advancements · Limitations · Integrated anaerobic–aerobic biodegradation · Stable-Isotope Probing

1 Introduction

Soil contamination is typically caused by human activities and considered as a “negative legacy” of industrial development. Different countries or regions with different industrial structures and economic histories suffer from different types of soil and groundwater contamination. European Environment Agency reported that the fractions of soil and groundwater contaminations across the countries in Europe were: heavy metals (37.3%), mineral oil (33.7%), polycyclic aromatic hydrocarbons (PAHs) (13.3%), aromatic hydrocarbons (BTEXs) (6%), phenols (3.6%), chlorinated

M. Zhang (✉) · M. Yoshikawa
Geological Survey of Japan, AIST, 1-1-1, Higashi, Tsukuba, Ibaraki 305-8567, Japan
e-mail: m.zhang@aist.go.jp

hydrocarbons (CHCs) (2.4%), and others (3.6%) [1]. In Japan, soil and groundwater contamination is divided into three categories: VOCs (category 1), heavy metals (category 2), and agricultural chemicals and polychlorinated biphenyls (PCBs) (category 3), according to the Soil Contamination Countermeasures Act (No. 53) enacted in 2002. The Geo-Environmental Protection Center (GEPC) in Japan estimated that up to 930,000 sites across Japan could potentially be contaminated, and the costs required for investigating these sites and for employing countermeasures would be 2 trillion yen and 11 trillion yen, respectively [2]. Statistical results issued by the Ministry of the Environment of Japan illustrated that more than 50% of the investigated sites were found to be contaminated. Among these, more than 60% and nearly 30% of the sites were contaminated with heavy metals and VOCs, respectively [3]. A total of more than 130,000 sites contaminated with VOCs that require remediation can be estimated from the statistical surveys. The fractions in Japan counter to those in Europe regarding heavy metals and organic contaminants, reflecting different industrial structures. Major contaminants of VOCs included trichloroethylene (TCE) (24%), tetrachloroethylene (PCE) (20%), benzene (19%), and *cis*-1,2-dichloroethylene (*cis*-DCE) (17%). In addition, 1,1-Dichloroethene (1,1-DCE) (6%), 1,1,1-trichloroethane (1,1,1-TCA) (4%), and dichloromethane (DCM) (3%) were also found as contaminants of VOCs in Japan [3].

In general, contamination of heavy metals is localized due to adsorption of heavy metals to soils. In contrast, contamination of VOCs is typically characterized as being nonhomogeneous in its distribution and concentration, and large plumes due to groundwater flow and diffusion of contaminants over long periods of time. Bioremediation technologies are applicable to remediate both contaminations with heavy metals and VOCs, but with different mechanisms. In Japan, however, bioremediation is rarely used to remediate the sites contaminated with heavy metals.

The mechanism for bioremediation of heavy metals is bio-immobilization through reductive precipitation [4]. Direct reductive precipitation is the use of microbes to precipitate heavy metals by changing their valency. For example, soluble and toxic Cr(VI) can be reduced to insoluble and less toxic Cr(III) by metal-reducing bacteria. Indirect reductive precipitation involves microbial reduction of other substances, such as Fe^{3+} or SO_4^- , which results in abiotic reduction and precipitation of heavy metals. The mechanism for bioremediation of VOCs is biodegradation with different kinds of processes. For example, microbial degradation processes for chlorinated ethenes may include reductive dechlorination, aerobic oxidation, anaerobic oxidation, and aerobic cometabolism [5].

With emphasis on biodegradation of volatile organic compounds (VOCs), one of the most common contaminants that occur both in developed and developing countries, this paper overviews some recent advancements and limitations associated with biodegradation, especially considering the use in engineering practice.

2 Advancements in Bioremediation of VOCs

2.1 *Understanding the Mechanisms of Biodegradation*

The existence of functional microorganisms is crucial to bioremediation. Molecular techniques such as genomics, metabolomics, proteomics, and transcriptomics have contributed to better understanding of microbial identification, functions, metabolic, and catabolic pathways. As for the chlorinated ethenes, a variety of microorganisms have been identified and reported that can degrade different chlorinated compounds under anaerobic and aerobic conditions (Table 1). Among those, *Dehalococcoides* is the only known microorganism that can completely degrade any of the chlorinated compounds. With such information, one can perform a feasibility study for a site by first investigating whether functional microorganisms exist or not in a contaminated site for targeted contaminants to be degraded.

2.2 *Biodegradation of Multiple Contaminants*

Bioremediation of soil and groundwater containing multiple contaminants remains a challenge because complete biodegradation of all components is necessary but very difficult to accomplish in practice. The difficulties are that not all functional microorganisms necessarily exist simultaneously in the same site. In addition, some components can only be degraded under anaerobic or aerobic condition, and sequential anaerobic–aerobic or aerobic–anaerobic biodegradation should be performed. However, most anaerobic microorganisms cannot survive under aerobic condition, and vice versa. Recently, the authors have challenged integrated anaerobic–aerobic biodegradation of 7 contaminants, specifically, PCE, TCE, *cis*-DCE, vinyl chloride (VC), DCM, benzene, and toluene [40]. PCE, TCE, *cis*-DCE, VC, and DCM degraded under anaerobic condition, and benzene, toluene, and DCM degraded under aerobic condition. A breakthrough finding was that *Dehalococcoides*, generally considered sensitive to oxygen, can survive aerobic conditions for at least 28 days, and can be activated during the subsequent anaerobic biodegradation. This finding is very useful to remediate the sites contaminated with chlorinated ethenes which are preferably degraded under anaerobic condition together with other contaminants which can only be degraded under aerobic condition.

2.3 *Identification of Functional Microorganisms Using Stable-Isotope Probing Technique*

Stable-isotope probing (SIP) is a technique in microbial ecology for tracing fluxes of nutrients in biogeochemical cycling by microorganisms [41]. A substrate, *e.g.*,

Table 1 Microorganisms capable of degrading chlorinated compounds

Contaminants								
Condition	Microorganism	PCE	TCE	<i>Cis</i> -	<i>Trans</i> -	1,1-	VC	References
				DCE	DCE	DCE		
Anaerobic	<i>Clostridium sp.</i> DC-1			+			+	[6]
	<i>Clostridium sp.</i> KYT-1	+	+					[7]
	<i>Dehalobacter restrictus</i> PER-K23	+	+					[8]
	<i>Dehalococcoides mccartyi</i> BAV1	+	+	+	+	+	+	[9]
	<i>Dehalococcoides mccartyi</i> CBDB1	+	+					[10]
	<i>Dehalococcoides mccartyi</i> FL2	+	+	+	+		+	[11]
	<i>Dehalococcoides mccartyi</i> GT		+	+		+	+	[12]
	<i>Dehalococcoides mccartyi</i> MB	+	+					[13]
	<i>Dehalococcoides mccartyi</i> UCH007		+	+		+	+	[14]
	<i>Dehalococcoides mccartyi</i> 195	+	+	+	+	+	+	[15]
	<i>Desulfitobacterium hafniense</i> TCE1	+	+					[16]
	<i>Desulfitobacterium hafniense</i> Y51	+	+					[17]
	<i>Desulfitobacterium sp.</i> PCE1	+	+					[18]
	<i>Desulfomonile tiedjei</i> DCB-1	+	+					[19]
	<i>Desulfuromonas chloroethenica</i> TT4B	+	+					[20]
	<i>Geobacter lovleyi</i> SZ	+	+					[21]
<i>Sulfurospirillum multivorans</i>	+	+					[22]	
Aerobic	<i>Burkholderia vietnamiensis</i> G4		+					[23]
	<i>Methylocystis sp.</i> SB2		+	+	+	+	+	[24]

(continued)

Table 1 (continued)

Contaminants								
Condition	Microorganism	PCE	TCE	<i>Cis</i> -	<i>Trans</i> -	1,1-	VC	References
				DCE	DCE	DCE		
	<i>Methylomonas methanica</i> 68-1		+					[25]
	<i>Mycobacterium aurum</i> L1			+	+	+	+	[26]
	<i>Mycobacterium ethylenense</i> NBB4			+			+	[27]
	<i>Mycobacterium rhodesiae</i> JS60						+	[28]
	<i>Mycobacterium vaccae</i> JOB5		+	+	+	+	+	[29]
	<i>Methylosinus trichosporium</i> OB3b		+	+	+	+	+	[30]
	<i>Nitrosomonas europaea</i>		+	+	+	+	+	[31]
	<i>Nocardioides</i> sp. CF8		+	+			+	[32]
	<i>Polaromonas</i> sp. JS666			+				[33]
	<i>Pseudomonas</i> sp. ENVBF1		+					[34]
	<i>Pseudomonas mendocina</i> KR1		+					[35]
	<i>Pseudomonas putida</i> F1		+	+	+	+		[36]
	<i>Ralstonia pickettii</i> PKO1		+					[37]
	<i>Rhodococcus rhodochrous</i> ATCC 21197		+	+		+	+	[38]
	<i>Thauera butanivorans</i>		+	+			+	[32]
	<i>Xanthobacter</i> sp. Py2		+	+	+		+	[39]

a contaminant, is enriched with a heavier stable isotope that is consumed by the microorganisms to be studied. Biomarkers, such as ^{13}C -DNA, with the heavier isotope incorporated into DNA can be separated from ^{12}C -DNA by density-gradient centrifugation. DNA isolated from the target group of microorganisms can be characterized taxonomically and functionally by gene probing and sequence analysis. Using the SIP technique, the authors identified a bacterial consortium that degrades multiple VOCs (DCM, benzene, and toluene) [42]. The results showed that *Hyphomicrobium* and *Propioniferax* were the main DCM and benzene degraders, respectively, under the coexisting condition. A more interesting finding was that the known benzene

degrader *Pseudomonas* sp. was present but not actively involved in the degradation. The results not only illustrated the effectiveness of the SIP technique, but also implied that the existence of a generally known functional microorganism for a targeted contaminant does not mean the microorganism can work under conditions contaminated with multiple contaminants. Cautions should be exercised when designing bioremediation for the sites contaminated with multiple contaminants.

3 Limitations and Challenges in Bioremediation

Although much progress and advancements have been made in bioremediation, especially in biodegradation of different kinds of contaminants at laboratory scales, limitations and challenges associated with the application of the technology in situ remain to be addressed.

Since microorganisms play a crucial role in bioremediation, the existence or introduction of functional microorganisms, the abundance and community structure of the microorganisms together with other environmental factors such as temperature and redox condition in situ become key factors that control the fate of a bioremediation. Low population or absence of functional microorganisms can be an obstacle to the application of bioremediation, though bioaugmentation can be considered as a countermeasure.

Stimulating materials, such as nutrients and/or electron donors are necessary for enhancing or maintaining the activities of functional microorganisms. Limitation of nutrients in situ can impede microbial activities and thus hinder the success of bioremediation. In engineering practice, the introduction of a nutrient or an electron donor into a contaminated site to be remediated is performed by injecting or hydrofracturing. In any case, it is difficult to ensure homogenous distribution of the nutrient or electron donor over the whole range for remediation. Uncertainty and incompleteness can be major pitfalls of bioremediation.

Bioremediation can be constrained by interactions among multiple contaminants due to the toxicity of coexisting contaminants and their by-products. In addition, catabolite repression, or competition between contaminant-degrading enzymes also constrain biodegradation of contaminants. Further studies on interactions among multiple contaminants are necessary toward a better understanding of the detailed mechanisms related to bioremediation of the sites contaminated with multiple contaminants [5].

4 Conclusive Remarks

Bioremediation has received much attention in recent years, because it is cost-effective, environmentally friendly, and applicable in situ. Most studies and/or applications, however, are still limited to remediate a single contaminant, or different

compounds but belong to the same category. In the real world, however, soil and groundwater contaminated sites are frequently contaminated with multiple contaminants rather than a single contaminant or a single type of contaminant. Under the multiple contaminants-polluted condition, the system becomes much more complicated. Interaction among coexisting contaminants and competition between microorganisms may occur. Bioremediation process can be enhanced or constrained. A known functional microorganism may not work as expected.

In any case, an ideal and effective bioremediation requires sufficient contacts among functional microorganisms, nutrients, and contaminants. This condition cannot be easily achieved in engineering practice. Uncertainty and incompleteness can be the major pitfalls of bioremediation.

Further studies on the interactions among multiple contaminants, and the development of engineering technologies that can increase certainty and efficiency of bioremediation are necessary in the future.

References

1. European Environment Agency Homepage, <http://www.eea.europa.eu/themes/soil/soil-threats>. Last accessed 16 June 2009
2. Geo-Environmental Protection Center (2000) Estimation of the costs of countermeasures to soil contamination in our country (In Japanese)
3. Ministry of the Environment, Japan (2005) The results of the survey on enforcement status of the soil contamination countermeasures act and numbers and trends of soil contamination investigations and countermeasures in the fiscal year 2013 (In Japanese)
4. Ojuederie OB, Babalola OO (2017) Microbial and plant-assisted bioremediation of heavy metal polluted environments: a review. *Int J Environ Res Public Health* 14:1504
5. Yoshikawa M, Zhang M, Toyota K (2017) Biodegradation of volatile organic compounds and their effects on biodegradability under co-existing conditions. *Microbes Environ* 32(3):188–200
6. Hata J, Miyata N, Kim E-S, Takamizawa K, Iwahori K (2004) Anaerobic degradation of *cis*-1,2-dichloroethylene and vinyl chloride by *Clostridium* sp. strain DC1 isolated from landfill leachate sediment. *J Biosci Bioeng* 97(3):196–201
7. Kim ES, Nomura I, Hasegawa Y, Takamizawa K (2006) Characterization of a newly isolated *cis*-1,2-dichloroethylene and aliphatic compound-degrading bacterium, *Clostridium* sp. strain KYT-1. *Biotechnol Bioprocess Eng* 11(6):553–556
8. Holliger C, Schraa G, Stams AJ, Zehnder AJ (1993) A highly purified enrichment culture couples the reductive dechlorination of tetrachloroethene to growth. *Appl Environ Microbiol* 59(9):2991–2997
9. He J, Ritalahti KM, Yang K, Koenigsberg SS, Löffler FE (2003) Detoxification of vinyl chloride to ethene coupled to growth of an anaerobic bacterium. *Nature* 424:62–65
10. Marco-Urrea E, Nijenhuis I, Adrian L (2011) Transformation and carbon isotope fractionation of tetra- and trichloroethene to *trans*-dichloroethene by *Dehalococcoides* sp. strain CBDB1. *Environ Sci Technol* 45(4):1555–1562
11. He J, Sung Y, Krajmalnik-Brown R, Ritalahti KM, Löffler FE (2005) Isolation and characterization of *Dehalococcoides* sp. strain FL2, a trichloroethene (TCE)- and 1,2-dichloroethene-respiring anaerobe. *Environ Microbiol* 7(9):1442–1450
12. Sung Y, Ritalahti KM, Apkarian RP, Löffler FE (2006) Quantitative PCR confirms purity of strain GT, a novel trichloroethene-to-ethene-respiring *Dehalococcoides* isolate. *Appl Environ Microbiol* 72(3):1980–1987

13. Cheng D, He J (2009) Isolation and characterization of “*Dehalococcoides*” sp. strain MB, which dechlorinates tetrachloroethene to trans-1,2-dichloroethene. *Appl Environ Microbiol* 75(18):5910–5918
14. Uchino Y, Miura T, Hosoyama A, Ohji S, Yamazoe A, Ito M et al (2015) Complete genome sequencing of *Dehalococcoides* sp. strain UCH007 using a differential reads picking method. *Stand Genomic Sci* 10(1):102
15. Maymo-Gatell X, Chien YT, Gossett JM, Zinder SH (1997) Isolation of a bacterium that reductively dechlorinates tetrachloroethene to ethene. *Science* 276(5318):1568–1571
16. Gerritse J, Drzyzga O, Kloetstra G, Keijmel M, Wiersum LP, Hutson R, Collins MD, Gottschal JC (1999) Influence of different electron donors and acceptors on dehalorespiration of tetrachloroethene by *Desulfitobacterium frappieri* TCE1. *Appl Environ Microbiol* 65(12):5212–5221
17. Suyama A, Iwakiri R, Kai K, Tokunaga T, Sera N, Furukawa K (2001) Isolation and characterization of *Desulfitobacterium* sp. strain Y51 capable of efficient dehalogenation of tetrachloroethene and polychloroethanes. *Biosci Biotechnol Biochem* 65(7):1474–1481
18. Gerritse J, Renard V, Pedro Gomes TM, Lawson PA, Collins MD, Gottschal JC (1996) *Desulfitobacterium* sp. strain PCE1, an anaerobic bacterium that can grow by reductive dechlorination of tetrachloroethene or ortho-chlorinated phenols. *Archives Microbiol* 165(2):132–140
19. Fathepure BZ, Nengu JP, Boyd SA (1987) Anaerobic bacteria that dechlorinate perchloroethene. *Appl Environ Microbiol* 53(11):2671–2674
20. Krumholz LR (1997) *Desulfuromonas chloroethenica* sp. nov. Uses Tetrachloroethylene and Trichloroethylene as Electron Acceptors. *Int J Syst Bacteriol* 47(4):1262–1263
21. Sung Y, Fletcher KE, Ritalahti KM, Apkarian RP, Ramos-Hernandez N, Sanford RA et al (2006) *Geobacter lovleyi* sp. nov. strain SZ, a novel metal-reducing and tetrachloroethene-dechlorinating bacterium. *Appl Environ Microbiol* 72(4):2775–2782
22. Scholz-Muramatsu H, Neumann A, Meßmer M, Moore E, Diekert G (1995) Isolation and characterization of *Dehalospirillum multivorans* gen. nov., sp. nov., a tetrachloroethene-utilizing, strictly anaerobic bacterium. *Archives Microbiol* 163(1):48–56
23. Nelson MJ, Montgomery SO, O’neill EJ, Pritchard PH (1986) Aerobic metabolism of trichloroethylene by a bacterial isolate. *Appl Environ Microbiol* 52(2):383–384
24. Im J, Semrau JD (2011) Pollutant degradation by a *Methylocystis* strain SB2 grown on ethanol: bioremediation via facultative methanotrophy. *FEMS Microbiol Lett* 318(2):137–142
25. Koh SC, Bowman JP, Saylor GS (1993) Soluble methane monooxygenase production and trichloroethylene degradation by a type I methanotroph, *Methylomonas methanica* 68-1. *Appl Environ Microbiol* 59(4):960–967
26. Hartmans S, de Bont JAM, Tramper J, Luyben KChAM (1985) Bacterial degradation of vinyl chloride. *Biotechnol Lett* 7(6):383–388
27. Le NB, Coleman NV (2011) Biodegradation of vinyl chloride, *cis*-dichloroethene and 1,2-dichloroethane in the alkene/alkane-oxidising *Mycobacterium* strain NBB4. *Biodegradation* 22(6):1095–1108
28. Coleman NV, Mattes TE, Gossett JM, Spain JC (2002) Phylogenetic and kinetic diversity of aerobic vinyl chloride-assimilating bacteria from contaminated sites. *Appl Environ Microbiol* 68(12):6162–6171
29. Wackett LP, Brusseau GA, Householder SR, Hanson RS (1989) Survey of microbial oxygenases: trichloroethylene degradation by propane-oxidizing bacteria. *Appl Environ Microbiol* 55(11):2960–2964
30. Oldenhuis R, Vink RL, Janssen DB, Witholt B (1989) Degradation of chlorinated aliphatic hydrocarbons by *Methylosinus trichosporium* OB3b expressing soluble methane monooxygenase. *Appl Environ Microbiol* 55(11):2819–2826
31. Arciero D, Vannelli T, Logan M, Hopper AB (1989) Degradation of trichloroethylene by the ammonia-oxidizing bacterium *Nitrosomonas europaea*. *Biochem Biophys Res Commun* 159(2):640–643
32. Hamamura N, Page C, Long T, Semprini L, Arp DJ (1997) Chloroform cometabolism by butane-grown CF8, *Pseudomonas butanovora*, and *Mycobacterium vaccae* JOB5 and methane-grown *Methylosinus trichosporium* OB3b. *Appl Environ Microbiol* 63(9):3607–3613

33. Coleman NV, Mattes TE, Gossett JM, Spain JC (2002) Biodegradation of *cis*-dichloroethene as the sole carbon source by a β -Proteobacterium. *Appl Environ Microbiol* 68(6):2726–2730
34. McClay K, Fox BG, Steffan RJ (1996) Chloroform mineralization by toluene-oxidizing bacteria. *Appl Environ Microbiol* 62(8):2716–2722
35. McClay K, Streger SH, Steffan RJ (1995) Induction of toluene oxidation activity in *Pseudomonas mendocina* KR1 and *Pseudomonas* sp. strain ENVPC5 by chlorinated solvents and alkanes. *Appl Environ Microbiol* 61(9):3479–3481
36. Wackett LP, Gibson DT (1988) Degradation of trichloroethylene by toluene dioxygenase in whole-cell studies with *Pseudomonas putida* F1. *Appl Environ Microbiol* 54(7):1703–1708
37. Leahy JG, Byrne AM, Olsen RH (1996) Comparison of factors influencing trichloroethylene degradation by toluene-oxidizing bacteria. *Appl Environ Microbiol* 62(3):825–833
38. Malachowsky KJ, Phelps TJ, Teboli AB, Minnikin DE, White DC (1994) Aerobic mineralization of trichloroethylene, vinyl chloride, and aromatic compounds by *Rhodococcus* species. *Appl Environ Microbiol* 60(2):542–548
39. Ensign SA, Hyman MR, Arp DJ (1992) Cometabolic degradation of chlorinated alkenes by alkene monooxygenase in a propylene-grown *Xanthobacter* strain. *Appl Environ Microbiol* 58(9):3038–3046
40. Yoshikawa M, Zhang M, Toyota K (2017) Integrated anaerobic-aerobic biodegradation of multiple contaminants including chlorinated ethylenes, benzene, toluene, and dichloromethane. *Water Air Soil Pollut* 228:25
41. Radajewski SR, Ineson P, Parekh NR, Murrell JC (2000) Stable-isotope probing as a tool in microbial ecology. *Nature* 403:646–649
42. Yoshikawa M, Zhang M, Kurisu F, Toyota K (2017) Bacterial degraders of coexisting dichloromethane, benzene, and toluene, identified by stable-isotope probing. *Water Air Soil Pollut* 228:418

Consolidation and Hydraulic Conductivity of Soil-Bentonite Backfill Containing SHMP-Amended Ca-Bentonite in CCR-Impacted Groundwater



Yan-Jun Du, Krishna R. Reddy, Yu-Ling Yang, and Ri-Dong Fan

Abstract This study presents an assessment of feasibility on using soil-bentonite (SB) cutoff wall to control the migration of coal combustion residual (CCR) impacted groundwater. One-dimensional consolidation tests were conducted on model backfill containing sodium hexametaphosphate (SHMP)-amended calcium bentonite. Both tap water and simulated CCR-impacted groundwater were used to prepare the backfill specimen. Hydraulic conductivities of the specimens calculated from the consolidation results were also evaluated. The results indicated that the compression and swell indices for backfill prepared with CCR-impacted groundwater were 0.15 and 0.009, which was slightly lower than those for backfill prepared with tap water. In contrast, the two backfills possess hydraulic conductivity lower than 10^{-9} m/s, even under low loading pressure of 24 kPa, with regardless of the solution type used for sample preparation. This indicates little impact of the CCR-impacted groundwater on consolidation and hydraulic conductivity of the tested specimens. Thus the SB wall containing SHMP-amended Ca-bentonite has the potential to be an effective containment system for groundwater in coal ash disposal sites.

Keywords Slurry wall · Bentonite · Hydraulic conductivity · Amendment · Contaminated solution

Y.-J. Du · Y.-L. Yang (✉)

Jiangsu Key Laboratory of Urban Underground Engineering & Environmental Safety, Institute of Geotechnical Engineering, Southeast University, Nanjing 211189, China
e-mail: 103200032@seu.edu.cn

Y.-J. Du

e-mail: duyanjun@seu.edu.cn

K. R. Reddy

Department of Civil & Materials Engineering, University of Illinois at Chicago, Chicago, IL 60607, USA

R.-D. Fan

School of Materials Science and Engineering, Southeast University, Nanjing 210096, China

© Springer Nature Switzerland AG 2020

K. R. Reddy et al. (eds.), *Sustainable Environmental Geotechnics*, Lecture Notes in Civil Engineering 89, https://doi.org/10.1007/978-3-030-51350-4_5

1 Introduction

More than 100 million tons of coal combustion residuals (CCRs) are released from coal-fired power plants in the United States every year [1]. Environmental toxicity of these CCRs has led to increasing interest of citizens and environmental groups as well as regulatory agencies. Small amount of the CCRs are reutilized in industries such as cement/concrete processing [2], structural fill, and wallboard, etc., while the remaining huge volume of CCRs are disposed in permitted landfills. However, there are many older abandoned coal ash disposal sites where CCRs are disposed in unlined landfills and surface impoundments, resulting in contamination of groundwater and posing risk to public health and the environment. In particular, the levels of contaminants such as boron, chromium, molybdenum, barium, mercury, selenium and nickel in groundwater are found to be elevated [1], thus requiring remedial action.

Soil-bentonite (SB) slurry trench cutoff walls are commonly used as in situ engineering barrier to control migration of the contaminated groundwater [3, 4]. Procedures for SB wall construction include excavating a narrow vertical trench firstly, and filling the trench with bentonite-water slurry simultaneously; mixing backfill mixture along the trench side; and then replacing the slurry within the trench by the backfill mixture. Sodium bentonite (Na-bentonite) is the important constitute of the backfill material, which allows the backfill a low Hydraulic conductivity (k), i.e., a k lower than 1×10^{-9} m/s [5].

For countries where resource of high-quality Na-bentonite is scarce, such as China and India, commonly available calcium bentonite (Ca-bentonite) is considered to be an alternate material for use after proper amendment. Sodium hexametaphosphate (SHMP) is found to be a beneficial amendment for improving the swelling ability of the Ca-bentonite and decreasing hydraulic conductivity of the sand/Ca-bentonite backfills in tap water permeated condition [6–8].

This study presents the results of one-dimensional consolidation tests performed to assess the compressing and swelling behaviors of backfill containing sand and SHMP-amended Ca-bentonite in either tap water or CCR-impacted groundwater. The hydraulic conductivity calculated from the consolidation results is also investigated.

2 Materials and Methods

2.1 Solid Materials

Clean sand and powered SHMP-amended Ca-bentonite were used to prepare the backfill mixture. The sand was obtained from a quarry in Beloit, Wisconsin, USA. The raw Ca-bentonite was supplied by the CETCO (Colloid Environmental Technologies Co., Hoffman Estates, IL). The SHMP-amended Ca-bentonite is the same as that used by Yang et al. [7], and possesses a SHMP-to-bentonite ratio of 2% (dry weight basis).

Table 1 Contaminants in simulated CCR-impacted groundwater [10, 11]

Contaminant ions	Source compound	Target concentration	
		($\mu\text{g/L}$)	(mM)
Antimony	SbCl_3	4	1.75E-5
Arsenic	As_2O_3	50	5.06E-4
Barium	BaSO_4	1000	4.28E-3
Boron	H_3BO_3	3000	4.85E-2
Cadmium	$\text{Cd}(\text{NO}_3)_2$	5	2.11E-5
Chloride	CaCl_2	320000	2.88
Chromium	$\text{K}_2\text{Cr}_2\text{O}_7$	50	5.15E-4
Iron	$\text{Fe}_2(\text{SO}_4)_3$	60000	0.30
Lead	$\text{Pb}(\text{NO}_3)_2$	33	9.96E-5
Manganese	MnCl_2	10000	7.94E-2
Nickel	$\text{Ni}(\text{NO}_3)_2$	500	2.74E-3
Selenium	SeO_2	60	5.41E-4
Sulfate	Na_2SO_4	850000	5.98
Thallium	TlNO_3	0.7	2.63E-6
Vanadium	$\text{V}(\text{NO}_3)_3$	54	2.28E-4

2.2 CCR-Impacted Groundwater

The information of types of contaminants and their concentrations on CCR-impacted groundwater was obtained by performing a review on data of coal ash disposal sites in the US (mostly North Carolina). Based on these data, a simulated CCR-impacted groundwater was prepared. Tap water was also used for comparison tests.

The simulated CCR-impacted groundwater was prepared by dissolving salts of desired contaminant constituents in a simulated groundwater which consisted of distilled water and 0.006 M sodium bicarbonate, 0.002 M calcium chloride, and 0.001 M magnesium chloride as described by Reddy et al. [9]. The specific contaminants and their targeted concentrations in the CCR-impacted groundwater are summarized in Table 1.

2.3 Consolidation Tests

Two specimens prepared with either tap water (denoted as SHMP-20CaB-water) or CCR-impacted groundwater (denoted as SHMP-20CaB-CCR) were used for one-dimensional consolidation. The SHMP-20CaB-CCR backfill was prepared by mixing 80% sand, 20% bentonite (by dry weight), and CCR-impacted groundwater at a moisture content of 30.0%, which corresponded to a target slump height of 125 mm. The 20% bentonite was adopted as recommended by Yang et al. [7]. The moist

Table 2 Composition and physical properties of the specimens prepared for hydraulic conductivity and consolidation tests

Specimen ID	Liquid for preparing the specimen	Initial moisture content, w_i (%)		Initial void ratio, e_0
		Target	Measured	
SHMP-20CaB-water	Tap water	30.0	33.1	0.88
SHMP-20CaB-CCR	CCR-impacted groundwater	30.0	30.6	0.86

mixture was then sealed in a plastic bag and cured for 15 days to allow chemical equilibrium. The mass of the mixture and plastic bag was monitored at the beginning and end of the curing period, and evaporation loss was then compensated by adding distilled water to the mixture. The SHMP-20CaB-water backfill was created in the same manner; except that tap water was used instead of CCR-impacted groundwater, and the curing time was shortened to 1 day.

The consolidation test was conducted with incremental loading as per ASTM D2435 [12]. Each backfill mixture was placed in a steel ring and tapped carefully to remove large voids within the specimen. The initial properties of the final specimen for the consolidation tests are shown in Table 2. The specimen was then placed in the oedometer and subjected to a small seating load (i.e., 1.3 kPa) for 24 h. The consolidation loading sequence used in this study began at 24 kPa and was doubled after each loading stage until it reached up to 1532 kPa. The specimens were then unloaded by decreasing the applied loads by a factor of four relative to the previous load.

3 Results and Discussion

Figure 1 presents consolidation results of void ratio (e) versus effective consolidation stress (σ') on semi-logarithmic coordinates. The compression index (C_c) and swell index (C_s) represent slopes of the loading and unloading portions of the e -log σ' curves, respectively. Higher C_c and C_s values are observed in SHMP-20CaB-water specimen in Fig. 1. For example, SHMP-20CaB-water exhibits C_c and C_s values of 0.18 and 0.017, respectively, while those of SHMP-20CaB-CCR are 0.15 and 0.009, respectively. This may be the result of condensed diffused double layer thickness of the bentonite induced by CCR-impacted groundwater, which diminished the compression and swelling of the bentonite. In addition, the SHMP-20CaB-water specimen is found to possess higher initial moisture content as compared to the SHMP-20CaB-CCR specimen (see Table 2), which might also be the reason for higher C_c and C_s of the former.

Figure 2 illustrates variation of coefficients of consolidation (c_v) with effective stress. The c_v values are calculated using square root of time (Taylor) method, and the

Fig. 1 Relationship between effective consolidation stress and void ratio

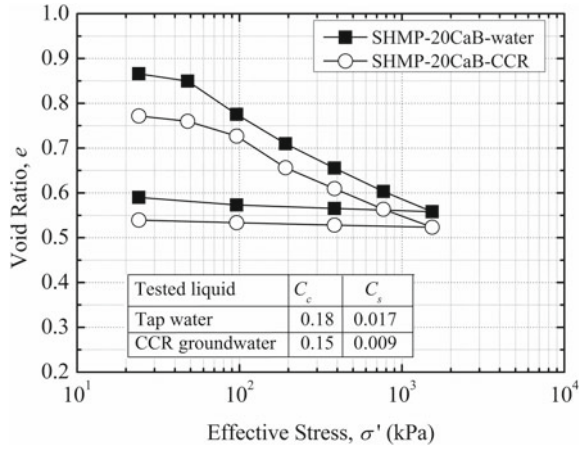
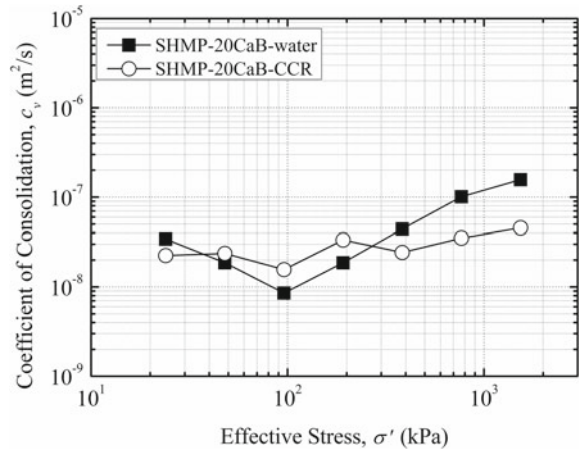


Fig. 2 Relationship between coefficients of consolidation based on Taylor's method and effective stress



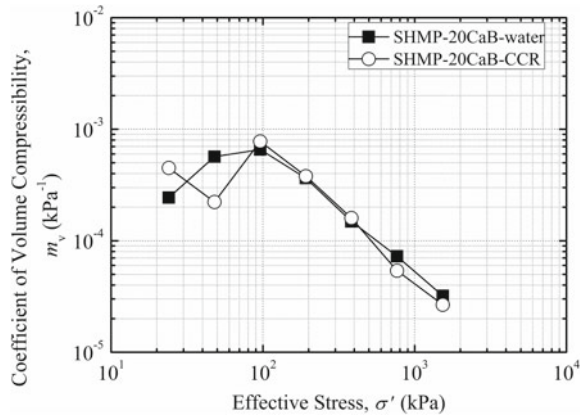
results generally fall within the range of 10^{-8} to 10^{-7} m^2/s with negligible differences found between the two tested specimens.

Figure 3 shows the relationship between the coefficient of volume compressibility (m_v) and effective stress (σ_0). The m_v value varies from 10^{-5} to 10^{-3} kPa^{-1} , with both specimens possess similar m_v value at a given effective stress. This implies insignificant effect of the CCR-impacted groundwater on the coefficient of volume compressibility of the tested backfill specimen.

The hydraulic conductivities were calculated using Terzaghi's one-dimensional consolidation theory which expressed as below equation:

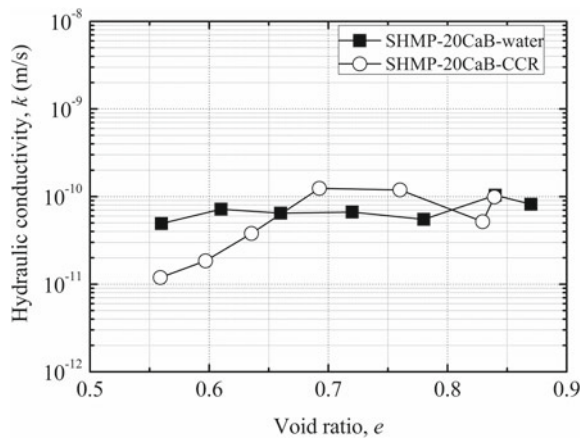
$$k = c_v m_v \gamma_w \tag{1}$$

Fig. 3 Relationship between coefficient of volume compressibility and effective stress



where k is the hydraulic conductivity (m/s), c_v is the coefficient of consolidation (m^2/s) determined using Taylor’s method, m_v and γ_w is the coefficient of volume compressibility (kPa^{-1}) and the unit weight of water (kN/m^3), respectively. The hydraulic conductivities are plotted versus void ratio in Fig. 4. Similar to findings showed in Figs. 2 and 3, in general, hydraulic conductivity of the backfill is insensitive to the CCR-impacted groundwater. In addition, even at higher void ratio which corresponds to low effective stress level, the k values of both specimens are lower than the target limit of 10^{-9} m/s for SB cutoff walls.

Fig. 4 Relationship between coefficient of volume compressibility and effective stress



4 Conclusions

This study investigated consolidation property of soil-bentonite backfill containing sodium hexametaphosphate (SHMP)-amended Ca-bentonite in either tap water or coal combustion residual (CCR)-impacted groundwater. Hydraulic conductivities of the tested specimens were also estimated via Terzaghi's one-dimensional consolidation theory.

The specimen prepared with tap water exhibited higher compression and swell indices than the specimen prepared using CCR-impacted groundwater. This might be attributed to shrinkage of the diffused double layer of the bentonite by CCR-impacted groundwater, as well as lower initial moisture content of the specimen with CCR-impacted groundwater. In contrast, The CCR-impacted groundwater had insignificant effects on coefficients of consolidation and coefficient of volume compressibility of the tested specimens.

The hydraulic conductivity (k) of the backfill specimen was found insensitive to the CCR-impacted groundwater. In addition, the k values of the tested specimens were lower than the target limit of 10^{-9} m/s for SB cutoff walls, indicating that the soil-bentonite slurry wall containing the tested backfill has potential to be an effective containment system for groundwater in coal ash disposal sites.

Acknowledgments Financial support for this project is provided by the National Key Research and Development Programme (Grant Nos. 2018YFC1803100, 2018YFC1802300 and 2019YFC1806000), Primary Research & Development Plan of Jiangsu Province (Grant No. BE2017715), and National Natural Science Foundation of China (Grant Nos. 41877248 and 41907248). The authors thank CETCO for providing the bentonites used in this study.

References

1. U.S. EPA (2015) Hazardous and solid waste management system; disposal of coal combustion residuals from electric utilities; final rule. EPA-HQ-RCRA-2009-0640, U.S. Environmental Protection Agency, Office of Resource Conservation and Recovery, Washington, D.C.
2. Zhang T, Yang YL, Liu SY (2020) Application of biomass by-product lignin stabilized soils as sustainable geomaterials: a review. *Sci Total Environ* 138830
3. D'Appolonia DJ (1980) Soil-bentonite slurry trench cutoffs. *J Geotech Eng Div* 106(4):399–417
4. Sharma HD, Reddy KR (2004) *Geoenvironmental engineering: site remediation, waste containment, and emerging waste management technologies*. Wiley, Hoboken, NJ
5. Evans JC (1993) Vertical cutoff walls. In: Daniel DE (ed) *Geotechnical practice for waste disposal*. Chapman and Hall, London, UK. pp 430–454
6. Du YJ, Yang YL, Fan RD, Wang F (2016) Effects of phosphate dispersants on the liquid limit, sediment volume and apparent viscosity of clayey soil/calcium-bentonite slurry wall backfills. *KSCE J Civil Eng* 20(2):670–678
7. Yang YL, Du YJ, Reddy KR, Fan RD (2017) Phosphate-amended sand/Ca-bentonite mixtures as slurry trench wall backfills: Assessment of workability, compressibility and hydraulic conductivity. *Appl Clay Sci* 142:120–127

8. Yang YL, Reddy KR, Du YJ, Fan RD (2018) Short-term hydraulic conductivity and consolidation properties of soil-bentonite backfills exposed to CCR-impacted groundwater. *J Geotech Geoenviron Eng* 144(6):04018025
9. Reddy KR, Khodadoust AP, Darko-Kagya K (2014) Transport and reactivity of lactate-modified nanoscale iron particles for remediation of DNT in subsurface soils. *J Environ Eng-ASCE* 140(12):04014042, 1–12
10. Naeem A, Westerhoff P, Mustafa S (2007) Vanadium removal by metal (hydr) oxide adsorbents. *Water Res* 41(7):1596–1602
11. NCDENR (2015) Duke energy groundwater assessment plans for coal-fired power stations. From http://portal.ncdenr.org/web/wq/coal_ash_gw_assessment_plans
12. ASTM (2011) Standard test methods for one-dimensional consolidation properties of soils using incremental loading. ASTM D2435, West Conshohocken, PA

Engineered Water Repellency for Applications in Environmental Geotechnology



John L. Daniels

Abstract Engineered water repellency offers a transformative approach to environmental geotechnology challenges. This paper reviews the use and potential for organosilanes to reduce leachability, control infiltration, increase strength, reduce erosion, reduce swell, and reduce effects of frost action. Organosilanes can be dissolved in water and mixed with soils and waste by-products using standard field compaction methodologies. Once cured, the treated material becomes hydrophobic. Treatment efficacy can be assessed in terms of contact angle and water entry head measurements. Evolving laboratory and field results will be summarized with a vision for future research and development.

Keywords Organosilane · Water repellency · Hydrophobicity

1 Introduction

Water repellency, as a natural phenomenon, has been well studied, with reports by Schreiner and Shorey [1]. DeBano [2] provides a review of the origin and development of related knowledge in his state-of-the-art report on hydrophobic soils. Naturally occurring repellency often derives from nonpolar organic matter such as humic substances, fungi, and microorganisms. When this matter is heated, as for example through a forest fire, the matter can be mobilized, distributed, and bonded to soil particles. DeBano [2] observes that intense water repellency can manifest when soils with hydrophobic compounds are heated between 176 and 204 °C, while increasing the temperature beyond 288 °C results in a destruction of these compounds. As such, forest fires generally create layers of water repellency at varying depths, according to the amount of organic matter and prevailing temperature gradient. While frequently viewed as a problem (e.g., erosion above and downgradient of water-repellent layer, and inhibition of plant growth), the benefits of water repellency have also been explored for “water harvesting” in agriculture. Water harvesting refers to methods to

J. L. Daniels (✉)
University of North Carolina at Charlotte, Charlotte, NC 28223, USA
e-mail: John.Daniels@unc.edu

collect and store water, often when other sources, such as groundwater and surface water or unavailable. Fink and Myers [3] and Fink [4] present data for intentionally creating water-repellent soils in the Phoenix, Arizona area for the purpose of increasing stormwater runoff for subsequent collection. Their results showed that it is possible to treat and transform high-infiltration capacity soils to become water repellent. While there is considerable literature available in soil science [5], hydrology [6], and agriculture [4], much less has been studied in geotechnical engineering. In geotechnical engineering, the use of engineered water repellency has been explored by Lambe and Kaplar [7], Daniels et al. [8], Bardet [9], Choi et al. [10], and others. Bardet [9] indicates that water repellency remains largely unexplored in geotechnical engineering while Daniels and Hourani [11] note that it may find wide application in geotechnical and geoenvironmental engineering. The objective of this paper is to concisely review such wide applications, including the use and potential for water repellency to reduce leachability, control infiltration, increase strength, reduce erosion, reduce swell, and reduce effects of frost action.

2 Background

Core concepts in water repellency include the contact angle and water entry head.

2.1 Contact Angle

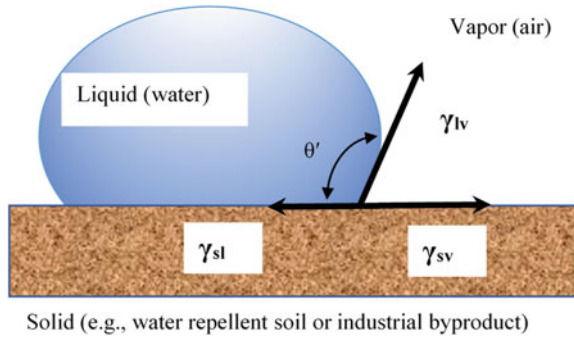
Contact angle measurements allow one to quantify that which is readily observable: the extent to which water will “bead” on the surface of a given substrate, i.e., soil, concrete, or some industrial by-product. This extent is attributed to the balance of adhesive and cohesive forces in the water while in contact with the substrate. This relationship is typically described by Young [12]:

$$\gamma_{sv} - \gamma_{sl} = \gamma_{lv} \cos \theta' \quad (1)$$

where γ_{sv} , γ_{sl} , and γ_{lv} represent the surface tension at the solid–vapor interface, solid–liquid interface, and liquid–vapor interface, respectively, and θ' is the apparent contact angle between the solid–liquid and liquid–vapor interface. This is illustrated in Fig. 1.

The measurement of contact angles has been the subject of extensive research for a wide variety of applications. A summary of the fundamental aspects of contact angle measurements and their interpretation may be found in Kock-Yee and Zhao [13]. For engineered water repellency of soils and industrial by-products, there are specific factors to consider. In the case of coal fly ash, Feyyisa et al. [14] provides background and makes recommendations, namely, the use of a dynamic, advancing method of contact angle measurement is more accurate than alternate methods.

Fig. 1 Contact angle formed of a water-repellent surface



2.2 Water Entry Head

The purpose of engineering water repellency is to prevent infiltration. Contact angle measurements can be used as an indication of water repellency and is particularly useful for solid substrates. In the case of porous media, i.e., soil or industrial by-products, we need a relationship that accounts for the pore space. This is often accounted for by using the same equation invoked for capillary rise and is often credited to Washburn [15]:

$$H = \frac{2\gamma \cos \theta}{r\rho g} \tag{2}$$

In Eq. (2), γ is the surface tension at the water/air interface, θ is the contact angle formed inside a capillary tube of radius r , ρ is the water density, g is the constant for gravity, and H is the height of water entry head. In practice, the contact angle measured on flat surfaces, θ' , is used interchangeably with θ , which represents the actual angle which manifests in the pore space. Natural soils are typically hydrophilic, and the water entry head is negative, i.e., capillary attraction holds water at pressures that are less than atmospheric. When engineered to be hydrophobic, the water entry head becomes positive. This is illustrated in Fig. 2 for a range of pore sizes.

As noted in Fig. 2, greater contact angles correspond to larger water entry heads. Smaller pore sizes correspond to larger values of suction and more negative values of water entry head for hydrophilic soils ($\theta < 90$) while for hydrophobic soils ($\theta > 90$), the water entry head values become more positive. What this means is that higher heads are required to force water into the pores in hydrophobic soils. For hydrophilic soils, it is the smaller pores which fill first, followed by the larger pores. In the case of hydrophobic soils, the large pores fill first, followed by the smaller pores. Soils and industrial by-products have a distribution of pores. Consider, for example Fig. 3, which presents the calculated pore size distribution for fine-grained and coarse-grained soil. Keatts et al. [16] used Eq. 2 to compare predicted water entry head with experimentally measured values for coal fly ash and sand engineered with organosilanes (OS) to become water repellent. Their results indicated that the water

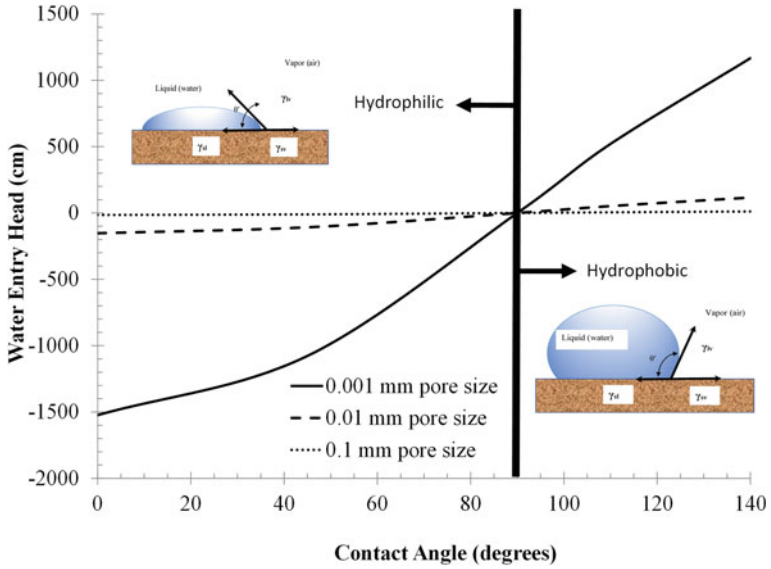


Fig. 2 Relationship between contact angle and water entry head

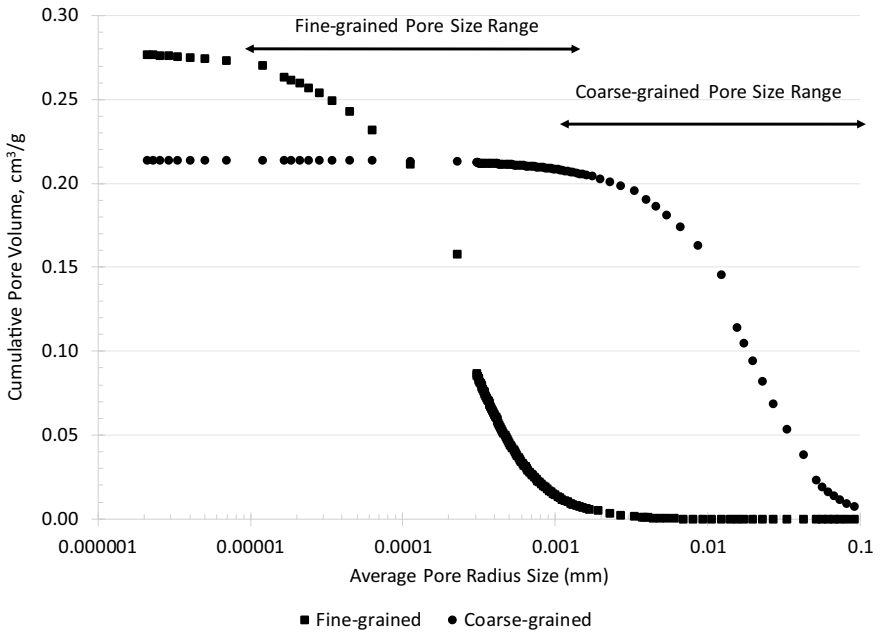


Fig. 3 Example distribution of pores for fine-grained and coarse-grained soils

entry head was increased to as high as 14 cm and 542 cm for sand and coal fly ash, respectively. Presuming a simple cubic packing, the authors estimated the pore diameters for the sand and coal fly ash to be 0.123 mm and 0.006 mm, respectively.

3 Applications

Water is the source of many challenges in environmental geotechnology. Uncontrolled moisture flux can result in increased leachability, reduced strength, increased erosion, increased swelling, and damaging frost action. Engineered water repellency has potential relevance in each of these areas. To achieve water repellency, a commonly used additive is organosilane (OS), as described in more detail in Daniels et al. [8] or Keatts et al. [16]. The OS can be applied to soils or industrial by-products in the same way that traditional moisture control for compaction is applied. For example, OS solutions can be mixed in a water truck and deployed with a sprayer bar. The soil can then be mixed, compacted, and allowed to cure. Curing durations vary, but the change from hydrophilic to hydrophobic occurs after the OS treatment is allowed to dry. Unless the OS is augmented with polymers or other additives, the resulting matrix is one in which the particles remain uncemented. Air can pass through pore space, however, water is limited according to the water entry head.

3.1 *Leachability/Infiltration Control*

Naturally occurring soils and industrial by-products can leach contaminants at concentrations that exceed various criteria. Likewise, infiltration control is a design requirement at municipal, hazardous, and nuclear waste sites. For example, the barrier layer in a municipal solid waste landfill is typically required to have a saturated hydraulic conductivity of no more than 10^{-5} cm/s. Barriers in hazardous waste landfills are required to have saturated hydraulic conductivities of no more than 10^{-7} cm/s. Engineered water repellency, by contrast, is designed to prevent any infiltration and thus saturation. If the prevailing head is less than the water entry head, then no water enters the matrix. This paradigm is similar to capillary barriers, in which a fine-grained layer is placed above a coarse-grained layer. Capillary barriers are designed to function while these layers are unsaturated, a condition that is easier to achieve in arid conditions. Under unsaturated conditions, the moisture gradient is typically upward in a capillary cover system (and away from the waste). The moisture which penetrates the fine-grained layer is designed to infiltrate the sand layer under unsaturated conditions. For a wide range of suction conditions, the unsaturated hydraulic conductivity of sand is lower than clay; i.e., the reverse condition as compared to saturated conditions [17]. Engineered water repellency is also intended to function under unsaturated conditions, however, it can be designed in any climate. Failure occurs when the water entry head is exceeded, at which point the hydraulic conductivity of a

water-repellent/hydrophobic soil may be no different than its untreated/hydrophilic counterpart. In the words of Bauters et al. [6], the hydrophobicity “functionally disappears” when saturation is forced. Keatts et al. [16] confirmed such disappearance, with measured values of saturated hydraulic conductivity ranging from 0.022 to 0.033 cm/s for contact angles ranging from 0 to 118°.

As the foregoing illustrates, the key design parameter for engineered water repellency is the water entry head. Jordan et al. [18] evaluated this parameter as a function of temperature and particle size. For a given pore diameter, increasing temperature resulted in a lower water entry head. For example, the water entry head for fine sand was 13.9, 12.7, and 7.1 for temperatures of 5, 20, and 50 °C. The authors provided a design chart that compared expected water entry head as a function of slope for various soil types and design storms. For slopes greater than 0.6%, the calculated runoff depth was less than the measured water entry head for 2, 10, and 50-year storm events at all temperatures.

3.2 Erosion

Forest-fire induced water repellency generally results in increased erosion. This occurs not at the water-repellent layer, but downstream, i.e., increased runoff from the water-repellent zone is directed to erodible soils. However, judicious use of engineered water repellency can reduce erosion locally. For example, Daniels and Hourani [11] observed that engineered water repellency of a 2:1 (horizontal: vertical) slope, at a monitored field site, resulted in a reduction in eroded mass by a factor approaching 50.

3.3 Strength and Swell

Swelling in soils is generally a function of changing moisture conditions, especially in the presence of certain clays, e.g., those with significant fractions of montmorillonite and similar minerals. Daniels and Hourani [11] observed a reduction in swell in response to treatment with OS, from 6.5% to 0.8%, for micaceous silt samples subjected to a 4.5 kg surcharge. Likewise, the California Bearing Ratio (CBR) values increased from 0.9 and 1.4, to 5.4 and 6.5, for values at 2.5 and 5.0 mm penetration. The precise mechanism for strength gain and swell reduction is unclear, however it appears the OS treatment interferes with hydration reactions and interlayer swelling. Limited data exist on the effect of water-repellent treatment on friction angle. Byun et al. [19] observed a reduction in friction angle in glass beads as a function of water repellency treatment. Daniels et al. [20], however reported that in the case of several coal fly ash samples, the reported peak and residual friction angles were similar.

4 Future Work

The use of engineered water repellency may find relevance wherever there is a need to control moisture conditions or infiltration. Another area is frost action, whereby there is a need to reduce the amount of water which is available to supply a growing ice lens. Work is beginning by the authors in this area, with preliminary (unpublished) results suggesting that water repellency can reduce frost heaving induced by the ice lensing process.

Water repellency may find use in improving pavement system performance and long-term durability, embankments, reuse of industrial by-products, landfill liners and covers, and general soil improvement. Water repellency is generally achieved with OS, and its use in the food and beverage industry suggests that environmental compatibility is of little concern Kregiel et al. [21]. Cost is another common concern, and that depends largely on the product chosen and the requisite dose. Preliminary, internal calculations indicate that OS treatment can be competitive with alternative additives or geosynthetics. Durability is another concern. Indeed, Jordan et al. [18] indicated that continued wet/dry cycles can reduce efficacy. Yet other applications of OS technology in concrete indicate that performance can perform for decades, consistent with other infrastructure life cycles [22]. Still, this technology needs further full-scale testing before design methodologies can be developed and deployed. The author suggests that engineered water repellency, as a design approach, is today where geosynthetics were in the 1970s. If true, this area of research is exceedingly fertile.

References

1. Schreiner O, Shorey EC (1910) Chemical nature of soil organic matter. USDA Bureau Soils Bull 74:2–48
2. DeBano, Leonard F (1981) Water Repellent Soils: A State-of-the-art. Tech. no. PSW-46. Pacific Southwest Forest and Range Experimentation Station, Berkeley
3. Fink DH, Myers LE (1969) Synthetic Hydrophobic Soils for Harvesting Precipitation. In Proceeding Symposium on Soil Wettability, Riverside, CA, pp 221–240
4. Fink DH (1970) Water repellency and infiltration resistance of organic-film-coated soils. Proc Soil Sci Soc Am, Madison, WI 34(2):189–194
5. Carrillo MLK, Yates SR, Letey J (1999) Measurement of initial soil-water contact angle of water repellent soils. Soil Sci Soc Am J 63(3):433
6. Bauters TWJ, Steenhuis TS, DiCarlo DA, Nieber JL, Dekker LW, Ritsema CJ, Parlange J-Y, Haverkamp R (2000) Physics of water repellent soils. J Hydrol 231–232:233–243
7. Lambe, T.W. and Kaplar, C.W (1971). Additives for modifying the frost susceptibility of soils. U.S. Cold Regions Research and Engineering Laboratory, Technical Report 123, part 1, March 1971
8. Daniels JL, Mehta P, Vaden M, Sweem D, Mason MD, Zavareh M, Ogunro VO (2009) Nano-scale organo-silane applications in geotechnical and geoenvironmental engineering. J. Terraspace Sci Eng 1(1):21–30
9. Bardet J-P, Jesmani M, Jabbari N (2014) Permeability and compressibility of wax-coated sands. Géotechnique 64(5):341–350

10. Choi Y, Choo H, Yun TS, Lee C, Lee W (2016) engineering characteristics of chemically treated water-repellent Kaolin. *Materials* 9:1–16
11. Daniels JL, Hourani MS (2009) Soil improvement with organo-silane. In *Advances in ground improvement: research to practice in the United States and China*, ASCE, GSP, vol 188, pp 217–224
12. Young T (1805) An essay on the cohesion of fluids. *Philoso Trans R Soc Lond* 01/1805 95:65–87
13. Kock-Yee L, Zhao H (2016) Surface wetting: characterization, contact angle, and fundamentals
14. Feyyisa JL, Daniels JL, Pando MA (2017) Contact angle measurements for use in specifying organosilane-modified coal combustion fly ash. *ASCE J Mater Civil Eng* 29(9):1–13
15. Washburn EW (1921) The dynamics of capillary flow. *Phys Rev* 17:273–283
16. Keatts MI, Daniels JL, Langley WG, Pando MA, Ogunro VO (2018) Apparent contact angle and water entry head measurements for organo-silane modified sand and coal fly ash. *ASCE J Geotech Geoenviron Eng* 144(6):1–9
17. Fetter CW (2001) *Applied hydrogeology*. 4th edn. Prentice Hall, p. 231
18. Jordan CS, Daniels JL, Langley W (2016) The effects of temperature and wet-dry cycling on water-repellent soils. *Environmental Geotechnics*, Institution of Civil Engineers, published online January 12, 2016, pp 1–10
19. Byun Y, Tran MK, Yun TS, Lee J (2012) Strength and stiffness characteristics of unsaturated hydrophobic granular media. *Geotech Test J* 35(1):1–8
20. Daniels JL, Pando MA, Ogunro VO, Feyyisa JL, Dumenu L, Moid M, Rodriguez C (2018) *Water Repellency for Ash Containment and Reuse*. Final Report submitted to the Environmental Research and Education Foundation
21. Kregiel D (2014) Advances in biofilm control for food and beverage industry using organo-silane technology: a review. *Food Control* 40(1):32–40
22. Basheer L, Cleland DJ (2011) Durability and water absorption properties of surface treated concretes. *Mater Struct* 44:957–967

Integrated Bioprocessing of Urban Organic Wastes by Anaerobic Digestion Coupled with Hydrothermal Carbonization for Value Added Bio-Carbon and Bio-Product Recovery: A Concept of Circular Economy



Sagarika Panigrahi, Hari Bhakta Sharma, and Brajesh K. Dubey

Abstract The major challenges associated with the anaerobic digestion of urban lignocellulosic biomass are its recalcitrance nature and the disposal of resulted digestate. In this study yard waste was thermally pretreated to overcome inherent recalcitrant nature during anaerobic digestion. The resulted digestate after anaerobic digestion, which poses a serious land disposal problem was hydrothermally treated to produce energy-rich solid biofuel known as hydrochar. After pretreatment the biogas production was improved from 328 to 364 mL/g VS. Then hydrochar prepared from the digestate at a temperature of 180 and 200 °C for a treatment duration of 6 h. The produced hydrochar had a calorific value in the range of 20–23.5 MJ/kg as compared to 15 MJ/kg for raw digestate. The present research on integration of anaerobic digestion and hydrothermal carbonization not only improved the bioenergy production but also minimized the waste production.

Keywords Hydrothermal carbonization · Anaerobic digestion · Yard waste

1 Introduction

Proper disposal of municipal solid waste is the key to sustainable management of solid waste. In 2017, 2.01 billion tons of municipal solid waste was generated and it has been expected that it will increase to 4.01 billion tons by the year 2050 [1]. However, organic waste is a major fraction of municipal solid waste in urban local bodies which ranges between 54 and 64% [2]. Additionally, due to poor source segregation practices, wet and dry waste gets mixed which increases the overall moisture content. Thermal treatment of high moisture and low calorific waste is not suitable as wet waste has to be pre-dried. Pre-drying itself is an energy-consuming

S. Panigrahi · H. B. Sharma · B. K. Dubey (✉)

Department of Civil Engineering, Indian Institute of Technology Kharagpur, Kharagpur, West Bengal 721302, India

e-mail: bkdubey@civil.iitkgp.ac.in

© Springer Nature Switzerland AG 2020

K. R. Reddy et al. (eds.), *Sustainable Environmental Geotechnics*, Lecture Notes in Civil Engineering 89, https://doi.org/10.1007/978-3-030-51350-4_7

process. Due to the mixed nature of waste owing to poor segregation and also due to poor demand, composting is not feasible technically as well as economically.

Energy harvesting from waste is the most feasible option to handle the society transition for sustainable solid waste management along with the implementation of promising renewable technologies such as Anaerobic Digestion (AD). However, organic wastes such as yard waste (YW) due to its recalcitrance nature needs to be pretreated before using it for an AD. Recalcitrant nature of organic waste is mainly due to lignin. These lignocellulosic components are a complex polymer of sugar and phenols which are difficult to degrade by microorganism, therefore yields longer hydrolysis rate. To overcome such defiant nature of an organic waste, it is pretreated. Hydrothermal carbonization (HTC) is another relatively newer thermochemical treatment technique which treats wet waste or dry waste in the presence of water [3]. Waste was heated in a closed reactor at the subcritical temperature range of water generally between 200 and 260 °C for 30 min to 3 h in an auto generated pressure. HTC takes advantage of special property of water that manifests during high temperature and pressure. In order to make AD of organic waste sustainable and profitable, the use of wet digestate as a direct feedstock during HTC for the hydrochar production seems interesting. YW used for the production of biogas has reached widespread application, and its water-rich fermentation residues, also known as digestate, typically show high concentrations of carbon and bear the potential risk of high greenhouse gas emissions. These characteristics make it an interesting feedstock for HTC.

Therefore, the aim of this study was to gain insights into the hydrothermal carbonization of digestate of microwave (MW) pretreated YW produced after AD. First, the MW pretreatment condition was optimized. Then the YW pretreated at optimum conditions was subjected to AD and the improvement in biogas production was checked. Finally the digestate produced after AD was hydrothermally carbonized and energy characteristics of hydrochar prepared was evaluated.

2 Materials and Methods

The YW (consisting of mainly dry leaves (65%), grass (33%), and fallen sticks (2%)) were collected in April 2018 from the Indian Institute of Technology Kharagpur in West Bengal, India. After receiving, the feedstock was dried in an ambient temperature to remove undesired moisture content then it was ground with a domestic mixture grinder (Havells Marathon, 2200 W, 230 V) to reduce its particle size and referred as prepared biomass. The prepared biomass was stored in an airtight bag. The effluent from liquid anaerobic digester handling wastewater of the Indian Institute of Technology Kharagpur was used as the inoculum. Prior to use, the collected inoculum was centrifuged to increase its density. The key initial characteristics of YW and inoculum are presented in Table 1.

Thermal pretreatment of the prepared biomass was carried out by a MW. All pretreatment was carried out in 250 mL glass conical flask bottles contained 5 mg YW and 150 mL water. One control sample was kept without any pretreatment named

Table 1 Initial characteristics of yard waste and inoculum

Parameter	Yard waste	Inoculum
TS (%)	93.45 ± 6.12	51.83 ± 0.09
VS (%)	84.75 ± 4.37	98.10 ± 6.11
pH	6.15 ± 0.2	7.23 ± 0.15
VFA (mg/L)	363.75 ± 20.16	157.45 ± 13.16
sCOD (mg/g TS)	189.35 ± 5.45	216.30 ± 4.92
C/N	49.73 ± 4.18	7.89 ± 1.09

as Untreated. The whole experiment and analysis was carried out in triplicate. Batch AD of pretreated and untreated samples were carried out to examine the effect of pretreatment on biogas production. The batch AD process was carried out in a 1L glass bottle under mesophilic conditions. Food to microorganism ratio of 2:1 was maintained in the reactor. The batch BMP test was conducted for approximately 30 days until biogas production was stopped.

The HTC experiment of resulted digestate from untreated (AD1) and treated (AD2) YW was carried out in a 50 mL Teflon lined autoclave. For each experiment 40 mL digestate slurry (AD1 and AD2) was used. Total solid (TS) content was 2.25 and 3.52 g for AD1 and AD2, respectively. The autoclave was closed and placed in an electric furnace and heated to the desired temperature at a heating rate of 13 ± 4 °C/min. The HTC was conducted at a temperature range of 180–200 °C for 3–6 h. After the desired reaction time, autoclave was immersed in a cold water bath to avoid any reaction beyond the desired residence time. Then the dark slurry (hydrochar) was vacuum filtered and washed with distilled water for multiple times and stored in a zip lock bag for further analysis. Then each sample was designated as per the reaction temperature and the time on which it was prepared. Digestate resulted from AD of untreated and pretreated YW was labeled as UT_Y and PT_Y. Hydrochar prepared at different temperatures and time was coded as “H”-“T (°C)”-“U/T”-“T (h)”. “H” represents hydrochar, “T (°C)” represent temperature, “U/T” represents digested type (Untreated/Treated YW digestate), and “T (h)” is time in hour. For example, “H-180-U-6” is the code name of the hydrochar prepared using digestate resulted from untreated YW at temperature–time of 180 °C–6 h. In a similar manner rest of the hydrochar were also coded.

Physiochemical parameters TS, volatile solid (VS), pH, alkalinity, and soluble COD (sCOD) of the samples were measured using standard methods [4]. Volatile fatty acids (VFA) were measured by the procedure described by [5]. Ultimate analysis in terms of carbon (C), hydrogen (H), and nitrogen (N) contents of YW was carried out using standard procedure of CHNS analysis by using EURO EA, fully automatic elemental analyzer.

3 Results and Discussion

3.1 Effect of Thermal Pretreatment on Organic Matter Solubilization

The effects of MW pretreatment temperature on YW digestibility were investigated in the temperature range from 110 to 200 °C because further increase in temperature might lead to the formation of significant inhibitors [6]. The characteristics of the supernatant for different temperature and time of untreated and MW pretreated biomass are shown in Fig. 1a, b, respectively. According to the data presented, MW pretreatment enhanced sCOD under all pretreatment conditions. MW pretreatment temperature at 110, 140, 170, and 200 °C led to increase in the sCOD by 14.4%, 40.7%, 39.0%, and 31.5%, respectively as compared to untreated one. A more pronounced effect of pretreatment temperature, manifested by a larger difference between values of sCOD, can be seen from 110 to 140 °C. It has been previously reported that MW pretreatment at high-temperature range (>100 °C) was likely to disintegrate biomass cell wall, composed of cellulose and hemicellulose, in the soluble form (e.g., sCOD) [7]. In order to study the effects of exposure time of MW pretreatment, the holding time at targeted temperature was analyzed. The targeted temperature was set at the optimum condition found previously, i.e., 140 °C. MW pretreatment at 140 °C confirmed that YW solubilization was increased with the increase in exposure time from 30 to 120 s. The sCOD increased more rapidly for the first 30 s, but the rate of solubilization was slower as the treatment time was further increased. The difference in sCOD between 30 and 70 s is almost negligible and the highest organic matter solubilization was found at 100 s.

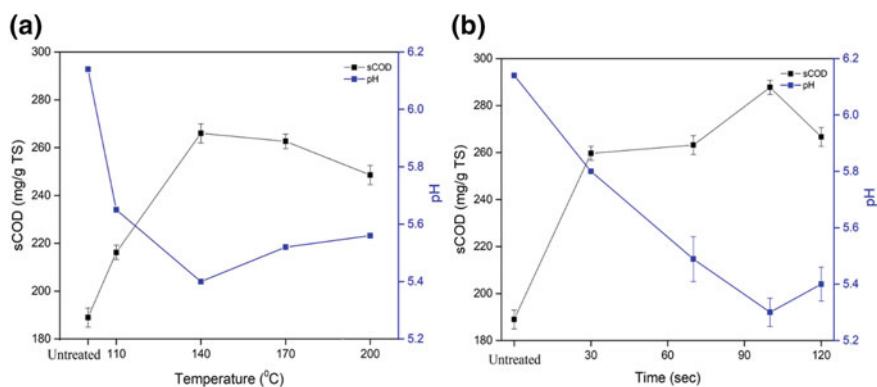
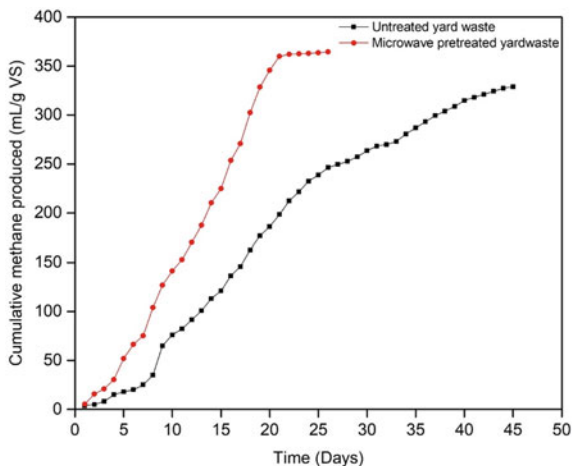


Fig. 1 a Variation in sCOD and pH of the effluent obtained after microwave pretreatment at different temperature for a duration of 2 min. b Variation in sCOD and pH of the effluent obtained for a treatment temperature of 140 °C at different duration

3.2 Effect of Thermal Pretreatment on Biogas Production

At high temperature (i.e., >150 °C) some part of structural constituents of biomass (hemicellulose and lignin) starts to solubilize. Solubilization of hemicellulose results in the formation of various acids and these acids help in further improvement in solubilization of hemicellulose. However, the solubilization of lignin is not desired in AD. The solubilization of lignin may produce inhibitory compounds like phenolic (furfural) and heterocyclic compounds like hydroxyl methyl furfural, which affects the activity of methanogens. In this scenario, BMP analysis was also conducted for MW pretreated YW and untreated YW to have a clear understanding of the effect of MW pretreatment on the improvement of hydrolysis rate and methane production. In order to determine the effect of thermal treatment on biogas production, AD assays were carried out over 45 days. Figure 2 shows the cumulative methane production achieved by untreated and MW pretreated YW. It was observed that MW pretreated YW produced higher cumulative methane yield than the untreated YW. In MW pretreated YW a sharp rise in cumulative methane production started from day 4 to day 20, and then gradually slowed down as the digestion period exceeded 21 days. On the other hand, in the case of the untreated YW, the cumulative methane production increased after day 9, which is 5 days later than MW pretreatment. The cumulative methane production of MW pretreated and untreated YW was 364.5 mL/g VS and 328.9 mL/g VS obtained after 26 and 45 days, respectively.

Fig. 2 Cumulative methane produced in untreated and microwave pretreated yard waste



3.3 Effect of Treatment Temperature and Time on Hydrothermal Carbonization

The ultimate analysis, proximate analysis, energy yield, fuel ration, hydrochar yield, and heating value (HHV) of the digestate and respective hydrochar produced at 180 and 200° for 6 h are summarized in Table 2. A significant change in the elemental composition was seen in the hydrochar after HTC. Carbon content for digestate, UTY and PTY was 44% and 44.35%, respectively. However, after HTC at 180 and 200°C for 6 h carbon content of Hydrochar; H-180-U-6, H-180-T-6, H-200-U-6, and H-200-T-6 was 51.60%, 53.26%, 53.35%, and 56.03%, respectively. HHV of all the hydrochar got increased after HTC and showed higher value at the higher temperature. HHV also called as calorific value is an important parameter if the hydrochar is intended to be used as fuel. To better understand, if the comparison is done with coal (lignite) which has a HHV of 24.98 MJ/kg [8] then digestate showed about 15.65 and 15.94 MJ/kg of heating value while hydrochar showed 20.47–23.31 MJ/kg. Aforementioned data proves that HTC of digestate produces energy-rich hydrochar which is comparable to lignite coal. The improvement in the HHV is mainly due to the increased value of fixed carbon.

Higher reaction condition during HTC promotes major reaction, i.e., dehydration and decarboxylation. The activities of dehydration and decarboxylation during HTC enhance energy densification (ED) [9]. Aforementioned point is evident from the improved value of ED seen presented in Table 2. ED for H-180-U-6 and H-180-T-6 was 1.30 and 1.33, respectively, while its value for H-200-U-6 and H-200-T-6 was 1.37 and 1.45, respectively. Fuel ratio, which is attributed to the volatile matter and

Table 2 Ultimate and proximate analysis of hydrochar prepared from digestate

Parameter		Untreated			Pretreated		
		UTY	H-180-U-6	H-200-U-6	PTY	H-180-T-6	H-200-T-6
^a Ultimate analysis	C	44	51.60	53.35	44.35	53.26	56.03
	H	6.17	7.10	7.10	6.34	7.06	7.37
	N	4.61	1.70	1.65	6.14	1.70	1.69
	O	45.01	39.75	37.29	45.34	37.89	34.91
^b Proximate analysis	A	18.32	19.31	20.23	17.56	19.67	20.57
	FC	16.57	22.04	26.16	15.44	23.59	28.2
	V	65.11	58.65	53.61	67	56.74	51.23
¹ #HHV (MJ/kg)		15.64	20.47	21.50	15.94	21.30	23.31
Energy Densification		–	1.30	1.37	–	1.33	1.45
Hydrochar yield (%)		–	68.18	65.62	–	64	55.55
Energy yield (%)		–	88.63	89.89	–	85.12	80.54

^adafb = dry ash free basis; ^bdb = dry basis

¹HHV = 0.3383 * %C + 1.422 * (%H – %O/8) [10]

#HHV of lignite is 24.98 MJ/kg [8]

fixed carbon content, gets affected by the extent of reaction severity. Improvement in fixed carbon content at higher reaction hydrochar prepared from UTY and PTY also improves fuel ratio. Fuel ratio for H-200-T-6 was 0.55 as compared to 0.48 for H-200-U-6. Similarly, fuel ratio for hydrochar H-180-T-6 was 0.42 as compared to 0.37 for hydrochar H-180-U-6. It is evident from abovementioned data that HTC of digested resulted from pretreated YW before AD exhibits better fuel quality, mainly due to accelerated and easy hydrolysis and dehydration reaction during HTC. Hence, pretreated YW not only removes recalcitrant nature for AD but also gives scope of producing better quality of fuel from its digestate.

4 Conclusions

The microwave pretreatment of yard waste at 140 °C for 100 s was an optimum condition for highest organic matter solubilization. The anaerobic digestion of microwave pretreated yard waste had an improvement in biogas production from 328.9 to 364.5 mL/g VS. The resulted wet digested when hydrothermally treated produces energy-rich hydrochar having calorific value up to 23.5 MJ/kg. The results of this study showed that the anaerobic digestion of the yard waste coupled with hydrothermal carbonization of the resulted digestate gives a unique opportunity to produce clean gas like methane and energy-dense solid fuel with a calorific value up to 24.59 MJ/kg which is comparable to lignite coal.

References

1. Kaza S, Yao LC, Bhada-Tata P, Van Woerden F (2018) What a waste 2.0. <https://doi.org/10.1596/978-1-4648-1329-0>, Accessed 04 Nov 2019
2. Hoorweg D, Bhada-Tata P (2012) a global review of solid waste management. World Bank Urban Development Series Knowledge Papers. <https://doi.org/10.1111/febs.13058>, Accessed 04 Nov 2019
3. Benavente V, Calabuig E, A. Fullana (2015) Upgrading of moist agro-industrial wastes by hydrothermal. *J Anal Appl Pyrolysis* 1(113):89–98
4. APHA (2005) Standard methods for the examination of water and wastewater, (20 edn), APHA American Public Health Association
5. DiLallo R, Albertson OE (1961) Volatile acids by direct titration. *Journal (Water Pollut Control Federation)* 356–365
6. Hu Z, Wen Z (2008) Enhancing enzymatic digestibility of switchgrass by microwave-assisted alkali pretreatment. *Biochem Eng J* 38(3):369–378
7. Kuglarz M, Karakashev D, Angelidaki I (2013) Microwave and thermal pretreatment as methods for increasing the biogas potential of secondary sludge from municipal wastewater treatment plants. *Biores Technol* 134:290–297
8. Liu Z, Quek A, Hoekman SK, Srinivasan MP, Balasubramanian R (2012) Thermogravimetric investigation of hydrochar-lignite co-combustion. *Biores Technol* 123:646–652

9. Hoekman SK, Broch A, Robbins C (2011) Hydrothermal carbonization (HTC) of lignocellulosic biomass. *Energy Fuels* 25(4):1802–1810
10. Xiao LP, Shi ZJ, Xu F, Sun RC (2012) Hydrothermal carbonization of lignocellulosic biomass. *Biores Technol* 118:619–623

Geoenvironmental Investigation Methods Used for Landfills and Contaminated Sites Management



Eugeniusz Koda, Piotr Osiński, Anna Podlasek,
and Magdalena D. Vaverková

Abstract One of the most important activities when preparing a land reclamation project of brownfields is a comprehensive analysis and documentation of subsoil conditions at the site. The paper presents the site investigation methodology applied for the purpose of preparing land reclamation project for a number of challenging case studies, located in Poland. These are mainly post-industrial brownfields like steel plants and old municipal landfill sites. The paper presents the range and methodology of contaminated soil survey, waste morphology and composition analyses as well as documentation of obtained results. The research consisted of both, site investigation and laboratory tests. A detailed analysis of the results allowed precise determination of soil contamination indicators, environmental impact zones, and volumetric capacity of contaminated soil. On the basis of methods such as geoelectrical tests, boreholes, geodetic surveys, and laboratory chemical analyses of samples, maps of contamination impact zones were prepared, which at the final stage allowed completing complex brownfield reclamation plans and works for a number of case studies.

Keywords Brownfield · Landfill · Reclamation works · Site investigation

1 Introduction

The main idea of carrying out geoenvironmental investigation of landfills' area and contaminated sites is to determine the degree of contamination and to support risk assessment studies or remediation plans [1, 2]. Geoenvironmental investigation methods combine environmental and geotechnical studies aiming at identifying the chemical, physical and mechanical properties of the soil-water environment. With

E. Koda · P. Osiński (✉) · A. Podlasek · M. D. Vaverková
Faculty of Civil and Environmental Engineering, Warsaw University of Life Sciences,
Nowoursynowska 159 St, 02-776 Warsaw, Poland
e-mail: piotr_osinski@interia.pl

M. D. Vaverková
Faculty of AgriSciences, Mendel University in Brno, Zemědělská 1, 61300 Brno, Czech Republic

respect to the protection of the environment, the use of geoenvironmental investigation methods that allow for the identification of areas which may constitute a threat to natural resources are becoming particularly important worldwide [3–5]. Several researchers suggest coupling standard geological investigations with geophysical field measurements and remote sensing tools to estimate the degree of anthropogenic transformation [2, 6–8]. The application of geophysical methods to recognize the environmental conditions is particularly important when identifying the lithology of a landfill subsoil, the depth to groundwater level, the range of the contaminated zones, or the direction of the pollutant migration [9]. Noteworthy is also the fact that geophysical methods can be used to image landfill interiors, which provide crucial information about leachate levels, waste thickness, and their geoelectrical properties [10]. Moreover, geophysical investigations can be used in preliminary site assessment as a very effective tool for creating spatial distribution of soil geochemical parameters within a field [11]. Nevertheless, it should be highlighted that a comprehensive interpretation of the geophysical test results is justified when reliable geological and geochemical data are available [12]. Regarding geophysical test methods, the monitoring strategies and environmental assessment of hazards associated with contaminated areas can be carried out with greater efficiency. In reference to the issues presented above, the main objective of this paper was to present several case studies (adopted methods and solutions) from Poland dealing with geoenvironmental investigations carried out for the purpose of preparation land reclamation projects.

2 Methods

The aim of the investigation on contaminated sites is usually to determine the boundaries of contaminated soil zones. The information obtained enables preparation of the reclamation and removal plan for the landfill area. The entire process of remedial working plan could be enclosed in five primary stages as presented in Table 1.

The most common methods used for such purposes are: geological boreholes, piezometers installation, penetration tests, soil and water sampling for laboratory chemical analyses [9]. All these methods are well established and accurate but also are labor-intensive, time and money consuming, and most importantly they are so-called invasive methods [13, 14]. The general approach of reclamation management on contaminated site is presented in Fig. 1. To complete the subsoil investigation, only when geotechnical and geological test results are reliable, it is highly recommended to apply also geophysical tests of the study site to sparsely confirm the extension of potential contamination. Among all the geophysical methods, electrical resistivity methods have been recognized as an attractive geophysical technique in the hydrogeophysical field because of its sensitivity to relative changes in the saturation of the water phase [15] and its wettability [16]. The approach behind the method is based on the observation of the electric field properties [17, 18]. The electric field is artificially excited by introducing electrodes to the ground, for which the differential potential is maintained. The method is used to measure the resistivity of a bedrock

Table 1 General approach of remedial works planning and execution

Contaminated site reclamation stages				
I	II	III	IV	V
Primary investigation	Detailed investigation	Proposing reclamation method	Reclamation plan	Remedial works
Archive documentation analyses; site inventory; primary boreholes; preliminary site assessment	Hydrogeological and geotechnical investigation; field and laboratory chemical analyses; detailed pollutants determination	Ex situ <i>physical methods</i> (soil excavation); <i>chemical methods</i> (pollutants extraction); <i>biological methods</i> (composting, bioremediation)	Technical solutions; work schedule; complementary investigation	Execution of works; quality control; monitoring
		In situ <i>physical methods</i> (barriers, thermal); <i>chemical methods</i> (sorption and stabilisation); <i>biological methods</i> (bio- and phytoremediation)		

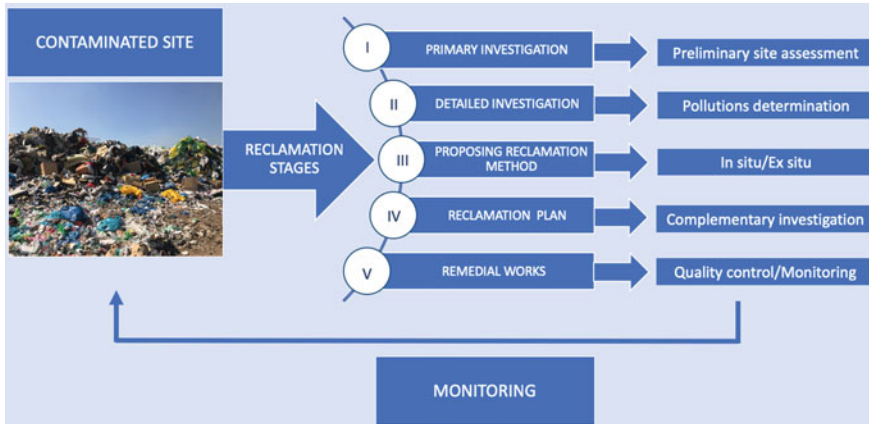


Fig. 1 Scheme of stages of contaminated sites reclamation performance

subjected to electrical field excitation, which allows precise location of layers of a different electrical resistivity potential. To perform comprehensive reclamation works at contaminated sites it is crucial to include complementary investigation tests at the stage of reclamation works design. It is also important to complete the working plan by quality tests and monitoring during the proposed reclamation process (Fig. 1).

The measurement method is based on electrical field excitation, in homogenous subsoil, by two electrodes A and B located on the ground surface subjected to different potentials. Electricity elliptic shaped lines distributed within the subsoil are limited by the surface soil layer. A depth of electrical filed presence strictly depends on the electrodes distance distribution.

3 Case Studies

3.1 Metallurgical Waste Landfill

Amount of wastes disposed and the boundary of contaminated zone. The landfill site is a part of the industrial facilities of the formal steel plant. The landfill was formed at the beginning of the 60 s. The material disposed on the landfill consisted of industrial waste products from the steel plant. The landfill was also used as a storage area for waste, such as metallurgical slag or noncombustible steel plant by-products, utilized for further development. A total area of the landfill is 34 ha, including the storage area of 26 ha. At the initial stage of the landfill operation, all materials from the steel plant were disposed without any appropriate waste management plan. First steps of reducing an environmental nuisance caused by inappropriate waste management on the landfill started in 70 and 80s and consisted of reducing the amount of wastes

disposed on the landfill, by utilizing it as a building material for the landfill roads and car parks (Figs. 2 and 3).

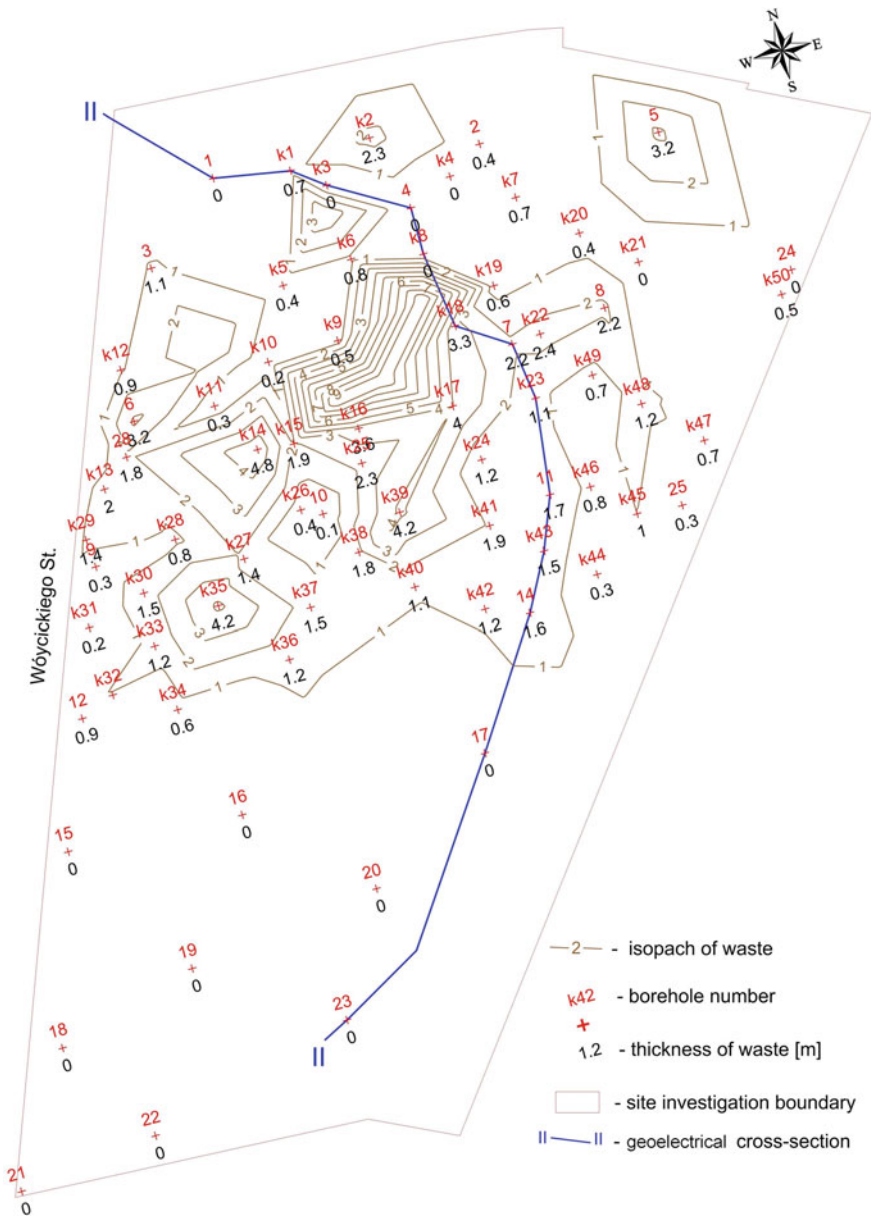


Fig. 2 Sampling location map, geoelectrical cross-section, and waste thickness [19]



Fig. 3 Areal distribution of selected contaminant indicators for metallurgical waste landfill [2]

In order to evaluate the amount of wastes actually disposed on the landfill, a geodetic survey of dumps and the landfill's body was conducted. The area of landfill was evaluated with the use of GPS methods. The bottom area was identified based on the interpretation of the borehole penetration test and geoelectrical measurement results (Figs. 2 and 3). Due to the performed investigation, it was revealed that the maximum thickness of waste dumps reaches ca. 10 m. The total cubic capacity of the waste actually disposed equals ca. 255000 m³. The total mass of waste body was estimated at the level of ca. 420000 Mg.

Works related to landfill reclamation were divided into several stages. Basically, the general aim of performed investigation was to identify the boundaries of the contaminated zones within the landfill surroundings. Site investigations concerned the accomplishment of 80 boreholes to the depth of 5–11 m and the collection of soil samples for laboratory studies.

Moreover, piezometers were installed for groundwater sampling. In order to determine zones of contaminated soil, the geophysical tests, based on the electrical resistivity method and laboratory studies, were performed. The soil samples were collected from each meter of the vadose zone in order to determine the potential emission of volatile organic compounds (VOC) following the photo-ionization measurement method (PID). Forty soil samples were selected for further detailed laboratory analyses. Results of laboratory studies revealed that the concentration of organic pollution indicators was exceeded several times which means that soil samples could have been contaminated by petroleum products. Obtained laboratory outcomes were compared with the Polish standards. It was stated that for a significant number of collected samples the values of soil quality indicators were exceeded (high levels of Cr, Zn, Cd, Mo, Pb, gasoline, and mineral oil). Based on the performed study it was assessed that the capacity of the soil requiring reclamation is around 110000 m³. Conducted geoenvironmental investigations allowed preparing the scope of required remedial works, i.e. direct soil excavation, ex situ soil washing, or phytoremediation more frequently used on degraded sites [20–22].

3.2 Municipal Solid Waste Landfills

Thickness of wastes disposed and the depth to the impermeable layer. Presented case study concerns the remediated municipal landfill site located at the north site of Lakeland mezoregion in Poland. Performed investigations consisted of geotechnical tests aiming at the determination of the soil and waste mechanical parameters and environmental surveys conducted to assess the soil-water quality. Based on geotechnical investigations it was possible to identify the thickness of wastes and layers within the subsoil (Fig. 4).

Waste thickness assessed on the basis of geophysical investigations falls in the range 4.2–7.5 m. The resistivity of wastes was identified between 12 and 29 Ωm. The depth to clay layers determined in geophysical investigation was within the range 9.5–19.7 m b.s.l. Results obtained from the geophysical tests were verified

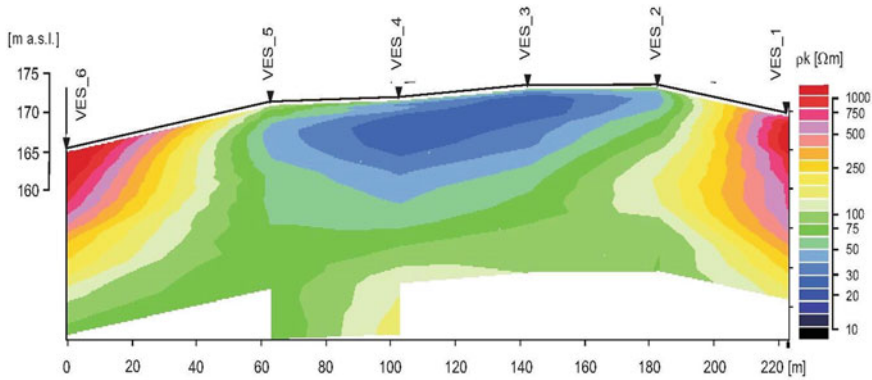


Fig. 4 Graphical interpretation of geophysical studies

by comparison with data obtained from geological boreholes and geotechnical cone penetration tests.

Leakage investigation. Geophysical investigations were performed to identify the leakage of contaminants from the municipal solid waste landfill located in the central part of Poland. The electrical resistivity measurements were conducted to distinguish the thickness of the soil layer, the groundwater level, the contaminated zone, as well as the direction of groundwater flow (Fig. 5).

The investigation was conducted due to increased concentrations of total organic carbon (TOC) and electrical conductivity (EC) measured in groundwater samples collected from the piezometer P-2 located on the outflow from the landfill. Based on monitoring results, it was stated that the leakage appeared and was the most visible in the next three years. Groundwater quality at that time was assigned to IV and V class according to Polish Regulations. The interpretation of monitoring results supported by geophysical surveys led to remedial works concerning the sealing of the area where the leakage was detected using injection methods. Moreover, contaminated water from piezometer was redirected to the pumping station at the landfill site. It was also confirmed by Pomposiello et al. [23] that the electrical resistivity imaging survey is useful in controlling the geometry of the landfill and monitoring early leakage detection [10].

Integrity of a cut-off wall around the landfill. The investigations were performed to identify the possibility of leakage of contaminants through a slurry wall installed around the municipal solid waste landfill in the central part of Poland. The field method based on the electrical resistivity tomography was applied along the cut-off wall at a distance of 5 m from the outside and inside part of the barrier. The results of investigations indicate that at the inside part from the cut-off wall, soil profile is contaminated with the landfill leachate what was confirmed by measured values of electrical resistivity (lower than 5 Ωm) (Fig. 6).

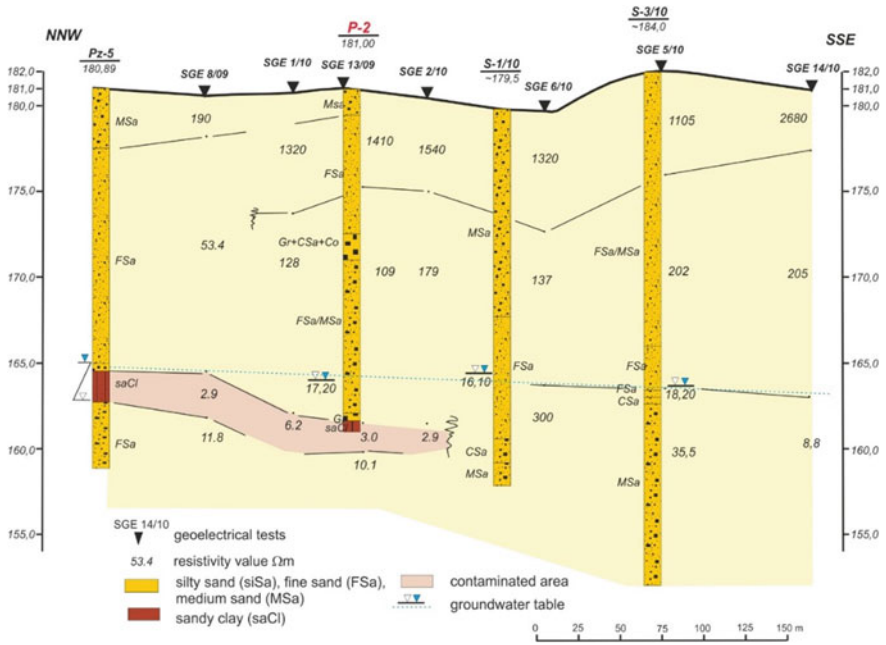


Fig. 5 Geoelectrical cross-section of the landfill subsoil [9]

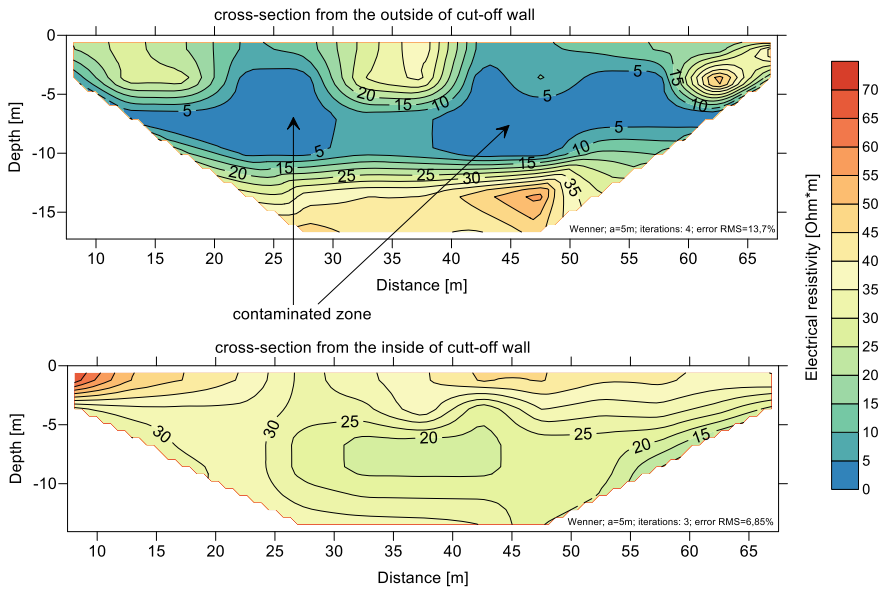


Fig. 6 The electrical resistivity cross-section made on the basis of the surveys conducted from the inside a and from the outside b part of the cut-off wall [9]

The electrical conductivity measured in the soil profile at the outside part from the cut-off wall demonstrates no contamination caused by the landfill. The values of electrical conductivity observed at that site were in the range 20–70 Ω m. In this case, the cut-off wall constitutes an impermeable barrier for the migration of contaminants to the surrounding environment. There were also several studies conducted to confirm the crucial role of vertical barriers in protection of the soil-water environment at the landfill sites [24–27].

4 Industrial Waste Landfill

Thickness of industrial wastes and the soil-water conditions. This study case concerns a closed industrial landfill with no liner applied. The landfill is located in the central part of Poland, in the neighborhood of environmentally protected areas. After the closure and reclamation works, the landfill is intended to be adapted for recreational purposes. Geoenvironmental investigations concerned geological surveys and geoelectrical tests. Based on conducted geophysical measurements, it was possible to assess the thickness of industrial wastes, paths of contaminant migration, and the depth to impermeable layers. Low levels of resistivity measured in the first aquifer layer indicate the long-term emission of pollutants from the landfill. It can be seen that the contaminated zone spread toward the soil layer with a lower permeability (Fig. 7). Umar et al. [27] and also revealed that geophysical investigations are useful in recognition of contaminated zones within the landfill site. In their case, the extremely low resistivity variation indicated the tendency to groundwater contamination.

Based on geophysical tests, it was also possible to determine the cubic capacity of wastes disposed and the amount of soil that is required to be removed during the reclamation. According to conducted tests, it was assessed that ca. 255000 m^3 of

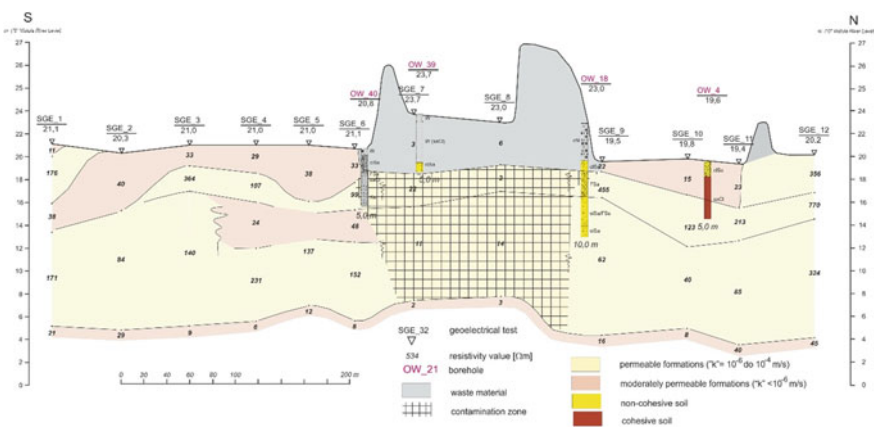


Fig. 7 The geoelectrical cross-Section. 4 of the industrial waste landfill subsoil

wastes is stored at the landfill and ca. 110000 m³ of soils should be removed during restoration works. For comparison, Belghazal et al. [29] revealed in their study that the geophysical investigations of industrial waste disposals allow to estimate the volumes of refuses required for reclamation and facilitate the recognition of the paths of leachate migration. Moreover, Gaël et al. [28] presented the ability of geophysical methods to characterize a large technical landfill installed in a former sand quarry.

5 Conclusions

A comprehensive reclamation working plan requires performing complex and detailed site investigation followed by proposed reclamation in situ or ex situ works, that at the final stage need to be quality controlled and monitored during the execution. With reference to the presented case studies, it can be concluded that the application of geophysical methods gives a great opportunity to assess the possible migration of contaminants from the landfill to the soil-water environment. In that case, geophysical measurements allow for quite precise determination of the range of contaminant spread, especially salts and bicarbonates. The interpretation of geophysical data, supported by geological surveys and geochemical tests, significantly facilitate the preparation of reclamation works for contaminated and industrial sites.

References

1. Mondelli G, Giacheti HL, Howie JA (2010) Geo-environmental investigation: a brief review and a few suggestions for Brazilian contaminated sites. *Soils and Rocks* 33(3):171–182
2. Koda E, Osiński P (2016) Site investigation of an industrial landfill for the purpose of a remedial works project. In: *Proceedings of the geo-Chicago 2016: sustainable waste management and remediation*, Chicago, IL, USA, pp 750–757
3. Rowe RK (ed) (2012) *Geotechnical and geoenvironmental engineering handbook*. Springer Science & Business Media
4. Di Fiore V, Cavuoto G, Punzo M, Tarallo D, Casazza M, Guarriello SM, Lega M (2017) Integrated hierarchical geo-environmental survey strategy applied to the detection and investigation of an illegal landfill: a case study in the Campania Region (Southern Italy). *Forensic Sci Int* 279:96–105
5. Babu GS, Reddy KR, De A, Datta M (eds) (2017) *Geoenvironmental practices and sustainability: linkages and directions*. Springer
6. Jodeiri Shokri B, Doulati Ardejani F, Moradzadeh A (2016) Mapping the flow pathways and contaminants transportation around a coal washing plant using the VLF-EM, geo-electrical and IP techniques—A case study. *NE Iran Environ Earth Sci* 75:62
7. De A (2017) Site characterization of landfills through in situ testing. In: Sivakumar BG, Reddy K, De A, Datta M (eds) *Geoenvironmental practices and sustainability. Developments in Geotechnical Engineering*, Springer, Singapore
8. Esposito G, Matano F, Sacchi M (2018) Detection and geometrical characterization of a buried landfill site by integrating land use historical analysis, digital photogrammetry and airborne lidar data. *Geosciences* 8:348

9. Koda E, Tkaczyk A, Lech M, Osiński P (2017) Application of electrical resistivity data sets for the evaluation of the pollution concentration level within landfill subsoil. *Appl Sci* 7:262
10. Carpenter PJ, Reddy KR (2017) Geophysical imaging of landfill interiors: examples from Northern Illinois, USA. In: Sivakumar Babu G, Reddy K, De A, Datta M (eds) *Geoenvironmental practices and sustainability. developments in geotechnical engineering*. Springer, Singapore, pp 1–11
11. Koda E, Siczka A, Osinski P (2016) Ammonium concentration and migration in groundwater in the vicinity of waste management site located in the neighborhood of protected areas of Warsaw. *Poland Sustain* 8(12):1253
12. De Carlo L, Perri MT, Caputo MC, Deiana R, Vurro M, Cassiani G (2013) Characterization of a dismissed landfill via electrical resistivity tomography and mise-à-la-masse method. *J Appl Geophys* 98:1–10
13. Liao Q, Deng Y, Shi X, Sun Y, Duan W, Wu J (2018) Delineation of contaminant plume for an inorganic contaminated site using electrical resistivity tomography: comparison with direct-push technique. *Environ Monit Assess* 190(4):187
14. Wang TP, Chen CC, Tong LT, Chang PY, Chen YC, Dong TH, Liu HC, Lin CP, Yang KH, Ho CJ (2015) Applying FDEM, ERT and GPR at a site with soil contamination: a case study. *J Appl Geophys* 121:21–30
15. Maurya PK, Rønne VK, Fiandaca G, Balbarini N, Auken E, Bjerg PL, Christiansen AV (2017) Detailed landfill leachate plume mapping using 2D and 3D electrical resistivity tomography—With correlation to ionic strength measured in screens. *J Appl Geophys* 138:1–8
16. Bichet V, Grisey E, Aleya L (2016) Spatial characterization of leachate plume using electrical resistivity tomography in a landfill composed of old and new cells (Belfort, France). *Eng Geol* 211:61–73
17. Oh TM, Cho GC, Lee C (2014) Effect of soil mineralogy and pore-water chemistry on the electrical resistivity of saturated soils. *J Geotech Geoenviron Eng* 140(11):06014012
18. Loke MH, Chambers JE, Rucker DF, Kuras O, Wilkinson PB (2013) Recent developments in the direct-current geoelectrical imaging method. *J Appl Geophys* 95:135–158
19. Koda E, Kotanka T, Osiński P (2013) Investigation of soil contamination level beneath the metallurgical waste landfill for the purpose of future reclamation works. *Anna Warsaw Univ Life Sci SGGW, Land Reclam* 45(1):5–16
20. Brtnický M, Pecina V, Hladký J, Radziemska M, Koudelková Z, Klimánek M et al (2019) Assessment of phytotoxicity, environmental and health risks of historical urban park soils. *Chemosphere* 220:678–686
21. Adamcová D, Vaverková MD, Bartoň S, Havlíček Z, Břoušková E (2015) Soil contaminations in landfill: a case study of the landfill in Czech Republic. *Solid Earth Discuss* 7(4)
22. Vaverková MD, Radziemska M, Bartoň S, Cerdà A, Koda E (2018) The use of vegetation as a natural strategy for landfill restoration. *Land Degrad Dev* 29(10):3674–3680
23. Pomposiello C, Dapeña C, Favetto A, Boujon P (2012) Application of geophysical methods to waste disposal studies. In: Yu X-Y (ed) *Municipal and industrial waste disposal*. <https://doi.org/10.5772/29615>
24. Hale J, Hubaut A, Vincent P (2015) Utilisation of deep groundwater barrier walls using soil bentonite and biopolymer slurries in geotechnical and environmental applications. In: *Australian geomechanics society sydney chapter symposium*, pp 1–14
25. Yang YL, Reddy KR, Du YJ (2016) A soil-bentonite slurry wall for the containment of CCR-impacted groundwater. *InGeo-Chicago 2016*:578–589
26. Koda E, Miskowska A, Siczka A, Osiński P (2018) Heavy metals contamination within restored landfill site in Poland. *Environ Geotech*. <https://doi.org/10.1680/jenge.18.00031>
27. Xie H, Wang S, Chen Y, Jiang J, Qiu Z (2018) An analytical model for contaminant transport in cut-off wall and aquifer system. *Environ Geotech*. <https://doi.org/10.1680/jenge.18.00021>
28. Umar M, Bala B, Garba MA, Muhammed MA (2017) Subsurface mapping of groundwater contamination pathway using geoelectric method at waste site of Kubanni Basin, Zaria, Kaduna State, Nigeria. *Bayero J Pure Appl Sci* 10(2):300–304

29. Belghazal H, Piga C, Lodo F, Stitou El Messari J, Ouazani Touhami A (2013) Geophysical surveys for the characterization of landfills. *Int J Innov Appl Stud* 4(2):254–263

Minimizing the Impact of Groundwater Pumping on the Environment: Optimization Strategies



S. Mohan

Abstract Long-term Groundwater pumping alters the environment and groundwater availability and thus affecting both the local and regional environment in a significant way. There are many purposes for which the groundwater has been abstracted in large quantity thus creating an unscientific way of management of the groundwater, leading to jeopardizing the sustainability of groundwater availability on a long-term basis. In this paper, we would be discussing one case study dealing with the groundwater modeling of open-cast mines with the development of an Integrated groundwater model to evaluate the impact of mining and the irrigated agriculture in the surrounding environs, on the groundwater status as well as to determine the time-period/year when the newly proposed mines without any increase in total pumping of groundwater. The study includes estimating groundwater recharge and developing a three-dimensional steady-state groundwater flow model exclusively for mine pumping simulation. The model has been utilized to evaluate the impacts of changes in groundwater pumping under the mine expansion scenario. In addition, simulation runs were made with the developed model to assess the impacts of recharging into the aquifer systems through the proposed recharge structures on groundwater and the surrounding environments and for various scenarios that vary depending upon the current as well as on the future conditions of water use. The other case study was in connection with the dewatering optimization in a metro rail tunneling construction. The requirement of maximum allowable drawdown necessitates the need for pumping and injection simultaneously and the optimal pumping wells and recharge wells location as well as the quantum of pumping and injection have been arrived at for 5 typical tunnel construction locations in a metro city of India. The engineering lessons learned, and the environment-friendly groundwater pumping plans are the major outcomes of these research works, which would be highlighted.

Keywords Groundwater · Pumping · Visual MODFLOW · Open pit mines · Environment · Optimization

S. Mohan (✉)

Environmental & Water Resources Engineering Division, Department of Civil Engineering,
Indian Institute of Technology Madras, Chennai 600036, India
e-mail: smohan@iitm.ac.in

© Springer Nature Switzerland AG 2020

K. R. Reddy et al. (eds.), *Sustainable Environmental Geotechnics*, Lecture Notes
in Civil Engineering 89, https://doi.org/10.1007/978-3-030-51350-4_9

1 Introduction

Mathematical models are conceptual descriptions or approximations that describe physical systems using mathematical equations. They are not exact descriptions of physical systems or processes. The applicability or usefulness of a model depends on how closely the mathematical equations approximate the physical system being modeled. To evaluate the applicability or usefulness of a model, it is necessary to have a thorough understanding of the physical system and the assumptions embedded in the derivation of the mathematical equations. Due to the simplifying assumptions embedded in the mathematical equations and many uncertainties in the values of data required by the model, a model must be viewed as an approximation and not as an exact duplication of field conditions.

1.1 Development of a Conceptual Model

The behavior of the system may be complicated, depending on the amount of details we wish or need to include in describing them. We need to simplify the description of the considered system and its behavior to a degree that will be useful for the purpose of planning and making management decisions in specific cases. These simplifications are introduced in the form of a set of assumptions that expresses our understanding of the nature of the system and its behavior, as far as the considered problem is concerned. For example, simplifying assumptions should be introduced concerning geometry of the domain, effects of heterogeneity, nature of solid and fluid phases involved, regimes of the flow, and various physical, chemical, and biological processes taking place within the domain.

The selection of the appropriate conceptual model for a particular case depends on the objectives of the investigation, available resources required for constructing and solving the model, and legal and regulatory framework, which pertains to a considered case.

1.2 Development of a Mathematical Model

In this step, the conceptual model is expressed in the form of a mathematical model. The mathematical model consists of:

- A definition of the geometry of the surfaces that bound the considered domain.
- Equations that express the balances of the considered quantities.
- Flux equations that relate the fluxes of the considered extensive quantities to the relevant state variables of the problem.
- Constitutive equations, that define the behavior of the particular phases and chemical species involved.

- Sources and sinks, often referred to as forcing functions, of the relevant extensive quantities.
- Initial conditions that describe the known state of the considered system at some initial time.
- Boundary conditions that describe the interaction of the considered domain with its environment across their common boundaries.

1.3 Development of a Numerical Model and Code

Numerical methods are usually employed for solving the mathematical models. This means that various numerical methods are employed to transform the mathematical model into a numerical one. In the latter, the partial differential equations appearing in the former are represented by their numerical counterparts. A computer program or code is required in order to solve the numerical model. Verification of the numerical code is essential, and it includes checking what it proclaims to do, namely, to solve the mathematical model. Verification involves comparing solutions obtained by using the code with those obtained by analytical method, whenever such solutions are available. This is usually done for cases of simplified domain geometry, homogeneous material, etc. In many cases, analytical solutions cannot be derived. The only procedure is then to compare code solutions with solutions obtained by other codes.

1.4 Model Calibration and Parameter Estimation and Validation

Model calibration is identifying the values of these model coefficients as inverse problem, or parameter estimation problem. It is essential that for any groundwater models to be interpreted and used properly its limitations should be understood. Hydrogeologic and hydrologic parameters used by the model are always just an approximation of their actual field distribution that can never be determined with 100% accuracy.

Model validation is the process of making sure that the model includes and describes all the relevant processes that affect the excitation-response relations of interest to an acceptable degree of accuracy. It is desirable to perform the model validation for the actual site of interest. Many features of field experiments cannot be controlled or even identified. Among them, field heterogeneity and anisotropy, which, in many cases, are very critical features that often, dominate the system's behavior.

1.5 Groundwater Flow Modeling Using Visual MODFLOW

Visual MODFLOW is a modular three-dimensional finite difference groundwater flow model where similar program functions are grouped together, and scientific computational and hydrologic options are constructed in such a manner that each option is independent of other options. The three-dimensional movement of groundwater of constant density through a porous medium may be described by

$$\frac{\partial}{\partial x}k_{xx}\frac{\partial h}{\partial x} + \frac{\partial}{\partial y}k_{yy}\frac{\partial h}{\partial y} + \frac{\partial}{\partial z}k_{zz}\frac{\partial h}{\partial z} - w = S_s\frac{\partial h}{\partial t} \quad (1)$$

where k_{xx} , k_{yy} , and k_{zz} are values of hydraulic conductivity along x , y , and z axes, respectively, h is the potentiometric head, w is the volumetric flux per unit volume, S_s is the specific storage, and t is the time. This parabolic differential equation with specified initial and boundary conditions constitutes a mathematical representation of groundwater flow system. In Visual MODFLOW this equation is solved using block centered finite difference approach where the groundwater system, represented by the Eq. (1), is replaced by a finite set of discrete points in space and time. These points are at the center of each cell. Then the partial differentials in the equation for each point are replaced by finite difference terms. This leads to a set of simultaneous linear equations which are solved by different methods such as Pre-Conditioned Conjugate Gradient method, Slice-Successive Overrelaxation method, etc.

2 Case Study 1: Groundwater Control for Mining Operations

Mining industries are significant contributors to a country's economy. The extraction of minerals from the earth often interferes with the groundwater after reaching specific depths below the ground level. As and when the overburden material is removed, the balancing pressure is disturbed, and as a result, the water present in the underlying confined aquifers which is under high pressure burst out and cause flooding of the mine floors [1]. The flooding of the mine floor can cause damage to life as well as machinery leading to a massive loss in terms of life and property [2]. Unexpected inflow in large quantities may also impede production, delay the project, and may lead to safety and environmental problems.

To ensure safe mining operations, it is essential to pump out the water flooding the mines by depressurization plans and ensure safe working conditions at the mine floor. The water levels at different stages of mining should be found out for carrying out safe operations. Groundwater management is essential as the water resources available on the earth's surface is getting depleted over time. If the groundwater resources are abstracted at a rate much faster than the rate at which it can be replenished, then it gets exhausted over time. Depletion of groundwater levels can have severe effects

on the ecosystem, such as reduction of flow to the streams during the dry season, reduction in the contribution to the groundwater supplied wetlands, reduction in the amount available to meet human demands, etc.

Thus, it becomes essential to focus on groundwater management as the resources are getting depleted with time. Simulation models are used to understand the system and to test specific water-resource management plans, in a trial-and-error approach, to select a single idea from a few alternative ones that gives the best solution strategy. Due to the complex behavior of groundwater systems, the selection of best-operating procedure or policy can be challenging. To address this difficulty, groundwater simulation models have been linked with optimization models to determine the best management strategies from among many possible approaches.

2.1 Simulation Models for Groundwater Control

Groundwater modeling is an efficient tool to understand the groundwater flow beneath the earth's surface [3]. Groundwater flow models have been used as interpretative tools for investigating groundwater system dynamics and understanding the flow patterns, as simulation tools for analyzing responses of the groundwater system to stresses, as assessment tools for evaluating recharge, discharge and aquifer storage processes, and for quantifying sustainable yield. Modeling of a system requires a sufficient amount of information about the aquifer, which includes the soil types that make up the lithological units.

The application of groundwater modeling is tremendously increased due to its vast capacity and simplicity. Especially in case of mines, where a huge quantity of water is extracted for safe mining purposes, a management strategy must be adopted to ensure that not more than what is essential is withdrawn from the underground reserves. To understand the subsurface system, groundwater models serve as a versatile tool. These models can also be used as predictive tools for predicting future conditions or impacts of human activities, supporting means for planning field data collection and designing practical solutions, screening tools for evaluating groundwater development scenarios, management tools for assessing alternative policies, visualization tools for communicating critical messages to public and decision-makers [4].

Finite element or Finite difference method are commonly employed for arriving at the solution for numerical models. MODFLOW (3D Finite-Difference Groundwater Flow Model) [5], which works based on the Finite Difference method is widely used as a tool for groundwater flow simulations. For modeling an aquifer system, the foremost thing required is the details of the aquifer system. A sufficient number of bore log information is needed to create the lithological profile of the aquifer. Properties such as conductivity, storage are assigned to each stratigraphic unit. Once the conceptual model is developed, then the numerical simulations can be performed by adding initial and boundary conditions (Fig. 1).

The recharge received from rainfall is also given as input to the model as a part of rainfall recharge to the groundwater. Usually, 15–20% of rainfall is taken as recharge

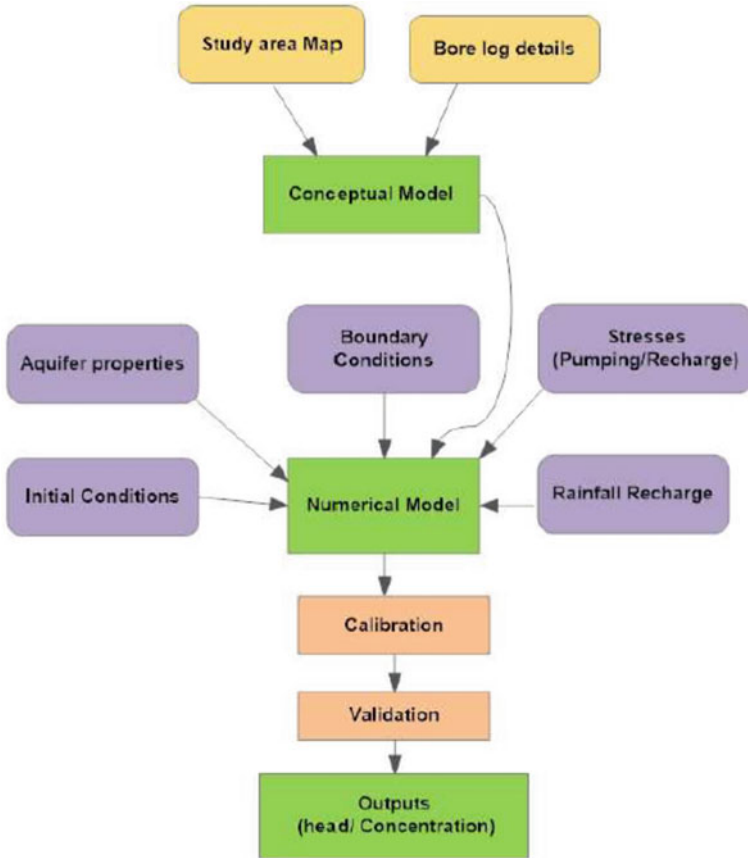


Fig. 1 Flow chart of groundwater simulation modeling

[6]. The boundary conditions are assigned based on the water level and flow condition that exists in the boundary region. Different boundary conditions such as Dirichlet, Cauchy, and Neumann can be applied based on the conditions that occur in the site. The pumping wells and recharge wells within the study area act as source or sinks in the model. The location of the wells and the rates at which they pump out/inject water needs to be incorporated into the model. The model gives head at various locations within the study area as output, along with that it provides the direction of groundwater flow, path lines for particle tracking, the velocity of groundwater flow, the mass balance between layers, etc.

After the model run, the model needs to be calibrated. Calibration is the adjustment of parameters such that the simulated head values are matched with the observations. The calibrated model is later used for predictions. Once a flow model is set up, it can be used for estimating the amount of water to be withdrawn from the mines for the

progress of the mining operation. It also gives an estimate of the amount of water that needs to be pumped out from the wells to avoid flooding of the mine floors.

2.2 Simulation: Optimization Framework for Groundwater Control

The pumping rates that are obtained from the simulation models need not necessarily be an optimal value. Since the depth of the mineral bed varies from region to region in the model domain, it is difficult to fix the pumping rate just by simulation. Or a constant rate of pumping throughout the mine bench may not be an ultimate solution. Thus, optimization plays a significant role in arriving at the most suitable pumping rates. The simulation models are generally linked with optimization models for this purpose.

The groundwater control operations in the mines while ensuring water conservation can be addressed with a good simulation model that replicates the aquifer system. A linked simulation—optimization framework (Fig. 2) ensures that the requirements are met within a certain set of constraints which corresponds to the safe operating limits for the mines, thereby ensuring safety and sustainability.

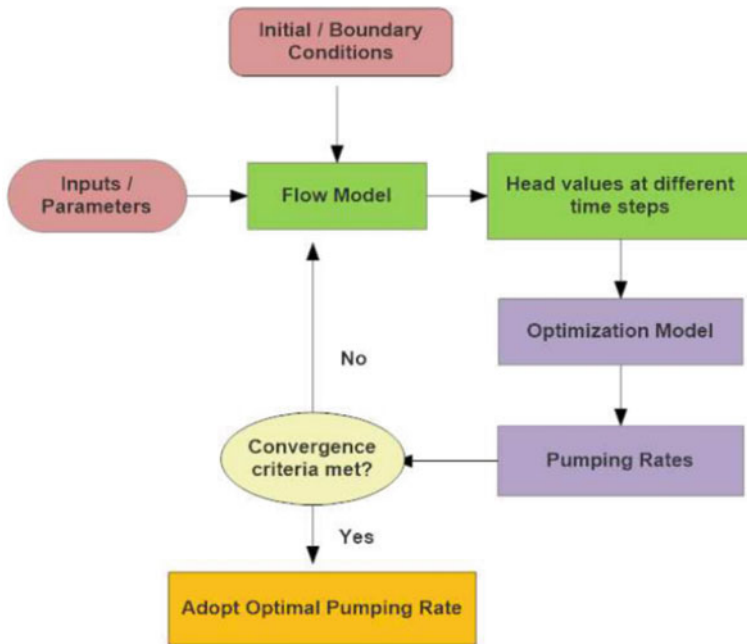


Fig. 2 Flow chart of a simulation—Optimization framework

3 Case Study 2: Dewatering for Construction of Delhi Metro

The Delhi Metro Rail Corporation (DMRC) proposes to construct an underground rail line in Delhi, India. The International Metro Civil Contractors (IMCC) have been awarded the contract MC1B for the section between the Inter-State Bus Terminal and Central Secretariat. The objective of the study is to optimize dewatering scheme for the station location. The scheme includes detailed design for the excavation dewatering scheme, impact on external drawdown and settlement, and surface water management system (Recharge well system).

3.1 Problem Description

Contract MC1B consists of the construction of 6.6 km underground railway in the bored tunnel and cut and cover section. The current proposal includes for the running tunnels between chainage 14105 and 17900 to be constructed using appropriate tunnel boring machines and the remaining running tunnels by cut and cover techniques using King Piles and diaphragm walls where necessary.

The six stations within contract section are Delhi Main Station, Chawri Bazaar Station, New Delhi Station, Connaught Place Station, Patel Chowk Station, and Central Secretariat Station. It is currently proposed that Delhi Main, New Delhi, and Connaught place stations will be constructed using Diaphragm walls. Patel Chowk will be constructed using the diaphragm wall and the King pile wall and Central Secretariat will be constructed using King Pile walls. Chawri Bazaar is a special case due to dense urban environment and it is proposed to be constructed by enlarging the running tunnels underground to form the platforms and constructing two top-down diaphragm wall shafts.

3.2 Geology

The geology of the Delhi area as given in the tender document consists of Proterozoic basement rocks belonging to the Alwar Series of the Delhi Super Group overlain by recent alluvium associated with the Yamuna River. The Delhi area is generally of flat and low topography associated with the Yamuna flood plain. Within this are discontinuous hillocks that are composed of basement rock representing the northern extent of the Aravalli Range (Table 1).

Table 1 Geology of the site

Formation	Age	Properties
Younger Alluvium	Present	Typically found as sand in close proximity with the Yamuna River
Older Alluvium	Pleistocene	Fine-grained soil with kankar and ferruginous concretions typically found at elevations above immediate river bank level on river terraces
Aeolian	Pleistocene	Possible occurrence of Aeolian silts
Intrusives		Quartz and pegmatite
Alwar Series	Proterozoic	Metasedimentary sequence consisting primarily of quartzite with schist and calcareous rocks

3.3 Hydrology

There are two main aquifers within the route area; the alluvium and the rock. Groundwater flow within the alluvium is controlled by intergranular flow and will be variable depending upon the spatial form of the historical channel deposits. Flow within the rock will be controlled by fissure flow. Recharge of the aquifers is from the Yamuna River catchment via the alluvium, and from the Aravalli Range via the basement rock. The recharge systems will be affected by the monsoon climate and groundwater levels can be expected to be seasonally affected with higher levels occurring during the monsoon season.

Groundwater within the Delhi area has been pumped for various uses and demand is increasing. As a result, the groundwater level has been reducing within the last few decades. An average annual decline rate of 0.22 m/year has been calculated by the Central Groundwater Board (CGWB). Pumping of groundwater occurs from both the shallow alluvial deposits and the deeper rock.

3.4 Groundwater Modeling of New Delhi Station

Areal discretization was done by dividing the area into rows and columns. The grid size within the excavation area is 1 m × 1 m and gradually varied up to 5m × 5m grid size. Vertical discretization was done by dividing the geohydrologic system into three layers. First layer top at +210.5, first layer bottom is varying as the variation of alluvium in boreholes. The second layer bottom is at +196.0 m and third layer bottom at +180 m.

Based on the borehole details the aquifer system in the New Delhi station is modeled as a three-layer system. The average ground level at this station is at +215.0 m. Groundwater table is at +210.5 m. The bottom of the excavation is at +197.0 m. The required drawdown is at +196. The total length of the station including shaft is 260.0 m. The top layer is fixed at +210.5 m.

Aquifer parameters such as hydraulic conductivity and storage properties (specific storage and specific yield) for the layers are important for flow modeling. The specific yield is taken as 0.014 based on Delhi main station/New Delhi pumping test results.

The soil profiles are heterogeneous in nature across the station area and the data available is from boreholes taken by different parties and at different times. No direct correlation is possible from different permeability test results. The possible approach is to do a sensitivity analysis of the model using different values of permeability followed by an observational approach as we proceed with work. Considering the above points different combinations of permeability values are considered for modeling.

To start of iterative model computation the initial values are necessary. These values must be higher than the elevation of the cell bottom. Initial hydraulic heads in transient simulation should closely resemble the head distribution derived from field data. The initial head is given at +210.5 m.

Based on the approximate calculation of the radius of influence the boundaries were fixed. Extreme boundaries were given as no-flow boundaries and these boundaries are sufficiently away from the area of influence. The top boundary water table and direct recharge due to rainfall were neglected for the present analysis. The bottom boundary is also assumed as no-flow boundary. The diaphragm wall was already constructed on the site at the box location and these walls were given around the station box.

3.5 Model Runs

In the run module, the user should specify the number of time steps and time step multiplier for each stress period (stress period is the time interval during which all external stresses are constant), type of solver (e.g., Pre-conditioned conjugate gradient package, strongly implicit procedure, slice-successive overrelaxation, WHS solver), type of layers (e.g., unconfined, confined or combination of both). Slice-Successive Overrelaxation method was adopted as the solver in which the Gauss elimination method is used to solve the system of linear equations.

For the different stages, optimum pumping quantity was determined to attain drawdown up to alluvium and excavation inflow when excavating up to rock was determined. The optimum locations and quantity of recharging also determined based on an initial guess suggested by DMRC.

3.6 Optimization of Pumping Quantity to Lower Water Table up to Alluvium

Different trials were carried out by varying the pumping quantity and number of wells. The optimal arrangement of pumping wells was arrived at with 23 wells based on drawdown criteria and 4 nos. of observation wells. Tables 2, 3 and 4 shows the pumping quantity required to lower the water table up to alluvium for the three cases. From these tables, the maximum quantity to be pumped from alluvium is 500 m³/d to achieve the drawdown up to the bottom of excavation (for case 3 between grid 26–21) of the sections.

3.7 Excavation Inflow When Excavating up to Rock

Using the drain package in MODFLOW the excavation inflow was determined. Tables 5, 6 and 7 shows inflow quantities when excavating up to rock.

3.8 Optimization of Recharge Well Quantity and Location

The optimum location of recharge wells has been fixed based on the site convenience. Table 8 shows the optimum recharge quantities.

The pumping quantities and excavation inflows are slightly increasing because of recharging.

The general observations of the study are:

- The drawdown inside the pit is achieved up to the required level with the proposed pumping arrangement.
- The number of wells required to lower the water table up to the bottom of the formation level is 23 wells of 300 mm diameter. The depth of well shall be 6 m into the rock layer/10 m below the formation level.
- Maximum quantity of water that is to be pumped to lower the water table in the alluvium is 500 m³/day for case 3 without recharge.
- Maximum excavation inflow from the rock aquifer is 3413 m³/day for case 3 without recharge.

4 Conclusions

Dewatering is critical to most mining operations through pumping groundwater. The optimal planning for the dewatering for safe mining purpose needs to extract the lowest volume of water, at a minimum cost. Accurately planning and modeling the multi-aquifer system proved to be a viable tool to derive the optimal groundwater

Table 5 Case-1 excavation inflow (m³/day) for drain (Without recharge)

Days	Grid VI	Grid VII
214	1052	
270	483	738
343	419	632
366		804

Table 6 Case-2 excavation inflow (m³/day) for drain (Without recharge)

Days	Grid VI	Grid VII
214	213	
270	104	160
343	87	126
366		135

Table 7 Case-3 excavation inflow (m³/day) for drain (Without recharge)

Days	Grid VI	Grid VII
214	3413	
270	1536	2324
343	1378	2067
366		2770

Table 8 Recharging quantities (No. of wells-11)

Cases	34-160 days (4 nos. of wells)	100-214 days (7 nos. of wells)	180-366 days (11 nos. of wells)
Case 1	140	245	790
Case 2	31	39	77
Case 3	355	525	1650

extraction for dewatering. Visual Modflow-based simulation of a multi-aquifer system has been demonstrated for effective pumping of groundwater without much environmental impact. The results of Visual MODFLOW for New Delhi station construction dewatering reveals that excavation inflows are varying from case to case with different values of permeability (i.e., from case 1 to case 3). It is recommended to have an observational approach for the dewatering and recharge system. An optimum well layout has been developed keeping in view of various possible cases that are analyzed in the MODFLOW. The dewatering scheme consists of 23 numbers of 300 mm diameter pumping wells. The depth of boring of each well is up to 6 m into rock/10 m below the excavation level. It is recommended to have 4 (in addition to pumping wells) observation wells (inside the pit) to observe water levels. Eleven number of recharge wells have been proposed to recharge the pumped water

into the aquifer. It is recommended to have 2 (Out of 11 recharge wells) observation wells outside the pit to observe water levels.

References

1. Lian Liang Z, Ren T, Ningbo W (2017) Groundwater impact of open cut coal mine and an assessment methodology: a case study in NSW. *Int J Min Sci Technol China Univ Min Technol* 27(5):861–866
2. Karmakar BHN, Das PK (2012) Impact of mining on ground and surface waters
3. Wang HF, Anderson MP (1982) Introduction to groundwater modeling: finite difference and finite element methods
4. Zhou Y, Li W (2011) A review of regional groundwater flow modeling. *Geosci Front (Elsevier B.V.)* 2(2):205–214
5. McDonald MG, Harbaugh AW (2003) The history of MODFLOW. Ground water
6. GEC (2009) Report of the ground water resource estimation committee ground water resource estimation ministry of water resources

Numerical Modeling of Landfill Processes: Complexity Versus Practicality



Girish Kumar and Krishna R. Reddy

Abstract Bioreactor landfills are emerging as a sustainable means of municipal solid waste (MSW) management due to enhanced rates of waste decomposition which leads to early waste stabilization in landfills along with other short-term and long-term benefits. Currently, no well-established procedures or design guidelines exist to design and operate such landfills safely and effectively. This largely stems from the fact that there is no clear understanding of the fundamental processes and their interdependencies that influences the behavior of the waste and consequently the overall performance of a bioreactor landfill. Mathematical modeling of the major landfill processes (hydraulic, mechanical, biochemical, thermal) and their interrelated behavior using numerical methods is a useful tool in understanding the landfill performance and has been carried out ever since the late 1980s. Several researchers have developed numerical models to simulate the behavior of MSW in landfills with varying mathematical complexity. However, most of these models don't find their application in the current state of practice, although many of the simpler models are increasingly welcomed by landfill owners and design professionals. This paper briefly summarizes the important concerns regarding the development of numerical models for modeling of landfill processes and their applicability in practice. Further, the key technical challenges that need to be addressed while developing a numerical model are discussed. The purpose of this paper is to have the landfill modelers embrace the need for a balance between the complexity and practical applicability of the model for the design and operation of bioreactor landfills.

Keywords Municipal solid waste · Leachate recirculation · Bioreactor landfills · Numerical modeling · Coupled processes

G. Kumar (✉) · K. R. Reddy
University of Illinois at Chicago, Chicago, IL 60607, USA
e-mail: gkumar6@uic.edu

© Springer Nature Switzerland AG 2020
K. R. Reddy et al. (eds.), *Sustainable Environmental Geotechnics*, Lecture Notes
in Civil Engineering 89, https://doi.org/10.1007/978-3-030-51350-4_10

1 Introduction

Landfills have been a major waste management option for the disposal of MSW in the United States (US) and many other developed and developing countries alike. In the US alone, it is reported that about 267.8 million tons of MSW was generated in the year 2017 of which about 139.6 million tons (52.1%) was disposed of in various fills across the country [1]. With the ever-growing population, rapid urbanization, and changing life-styles, the amount of waste generation is expected to increase over the years. Although the number of landfills has decreased, the capacity of landfills has increased to accommodate the increased waste generation. Currently, there are well-established procedures to design and construct landfills with engineered components to effectively contain the waste and its byproducts [2]. However, in conventional landfills, the organic matter of the MSW within the landfill undergoes slow decomposition due to the low moisture within the MSW thereby leading to several problems including, low methane (CH_4) gas generation rates and hence low gas to energy conversion, low settlement rates of the waste, increased leachate treatment and disposal costs, prolonged waste stabilization period, and associated emissions over the period, among others.

Ever since the pioneering work on leachate recirculation in landfills in the 1970s by Pohland [3], leachate recirculating landfills (bioreactor landfills) have evolved as a sustainable means of waste management offering numerous benefits over the conventional landfills [4]. But, unlike the design of conventional landfills, the design of bioreactor landfills needs careful consideration to the flow and distribution of the injected liquid within the landfill, the liquid pressures developed and its influence on the stability of the landfill slopes, the enhanced decomposition rates, the thermal conditions within the waste due to enhanced heat generation from rapid waste decomposition, the changing waste properties, and its influence on the settlement and the stability and integrity of the major landfill components including liner, cover and leachate injection systems. The holistic performance of a bioreactor landfill is primarily dictated by the coupled interactions of the hydraulic, mechanical, biochemical, and thermal processes within the MSW. A comprehensive understanding of these individual processes and their interdependencies will aid in realistic predictions about the performance of bioreactor landfills [5].

Numerical models simulating the landfill processes began with the work of Young [6] and El Fadel et al. [7]. Over the last decade, several other researchers have taken inspiration from this prior work and have proposed numerical models that simulate the landfill processes and the coupled interactions with varying mathematical complexity. Some of the studies proposed and developed numerical models to simulate individual system processes (e.g., fluid flow, waste settlement, biochemical reactions, temperature distribution) [8–15] while a few others proposed models to simulate the coupled or interrelated behavior (e.g., fluid-mechanical interaction, bio-mechanical interaction, hydro-bio-mechanical interaction) [16–22]. Despite the accuracy and comprehensive inclusion of various processes/interactions in the advanced coupled models, their applicability in the field for landfill design is limited

as compared to the much simpler uncoupled models. Yet, the waste management industry calls for the need for a numerical model that is mathematically involved and is readily usable by landfill design professionals. There are major issues concerning the practical use of the models developed as well as the relevance of the model to meet the needs of the waste management industry. This paper intends to bring a sound understanding of what is of utmost importance to the landfill owners and designers in their practice and have the landfill modelers/research groups to incorporate/address those concerns and challenges in their efforts toward modeling of landfill processes.

2 Research Status on Modeling of Landfill Processes

Modeling of landfill processes including fluid transport, gas and heat generation, and their transport, biochemical reactions kinetics, and leachate chemistry using numerical methods had been carried out in 1990s and was a precursor to the development of many of the new models that are published in the recent years. It is important to note that most of the recently published models are focused toward accurate simulation of the biochemical processes and its impact on other system processes (fluid flow, mechanics, and thermal regime within the landfills). It is invariably believed that the biodegradable aspect of MSW is what makes the understanding of the waste behavior and its influence on the performance of the landfill a complex and unique issue.

There is a varied complexity in the models that are available to simulate one or more landfill processes. The simpler uncoupled models such as the USEPA's LandGEM model [23] and the UK Environment Agency's GasSim2 [24] are widely used in the landfill industry for the estimation of CH₄ gas generation. These simpler models are in most cases based on simplifying the waste degradation and subsequently the gas generation as a first order decay (exponentially decreasing function) process. The model parameters are empirically derived based on curve fitting thus having limited applicability to different site conditions. These models do not explicitly account for, in most cases, the different factors that influence the rate of waste degradation and therefore can grossly overpredict or underpredict the CH₄ gas production in landfills. On the other hand, there exists complex multi-component models that include biochemical reaction kinetics of the aerobic and mostly anaerobic degradation processes involving the growth and decay of different chemical species and the microbial communities along with their transport within the landfill. These models also account for the influence of different factors such as relative digestibility of different waste components, moisture availability, pH of the aqueous medium, and temperature, on the rate of reactions [6, 7, 17, 25, 26]. These models closely predict the biochemical behavior of the waste and thus the CH₄ gas generation and the leachate chemistry. However, the landfill designers are less likely to use such models because they are highly parameter intense and many of the parameters required by the model would be expensive and difficult to evaluate at full scale or the historical data needed to evaluate them may not be available [27].

In the last decade, there have been considerable efforts in developing the understanding of different system processes within MSW and consequently on the landfill performance in those different respects. Some studies used the concepts of fluid flow in unsaturated porous media and focused particularly on the hydraulic (leachate flow and pore pressures) performance of the leachate recirculating landfills by simulating the fluid flow and its distribution by different leachate injection systems [8, 9]. Based on different parametric analyses, design guidelines were established for designing the appropriate leachate injection systems for the safe operation of the landfill while obtaining a nearly uniform distribution of the injected leachate [28–30]. However, the conditions simulated were more idealized and they did not consider the effects of biodegradation and settlement on the fluid flow and its distribution. Similarly, some researchers investigated the thermal behavior, mechanical behavior, and biochemical behavior separately without considering the influence of other processes [10–15]. Although this helped bolster the understanding of the nuances among the individual behaviors, it is essential to incorporate the interrelated behavior into the model to simulate the realistic behavior of MSW.

In the recent years, several models were proposed and developed to account for the coupled interactions between the hydraulic, mechanical, biochemical, and thermal processes and their influence on the various aspects of landfill performance (e.g., gas generation, leachate chemistry, leachate distribution, and waste settlement) [17–19, 21, 25, 26]. However, the mathematical and in some cases the numerical complexity of the model, the accuracy of the model predictions with respect to reality, the reliability in the model predictions for heterogeneous waste conditions are still unclear. Moreover, none of these models holistically assess the performance of the landfill systems (e.g., the stability of waste slopes, integrity of leachate injection systems, stability, and integrity of the liner and cover systems) under the influence of the coupled interactions of thermo-hydro-bio-mechanical processes. In the light of many studies discussed above, there are a few major challenges that need to be addressed to develop a numerical model that is more inclusive of the mathematical complexity and yet is readily usable for practical application.

3 Challenges and Concerns

3.1 *Lack of Consensus Among the Landfill Modelers*

The numerous models that are available and the new numerical investigations that continue to be published each year addressing one or the other aspect of landfill processes demonstrates the importance of research on this topic. Despite the various developments made by different research groups, there is still a lack of consensus among the modelers about the essential technical requirements for a good and useful numerical model. For example, Fig. 1 shows the prediction of waste settlement by various simple settlement models [31] and this figure is a good indicator of how

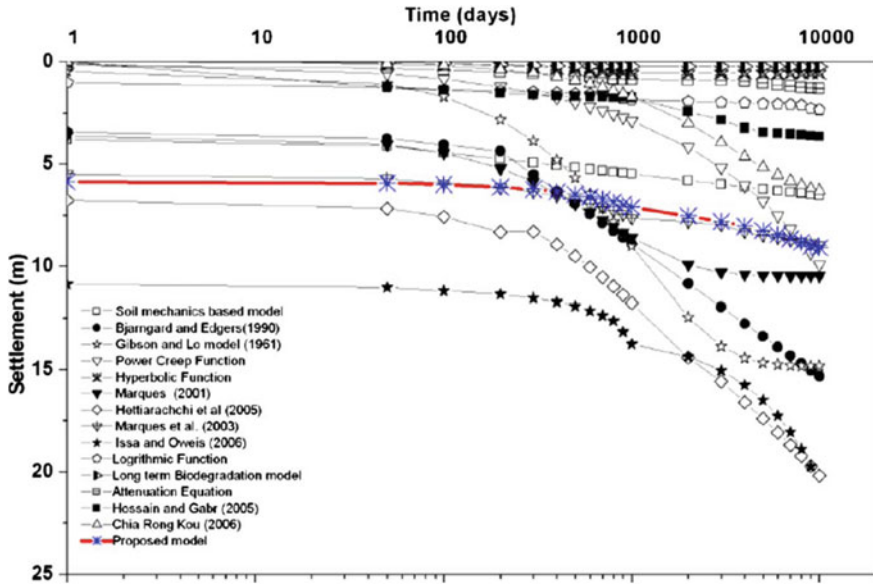


Fig. 1 Settlement prediction of various simple mechanical models [31]

much of variability exists among the different models in their predictions. With such uncertainty in the prediction, it is difficult for the user (the landfill owners, operators, and designers) to choose or substantiate the use of one model over the other. This gap is perhaps mainly due to the variability in the conceptual models. Moreover, there is also a considerable duplication of the concepts involved in earlier models thereby eventually ending up in having more models than we already have but with no apparent benefits to the landfill industry. This concern was earlier pointed out by Beaven et al. [32] in their efforts to begin a dialogue between different landfill research groups/modelers and help identify the important aspects of the models they have developed. The study also revealed the variability in several advanced models in their prediction of landfill performance parameters such as cumulative CH₄ gas generation (Fig. 2), indicating variability in how different research groups understand and interpret the fundamental processes in a landfill.

The study was also meant to help identify the crucial elements of a model for accurate prediction of landfill processes. This study is quintessential to future discussions on this topic and to devise a feasible and useful tool for the landfill industry to use.

3.2 Complexity of the Model

As discussed earlier, the numerical models developed to date have varying mathematical complexity. Given the heterogeneity of the waste for different regions or even

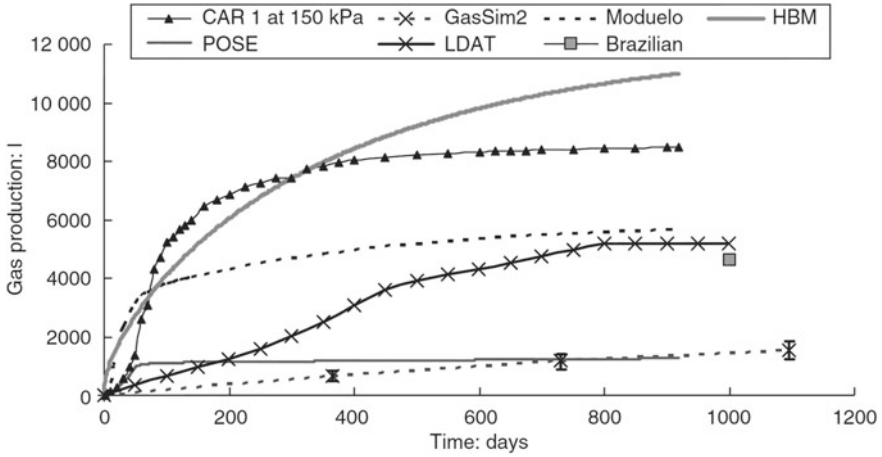


Fig. 2 Prediction of cumulative CH₄ gas production in a laboratory simulation of the consolidated anaerobic reactor by different landfill models [32]. Note CAR 1 at 150 kPa represent the laboratory-measured results

within the same landfill, there is no clear evidence as to how much of a difference in the accuracy would a complex coupled model have in comparison to a simple uncoupled model which is sufficient in many cases. Moreover, with the introduction of mathematical complexity comes the question about the feasibility in numerical implementation and its associated problems. The end-user to whom the model is intended for (landfill designers and operators) must be able to obtain the relevant input parameters easily, comprehend the analysis, and interpret the results. Most of the models developed are mostly like “black-box” software which feeds on some input and generates some output. The approach for modeling of landfill processes should be a balance between the accuracy and complexity, in that the number of parameters required for the model, the ease of use, and the reliability of the model predictions should be desirable. So, getting the conceptual model right (with coupled effects of different processes) while keeping the number of relevant parameters of the model minimal would be fruitful for its potential use in practice. More complex coupled models with rigorous mathematical detail could be used to validate and provide bounds to the predictions of the simple models that account for interrelated behavior of different landfill processes. In addition, design charts based on a parametric study involving different modeling scenarios could be developed to facilitate the use of the analyses results by landfill design professionals.

3.3 Relevance of the Model to the Landfill Industry

Many of the numerical models developed for the prediction of landfill processes are mathematically sound and reasonably accurate but are still not used in practice. A

major reason for which is the lack of the relevance of the model to the landfill design. The most advanced coupled models developed to date use complex mathematical descriptions for the different landfill processes and their interactions to accurately predict the behavior of the waste. However, it is equally important that the model addresses the influence such behavior would have on the other vital components of a bioreactor landfill. For example, the rapid waste decomposition influences changes in the mechanical properties of the waste and induces settlement that can influence the stresses imposed on the liner underneath the waste. The interface shear responses are often dictated by the waste-liner interaction and govern the long-term stability and integrity of the liner system and thereby the integrity of the whole waste containment system. Likewise, the stability of waste slopes, the integrity of the cover system, and the leachate injection systems are dependent on the differential settlement of the waste and there is in fact clear evidence of excessive differential settlements in bioreactor landfills with different regions having different rates of biodegradation, thereby different rates of waste settlement (see Fig. 3). However, most published models still consider only a 1D settlement of the waste in their model formulation, which is inadequate.

The elevated temperatures within the landfill and especially near the liners can significantly affect the integrity and performance of the liner system and hence the prediction of thermal behavior of landfills is important. Prediction of landfill waste stabilization time reasonably and reliably is another important aspect pertinent to the landfill designers and operators to plan the closure and monitoring. Prediction of the major chemical constituents of leachate that are indicative of the strength of the leachate is important to the landfill owners. Many of the models developed do not assess the influence of landfill processes on the above-mentioned broader aspects of bioreactor landfill performance and thus do not attract the landfill industry to utilize

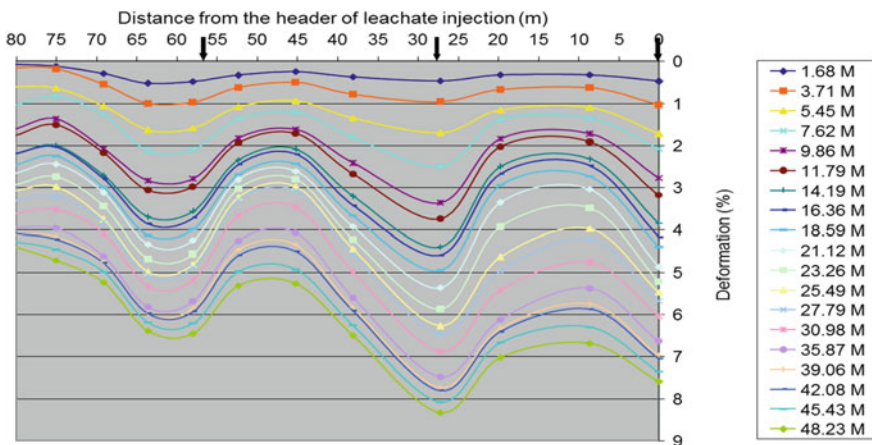


Fig. 3 Field monitoring data showing transient differential surface settlements at a leachate recirculating landfill. *Courtesy* Veolia Environment. *Note* The arrows indicate injection location

the model. Thus, the future efforts toward modeling landfill processes should focus toward addressing these issues for practical use of the model.

4 Summary

Modeling of landfill processes, which began in the late 1980s was a major intervention in making landfill design and operations more effective and efficient. In light of the discussion on bioreactor landfills, the numerical modeling of landfill processes has gained more prominence in that the holistic performance of the landfill is dictated primarily by the hydraulic, mechanical, biochemical, and thermal behavior and their interactions within the MSW. In this regard, several simple uncoupled as well as complex multi-component coupled models have been formulated, proposed and some are still continuously developed. Despite their technical efficiencies and predictive capabilities, the published models don't find wide acceptance with the landfill industry as a design tool that aids in designing and operating safe and effective bioreactor landfills. This is due to many factors including the undue importance given to the mathematical detail over the practical implications of the model to the users (landfill designers, operators, owners), overtly parameter intensive model formulations, unaddressed issues that matter the most to the landfill owners. This paper has highlighted some of the important technical and practical challenges that are relevant and those that need to be addressed by the landfill modelers to make their models practically useful. Most of the challenges are comprehensively being addressed in the authors' ongoing research [22, 33–36].

Acknowledgments This material is based upon work supported by the National Science Foundation (NSF) (CMMI #1537514), Itasca Education Program (IEP) by Itasca Consulting Group Inc. (ICGI), and Environmental Research and Education Foundation (EREF). Any opinions, findings, conclusions, and recommendations expressed in this material are those of the authors and do not necessarily reflect the views of the NSF, ICGI, or EREF.

References

1. USEPA (2019) Advancing sustainable materials management: 2017 fact sheet. <https://www.epa.gov/>, Accessed 8 July 2020
2. Sharma HD, Reddy KR (2004) Geoenvironmental engineering: site remediation, waste containment, and emerging waste management technologies. Wiley
3. Pohland FG (1975) Sanitary landfill stabilization with leachate recycle and residual treatment, EPA-600/2-75-043
4. Townsend TG, Powell J, Jain P, Xu Q, Tolaymat T, Reinhart D (2015) Sustainable practices for landfill design and operation. Springer, New York
5. Reddy KR, Kumar G, Giri RK (2017) Modeling coupled processes in municipal solid waste landfills: an overview with key engineering challenges. *Int J Geo-Synth Ground Eng* 3(1):6

6. Young A (1989) Mathematical modelling of landfill degradation. *J Chem Technol Biotechnol* 46(3):189–208
7. El-Fadel M, Findikakis AN, Leckie JO (1996) Numerical modelling of generation and transport of gas and heat in landfills I. Model formulation. *Waste Manag Res* 14(5):483–504
8. Reddy KR, Kulkarni HS, Khire MV (2013) Two-phase modeling of leachate recirculation using vertical wells in bioreactor landfills. *J Hazard Toxic Radioact Waste* 17(4):272–284
9. Reddy KR, Kulkarni HS, Srivastava A, Sivakumar Babu GL (2013) Influence of spatial variation of hydraulic conductivity of municipal solid waste on performance of bioreactor landfill. *J Geotech Geoenviron Eng* 139(11):1968–1972
10. Machado SL, Carvalho MF, Vilar OM (2002) Constitutive model for municipal solid waste. *J Geotech Geoenviron Eng* 128(11):940–951
11. Machado SL, Vilar OM, Carvalho MF (2008) Constitutive model for long term municipal solid waste mechanical behavior. *Comput Geotech* 35(5):775–790
12. Machado SL, Vilar OM, de Fátima Carvalho M, Karimpour-Fard M (2017) A constitutive framework to model the undrained loading of municipal solid waste. *Comput Geotech* 85:207–219
13. Gawande NA, Reinhart DR, Yeh GT (2010) Modeling microbiological and chemical processes in municipal solid waste bioreactor, part I: development of a three-phase numerical model BIOKEMOD-3P. *Waste Manag* 30(2):202–210
14. Haarstrick A, Hempel DC, Ostermann L, Ahrens H, Dinkler D (2001) Modelling of the biodegradation of organic matter in municipal landfills. *Waste Manag Res* 19(4):320–331
15. Hanson JL, Yeşiller N, Onnen MT, Liu WL, Oettle NK, Marinos JA (2013) Development of numerical model for predicting heat generation and temperatures in MSW landfills. *Waste Manag* 33(10):1993–2000
16. Reddy KR, Giri RK, Kulkarni HS (2015) Modeling coupled hydromechanical behavior of landfilled waste in bioreactor landfills: Numerical formulation and validation. *J Hazard Toxic Radioact Waste* 21(1):D4015004
17. White J, Robinson J, Ren Q (2004) Modelling the biochemical degradation of solid waste in landfills. *Waste Manag* 24(3):227–240
18. White JK, Beaven RP (2013) Developments to a landfill processes model following its application to two landfill modelling challenges. *Waste Manag* 33(10):1969–1981
19. McDougall J (2007) A hydro-bio-mechanical model for settlement and other behaviour in landfilled waste. *Comput Geotech* 34(4):229–246
20. Feng SJ, Cao BY, Bai ZB, Yin ZY (2016) Constitutive model for municipal solid waste considering the effect of biodegradation. *Géotech Lett* 6(4):244–249
21. Hubert J, Liu XF, Collin F (2016) Numerical modeling of the long term behavior of Municipal Solid Waste in a bioreactor landfill. *Comput Geotech* 72:152–170
22. Reddy KR, Kumar G, Giri RK (2017) Influence of dynamic coupled hydro-bio-mechanical processes on response of municipal solid waste and liner system in bioreactor landfills. *Waste Manag* 63:143–160
23. USEPA (2005) Landfill gas emissions model (LandGEM) version 3.02, User's Guide. Washington D.C., EPA-600/R-05/047
24. Gregory RG, Revans AJ, Hill MD, Meadows MP, Paul L, Ferguson CC (1999) A framework to assess the risks to human health and the environment from landfill gas. Environment Agency, Bristol, Technical report P271, under contract CWM168/98
25. Reichel T, Haarstrick A (2008) Modelling decomposition of MSW using genetic algorithms. *Proc Inst Civil Eng-Waste and Resour Manag* 161(3):113–120
26. Lobo A, Tejero I (2007) MODUELO 2: A new version of an integrated simulation model for municipal solid waste landfills. *Environmen Modell Softw* 22(1):59–72
27. Lamborn J (2010) Modelling landfill degradation behaviour, Ph.D. thesis. Swinburne University of Technology
28. Reddy KR, Giri RK, Kulkarni HS (2014) Design of drainage blankets for leachate recirculation in bioreactor landfills using two-phase flow modeling. *Comput Geotech* 62:77–89

29. Reddy KR, Giri RK, Kulkarni HS (2015) Design of horizontal trenches for leachate recirculation in bioreactor landfills using two-phase modelling. *Int J Environ Waste Manag* 15(4):347–376
30. Reddy KR, Giri RK, Kulkarni HS (2015) Design of vertical wells for leachate recirculation in bioreactor landfills using two-phase modeling. *J Solid Waste Technol Manag* 41(2):203–218
31. Sivakumar Babu GL, Reddy KR, Chouskey SK, Kulkarni HS (2010) Prediction of long-term municipal solid waste landfill settlement using constitutive model. *Pract Period Hazard Toxic Radioact Waste Manag* 14(2):139–150
32. Beaven RP (2008) Review of responses to a landfill modelling challenge. *Proc Inst Civil Eng-Waste Resour Manag* 161(4):155–166
33. Reddy KR, Kumar G, Giri RK (2017c) Numerical modeling of the shear response of a composite liner system with municipal solid waste degradation in landfills. *Geotech Front* 52–63
34. Reddy KR, Kumar G, Giri RK (2018) Modeling coupled hydro-bio-mechanical processes in bioreactor landfills: framework and validation. *Int J Geomech* 18(9):04018102
35. Reddy KR, Kumar G, Giri RK (2018) System effects on bioreactor landfill performance based on coupled hydro-bio-mechanical modeling. *J Hazard Toxic Radioact Waste* 22(1):04017024
36. Reddy KR, Kumar G, Giri RK, Basha BM (2018) Reliability assessment of bioreactor landfills using Monte Carlo simulation and coupled hydro-bio-mechanical model. *Waste Manag* 72:329–338

Status of C&D Waste Recycling in India



Mohan Ramanathan and V. G. Ram

Abstract A major portion of C&D waste is generally dumped in landfills or unauthorized places in India causing considerable ecological damage. Several barriers such as inadequate regulations, lack of incentives, lack of awareness about recycling techniques, and unavailability of guidelines have been reported to hinder setting up recycling facilities in India. Amidst challenges, few recycling facilities have been commissioned and are operational in different Indian cities. A rich description of the cases helped us in tracing the evolution of recycling in India over a timeline. A multitude of factors including a pro-active urban local body, R&D efforts from PPP partner cum recycler, demonstration projects using recycled aggregates with the support of Central Road Research Institute, extensive support from the Government of India's Ministry of Urban Development, the framing of standards and guidelines with the help of various professional bodies were found to be contributing to the successful development and operation of India's first C&D waste recycling facility. Following this success, several plants were commissioned in other cities mimicking the same operational model. Insights discussed in the paper could be very useful for policymakers in evaluating various interventions for promoting C&D waste recycling practices in other regions and countries.

Keywords C&D waste · Recycling · Initiatives · Waste management · India

1 Introduction

The Indian construction industry is growing at an annual growth rate of 10% over the last 10 years. Indian real estate operations are estimated to reach a market size of 180 million USD by 2020 and about 170 million houses are expected to be built by 2030. Such rapid urbanization puts enormous stress on the environment toward satisfying

M. Ramanathan (✉)

Advanced Construction Technologies, Chennai, India

e-mail: mohanact@gmail.com

V. G. Ram

Department of Civil Engineering, IIT Madras, Chennai, India

© Springer Nature Switzerland AG 2020

K. R. Reddy et al. (eds.), *Sustainable Environmental Geotechnics*, Lecture Notes in Civil Engineering 89, https://doi.org/10.1007/978-3-030-51350-4_11

the growing demands for natural resources such as aggregates in the construction industry. Moreover, estimates of Construction and Demolition waste generation in India range from 112 to 700 million tonnes/year. C&D waste recycling, one of the sustainable solutions for managing this sector of waste is gaining popularity worldwide. However, very few recycling facilities are available in India presently to recycle C&D waste being generated.

Tracing the evolution of recycling in pioneer Indian cities that had established recycling facilities could help us understand the challenges being faced in developing recycling systems and thereby identify better ways of managing them in the coming years. In this paper, a historical account of C&D waste recycling status in India has been presented. Primary data including direct observation and several other data sources such as technical reports published by expert organizations, proceedings of sensitizing workshops being conducted all over the country, administrative procedures, and forms from Corporation' websites, newspaper articles, and other related documents form part of our evidence. Data triangulation technique was used to ensure internal validity. While Indian data are presented and discussed in this paper, it might provide insights to other jurisdictions that aspire to improve construction waste management.

2 Historical Background

The waste management operations in India are being handled by the urban local bodies in each city, continuing the practice as it is as inherited from the British rule. British ruled India for about 200 years, which ended in 1947. When they developed cities in India, they adopted the same system of solid waste management as that prevailed in the United Kingdom. The city corporations were responsible for collecting the waste from the cities and dispose in the designated dump yards developed outside the city. Bullock carts were initially used for collection and later it evolved to using powered vehicles. However, the process of dumping the waste without any processing or beneficiation continued even after the independence for the past 70 plus years (Fig. 1).

Blind Eye to Pollution. The industrial revolution made sure the focus was on development and hence, there was no importance given to curb pollution including waste management. There were no governing rules to tackle the situation then. People also did not focus on the clean-up afterward and the awareness of healthy living was not good either. It was believed that C&D waste contributes fewer pollutants to the environment as compared to other wastes and therefore the least importance was given to manage it. While waste-to-energy (WTE) plants started picking up, it is mainly restricted to organic matter in the solid waste, which can be converted to fuel. Various models emerged to set up WTE plants and the construction waste, the inert portion of the solid waste was out of the radar.



Fig. 1 Overflowing dump yards of Chennai city

Gross Underestimation of C&D Waste. In the Indian urban areas, there are no reliable estimates available regarding the quantity of C&D waste that is getting generated. The Technology Information, Forecasting and Assessment Council (TIFAC) reported that the quantity of C&D waste getting generated in India is around 10–12 million tons annually [1]. Government reports indicate about 12–15 million tonnes of C&D waste generation every year [2]. However, the estimate has been criticized to be a gross underestimation with scientific evidence [3]. The Centre for Science and Environment (CSE) came up with an estimate of 626 million tons of C&D waste generated in a span of eight years (2005–2013) [4]. An independent organization named Development Alternatives projected a massive amount of 750 million tons of C&D waste generation annually [5]. Using Materials flow analysis, a research paper showed that the generation of C&D waste in India could range between 112 and 431 million tons [6]. Thus, the available estimates vary to a wide extent and reliability is lacking. Since the knowledge on the quantity of C&D waste being generated helps in understanding the needs and in designing the facilities required, lack of reliable estimates was accused to be one of the reasons for lack of proper policies to improve C&D waste management in India.

Pilot Recycling Facility: One of the biggest milestones in the steps to improve C&D waste management in India was the setting up of a pilot recycling facility in New Delhi. In New Delhi (the capital city of India), around 4000 tons of C&D waste is being generated every day. On an average, around 2000 TPD of waste is being dumped in the corporation run landfills. The remaining waste gets dumped in unauthorized sites such as on river beds, low lying areas, and roadsides, which pose several downstream issues in the city. Amidst these problems faced by MCD, the development activities related to hosting Commonwealth Games (CWG) in 2010 added more pressure to the corporation. The anticipation of a huge quantity of C&D

waste generation due to an enormous amount of construction activities related to hosting CWG led the city corporation to realize the problem of C&D waste and its impact on the environment if not properly managed. In an attempt to solve this problem in a sustainable manner, the Municipal Corporation of Delhi initiated the establishment of setting up a pilot C&D waste processing facility in its jurisdiction.

Municipal Corporation of Delhi (MCD) in collaboration with IL&FS Environmental Infrastructure & Services Ltd (IEISL) developed a C&D waste processing facility operating on a PPP model involving MCD & IEISL. While the plant was developed with a capacity to process about 500 TPD initially, the capacity has been upgraded later (after few years) to about 2000 TPD. This C&D waste processing facility is the largest in India presently and sits on approximately seven acres of low and marshy land provided by the MCD for a period of 15 years. The land was originally owned by the Indian Army (about 40 Hectares) which was taken on lease by MCD in a long-term contract. In return, the Army will get its low and marshy land rehabilitated which can then be used for development purposes and thus a synergistic arrangement was arrived at.

There are about 168 designated locations that have been authorized by the Municipal Corporation of Delhi as collection points in and around the city where the waste generators can dispose of the waste generated by them. IEISL will haul the C&D waste dumped in the collection points to the recycling facility through own/hired trucks. Transportation fee is collected from the MCD in cases of transporting waste from the collection points or illegally dumped sites. The waste generated in the government projects is disposed of in the recycling facility itself along with the processing fee as well.

The plant initially had a mobile crushing unit and was indulged in de-sizing and desilting operations. Once the aggregates are recovered from the processed waste, value-added products such as the production of RMC, pavement blocks, kerb stones, concrete blocks, and bricks were produced and sold. These downstream products helped to consume the produced recycled aggregates as well as increased the returns from the facility. The main source of income for the facility is from the sale of the recycled products and value-added products. Tipping fee that includes the transportation and processing fee forms the second major source of income. The municipal corporation also plays the role of a customer by utilizing the recycled products in the projects being handled by it (Fig. 2).

Barriers and lessons learnt: The management of the facility faced many barriers in the C&D waste recycling process as well as in the sale of recycled products. The market acceptance of the recycled aggregates was also low. Hence various value-added products were produced and sold as a finished product instead of selling as a raw material. The design of concrete mixes was also carefully prepared such that the quality of the product does not get affected because of the use of recycled aggregates which are slightly inferior in quality as compared to quarried aggregates.

The taxes on finished goods such as ready-mixed concrete and other precast products were also influencing the economic viability of the recycled products. During the discussion with the IEISL, it was inferred that some tax concessions on these



Fig. 2 Machinery and output products of recycling facility at Burari, New Delhi

products might help them market the recycled products much effectively and will make it possible to compete with other products available in the market.

In order to improve the market acceptance of recycled aggregates, a pilot project was taken up by IEISL in collaboration with Central Road Research Institute (CRRI) wherein the access roads to the recycling plant have been constructed with recycled materials and the performance was monitored closely. Even though the roads were subjected to the movement of heavy trucks carrying C&D waste, it was showcased that the need for maintenance in the constructed stretch has been very low reinforcing the safe use of recycled materials. The need for incorporation of the clauses allowing the use of recycled aggregates in codes and standards for design was emphasized to improve the acceptance of recycled products.

2.1 Initiatives of Expert Organizations and Professional Bodies

Awareness of C&D waste management was still low even among the policymakers. Several expert organizations from all over the country started to work on it. Indian Concrete Institute (ICI) was one of the professional bodies that organized many sensitizing workshops about C&D waste recycling along with Central Public Works Department (CPWD) and IIT Madras. The first of the workshop series was held in New Delhi along with the support of the Ministry of Urban Development (MoUD) and included a visit to the pilot recycling facility operating in the region. A series

of workshops followed it in several cities all over the country such as Chennai, Hyderabad, Mangalore, etc. Participants in those workshops included Government officials handling solid waste management in the region, construction contractors, demolition experts, equipment manufacturers, recyclers, and academicians. Experts from all over the world shared their experiences on C&D waste management with the participants and brainstorming sessions were conducted to create a roadmap for the evolution of C&D waste management in the country.

IIT Madras did one of the pioneering scientific studies on C&D waste generation in India and proved that there is gross underestimation in the estimates that are available at the national level. It also worked closely with several local authorities and helped them draft C&D waste management plans for their jurisdictions. Institutions such as Central Building Research Institute (CBRI), Central Road Research Institute (CRRI), and IIT Bombay have also been working on several topics of C&D waste management and contributed in various ways in improving the awareness about better C&D waste management.

2.2 C&D Waste Management Rules (2016)

Until 2016, Municipal Solid Waste (management & handling) rules, 2000 provided the overarching framework that governs the management of all solid waste generated in Indian cities. Because of the lack of awareness and the historical background explained, this regulation lacked details about C&D waste management. Improving awareness led to understand the need for importance of proper C&D waste management and guidelines on how to handle the C&DW being generated were given in detail in this new set of rules. Ministry of Environment, Forest and Climate change notified this new set of rules superseding MSW rules, 2000, to be called as the Construction and Demolition Waste Management Rules, 2016. This became one of the very big milestones for C&D waste management in India.

According to the rules issued in 2016, various stakeholders involved in the C&DW management have been assigned a specific role to be played in the process. The waste generators were thrust with the responsibility to collect, segregate, and store the C&D waste generated within the site premises. The generators of waste are also required to pay the cost for storage, collection, and transportation. Large generators (generating more than 20 tons per day or 300 tons per project in a month) were also required to bear the costs for processing and disposal of the generated waste. It is also their responsibility to give an undertaking for proper disposal of C&D waste as per the local bye-laws, requiring submitting waste management plans for approvals before construction or renovation activities.

Urban local bodies have also been assigned various duties for the management of C&D waste. Issuing detailed directions for the management of waste including arrangements for collection, transportation, processing, and disposal. Planning incentives for deconstruction and promoting in situ recycling have also been delegated. The state government has been given the responsibility to help identify the land

needed for setting up recycling plants for C&D waste. For improving the acceptance of recycled aggregates for reuse in concrete, the BIS and IRC have the responsibility to bring out changes in the design codes and guidelines. These rules also set the standards for the setting up of a recycling plant, including the various types of machinery needed, along with various environmental factors for its safe operation. It also prescribes the various forms to be submitted by the plant to the state and central pollution control boards and various other operating standards that must be adhered to in the operation of C&DW recycling facilities.

The timeframe for implementation of these rules including developing and commissioning a recycling facility in jurisdictions was set at about 18 months for cities with population not exceeding a million and 24–36 months for cities having more than a million population. However, the state governments were not very serious about it and none of the deadlines stipulated were met by most of the cities in India. The central government had also become busy with other political issues and the timeframes of implementation were not achieved. Strict enforcement was also found to be lacking in the cities.

2.3 National Initiatives

The Government of India launched ‘Swacch Bharat Mission’ in 2014 (translates to ‘clean India mission’ in English) to clean up the streets, roads, and other infrastructure of India’s cities, towns, and villages. It has become one of the massive sanitation campaigns that made people think about having a clean street and raised awareness on several issues including open defecation, littering in the public streets, etc. Clean Ganga projects being run by the government also notifies its strong stand toward cleanliness to the public.

The Government of India also launched ‘Smart Cities Mission’ in 2015 to develop 100 cities that are sustainable and citizen-friendly. One of the requisite clauses of a smart city is to have an operational C&D waste recycling facility. Since the involvement of the central government in developing smart cities was higher and so did the funding available, the pressure of implementing transcended to the ground and a rapid pace in the development was seen. Several cities improved their infrastructure and the number of recycling facilities in the country to process C&D waste touched double digits. Following the successful model of the Burari plant in New Delhi, several cities including Ahmedabad, Mumbai, Vijayawada, and Indore have all developed and commissioned a recycling facility. Two more facilities have been developed in New Delhi itself making a total of three operational facilities in the city.

2.4 Publications Available for Practicing Engineers

The concept of recycling is still new to India and understanding the need for guidelines to help practicing engineers; some of the professional bodies with the help of experts have come up with publications relating to collection, processing, and utilization of C&D waste. Indian Concrete Institute (ICI) had set up a technical committee to work on the issue and drafted the document titled “Recycling, Use and Management of C&D wastes.” The Building Materials & Technology Promotion Council (BMTPC) has also issued guidelines about C&D waste recycling and recycled products. The statutory bodies such as Central and state pollution control boards have also issued guidelines for proper handling of C&D waste.

Delhi Government had issued an advisory note to all Delhi government agencies in New Delhi to consider using recycled aggregates in all of their projects mandatorily for a minimum amount of 2% in building works and 10% in road works. The local authorities have also been asked to mandate builders to use 5% C&D waste recycled products in non-structural applications during plan approvals. During a sensitizing workshop conducted in Mangalore, the participants formed an association, called Federation of C&D waste recycling, to be registered in New Delhi. The main purpose of this association would be to disseminate the knowledge available in the literature to everyone interested in C&D waste recycling and also for professional lobbying to push policies that support C&D waste recycling.

3 Today’s Scenario

Increasing awareness about conserving natural resources and C&D waste management is a booster for the country with respect to resource efficiency. Having implemented several recycling projects in multiple cities, technological expertise to recycle C&D waste is not a problem anymore. The focus of the government toward resource efficiency, clean India, and several other campaigns has sent out a clear message to the public about its interests in implementation and expectations from the industry.

The works of several organizations and professional bodies in the area of C&D waste recycling led to the change in the codal provisions that earlier prevented the usage of recycled aggregates for the production of concrete used in construction. IS 383 (Indian Standards for specifications for coarse and fine aggregates) was revised in 2016 to include recycled aggregates also as one of the sources of coarse and fine aggregates for concrete. While this change was supposed to improve the utilization of recycled aggregates in the construction projects, there were hesitations still to use recycled products. The concerns over long-term performance of recycled products kept designers from not specifying their usage in concrete. While experts have backed the usage of recycled aggregates and products, bold specifications from consultants to use them are lacking in the construction industry.

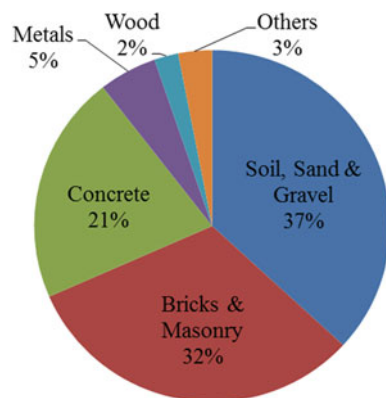
Problems peculiar to Indian urban areas. While a lot has been changing in recent times, several problems are very peculiar to Indian urban areas with regard to C&D waste management. One of the big problems is with respect to the data that we have with respect to the quantum of generation and its composition. There are several estimates that are out there at the national level. Lack of proper bookkeeping practices about C&D waste and reliable data from the cities raises doubts about the accuracy of the estimates. Based on the experts’ opinions and data in refereed journals, 500 million tonnes of annual C&D waste generation in the country looks very much possible. Such a huge volume of waste generation demands an explicit ‘C&D Mission’ to address and improve the situation before it gets aggravated further. Moreover, the fact that illegal disposal of almost half of the waste quantity being generated in the Indian urban areas still is alarming.

The composition studies in India indicate that the proportion of soil and brick masonry debris form major components of C&D waste rather than concrete as shown in Fig. 3. This is in contrast with some other Asian and European countries wherein concrete waste is one of the biggest constituents. Because of this, the business model and output of recycling facilities need to be tailored to the local conditions. The composition of primary materials in the total quantity of waste generated as quoted in the TIFAC study is shown in Fig. 3.

Availability of river sand has become scarce in the Indian cities owing to local ban on quarrying sand from river beds in recent years. Manufactured sand (crushed rock to fine aggregates size), a material produced during the process of quarrying and crushing for coarse aggregates, is increasingly becoming popular as a substitute to river sand. The crushed recycled fine aggregate could be pitched in as a substitute for fine aggregates instead, if the recycling facilities are equipped with crushing and screening facilities that can produce fine aggregates as well.

The demand for aggregates in the Indian construction sector is projected to be about 2 billion tonnes of coarse aggregates and 1.4 billion tonnes of sand (fine aggregates) by 2020 as shown in Fig. 4 [7]. Even if we consider that about 500 million tonnes of the entire C&D waste generation in the country is recycled, it can

Fig. 3 Composition of C&D waste in India. *Source* TIFAC [1]



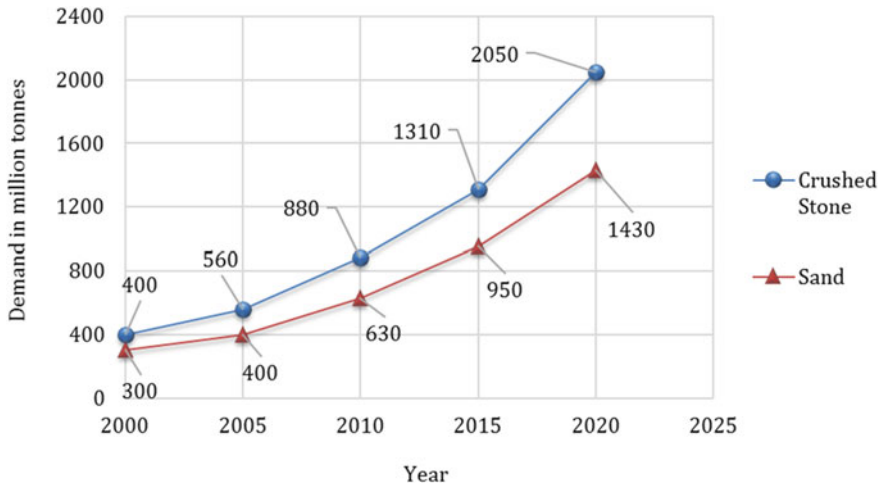


Fig. 4 Demand for aggregates in India

just partially substitute the demand that exists in the sector. Hence, if C&D waste recycling is not pursued, very high amounts of domestic resource extraction are the most probable response to meeting the growing demands.

4 Concluding Comments

The National Green Tribunal, playing the role of a watchdog, is very active and has made it clear that the natural resource (be it in quarry or riverbed) cannot be exploited anymore and need to be protected. Since there is a huge demand that exists in the construction sector and a large amount of C&D waste being generated, C&D waste recycling seems to be a sustainable solution and could potentially be a partial substitute that can alleviate several problems of the society.

The cost of quarried aggregates is close to about 50–60 rupees per cft and cost–benefit analysis in the literature shows that recycled aggregates could be produced at a much lower cost than quarried aggregates provided a pro-recycling environment exists in the city. Thus, utilizing recycled products makes sense not just from the environmental point of view but also economically.

Some of the incentives such as tax credits for recycling and recycled products, providing land and other crucial resources for setting up recycling infrastructure on low rates could help the recycling environment to thrive. The city authorities need to take a serious stand on this subject and their response to public actions and demands might be closely watched to improve C&D waste management in their jurisdictions. The regulatory framework has evolved quite well and is supportive. Strict enforcement and the willingness of people to use recycled products are needed.

The carbon footprint reduction potential in utilizing recycled aggregates instead of quarried aggregates is to be factored in the equations while proposing incentives and other mechanisms to boost the recycling industry.

References

1. TIFAC (2001) Utilisation of waste from construction industry. http://tifac.org.in/index.php?option=com_content&id=710&Itemid=205, Last accessed 16 Nov 2016
2. MoEF. Ministry of Environment and forests. <http://www.moef.nic.in/downloads/public-information/Roadmap-Mgmt-Waste.pdf>. Last accessed 18 Feb 2019
3. Ram VG, Kalidindi SN (2017) Estimation of C&D waste using waste generation rates in Chennai, India. *Waste Manag Res* 6(5):610–617
4. Centre for Science and Environment. <http://www.cseindia.org/content/waste-resource-briefing-note-cse-warns-cities-are-choking-and-because-their-own-construction>, Last accessed 12 Nov 2016
5. Development Alternatives (2015) Resource efficiency in the Indian construction sector: market evaluation of the use of secondary raw materials from construction and demolition waste. New Delhi: Deutsche Gesellschaft Internationale Zusammenarbeit (GIZ) GmbH
6. Jain S, Singhal S, Jain NK (2018) Construction and demolition waste (C&DW) in India: generation rate and implications of C&DW recycling. *Int J Constr Manag*. <https://doi.org/10.1080/15623599.2018.1523300>
7. Aggregate Business International. <http://www.aggbusiness.com/sections/market-reports/features/booming-indian-aggregates-market/>, Last accessed 18 Feb 2019

An Ontological Analysis of Challenges Involved in Urban Solid Waste Management



Shwetmala Kashyap, Arkalgud Ramaprasad, and Chetan Singai

Abstract Solid waste is a heterogeneous mixture of solid material (biodegradable, non-biodegradable, and inert) that does not have any further use to the society. Research studies suggest an annual per capita rate of increase in solid waste of 1–1.33%. The increasing quantity of such waste is resulting in serious health, aesthetic, environmental, social, and economic problems due to lack of appropriate planning and management. This necessitates the implementation of suitable policies to reduce the risk at all the stages starting from generation and ending with disposal of waste. Generally, the management of solid waste encompasses generation, segregation, storage, collection, transportation, recycling, processing, and disposal. This article presents a logically constructed ontological framework of urban solid waste management. It gives importance to waste management policy, functional elements of waste management, types of waste, sources of waste generation, people involved in waste management, and benefits of solid waste management. It shows the pathways to address the challenge to achieve sustainable solid waste management in the cities. The ontological framework encapsulates a total of $7 * 8 * 3 * 6 * 11 * 5 = 55,440$ possible components of the challenge. A critical analysis based on primary and secondary data on urban solid waste management using the framework in Bengaluru, India will help in developing strategies to deal with solid waste. It can be used to systematically map the state-of-the-research on and the state-of-the-practice of urban solid waste management, to discover the gaps, and to bridge the gaps in waste management policy-making.

Keywords Urban solid waste · Sustainable management · Ontology · Framework

S. Kashyap (✉) · A. Ramaprasad · C. Singai
Ramaiah Public Policy Center, Bengaluru, Karnataka, India
e-mail: shwetmala.kashyap@rppc.ac.in

A. Ramaprasad
University of Illinois at Chicago, Chicago, IL, USA

1 Introduction

An Urban Solid Waste Management (USWM) system is complex as it involves many elements and sub-elements. A typical USWM system comprises of generation, segregation, storage, collection, transportation, recycling, processing, and disposal of waste. The purpose of USWM is to provide resource recovery from waste, to encourage reuse of materials within the society, and ultimately to reduce the risk to the human and the environment [1].

With rapid urbanization, the quantity of solid waste is increasing, thus mandating a systematic and systemic USWM. Indian cities’ average annual per capita increase in waste generation rate is 1–1.33% [2–4]. This increase can be attributed to the rapid increase in population, industrialization, and other economic activities in the cities.

The approach to solving the USWM problem, in most cases, has been focused on a part of the problem based on the immediate requirement, thus missing the big picture of the problem. The challenge is to address this problem in a more systematic way to give a complete picture of USWM. Visualization of USWM will help determine the gaps and problems to achieve effective waste management. We present an ontological framework as a systematic approach to make the USWM problem whole and visible.

2 Ontology of USWM

An ontology is an explicit specification of a conceptualization [5]. The ontology of USWM is a combinatorial representation, effective in capturing its complexity, while making it simple, visible, and comprehensible. An ontology of USWM is shown in Fig. 1 and a glossary of all the elements of the ontology is shown in Appendix A. We will discuss the construction of the ontology, its dimensions, taxonomies, elements, and the pathways for USWM encapsulated within.

A USWM system can be defined by six dimensions, each of which is a complex construct. Thus:

Urban Solid Waste Management					
Policy	Function	Solid Waste	Source	Stakeholder	Outcome
[Implementation of] Legislative Instrument	[Instruments for] Generation	[of solid] Biodegradable	[Σ] Residential	[waste by/for] Waste generator	[for] Health
Regulatory	Segregation	Non-biodegradable	Non-Residential	Urban planner	Aesthetic
Economic	Storage	Inert	Institutional	Waste picker	Environmental
Fiscal	Collection		Commercial	Service provider	Social
Contractual	Transportation		Construction & Demolition	Resident welfare assoc.	Economic
Information	Recycling		Industrial process	NGO	
Social	Processing		Municipal service	Academia	
	Disposal			Business	
				Government	
				Local/Municipal	
				Provincial/State	
				Central/Federal	

Fig. 1 An ontological framework of urban solid waste management (USWM)

$$USWM = f \left(\begin{array}{l} \text{Policy Instrument} + \text{Function} + \text{Solid Waste} \\ + \text{Source} + \text{Stakeholder} + \text{Outcome} \end{array} \right)$$

The policy instrument of USWM are legislative, regulatory, economic, fiscal, contractual, information, and social. Thus:

$$\text{Policy instrument} \subset [\text{Legislative, Regulatory, Economic,} \\ \text{Fiscal, Contractual, Information, Social}]$$

The functional elements of USWM include waste generation, segregation, storage, collection, transportation, recycling, processing, and disposal. Thus:

$$\text{Function} \subset [\text{Generation, Segregation, Storage, Collection,} \\ \text{Transportation, Recycling, Processing, Disposal}]$$

The solid waste may be biodegradable, non-biodegradable and inert. Thus:

$$\text{Solid Waste} \subset [\text{Biodegradable, Non – biodegradable, Inert}]$$

The source of solid waste generation in an urban area are mainly residential and non-residential areas. Non-residential waste generation sources are institutional, commercial, construction and demolition, industrial processes, and municipal services. Thus:

$$\text{Source} \subset [\text{Residential, Non – Residential}_{(\text{Institutional})}, \text{Non – Residential}_{(\text{Commercial})}, \\ \text{Non – Residential}_{(\text{Construction and demolition})}, \text{Non – Residential}_{(\text{Industrial processes})}, \\ \text{Non – Residential}_{(\text{Municipal services})}]$$

The stakeholders involved in USWM include waste generators, urban planners, waste pickers, service providers, resident welfare associations, NGO, academia, business, and government. The government may be local or municipal, provincial or state, and central or federal. Thus:

$$\text{Stakeholder} \subset [\text{Waste generator, Urban planner, Waste picker,} \\ \text{Service provider, Resident Welfare Association,} \\ \text{NGO, Academia, Business, Govt.}_{(\text{Local/Municipal})}, \\ \text{Govt.}_{(\text{Provincial/State})}, \text{Govt.}_{(\text{Central/Federal})}]$$

The desirable outcomes of USWM are health, aesthetics, environmental (improvement), social wellbeing, and economic wellbeing. Thus:

$$\text{Outcome} \subset [\text{Health, Aesthetic, Environmental, Social, Economic}]$$

The six dimensions arranged left to right with connecting terms (symbols/words/phrases) form natural English sentences that represent potential pathways for USWM. Thus, the total number of pathways in the framework are $7 * 8 * 3 * 6 * 11 * 5 = 55,440$ components. Three illustrative pathways derived from the framework are:

Implementation of legislative instruments for the segregation of solid biodegradable residential waste by waste pickers for environmental (wellbeing) of the community.

Implementation of contractual instruments for disposal of solid non-biodegradable non-residential for businesses for economic (wellbeing) of the community.

Implementation of social instruments for recycling non-biodegradable residential waste by waste pickers for the health of the community.

The ontology is constructed logically incorporating the empirical elements of USWM. The 55,440 pathways encapsulated in the ontology represent the complete requirement to manage urban solid waste systematically and systemically. Some of the combinations may be infeasible or not instantiated, but many pathways can be used for research, making Government policy and waste management practice.

3 Applications of the Ontology

The ontology provides a complete visual picture of USWM, without reducing its combinatorial complexity. The multidisciplinary framework incorporates elements of urban planning, policy, social science, science, and engineering. It can be a tool for researchers, policy-makers, and practitioners to visualize the important pathways to USWM, and to develop strategies to deal with solid waste.

It can be used to systematically map the state-of-the-research in, and state-of-the-practice of USWM, to discover the gaps within each and between the two, and to bridge the gaps in waste management policy-making.

4 Conclusions

In this paper, an ontology of USWM is proposed that encapsulates its complexity. It can be used to study the system from many perspectives and to explore different pathways. A comprehensive framework of USWM such as this will help achieve sustainable waste management in an urban area.

Appendix: Glossary of Urban Solid Waste Management Framework

<i>Policy instrument</i>	<i>Means of government intervention to manage solid waste management</i>
Legislative	Legislative means to manage solid waste management
Regulatory	Regulatory methods to manage solid waste
Economic	Economic incentives/penalties to manage solid waste
Fiscal	Fiscal measures to manage solid waste
Contractual	Licensing/contracts to manage solid waste
Information	Informational means to manage solid waste
Social	Popularly practiced social norms to manage solid waste
<i>Function</i>	<i>Means of functional elements involved in solid waste management</i>
Generation	Generation means quantity of materials that enter the waste stream
Segregation	Segregation means to separate solid waste into the groups of organic, inorganic, recyclables and hazardous wastes
Storage	Storage means the temporary containment of solid waste in a covered bin or container
Collection	Collection means lifting and removal of solid wastes from collection points or any other location.
Transportation	Transportation means conveyance of municipal solid waste, either treated, partly treated or untreated from a location to another location in an environmentally sound manner
Recycling	Recycling means the process of transforming segregated recyclable solid waste into a new product or raw material for producing new products
Processing	Processing means the process by which solid waste is transformed into new or recycled products
Disposal	Disposal means the final and safe disposal of solid waste on land to prevent contamination of ground water, surface water, ambient air and attraction of animals or birds
<i>Solid Waste</i>	<i>Heterogeneous mixture of solid materials that does not have any use to society</i>
Biodegradable	Biodegradable means any organic material that can be degraded by micro-organisms into simpler stable compounds
Non-recyclable	Non-biodegradable means a substance that cannot be degraded by micro-organisms
Inert	Inert means solid wastes or remnant of processing which are not biodegradable, recyclable or combustible and includes non-recyclable fraction of construction and demolition waste, street sweeping, or dust and silt removed from the surface drains

(continued)

(continued)

<i>Policy instrument</i>	<i>Means of government intervention to manage solid waste management</i>
<i>Source</i>	<i>The premises/community in which waste is generated</i>
Residential	Residential source includes waste generated from single and multifamily dwellings
Non-residential	Waste generated from sources excluding residential area
Institutional	Institutional source includes waste generated from schools, hospitals, prisons, government centers
Commercial	Commercial source includes waste generated from stores, hotels, restaurants, markets, office buildings, etc.
Construction and demolition	Construction and demolition source includes waste generated from new construction sites, road repair, renovation sites, demolition of buildings
Industrial process	Industrial process includes waste generated from light and heavy manufacturing, fabrication, construction sites, power and chemical plants, heavy and light manufacturing, refineries, chemical plants, power plants, mineral extraction and processing
Municipal services	Municipal services include waste generated from street cleaning, landscaping, parks, beaches, other recreational areas, water and wastewater treatment plants
<i>Stakeholder</i>	<i>People, organization or system involved in solid waste management actions</i>
Waste generator	Waste generator means persons and establishments generating municipal solid waste
Urban planner	Urban planners need to keep waste management in mind while developing city/town plans
Waste picker	Waste picker means a person or groups of persons engaged in collection of reusable and recyclable solid waste from the source of waste generation as well as picking up of wastes from the streets, bins, processing and waste disposal facilities for sale to recyclers directly or through intermediaries to earn their livelihood
Service provider	Service provider means an authority providing public utility services like water, sewerage, electricity, telephone, roads, drainage etc.
Resident welfare association	Resident welfare association means a group of owners or occupiers of residential premises or association of such owners that represents the interests of the residents
NGO	NGOs take lead in forming ward committees and community participation
Academia	Academia can influence minds on solid waste management and can also carry out relevant research and development
Business	Businesses availing solid waste management
Government	The different levels of government

(continued)

(continued)

<i>Policy instrument</i>	<i>Means of government intervention to manage solid waste management</i>
Local/Municipal	The lowest level of government
Provincial/State	The government of a province or state, above the local/municipal government
Central/Federal	The government of the country
<i>Outcome</i>	<i>Outcome of solid waste management</i>
Health	Health improvement includes better public health, hygiene and sanitation with management of solid waste
Aesthetic	Aesthetic improvement includes reduction in public nuisance due to unsightliness and bad smell with management of solid waste
Environment	Environment improvement includes reduction in effects on air, water and land with management of solid waste
Social	Social development includes social acceptability of implemented solid waste management system
Economic	Economic development includes income and output resulting from solid waste management

References

1. Tchobanaglou G, Theisen H, Eliassen R (1997) Solid wastes: engineering principles and management issues. McGraw-Hill publications, New York, USA
2. Shekdar AV (1999) Municipal solid waste management—The Indian perspective. *J Indian Assoc Environ Manag* 26(2):100–108
3. Pappu A, Saxena M, Asokar SR (2007) Solid waste generation in India and their recycling potential in building materials. *J Build Environ* 42(6):2311–2324
4. Sharholi M, Ahmed K, Mahmood G, Trivedi RC (2008) Municipal solid waste management in India cities—A review. *Waste Manag* 28:459–467
5. Gruber TR (1995) Toward principles for the design of ontologies used for knowledge sharing. *Int J Hum-Comput Stud* 43:907–928

Development of New Precursors for One-Part Alkali-Activated Geopolymer Using Industrial Wastes



Monower Sadique, Abdullah Kadhim, William Atherton, and Patryk Kot

Abstract Conventional two-part alkali activation has many drawbacks: the hazardous activating solution, which makes it less friendly to handle and the absence in long-term availability of its main precursors such as fly ash and ground granulated furnace slag. This research aimed to develop a one-part alkali-activated cement, which is free of chemical solutions. A blend of alumina-silicate rich materials with adequate alkaline content to minimise the limitations associated with the current (AAC) relating to source materials was utilised. At the same time, applying alternative activation methods such as thermo-mechanical activation, alkali-thermal activation or thermo-chemical activation of new (AAC) precursors were investigated. Materials were analysed in terms of their physical, chemical and metallurgical properties to understand the changes after thermal activation. Enhanced compressive strength was recorded from individual thermal activation of the materials at 450 °C and 950 °C.

Keywords One-part geopolymer · Alkali activation · Thermal activation

1 Introduction

Recently, Alkali-Activated Cement (AAC) or geopolymer cement has attracted global considerations for its high engineering and mechanical properties. Conventional two-part AAC is produced by activating solid alumina-silicate sources with alkali metal (Na or K) or alkaline earth (Ca or Mg) hydroxide or silicate solution from a sequence of dissolution–reorientation–solidification reactions [1, 2]. However, this process of manufacturing has many drawbacks including chemical handling difficulties and hazards from these solutions which in terms of rising impracticality of using these novel materials for in situ applications. Therefore the need for

M. Sadique (✉) · W. Atherton · P. Kot
Department of Civil Engineering, Liverpool John Moores University, Peter Jost Centre, Byrom Street, Liverpool L3 3AF, UK
e-mail: m.m.sadique@ljmu.ac.uk

A. Kadhim
Department of Civil Engineering, Liverpool John Moores University, Henry Cotton Building, Webster Street, Liverpool L3 2ET, UK

one-part dry AAC that just needs water to create a binding material started to be very significant [3]. This means that AAC can be similar to OPC but with exceptional engineering and ecological properties. One-part AAC can be synthesised by providing sources of (alkali+silicate+aluminate) as solid powder form with utilising various assisted activation methods such as thermal (calcination), mechanical (grinding) or combination of both methods. A wide range of alumina-silicate materials can be incorporated in the process including (natural and artificial) pozzolans and industrial (by-products and wastes). Sturm, Gluth [4] synthesised one-part Geopolymer mix by mixing calcined (600 °C) Rice Husk Ash and solid sodium aluminate which was considered as an activator in the system as it is easy to dissolve on water. Therefore, water just added to the binder with a water/binder ratio 0.5. The samples were cured in open moulds for an 80 °C to increase the reactivity of the mixtures. The obtained compressive strength was 30 Mpa after one day curing. Alkaline source can be either (Na, K or Ca, Mg), however, past studies proved that using CaO or Ca (OH)₂ can be alternative activators as these sources are cheaper than (NaOH or KOH) [5, 6]. Kim, Jun [6] used synthetic commercial CaO solid powder to create cement-free binder with ground granulated blast furnace slag as Si/Al source material. After comparing with Ca (OH)₂, CaO activator was discovered to present developed mechanical properties with 53 MPa strength of 56 days because of the fabrication of additional C-S-H than Ca (OH)₂.

In this research, attempts were targeting towards synthesising a dry one-part AAC utilising a waste material from quick lime production which is mostly rich in alkaline source (CaO) instead of the commercial synthetic CaO chemical powder which was used by past studies. This lime waste (LW) is used to activate the source of alumina-silicate (Al/Si) materials offered by a blend of metakaolin (MK) and a natural pozzolan material from volcanic tuff (NP).

2 Materials and Experimental Work

2.1 Material Characterisation

Initially, all materials were assessed and characterised to evaluate their chemical and physical properties. Table 1 shows the physical properties of materials including specific surface area, alkalinity and density. MK and NP having higher surface area

Table 1 Physical properties of undisturbed materials

Material	Specific surface area (Blaine) (m ² /g)	pH	Density (g/cm ³)
MK	19.6	6	2.69
NP	17.2	6	2.57
LW	10.1	12.3	2.7

than LW which has high alkalinity with pH of 12.3 is favourable for alkalination of MK and NP. The specific surface area was determined by Blaine Air Permeability Apparatus according to the British standard (EN 196-6). Mineralogy of materials was evaluated by X-Ray Diffraction (XRD) and Thermogravimetric analysis (TGA) methods. XRD has been conducted for undisturbed materials and after calcination with two levels 450 °C and 950 °C.

Particle size distribution (PSD) was determined by a laser diffraction particle size analyzer as displayed in Table 2. MK and NP were nearly similar with (D_{50}) is 7.88 and 9.68 μm , respectively. Conversely, LW was coarser with D_{50} 15.9 μm .

All materials were provided by local suppliers in the UK. Materials were characterised chemically to determine their composition by using X-Ray fluorescence (XRF) as shown in Table 3. MK and NP are mostly composed of SiO_2 and Al_2O_3 with fewer amounts of CaO , Na_2O , K_2O and MgO in NP. In contrast, LW is mostly rich in CaO of 80.1 Wt. % with small amounts of SiO_2 and Na_2O .

Table 2 Particle size distribution (PSD) of starting materials

	Amount (%)	Mean (μm)	Median (μm)	S.D (μm)	C.V	d10 (μm)	d50 (μm)	d90 (μm)
LW	100	23.6	15.9	22.1	93.70%	0.965	15.9	59.6
MK	100	13.9	7.88	15.2	110%	1.2	7.88	38
NP	100	15.1	9.68	14.5	95.70%	0.972	9.68	39
(Average)	100	17.5	11.2	17.3	99.60%	1.05	11.2	45.5
(C.V.)	0.00%	30.20%	37.90%	24.50%	8.70%	12.80%	37.90%	26.80%
(Maximum)	100	23.6	15.9	22.1	110%	1.2	15.9	59.6
(Minimum)	100	13.9	7.88	14.5	93.70%	0.965	7.88	38

Table 3 Chemical composition of undisturbed materials by XRF

Component	MK	NP	LW
SiO_2	46.2	46.6	14.6
Al_2O_3	33	18.6	0.27
Fe_2O_3	0.9	3.8	0.1
CaO	0.3	4.5	80.1
Na_2O	0.9	3.9	1.8
K_2O	0.4	6	0.5
MgO	0.1	4.2	0.6
TiO_2	1.6	0.6	0.1

Table 4 Mixing proportions of blends

Mix ID	Binder contents	Calcined constituent
M1	35%MK 35%LW 30%NP	NP
M2	35%MK 35%LW 30%NP	MK
M3	35%MK 35%LW 30%NP	LW
M4	35%MK 35%LW 30%NP	NP, MK, LW

2.2 Tests Preparation and Procedures

The mixing method was followed consistent with the requirements of (BS EN 196-1:2016). Water/binder ratio w/b was fixed of 0.45 for all the mortars after exploring the appropriate w/b for the selected materials. Primarily, 0.55 ratio was chosen but it was found that the mortars were very workable. Consequently, it was decreased to 0.45 and mortars with suitable uniformity was attained at this stage. Mortars were mixed using sand passing through 2.0 mm BS sieve with a specific gravity of 2.62 with mixing ratio (1:2). The mortars were mixed using Hobart mixer and cast in steel moulds of prisms with (40 mm × 40 mm × 160 mm). Mortars were blended in ternary procedure with magnitudes as shown underneath in Table 4. The mortars were cured in hot water curing regime to improve the reactivity and the hydration rate of the mortars and to avoid possible problems such as efflorescence and micro-cracking at this stage which can lead to a reduction in compressive strength [7]. The curing temperature was fixed to 50 °C for 7 days and then cured in normal 20 °C water until 28 days. This curing procedure was selected based on past reports and studies that proved the best curing temperatures for alkali-activated cement [8, 9].

The calcination of materials in muffle furnace was individually to assess the influence of each material on the mixture's properties. Two levels of calcination were based (950 and 450 °C) for 2 h with 20 °C/min calcining rate. Calcination temperatures were chosen depending on the characterisation (XRD & TGA) results which presented that most phase's changes take place at these levels.

3 Results and Discussions

3.1 Mineralogical Analysis

It is noticeable from the diffractions of MK in Fig. 1 that MK encompasses of minerals comprising kaolinite and quartz in main phases. Minor phases involve mullite, anatas and illite. Noteworthy decrease and even disappearance of kaolinite and quartz peaks were noted after both levels of calcination indicating semi-transformation of material to an amorphous phase.

In Fig. 2, XRD spectrums of NP which shows vast transformation of crystalline to

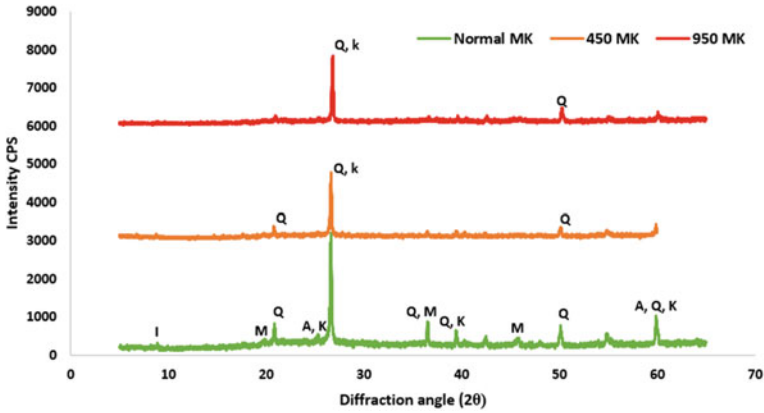


Fig. 1 XRD of MK before and after calcination. Q: Quartz (SiO_2), K: kaolinite ($\text{Al}_2\text{Si}_2\text{O}_5(\text{OH})_4$), M: Mullite $\text{Al}_6\text{Si}_2\text{O}_{13}$, A: Anatas (TiO_2), I: Illite ($\text{K,H}_3\text{O}(\text{Al,Mg,Fe})_2(\text{Si,Al})_4\text{O}_{10}[(\text{OH})_2,(\text{H}_2\text{O})]$)

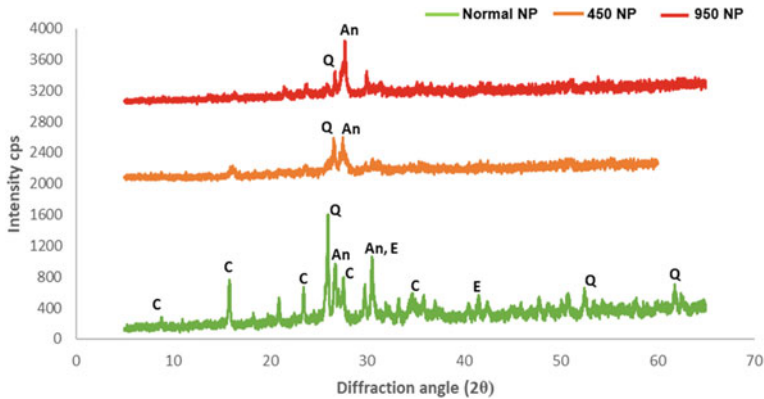


Fig. 2 XRD of NP before and after calcination. Q: Quartz (SiO_2), C: Clinoptilolite ($\text{KNa}_2\text{Ca}_2(\text{SiO}_{29}\text{Al}_7)\text{O}_{72}\cdot 24\text{H}_2\text{O}$), An: Anorthite ($\text{CaAl}_2\text{Si}_2\text{O}_8$), E: Edenite ($\text{Ca}_2\text{NaMg}_5(\text{AlSi}_7)\text{O}_{22}(\text{OH})_2$)

amorphous phases through the loss of Clinoptilolite and Anorthite peaks. Moreover, substantial decreasing in crystalline quartz at 950 °C calcination level.

Figure 3 displays the diffraction patterns of LW which can be seen clearly that the strong crystalline diffraction peak of lime (CaO) in LW was reduced significantly when calcined to 450 °C and entirely disappeared in 950 °C calcination. The presence of new diffraction peaks at new angles of calcined LW at 950 °C representing the formulation of new compounds but composed of same elements of undisturbed LW (CaO, SiO_2 and Na_2O) in form of wollastonite minerals [10, 11].

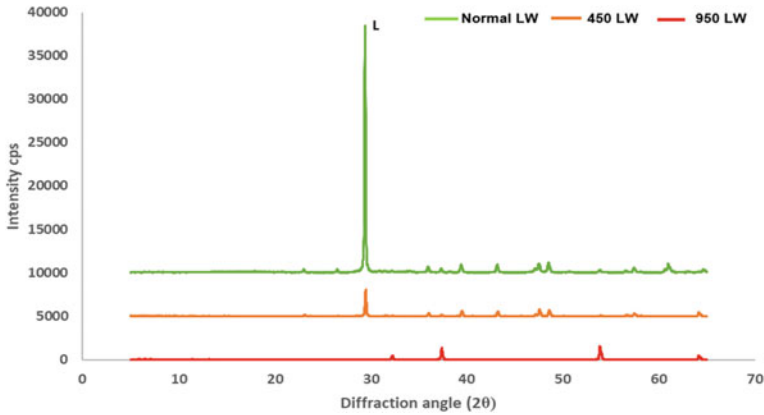


Fig. 3 XRD of LW before and after calcination. L: Lime (CaO)

3.2 Thermogravimetric Analysis (TGA)

TG-DTA thermal analysis was used to assess the thermal behaviour of raw materials when calcined to higher temperatures up to 900 °C. Figure 4a displays mass loss of NP up to 7% from initial weight when calcined from room temperature to 900 °C. While DTA curve is indicating exothermic concavity at 250 °C tailed by an endothermic drop in the curve reaching around 450 °C representing a start of phase's conversion process at this temperature. DTA curve of MK has revealed minor phase change about 700 °C as in Fig. 4b. Weight loss of LW started to drop intensely at 620 °C with 35% from the original weight with an intense and severe exothermic peak of DTA curve as demonstrated in Fig. 4c. This peak accredited to the disappearance of (CaO) crystalline peak in XRD of calcined LW.

3.3 Compressive Strength

Figure 5 shows compressive strength of mortars after individual calcination for 950 °C. A higher strength was gained from M3 that consists of calcined LW with 27.3 MPa in 28 days. This strength is attributed to the large transformation to vitreous mineralogy and disappearance of crystalline CaO peak because of calcination to 950 °C. Reduced dissolution of alumina-silicate compounds from NP and MK due to high amounts of amorphous compounds and lesser amounts of CaO when all materials calcined led to a fall of strength in M4.

Both XRD and TG-DTA results have shown that changes in phases of this ternary blend components starting in temperatures ranging from 350–500 °C. Hence, blends were mixed after calcination of 450 °C with the same method of proportioning that is mentioned in Table 4. Noticeably as shown in Fig. 6, comparative strength was

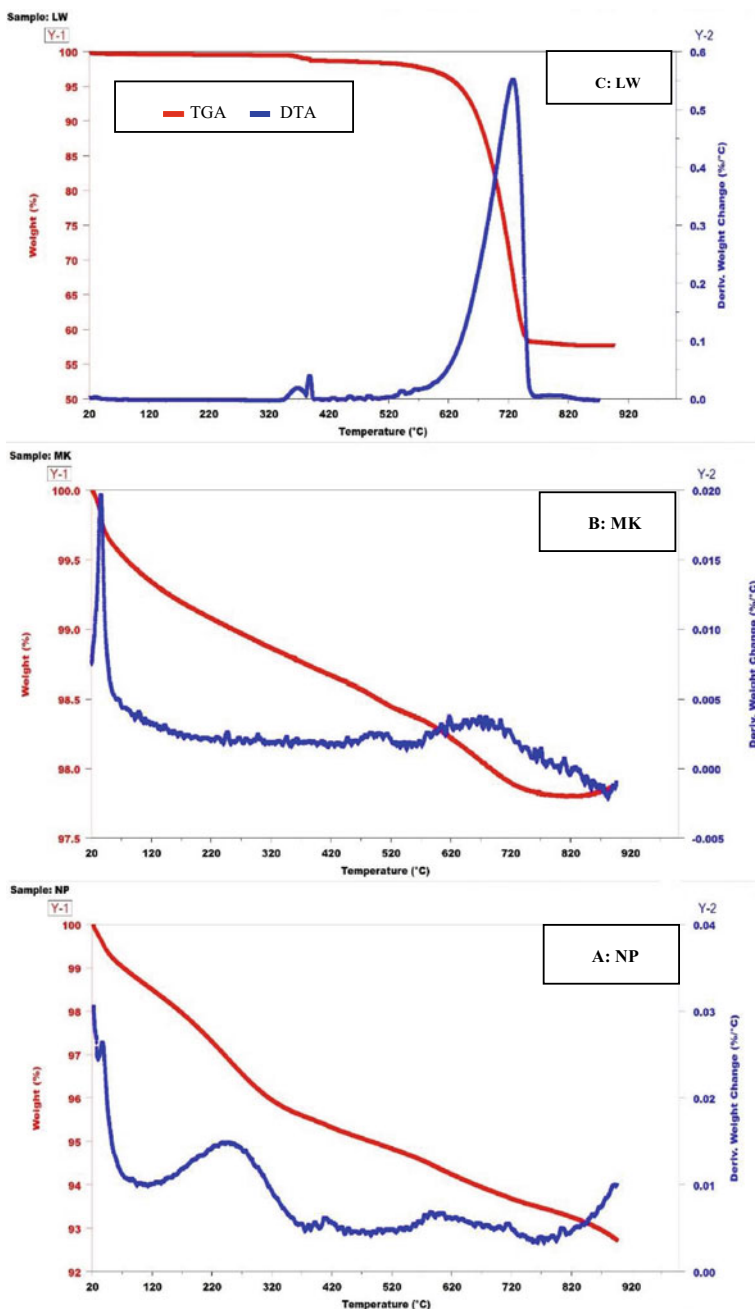


Fig. 4 TG-DTA analysis of A: NP, B: MK, C: LW

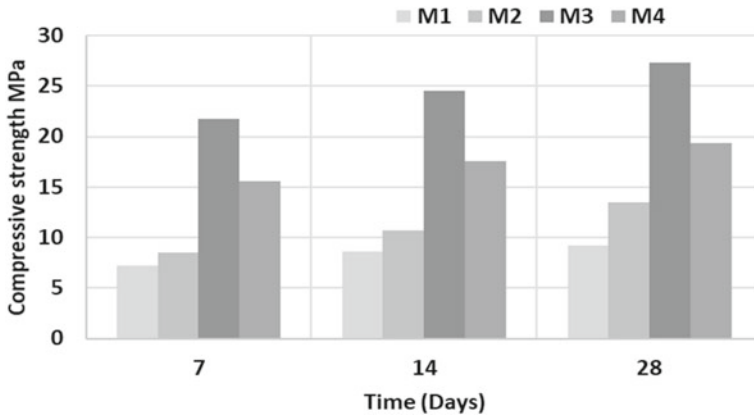


Fig. 5 Compressive strength after 950 °C calcination

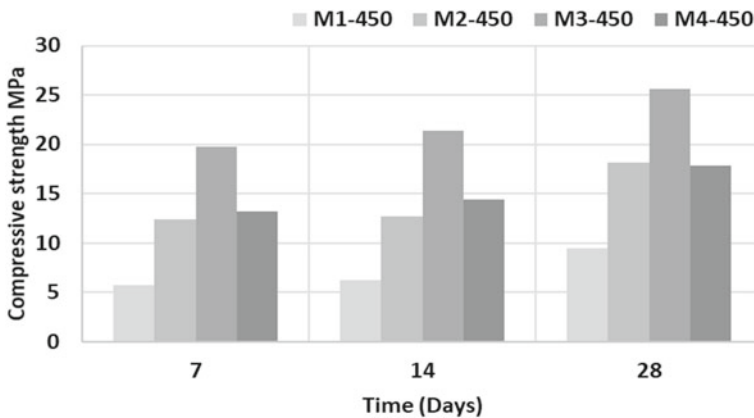


Fig. 6 Compressive strength after 450 °C calcination

obtained at this level of calcination with developed strength reached for 25.6 MPa at 28 d for M3-450 that has LW of 35%. This comparable growth of strength is attributed to mineralogical and chemical variations that were remarked in both XRD and DT-TGA results which designated that most diffraction patterns were starting to convert before and around 450 °C.

4 Conclusions

- Calcination was chosen assisted thermal activation for producing one-part AAC from a combination of alkali alumina-silicate materials. Calcination of materials

was conducted to 450 and 950 °C individually to assess the contribution of each material.

- Raw materials were characterised physically and chemically. Mineralogy and thermal behaviour and change due to calcination were assessed.
- Maximum compressive strength was recorded of 27.3 MPa in 28 d for mortar containing calcined (LW) of 950 °C. Relative compressive strength was gained at 450 °C calcination level demonstrating that reactivity of materials started to increase at this temperature.
- This strong growth was attributed to the massive conversion of LW mineralogy to be amorphous which initiated by calcination which was considered as an assisted activation factor.
- The outcomes of the study have shown that lime waste (LW) has high probability to be solid alkaline activator if treated correctly and its impurities are removed.

References

1. Palomo A et al (2014) A review on alkaline activation: new analytical perspectives 64(315)
2. Provis JL (2017) Alkali-activated materials. *Cem Concr Res*
3. Luukkonen T et al (2018) One-part alkali-activated materials: a review. *Cem Concr Res* 103:21–34
4. Sturm P et al (2016) Synthesizing one-part geopolymers from rice husk ash. *Constr Build Mater* 124:961–966
5. Vaccari M, Gialdini F, Collivignarelli C (2013) Study of the reuse of treated wastewater on waste container washing vehicles. *Waste Manag* 33(2):262–267
6. Kim MS et al (2013) Use of CaO as an activator for producing a price-competitive non-cement structural binder using ground granulated blast furnace slag. *Cem Concr Res* 54:208–214
7. Chithra S, Dhinakaran G (2014) Effect of hot water curing and hot air oven curing on admixed concrete. *Int J ChemTech Res CODEN (USA): IJCRGG*:1516–1523
8. Perera DS et al (2007) Influence of curing schedule on the integrity of geopolymers. *J Mater Sci* 42(9):3099–3106
9. Singh B et al (2015) Geopolymer concrete: a review of some recent developments. *Constr Build Mater* 85:78–90
10. Eilers LH, Nelson EB, Moran LK (1983) High-temperature cement compositions—Pectolite, Scawtite, Truscottite, or Xonotlite: which do you Want? *J Petrol Technol* 35(07):1373–1377
11. Garbev K et al (2008) First observation of α -Ca₂[SiO₃(OH)](OH)–Ca₆[Si₂O₇][SiO₄](OH)₂ phase transformation upon thermal treatment in air. *J Am Ceram Soc* 91(1):263–271

Waste Management in Textile Industry—A Novel Application of Carbon Footprint Analysis



S. Mohan and Ninad Oke

Abstract The higher quantities of water and a wider spectrum of dyes and auxiliary chemicals used impart a complex nature to combined effluent from various textile manufacturing units. Standards for color, organics, and dissolved solids are becoming stringent with time and regulators are in demand of zero liquid discharge units. For any zero liquid discharge facility, the major concerns include higher energy consumption for reject management and the generation of hazardous solid waste. As per the government regulations in Tamil Nadu, India, all the textile industries with a daily effluent discharge of more than 25 kiloliters must set up a zero liquid discharge facility. This has led to the accumulation of million tons of hazardous solid waste in the premises of textile manufacturing units. A carbon footprint is a measure of the total amount of greenhouse gases emissions of a defined person, organization, or a region associated with certain activities, production processes and life cycle of a product. The application of carbon footprint analysis to different waste management options can effectively help in the quantification of the overall environmental impact. The analysis performed can give key inputs to the stakeholders in the decision-making process regarding waste management in textile industries. Based on the methodology applied as per IPCC guidelines, the carbon footprint of a zero liquid discharge textile manufacturing facility in south India was found to be 10598.31 tCO₂ equivalents per year. Sustainable waste management in textile industries plays an important role in minimizing the overall environmental impact of this continuously growing industry.

Keywords Carbon footprint · Zero liquid discharge · Hazardous solid waste · Sustainability

S. Mohan · N. Oke (✉)
Indian Institute of Technology Madras, Chennai, India
e-mail: okeninad@gmail.com

© Springer Nature Switzerland AG 2020
K. R. Reddy et al. (eds.), *Sustainable Environmental Geotechnics*, Lecture Notes
in Civil Engineering 89, https://doi.org/10.1007/978-3-030-51350-4_14

125

1 Introduction

Global climate change, also known as global warming, is caused by the increasing emission of greenhouse gases due to various anthropogenic activities. The increased concentration of greenhouse gas in the atmosphere directly leads to global temperature rise, which in turn causes sea-level rise, flooding, and extreme weather.

In the year 2010, global greenhouse emission was reported as 48629 MT CO₂-equivalent out of which, nearly 3% of the global emissions were contributed by the waste management sector [1]. Whereas, in the Indian scenario the contribution from the waste management sector was 3.34%, slightly above the global average [2]. It underlines the immediate need of a well-developed methodology to quantify greenhouse gas emissions from this sector to further implement focused emission mitigation practices. The three major greenhouse gases generally considered in carbon footprint calculation are carbon dioxide, methane, and nitrous oxide.

The wastewater treatment plants have a positive contribution toward environmental impact mitigation through wastewater treatment but, the energy consumption by them must be also considered. Recent developments in the concept of Zero Liquid Discharge facilities are very important from the resource recovery approach. High energy consumption by the reject management system in Zero Liquid Discharge facilities demands a need for well-developed methodology to quantify the environmental impact of the wastewater treatment plants.

An important point to be considered in the establishment of Zero Liquid Discharge facilities is the ultimate disposal of the generated solid waste. As the heavy metal-based azo dyes widely used in cellulose dyeing processes in India, the generated solid waste is considered of hazardous nature. The huge accumulation of the hazardous solid waste at the textile manufacturing facilities as a result of the establishment of Zero Liquid Discharge facility needs to be well addressed.

2 Zero Liquid Discharge Facility

South India is also known as the Manchester of India as the textile manufacturing has very well thrived in southern parts of the country [3]. The enough availability of raw materials and cheap labor further enhance the socio-economic growth associated with the textile manufacturing activities. With the ever-increasing textile manufacturing practices in southern India, the adverse environmental impacts have started becoming a major concern for regulatory authorities.

The practice of setting up the Common Effluent Treatment Plant (CETP) for textile manufacturing industry clusters has been implemented by the regulatory bodies in India. In the textile dyeing process, salts like NaCl and Na₂SO₄ are added for enhanced dye fixation on the cellulose fiber [4]. The combined effluent from textile manufacturing processes is highly colored, having high organic load and very high total dissolved solids. As the CETP generally provides treatment only up to the

secondary level, the total dissolved solids were not removed from the discharged treated textile effluent. The higher salt content is a major concern for the natural receiving water bodies. Therefore, regulatory bodies made it mandatory for all the textile industries with a daily effluent discharge of more than 25 kiloliters to set up a zero liquid discharge facility.

In the Zero Liquid Discharge effluent treatment facility, reverse osmosis is provided as the tertiary treatment. The permeate stream can be reused as the process water by textile industries. The reject stream is further fed to multiple-effect evaporator for enhanced water recovery. The residual solids from the multiple-effect evaporator are dried on the solar drying pans. The wastewater from textile manufacturing activities can be effectively reused by the implementation of above concept. The uniform water quality parameters of the reused water are advantageous for the industries, as they can get a constant source of high-quality process water.

There are two major sources of hazardous solid waste in the Zero Liquid Discharge facility. Firstly, the sludge generated from primary and secondary settling tanks and second is the residual salt obtained from multiple-effect evaporator. The effective hazardous solid waste management system is required at such facilities. Following Fig. 1 gives a schematic flow diagram of the Zero Liquid Discharge facility.

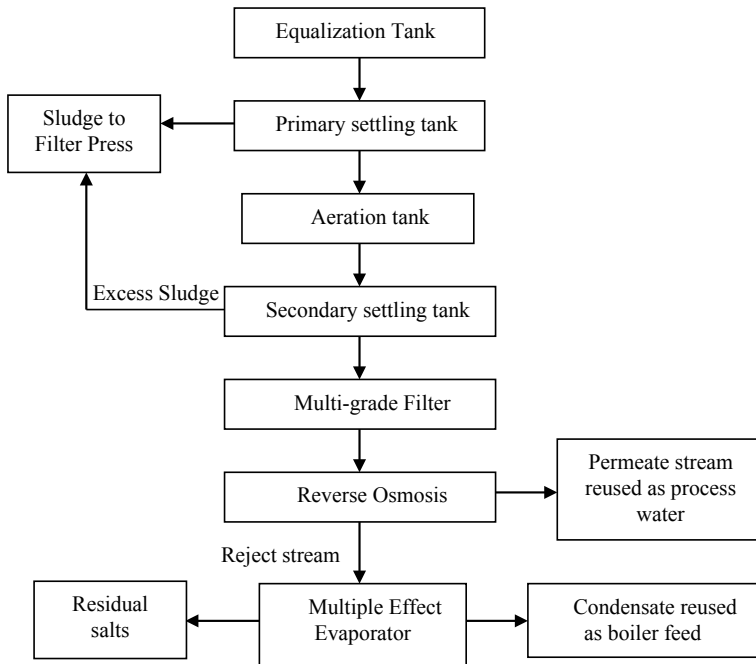


Fig. 1 Schematic flow diagram of a zero liquid discharge effluent treatment facility

Table 1 Definitions of carbon footprint

Definition	Reference
The CF stands for the total amount of CO ₂ and other greenhouse gases, emitted over the full life cycle of a process or product	[6]
The CF is the result of life cycle thinking applied to global warming	[7]
The CF stands for the land area required for the sequestration of fossil-fuel CO ₂ emissions from the atmosphere through afforestation	[8]
The CF is a measurement of the exclusive direct and indirect CO ₂ emissions over a life cycle	[9]

3 Carbon Footprint

The quantification of greenhouse gas emissions due to certain human activity is very important as only after a proper quantification, proper monitoring is possible. This quantification process in case of a product manufacturing step, product disposal option or for an organization cannot be a subjective analysis as it will hinder the comparativeness of different studies. Therefore, the application of the concept of carbon footprint is important as it provides a platform to compare the greenhouse emissions from various sources reported globally.

Carbon footprint can clearly reflect the overall emission of greenhouse gases in the whole life cycle of a certain human activity. The specific time horizon considered for carbon footprint calculation is generally 100 years [5]. Various definitions of carbon footprint are available in the literature. Table 1 gives a list of key definitions of carbon footprint available from various literature.

There exists a clear lack of quick and reliable tools for carbon footprint calculation considering the data limitations in the case of developing countries. The understanding of the concept of carbon footprint and its appropriate field-scale application is important for the reporting of anthropogenic greenhouse emissions.

4 Methodology

In the present research work, carbon footprint has been calculated for a zero liquid discharge textile effluent treatment facility. The overall treatment capacity of the plant is 4.4 MLD out of which, 2.2 MLD was operation at the time of data collection.

The methodology of calculation of carbon footprint for the wastewater treatment plants can be divided into three major steps. The first step involves the identification of key sources of direct and indirect greenhouse gas emissions. It is followed by the quantification step in which one attempts to quantify the emissions from each of the identified sources. The third and final step involves the use of appropriate emission factors to report the data in terms of carbon dioxide equivalents calculated over a time horizon of 100 years.

The capacity to trap the energy in the atmosphere is different for different greenhouse gases. It is quantified in terms of “global warming potential” which is based on the radioactive effect of 1 kg of the gas over 100 years, compared to the effect of 1 kg of CO₂ and it is expressed as CO₂ equivalents. As per the IPCC fifth assessment report published in 2014, the global warming potential values for methane and nitrous oxide are 28 and 265, respectively [10]. After calculation of the methane and nitrous oxide emissions from the transportation activity they need to be converted to carbon dioxide equivalents by multiplying by the respective global warming potential values.

5 Results and Discussion

The following section presents the results obtained from the carbon footprint calculation for the considered Zero Liquid Discharge effluent treatment facility. From the field visits and data provided by plant operators, the major carbon emission sources were identified.

Within the premise, wood was being used as the fuel for boiler units. Possible methane emissions during the biological treatment of the effluent were considered and calculated as per the IPCC guidelines [11].

Carbon emissions associated with the electricity consumption contributed the most significant portion of the calculated carbon footprint. The carbon emissions associated with the transportation of hazardous solid waste to the hazardous waste landfill site in trucks or lorries have been included in the present carbon footprint calculation. The details of the calculation are presented in the Table 2.

The total carbon footprint was observed to be 10598.31 tCO₂ equivalents per year. The carbon footprint can also be reported as 13.1 kg CO₂ equivalent per m³ of textile industry effluent being treated. The obtained carbon footprint was found to be significantly higher than the global average values [12]. It underlines the need of minimizing the fuel and energy consumption at the Zero Liquid Discharge effluent treatment plants.

Table 2 Carbon footprint calculation of zero liquid discharge facility

Sr. No	Carbon emission source	Total tCO ₂ equivalent per year
1	Fuel use on site	7200.70
2	Electricity consumption	2675.06
3	Transportation	160.45
4	CH ₄ emissions from treatment plant	562.10
Total		10598.31

6 Conclusion

The Carbon Footprint analysis can be used as an effective tool to quantify carbon emissions from the effluent treatment plants, which supports further understanding of the pollution hotspots at the effluent treatment plants.

The concept of establishment of Zero Liquid Discharge effluent treatment facilities needs to be widely implemented as it prevents environmental pollution along with resource recovery. All the new effluent treatment facilities for the textile industry effluent need to be established as Zero Liquid Discharge facilities. The dissolved solids being discharged from the existing common effluent treatment plants are affecting many hectares of good fertile agricultural land.

For the Zero Liquid Discharge facilities also, we need to manage the hazardous solid waste effectively to prevent any further environmental impact. The accumulation of the residual salts at the textile manufacturing units needs to be avoided. The development of a cost-effective and carbon neutral waste management option for the hazardous residual salts will be a major step toward sustainable textile manufacturing practices in India.

References

1. Singh P, Kansal A, Carliell-Marquet C (2016) Energy and carbon footprints of sewage treatment methods. *J Environ Manag* 165:22–30
2. Singh DP, Maurya NS (2016) Estimation of greenhouse gas emissions: a case of Beur municipal wastewater treatment plant Unit-I, Patna India. *Desalin Water Treat* 57(58):28250–28261
3. Manikandan P, Palanisamy PN, Baskar R, Sivakumar P, Sakthisharmila P (2015) Physico chemical analysis of textile industrial effluents from Tirupur city, TN, India. *Int J Adv Res Sci Eng* 4(2):93–104
4. Holkar CR, Jadhav AJ, Pinjari DV, Mahamuni NM, Pandit AB (2016) A critical review on textile wastewater treatments: possible approaches. *J Environ Manag* 182:351–366
5. IPCC Guidebook: good practice guidance and uncertainty management in national greenhouse gas inventories (2006)
6. UK POST (Parliamentary Office of Science and Technology) (2006) Carbon footprint of electricity generation. No 268
7. EC (European Commission) (2007) Carbon Footprint e what it is and how to measure it. www.to-be.it/wp-content/uploads/2015/07/Carbon-footprint.pdf. Accessed 11 Jan 2019
8. De Benedetto L, Klemes JJ (2009) The environmental performance strategy map: an integrated LCA approach to support the decision making process. *J Clean Prod* 17:900e906.
9. Wiedmann T, Minx J (2008) A definition of ‘carbon footprint’. In: Pertsova CC (ed) *Ecological economics research trends*. Nova Science Publisher, Hauppauge, NY, US. Ch 1, 1e11
10. Yan Y, Wang C, Ding D, Zhang Y, Wu G, Wang L, Zhao C (2016) Industrial carbon footprint of several typical Chinese textile fabrics. *Acta Ecol Sin* 36(3):119–125
11. IPCC Guidelines for National Greenhouse Gas Inventories (2006) *Wastewater treatment and discharge*, vol 5, ch 6
12. Pagilla K, Shaw A, Kunezt T, Schiltz M (2009) A systematic approach to establishing carbon footprints for wastewater treatment plants. *Proc Water Environ Fed* 2009(10):5399–5409

New Ternary Blend Limestone Calcined Clay Cement for Solidification/Stabilization of Pb²⁺ Contaminated Soil



Anand V. Reddy, Chandresh H. Solanki, Shailendra Kumar,
and Krishna R. Reddy

Abstract The use of supplementary cementitious materials (SCMs) in engineering applications has been gaining more attention recently. SCMs such as calcined clay (CC) and limestone (LS) used for the clinker substitution over 50% during the cement manufacturing process makes an effective low clinker cement blend called limestone calcined clay cement (LC³). In the present study, the effects of LC³ binder on pH, leaching, and strength performance of lead (Pb) contaminated soil are investigated. Toxicity characteristics leaching procedure (TCLP) test was conducted to evaluate the leaching potential, and unconfined compressive strength (UCS) test was conducted to assess strength characteristics. The TCLP test results show that the leached Pb concentrations in the LC³ stabilized samples were well below the regulatory limits after 14 days of curing, and the UCS strength values increased with the increase in the curing time. Therefore, the use of new ternary blend LC³ can be used as a sustainable and environmental-friendly additive for the remediation of heavy metal contaminated soils.

Keywords Supplementary cementitious materials · Solidification/stabilization · Lead stabilization · Leaching and strength

A. V. Reddy (✉) · C. H. Solanki · S. Kumar
Civil Engineering Department, Sardar Vallabhbhai National Institute of Technology (SVNIT),
Surat, Gujarat, India
e-mail: vemulaanandreddy@gmail.com

C. H. Solanki
e-mail: chandresh1968@yhoo.co.in

S. Kumar
e-mail: skumar1863@gmail.com

K. R. Reddy
Department of Civil and Materials Engineering, University of Illinois, Chicago, IL 60607, USA
e-mail: kreddy@uic.edu

1 Introduction

Lead contamination is one of the serious environmental problems around the globe and has received increased attention over the years [1, 2]. The sources include mining activities, smelter operations, chemical industries, etc. Heavy metals introduced into the ground from such sources are difficult to treat because of their complex behavior. The remediation of such sites has become a major concern for both engineers and researchers. Although various methods such as phytoremediation, bioremediation, and soil washing are available for the treatment of contaminated sites [3, 4], solidification/stabilization (SS) has received utmost attention due to the ease in construction and cost-effectiveness over years. SS has been considered as the “best demonstrated available technology” (BDAT) to treat toxic contaminants [5–7]. The term stabilization of contaminated soils involves fixing agents chemically, hinder the solubility and mobility of contaminants. Besides, the addition of cement-based additives to the contaminated soils to form a “monolith” is referred to as solidification [8]. Published studies have extensively addressed the treatment of heavy metals using various cement-based materials and have been successfully demonstrated [7, 9–11]. The use of supplementary cementitious materials (SCMs) is gaining attention due to low carbon emissions during their manufacturing process [12–16]. In the present study, the pH, leaching and compressive strength tests were performed to investigate the performance of LC³ stabilized lead-contaminated soils at various curing times. The objective of the study is to investigate: (1) soil pH changes due to LC³ stabilizer; and (2) unconfined compression strength and leaching characteristics of untreated and LC³ stabilized soils.

2 Materials and Methods

The soil used in the study was collected from SVNIT Campus, Surat, India. The basic physicochemical parameters are given in Table 1. The binder limestone calcined clay cement (LC³) at 6% used in the study was procured from technology and action for

Table 1 Basic physicochemical parameters of the soil used in the study

Property	Value
Specific Gravity, G_s	2.67
Untreated soil pH	5.79
Liquid limit (%)	60.6
Plastic limit (%)	28.3
Plasticity index (%)	32.3
Soil classification (%)	CH
Sand (%) (4.75–0.075 mm)	7.3
Silt (%) (0.002–0.075 mm)	22.7
Clay (%) (<0.002 mm)	69.7

rural advancement, TARA, New Delhi, India. The target heavy metal lead Pb^{2+} was used in the study because it is considered as one of the potentially toxic heavy metal commonly found at polluted sites [17, 18]. Lead nitrate $(PbNO_3)_2$ solution at 0.5% and 1.0% solution was used to prepare artificial contaminated soil. Lead nitrate $(PbNO_3)_2$ (Analytical reagent was dissolved in deionized double distilled water for preparing the solutions. The reason for using in nitrate form is that it is inert to hydration [19]. The unconfined compression strength (UCS) tests were conducted on the stabilized lead-contaminated specimens as per ASTM (2008) (ASTM standard D4219) [20] with a controlled strain rate of 1%/min. The pH of the soil was measured using ASTM D4927 [21]. Leaching tests were performed as per the toxicity characteristic leaching procedure TCLP-USEPA method 1311 [22]. The extraction fluid #1 glacial acetic acid (CH_3COOH and NaOH pellets diluted in distilled water) at pH (4.93 ± 0.05) was used.

3 Results and Discussion

3.1 Soil pH

Figure 1 shows the pH variation of untreated soil and LC^3 stabilized soil with curing time. It is evident that the pH of LC^3 stabilized soil increases by 1.33–1.53 units after 7 days of curing when compared to untreated soil at 0 days curing. In addition, the pH values of LC^3 stabilized soil at 28 days curing increases to 9.06 to 8.89 and continues to be constant. The values are consistent with Du et al. [23] using KMP binder. Moreover, the lead concentrations become undetectable when the pH of the soils is between 9 and 11 as discussed by Paria and Yuet [9]. Results are essentially similar to reported studies on cementitious based materials.

3.2 Unconfined Compressive Strength

Figure 2 shows the unconfined compressive strength variation of untreated soil and LC^3 stabilized soil with curing time. The strength improvement was observed to be 466.35 kPa and 401.29 kPa, which is 3.32 and 2.86 times compared to untreated sample at a 7-day curing period. The binder has shown a moderate effect on higher lead concentration i.e. Pb 1.0 (1% Pb conc). For instance, at 28 days curing period the UCS value of Pb 0.5 (0.5% Pb conc) is 744 kPa, Pb 1.0 is 681 kPa. The values are increased to 3.49 and 3.19 times of untreated specimens. This agrees well with Wang et al. [24] using ordinary Portland cement (OPC) and magnesium phosphate cement. The hydration products of LC^3 could provide the bonding strength of the soil particles in filling the pore spaces to form a denser structure that promotes the insoluble compounds [24–26]. Further, the UC strength values tend to be stabilized

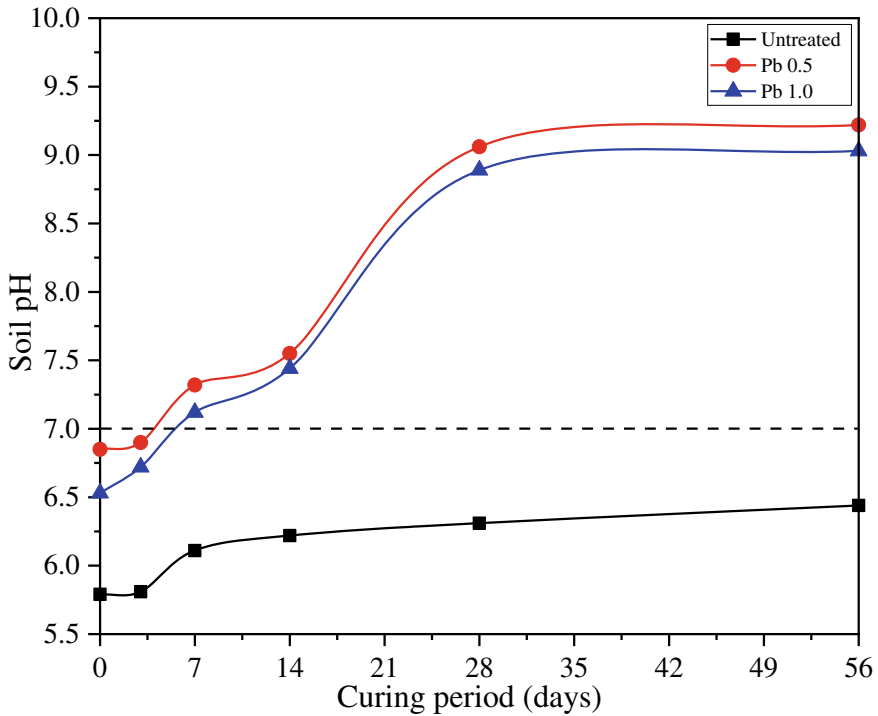


Fig. 1 Soil pH variation with (7, 14, 28, 56 Days) curing times

in the long term at 56 days curing. Overall, the effects of Pb products on the hydration of LC^3 based-SS process were notable.

3.3 Toxicity Characteristic Leaching Procedure Test

Figure 3 shows the leached Pb concentrations of untreated and LC^3 stabilized soils. For the 14 days curing period, Fig. 3. shows that 6% LC^3 content is able to reduce the Pb concentrations to 5 mg/L, which is toxicity characteristic limit specified by Hazardous Waste Management (HWM-2016, India) [27] regulatory limit for disposal of contaminated waste. The results are higher than Wang et al. [24] after 28 days curing compared to ordinary Portland cement (OPC). The incorporation of LC^3 could physically encapsulate the soluble Pb species in forming hydration products as discussed in the earlier Sect. 3.2. The formation of a denser structure during the hydration can immobilize the Pb products to make insoluble compounds thereby reducing the leaching and potential toxicity.

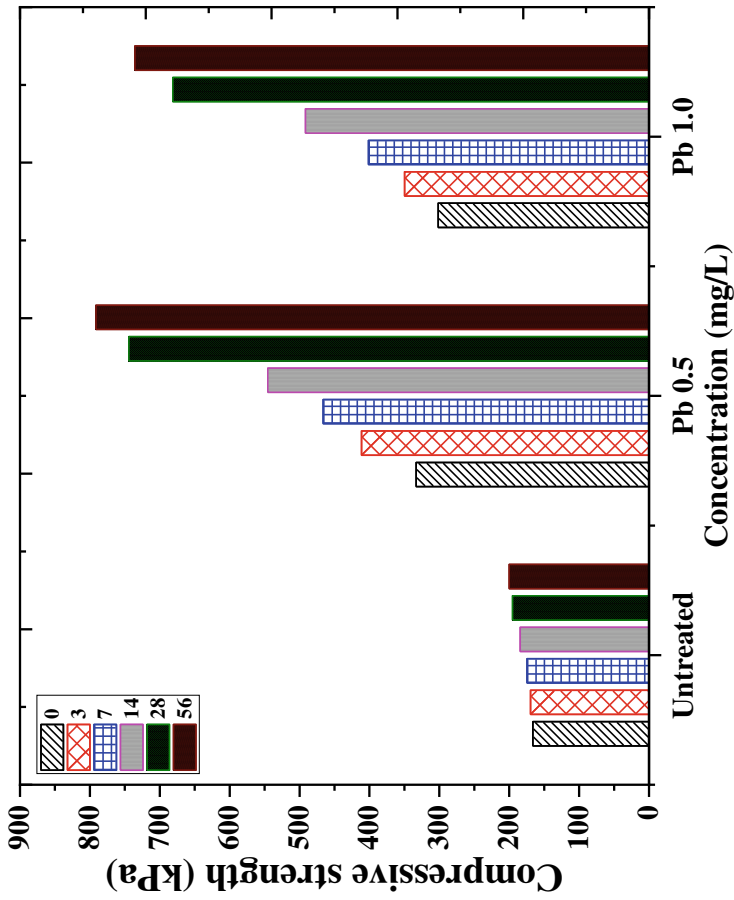


Fig. 2 Variation of compressive strength in untreated and stabilized soil with different curing times

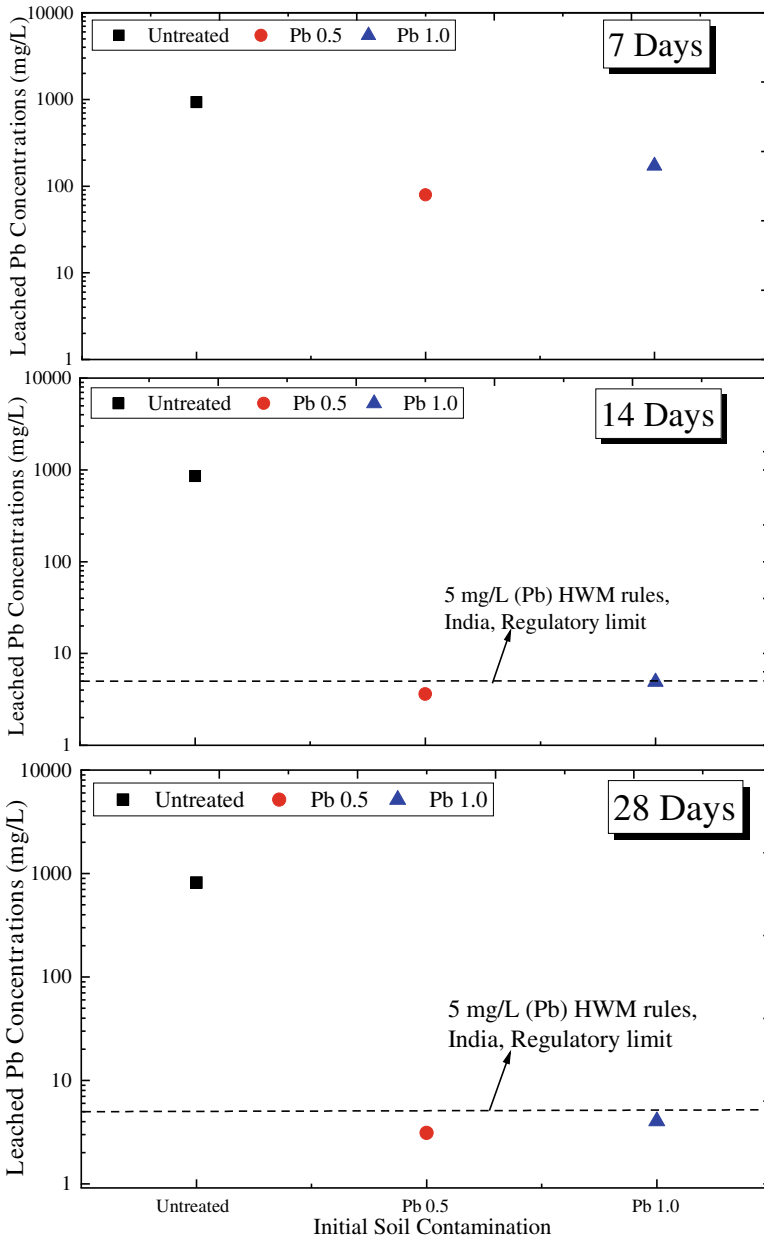


Fig. 3 Leached Pb concentrations in untreated and stabilized soil for 7 and 14 and 28 days curing time

4 Conclusions

Lead-contaminated soils were stabilized using 6% LC³ cement to investigate the response on pH, strength and Pb leaching. The following conclusions were drawn from this study:

- 1 Addition of LC³ content to lead-contaminated soil changes the pH from acidic to alkaline after 7 days curing and then increases marginally over time.
- 2 LC³ cement stabilization can promote early strength within 7 days of curing in filling the pore spaces and improved strength development.
- 3 The leached Pb concentrations were significantly reduced by the addition of LC³ content that is below the TCLP regulatory limit (HWM-2016), India.
- 4 LC³ cement supports the utilization of contaminated materials in forming sustainable engineered materials with reduced environmental risks and potential toxicity.

References

1. Beiyuan J, Tsang DCW, Valix M, Zhang W, Yang X, Sik Y, Li X (2017) Chemosphere selective dissolution followed by EDDS washing of an e-waste contaminated soil : extraction efficiency, fate of residual metals, and impact on soil environment. *Chemosphere* 166:489–496
2. Wang C, Li XC, Ma HT, Qian J, Zhai JB (2006) Distribution of extractable fractions of heavy metals in sludge during the wastewater treatment process. *J Hazard Mater* 137:1277–1283
3. Sharma HD, Reddy KR (2004) *Geoenvironmental engineering: site remediation, waste containment, and emerging waste management technologies*. John Wiley & Sons, Inc.
4. Reddy K, Adams J (2015) *Sustainable remediation of contaminated sites*. Momentum Press
5. Xia WY, Feng YS, Jin F, Zhang LM, Du YJ (2017) Stabilization and solidification of a heavy metal contaminated site soil using a hydroxyapatite based binder. *Constr Build Mater* 156:199–207
6. Singh TS, Pant KK (2006) Solidification/stabilization of arsenic containing solid wastes using portland cement , fly ash and polymeric materials. 131:29–36
7. Wang L, Yu K, Li JS, Tsang DCW, Poon CS, Yoo JC, Baek K, Ding S, Hou D, Dai JG (2018) Low-carbon and low-alkalinity stabilization/solidification of high-Pb contaminated soil. *Chem Eng J* 351:418–427
8. Patel H, Pandey S (2012) Evaluation of physical stability and leachability of Portland Pozzolona Cement (PPC) solidified chemical sludge generated from textile wastewater treatment plants. *J Hazard Mater* 207–208:56–64
9. Paria S, Yuet PK (2006) Solidification–stabilization of organic and inorganic contaminants using portland cement: a literature review. *Environ Rev* 14:217–255
10. Du YJ, Wei ML, Reddy KR, Liu ZP, Jin F (2014) Effect of acid rain pH on leaching behavior of cement stabilized lead-contaminated soil. *J Hazard Mater* 271:131–140
11. Du Y, Jiang N, Liu S, Jin F, Singh DN, Puppala AJ (2014) Engineering properties and microstructural characteristics of cement-stabilized zinc-contaminated kaolin. 302:289–302
12. Bishnoi S, Maity S, Mallik A, Joseph S, Krishnan S (2014) Pilot scale manufacture of limestone calcined clay cement : the Indian experience. *Indian Concr J* 88:22–28
13. Scrivener K, Martirena F, Bishnoi S, Maity S (2017) Calcined clay limestone cements (LC3). *Cem Concr Res.* 1–8 (2017)

14. Juenger MCG, Siddique R (2015) Recent advances in understanding the role of supplementary cementitious materials in concrete. *Cem Concr Res* 78:71–80
15. Hollanders S, Adriaens R, Skibsted J, Cizer Ö, Elsen J (2016) Pozzolanic reactivity of pure calcined clays. *Appl Clay Sci* 132–133:552–560
16. Maraghechi H, Avet F, Wong H, Kamyab H, Scrivener K (2018) Performance of Limestone Calcined Clay Cement (LC3) with various kaolinite contents with respect to chloride transport. *Mater Struct/Materiaux et Constr* 51:1–17
17. Mohmand J, Ali S, Akber M, Eqani S, Fasola M, Alamdar A, Mustafa I, Ali N, Liu L, Peng S, Shen H (2015) Human exposure to toxic metals via contaminated dust : bio-accumulation trends and their potential risk estimation. *Chemosphere* 132:142–151
18. Gatsios E, Hahladakis JN, Gidarakos E (2015) Optimization of electrocoagulation (EC) process for the purification of a real industrial wastewater from toxic metals. *J Environ Manag* 154:117–127
19. Cuisinier O, Le Borgne T, Deneele D, Masroufi F (2011) Quantification of the effects of nitrates, phosphates and chlorides on soil stabilization with lime and cement. *Eng Geol* 117:229–235
20. ASTM standard D4219: Standard test method for unconfined compressive strength index of chemical-grouted soils. American Society for Testing and Materials (ASTM), West Conshohocken, PA, 2008
21. ASTM standard D4972: Standard Test Method for pH of Soils. West Conshohocken, PA, American Society for Testing and Materials, 2001, pp 1–3
22. USEPA Method 1311: Toxicity characteristic leaching procedure (TCLP). United States Environmental Protection Agency (USEPA), Washington, DC
23. Du Y-J, Wei M-L, Reddy KR, Jin F, Wu H-L, Liu Z-B (2014) New phosphate-based binder for stabilization of soils contaminated with heavy metals: leaching, strength and microstructure characterization. *J Environ Manag* 146:179–188
24. Wang YS, Dai JG, Wang L, Tsang DCW, Poon CS (2018) Influence of lead on stabilization/solidification by ordinary Portland cement and magnesium phosphate cement. *Chemosphere* 190:90–96
25. Dhandapani Y, Santhanam M (2017) Assessment of pore structure evolution in the limestone calcined clay cementitious system and its implications for performance. *Cem Concr Compos* 84:36–47
26. Dhandapani Y, Sakthivel T, Santhanam M, Gettu R, Pillai RG (2018) Mechanical properties and durability performance of concretes with Limestone Calcined Clay Cement (LC3). *Cem Concr Res* 107:136–151
27. Government of India (2016) New Delhi: Waste Management Rules. 1981, pp 1–68

A Study on Evaluating the Usefulness and Applicability of Additives for Neutralizing Extremely Alkaline Red Mud Waste



Manas Chandan Mishra, N. Gangadhara Reddy , B. Hanumantha Rao, and Sarat Kumar Das

Abstract The chemico-mineralogical compositions of red mud lead to its abnormal pH (>11), rendering it unusable as a resource material for civil engineering applications. Such extreme alkalinity accentuates the dearth of contriving a solution to ensure the acceptability and reutilization of the waste. Curing period has considerable significance in the context that the previous studies reported reversal of pH of the red mud after neutralization. Thus, efforts are made in the present study to evaluate the usefulness and applicability of a variety of additives for neutralizing the red mud waste. Additives such as lime, ground granulated blast furnace slag, fly ash, gypsum in different proportions, and acids such as nitric acid and hydrochloric acid of varying strengths were employed, aiming at investigating the alkalinity mitigation capacity in the red mud. The results demonstrated a substantial reduction in the alkalinity levels of the red mud immediately after treatment, but the post-neutralization pH results exhibited noteworthy reversal with time. It has also been found that the type of neutralizing additives has considerable influence on the chemistry which in turn might have affected alkalinity levels in the red mud.

Keywords Red mud · Additives · Alkalinity reduction · Neutralization · pH rebound

M. C. Mishra · N. Gangadhara Reddy · B. Hanumantha Rao (✉)
School of Infrastructure, IIT Bhubaneswar, Khordha 752050, Odisha, India
e-mail: bhrao@iitbbs.ac.in

M. C. Mishra
e-mail: mcm10@iitbbs.ac.in

N. Gangadhara Reddy
e-mail: gn11@iitbbs.ac.in

S. Kumar Das
Department of Civil Engineering, IIT (ISM) Dhanbad, Dhanbad 826004, Jharkhand, India
e-mail: saratdas@rediffmail.com

© Springer Nature Switzerland AG 2020

K. R. Reddy et al. (eds.), *Sustainable Environmental Geotechnics*, Lecture Notes in Civil Engineering 89, https://doi.org/10.1007/978-3-030-51350-4_16

1 Introduction

A slurry-based residue is generated along with alumina from bauxite ore by Bayer process. This bauxite residue, also known as red mud (RM), is classified as extreme alkaline waste material primarily due to its pH in excess of 11.5 and high sodic content. A few other associated problems of RM include dispersivity, low compressive strength, a variable degree of compactibility, dusting behavior, and leaching, which undergo changes with variations in pH conditions [1–5]. Of the total RM produced worldwide in a year, the utilization is limited to a bare 2–3% [6]. The utilization of RM has been limited to a few applications in the construction industry [7, 8]. However, it should be noted that resource materials with pH more than 8.5 have been recommended not to be used for civil engineering applications as per Indian Standards [9, 10]. Therefore, it is essential not only to stabilize the RM but also to maintain a lower pH of the waste to render it environmentally benign enough to be utilized as a resource material.

Of late, endeavors [11–15] are made at the reutilization of RM as an adsorbent to retrieve phosphates, fluorides, and heavy metals like arsenic. However, the contributions of such efforts toward the utilization or neutralization of RM at large scale are negligible vis-à-vis its annual production. Furthermore, various attempts have been made over the years at improving the engineering properties of weak soils using different additives, most of which accentuate the material characteristics by cementation, cation exchange, and carbonation processes [16–19]. However, the effect of such treatments on the alkalinity of the material to be treated is not explored in-depth.

It was reported by several studies that various naturally available chemicals and industrial wastes such as lime, gypsum, fly ash (FA), and ground granulated blast furnace slag (GGBS) are effective in stabilizing alkaline wastes like RM to be used as construction resource materials [3, 20–23]. Red mud has also been reported as an excellent neutralizing agent for wastewater and recovering oxides from acidic media [24]. It is, however, pertinent to note that no study has explored in detail the comparative efficacy of these additives for the reduction of RM alkalinity: thereby providing an opportunity to explore the competence of these additives as neutralizing agents for the RM.

To cap it all, it can be stated based on the available literature that the effectiveness of strong organic acids and traditional stabilizing agents such as lime and gypsum, and industrial wastes such as GGBS and FA has not been investigated in detail with respect to the neutralization of RM. Moreover, the effect of curing time on various methods of neutralization of the alkaline waste still remains unexamined. With this in mind, efforts are taken in this study to analyze the performance of various additives, such as nitric acid (HNO_3), hydrochloric acid (HCl), lime, ground granulated blast furnace slag (GGBS), gypsum, and fly ash (FA) on the neutralization of RM over different curing periods. The main objectives of this study are two-fold: it targets providing an effective alternative for neutralization of the waste, and it also focusses on discerning the efficacy of implemented additives in maintaining the pH after treatment. In addition to that, endeavors are also made in developing a lucid

understanding of the chemistry behind the high pH of the RM and its reduction. The results of this study bring out an efficient and practical alternative toward the reduction of the extreme alkalinity levels of RM, so as to encourage more research into developing reutilization alternatives of the same in various geotechnical engineering applications.

2 Materials and Testing Methodology

Disturbed samples of the RM were collected from a disposal pond of M/s. Vedanta Aluminium Limited situated at Lanjigarh in Kalahandi, Odisha, for detailed experimental investigations. The samples were collected from the disposal site in the moist state and were subjected to oven drying before experimentation, wherever deemed necessary. Basic characterization of the RM samples was done by laboratory-based experimental studies according to various code provisions as per American Society for Testing and Materials (ASTM) standards. The RM sample was classified as a silt of low plasticity (ML). It was found that the majority of particles are in the range of silt size (56%), in addition to particles in the range of clay size (26%) and sand size (18%). Liquid limit, w_L , and plasticity index, w_{PI} , was measured as 40% and 11%, respectively. The grain size distribution and Atterberg's limits results were used to classify the soil according to the Unified Soil Classification System (USCS) [25]. The specific gravity and pH of the RM samples were found to be 3.09 and 12.5, respectively. X-ray fluorescence (XRF) analysis was performed to obtain the chemical compositions of the waste. It was found that Fe_2O_3 is the major constituent (39.89%), followed by 22.72%, 13.43%, 10.17%, 6.48%, and 4.06% of Al_2O_3 , SiO_2 , TiO_2 , Na_2O , and CaO , respectively.

Nitric acid (HNO_3) and hydrochloric acid (HCl) are used in this study to neutralize and reduce the alkalinity of RM. The effect of the inorganic acids is also studied by preparing acid solutions of molarity varying from 1 to 3 pH from commercially available aqueous solutions of HNO_3 and HCl at designated assays. The pH of prepared solutions is cross-checked before further experimentation.

In this study, quicklime was used to treat the RM in an effort to reduce its pH. Quicklime was preferred over hydrated lime for stabilization as it has been observed in previous studies [26] that the strength gain is higher and faster for quicklime than for hydrated lime; however, it is also to be accounted for that quicklime requires higher moisture content during curing than hydrated lime. Commercial grade lime was procured from the local market to investigate the effect of lime treatment on the strength parameters of RM. Ground Granulated Blast Furnace Slag (GGBS) used in the study was procured from M/s. Counto Microfine Products Pvt. Ltd., Panaji, Goa, India. The pH of the GGBS used in this study was measured as 8.32. Commercially available gypsum ($CaSO_4 \cdot 2H_2O$) was used to evaluate the efficacy of the additive as a neutralizing agent. Fly ash (FA) used as an additive for alkalinity reduction treatment was collected from the fly ash ponds of M/s. Vedanta Power Plant, Lanjigarh, Odisha.

3 Testing Methodology

A mixture of untreated or treated RM and deionized water (weight ratio 1:1) was stirred constantly for 4 h, filtered through 0.2 microns, and then the filtrate was used as the sample for pH measurement using glass electrodes [27]. A standard calibrated pH meter Systronics 335 was used for measurement purposes. Samples were put in 100 mL high borosil beakers in a controlled environment where the temperature was maintained at 20 °C. Tests were run with samples of RM alone, RM mixed with various proportions of HNO₃, HCl, lime, GGBS, gypsum, and FA. The pH meter was calibrated before experimentation with pH buffer solutions of 4, 7, and 9.1.

4 Results

Red mud is a highly alkaline waste material, thereby requiring reduction of pH in order for qualifying it suitable as a material for geotechnical applications or for agricultural purposes. Acid neutralization technique was chosen for reducing RM alkalinity based on the available literature [28]. A variety of acids can be used to neutralize highly alkaline soils and waste materials, which are exhibiting pH as high as above 12. Table 1 shows the pH values of all samples treated with inorganic acids such as HNO₃ and HCl. In general, it is known that HNO₃ and HCl are strong acids and are considered as good neutralizing agents as they completely dissociate into H⁺ ions, thereby facilitate higher and faster reaction with available alkalinity. Therefore, these inorganic acids were used in this study at various molar concentrations to reduce RM alkalinity. It can be observed that treatment with 0.1, 0.03, 0.01, 0.001, and 0.0001 M HCl led to decrease in pH to 6.59, 8.20, 9.73, 10.48, and 10.52, respectively, from the extortionate initial pH of >11. As per the guidelines of [14, 15], the results obtained on the 0th day with an HCl molarity of 0.01 M onwards, qualify the RM to be used as resource material for geotechnical purposes. However, the pH rebound in 7 days was as high as 8.16 and 9.86 after an immediate substantial plunge on the addition of 0.1 and 0.01 M HCl solution, respectively.

On a similar note, the addition of HNO₃ also drastically lowered the pH to 7.54, 8.39, 9.91, and 10.62, respectively, for molarity of 0.1, 0.03, 0.01, and 0.001 from the initial greater value of 11 on the 0th day. Nevertheless, the rebound in pH for HNO₃ also seemed prominent but observed to be comparatively slower than that of HCl. An acceptable pH was maintained after the addition of 0.1 M HNO₃ up to 28 days. However, the pH of RM should be maintained at a required level for a practical duration of 6–12 months in order to render acceptability to the waste as a viable geomaterial for engineering purposes, such as in pavement constructions. Thus, it may be interpreted that the efficiency of HCl and HNO₃ as neutralizing agents for RM is acceptable. On the other hand, they may not be recommended as their efficacy to sustain the reversal of alkalinity after treatment is failed.

Table 1 Measured pH of red mud samples neutralized using varying combinations of gypsum and acids at different curing periods

Additive	Proportion	pH at different curing periods					
		0	7	28	45	90	180
Gypsum (G) alone	RM + 1% G	10.08	10.28	10.52			
	RM + 2% G	9.80	9.85	9.91	9.97	10.09	
	RM + 4% G	8.68	8.88	9.01	8.82	8.63	
	RM + 6% G	8.16	8.22	8.29	8.37	8.51	
	RM + 8% G	8.12	8.37	8.16	8.29	8.42	
	RM + 10% G	8.23	8.34	8.15	8.33	8.47	
	RM + 12% G	8.31	8.41	8.48	8.52	8.59	
HNO ₃	RM + pH 1 HNO ₃	7.54	8.11	8.42	8.83	9.12	9.78
	RM + pH 1.5 HNO ₃	8.39	8.69	9.98	10.19	10.56	10.72
	RM + pH 2 HNO ₃	9.91	10.11	10.79	11.01		
	RM + pH 3 HNO ₃	10.62	10.71	10.93	11.35		
HCl	RM + pH 1 HCl	6.59	8.16				
	RM + pH 1.5 HCl	8.20	9.86				
	RM + pH 2 HCl	9.73	10.44				
	RM + pH 3 HCl	10.48	10.90				
	RM + pH 4 HCl	10.52					

Lime, also found to have high alkalinity, has always been considered as an excellent stabilizing agent making it a viable alternative for the improvement of RM engineering properties. Thus, it is obvious to interpret that its addition may not fetch the advantage of pH neutralization. Table 2 shows the pH of samples treated with lime alone in various combinations. It can be observed that the alkalinity of lime alone treated samples on the 0th day were beyond the acceptable limits in accordance with IRC guideline. It was thus deemed inessential to further explore the effect of lime alone on the pH of RM for higher curing periods. An increase in lime content provides a basic medium after treatment. It was evident from Table 2 that lime treatment caused a rise in pH of treated RM vis-à-vis with that of raw one in the presence of water. These results substantiated the reason behind combining lime treatment with some neutralizing agent so that the stabilized RM can be rendered suitable enough to be accepted for diverse engineering applications.

Table 2 Measured pH of red mud samples neutralized using varying combinations of lime, gypsum plus fly ash, and GGBS immediately after treatment

Additive proportions	0 th day pH	Additive proportions	0 th day pH
RM + 0% Lime	12.47	RM 95% + 5% GGBS	12.02
RM + 0.5% Lime	11.90	RM 90% + 10% GGBS	11.77
RM + 1% Lime	12.44	RM 85% + 15% GGBS	11.23
RM + 2% Lime	12.69	RM 80% + 20% GGBS	10.38
RM + 5% Lime	12.95	RM 75% + 25% GGBS	9.65
85% RM + 15% FA + 4% G	10.52	70% RM + 30% FA + 4% G	10.73
85% RM + 15% FA + 6% G	10.65	70% RM + 30% FA + 6% G	10.84
85% RM + 15% FA + 8% G	10.53	70% RM + 30% FA + 8% G	10.72
85% RM + 15% FA + 10% G	10.54	70% RM + 30% FA + 10% G	10.64
80% RM + 20% FA + 4% G	10.75	65% RM + 35% FA + 4% G	10.28
80% RM + 20% FA + 6% G	10.62	65% RM + 35% FA + 6% G	10.35
80% RM + 20% FA + 8% G	10.64	65% RM + 35% FA + 8% G	10.47
80% RM + 20% FA + 10% G	10.70	65% RM + 35% FA + 10% G	10.58
75% RM + 25% FA + 4% G	10.81	60% RM + 40% FA + 4% G	10.44
75% RM + 25% FA + 6% G	10.78	60% RM + 40% FA + 6% G	10.51
75% RM + 25% FA + 8% G	10.62	60% RM + 40% FA + 8% G	10.53
75% RM + 25% FA + 10% G	10.64	60% RM + 40% FA + 10% G	11.00

The results of pH changes in RM due to the addition of the industrial waste FA and naturally available chemical gypsum in various proportions are also presented in Table 2. The addition of gypsum alone (refer to Table 1) does not bring out any reassuring improvements at lower contents up to 2%. However, on further increments of gypsum, reasonable curtailment in RM pH is visible. The pH measured after 45 days of treatment with 6, 8, 10, and 12% gypsum content were 8.37, 8.29, 8.33, and 8.52, respectively, which fall in the acceptable range of pH for resource materials

in pavement constructions recommended by IRC. Be that as it may, the replacement of RM with FA with the addition of gypsum was not found to have any promising outcome in terms of neutralization. It is clearly observed from Table 2 that the post-treatment pH values for the same were well above 10 units. As such, this marginal reduction from the pH of raw RM does not endorse the combination as an acceptable alternative. A similar outcome was observed for the treatment of RM with GGBS as an additive. The alkaline industrial waste, RM was supplanted with GGBS at different proportions with the contents of the latter varying from 5 to 25%. There was an insignificant reduction in pH (12.5–12.02) of raw RM for the replacement of 5% GGBS. However, the maximum reduction to 9.65 units was observed for the highest GGBS content of 25%. Nonetheless, the amelioration of RM alkalinity using GGBS as an additive was not found to be an acceptable alternative.

5 Discussion

It is evident from Table 1 that the neutralization of RM using HCl yields a better result than those by its inorganic counterpart. It is to be noted that the reduction in pH immediately after treatment with the acids is higher for HCl. However, it is worrisome that the rebound in RM alkalinity is also higher for HCl than for HNO₃. It is well known that iron oxidizes in acidic media gets converted to a more soluble form. Thus, it is safe to infer that the oxidation of available iron in RM plays an important role in the immediate pH reduction. It is reported in previous studies [29] that the dissolution rate of iron is higher for HCl than that for HNO₃. This might be a reason for the faster and greater reduction in RM alkalinity upon treatment with HCl. While comparing the neutralization results for nitric acid and hydrochloric acid from Table 1, it is clearly observed that the latter serves as a better neutralizing agent for RM than the former. This might be due to a simple reason of higher ability of the latter to release H⁺ ions, thereby allowing higher reaction rates. The dissociation constant of HCl is around 10⁵ times more than that of HNO₃, making it a considerably stronger acid. The same can be observed from the efficacy of pH reduction for corresponding acids upon being used as the neutralizing agent. This might be a dominant factor contributing toward the variation in pH reduction for these additives.

Table 2 shows the measured pH of gypsum and FA together treated RM samples. It is clear from the results that the availability of moisture in RM and its high alkalinity might be triggering the dissociation of gypsum allowing the sulfates available for further reactions. This might have led to the formation of sulphuric acid in the RM samples treated with gypsum, thereby aiding in the reduction of its alkalinity. However, the variation in the efficacy of gypsum with different proportions of replaced FA suggests the role of FA in affecting the neutralization mechanism. But, it can also be said that the replacement of FA up to 35% might reduce the overall alkalinity of the mixture without compromising the availability of readily available ions which can thus be utilized for neutralizing the RM by the sulphuric acid produced on dissociation of gypsum.

The results of pH change in RM with the addition of GGBS are presented in Table 2. It is interesting to observe that replacing RM with increasing proportions of GGBS has an abating effect on the pH of the alkaline waste. However, on closer scrutiny, it can be deduced that the reduction in GGBS treated RM samples might be due to the replacement with substantial proportions of lower pH material, i.e. GGBS, as the pH measurement of GGBS yielded a value of 8.32. It is to be noted that GGBS is a pozzolan showing affinity to undergo hydration reactions in the presence of water, which increases the pH of the mixture due to the formation of cementitious products, as is commonly found with the hydration of cement. This might further increase the pH of RM + GGBS mixture up to 28 days or more depending on the time required for the completion of pozzolanic hydration reactions. Thus, the addition of GGBS alone does not pose as a prudent solution toward RM treatment as it cannot address the alkalinity related issues of the waste. However, when combined with an appropriate neutralizing agent, GGBS might prove as an expedient alternative for remediation of RM.

Moreover, it can also be observed from Table 1 that there is a significant increase in pH with an increase in the curing period of 0–90/180 days across all the additives. This increase in alkalinity with time might possibly be triggered by the gradual release of Na^+ ions in RM after treatment. The availability of fewer free cations might be the reason for lower rates of cation exchange and flocculation in the stabilization of RM effecting negligible immediate improvement. The effect of curing may be envisaged by considering RM as a pozzolan, as reported by [30] which forms cementitious gels leading to the formation of hydrates upon its reaction with calcium and alumina in the presence of water, while the abundantly available Na^+ ions might not be participating in the reactions. Moreover, the gradual release of Na^+ ions might be a distinct contributor towards pH rebound post-neutralization. The initial reduction in alkalinity may be attributed to the immediate reaction of additives with freely available ions. However, this is considerably less as compared to the long-term pH reduction exhibited after 90 days, which might be caused by the release and availability of Na^+ ions along with the reaction with aluminates and silicates present in RM. It is further seen from Table 1 that there is a sudden drop in the pH of RM samples after adding various acids. This may be attributed to the acidic and basic media provided by acids and RM, respectively, which can be validated by a reduction in pH with an increase in acid concentration.

On the basis of the results presented in this study, it can be understood that strong acids such as HNO_3 and HCl present excellent alternatives as neutralizing agents for RM. Nonetheless, it is essential to remember that these additives could reduce the alkalinity but were found incapable of inhibiting the pH reversal of RM. These chemical additives can thus be recommended as neutralizing agents of RM for various applications where reduced pH levels are required to be maintained up to 28 days. However, the limitations of these additives are handling and storage of such strong reagents at site conditions, which once taken care of, provide a remarkable alternative. In addition, additives such as lime, FA, and GGBS might be considered as an admixture to address problems associated with RM only when combined with other additives which can bring down the extreme alkalinity of the industrial waste.

These may not be used as standalone treating agents for neutralization purpose of RM. Gypsum can be endorsed to be used as an RM neutralizing agent within a range of 4–12%. In this study, results of gypsum addition present acceptable results up to 45 days, making it a viable additive for applications where the RM alkalinity is to be curtailed and maintained below 8.5 for 1–2 months. However, the chemical composition of RM is complicated, consisting of various dominant oxides. Therefore, further chemical, elemental and mineralogical investigations are required for strong recommendations of any of these additives as harmful byproducts such as chlorides, nitrates or sulfates might be formed beyond acceptable limits due to the reactions of RM with HCl, HNO₃ and gypsum.

6 Concluding Remarks

In the present study, the usefulness and applicability of various additives for reducing the alkalinity with simultaneously neutralizing capability of the red mud was investigated in a comprehensive way. The changes in pH were monitored up to six months after treating with the additives. The various results presented in the paper demonstrate a fact that treating the red mud for pH reduction can assume practical significance and treated RM can be considered as potential resource material for geotechnical engineering applications. The following salient conclusions are drawn based on the results of the study:

- Application of chemical additives proved effective in reducing the pH of the RM substantially, but failed to maintain the post-treatment pH at desired levels as required by code provisions. A significant reversal in the RM alkalinity is observed with an increase in post-neutralization time beyond one month.
- The addition of lime proved to exhibiting a nil effect in the alkalinity of the RM. On the contrary, lime treatment yielded adverse results. However, replacing red mud with increasing proportions of GGBS showed a considerable reduction in its pH with a value of 9.65 achieved with a replacement of 25%.
- Gypsum, when used as an additive, was found to demonstrate better neutralizing efficacy than being used along with the replacement of red mud with FA. An addition of 8% gypsum alone exhibited the maximum reduction in alkalinity leading to a pH of 8.12 immediately after treatment, which was found to have regained to 8.42 after 90 days. The optimal combination was found to be 4% gypsum with 65% RM + 35% FA, which yielded a pH of 10.28.
- Among the acid solutions used in this study, 0.1 M HCl and 0.1 M HNO₃ alone treatments exhibited an abridged pH of 6.59 and 7.54, respectively.

Further extensive elemental, mineralogical and morphological investigations are recommended for the better knowledge of the factors affecting the neutralization mechanism of red mud in order to arrive at a more lucid understanding as to ascertain the efficiency of different additives and physical treatments used in this study.

References

1. Nikraz HR, Bodley AJ, Cooling DJ, Kong PY, Soomro M (2007) Comparison of physical properties between treated and untreated bauxite residue mud. *J Mater Civ Eng* 19(1):2–9
2. Gräfe M, Power G, Klauber C (2011) Bauxite residue issues: III Alkalinity and associated chemistry. *Hydrometallurgy* 108(1–2):60–79
3. Reddy NG, Rao BH (2016) Evaluation of the compaction characteristics of untreated and treated red mud. *GSP, ASCE* 272:23–32
4. Reddy NG, Rao BH (2017) Assessment of dispersion characteristics of red mud waste from physical tests. In: *Indian geotechnical conference-2017, Theme 5, Article 546*, p. 4, 14–16 Dec 2017, IIT Guwahati, India
5. Reddy NG, Rao BH, Reddy KR (2018) Biopolymer treatment for mitigating dispersive characteristics of red mud waste. *Geotech Lett* 8(3):201–207
6. Sutar H, Mishra SC, Sahoo SK, Chakraverty AP, Maharana HS (2014) Progress of red mud utilization: an overview. *Am Chem Sci J* 4(3):255–279
7. Pontikes Y, Angelopoulos GN (2013) Bauxite residue in cement and cementitious applications: current status and a possible way forward. *Resour Conserv Recycl* 73:53–63
8. Reddy NG, Rao BH, Reddy KR (2018) Chemical analysis procedures for determining the dispersion behavior of red mud waste. In: *Proceedings of international conference on environmental geotechnology, recycled waste materials and sustainable engineering (EGRWSE-2018)*, organized by Department of Civil Engineering, NIT Jalandhar, India, 29–31 March 2018
9. IRC (Indian Road Congress) SP 20-2001a: Rural roads manual. IRC, New Delhi, India (2001)
10. IRC (Indian Road Congress) SP 58-2001b: Guidelines for use of fly ash in road embankment. IRC, New Delhi, India (2001)
11. Genç-Fuhrman H, Tjell JC (2003) Effect of phosphate, silicate, sulfate and bicarbonate on arsenate removal using activated seawater neutralized red mud (Bauxsol). *J Phys IV*(107):537–540
12. Shen F, Chen X, Gao P, Chen G (2003) Electrochemical removal of fluoride ions from industrial wastewater. *Chem Eng Sci* 58(3–6):987–993
13. Liu CJ, Li YZ, Luan ZK, Chen ZY, Zhang ZG, Jia ZP (2007) Adsorption removal of phosphate from aqueous solution by active red mud. *J Environ Sci* 19(10):1166–1170
14. Bhatnagar A, Kumar E, Sillanpää M (2011) Fluoride removal from water by adsorption—A review. *Chem Eng J* 171(3):811–840
15. Zhao Y, Yue Q, Li Q, Xu X, Yang Z, Wang X, Gao B, Yu H (2012) Characterization of red mud granular adsorbent (RMGA) and its performance on phosphate removal from aqueous solution. *Chem Eng J* 193:161–168
16. Eades JL, Grim RE (1960) Reaction of hydrated lime with pure clay minerals in soil stabilization. *Highw Res Board Bull* 262:51–63
17. Diamond S, Kinter EB (1965) Mechanisms of soil-lime stabilization. *Highway Res Rec* 92:83–102
18. Arman A, Munfakh GA (1970) Stabilization of organic soils with lime. Bulletin No. 103, Baton Rouge, Division of Engineering Research (LSU)
19. Jacobson JR, Filz GM, Mitchell JK (2003) Factors affecting strength gain in lime-cement columns and development of a laboratory testing procedure. Report No. VTRC 03-CR16, Virginia Transportation Research Council, Charlottesville, VA
20. Chen H, Wang Q (2006) The behaviour of organic matter in the process of soft soil stabilization using cement. *Bull Eng Geol Env* 65(4):445–448
21. Burke IT, Peacock CL, Lockwood CL, Stewart DI, Mortimer RJ, Ward MB, Renforth P, Gruiz K, Mayes WM (2013) Behavior of aluminum, arsenic, and vanadium during the neutralization of red mud leachate by HCl, gypsum, or seawater. *Environ Sci Technol* 47(12):6527–6535
22. Nagaraj HB, Sravan MV, Arun TG, Jagadish KS (2014) Role of lime with cement in long-term strength of compressed stabilized earth blocks. *Int J Sustain Built Environ* 3(1):54–61
23. Reddy NG, Rao BH (2018) Compaction and consolidation behaviour of untreated and treated waste of Indian red mud. *Geotech Res* 5(2):106–121

24. Cengeloglu Y, Tor A, Ersoz M, Arslan G (2006) Removal of nitrate from aqueous phase by using red mud. *Sep Purif Technol* 51:374–378
25. ASTM D2487–11: Standard practice for classification of soils for engineering purposes (unified soil classification system). Annual Book of ASTM Standard, ASTM International, 04–08, West Conshohocken, PA (2011)
26. Ahnberg H, Bengtsson PE, Holm G (1989) Prediction of strength of lime columns. In: Proceedings of 12th international conference on soil mechanics and foundation engineering, vol. 2. Rio de Janeiro, pp 1327–1330
27. ASTM D4972–13: Standard test methods for pH of soils. Annual Book of ASTM Standards. ASTM International, West Conshohocken, PA (2013)
28. Sahu RC, Patel RK, Ray BC (2010) Neutralization of red mud using CO₂ sequestration cycle. *J Hazard Mater* 179(1–3):28–34
29. Borra CR, Pontikes Y, Binnemans K, Gerven TV (2015) Leaching of rare earths from bauxite residue (red mud). *Miner Eng* 76:20–27
30. Ribeiro DV, Labrincha JA, Morelli MR (2011) Potential use of natural red mud as pozzolan for Portland cement. *Mater Res* 14(1):60–66

Contribution to the Remediation of Saline Soils by Electrokinetic Process: Experimental Study



Faiza Klouche, Karim Bendani, Ahmed Benamar, Hanifi Missoum, Mustapha Maliki, and Laila Mesrar

Abstract Salinization affects ecosystem biodiversity, human health, agricultural productivity, as well as engineering and construction infrastructure. In Algeria, many arid, semi-arid, and near-coastal areas are suffering from soil salinization for more than two decades. In order to restore contaminated soils (saline), the electrokinetic process was tested in laboratory to study the mobility, migration, and elimination of ions (salts) in the soils of two regions of Mostaganem and Relizane (north-west of Algeria). The electrokinetic method is one of the most promising fine-grained soil decontamination processes. In this work, the variation of the electric current, the electro-osmotic flow, the pH, and the rate of elimination of the cations, such as sodium and calcium according to the treatment duration, were determined. According to the results obtained, the electrokinetic treatment proves to be a new technique used successfully, reliably, and inexpensively. It allows the remediation and restoration of fine-grained soils affected by salts. Our research demonstrates the economic and environmental value and the efficiency of electrokinetic technology, which is an innovative process. It deals very effectively with the depollution and remediation of saline soils and helps to inhibit the scourge of soil salinization and environmental pollution.

Keywords Saline soils · Electrokinetic · Remediation · Removal efficiency

F. Klouche (✉) · K. Bendani · H. Missoum · M. Maliki
Faculty of Sciences and Technology, Civil Engineering and Architecture Department, University Abdelhamid Ibn Badis of Mostaganem, 27000 Mostaganem, Algeria
e-mail: faiza.klouche@univ-mosta.dz

Construction, Transport and Protection of Environment Laboratory (LCTPE), Mostaganem, Algeria

A. Benamar · L. Mesrar
LOMC Laboratory, UMR 6294, CNRS-University of Le Havre Normandy, Le Havre, France

1 Introduction

Soil is a heterogeneous assemblage of particles with very different properties. It is a living resource for agricultural productivity and human activities.

Soil salinization continues to be a scourge of land degradation globally. The rate of soils affected by salinity in Algeria is of the order of 3.2 million hectares, particularly in arid and semi-arid zones. Soil salinization can be caused by several environmental factors, such as marine intrusion, deposition of marine salts carried by winds, or by inadequate human intervention (inadequate drainage, excessive irrigation with salt water). During recent two decades, contaminated (saline) land has become an area of increasing importance for the geotechnical and agricultural fields. Recently in Algeria, an extensive construction program has been planned in several parts of the country, while saline agricultural lands will be converted to receive infrastructure for future use.

Extreme concentration of ionic species, such as cations (sodium, potassium, and calcium), and anions, (chloride, sulfate, and nitrate), result in an increase of osmotic pressure, leading to a significant deterioration of the soil surface affecting as a result, on the civil engineering infrastructure and productivity of farmland [1, 2] Currently, geo-environment specialists are facing challenges related to the improvement of natural soils for the protection of the environment. In this context, it should be emphasized that the evaluation and control of the geo-environmental impact of saline soils in Algeria could guarantee better management and better elimination of pollutants, with a focus on development mechanisms adequate.

Several researches have been conducted on the remediation of contaminated soils, developing several processes, such as solidification, excavation, thermal desorption, and biological treatment, in order to remediate and restore such soils.

Nevertheless, many of these soil remediation methods have not been followed up in depth, since most of them remain inadequate, too expensive, and inefficient, especially for fine-grained soils because of their low permeability and mineralogical complexity.

Innovative and inexpensive EK technology has become an alternative method to conventional soil improvement methods, which involves electrochemical stabilization by electro-osmosis of fine-grained soils. This process was chosen in our research because it is easy to install, quick to use and can be used in the laboratory and in situ.

This new method of EK treatment has now begun to be used in several countries for stabilization and remediation of soils in general and fine sediments in particular [3–9].

Electrokinetic technology, inserted as part of the sustainable development strategy, combines social and economic progress with the protection and improvement of the environment.

The principles of electrokinetics involve the application of a low direct current (DC) or a low potential gradient to the electrodes inserted into fine and low permeability soils. These soils have specific mineralogical properties and are therefore electrically and chemically active. When a continuous electrical potential is applied

to the sample, it activates the migration of electrical charges, pore fluid, ions, and fine particles through the soil-liquid medium to the opposite charged electrodes, thereby creating chemical combined effects, hydraulic and electric processes [10].

The electrochemical process depends on several parameters, such as the concentration and mobility of ions, the potential voltage, and the viscosity of pore water.

In recent years, many researchers have been interested in EK through the implementation of several successful applications [11–18]. For example, the technology of electro-osmosis has been used for several decades to remove water from clay and loam soils and to clean poorly permeable saline soils [19].

In this paper, the physicochemical characteristics of two local soils in the study areas of Ain Nouissy -Mostaganem and Hmadna - Relizane, Algeria, in particular pH variations, electro-osmotic flow, and ion mobility such as that sodium (Na^+) and calcium (Ca^{2+}) are studied and analyzed in the LCTPE research laboratory of the University of Mostaganem. The objective of this research is to study the efficiency and performance of the EK method to accelerate the treatment process and the effective remediation of fine saline soils.

2 Materials and Methods

2.1 Material Sampling

The first study area is located in northwestern Algeria, in the lower valleys of west Mostaganem, and more particularly in the region of Ain Nouissy, whose area is 680 Km^2 . As for the second zone, it is also located in north-west of Algeria, precisely Hmadna in the region of Relizane. The salinity problems of these two soils have worsened over the last twenty years, due to low rainfall rates that have led to an accumulation of salts at the surface of the soil at an alarming rate. Samples from both soils were collected at a depth of approximately 0.5–1 m. The soil masses were contained in plastic bags and transported to the laboratory where they were air-dried and ground into a fine powder for analysis.

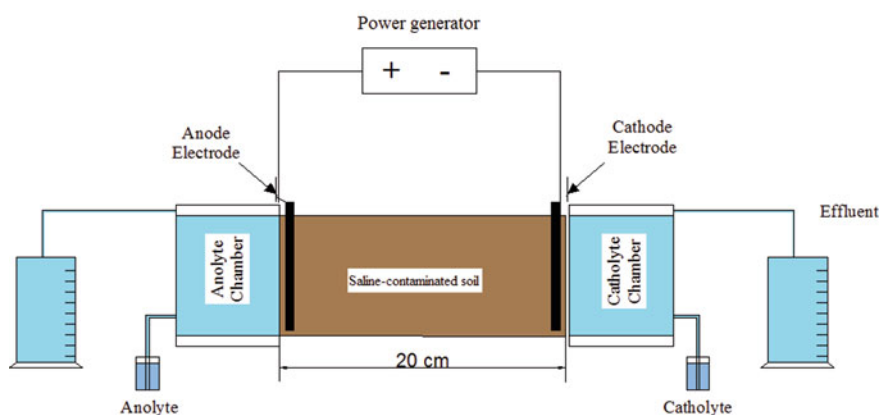
Table 1 shows the physicochemical properties of the two saline soils studied.

2.2 Experimental Cell

The electrokinetic experiments were conducted in a parallelepiped shaped cell with glass walls of 8 mm thick and whose dimensions are as follows: length 30 cm; width 10 cm, and height 10 cm, comprising three compartments: anode, sample cell floor, and cathode (Fig. 1). The tanks are made of glass because the latter is relatively, chemically, and electrically neutral, in order to minimize the ground reactions. The

Table 1 Physicochemical properties of used material

Soil properties	Ain Nouissy	Hmadna
pH	15	7.49
EC (dS/cm)	8.5	11.09
<i>Particle size analysis (%)</i>		
Clay (%)	30	6
Silt (%)	62	78
Sand (%)	8	16
Organic content (%)	1.7	16.66
<i>Initial soluble concentration (mg/kg)</i>		
Na ⁺	1917.2	905.2
Ca ²⁺	1165	1421.6

**Fig. 1** Schematic draw of the electrokinetic test apparatus

two electrodes compartments of the anode and cathode contain an outlet, allowing the flow of electro-osmotic flow (amount of water collected in a graduated tank cylinder). The walls separating the compartments are perforated grids wrapped in geosynthetic material. Filter papers [Whatman No. 4] are placed against the grids separating the soil from the anode and cathode compartments, to prevent the movement of the fine particles from the soil toward these compartments (anode and cathode chambers). Soil samples were continuously fed with distilled water through the anode, using a pipe connected to an external tank to facilitate electro-osmotic flow.

2.3 Test Procedure

A mass of 2600 g each of the two soils was mixed with deionized water for each test, to obtain a water content of 5% above the liquid limit. The material is mixed for one hour, until a homogeneous and smooth paste is obtained, then placed in the central reservoir of the experimental cell in three successive compacted layers at a density of 1300 kN/m^3 , in order to completely eliminate the air bubbles formed during installation. Then, two perforated cylindrical copper tubes were inserted into the cell 2 cm from the ends of the transverse walls to serve as electrodes. The experiments were carried out under a voltage gradient of 1.5 V/cm. Different successive tests of duration of 5, 8, 10, and 15 days were carried out for the two soils to measure the different parameters, such as: the intensity of the electric current, the electro-osmotic flow, the pH, the CE, as well as the elimination of ions.

Also, the electro-osmotic flow contained in the cathode compartment was collected in graduated test tubes and measured daily. Under a constant voltage gradient, current intensity was measured at regular time intervals.

At the end of each test, the soil compartment was cut into equal sections from the anode at 4, 8, 12, and 16 cm and then analyzed. After the required electrochemical treatment period, samples from each of the two soils were taken from different sections to analyze their chemical and physical properties. pH and EC were determined using a Hach sension 156 pH/conductivity/dissolved oxygen multi-parameter digital apparatus. The flame spectrophotometer equipment was used to analyze the cations.

3 Results and Discussion

3.1 Variation of Current Intensity

The EK process involves the application of a potential gradient in the soil matrix. This imposed electric field, leads to the movement and migration of ionic species in the soil, which induces changes in electrical intensity. Figure 2 shows the variation of the intensity of the electric current with the treatment time for both each of the two studied soils. The current gradually increased at the beginning of the experiments because the electro-osmotic flow passed through the soil and increased the dissolution of the salts in the interstitial water. Over time, the current flowing through the soils decreased, falling to less than 10 mA in the test period of about 10–15 days. The current distribution is influenced by the concentration of soluble salt ions in the interstitial water. The large initial values are due to the solubilization of the salts contained in the soil, which also leads to an increase of the EC, which is in agreement with the work of Gray et al. [20]. Therefore, soil pH plays an important role in the variation of electrical intensity. The highly alkaline medium, in the cathodic zones,

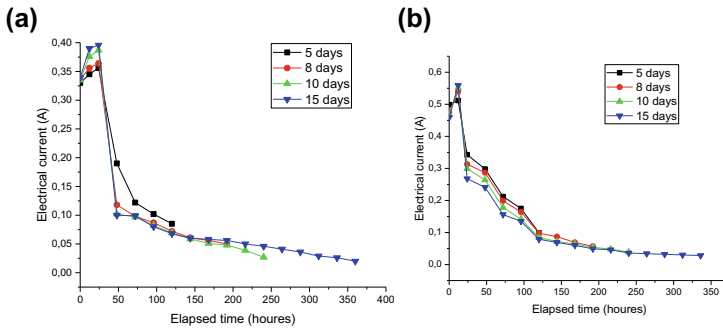


Fig. 2 Variation of electric current intensity with time, **a** Ain Nouissy and **b** Hmadna

causes the precipitation of ionic compounds in the soils, thus leading to a decrease of the current intensity [8, 21].

3.2 pH Distribution After the Test

Figure 3 shows the change in soil pH as a function of time for the two tested soils considered. Consequently, it can be observed that the pH value increases over the entire distance between the anode and the cathode for the two soils of Ain nouissy such as that of Hmadna. When an electric field is applied, electrolysis takes place and H^+ and OH^- ions are generated at the anode and at the cathode, respectively. The low pH near the anode allows the solubility and desorption of salts, and consequently its mobility by electro-osmotic and electro-migration mechanisms. The same trend was reported by Li et al., Peng et al., Cho et al., and Kim et al. [1, 22–24].

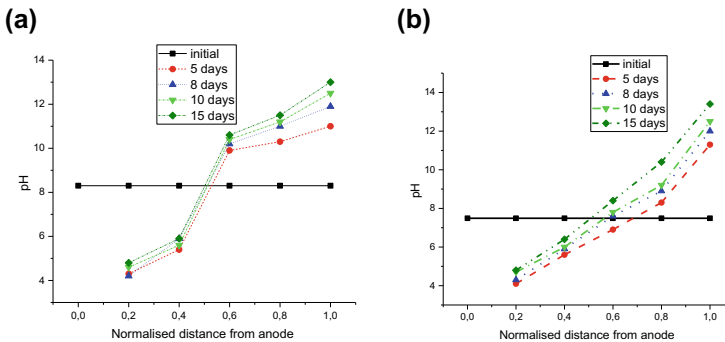


Fig. 3 pH variation along distance from anode after test. **a** Ain Nouissy and **b** Hmadna

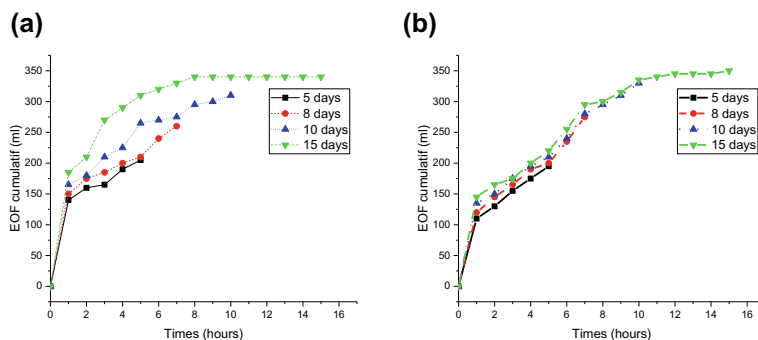


Fig. 4 Evolution of electro-osmotic volume during electrokinetic treatment **a** Ain Nouissy and **b** Hmadna

3.3 Cumulative Electro-Osmotic Flow

The electro-osmotic flow during the electrokinetic process as a function of time for each of the two soils is illustrated in Fig. 4. It may be noted that the flow rate increased with increasing processing time, where flow direction was valid for all anode tests at the cathode. This increase is the result of the mobilization of ionic species to which the applied voltage tends to increase the intensity of the electric current in the soils and thus the electro-osmotic output flow. The same results have been reported by several researchers [8, 24–26].

3.4 Removal Efficiency of Cationic Salts

During EK treatment, the applied electric current includes two phenomena: electro-osmosis and electro-migration, which allows the mobilization of salts and the facilitation of their transport and their elimination. Electro-migration allows the transport of ionic species such as bonds through the cathode, while electro-osmosis is related to the displacement of the pore water from the anode to the cathode, thus providing, the transport of salts in the pore solution. Figure 5 shows the removal of ions (salts) in samples from both soils after treatment with EK. The charged ions are mainly displaced by phenomena, such as: electro-migration, electro-osmosis, electrophoresis, and diffusion in the electrokinetic process. The two mechanisms of electro-osmosis and electro-migration improve the transport of cations (sodium, potassium, calcium, and magnesium) from the anode to the cathode. Electro-osmosis is the key phenomenon, which allows the removal and extraction of contaminants (salts) in the electro-osmotic flow collected to the cathodic compartment.

Also, the soil pH influences the migration and the elimination of the contaminants, an acidic environment near the anode allows the desorption and the dissolution of the contaminants, which lead to their better mobilization and extraction of the latter.

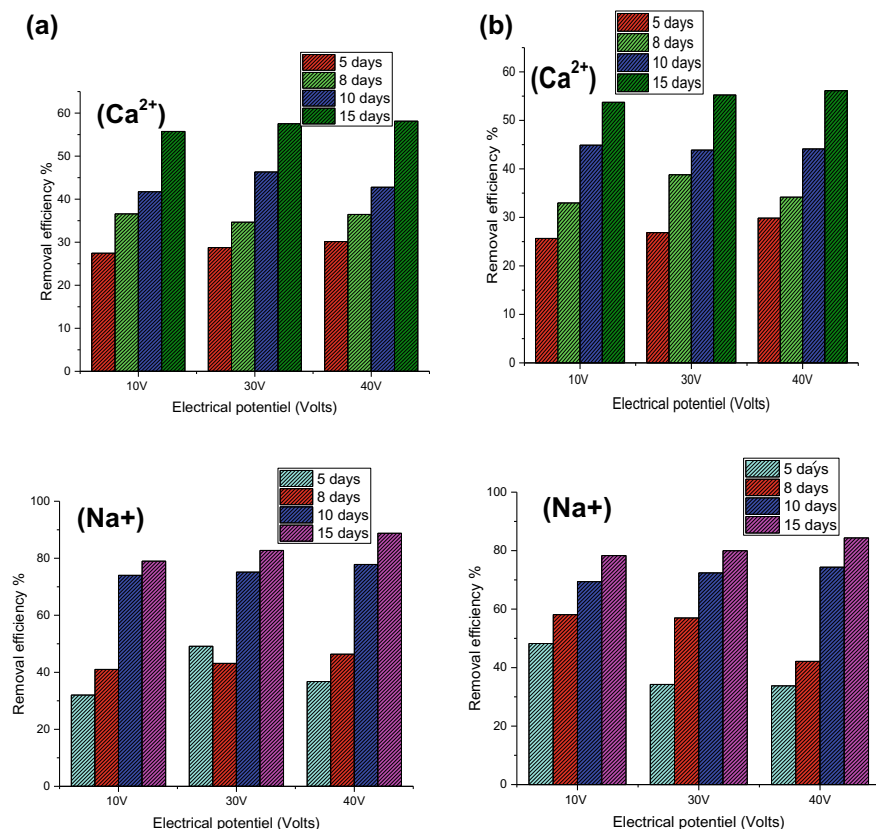


Fig. 5 Salt removal efficiency at the end of treatment. (Sodium and Calcium) **a** Ain Nouissy and **b** Hmadna

With the increase in the duration of the treatment, it is found that the efficiency of the removal of ions increases. This is due to the EOF, which has contributed to the transport and elimination of salts. Ion mobility is a parameter to control the efficiency of salt removal, which is more effective for Na^{+} than for Ca^{2+} , even if the ionic mobility of Na^{+} is lower. Divalent ions require more energy to be removed than monovalent ions. Divalent cations such as Ca^{2+} appear to be less mobile than monovalent cations, such as Na^{+} .

It is also necessary to show that monovalent cations have a lower atomic size than divalent cations, resulting in high ionic mobility in aqueous solution, implying a strong extraction of sodium with respect to calcium.

According to the results obtained for each of the two soils, we can say that the Ain Nouissy soil is a very saline clay loam very little plastic.

On the other hand, the soil of Hmadna is an extremely salty silty soil. It can be seen from the parameters obtained that cation extraction is more important for the Ain Nouissy soil than for the Hmadna soil.

4 Conclusion

In our research, sustainable management practices are being considered for application to saline soil remediation at the two study sites to maximize the economic, environmental, and social benefits of the electrokinetic process.

An EK experiment was carried out using a research laboratory-wide cell allowing the treatment and the decontamination of the saline soils from the regions of Ain Nouissy and Hmadna, in order to make profitable these lands for their effective and optimal use.

The results showed that: The pH data for each of the two soils is combined with the removal efficiency at different locations in the soil cell. The influence of the migration of the acid front from the anode to the cathode should be taken into account because of the effect of the dissolution and desorption of the ions.

In addition, it can be noted that the trend of EC soil Hmadna is less, compared to that of the soil of Ain Nouissy and this can be due to many factors, which include: the temperature, the content of water, soil porosity, interstitial fluid resistivity, soil composition, and salinity.

With the application of the continuous electrical potential on both soil samples, the soil-liquid medium undergoes several physical, chemical, and electrical changes, due to several EK processes, which take place in the middle of the soil.

Monovalent cations are strongly eliminated as divalent cations because of their ionic mobility, atomic size, and intensity of attraction. The proposed method achieved a removal rates of 89 and 58% for sodium and calcium ions respectively for Ain nouissy soil and 84 and 56% for Hmadna soil at 40 V electrical potential and a treatment duration of 15 days. It can be deduced that the increase of the treatment time allows a better electrical transport, leading to an optimal transport of the ionic species.

EK treatment is considered as an inexpensive and innovative technology applied in situ and in the laboratory. It is used to treat and remove salts from fine-grained soils to improve agricultural productivity on the one hand, and to protect construction and engineering facilities from deteriorating effects of salinity, on the other hand.

References

1. Kim KJ, Cho JM, Baek K, Yang JS, Ko SH (2010) Electrokinetic removal of chloride and sodium from tidelands. *J Appl Electrochem* 40(6):1139–1144
2. Jo S, Shin YJ, Yang JS, Moon DH, Koutsospyros A, Baek K (2015) Enhanced electrokinetic transport of sulfate in saline soil. *Water Air Soil Pollut* 226:199
3. Acar YB, Alshawabkeh AN (1996) Electrokinetic remediation. I: Pilot-Scale tests with Lead-Spiked Kaolinite. *J Geotech Eng* 122(3): 173–185
4. Micic S, Shang JQ, Lo KY, Lee YN, Lee SW (2001) Electrokinetic strengthening of a marine sediment using intermittent current. *Can Geotech J* 38(2):287–302

5. Ammami MT, Benamar A, Wang H, Bailleul C, Legras M, Le Derf F, Portet-Koltalo F (2013) Simultaneous electrokinetic removal of polycyclic aromatic hydrocarbons and metals from a sediment using mixed enhancing agents. *Int J Environ Sci Technol* 11(7):1801–1816
6. Gupta VK, Yola ML, Atar N, Solak AO, Uzun L, Üstündağ Z (2013) Electrochemically modified sulfoxazole nanofilm on glassy carbon for determination of cadmium (II) in water samples. *Electrochim Acta* 105:149–156
7. Gupta VK, Yola ML, Atar N, Ustündağ Z, Solak AO (2013) A novel sensitive Cu (II) and Cd (II) nanosensor platform: graphene oxide terminated p-aminophenyl modified glassy carbon surface. *Electrochim Acta* 112:541–548
8. Yuan L, Li H, Xu X, Zhang J, Wang N, Yu H (2016) Electrokinetic remediation of heavy metals contaminated kaolin by a CNT-covered polyethylene terephthalate yarn cathode. *Electrochim Acta* 213:140–147
9. Faisal AAH, Sulaymon AH, Khaliefa QM (2018) A review of permeable reactive barrier as passive sustainable technology for groundwater remediation. *Int J Environ Sci Technol* 15(5):1123–1138
10. Jayasekera S (2008) An investigation into modification of the engineering properties of salt affected soils using electrokinetics, PhD thesis, University of Ballarat, Australia
11. Chien SC, Ou CY, Lee YC (2010) A novel electroosmotic chemical treatment technique for soil improvement. *Appl Clay Sci* 50(4):481–492
12. Chien SC, Ou CY, LoWW (2014) Electroosmotic chemical treatment of clay with interbedded sand. *Proc Inst Civ Eng-Geotech Eng* 167(1):62–71
13. Ou CY, Chien SC, Yang CC, Chen CT (2015) Mechanism of soil cementation by electroosmotic chemical treatment. *Appl Clay Sci* 104:135–142
14. Ou CY, Chien SC, Liu RH (2015) A study of the effects of electrode spacing on the cementation region for electroosmotic chemical treatment. *Appl Clay Sci* 104:168–181
15. Peng J, Ye H, Alshwabkeh AN (2015) Soil improvement by electroosmotic grouting of saline solutions with vacuum drainage at the cathode. *Appl Clay Sci* 114:53–60
16. Rittirong A, Douglas RS, Shang JQ, Lee EC (2008) Electrokinetic improvement of soft clay using electrical vertical drains. *Geosynth Int* 15(5):369–381
17. Klouche F, Bendani K, Benamar A, Missoum H, Laredj N (2018) Remediation of the saline soil of the Mostaganem region by electrokinetic technique. *Innov Infrastruct Solut* 3:73
18. Reddy KR, Saichek RE (2004) Enhanced electrokinetic removal of phenanthrene from clay soil by periodic electric potential application. *J Env Sci Health Part A – Toxic/Hazardous Subst Env Eng* 39(5):1189–1212
19. Bruell CJ, Segall BA, Walsh MT (1992) Electroosmotic removal of gasoline hydrocarbons and TEC from clay. *J Environ Eng* 118(1):68–83
20. Gray DH, Mitchell JK (2005) Fundamental aspects of electro-osmosis in soils. *ASCE, J Soil Mech Found Eng* 93:209–236
21. Ammami MT, Portet-Koltalo F, Benamar A, Duclairoir-Poc C, Wang H, Le Derf F (2015) Application of biosurfactants and periodic voltage gradient for enhanced electrokinetic remediation of metals and PAHs in dredged marine sediments. *Chemosphere* 125:1–8
22. Li T, Guo S, Wu B, Li F, Niu Z (2010) Effect of electric intensity on the microbial degradation of petroleum pollutants in soil. *J Environ Sci* 22:1381–1386
23. Peng C, Almeida JO, Gu Q (2013) Effect of electrode configuration on pH distribution and heavy metal ions migration during soil electrokinetic remediation. *Environ Earth Sci* 69(1):257–265
24. Cho J, Park S, Baek K (2010) Electrokinetic restoration of saline agricultural lands. *J Appl Electrochem* 40:1085–1093
25. Jayasekera S, Hall S (2007) Modification of the properties of salt affected soils using electrochemical treatments. *Geotech Geol Eng* 25(1):1–10
26. Cameselle C (2015) Enhancement of electro-osmotic flow during the electrokinetic treatment of a contaminated soil. *Electrochim Acta* 181:31–38

A Case Study Sequel: Sustainable Remediation Using Succession Crops for PAH Impacted Soil



Linda C. Yang, Matt Catlin, and Michael Jordan

Abstract A site in northern Illinois was impacted with polycyclic aromatic hydrocarbons (PAHs) in soil from historical foundry operations. Three PAHs—benzo(a)pyrene, benzo(b)fluoranthene, and dibenzo(a,h)anthracene were identified with concentrations exceeding their site remedial objectives in the upper three feet of soil. The remedial remedy was complicated due to the large volume of impacted soil, project funding limitations, and the site’s location within a flood plain, preventing the importation of fill to create an engineered barrier. To address these challenges a sustainable design relying on phytoremediation was employed. In an effort to accommodate a short remedial timeframe, a unique approach was selected that was predicated on employing unique phytoremediation agents. The chosen planting regime allowed for maximum root production using rapidly maturing crops where multiple succession crops could be grown during the traditional growing season. The growing season was extended by using cold hardly winter crop, which allowed nearly year-round plant activity. The design and initial implementation was presented in Geo-Chicago 2016: Sustainability, Energy, and Geoenvironment in 2016. This paper summarizes the phytoremediation’s operation and monitoring, follow up planting, and soil sampling results.

Keywords Phytoremediation · Sustainability · PAH impacted soil remediation

L. C. Yang (✉)

Terracon Consultants, Inc., 192 Exchange Blvd., Glendale Heights, IL 60139, USA
e-mail: linda.yang@terracon.com

M. Catlin

Terracon Consultants, Inc., 11600 Lilburn Park Road, St. Louis, MO 63146, USA

M. Jordan

Terracon Consultants, Inc., 2401 Brentwood Rd., Raleigh, NC 27604, USA

© Springer Nature Switzerland AG 2020

K. R. Reddy et al. (eds.), *Sustainable Environmental Geotechnics*, Lecture Notes in Civil Engineering 89, https://doi.org/10.1007/978-3-030-51350-4_18

1 Introduction

This paper discusses the continuation and site closure strategy of phytoremediation at a site where historical foundry operations generated a significant volume of foundry sands impacted with PAHs.

Since the late 1990s phytoremediation of soils impacted with PAHs has increased in popularity. The appeal of phytoremediation lies in its inexpensive, relatively non-invasive implementation and waste reduction. Of particular interest with regard to remedy evaluation criteria, phytoremediation scores high as a green and sustainable remedy as well as providing multiple secondary benefits not realized through excavation, thermal destruction, in-situ oxidization, or other applicable PAH remedies.

The phytoremediation design incorporates a new approach selected to address the difficult site conditions by incorporating readily available agricultural implements, conventional planting methods, and cold hardy cover crops to extend the growing seasons. The approach combines successional conventional tillage to take advantage of green manure plowdown to build organic matter, increase soil tilth, water retention field capacity, and increase the diversity of soil fauna bacteria fungi facultative groups.

Remedy evaluation and design were conducted at the subject site in 2014, and the initial growth cycle included planting of buckwheat in June, July and August of 2015 and winter rye in September 2015. Repeated planting of successional crops took place annually from 2016 to 2018 where two stands of buckwheat were followed by winter rye. Each crop was disced followed by immediate replanting. Soil sampling and analyses of PAHs has been performed since 2016 and the results show significant reduction of PAHs concentrations in soil.

1.1 Background

The Corner Parcel Site (Site) is located at the northeast corner of Gardner Street (IL-75) and Blackhawk Boulevard (IL-2) in South Beloit, Illinois. The Site is approximately 4.94 acres and is currently unoccupied and vacant. It is fenced with access on both Gardner Street and Blackhawk Boulevard.

The Site was operated as Beloit Foundry/Prime cast Foundry producing ductile, gray iron, and stainless steel castings from 1852 through 2003. From at least 1939 and until late 1960s or early 1970s, the site was also occupied by two gasoline service stations. The City of South Beloit acquired the Site in 2002 and the onsite buildings were demolished in 2003. The Site has been vacant since that time.

1.2 Site Setting

The Site is at a major intersection near the Illinois/Wisconsin border and is close to Turtle Creek and Rock River. South Beloit has developed a draft Comprehensive Plan including well-maintained parks and open spaces centered on and showcasing the Rock River, Turtle Creek, and City Parks. The City desires to develop the Site into a public green space in a safe and environmentally sustainable way, while not exceeding the limited funding available.

1.3 Site Investigation and Cleanup Objectives

A series of environmental assessments and subsurface investigations were conducted; and the Site was entered into the Illinois Environmental Protection Agency's (IEPA) voluntary cleanup program, Site Remediation Program (SRP). Initial investigations identified volatile organic compounds, semi-volatile organic compounds, pesticides, polychlorinated biphenyls, and metals at concentrations above the IEPA's Tier I cleanup objectives. The main challenge or driver to the closure of the site was the widespread PAH concentrations.

In accordance with the IEPA SRP regulations, a 95% upper confidence limit (95UCL) was established for the individual PAH concentrations at the site. The site-wide 95UCLs were then compared to the remedial objectives. Three PAHs exhibited 95UCLs in the upper three feet of soil at concentrations exceeding their respective site specific remedial objectives. Table 1 illustrates the IEPA approved remedial objectives and maximum concentrations of the PAHs detected at the Site before phytoremediation. The site investigation results indicated that six areas of the Site contain three PAHs concentrations over the remedial objectives. The contaminant distribution does not exhibit a pattern, which is likely due to the historical industrial operations and nonpoint source contamination nature of the Site.

Figures 1 and 2 illustrate the site general location and the areas with PAHs exceedances.

Table 1 PAHs concentration and remedial objectives

Parameters	Remedial objectives (mg/kg)	Maximum concentrations (mg/kg)
Benzo(a)pyrene	2.1	130
Benzo(b)fluoranthene	8	190
Dibenzo(a,h)anthracene	0.8	40



Fig. 1 The corner parcel site, South Beloit, Illinois

2 Remedy Design

Phytoremediation was selected to remediate PAH impacts in soil. Of the potential remedies evaluated, phytoremediation was selected based on the sustainability goal, Site end use, and budget allocation [1].

A comprehensive review of available literature was conducted in an attempt to identify low maintenance plant species with demonstrated abilities to degrade PAHs; and ideally, degrade them in soil and climate conditions similar to the Site. Installation of multiple plant species offers a greater chance for success than planting of a monoculture [2]. Several plants including rye grass [3], black willows [4], and prairie grasses [5] have established track records of success with PAHs. While effective, grasses are limited by a shallow rooting depth and trees and prairie grasses are hampered by slow development.

To overcome this challenge, an innovative solution of succession crops (buckwheat and cereal rye grain) was selected [6]. The successive approach (two rounds of buckwheat planting in the summer and early fall, followed with winter rye planting in late fall) takes advantage of the specific natures of the plants and the seasons. Given

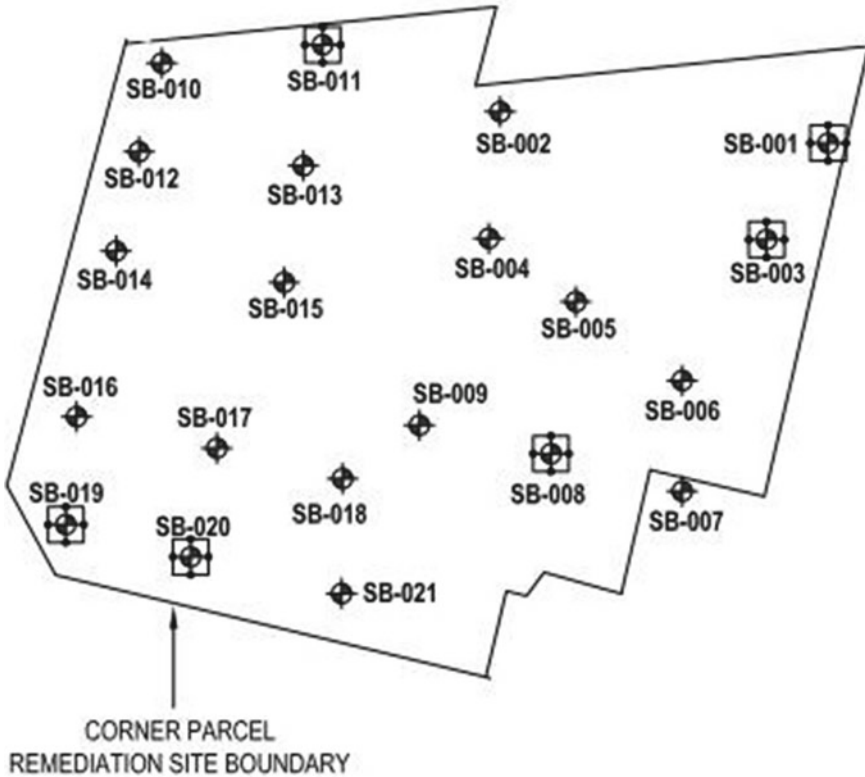


Fig. 2 Site Plan (PAH exceedance around SB-001, SB-003, SB-008, SB-011, SB-019, and SB-020)

the less than ideal soil conditions at the site, a succession planting regimen offers the additional benefit of rapidly improving soil [1].

Buckwheat rapidly matures; and once soil conditions reach approximately 80 degrees F, it can produce substantial biomass and a dense root system within approximately 35 days. The rapid growth of buckwheat allows multiple crops to be sown and tilled in a single season. Buckwheat also readily grows on poor soils and is drought resistant. It is so vigorous, organic farmers often utilize it as a smother crop during fallow periods as it will rapidly outcompete most weed species. The buckwheat crop’s substantial root and biomass production is conventionally tilled in using a large double gang disc harrow with aggressive disc angles pulled by a farm tractor. The incorporation of the green plants into the soil rapidly builds soil tilth, increases organic matter and begins to break down hardpan while increasing the diversity and population of soil fauna.

Buckwheat is a plant that is cultivated for its grains and is commonly used as a cover crop. It has a branching root system, with one primary root reaching deeply in the moist soil, causing a better adaption to its environment than other cereal crops

[7]. The life cycle of buckwheat is shorter than others, approximately 6–12 weeks. It is considered that the buckwheat's adaptation to the northern Illinois environment, short life cycle, and dense root system will enhance the biomass in the shallow soil, biodegradation of the PAHs, and maximize the relatively short growing season length in northern Illinois.

Buckwheat in this regimen is followed by cereal rye. Cereal rye extends the growing season as it will germinate and grow when temperatures are above 33 degrees F. Cereal rye produces an extremely large network of root mass in the soil, providing one of the largest root surface areas per acre of readily available plants. Cereal rye also provides a deep root system capable of encompassing the depth of impact identified at the site.

Winter rye is an excellent winter cover crop because it rapidly produces a ground cover that holds soil in place against the forces of wind and water. The extensive root system of rye helps prevent compaction in annually tilled fields. Winter rye also has a positive effect on soil tilth. Compared to other cereal grains, rye grows faster in the fall and produces more dry matter the following spring. Rye is the most winter-hardy of all cereal grains, tolerating temperatures as low as -30°F once it is well established. It can germinate and grow at temperatures as low as 33°F [8]. The deep root of winter rye has a significantly greater root surface compared to other plants. This allows the plant to extend to deeper areas below the surface, access the vertical extent of contamination, and increase drought existence, therefore, reducing the operation and maintenance costs.

It is considered that the buckwheat and winter rye's adaptation to the northern Illinois environment, reduced maintenance including no irrigation requirements, and their extensive root systems will enhance the biomass in the shallow soil and biodegradation of the PAHs.

3 Succession Crops Installation and Monitoring

The site was prepared for planting by mowing the existing vegetation and tilling the surface using a double gang disc harrow pulled by a tractor. The disc harrow exposed the soil and generated an appropriate seed bed for planting. A conventional grain drill was used to drill the buckwheat into the soil at a typical rate of 60 lb per acre. Cereal rye grain was drilled using the same methodology after discing in the second buckwheat crop.

The first planting of buckwheat took place in the first week of June 2015. Site visits were conducted on a weekly basis to observe the site conditions. Buckwheat was observed to germinate approximately 1.5 weeks after the planting. Plants were observed to be fully blossoming one month after the planting. The second round of planting occurred in the seventh week after the first planting. It was observed that the buckwheat height ranged from approximately 51 inches in most of the site to 3 inches in the area that was poorly drained. Some plants were removed from the

ground and the roots were observed to be dense and approximately 4 inches in length (Photos 1 and 2).

In late September 2015, winter rye was planted after the second round of buckwheat was terminated. In about three weeks, the plant grew to approximately 2–4 inches. The plant was observed to germinate slower than buckwheat and continued to grow in colder temperatures in October and November. In about five weeks, winter



Photo 1 Preparation for first planting



Photo 2 Buckwheat blossoming (5 weeks after planting)



Photo 3 Winter Rye

rye grew to approximately 3 inches (in the poorly drained area) to 9 inches tall. By May 2016, winter rye grew to approximately 36 inches in height in the good growth area (Photo 3).

It is well known that winter rye has a very intense root system and can improve soil significantly. It was reported anecdotally that winter rye roots could grow to 45 inches in north-central Indiana in May. During the project monitoring, particular attention was paid to the roots system. The observation showed that winter rye had very dense root system. In May 2016, the plant was removed from the ground using a hand auger. The measurement showed that the width of one plant root ball was approximately 9 inches wide and the root was approximately 11 inches long. The dense root system attached a lot of soil to it (Photo 4).

4 Soil Sampling and Analyses

After one cycle of the buckwheat and winter rye crop, soil sampling was conducted from (0–3) feet below grade interval at the original sampling locations (Fig. 1) to evaluate remedial progress and obtain another set of entire site condition of PAHs of concerns.

Analytical results showed that soil samples at three locations (SB-004, SB-010, and SB-012) exceeded site specific remedial objectives for benzo(a)pyrene, benzo(b)fluoranthene, and dibenzo(a,h)anthracene. 95UCL of the three PAHs of concern were calculated using the USEPA statistical tool. Benzo(a)pyrene exceedance in sampling location SB-010 was eliminated by the statistical evaluation.



Photo 4 Winter Rye Root System (May 2016)

In June 2017, after two cycles of succession crops treatment at the site, lateral delineation samples were collected from sampling locations SB-004 and SB-012. Four soil samples were collected in the four cardinal directions approximately 10 to 15-foot distance from the 2016 sampling locations, and the samples were analyzed for PAHs of concern. The objectives of the 2017 sampling were to (1) assess the remedial progress near the sampling locations that exceeded site specific remedial objectives in 2016; and (2) identify the areas of exceedance that potential soil removal might be necessary in order to achieve the objectives more quickly. The statistical evaluation using 95UCL was performed on the entire data set. The 95UCL statistical calculations eliminated the sampling area of SB-004.

In summer 2018, after three cycles of the succession crops planting, one soil sample was collected from SB-012 N location, the only remaining location with benzo(a)pyrene and dibenzo(a,h)anthracene concentrations exceeding the site specific remedial objectives. The 2018 sampling results illustrated that the PAHs concentrations decreased significantly from 2017, and the 95UCL calculations indicated that the entire data set met site specific remedial objectives for PAHs of concern.

Soil analytical results and 95UCL calculation demonstrated that phytoremediation achieved the site specific remedial goals of PAHs of concern (Tables 2 and 3).

Table 2 Remediation progress soil sampling analytical results

Polynuclear Aromatic Hydrocarbon (PAHs) Parameters			Benzo(a) pyrene	Benzo(b) fluoranthene	Dibenzo(a,h) anthracene
			(mg/kg)	(mg/kg)	(mg/kg)
IEPA Approved Site-Specific Remedial Objectives			2.1	8	0.8
Site Specific Soil Remedial Objectives					
Sample Identification	Sample Date	Units			
SB-001	10/10/2016	mg/kg	0.75	1	0.31
SB-002	10/10/2016	mg/kg	1.4	1.7	0.55
SB-003	10/10/2016	mg/kg	0.26	0.34	0.11
SB-004	10/10/2016	mg/kg	6	8.9	2.3
SB-004	10/26/2017	mg/kg	0.05	NA	7.4
SB-004N	6/20/2017	mg/kg	0.26	0.28	0.089
SB-004E	6/20/2017	mg/kg	0.32	0.37	0.11
SB-004S	6/20/2017	mg/kg	0.044	<0.034	<0.034
SB-004W	6/20/2017	mg/kg	0.8	1	0.25
SB-005	10/10/2016	mg/kg	0.31	0.42	0.13
SB-006	10/10/2016	mg/kg	0.74	0.9	0.31
SB-008	10/10/2016	mg/kg	0.1	0.14	< 0.046
SB-009	10/10/2016	mg/kg	1.6	2.1	0.61
SB-010	10/10/2016	mg/kg	2.7	2.8	0.72
SB-011	10/10/2016	mg/kg	0.52	0.68	0.21
SB-012	10/10/2016	mg/kg	6.2	6.7	1.8
SB-012	10/26/2017	mg/kg	<0.045	NA	2.3
SB-012N	6/20/2017	mg/kg	19	24	28
SB-012N	7/6/2018	mg/kg	3.2	NA	0.95
SB-012N1	6/20/2017	mg/kg	2	2.3	0.48
SB-012E	6/20/2017	mg/kg	0.57	0.65	0.17
SB-012S	6/20/2017	mg/kg	0.88	1	0.28
SB-012W	6/20/2017	mg/kg	6.4	7.7	2.3
SB-013	10/10/2016	mg/kg	0.043	0.048	< 0.036
SB-014	10/10/2016	mg/kg	< 0.042	< 0.042	< 0.042
SB-015	10/10/2016	mg/kg	< 0.034	< 0.034	< 0.034
SB-016	10/10/2016	mg/kg	< 0.037	< 0.037	< 0.037
SB-017	10/10/2016	mg/kg	1	1	0.34
SB-018	10/10/2016	mg/kg	0.074	0.096	< 0.043
SB-019	10/10/2016	mg/kg	0.36	0.64	0.25
SB-020	10/10/2016	mg/kg	0.75	1	0.23
SB-021	10/10/2016	mg/kg	0.099	0.13	0.045

Notes

1. Site Specific Remedial Objectives were approved by the IEPA in the April 16, 2012 Remedial Action Plan
2. Cells highlighted in yellow indicate exceedances of IEPA approved remedial objectives
3. NA = Not Analyzed
4. Soil samples were collected from (0–3) foot interval below ground

Table 3 PAHs Remedial objectives and 95UCL results

Parameters	Remedial objectives (mg/kg)	95UCL (mg/kg)
Benzo(a)pyrene	2.1	1.79
Benzo(b)fluoranthene	8	6.08
Dibenzo(a,h)anthracene	0.8	0.59

5 Conclusions

A phytoremediation approach including succession crops of buckwheat and winter rye was successfully employed to reduce PAHs in soils resulted from historical foundry operations to site specific cleanup objectives in a sustainable and cost effective way.

Additional benefit of phytoremediation was aesthetical. The desirable appeal of blossoming buckwheat in summer and fall, and ground covering plant of winter rye in winter and spring improves the negative perception from the dilapidated vacant brownfields site prior to phytoremediation.

Acknowledgments The authors appreciate the support of the following individuals and organizations.

Theodore Rehl, Mayor, City of South Beloit, Illinois
 Tracy Patrick, City Clerk, City of South Beloit; Illinois
 Jeff Reininger, Public Works Director, City of South Beloit, Illinois
 Keary Cragan, USEPA Region 5
 Steve Colantino, former Illinois EPA, Office of Brownfields Assistance
 Krishna Reddy and Erin Yangicoglu, The University of Illinois Chicago
 Junaluska Williams and Rich O'Brien, P.E., Terracon Consultants, Inc.

References

1. Yang L, Catlin M, Jordan MT (2016) Development and installation of a sustainable remediation system using succession crops for pah impacted soil. In: Geo-Chicago 2016: sustainable waste management and remediation proceedings, pp 286–294
2. ITRC (Interstate Technology & Regulatory Council) (2009) Phytotechnology technical and regulatory guidance and decision trees, revised. PHYTO-3. Interstate Technology & Regulatory Council, Phytotechnologies Team, Tech Reg Update, Washington, D.C.
3. Ferro AM, Rock SA, Kennedy J, Herrick JJ, Turner DL (1997) Phytoremediation of soils contaminated with wood preservatives: greenhouse and field evaluations. *Int J Phytorem* 1(3):289–306
4. Spriggs T, Banks MK, Schwab P (2005) Phytoremediation of polycyclic aromatic hydrocarbons in manufactured gas plant-impacted soil. *J Environ Qual* 34:1755–1762
5. Nedunuri KV, Lowell C, Meade W, Vonderheide AP, Shann JR (2010) Management practices and phytoremediation by native grasses. *Int J Phytorem* 12(2):200–214
6. Jordan MT (2015) Phytoremediation of PAHs: designing for success. In: Third international symposium on bioremediation and sustainable environmental technologies

7. Stone JL (1906) Buckwheat. In: Agricultural experiment station of the college of agriculture department of agronomy (Bulletin 238 ed). Cornell University, Ithaca, New York, United States, pp 184–193
8. Grubinger V (2010) Winter Rye: A reliable cover crop. The University of Vermont, A publication of UVM extension's vermont vegetable and berry program

Characterization and Ecotoxicological Evaluation of Nanostructured Chitosan Particles



Fabiana Pereira Coelho, Thaynara Santana Rabelo, Louise da Cruz Felix, Daniele Maia Bila, and Elisabeth Ritter

Abstract Today there are several areas impacted by contaminants dangerous to the environment and there is a growing need to recover, with the use of materials that generate less environmental impacts. In this environmental line the use of green materials, such as chitosan, an amino polysaccharide derived from a very abundant Chitin and is capable of adsorbing heavy metals and anionic and cationic dyes due to the presence of amino and hydroxyl groups. Another very growing aspect is the new technologies as the nanoparticles can be classified by the structure or size of the material. Therefore, the challenge is to use new technologies and also to know the influence of nanoparticles in the environment. The objective of this work was to characterize the nanostructured chitosan and to evaluate its toxicity. The characterization test is Thermogravimetric Analysis (TGA) and High Resolution Scanning Microscopy (SEM-FEG). To evaluate the toxicity of nanostructured chitosan (green material) magnetized chitosan in different percentages (with iron oxide II, III nanoparticles) and metallic nanoparticles were considered the organisms: *Euruca sativa* (arugula) and *Allivibrio fischeri*, using lyophilized bacteria. The results indicated the difference of the structures in relation to the percentage of Chitosan used, being Chitosan 1% with higher magnetic frequency. They also indicated a decrease in growth in samples with magnetic nanoparticles and acute toxicity to *Allivibrio fischeri* in contact with magnetized chitosan and magnetic nanoparticles.

Keywords Chitosan nanoparticles · Characterization · Toxicity

F. P. Coelho (✉) · T. S. Rabelo · L. da Cruz Felix · D. M. Bila · E. Ritter
Universidade do Estado do Rio de Janeiro, Rio de Janeiro, Brazil
e-mail: fpcoelho@firjan.com.br

F. P. Coelho
Instituto SENAI de Tecnologia Química e Meio Ambiente, Rio de Janeiro, Brazil
Instituto SENAI de Inovação Em Química Verde, Rio de Janeiro, Brazil

1 Introduction

Nanoscience and Nanotechnology seek to study the properties of nanometer-sized objects and to develop their use in systems in which at least one of the dimensions is on this scale. In order to obtain the desired property, it is necessary to look not only for the chemical and structural composition of the material, but also for the size and shape of its particles [1]. In the last decades, the use of nanomaterials has become increasingly used in industrial processes, consumer and medical products, [2] and more recently in environmental treatment [3].

The high surface areamass ratios (i.e., specific surface area) of these materials can benefit any technology that depends on reactions at solids and solid gas interfaces. Such technologies include adsorption used for treatment of water and exhaust gases, as well as photocatalytic processes for the degradation of contaminants [4].

The characterization of structured or nanostructured materials is important because it has to define the physico-chemical properties of materials (size, functional groups, morphology and thermal stability) and adsorption performance of materials, especially those used for water treatment.

According to Reddy and Lee [5] the production of magnetic materials is a multi-stage process and therefore it is important to observe and evaluate the products (structural, thermal, morphological, and chemical properties) at each stage. Therefore, it is essential to use different analytical techniques for this purpose.

Due to the increased production of these nanoparticles, there are concerns about the use and disposal of these nanomaterials in the environment. Studies demonstrate evidence of the actual toxicity of nanosystems [6]. In relation to the germination test results, it can be observed that in some cases the type of contaminant influences more than the use of nanomaterials, Rede et al. [7] already indicated this type of influence. For more efficient use and with less impact to the environment, the use of green materials is increased, being more available in the environment and with less impact to the environment. Chitosan is a natural material derived from chitin and found from the exoskeleton of crustaceans.

In the present study, unstructured chitosan and magnetic nanoparticles with chitosan were produced. The organisms *Aliivibrio fischeri* (gram-negative marine bacteria with bioluminescent properties) and *Euruca sativa* (scientific name of rocket seeds) were also used to evaluate the toxicology of nanoparticles.

2 Material and Methods

2.1 Preparation of Nanomaterials

The commercial chitosan used was first weighed 5 g and oven dried at 100 °C for 2 h, with repetition of the procedure to ensure the reliability of the result. After drying

there was a mass reduction of 0.6 g. Low molecular weight chitosan (Sigma Aldrich), Iron oxide II/III nanopowder >50 nm (Sigma Aldrich) were used.

The synthesis of materials sensitive to magnetization and chitosan derivatives was performed using FeCl_3 (3.7 g) and $\text{FeSO}_4 \cdot 7\text{H}_2\text{O}$ (4.17 g) (Fe (III) / Fe (II) molar ratio = 1.5) these were dissolved in 100 ml of deionized water at room temperature and warmed to 90 °C. Two other solutions were also prepared:

- (a) 10 mL of 25% vol ammonium hydroxide;
- (b) 50 ml of an aqueous solution of chitosan previously prepared in a weak acidic environment (i.e., to favor the solubility of chitosan). A stock solution with chitosan (1% and 3% by weight) using HCl (2% and 6% by volume, respectively).

As soon as the desired temperature was reached in the ferrous solution, the two other solutions were added in sequence. The mixtures were stirred at 90 °C for 30 min and then cooled to room temperature. Magnet-sensitive solutions were washed twice with deionized water. For better washing they were centrifuged twice with removal of the supernatant. To reduce the volume generated, the samples were dried until the volume was reduced. After washing the samples and reducing the volume they were dried at 100 °C overnight.

According to this procedure adapted from Nístico et al. [8], the dispersions of iron oxide particles in the chitosan matrix are expected to form. The materials thus obtained (referred to as $Q_{\text{pm}1\%}$ and $Q_{\text{pm}3\%}$) were pyrolyzed in a muffle for heat treatments at 700° C for 1 h. The pyrolyzed materials were encoded as $Q_{\text{pm}1\%}$ and $Q_{\text{pm}3\%}$. The pure chitosan was pyrolyzed in the muffle for heat treatment at 700 °C for 1 h. The samples were identified as Q for chitosan, Q_{p} for pyrolyzed chitosan, $Q_{\text{pm}1\%}$, (Fig. 1) for magnetized and pyrolyzed chitosan with 1% chitosan concentration, $Q_{\text{pm}3\%}$ with 3% chitosan concentration, and NP_{Fe} for ferrous nanoparticles.

Fig. 1 Sample of $Q_{\text{pm}1\%}$ —volume e magnetism



2.2 *Characterization of Nanomaterials*

Thermogravimetric analysis was performed at the SENAI Institute for Innovation in Green Chemistry (ISI of Green Chemistry) using the Simultaneous Thermal Analyzer TGA-DTA STA 6000 (Perkin Elmer) on heating from room temperature to 600 °C with a heating rate of 10 °C/min and Nitrogen atmosphere. The temperature at the start of the decomposition, the temperature at the maximum process rate and the percentage weight loss were evaluated from thermogravimetric (TG) curves. Opened corundum crucibles were used to contain 7 mg sample.

High resolution scanning microscopy analysis was performed at the Nanomaterials Laboratory of the Department of Mechanical Engineering of the State University of Rio de Janeiro using the JSM-7100F (JEOL) Thermal Field Scanning Electron Microscope with a resolution of up to 1.2 nm. A sample is inserted into a 12 mm pipe and it is through the air chamber keeping the sample in a vacuum of 9.6 E-5 Pa. This equipment has the advantage of not generating magnetic fields so it is possible to analyze the magnetic samples. Several images of morphology and surface structures are obtained.

2.3 *Ecotoxicological Tests—Germination*

The direct germination test was adapted from Piazza et al. [9], Tang et al. [10], and France [11]. The tests used Arugula seeds (248), Isla brand, having the following specification of seeds: Lot 117427, Germination Rate 96 ¢, Date / Analysis on 08/18, Validity up to 08/20, and purity 99.9%. Lots of 10 seeds were sown on a 9.00 Ø thickness filter paper of the Quality brand in Petri dishes (9 cm) in five replicates. In order to evaluate the seed germination variation when exposed to samples of the industrialized and ready-made materials (Q, Q_p, Q_{pm1%}, Q_{pm3%} and NP_{fe}), 5 ml solutions of each compound with a concentration of 300 mg/l were added. Distilled water was used as a negative control and NaCl solution was used as a positive control (0.25 mol). The assay was performed in the dark at 22 °C for 72 h. The number of germinated seeds was evaluated after 24, 36, 48, and 72 h. After this period, the root lengthening and the aerial part length of the seedlings were evaluated.

2.4 *Ecotoxicological Tests—Microtox*

The test was performed using the organism *Aliivibrio fischeri* a gram-negative marine bacterium commonly found in symbiosis with other organisms in the oceans. The test was performed in duplicate, previously screening all samples without dilution in order to determine the working range that best identified the concentration that causes deleterious effect in 50% and 20% of the observed population (CE 50 and CE

20, respectively) when exposed to contaminants for 30 min at a constant temperature (15 ± 2 °C). The ABNT standard NBR 15411-3 (2012) was used as reference for the test. A Microtox[®] Model 500 luminometer from Analyzer was used and the results statistic was calculated with Microtox OMNI TM software, version 4.1, with results that showed r^2 above 0.98 being accepted.

3 Results

3.1 Characterization of Nanomaterials

Figure 2 shows the thermal analysis curve (Blue Curve), being the temperature (°C) in the abscissa and loss of mass (%/min) and Endothermic Heat Flow (mW) in the ordinate. Thermogravimetric measurements under non-oxidized conditions (nitrogen atmosphere) indicated that the chitosan sample contains 6.34% of adsorbed water, which is evaporated at a relatively low temperature (below 100 °C—1st Stage).

The predominant stage of thermal degradation occurs in the range of 250–340 °C (maximum 270 °C) during which 44.45% decrease in the chitosan mass (2nd Stage) caused by the depolymerization of chitosan chains, decomposition of pyranose rings through dehydration and deamination and finally ring opening reaction. A small loss is observed with reduction of 17.90% (3rd Stage). The residue of coal of 30.82% is constant at least up to 618 °C (4th Stage).

The DTG curve (Green Curve) of the chitosan recorded in N₂ shows an endothermic effect accompanied by the thermal decomposition of the sample. The

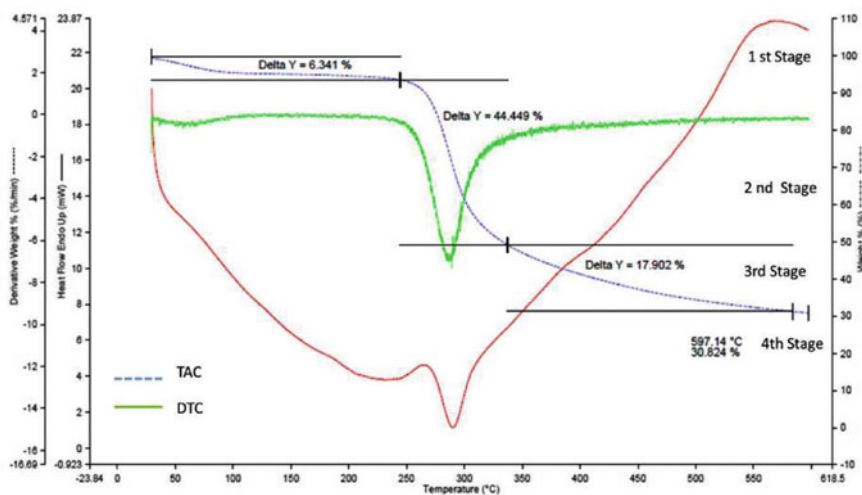


Fig. 2 Thermal analysis curve in blue—TAC and green derived thermogravimetry curve—DTC

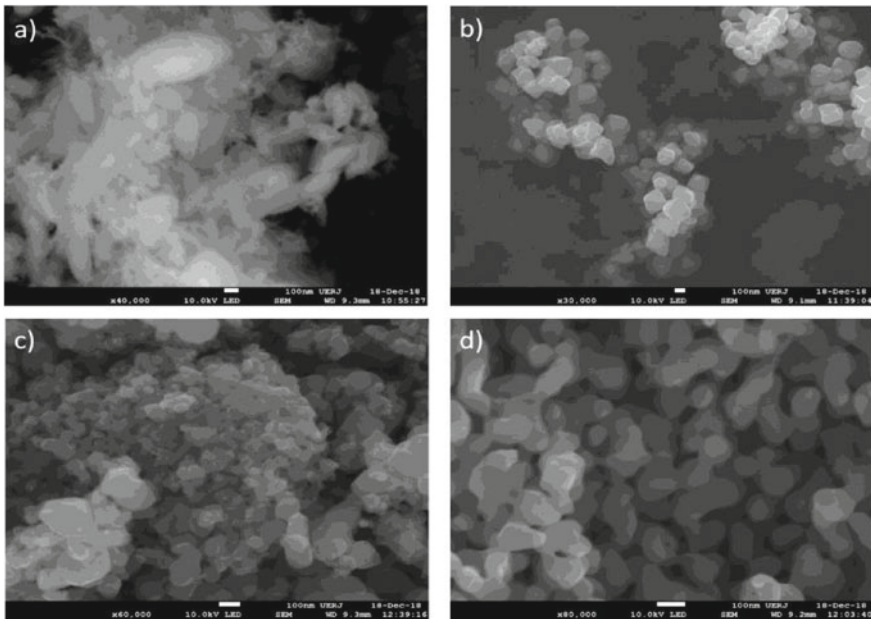


Fig. 3 Surface images obtained with the SEM: **a** Q_p , **b** NP_{Fe} , **c** $Q_{pm1\%}$ and **d** $Q_{pm3\%}$

thermogravimetric analysis allows to conclude that the studied chitosan is thermally stable up to 270 °C in nitrogen. However, the evolution of differently bound water starts at very low temperatures.

The SEM images of the Q_p , $Q_{pm1\%}$, $Q_{pm3\%}$, and NP_{Fe} samples are shown in Fig. 3. It can be seen that the morphological surface of the chitosan samples is spherical in shape, which translates into a large surface area and is a propensity to maximize the adsorption of target pollutants.

In the Q_p sample it was possible to observe in the images the presence of mesopores, Fig. 4, besides the rounded morphology of the grains. However the morphology of the ferrous nanoparticle (NP_{Fe}) presents cubic geometry, and without the presence of pores. For the sample of $Q_{pm1\%}$ and $Q_{pm3\%}$, the morphology presented in the images indicates more elongated forms, identifying the iron presence in the sample. In both magnetized samples it was not possible to verify the presence of chitosan in the pore structure. Regarding grain size, the presence of 100 nm size grains was observed for $Q_{pm1\%}$, $Q_{pm3\%}$, and NP_{Fe} samples. Already the sample of Q_p was observed that mesopores with dimensions between 50 and 100 nm.

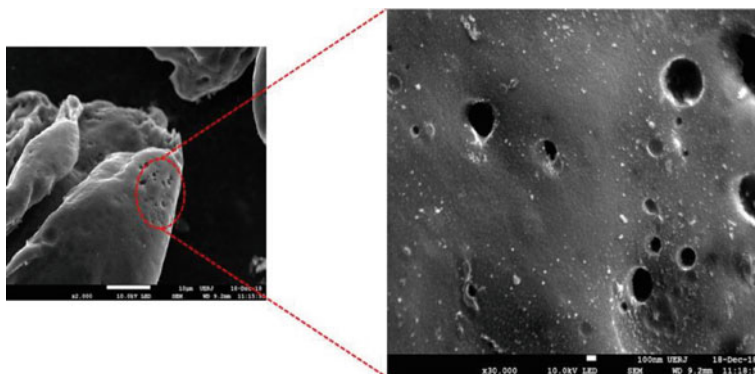


Fig. 4 Mesopores in Qp, scale—100 nm

3.2 Results Germination

In relation to the germination rate, it was possible to observe that there was no variation between the chitosan and the other solutions with the nanoparticles, since all presented a germination rate similar to the control. In addition, it is observed that the germination rate reaches the maximum limit in 48 h. Thus, in the next tests, this time can be adopted as the standard for nanoparticle analysis. In relation to the germination rate, it can be seen that after 48 h of incubation there was a stabilization in the seeds growth, with 98% of germination.

It is noteworthy that during the NP_{Fe} test these were adhered both in the seed and the filter paper (black dots in Fig. 5).

In relation to root elongation rates (Fig. 6a) it can be observed that the $Q_{pm1\%}$ obtained a larger mean in the root size, while the NP_{Fe} showed the lowest average, and its value was still similar to the white.

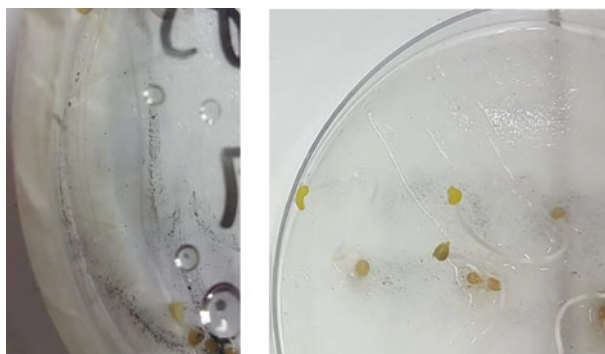


Fig. 5 Examples of particles adhered to the root and to the film paper

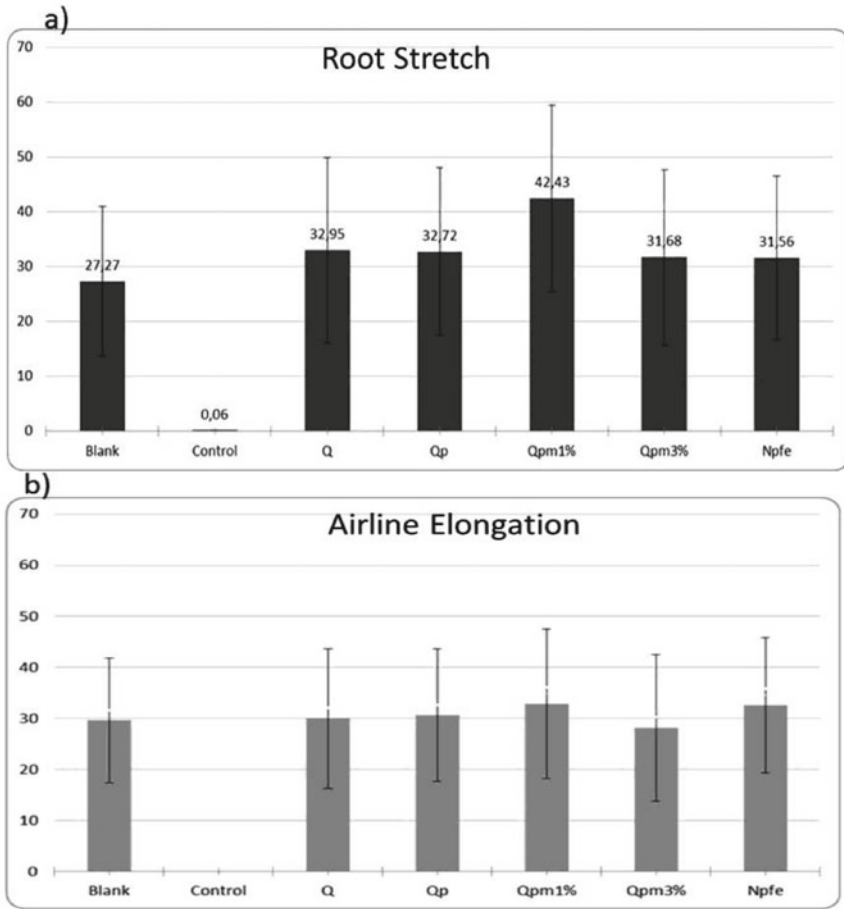


Fig. 6 a Root Stretch and 1b Airline Elongation

For the aerial elongation rates (Fig. 6b), it was observed that the lowest average presented to $Q_{pm3\%}$, being below white, indicating a small influence on the germination of the seeds possibly associated with a higher concentration of chitosan in the solution as already studied [6].

3.3 Results Bioluminescence

The results of the test with the bioluminescent bacterium *Aliivibrio fischeri* are presented in Table 1. In the first test the samples were screened for nanomaterials with concentration 300 mg/L. In this case, a bioluminescence emission inhibitory effect of more than 20% was observed in all the samples, with two results higher than

50%, indicating the need to carry out a series of dilutions in order to find the values of CE 50 and CE 20. The highest inhibition rate of bioluminescence was observed in non-pyrolyzed chitosan. This greater effect may be related to the structure of the material and the organic origin of this compound.

After the screening, dilutions were made in order to determine the CE50, when applicable, and the CE 20 of the nanomaterial solutions. CE50 of chitosan and pyrolyzed Chitosan with 1% of nanoferro were obtained. Again, Chitosan had a higher toxic effect, obtaining an EC50 of 26.54%.

For the CE20, the nanoferro particles showed less toxicity. This result is consistent with that presented by Dutra (2015), who, when performing tests with *Aliivibrio fischeri*, concludes that iron particles do not represent toxic effects to organisms and the results of acute toxicity with *C. silvestrii* were carried out by Gerbara [12]. However more detailed tests are needed to evaluate the chronic effect of these particles. Gerbara [13] obtained values of CENO (I) (initial concentration of not observed effect) and CEO (I) (initial concentration of observed effect) around 2500 and 5000 mg L⁻¹ of nano-Fe₃O₄ for the growth parameter, respectively.

4 Conclusions

The methodology of preparation of the nanoparticles Q_{pm1%} and Q_{pm3%} is adequate resulting in magnetic nanoparticles, but should be reviewed contemplating the increase of the percentage of chitosan used in the preparation of the sample, because the final volume generated, 0.51 g of Q_{pm1%} and 0.40 g of Q_{pm3%}, is very low. For Q_p the increase of the preparation temperature could generate more nanostructures in the sample.

Thermal analysis indicated that the temperature of 600 °C still shows a significant residual rate. From this result the material pyrolysis was carried out up to 700 °C and with this carbonization temperature samples were obtained with a better quantitative mesopores and the generation of more nanoparticles. Scanning images were obtained, which allowed to observe the presence of mesopores in the Q_p particle, with a well rounded arrangement. For an increase in the number of pores, there should be an increase in the carbonization temperature. The images of Q_{pm1%} and Q_{pm3%} presented only the evidence of nanoferro and not indicating the occurrence of chitosan, therefore the increase of the percentage of chitosan will be valid in the next tests.

In relation to the germination, result indicates that the influence on the germination rate is more associated, for example, with the remediation method and the contaminant than with the use of nanoparticles in the medium. Thus, due to the similarity of germination results obtained with white, it suggests the proposal to reduce the test time to 48 h in the next works.

For the result of acute toxicity with the bacterium *Aliivibrio fischeri*, it can be concluded that Chitosan in nature presented higher toxicity than the structured nanoparticles. For the nanoparticles, the pyrolyzed Nanoquitosana presented higher toxicity (CE20 = 11.01%). The order of toxicity (CE20) was Q > Q_{pm1%} > Q_{pm3%}

Table 1 Results of CE 50 and CE 20 obtained from the toxicity tests with the bacterium *Aliivibrio fischeri*

Compound	Size (nm)	Conc. (mg/L)	Screening* (%)	CE50 (%)	CE20 (%)
Q		300	100	26.54	11.01
Q _p	100	300	NO**	NO**	14.80
Q _{pm1%}	200	300	53.13	91.99	41.88
Q _{pm3%}	200	300	35.02	NO	60.68
NP _{fe}	> 100	300	28.86	NO	91.11

* Inhibition at initial concentration., ** NO—Not Observed

> NP_{fe} > Q_p. Only the tests with Q and Q_{pm1%} showed CE50. Further studies are needed to detail the structure of these nanoparticles and the toxic effect associated with them for more complex organisms.

References

1. Macêdo, MIF, Ferreira CA, Rangel MLSS (2011) Preparação de nanopartículas de magnetita e maghemita superparamagnéticas. In: XVI congresso brasileiro de catálise, Campos do Jordão, SP
2. Batley GE, Kirby JK, McLaughlin MJ (2013) Fate and risks of nanomaterials in aquatic and terrestrial environments. *Accounts Chem Res* 46(3):854–862
3. Sanchez A, Recillas S, Font X, Casals E, Gonzalez E, Puentes V (2011) Ecotoxicity of, and remediation with, engineered inorganic nanoparticles in the environment. *Trac-Trends Anal Chem* 30(3):507–16
4. Kanatzidi MG, Poeppelmeier KR (2007) Report from the third workshop on future directions of solid-state chemistry: the status of solid-state chemistry and its impact in the physical sciences. *Prog Solid State Chem* 36:1–133
5. Reddy HK, Lee S (2013) Application of magnetic chitosan composites for the removal of toxic metal and dyes from aqueous solutions. *Adv Colloid Interf Sci* 201–202: 68–93
6. Wang Y, Zhou J, Liu L, Huang C, Zhou D, Fu L (2016) Characterization and toxicology evaluation of chitosan nanoparticles on the embryonic development of zebrafish, *Danio rerio*. 141: 7p. *Carbohydrate Polymers*
7. Rede D, Santos LHMLM, Ramos S, Oliva-Teles F, Antão C, Souza S, Delerue-Matos C (2016) Ecotoxicological impact of two soil remediation treatments in *Lactuca sativa* seeds. *Chemosphere* 199:193–198
8. Nisticò R, Francozo F, Cesano F, Scarano D, Magnacca G, Parolo ME, Carlos L (2016) Chitosan-derived iron oxide systems for magnetically-guided and efficient water purification processes from polycyclic aromatic hydrocarbons. *ACS Sustain Chem Eng*
9. Plaza G et al (2005) The application of bioassays as indicators of petroleum-contaminated soil remediation. *Chemosphere* 59: 289–296
10. Tang J et al (2011) Eco-toxicity of petroleum hydrocarbon contaminated soil. *J Environ Sci* 23:845–851
11. França, Fernanda de Oliveira Mury. Avaliação de Atividade Estrogênica e Toxicidade de Lixiviados de Resíduos Sólidos Urbanos. Dissertação de Mestrado

12. Dutra MC (2015) Síntese e Caracterização de Nanopartículas de Ferro-zero Valente (Nzvi) Aplicadas ao Tratamento de Águas Contaminadas com 4- Clorofenol. Dissertação de Mestrado. Universidade Federal de Santa Catarina
13. Gebara, RC (2017) Toxicidade de nanopartículas de óxido de ferro (Fe₃O₄) para o cladóceros tropical *Ceriodaphnia silvestrii*. Dissertação de Mestrado. Universidade do Estado do Rio de Janeiro

Clean Hydraulic Reclamation Technology and Clean Foundation Treatment Technology—Countermeasures to Contaminated Fills



Jianxiu Wang, Linbo Wu, Xuexin Yan, Zhao Wu, Guanhong Long, Hanmei Wang, and Na Xu

Abstract On basis of amount of collected information on geotechnic features and pollution distribution within reclaimed soils in China, well transportable heavy metal contaminants (both Zn and Ni) within China's major reclaimed lands were focused herein. Accordingly, both CHRTs and CFRTs proposed by the authors were summarized. To verify the injection and pumping method transformed from the clean pit dewatering method, FDN modeling was done taking stochastic dredge fills within Hengsha Island of Shanghai as the object soils. Numerical analysis results showed the injection and pumping method worked well when acting as a type of CFRT, remediating the stochastic dredge fills and quickening their consolidation simultaneously.

Keywords Land reclamation · Soil pollution · Clean hydraulic reclamation technology · Clean foundation treatment technology

1 Introduction

Coastal land reclamation in mainland China, excluding Hong Kong, Macao, and Taiwan, has been developed rapidly since the early twenty-first century. China's large-scale reclaimed fields were formed since early this century to the end of 2016.

J. Wang (✉) · L. Wu · Z. Wu · G. Long · N. Xu
College of Civil Engineering, Tongji University, Shanghai 200092, China
e-mail: wang_jianxiu@163.com

J. Wang
Key Laboratory of Geotechnical and Underground Engineering of Ministry of Education, Tongji University, Shanghai 200092, China

CCCC Key Laboratory of Environment Protection & Safety in Foundation Engineering of Transportation, Guangzhou 510230, China

X. Yan · H. Wang
Key Laboratory of Land Subsidence Monitoring, Prevention and Control of Ministry of Land and Resources, Shanghai Institute of Geological Survey, Shanghai 200072, China

These fields exceed 1860 km², and over 80% of these areas are involved in hydraulic reclamation technology. China's Shanghai reclaimed over 300 km² new coastal land during this period, acting as one of the major land reclamation zones in China [1].

Evaluation on potential pollution of eight heavy metal elements and five types of organic contaminants within reclaimed soils from China's major reclaimed zones, show worrying contamination probably exists in many large-scale reclaimed zones. Taking well transportable heavy metal contaminants Zn and Ni as examples, we can find that the two contaminants show points over the China's limit in Jinzhou Gulf in the city of Huludao (L8), Yangtze River estuary- Hangzhou Gulf (L28-L37), Ou River estuary (L39), Xiamen Gulf-Jiulong River estuary (L47-L49) and Pearl River estuary (L53-L57), and Ni also appears over limit in Bohai Gulf (L11-L13) and Qinzhou Gulf (L62) [1]. Land subsidence evaluation using data from over one thousand boreholes, shows the large-scale reclaimed zone in Shanghai would suffer from long term remarkable surface subsidence caused by land reclamation, indicating effective foundation treatments should be done before those fields are used for construction [2].

Given the potential geo-hazards revealed in China's major reclaimed zones, Wang et al. [1] proposed clean foundation treatment technology (CFTT), integrating foundation treatment and field remediation into one process, and clean hydraulic reclamation technology (CHRT) depolluting polluted sediments when using them for land reclamation. This paper introduced several CFTTs and CHRT developed by the authors. Considering widespread heterogeneity of reclaimed soils in Shanghai, we built stochastic geo-model for one typical reclaimed field in Hengsha Island, Shanghai, and verified validation of one of the introduced CFTTs using finite difference numerical (FDN) modeling.

2 Clean Foundation Treatment Technologies

Three Chinese patents applied by the authors are introduced herein. Firstly, a draining and depollution apparatus is mainly constituted of transferred PVD and depollution pocket, the PVC wick conducts groundwater from the soil to the depollution pocket, and detergent within the depollution pocket would adsorb contaminants within the polluted water, the detergent is chosen according to chemical properties of contaminants (Fig. 1) [3]. This apparatus is designed for slightly polluted fields, and the contaminants should be well transportable in groundwater. Given that it needn't other supports (e.g., electric power) and is convenient to be produced and set, this apparatus can be used for large-scale field and work for long term (e.g., several years).

Secondly, a clean pit dewatering method (CPDM) couples pit dewatering technologies and reaction barrier together (Fig. 2) [4]. Part of the wall used for pit dewatering is designed as reaction barrier, to depollute contaminated water within confined layers. These patents can also be used in reclaimed fields after some transformation. Given newly reclaimed layers in Shanghai usually show 3–10 m thick, no significant confined water exists in them, but excess pore pressure exists for long

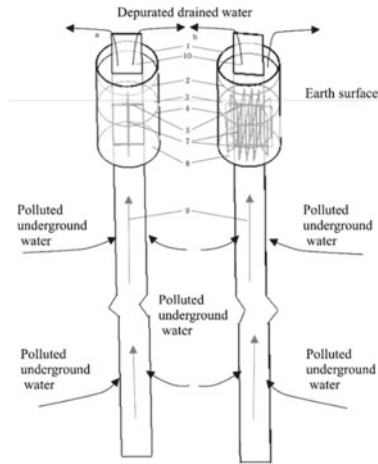


Fig. 1 Structure of the draining and depollution apparatus. 1. Upper geopocket, 2. Upper geomembrane, 3. Buffer material, 4. Separating geomembrane, 5. Geomembrane sleeve, 6. Rubber block, 7. Wick drain, 8. Detergent, 9. Filter membrane, 10. PVC wick [3]

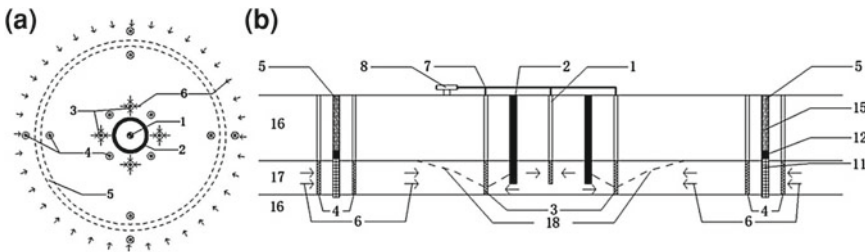


Fig. 2 Structure of the clean pit dewatering method. 1. Draining well, 2. Water-proof curtain, 3. Head-lowering well, 4. Monitoring well, 5. Permeable reaction ditch, 6. Seepage, 7. Draining pipe, 8. Pump, 9. Steel pipe, 10. Well screen, 11. Permeable reaction barrier, 12. Clayey fill, 13. Sandy fill, 14. Cone piece, 15. Blocky fill, 16. Aquitard, 17. Aquifer, 18. Water table [4]

term due to land reclamation construction process, and the shallow sedimentary layer widely shows as well conductive sandy-silty layer. Thus injection-pump wells work together with walls can act as a CFTT, verified in the FDN analysis section.

The vacuum preloading and flushing method (VPFM) couples vacuum preloading foundation treatment with in-site soil flushing (Fig. 3) [5]. Given that vacuum preloading method usually is utilized in fine soils, and that in-site soil flushing method requires the soil to be coarse, the vacuum preloading and flushing method probably works well in silty soils.

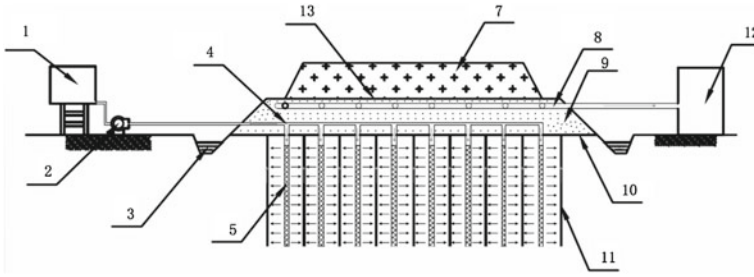


Fig. 3 Structure of VPFM with drift preloading method. 1. Eluent box, 2. Booster pump, 3. Seal groove, 4. Injection system, 5. Injection, 7. External load, 8. Outlet pipe, 9. Sand layer, 10. Geotextile, 11. Wick drain, 12. Vacuum pump, 13. Geomembrane

3 Clean Hydraulic Reclamation Technologies

The presetting sand well-PVD drain and depollution apparatus integrates sand well, PVD, and depollution pocket together (Fig. 4) [6]. The component of sand well and the center tube in the core column enables its stability when preset in the construction water. Comparing with common PVD or sand well drain methods, the component of buoyance-controlling layered horizontal PVDs allows larger distance between neighboring drain apparatus, and this enables easier transportation of workers and instruments in the field without disturbing the presetting apparatus significantly. Some similar to the draining and depollution apparatus, this patent is also aimed at depollution of well transportable contaminants. Actually, preinstalled cube grid

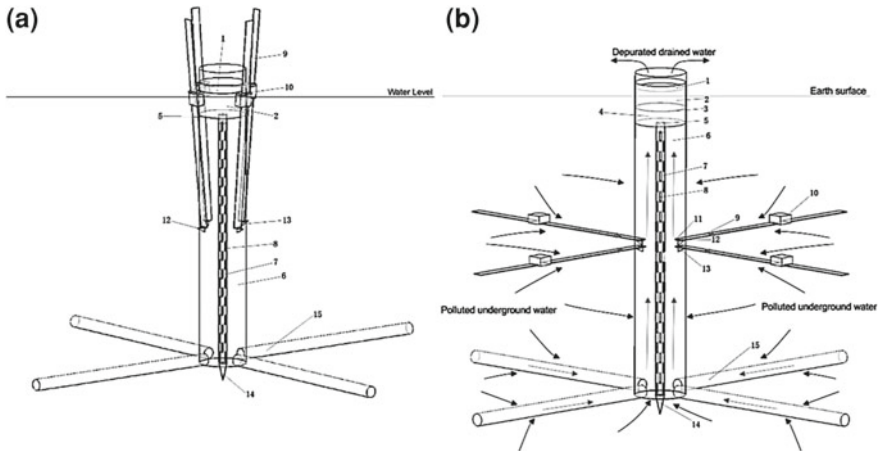


Fig. 4 A presetting pack-wick drain for both draining and decontamination. 1. Upper geopocket, 2. Fine sand, 3. Geomembrane, 4. Detergent, 5. Sleeve, 6. Lower geopocket, 7. Centre tube, 8. Permeable hole, 9. Wick drain, 10. Float piece, 11. Fastener, 12. Backing plate, 13. Dunnage, 14. Tube tip, 15. Bottom pack drain [6]

of plastic drain boards structure was proved to work well in boosting dredger fill consolidation [7], indicating the validation of in this apparatus.

4 Stochastic Geo-Modeling

On basis of detailed survey in reclaimed zone of Hengsha Island, this paper chose a typical reclaimed field therein of around 6 km² to do the stochastic geo-modeling and numerical analysis. Analyzing borehole data detected in 2016–2017 of the study field and the neighboring zones, we found the fills above –2 m are all silty fills, but the below fills shows six major types of fills distribute heterogeneously. Analyzing geotechnic data of the six types of fills below –2 m, we found that fills can be divided into two groups on basis of these hydraulic conductivity, compression modulus, and porosity. The two groups of soils, i.e., the clayey fill and the silty-sandy fill, get their geotechnic parameters using means of the detected data in 2016. T-PROGS is a program building stochastic geo-models on basis of transitional probability geo-statistics [8]. Stochastic geo-model of the fills below –2 m was built. Considering the borehole data and the requirement of Peclet number and Courant number for the contaminant transport numerical analysis, the grids distribute homogeneous in horizontal directions, 15 m × 15 m per grid horizontal plane, and the height of per grid is 0.4 m (Fig. 5c). Using borehole Hg04 and borehole Hg05 to cross-validate the stochastic geo-model, we found that spatial order of the different fill layers fit well to the facts, although some differences exist in exact positions of each fill layer (Fig. 5d).

5 Finite Difference Numerical (FDN) Analysis

On basis of field survey data, we took 11.6 m thick reclaimed layer and the 4 m thick sandy-silty layer below the fills for the numerical model (Fig. 5). The contaminant is Zn showing over limit in some reclaimed points of Shanghai [1], Zn concentration in each type of soil and other key parameters is shown in Table 1. CFTT transformed from CPDM was modeled in the analysis. Arrangement of wells and water-proof curtain in the treatment field are shown in Fig. 6. Given groundwater PH within the study zone ranges from 7.7 to 8.2, indicating a very low Zn concentration in the groundwater due to low solubility of Zn²⁺ in alkalic solution [9], and the major Zn contamination within the fills was considered in format of Zn(OH)₂. To depollute the Zn contamination, acid water of PH = 2 was injected in the field.

Subsidence and Aquifer-System Compaction program (SUB) can be used to build 3D groundwater flow field and 1D vertical consolidation model [10]. PHT3D program, coupling PHREEQC-2 and (Nonreactive transport model) MT3DMS together, can be applied to simulate transport of multi chemical components, and influence of changing PH [11]. Using the stochastic geo-model data, we built the

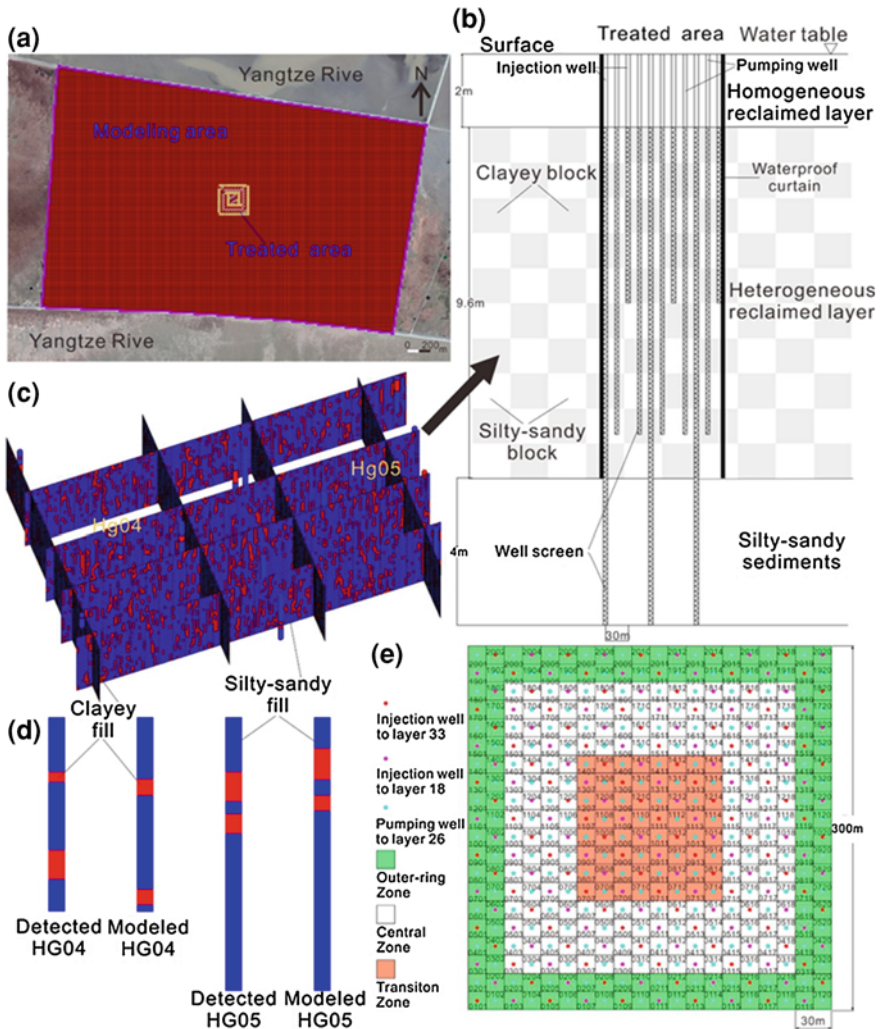


Fig. 5 Geo-model for the numerical analysis. **a** Plane distribution of the modeling area, **b** Schematic section of the treated area, **c** Stochastic model for the heterogeneous reclaimed layer, **d** Verification for the geo-modeling, **e** Distribution of wells in the treated area

comprehensive geo-model (Fig. 6b). Evolution of Zn^{2+} , $Zn(OH)_2$, and PH distribution within the layers was analyzed using PHT3D, and evolution of vertical displacement under the same treatment was analyzed using SUB. The injection and pumping treatment can be divided into two stages, the remediation stage (0–450.5 d) and the field consolidation stage (450.5–454.1 d). In the remediation stage, eluent was injected into the field using the injection wells, and flushing water was pumped out from the pumping wells. In the field consolidation stage, pore water within the field

Table 1 Key soil parameters in the numerical model

Layer	Kv(m/d)	Kh(m/d)	Porosity	Se(m ⁻¹)	Si(m ⁻¹)	SY	SS(m ⁻¹)	LD (m)	PH	Zn ²⁺ (mol/L)	Zn(OH) ₂ (mol/L)
Homogeneous fill	2.39×10^{-1}	3.92×10^{-1}	0.50	5.10×10^{-4}	1.53×10^{-2}	0.28	1.58×10^{-2}	10	8	3.06×10^{-6}	4.25×10^{-3}
Inter blocks	4.13×10^{-3}	5.73×10^{-3}	0.51	2.55×10^{-3}	7.64×10^{-2}	0.05	7.90×10^{-2}	10	8	3.06×10^{-6}	4.25×10^{-3}
Aquifer blocks	2.39×10^{-1}	3.92×10^{-1}	0.43	5.10×10^{-4}	1.53×10^{-2}	0.28	1.58×10^{-2}	10	8	3.06×10^{-6}	4.25×10^{-3}
Underlying sediments	1.62×10^{-1}	2.34×10^{-1}	0.45	1.96×10^{-4}	5.88×10^{-3}	0.21	6.08×10^{-3}	10	8	3.06×10^{-6}	4.25×10^{-4}

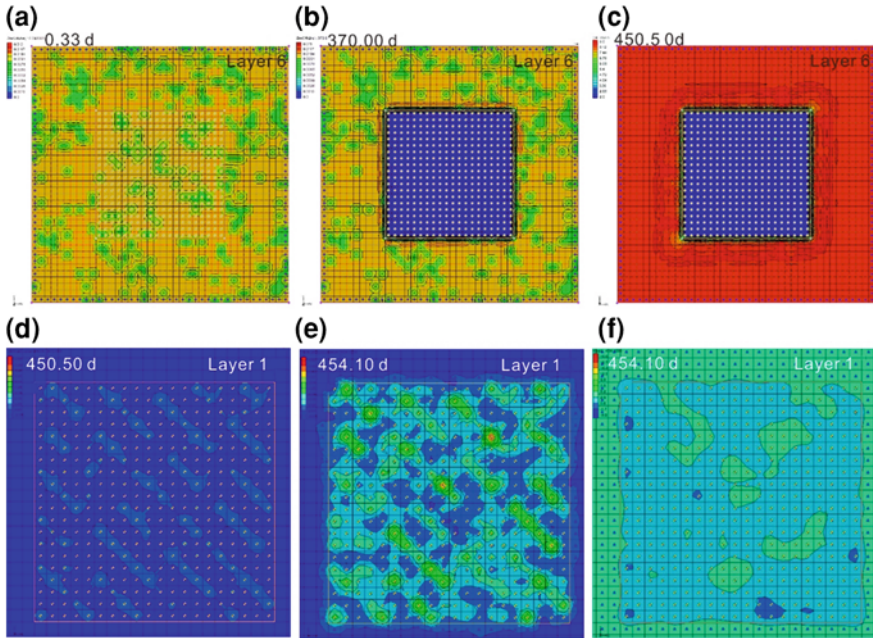


Fig. 6 Numerical modeling results. Zn(OH)_2 concentration within layer 6 at 0.33 d (a) and 370.00d (b), c. PH distribution within layer 6 at 450.50 d, d. Surface subsidence at 0.33 d (d) and 370.00d (e), f. Surface head distribution at 454.10 d

was pumped out using both the injection wells and pumping wells to facilitate the layers to consolidate.

PHT3D requires the simulated area to be saturated, majority of Zn contaminant should be removed during the remediation stage, and the field contaminated reclaimed layers kept saturated during this stage, but it would become unsaturated during the field consolidation stage. Thus only the remediation stage was analyzed using PHT3D, and the numerical model parameters are shown in both Fig. 6 and Tables 1 and 2. The vertical displacement evolution within the field during both the remediation stage and field consolidation stage was numerically modeled using SUB, and the model parameters are listed in Fig. 6 and Tables 1 and 2.

The chemical equilibriums considered herein are [11]:



Table 2 Key well parameters in the numerical model

Wells	Time since start (d)	Flow rate(m ³ /d)		PH	Zn ²⁺ (mol/L)	Zn(OH) ₂ (mol/L)
		Injection well	Pumping well	Injection well	Injection well	Injection well
Outer-ring Zone, W1110	450	1	-1	2	0	0
	450.5	0	-1	2	0	0
	451.7	-1	-1	2	0	0
	454	-1(-0.8)	0	2	0	0
Transiton Zone	450	1	-0.9	2	0	0
	450.5	0	-0.9	2	0	0
	451	-1	-0.9	2	0	0
	454	-1(-0.8)	0	2	0	0
Central Zone	450	1	-1.1	2	0	0
	450.5	0	-1.1	2	0	0
	451.7	-1	-1.1	2	0	0
	454	-1(-0.8)	0	2	0	0

6 Results

The Numerical modeling analysis using PHT3D shows that Zn(OH)₂ within the whole 24 layers of dredge fill was depolluted to a safe level after 370 d remediation treatment (Fig. 6a, b), given that China's Zn contamination threshold for soils (PH > 7.5) is 2.55e-3 mol/L (300 ppm). During the remediation stage, Zn(OH)₂ in the clayey fill shows a quicker depollution than that in the silty-sandy fill, and the acid eluent did not significantly intrude into the neighboring area (Fig. 6c). No significant subsidence happened during the remediation stage (Fig. 6d). Surface subsidence increased rapidly during the 3.6 days of foundation treatment (450.5–454.1 d), the subsidence distributed heterogeneously and mainly happened within the treated area. The largest subsidence can reach 50 cm ±, and controlled mainly by location of wells pumping groundwater out (Fig. 6e). The surface water head in the treated area generally recovered to the start head level (Fig. 6f).

7 Discussion and Conclusions

The injection and pumping method herein couples injection wells, pumping wells, and water-proof barrier into a CFFT. Using acid water (PH = 2) as eluent, it can be used to depollute Zn(OH)₂ contamination within the dredger fills with the layers to be significantly compacted simultaneously. Considering the VPFM proposed by Wang et al. [5], efficiency of the injection and pumping method probably can be improved

through adding vacuum load into the object layers. The real layer compaction caused by the injection and pumping method is probably larger, because the SUB only takes head change into consideration for soil compaction analysis. And further theory studies and field practices should be conducted to enable the proposed CHRTs and CFTTs more practical.

Acknowledgments This work is supported by China's National Key R&D Program (2017YFC0806000), China's National Key Basic Research Program (2014CB046901); Shanghai Pujiang Program (15PJD039); Shanghai Municipal Science and technology project (18DZ1201301); Opening fund of State Key Laboratory of Geohazard Prevention and Geoenvironment Protection (SKLGP2018K019); Fund of Shanghai Institute of Geological Survey.

References

1. Wang JX, Wu LB, Deng YS, Song DS, Liu WJ, Hu MZ, Liu XT, Zhou J (2018) Investigation and evaluation of contamination in dredged reclaimed land in China. *Mar Georesour Geotechnol* 36(5):603–616
2. Wang JX, Wu LB, Yang TL, Jiao X, Deng YS, Liu XT (2017) Spatio-temporal reconstruction of multiphase reclaimed Layers and prediction on corresponding land subsidence in Shanghai, China. In: 15th IACMAG. October. Wuhan, China, pp 730–740
3. Wang JX, Wu LB, Liu WJ, Zhang YC, Liu YY (2018) A draining and depollution apparatus. CN106638550A
4. Wang JX, Wu LB, Deng YS, Song DS, Zhang YC (2017) A clean pit dewatering method. CN105839655A
5. Wang JX, Wu LB, Deng YS, Gu QW, Liu XT, Zhang YC (2018) A vacuum preloading and flushing method. CN108005057A
6. Wang JX, Wu LB, Deng YS, Gu QW, Song DS (2018) A presetting sand well-PVD drain and depollution apparatus. CN106638549A
7. Yang P, Tang YQ, Wang JX, Yang Y, An X (2012) Test on consolidation of dredger fill by cube grid of plastic drain board preinstalled. *Eng Geo* 127:81–85
8. Carle SF (1999) T-PROGS: Transition probability geostatistical software Version 2.1, Hydrologic Sciences Graduate Group University of California, Davis
9. Reichle RA, Mccurdy KG, Hepler LG (1975) Zinc hydroxide: solubility product and hydroxy-complex stability const. *Revue Canadienne De Chimie* 53(24):3841–3845
10. Hoffmann J, Leake SA, Galloway DL, Wilson AM (2003) MODFLOW-2000 ground-water model—user guide to the subsidence and aquifer-system compaction (SUB) package. Open-File Report 03–233, US Geological Survey
11. Prommer H, Post V (2010) PHT3D: A reactive multicomponent transport model for saturated porous media (Version 2.10), User's Manual. <https://www.pht3d.org>

Nanobioremediation of Soils Contaminated with Lindane: Overview and Research Challenges



Liang Zhao, Jyoti K. Chetri, and Krishna R. Reddy

Abstract γ -hexachlorocyclohexane (γ -HCH, also called γ -BHC and lindane) as a halogenated organic insecticide has become an issue of environmental concern over the years. The isomers of hexachlorocyclohexanes (HCHs) mainly consist of α -HCH, β -HCH, γ -HCH, and δ -HCH. Among these isomers, only γ -HCH has insecticidal applications and thus, leading to cumulative toxic effects through bioaccumulation in food chains. The demand for techniques to decontaminate γ -HCH in soils is gradually growing. The previous studies investigated integrated nanobioremediation techniques involving the use of nanoparticles and indigenous microbes, on the degradation of halogenated organic contaminants, especially lindane, in soils and groundwater. The application of nanomaterials, for instance nanoscale zero-valent iron (nZVI), has recently been researched extensively. However, its efficiency is limited by low aqueous solubility and high hydrophobicity of the contaminants. Moreover, the degradation of contaminants by nanomaterials may not be complete resulting relatively high levels of toxic intermediates. This critical review highlights (i) the applications of nanoparticles for the degradation of γ -HCH (nanoremediation); (ii) the applications of microorganisms for γ -HCH remediation (bioremediation); and (iii) the combination of nanoremediation and bioremediation through the application of nanomaterials and microbes, respectively, in order to achieve effective remediation of γ -HCH (nanobioremediation). Further research on effective biological methods complementing nanoremediation is needed to the development of effective and efficient remediation strategies for recalcitrant halogenated organic contaminants in the subsurface environments.

Keywords Nanoremediation · Bioremediation · Nanobioremediation · Lindane · Nanoscale iron particles · Microorganisms · Contaminated soils

L. Zhao (✉) · J. K. Chetri · K. R. Reddy
University of Illinois at Chicago, Chicago, IL 60607, USA
e-mail: lzhao42@uic.edu

1 Introduction

γ -Hexachlorocyclohexane (γ -HCH/ γ -BCH), commonly and commercially known as lindane, is a notorious organochlorine pesticide severely affecting the public health and environment due to its persistence, high toxicity, mobility in soils and groundwater, bioaccumulation in the food chain, long-range transport potential, and recalcitrant characteristics in the atmosphere, which led to the prohibition of the production of lindane in most countries [1]. The Stockholm Convention on persistent organic pollutants (POPs) is a global treaty which was started in 2001 to protect human health and environment from the adverse effects of the chemicals that are persistent and toxic [2]. The 2001 convention obliged the involved parties to limit and restrict the production and use of the twelve POPs which are also referred as the “dirty dozen.” Nine new chemicals were listed under the Stockholm Convention in 2009 and lindane was one of those nine chemicals [3]. Lindane is banned for agricultural use in the countries that signed the Stockholm Convention on POPs; however, the use of lindane in pharmaceutical applications such as in shampoos for treatment of lice is in practice in many countries [4]. The major lindane production sites were reported to exist in India and China [5]. About 600,000 tons of lindane was estimated to be applied globally in agriculture, medicine, and other industries between 1950 and 2000, and around 1,600,000–1,900,000 million tons of HCH residues were estimated to be present worldwide [6].

Once lindane enters the soil, it can be either adsorbed onto the soil particles or enter atmosphere through volatilization, leach into groundwater, and infiltrate into subsurface [7]. Thus, the lindane and its isomers have the potential to be present in soils, groundwater, and air, hence threatening the public health and the environment [1, 8]. The health effects of lindane have been studied extensively for many decades and still being studied. The recent studies include study of the toxic effects of lindane on soil [8], groundwater, mammals [9], and plants [10]. It has been shown that the HCH isomers, especially lindane, may cause serious consequences to public health in either short or long term. Lindane has carcinogenic, teratogenic, genotoxic, and mutagenic effects on mammals [11] Likewise, Pesce et al. [12] reported that certain dose of lindane may cause respiratory dysfunctioning, trembling, hyper-salivation, and convulsions, which may be lethal in extreme situations. Lindane has been linked to the adverse effects on female reproductive system including adverse effects on gestation and labor [13, 14]. The U.S. Environmental Protection Agency (USEPA) has classified lindane as B₂ carcinogens.

Lindane, like other organochlorine pesticides, is known to be recalcitrant in the environment and has the propensity of bioaccumulation and biomagnification resulting in chronic health effects. The severity of the adverse effects of lindane on the public health and environment makes lindane contamination a widespread and intractable problem in the environmental protection. Therefore, mitigation of lindane contamination in soils, groundwater, and air has been given due attention for many years. Many researchers have been involved in exploring remedial measures for lindane contamination. There are several methods developed for treatment of

lindane contaminated soils and water sources which include conventional methods such as soil washing [4], soil flushing [15, 16], vitrification [15], phytoremediation [17–19], thermal desorption [20], and electrochemical remediation [21–23]. Recently, nanobioremediation is considered as an emerging approach toward lindane degradation. This paper first reviews the properties of lindane, and then provides an overview of nanoremediation, bioremediation, and their combination known as nanobioremediation. Finally, future research needed to overcome the current limitations of nanobioremediation and understand the fundamental biochemical processes involved is discussed.

2 Properties of Lindane

HCH isomers are the most commonly used and easily detectable organochlorine pesticides in the environmental samples [24]. Lindane is the γ isomer of the eight isomers (α , β , γ , δ , ϵ , η , and θ) of 1, 2, 3, 4, 5, 6-hexachlorocyclohexane. Among all the isomers, γ -HCH is the most commonly applied insecticide and could potentially be transferred to α -HCH and β -HCH with higher toxicity (ATSDR [25]). γ -HCH is commonly produced by the photochemical chlorination of benzene with UV light. Some other isomers such as α , β , ϵ , and δ HCH are also produced as by-products during this process. γ -HCH is the most effective or strongest insecticide among all the isomers of HCH [26]. Table 1 summarizes important physical and chemical properties of γ -HCH or lindane. Lindane is characterized with low water solubility and high hydrophobicity (high $\log K_{ow}$ (Octanol-water partition coefficient)) and tendency for bioaccumulation in biota.

3 Nanoremediation

Persistent and bioaccumulative nature of γ -HCH in the environment warrants serious remedial measures for lindane contamination. The natural degradation of lindane is a slow process and may require very long period of time. Hence, some active treatment methods are preferred. Nanoremediation has emerged as a fast and efficient chemical treatment method.

Nanoremediation involves the application of reactive nanomaterial such as nanoscale zero-valent iron (nZVI), iron sulfide (FeS) nanoparticles, metal nanoparticles (such as iron nanoparticles (FeNPs)), bimetallic nanoparticles (such as Ag/Fe, Ni/Fe, and Cu/Fe), etc. for the transformation and detoxification of pollutants. Nanoremediation has emerged as a novel and effective solution for environmental clean-up which is applicable for wide range of contaminants such as chlorinated compounds, hydrocarbons, and organic compounds. It plays a crucial role in the pollution prevention, detection, monitoring, and remediation of the environmental pollutants [27]. Many researchers have explored the application of nanoparticles

Table 1 Physical and chemical properties of γ -HCH

Properties	γ -HCH
Molecular formula	C ₆ H ₆ Cl ₆
Molecular weight	290.830
Boiling point	311 °C
Melting point	112-113 °C
Solubility in water	7.3 mg/L at 25 °C
Solubility in acetone	>200 g/L at 25 °C
Solubility in hexane	12.6 g/L at 20 °C
Specific gravity	1.85
Corrosivity	Corrosive to metals
Color/form	White crystalline powder
Stability	Stable under recommended storage conditions
log K _{ow}	3.7 ± 0.5
Bioconcentration factor in human fat	19 ± 9
Bioconcentration factor in aquatic animals	2.5 ± 0.4
EPA toxicity classification	Class II

in remediating various pollutants in the environment. For example, Li et al. [28] highlighted the methods of synthesis and characterization of nZVI and its application in the treatment of organic and inorganic pollutants. nZVI showed significant removal of lindane from contaminated groundwater [28]. Similarly, Román et al. [29] reported lindane degradation by laboratory-synthesized polymer-stabilized iron nanoparticles in aqueous solution. Dominguez et al. [30] studied degradation of lindane in soil, water, and groundwater using five commercial iron microparticles with different physical and chemical properties. In addition to the nZVI, Paknikar et al. [31] explored lindane degradation approach by FeS nanoparticles and proposed a cost-effective solution to the problem of removal of lindane from water. Román et al. [32] investigated use of nZVI and polymer-stabilized nanoparticles for lindane degradation and developed analytical methods to measure and detect lindane and its by-products formed during degradation. Recently, Rawtani et al. [33] compared the degradation potential of nZVI and polymer-stabilized nZVIs and reported dichloro elimination and dehydrohalogenation as the prime mechanism behind lindane degradation.

Among all nanoscale particles that are available for degradation of lindane, nZVI is currently the most widely used nanoparticles [27]. Metal nanoparticles, such as NANOFER 25S suspension and NANOFER STAR powder are among the few commercially available nZVI particles manufactured in Europe and have the potential for effective remediation of soils and groundwater contamination. However,

only a few studies have explored the performance of these particles in remediating pollutants. For example, Zhuang et al. [34] and Laumann et al. [35] evaluated the remediation capability of one of the types of NANOFER particles. However, to our knowledge, none of the studies in the past have explored the abilities of NANOFER to degrade lindane in contaminated soils. Vinod et al. [36] explored the application of commercial stabilized nZVI called NANOFER STAR powder for the removal of chromium and volatile organic compounds such as cis-dichloroethene, perchloroethene, and trichloroethene from water.

Some researchers explored the effect of iron nanoparticles on the surrounding environment. Keller et al. [37] studied the toxic effects of three commercial nZVIs (NANOFER 25, NANOFER 25S, and NANOFER STAR) and recommended to prevent the transport of injected nZVI beyond the target remediation area. NANOFER STAR is a dry air-stable, flammable powder which contains 65–80% of Fe⁰ and 35–20% of iron oxide content. The surface of nanoparticles is stabilized by a thin layer of iron oxide preventing nZVI from its immediate oxidation in contact with atmospheric oxygen. NANOFER 25S is aqueous suspension of water (77%), iron (14–18%), magnetite (2–6%), surfactant (3%), and carbon (0–1%) [38].

4 Bioremediation

Bioremediation is a technique for degrading contaminants in soils and water, which involves creating favorable conditions to stimulate the growth of microorganisms to degrade or immobilize the pollutants [39]. Bioremediation technique has been commonly used for remediating wide range of contaminants. In the recent years, several researchers have explored the potential of bioremediation by using consortia of several bacterial and fungal species for degrading lindane in contaminated soils and water. For instance, Rigas et al. [40] explored the ability of the fungus *Pleurotus ostreatus* to facilitate the degradation of lindane and reported an optimum lindane degradation rate of 0.16 g kg⁻¹ month⁻¹. Nagata et al. [41–43], and Tabata et al. [44] reported the degradation potential, degradation pathways, genes, and enzymes for lindane degradation in *Sphingomonas paucimobilis* UT26. Likewise, Benimeli et al. [45, 46] reported the lindane bioremediation abilities in bacterial strain *Streptomyces* sp. M7 which was isolated in the laboratory from wastewater sediment samples of a copper filter plant, a pesticides-contaminated site. Guillén-Jiménez et al. [1] isolated a fungal strain, the *Fusarium verticillioides* AT-100 strain, from Agava tequilana leaves that is able to use lindane as a carbon and energy source under aerobic condition. Salam et al. [47] and Salam and Das [48] reported a novel yeast strain, *Rhodotorula* sp. VITJzN03, isolated from sorghum cultivation field, and *Candida* VITJzn04, isolated from sugarcane cultivation fields, respectively, both utilizing lindane as a sole source of carbon for growth, thereby degrading lindane.

Recently, Egorova et al. [49] showed that the bioaugmentation of the contaminated soil with the bacterial strain *Rhodococcus wratislaviensis* Ch628 led to a significant reduction in the toxicity of the HCH contaminated soil, especially γ -HCH. Bajaj

et al. [50] found the halophilic bacterium *Chromohalobacter* sp. LD2 isolated from HCH dumpsite to be an effective degrader of γ -HCH in saline environments. The bacterial strain showed 89.6% removal of lindane in 7 days. Umadevi et al. [51] listed *Bacillus* sp., *Exiguobacterium aurantiacum*, *Pandoraea* sp., *Pseudomonas pseudoalcaligenes*, and *Micrococcus luteus* as the microorganisms capable of degrading lindane. Similarly, Manickam et al. [5] isolated a bacterial strain *Xanthomonas* sp. ICH12 from HCH contaminated site, which was capable of degrading lindane. In addition, Manickam et al. [5] showed dechlorination of all four isomers of HCH (α , β , γ , δ) by *Sphingomonas* sp. NM05 which was isolated from HCH contaminated sites. Okeke et al. [52] isolated bacterial strain *Pandoraea* sp. From enrichment culture, which showed lindane removal of 25 and 45.5% in liquid cultures of two bacterial isolated LIN-1 and LIN-3, respectively.

Among the microorganisms, actinobacteria have been studied for degradation of lindane in recent years. *Arthrobacter citreus* BI-100 was able to completely degrade lindane [53] and *Microbacterium* ITRC1 had the ability to degrade all the major four isomers of HCH including lindane [54]. Most of the extensive research studies that have been done in recent years on bioremediation of lindane contamination in laboratory scale are leading to the pervasive problem of massive field application. Hence, a new approach toward degradation of lindane was developed by few researchers which combined the methods of nanoremediation and bioremediation and proposed a concept of nanobioremediation (NBR).

5 Nanobioremediation

Recently, the application of nanobioremediation for environmental clean-ups is proposed as it is realized that one single technique may not be economically sustainable and/or feasible for all ranges of pollutants. It is significant to develop combined technologies which involve multiple techniques in sequence to overcome the defects in each single technology and save resources [55]. Nanobioremediation is an emerging technology for remediation of recalcitrant contaminants and with the aid of biosynthetic nanoparticles, this technology can be deployed at the sites where conventional remediation technologies proved ineffective [55].

The integrated remediation technology aims for effective, efficient, sustainable remediation, and possible field scale application. Nanobioremediation involves the application of nanoremediation including nanoparticles such as nZVI and nanoscale FeS initially to reduce the contaminants to the conducive levels to microbes, bacteria and fungi and subsequently apply bioremediation of the contaminants to reach the risk-based levels. Few pioneering research studies have been published in the field of nanobioremediation of lindane. Paknikar et al. [31] reported the potential of biopolymer-stabilized iron nanoparticles on lindane degradation. Singh et al. [56] proposed an integrated nanobioremediation technique involving the initial application of Pd/Fe and then *Sphingomonas* sp. strain NM05 for the degradation of lindane

in soil. Their study showed that the integrated system or nanobioremediation had 1.7–2.1 times more efficiency than the individual systems.

To date, very few studies have explored the nanobioremediation technique to degrade lindane. Hence, there is profound scope to further investigate the effects of nanobioremediation technique involving the use of various types of nanoparticles, such as nZVI, FeS, FeNPs, and various types of bacterial strains such as *Spingomonas paucimobilis* and *Streptomyces* sp., for the degradation of lindane, a pervasively utilized pesticide and well-documented recalcitrant organic contaminant. Biological processes occurring in the soil subsequent to nanoremediation should also be explored and optimized.

6 Conclusions

Lindane is one of the legacy contaminants which is highly persistent, bioaccumulative, and possesses adverse effects on human health and the environment. Although, the manufacture and agricultural use of lindane is banned in many countries, the risks of contamination are still prevalent as it is highly persistent in nature. This paper summarized the remedial measures for lindane contamination with the main focus on nanoremediation, bioremediation, and nanobioremediation. The investigation demonstrates the development, fate, and future prospective of lindane degradation technologies. Although the results of lindane remediation are advanced, there are still some challenges that need to be overcome. Firstly, since the complicated and variable environmental factors affect the physical and chemical properties of nanoparticles, such as nZVI and the negative impacts of nanoparticles on microorganisms induce adverse consequences on the results of degraded lindane concentration, the combined nanobioremediation needs further investigations. Secondly, majority of the past studies were conducted on a laboratory scale, which necessitates extensive additional research on field applications of lindane remediation as the field conditions are complicated and difficult to predict.

References

1. Guillén-Jiménez FDM, Cristiani-Urbina E, Cancino-Díaz JC, Flores-Moreno JL, Barragán-Huerta BE (2012) Lindane biodegradation by the *Fusarium verticillioides* AT-100 strain, isolated from Agave tequilana leaves: kinetic study and identification of metabolites. *Int Biodeterior Biodegradation* 74:36–47
2. Lallas PL (2001) The Stockholm Convention on persistent organic pollutants. *American Journal of International Law* 95(3):692–708
3. Stockholm Convention. Talks to spotlight nine new chemicals, alternatives to DDT and the challenges of a POPs-free Future. Press release - COP4 - Geneva (2009). Available at: <http://chm.pops.int/Implementation/PublicAwareness/PressReleases/COP4Geneva,4May2009/tabid/509/Default.aspx>

4. Muñoz-Morales M, Braojos M, Sáez C, Cañizares P, Rodrigo MA (2017) Remediation of soils polluted with lindane using surfactant-aided soil washing and electrochemical oxidation. *J Hazard Mater* 339:232–238
5. Humphreys EH, Janssen S, Heil A, Hiatt P, Solomon G, Miller MD (2007) Outcomes of the California ban on pharmaceutical lindane: clinical and ecologic impacts. *Environ Health Perspect* 116(3):297–302
6. Vijgen J, Yi LF, Forter M, Lal R, Weber R (2006) The legacy of lindane and technical HCH production. *Organohalogen Comp* 68:899–904
7. Walker K, Vallero DA, Lewis RG (1999) Factors influencing the distribution of lindane and other hexachlorocyclohexanes in the environment. *Environ Sci Technol* 33(24):4373–4378
8. Saez JM, Bigliardo AL, Raimondo EE, Briceño GE, Polti MA, Benimeli CS (2018) Lindane dissipation in a biomixture: Effect of soil properties and bioaugmentation. *Ecotoxicol Environ Saf* 156:97–105
9. Steffan JJ, Brevik EC, Burgess LC, Cerdà A (2018) The effect of soil on human health: an overview. *Eur J Soil Sci* 69(1):159–171
10. Bragança I. et al. Ecotoxicological Effects of Insecticides in Plants Assessed by Germination and Other Phytotoxicity Tools. In: Vats S. (eds) *Biotic and Abiotic Stress Tolerance in Plants*. Singapore (2018)
11. Salam JA, Das N (2012) Remediation of lindane from environment-an overview. *International Journal Advanced Biology Research* 2:9–15
12. Pesce SF, Cazenave J, Monferran MV, Frede S, Wunderlin DA (2008) Integrated survey on toxic effects of lindane on neotropical fish: *Corydoras paleatus* and *Jenynsia multidentata*. *Environ Pollut* 156(3):775–783
13. Fanning RA, Champion DP, O’Shea M, Carey MF, O’Connor JJ (2017) A comparison of the effects of lindane and FeCl₃/ADP on spontaneous contractions in isolated rat or human term myometrium. *Reprod Toxicol* 74:164–173
14. Tiemann U (2008) In vivo and in vitro effects of the organochlorine pesticides DDT, TCPM, methoxychlor, and lindane on the female reproductive tract of mammals: a review. *Reprod Toxicol* 25(3):316–326
15. Jiang Danni, Zeng Guangming, Huang Danlian, Chen Ming, Zhang Chen, Huang Chao, Wan Jia (2018) Remediation of contaminated soils by enhanced nanoscale zero valent iron. *Environ Res* 163:217–227
16. Lemaire J, Buès M, Kabeche T, Hanna K, Simonnot MO (2013) Oxidant selection to treat an aged PAH contaminated soil by in situ chemical oxidation. *Journal of Environmental Chemical Engineering* 1(4):1261–1268
17. Abhilash PC, Singh B, Srivastava P, Schaeffer A, Singh N (2013) Remediation of lindane by *Jatropha curcas* L: utilization of multipurpose species for rhizoremediation. *Biomass Bioenerg* 51:189–193
18. Nagpal V, Paknikar KM (2006) Integrated biological approach for the enhanced degradation of lindane. *Indian Journal of Biotechnology* 5:400–406
19. Salam JA, Hatha MA, Das N (2017) Microbial-enhanced lindane removal by sugarcane (*Saccharum officinarum*) in doped soil-applications in phytoremediation and bioaugmentation. *J Environ Manage* 193:394–399
20. León VM, Alvarez B, Cobollo MA, Muñoz S, Valor I (2003) Analysis of 35 priority semivolatiles in water by stir bar sorptive extraction–thermal desorption–gas chromatography–mass spectrometry: I. Method optimization. *J Chromatogr A* 999(1–2):91–101
21. Reddy KR, Darko-Kagya K, Al-Hamdan AZ (2011) Electrokinetic remediation of chlorinated aromatic and nitroaromatic organic contaminants in clay soil. *Environ Eng Sci* 28(6):405–413
22. Rodrigo MA, Oturan N, Oturan MA (2014) Electrochemically assisted remediation of pesticides in soils and water: a review. *Chem Rev* 114(17):8720–8745
23. Waclawek S, Antoš V, Hrabák P, Černík M, Elliott D (2016) Remediation of hexachlorocyclohexanes by electrochemically activated persulfates. *Environ Sci Pollut Res* 23(1):765–773
24. Willett KL, Ulrich EM, Hites RA (1998) Differential toxicity and environmental fates of hexachlorocyclohexane isomers. *Environ Sci Technol* 32(15):2197–2207

25. Agency for Toxic Substances and Disease Registry (ATSDR). U.S. Department of Health and Human Services. Toxicologic profile for alpha-, beta, gamma- and delta-hexachlorocyclohexane. (2005)
26. Mullins LJ (1955) Structure-toxicity in hexachlorocyclohexane isomers. *Science* 122(3159):118–119
27. Patil SS, Shedbalkar UU, Truskewycz A, Chopade BA, Ball AS (2016) Nanoparticles for environmental clean-up: a review of potential risks and emerging solutions. *Environmental Technology & Innovation* 5:10–21
28. Li XQ, Elliott DW, Zhang WX (2006) Zero-valent iron nanoparticles for abatement of environmental pollutants: materials and engineering aspects. *Crit Rev Solid State Mater Sci* 31(4):111–122
29. San Román I, Galdames A, Alonso ML, Bartolomé L, Vilas JL, Alonso RM (2016) Effect of coating on the environmental applications of zero valent iron nanoparticles: the lindane case. *Sci Total Environ* 565:795–803
30. Dominguez Carmen M, Rodríguez Sergio, Lorenzo David, Romero Arturo, Santos Aurora (2016) Degradation of Hexachlorocyclohexanes (HCHs) by Stable Zero Valent Iron (ZVI) Microparticles. *Water Air Soil Pollution* 227:446
31. Paknikar KM, Nagpal V, Pethkar AV, Rajwade JM (2005) Degradation of lindane from aqueous solutions using iron sulfide nanoparticles stabilized by biopolymers. *Sci Technol Adv Mater* 6(3–4):370–374
32. San Román I, Alonso ML, Bartolomé L, Galdames A, Goiti E, Ocejo M, Vilas JL (2013) Relevance study of bare and coated zero valent iron nanoparticles for lindane degradation from its by-product monitorization. *Chemosphere* 93(7):1324–1332
33. Rawtani D, Khatri N, Tyagi S, Pandey G (2018) Nanotechnology-based recent approaches for sensing and remediation of pesticides. *J Environ Manage* 206:749–762
34. Zhuang Y, Jin L, Luthy RG (2012) Kinetics and pathways for the debromination of polybrominated diphenyl ethers by bimetallic and nanoscale zerovalent iron: effects of particle properties and catalyst. *Chemosphere* 89(4):426–432
35. Laumann S, Micić V, Lowry GV, Hofmann T (2013) Carbonate minerals in porous media decrease mobility of polyacrylic acid modified zero-valent iron nanoparticles used for groundwater remediation. *Environ Pollut* 179:53–60
36. Vinod VTP, Wactawek S, Senan C, Kupčák J, Pešková K, Černík M, Somashekarappa HM (2017) Gum karaya (*Sterculia urens*) stabilized zero-valent iron nanoparticles: characterization and applications for the removal of chromium and volatile organic pollutants from water. *RSC Advances* 7(23):13997–14009
37. Keller AA, Garner K, Miller RJ, Lenihan HS (2012) Toxicity of nano-zero valent iron to freshwater and marine organisms. *PLoS ONE* 7(8):e43983
38. Gil-Díaz M, Díez-Pascual S, González A, Alonso J, Rodríguez-Valdés E, Gallego JR, Lobo MC (2016) A nanoremediation strategy for the recovery of an As-polluted soil. *Chemosphere* 149:137–145
39. Sharma, H. D., and Reddy, K. R. *Geoenvironmental engineering: site remediation, waste containment, and emerging waste management technologies*. John Wiley & Sons (2004)
40. Rigas F, Papadopoulou K, Philippoussis A, Papadopoulou M, Chatzipavlidis J (2009) Bioremediation of lindane contaminated soil by *Pleurotus ostreatus* in non sterile conditions using multilevel factorial design. *Water Air Soil Pollut* 197(1–4):121–129
41. Nagata Y, Miyauchi K, Damborsky J, Manova K, Ansorgova A, Takagi M (1997) Purification and characterization of a haloalkane dehalogenase of a new substrate class from a gamma-hexachlorocyclohexane-degrading bacterium, *Sphingomonas paucimobilis* UT26. *Appl Environ Microbiol* 63(9):3707–3710
42. Nagata Y, Miyauchi K, Takagi M (1999) Complete analysis of genes and enzymes for γ -hexachlorocyclohexane degradation in *Sphingomonas paucimobilis* UT26. *Journal of Industrial Microbiology and Biotechnology* 23(4–5):380–390
43. Nagata Y, Natsui S, Endo R, Ohtsubo Y, Ichikawa N, Ankai A, Tsuda M (2011) Genomic organization and genomic structural rearrangements of *Sphingobium japonicum* UT26, an

- archetypal γ -hexachlorocyclohexane-degrading bacterium. *Enzyme and Microbial Technology* 49(6–7):499–508
44. Tabata M, Ohhata S, Nikawadori Y, Kishida K, Sato T, Kawasumi T, Nagata Y (2016) Comparison of the complete genome sequences of four γ -hexachlorocyclohexane-degrading bacterial strains: insights into the evolution of bacteria able to degrade a recalcitrant man-made pesticide. *DNA Res* 23(6):581–599
 45. Benimeli, C. S., Castro, G. R., Chaile, A. P., and Amoroso, M. J. (2006). Lindane removal induction by *Streptomyces* sp. M7. *Journal of Basic Microbiology*, 46(5), 348–357 (2006)
 46. Benimeli, C. S., Fuentes, M. S., Abate, C. M., and Amoroso, M. J. Bioremediation of lindane-contaminated soil by *Streptomyces* sp. M7 and its effects on *Zea mays* growth. *International Biodeterioration and Biodegradation*, 61(3), 233–239 (2008)
 47. Salam, J. A., Lakshmi, V., Das, D., and Das, N. Biodegradation of lindane using a novel yeast strain, *Rhodotorula* sp. VITJzN03 isolated from agricultural soil. *World Journal of Microbiology and Biotechnology*, 29(3), 475–487 (2013)
 48. Salam JA, Das N (2014) Lindane degradation by *Candida* VITJzN04, a newly isolated yeast strain from contaminated soil: kinetic study, enzyme analysis and biodegradation pathway. *World J Microbiol Biotechnol* 30(4):1301–1313
 49. Egorova Darya O, Buzmakov Sergei A, Nazarova Elmira A, Andreev Dmitryi N, Demakov Vitaly A, Plotnikova Elena G (2017) Bioremediation of Hexachlorocyclohexane-Contaminated Soil by the New *Rhodococcus wratislaviensis* Strain Ch628. *Water Air Soil Pollution* 228:183
 50. Bajaj, S., Sagar, S., Khare, S., and Singh, D. K. Biodegradation of γ -hexachlorocyclohexane (lindane) by halophilic bacterium *Chromohalobacter* sp. LD2 isolated from HCH dumpsite. *International Biodeterioration and Biodegradation*, 122, 23–28 (2017)
 51. Umadevi, S., Ayyasamy, P. M., and Rajakumar, S. Biological Perspective and Role of Bacteria in Pesticide Degradation. In *Bioremediation and Sustainable Technologies for Cleaner Environment* (pp. 3–12). Springer, Cham (2017)
 52. Okeke BC, Siddique T, Arbertain MC, Frankenberger WT (2002) Biodegradation of γ -hexachlorocyclohexane (lindane) and α -hexachlorocyclohexane in water and a soil slurry by a *Pandora* species. *J Agric Food Chem* 50(9):2548–2555
 53. Datta, J., Maiti, A. K., Modak, D. P., Chakrabarty, P. K., Bhattacharyya, P., Ray, and P. K. Metabolism of γ -hexachlorocyclohexane by *Arthrobacter citreus* strain BI-100: Identification of metabolites. *Journal of General and Applied Microbiology*, 46, 59–67 (2000)
 54. Manickam, N., Mau, M., and Schlömann, M. Characterization of the novel HCH-degrading strain, *Microbacterium* sp. ITRC1. *Applied Microbiology and Biotechnology*, 69(5), 580–588 (2006)
 55. Koul, B., and Taak, P. *Biotechnological Strategies for Effective Remediation of Polluted Soils*. (2018)
 56. Singh R, Manickam N, Mudiam MKR, Murthy RC, Misra V (2013) An integrated (nano-bio) technique for degradation of γ -HCH contaminated soil. *J Hazard Mater* 258:35–41
 57. American Type Culture Collection Product Sheet: *Sphingomonas paucimobilis* (ATCC 29837) and *Streptomyces* sp. (ATCC 55186). (2018)
 58. Barsan, M. E. NIOSH pocket guide to chemical hazards. Department of Health and Human Services. Center for Disease Control and Prevention, DHHS (NIOSH). Publication (2007)
 59. Mulligan Catherine N, Eftekhari Farzad (2016) Remediation with surfactant foam of PCP-contaminated soil". *Eng Geol* 70(3–4):269–279
 60. Cecchin I, Reddy KR, Thomé A, Tessaro EF, Schnaid F (2017) Nanobioremediation: Integration of nanoparticles and bioremediation for sustainable remediation of chlorinated organic contaminants in soils. *Int Biodeterior Biodegradation* 119:419–428
 61. Giácoman-Vallejos G, Lizarraga-Castro I, Ponce-Caballero C, González-Sánchez A, Hernández-Núñez E (2018) Presence of DDT and Lindane in a Karstic Groundwater Aquifer in Yucatan, Mexico. *Groundwater Monitoring & Remediation* 38(2):68–78
 62. Haynes WM (2014) *CRC Handbook of Chemistry and Physics*, 95th edn. CRC Press LLC, Boca Raton, pp 3–292
 63. Lewis, R. J. *Sax's dangerous properties of industrial materials*, Vol. 8, New York (1996)

64. Manickam, N., Reddy, M. K., Saini, H. S., and Shanker, R. Isolation of hexachlorocyclohexane-degrading *Sphingomonas* sp. by dehalogenase assay and characterization of genes involved in γ -HCH degradation. *Journal of Applied Microbiology*, 104(4), 952–960 (2008)
65. Manickam, N., Misra, R., and Mayilraj, S. A novel pathway for the biodegradation of γ -hexachlorocyclohexane by a *Xanthomonas* sp. strain ICH12. *Journal of Applied Microbiology*, 102(6), 1468–1478 (2007)
66. MacBean, C. e-Pesticide Manual. Alton (UK). British Crop Protection, Council. Glyphosate (1071-83-6) (2008)
67. Richardson LT, Miller DM (1960) Fungitoxicity of chlorinated hydrocarbon insecticides in relation to water solubility and vapor pressure. *Can J Bot* 38(2):163–175
68. Tripathi V, Abhilash PC, Singh HB, Singh N, Patra DD (2015) Effect of temperature variation on lindane dissipation and microbial activity in soil. *Ecol Eng* 79:54–59

Spirodela Polyrhiza: An Efficient Hyperaccumulator of Nickel at Low Concentration



Chandrima Goswami, Kaushik Bandyopadhyay, and Arunabha Majumder

Abstract Over a few years of time, heavy metal pollution in surface water has increased manifold owing to large scale dependency upon industrialization and modernization. Therefore, an effective removal of heavy metal pollution is important. Phytoremediation is an eco-friendly and cost-effective method of heavy metal removal by different plant species from water. The process has been utilised in the present investigation to remove Ni from contaminated water by duckweed *Spirodela polyrhiza*. At three different initial concentrations 2.92, 3.9, and 4.9 mg/L of Ni in contaminated water, removal of Ni by *Spirodela polyrhiza* has been studied together with their morphological changes. Bio concentration factor for Ni removal was obtained to be greater than 1000 at initial Ni concentrations of 2.92 and 3.9 mg/L, respectively. The results therefore suggest that duckweed *Spirodela polyrhiza* can efficiently remove as well as uptake Ni from contaminated water with minimal signs of toxicity symptoms.

Keywords Nickel · *Spirodela polyrhiza* · Bio concentration factor

1 Introduction

Today heavy metal pollution in water is a global environmental problem. Heavy metal pollution in urban waterbodies has been increasing due to its large scale usage in different industries and the simultaneous discharge of untreated or partially treated wastewater into the nearby aquatic bodies. There are different conventional treatment methods like adsorption, chemical precipitation, membrane filtration, etc. for remediation of heavy metal pollution in water [1]. Apart from other chemical treatment

C. Goswami (✉)

School of Environmental Studies, Jadavpur University, Kolkata, WB, India

e-mail: chandrima2345@gmail.com

K. Bandyopadhyay

Department of Construction Engineering, Jadavpur University, Kolkata, WB, India

A. Majumder

School of Water Resources Engineering, Jadavpur University, Kolkata, WB, India

© Springer Nature Switzerland AG 2020

K. R. Reddy et al. (eds.), *Sustainable Environmental Geotechnics*, Lecture Notes in Civil Engineering 89, https://doi.org/10.1007/978-3-030-51350-4_22

207

processes, phytoremediation is a green technology that is not only environment-friendly but also cost-effective [2]. In this process, plants are used to remediate pollution from water or soil. Plants have an innate ability to remove and uptake different toxic metals in their biomass and arrest them [3, 4]. This bioaccumulation capacity of plant is known to vary from species to species [5] and is a sustainable method of managing water pollution. Duckweeds are small, free-floating aquatic macrophytes belonging to Lemnaceae family and are known to accumulate different toxic metals in their biomass [5]. The pollutant removal efficiency of duckweeds has been utilised by many researchers for different heavy metals like cadmium, copper [5, 6]; chromium [2], and lead, etc. The aim of the present investigation includes the study of effectiveness of *Spirodela polyrhiza* to tolerate, remove as well as uptake Ni from contaminated water. The effect of Ni on growth of *Spirodela polyrhiza* as well as the accumulation potential of the duckweed was therefore studied. In India, application of phytoremediation is in the initial stages and therefore further investigations are required to be done. Its application can definitely bring about a green solution to the sustainable management of toxic wastes.

2 Materials and Methods

Spirodela polyrhiza were collected from an unpolluted pond near Salt Lake Campus of Jadavpur University, Kolkata to study its efficiency in removal and uptake of Ni from contaminated water. Further they were washed with tap water followed by distilled water to remove the debris and were further acclimatized with the pond water collected from the same pond in 25L plastic tubs over an experimental period of 22 days.

The experimental set up was run in duplicates. It included 40 g of *Spirodela polyrhiza* exposed to different concentrations 2.92, 3.9, and 4.9 mg/L of Ni. The 20L Ni contaminated water in each tub was prepared by dilution of stock solution of Ni prepared with nickel chloride salt. A control set up was also maintained with the same amount of *Spirodela polyrhiza* cultured with the same pond water with no Ni. Evaporation loss from the experimental tub was compensated with the addition of pondwater from outside, whenever necessary. pH of the working solution was monitored regularly. Water samples from the experimental tubs were collected on certain interval of days. Ni in the contaminated water was estimated by Atomic Absorption Spectrophotometer (AAS). On completion of experimental period of 22 days, *Spirodela polyrhiza* were harvested, dried, and digested. Further, the Ni content in the duckweed was analysed with AAS.

3 Results and Discussion

3.1 Morphological Symptoms

With increase in initial concentration of Ni in aqueous solution, fresh biomass of duckweed *Spirodela polyrhiza* was found to decrease compared to that of control after 22 days of experimental period. Chlorosis in the fronds was noticed after 10th day of exposure of duckweeds to 4.9 mg/L Ni initial concentration. At initial Ni concentrations of 2.92 and 3.9 mg/L, no visible sign of toxicity symptoms was noticed that suggests Ni does not generate toxic effect on *Spirodela polyrhiza* at such lower concentrations. In earlier research, authors have found duckweeds *Lemna minor* as well as *Spirodela polyrhiza* to be highly sensitive to the presence of Ni in contaminated water and therefore utilised them in ecotoxicological testing [7].

3.2 Percentage Removal of Nickel

Duckweeds have an innate ability to remove and uptake heavy metals in their biomass. Axtell et al. [8] obtained 82% preferential Ni removal when they exposed *Lemna minor* to different concentrations of Ni and Pb. Othman et al. [4] obtained *Lemna minor* to be a potential phytoremediator that had the ability to clean up heavy metal pollution from aquatic bodies. In the present investigation, results presented in Fig. 1 showed significant critical differences ($p = 0.05$) for removal of Ni by *Spirodela polyrhiza* at different initial concentrations of Ni. At initial Ni concentration of 2.92 mg/L, maximum Ni removal (72.26%) was obtained over an experimental

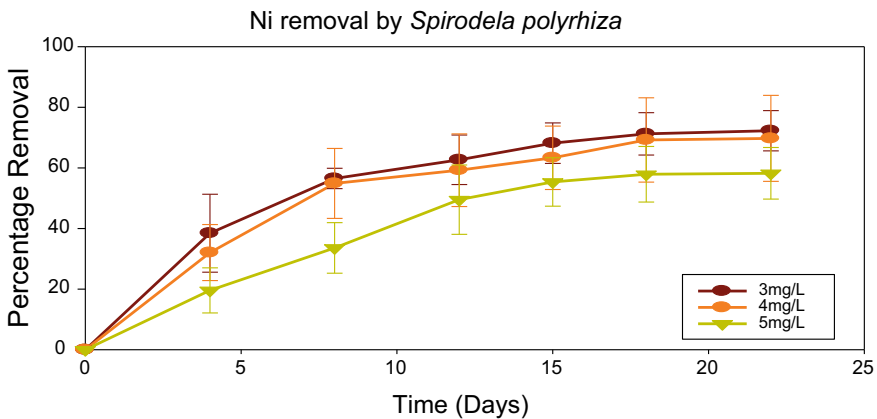


Fig. 1 Percentage removal of Ni by *Spirodela polyrhiza* at different initial concentrations. Bars denote \pm standard deviation from the mean of three replicates

period of 22 days. With further increase in initial Ni concentration, percent removal of Ni was found to decrease [9]. The reduction in percentage removal at higher initial Ni concentrations was probably due to increase in Ni ions with the sites of adsorption for the metal ions on the plant biomass remaining the same. At lower initial metal concentrations, adsorption sites on plants were sufficient enough for the sorption of metal ions. With increase in exposure period, removal of Ni increased but the rate of removal was found to decrease gradually. Positive correlation was obtained ($R^2 = 0.84$, $p < 0.005$) between the initial Ni concentration in the ambient solution and the concentration of Ni removed from the solution after 22 days.

3.3 Bio Concentration Factor

At a lower Ni concentration of 2.92 mg/L, Bio Concentration Factor (BCF) of *Spirodela polyrhiza* exposed to Ni was found to be maximum. BCF values at 2.92 mg/L and 3.9 mg/L were obtained to be more than 1000 and the values are 2383.9 and 1153.48 for initial concentrations of 2.92 and 3.9 mg/L, respectively. Thus we obtain that at lower Ni concentrations, *Spirodela polyrhiza* can hyperaccumulate Ni.

At higher concentration of 4.9 mg/L, BCF was found to decrease to 750.88 (Fig. 2). Correlation between Ni in ambient solution and BCF of Ni by *Spirodela polyrhiza* was strongly negative and significant ($r = -0.94$, $p < 0.005$). Other researchers also obtained similar results of efficient bioaccumulation of heavy metals (Ni, Cu, Cd) at lower concentrations by duckweeds [10]. When *Spirodela polyrhiza* L. was exposed to different metals at different concentrations, it was reported that the accumulation of metals was directly related to their individual concentrations in the medium [11]. To study the toxicity of Ni on the chloroplasts of *Spirodela polyrhiza*, Appenroth et al.

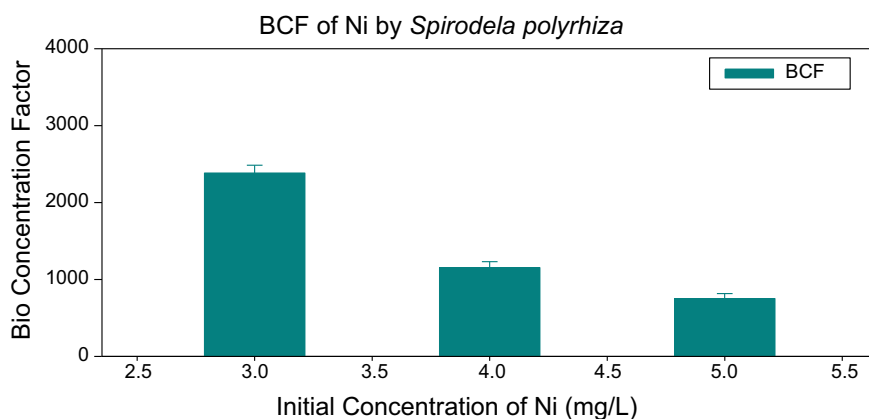


Fig. 2 Bio Concentration Factor of *Spirodela polyrhiza* exposed to Ni at different concentrations. Bars denote \pm standard deviation from the mean of three replicates

[7] exposed the duckweeds to 4 and 100 μM Ni concentrations over an experimental period of 7 days, and the bio concentration factors were obtained to be 100 and 80, respectively. This explains moderate toxic effect of Ni with reduced accumulation by the duckweed.

4 Conclusion

Phytoremediation is a well-defined remedial technology for heavy metals. From the present investigations, we can suggest that *Spirodela polyrhiza* could be utilised for the removal of Ni from contaminated water. A maximum of 72.26% Ni removal was obtained at initial Ni concentration of 2.92 mg/L and the removal rate decreased with increase in concentration further. The duckweed is very less affected with Ni at low concentrations of 2.92 and 3.9 mg/L with minimal signs of toxicity. From the Bio Concentration Factor (BCF), the duckweed is found to be an efficient accumulator and hence hyper accumulates Ni at low concentrations of 2.92 and 3.9 mg/L. There are scopes for research work further to obtain removal and accumulation at higher concentrations as well. This is a novel work which highlights a green solution to the sustainable management of toxic wastes.

References

1. Appenroth KJ, Krech K, Keresztes A, Fischer W, Koloczek H (2010) Effects of nickel on the chloroplasts of the duckweeds *Spirodela polyrhiza* and *Lemna minor* and their possible use in biomonitoring and phytoremediation. *Chemosphere* 78:216–223
2. Axtell NR, Sternberg SPK, Claussen K (2003) Lead and nickel removal using *Microspora* and *Lemna minor*. *Bioresource technology* 89:41–48
3. Bennicelli R., Stepniewska Z., Banach A., Szajnocha K., Ostrowski J.: The ability of *Azolla caroliniana* to remove heavy metals (Hg(II), Cr (III), Cr (VI) from municipal waste water. *Chemosphere* 55, 141-146 (2004).
4. Duman F, Leblebici Z, Aksoy A.: Bioaccumulation of Nickel, Copper, and Cadmium by *Spirodela polyrhiza* and *Lemna gibba*. *Journal of freshwater Ecology*, 24 (1), 177-179 (2009).
5. Gaur J.P, Noraho N., Chauhan Y.S.: Relationship between heavy metal accumulation and toxicity in *Spirodela polyrhiza* L. *Schleid* and *Azolla pinnata* R.Br., *Aquatic botany*, 49 (2-3), 183-192 (1994).
6. Goswami C., Majumder A., Misra A.K., Bandyopadhyay K.: Efficiency of *Spirodela polyrhiza* for the removal of nickel and chromium from wastewater, Proc. of Vth World Aqua Congress, Conference, New Delhi, (2011).
7. Khellaf N, Zerdaoui M (2010) Growth, Photosynthesis and respiratory response to copper in *Lemna minor*: a potential use of duckweed in biomonitoring toxic. *Iran J. Environ Health Sci Eng.* 7(2):299–306
8. Mishra V.K., Upadhyay A.R., Pathak V., Tripathi B.D.: Phytoremediation of Mercury and Arsenic from Tropical Opencast Coalmine Effluent Through Naturally Occurring Aquatic Macrophytes, *Water Air Soil Pollution* 192, 303– 314 (2007).

9. Othman R, Ramya R, Baharuddin ZM, Hashim KSH-Y, Yaman M (2015) Response of Lemna minor and Salvinianatans as phytoremediation agents towards Fe, Cu and Zn toxicities via in vivo model system. *JurnalTeknologi* 77(30):101–109
10. Soltan ME, Rashed MN (2003) Laboratory study on the survival of water hyacinth under several conditions of heavy metal concentrations. *Advances in Environmental Research* 7:321–334
11. Verma R. And SutharSurindra: Lead and cadmium removal from water using duckweed-Lemnagibba L.: impact of pH and initial metal load. *Alexandria Engineering Journal*, 54, 1297-1304 (2015).

Enhancement of Water Reuse by Treating Wastewater in Constructed Wetlands: Minimization of Nutrients and Fecal Coliform



B. Lekshmi, Rahul S. Sutar, Dilip R. Ranade, Yogen J. Parikh, and Shyam R. Asolekar

Abstract “CW4Reuse” *i.e.*, Constructed Wetland for Reuse technology, the eco-centric, low-cost approach for the management of domestic wastewaters has been developed at IIT Bombay, Mumbai. The Town of Mhaswad in the State of Maharashtra, India (population 25,000) has been perpetually facing drought to the extent that the livestock suffers death or migration during the summer months. In this study, the performance of the wastewater treatment plant based on ‘CW4Reuse’ technology has been investigated. Raw untreated wastewater polluted the Manganga River till the constructed wetland was commissioned. The treatment plant consists of nine horizontal subsurface flow constructed wetland beds each having dimension of 18 m × 4 m and 0.6 m depth. The constructed wetland beds are vegetated with *Canna indica* species. The present study investigates the system’s performance with respect to BOD₅, COD, TP, TKN as well as fecal coliform. The operating conditions and routines shall be mapped with the corresponding efficiencies of removal of TP, TKN, and fecal coliform with the aim to maximize the removal of nutrients and pathogenicity. Currently, the treatment system is removing 74% COD and 92% of BOD₅, while the treatment plant is subject to around 250 mg/L of COD and 100 mg/L BOD₅. It is recognized that the community would like to put the treated water for high-end reuse applications including toilet flushing, floor washing, and other body contact applications for vegetables and cash-crop cultivation. Kinetic studies are being conducted in the existing treatment systems by varying different operating conditions to achieve improved performance.

Keywords Constructed wetland · Natural treatment system · Wastewater treatment · Rural sanitation · Fecal coliform · Nutrients

B. Lekshmi · R. S. Sutar · D. R. Ranade · Y. J. Parikh · S. R. Asolekar (✉)
Centre for Environmental Science and Engineering, IIT Bombay, Mumbai, India
e-mail: asolekar@gmail.com

© Springer Nature Switzerland AG 2020

K. R. Reddy et al. (eds.), *Sustainable Environmental Geotechnics*, Lecture Notes in Civil Engineering 89, https://doi.org/10.1007/978-3-030-51350-4_23

1 Introduction

Direct discharge of wastewaters or partially treated wastewaters is one of the prime sources of pollution in coastal zones and drinking water reservoirs. Eutrophication in the surface waters is directly governed by the nutrients such as nitrogen and phosphorous in the wastewater. Conventional wastewater treatment technologies for domestic wastewaters often fail to meet the discharge standards in the long run. Moreover, the operational costs of those treatment systems are often the most expensive. In recent years, stringent environmental regulations on discharge standards are stipulated to control the pollutant discharge into water bodies. Therefore, developing sustainable decentralized solutions for wastewater treatment is inevitable. Sustainable solutions continuously benefit the ecosystem in the long run.

Low maintenance costs, greater economic, environmental, and social sustainability are the main features of natural treatment systems. Constructed wetlands (CWs) are one of the promising natural treatment technologies. Some of the other treatment technologies in this class happen to be waste stabilization ponds, duckweed ponds, oxidation ditches, etc. CWs are an optimistic prospect as it eliminates macro and well as micro-pollutants while preserving the ecosystem. Horizontal subsurface flow constructed wetlands (HSSF-CWs) are one of the most common engineered wetlands used in the treatment of domestic wastewater [1].

HSSF-CWs utilize plants, substrate, and associated rhizosphere microorganisms to remove or transform contaminants from wastewaters and provide better landscape integration. Several worldwide studies have reported that the CWs found to be efficient technology in the treatment of wastewater by the removal of organics, nutrients, suspended solids, pathogens, heavy metals including other emerging contaminants. Removal of organic pollutants and nutrients from wastewater using CWs are exclusively studied by various researchers [2–6].

CWs are eco-friendly, cost-effective treatment technology recommended for the treatment of wastewaters, especially in peri-urban and rural areas in India. However, CWs treatment technology is less explored in India and also there were less successful real-life WWTPs currently operated with this technology for domestic wastewater [4]. Kinetic studies on pollutant removal and significance of rate constants in the design and operation of constructed wetlands have been reported by various researchers [7–11]. The removal performance for pollutants in constructed wetlands are well predicted using the first-order degradation kinetic model even though the limitations are well recognized by many researchers [12]. The aim of the present study is to evaluate the system's performance in terms of removal of BOD₅, COD, TP, TKN, as well as fecal coliform in HSSF-CWs since there is lack of data for calibration of kinetic models in the tropical climate.

2 Materials and Methods

2.1 Study Area

The study area was constructed wetland based wastewater treatment plant ($17^{\circ}37'54.0''\text{N } 74^{\circ}47'06.4''\text{E}$) located in the Town of Mhaswad in the State of Maharashtra, India (Fig. 1). The Town of Mhaswad has a population of 25,000 [13]. The average rainfall in the study area for the period of 2013 to 2017 from Jul to Oct is around 173 mm and from Nov to Jun is around 10 mm [14]. Similarly, the annual daily minimum and maximum temperature in the region is observed to be 12.8°C and 37.2°C , respectively [15]. Consequently, the study area falls under the tropical dry climate and has been perpetually facing drought to the extent that the livestock suffers death or migration during the summer months from March to June. As a result, the community has been hoping to supplement their water supply with alternate renewable water sources within the prevailing water-cycle in the community to fulfill water demand for gardening, irrigation, fodder production, cattle rearing, (bathing, drinking, floor flushing), etc. The average domestic wastewater generated for the Town is around $750\text{ m}^3/\text{day}$ and the wastewater generated was previously discharged into the nearby Manganga River flowing through the town. In the current scenario, the 'CW4Reuse' wastewater treatment plant commissioned as shown in Fig. 1 is treating around $250\text{ m}^3/\text{day}$ of wastewater (generated by 30% population), followed by reuse for various applications.



Fig. 1 Aerial View of 'CW4Reuse' Treatment Plant at Mhaswad Town (Source: Google Maps)

2.2 Constructed Wetland Wastewater Treatment Plant

The wastewater treatment system is devised for bringing the raw wastewater (250 m³/day) from the Mhaswad community to the treatment plant by gravity. The wastewater is settled in the settling tank and subjected to treatment in nine beds of “CW4Reuse”- based treatment systems that are designed and constructed along the Riverfront of Manganga Lake in the Town. The “CW4Reuse” beds are planted with different flowing varieties of *Canna indica* (common name: Canna lily) species with yellow, orange, and red flowers. These plants are hydroponic in nature with broad leaves, ginger-like roots, and typically grow up to 2 m height. They are tropical herbs that belong to the Cannaceae family and have antibacterial, antiviral, anti-inflammatory, analgesic, antioxidant as well as cytotoxic effects [16]. Moreover, they have high nutrient removal efficiency and aesthetic value [17–19]. For the public acceptance of wastewater treatment plants, ornamental plants like *Canna* are recommended to enhance the aesthetic appearance in tropical climates [10].

In HSSF-CWs, wastewater is intended to stay behind the media (substrate) and flow of the water will be in and around media, root, and rhizome of plants. Organics, nutrients, and pathogen removal in CWs are governed by various processes, such as, aerobic microbial processes, anaerobic microbial processes, sedimentation, filtration, etc. [20]. Nitrification, denitrification, plant/microbial uptake, sorption/desorption, etc., are the main nitrogen removal mechanisms in CWs. Similarly, phosphorous removal is governed by adsorption/desorption, precipitation, plant/microbial uptake, etc. [21].

Each of the nine beds of “CW4Reuse” in the study site has dimensions of 18 m X 4 m X 0.6 m. The substrate used in the wetland beds have porosity previously estimated to be 0.5. The plant is fully operational from September 2017. The wetland beds are operated in batch mode with a hydraulic retention time (HRT) of 24 h. The treated water is collected in the collection tank and is pumped to the recreational garden which is around 5 m near the treatment plant (Fig. 1). During the summer months, the treated water is also transported by tankers to the “summer-fodder camp” to cater to nearly 3500 cattle. In the non-summer months, the excess treated water flows to the Manganga River adjoining the treatment plant and is eventually collected downstream in the water reservoir.

2.3 Kinetic Studies on Removal of Pollutants

Kinetic studies will allow comparison of uptake efficiency among different plant species, behavior in high pollutant loads, nutrient uptake, etc., of CWs [22, 23]. Kinetic studies on *Canna indica* for nutrient removal from wastewater was previously reported by Zhang et al. [24]. Kinetic studies are most significant to optimize the design criteria for constructed wetland systems. Kinetics of biodegradation of pollutants in CWs is conservatively assumed to be the first-order reaction [1]. The

first-order or pseudo-first-order rate expression is solved for the initial value problem, at $t = 0$, $C(t) = C_0$. Rate constants for CWs can be estimated by plotting $-\ln[C(t)/C_0]$ vs. batch reaction time (t) to give slope k (h^{-1}), where k is the pseudo-first-order rate constant (h^{-1}), $C(t)$ is the instantaneous concentration and t is the time in hours. In the present study, this model is used for interpreting rate constants for pollutant removal of domestic wastewater in HSSF-CW reactor beds.

Kinetics of pollutant uptake by wetland beds for this study was investigated in batch mode. Batch mode operations in horizontal subsurface flow reactors were more efficient than that of continuous flow operation as reported by various researchers [4, 25]. Year-round monitoring of wastewater treatment efficiency is carried out and the samples were collected during alternate months from January to December 2018. Inlet composite samples after the primary treatment (at 0 h) and outlet composite samples from the collection tank were collected (after 24 h of HRT) and transported to the IIT Bombay research laboratory for analysis. The removal rates were estimated from performance data for the pollutants COD, BOD, TKN, TP. Total of six batch experiments was conducted. The volumetric rate constant (k_v) of each of the parameters was determined from an average of all the batch experiments conducted.

2.4 Analysis of Wastewater

On each sampling event, influent and effluent composite samples from the nine beds of CW were collected, stored, and transported under refrigeration at 4 °C to IIT Bombay research laboratory. All analyses were performed as per standard procedures of the American Public Health Association [26]. The pH, dissolved oxygen (DO), the temperature, nitrate of the water samples collected were analyzed using portable HACH USA (HQ40d) meter. Total Suspended Solids (TSS) were analyzed by gravimetric method. Total phosphorus (TP) was analyzed by the ammonium molybdate spectrophotometric method, chemical oxygen demand (COD) was analyzed using closed reflux method and biochemical oxygen demand (BOD_5) was measured after incubation at 20 °C [26]. Total Kjeldahl Nitrogen (TKN) was analyzed using Kjeldahl block digestion unit (Borosil, India) and semi-automatic steam distillation unit (Borosil, India). All samples were analyzed in triplicates. Fecal coliforms (CFU) are analyzed by the membrane filtration method followed by incubation [26].

3 Results and Discussion

3.1 Removal Performance of 'CW4Reuse' WWTP

Influent pH (7.2–7.4) and effluent pH (7.6–7.9) of the samples were observed to be in the neutral range. The “CW4Reuse” removal efficiency of COD for HRT of 24 h

was observed to be $74 \pm 5\%$ with inlet concentrations in range of 160 to 360 mg/L after settling. Correspondingly, BOD_5 was removed for around $92 \pm 5\%$ ($n = 6$) for HRT of 24 h with inlet concentrations of around 100 ± 40 mg/L BOD_5 . For the treatment of different kinds of wastewater using HSSF-CWs, BOD and COD removal was reported to be highest in municipal wastewater [20]. As reported by the author, removal efficiencies for municipal wastewater using HSSF-CWs fall between 75 to 93% and between 64 to 82%, respectively, for BOD_5 and COD. Thus, the present study also demonstrates removal efficiencies in the similar range, especially towards the higher side despite the fact that there can be discrepancies in the operating conditions.

Nutrient removal in constructed wetlands are mainly governed by accumulation in plants, microbial action, adsorption, precipitation, etc. [21]. The nitrate concentrations in the inlet wastewater are considerably very low (<0.08 mg/L) and henceforth, organic and ammonia nitrogen removal is studied. The system performance for TKN removal is around $69 \pm 11\%$ with year-round inlet concentrations of 82 ± 14 mg/L. A review by Vymazal [21] reports mean total nitrogen removal of around 42% for HSSF-CWs studied by the author globally. Evidently, it reflects the fact that the performance of TKN removal in the present study is observed to be significant. The TP removal efficiencies were observed to be 48%, apparently less than that of other organics and nutrient removal. However, the reported range of TP varies between 40 to 60%, and TP removal in the HSSF-CWs are mainly governed by adsorption, plant uptake, and microbial uptake [21]. Preliminary analysis indicates 4 log removal for FC. Studies are in progress to authenticate the results. Hence, rate constants for FC were not determined due to less data points.

3.2 Kinetic Rate Constants for HSSF-CWs

Sutar et al., [7] have extensively reviewed various studies reporting the influence of rate kinetics in the treatment of wastewaters using constructed wetlands. In general, the studies reporting kinetic removal rates are limited to pilot-scale or laboratory scale CW systems. A small number of studies across the globe accounts for kinetic studies on the removal of pollutants in the full-scale CW treatment plants (Table 1). Volumetric rate constants (k_v) estimated from the study is presented in Table 1. Spatial variations in kinetic rate constants for BOD, TSS, and TP are less affected by the temperature of the wetland site [12]. Areal rate constants and volumetric rate constants reported from various studies were corrected to volumetric rate constants in h^{-1} basis for comparison [11]. The estimated volumetric rate constants k_V (h^{-1}) derived from areal rate constants, k_A (mh^{-1}) or k_A (my^{-1}) or volumetric rate constant, k_V (d^{-1}) reported in the literature given in Table 1. The rate constants discussed in further sections are limited to HSSF-CWs.

In the present study high organic and nutrient removal rate constants were observed. The rate constant for BOD_5 (0.0802 ± 0.017) was observed to be the highest. BOD rate constant for livestock wastewater treatment reported by Jamieson

Table 1 Estimated values of k (h^{-1}) for organics, nutrients and pathogens in removal kinetics of HSSF-CWs. For the present study, estimates were calculated from pseudo first-order rate expression for COD, BOD, TKN and TP

Sr. No	Scale of CW, Q (m^3/day) & No. of Beds	Type of Wastewater & Location	Species	Dimensions (L, W, D), Porosity (ϵ)	Parameters	Inlet and Outlet conc. (mg/L)	HRT, h	Rate Constant k_v (h^{-1})	Ref
1	Full scale, 250, 9	Domestic wastewater, Mhaswad, India	<i>Canna indica</i>	18 m (L), 4 m (W), 0.6 m (D), 0.5 (ϵ)	COD	365 - 164, 76 - 49	24	0.0553 ± 0.0071	This Study
					BOD ₅	199 - 62, 45-7	24	0.0802 ± 0.017	
					TKN	78-92, 33 - 16	24	0.0485 ± 0.0119	
2	Pilot-scale, 5.04, 4	Arusha, Tanzania	<i>Typha latifolia</i>	1.5 m (L), 0.5 m (W), 1 m (D), 0.35	COD	85, 19	144	0.0288	[9]
					FC	2.0 X 10 ⁶ , 2.4 X 10 ⁵	7	*0.1729	[28]
3	Full Scale, 95, 1	Domestic wastewater, Nunavut, Canada	<i>Salix spp</i> , <i>Bryophyte spp.</i> , <i>Hippuris vulgaris.</i> , <i>Carex spp.</i>	8374 m ² (SA), 0.07 m (D)	COD	127, 33	7	*0.1729	[28]
					FC	2.0 X 10 ⁶ , 2.4 X 10 ⁵	7	*0.3865	
					TN	47, 31	7	*0.0326	
4	Full Scale, 33	Waste water from the bird life, Beijing, China	<i>Lytthrum salicaria</i> , <i>Iris tectorum</i> , <i>Scirpus validus</i> ,	170 m ² (SA), 0.3 m (D); 160 m ² (SA), 0.1 m (D); 81 m ² (SA), 0.1 m (D)	NO ₃ -N	3.4, 1.22	-	*0.0185	[36]
					NH ₄ ⁺ -N	0.36, 0.27	-	*0.0096	
5	Pilot-scale, -, 6	Domestic wastewater, Thailand	<i>Canna</i>	2 m (L), 1 m (W), 1 m (D), 0.4 (ϵ)	COD	93 - 135, -	12-96	0.0295	[10]
					TN	17 - 27	12-96	0.0017	
					TP	6.7-9.8	12-96	0.0016	

(continued)

Table 1 (continued)

Sr. No	Scale of CW, Q (m ³ /day) & No. of Beds	Type of Wastewater & Location	Species	Dimensions (L, W, D), Porosity (ε)	Parameters	Inlet and Outlet conc. (mg/L)	HRT, h	Rate Constant <i>k_v</i> (h ⁻¹)	Ref
6	Pilot-scale, 0.18–1.35, 1	Aquaculture wastewater, Taiwan	<i>Phragmites australis</i>	5 m (L), 1 m (W), 0.8 m (D), 0.4 (ε)	NH ₄ ⁺ -N	0.18, 0.11	14.4	0.0071	[37]
					Ortho P	4.30, 3.53	14.4	0.0090	
7	Laboratory Scale, -, 16	Synthetic wastewater, Montana, USA	<i>Carex utriculata</i> , <i>Schoenoplectus acutus</i> , <i>Typha latifolia</i>	0.2 m (Ø), 0.5 m (D)-	COD	484-508, -	-	0.0373	[33]
					COD	484-508, -	-	0.0326	
					COD	484-508, -	-	0.0287	
8	Pilot-scale	Livestock wastewater, Nova Scotia, Canada	<i>Typha latifolia</i> , <i>Lenna spp</i>	20 m (L), 5 m (W) 0.8 m (D) & 0.15 m (D), -	BOD	1747, 34	2160	*0.0010	[29]
					TKN	237, 19	2160	*0.0006	
					TP	36.9, 7.1	2160	*0.0002	
					FC	216780, 3150	2160	*0.0012	
9	Full scale, 6.38, 6	Swine lagoon wastewater, Greensboro, North Carolina	<i>Typha latifolia</i> , <i>Schoenoplectus americanus</i>	40 m (L), 11 m (W), 0.75 m (D) 0.15 m (D), 0.45 (ε)	TN	116, 70	393.6	0.00113	[30]
					TP	56, 48	393.6	0.00042	

*Rate constants that are not corrected for ε factor due to unavailability of porosity data

et al. (2007) was quite low compared to the present study. COD rate constant (0.0553 ± 0.0071) for the present study was higher than similar studies conducted by Konnerup et al. [10] and Stein et al. [27]. On the other hand, the studies of Konnerup et al. [10] and Stein et al. [27] were pilot-scale compared to the present study. Only available removal rate constant for COD in full-scale treatment systems as per the knowledge of the author is reported by Hayward and Jamieson [28]. Hayward and Jamieson [28] reported the highest rate constants for COD and FC, which can be primarily due to the influence of HRT (7 h) maintained in the system. Generally, short term rate constants are observed to be higher than long term rate constants.

The TKN removal rates in the present study were comparable with Hayward and Jamieson [28]. Remarkably, removal rates of TKN (0.0485 ± 0.0119) and TP (0.0274 ± 0.0197) were observed higher than similar studies conducted by Jamieson et al. [29]; Stone et al. [30] and Konnerup et al., [10]. HRT is one of the factors governing the removal of nutrients in HSSF-CWs. Furthermore, the type of wetland vegetation and mode of operation must have influenced the reaction rate constants. Nitrogen and phosphorus removal are enhanced by batch mode of operations in HSSF-CWs [31–33]. On the other hand, BOD removal rate kinetics was not affected by batch or continuous mode operation [32]. Batch operational strategy is preferred for full-scale subsurface flow CWs when nutrient removal is desired [6]. One of the significant factors governing high nutrient uptake rates is reported to be the type of vegetation. Plants with fibrous roots (diameter ≤ 3 mm) like *Canna indica* reported to have high activity in the root zone, high photosynthetic and transpiration rate which governs the high removal rate of TP and TN [34, 35].

4 Conclusions

The present study successfully demonstrates the reuse of domestic wastewater using a community scale wastewater treatment plant based on HSSF-CWs. In summary, “CW4Reuse” based treatment system for domestic wastewater demonstrated high removal efficiencies for organics and nutrients with low HRT compared to other full-scale HSSF-CWs. The treated wastewater meets the reuse standards and is suitable for high-end applications. Type of vegetation, operational conditions, and adequate retention period may have influenced the high rate of removal of organics and nutrients in the present study. However, the influence of these parameters is not well determined due to the limited variability of HRT in our study. Further studies are desirable for assessing the factors governing removal rate constants. Kinetic studies using different HRTs will be beneficial for profoundly comprehending the influencing factors that govern rate constants in subsurface flow constructed wetlands.

Acknowledgments The authors hereby acknowledge the Rajiv Gandhi Science and Technology Commission, Government of Maharashtra, India, and Indian Institute of Technology Bombay, India for funding for this research work.

References

1. S.J. Arceivala, S.R. Asolekar: Wastewater Treatment for Pollution Control and Reuse. 3rd ed., 11th Reprint, McGraw Hill Education India Pvt. Ltd., New Delhi (2006)
2. Bustamante MAO, Mier MV, Estrada JAE, Domínguez CD (2011) Nitrogen and potassium variation on contaminant removal for a vertical subsurface flow lab scale constructed wetland. *Biores Technol* 102(17):7745–7754
3. Butterworth E, Richards A, Jones M, Mansi G, Ranieri E, Dotro G, Jefferson B (2016) Performance of four full-scale artificially aerated horizontal flow constructed wetlands for domestic wastewater treatment. *Water* 8(9):365
4. Kumar D, Asolekar SR (2016) Significance of natural treatment systems to enhance reuse of treated effluent: A critical assessment. *Ecol Eng* 94:225–237
5. Vymazal J (2010) Constructed wetlands for wastewater treatment: five decades of experience. *Environ Sci Technol* 45(1):61–69
6. Zhang DQ, Jinadasa KBSN, Gersberg RM, Liu Y, Ng WJ, Tan SK (2014) Application of constructed wetlands for wastewater treatment in developing countries—a review of recent developments (2000–2013). *J Environ Manage* 141:116–131
7. Sutar RS, Lekshmi B, Kamble KA, Asolekar SR (2018) Rate constants for the removal of pollutants in wetlands: A mini review. *Desalination and Water Treatment* 122:50–56
8. Kadlec RH (2000) The inadequacy of first-order treatment wetland models. *Ecol Eng* 15(1–2):105–119
9. Rugaika, A. M., Kajunguri, D., Van Deun, R., Van der Bruggen, B., Njau, K. N.: Mass transfer approach and the designing of horizontal subsurface flow constructed wetland systems treating waste stabilisation pond effluent. *Water Science and Technology*, (2019)
10. Konnerup D, Koottatep T, Brix H (2009) Treatment of domestic wastewater in tropical, subsurface flow constructed wetlands planted with *Canna* and *Heliconia*. *Ecol Eng* 35(2):248–257
11. Rousseau DP, Vanrolleghem PA, De Pauw N (2004) Model-based design of horizontal subsurface flow constructed treatment wetlands: a review. *Water Res* 38(6):1484–1493
12. Kadlec RH, Knight RL (1996) *Treatment wetlands*. CRC Press, Boca Raton, FL
13. Office of the Registrar General and Census Commissioner, India Homepage, <http://censusindia.gov.in/>, last accessed 2018/07/30
14. IMD Homepage, [http://hydro.imd.gov.in/hydrometweb/\(S\(trk2ok55gnoq2w45zureqbk\)\)/DistrictRaifall.aspx](http://hydro.imd.gov.in/hydrometweb/(S(trk2ok55gnoq2w45zureqbk))/DistrictRaifall.aspx), last accessed on 2019/02/13
15. IMD Homepage, http://www.imd.gov.in/pages/city_weather_show.php, last accessed on 2019/02/13
16. Al-Snafi AE (2015) Bioactive components and pharmacological effects of *Canna indica*-An Overview. *International Journal of Pharmacology and Toxicology* 5(2):71–75
17. Tanner CC (1996) Plants for constructed wetland treatment systems—a comparison of the growth and nutrient uptake of eight emergent species. *Ecol Eng* 7:9–83
18. Yang Q, Chen ZH, Zhao JG, Gu BH (2007) Contaminant removal of domestic wastewater by constructed wetlands: effects of plant species. *J Integr Plant Biol* 49:437–446
19. Zhang Z, Rengel Z, Meney K (2007) Nutrient removal from simulated wastewater using *Canna indica* and *Schoenoplectus validus* in mono- and mixed culture in wetland microcosms. *Water Air Soil Pollut* 183:95–105
20. Vymazal J, Kröpfelová L (2009) Removal of organics in constructed wetlands with horizontal sub-surface flow: a review of the field experience. *Sci Total Environ* 407(13):3911–3922
21. Vymazal J (2007) Removal of nutrients in various types of constructed wetlands. *Sci Total Environ* 380(1–3):48–65
22. Durai G, Rajamohan N, Karthikeyan C, Rajasimman M (2010) Kinetics studies on biological treatment of tannery wastewater using mixed culture. *International Journal of Chemical and Biological Engineering* 3(2):105–109
23. Kadlec, R. H., Wallace, S. *Treatment Wetlands*. CRC press (2008)

24. Zhang Z, Rengel Z, Meney K (2009) Kinetics of ammonium, nitrate and phosphorus uptake by *Canna indica* and *Schoenoplectus validus*. *Aquat Bot* 91(2):71–74
25. Zhang DQ, Tan SK, Gersberg RM, Zhu J, Sadreddini S, Li Y (2012) Nutrient removal in tropical subsurface flow constructed wetlands under batch and continuous flow conditions. *J Environ Manage* 96(1):1–6
26. American Public Health Association (APHA): Standard Methods for the Examination of Water and Wastewater. 21st ed. American Public Health Association, Washington DC, 1220p (2005)
27. Stein OR, Towler BW, Hook PB, Biederman JA (2007) On fitting the k - C p first order model to batch loaded sub-surface treatment wetlands. *Water Sci Technol* 56(3):93–99
28. Hayward J, Jamieson R (2015) Derivation of treatment rate constants for an arctic tundra wetland receiving primary treated municipal wastewater. *Ecol Eng* 82:165–174
29. Jamieson R, Gordon R, Wheeler N, Smith E, Stratton G (2007) Determination of first order rate constants for wetlands treating livestock wastewater in cold climates. *J Environ Eng Sci* 6(1):65–72
30. Stone KC, Poach ME, Hunt PG, Reddy GB (2004) Marsh-pond-marsh constructed wetland design analysis for swine lagoon wastewater treatment. *Ecol Eng* 23(2):127–133
31. Busnardo MJ, Gersberg RM, Langis R, Sinicrope TL, Zedler JB (1992) Nitrogen and phosphorus removal by wetland mesocosms subjected to different hydroperiods. *Ecol Eng* 1(4):287–307
32. Burgoon PS, Reddy KR, DeBusk TA (1995) Performance of subsurface flow wetlands with batch-load and continuous-flow conditions. *Water Environ Res* 67(5):855–862
33. Stein OR, Hook PB, Biederman JA, Allen WC, Borden DJ (2003) Does batch operation enhance oxidation in subsurface constructed wetlands? *Water Sci Technol* 48(5):149–156
34. Chen WY, Chen ZH, He Q, Wang XY, Wang C, Chen DF, Lai ZL (2007) Root growth of wetland plants with different root types. *Acta Ecol Sin* 27(2):450–458
35. Lai WL, Wang SQ, Peng CL, Chen ZH (2011) Root features related to plant growth and nutrient removal of 35 wetland plants. *Water Res* 45(13):3941–3950
36. Cui L, Li W, Zhang Y, Wei J, Lei Y, Zhang M, Ma W (2016) Nitrogen removal in a horizontal subsurface flow constructed wetland estimated using the first-order kinetic model. *Water* 8(11):514
37. Lin YF, Jing SR, Lee DY, Wang TW (2002) Nutrient removal from aquaculture wastewater using a constructed wetlands system. *Aquaculture* 209(1–4):169–184

Evaluation of Sodium Adsorption in Clay Soil in the Presence of Crude Oil



Thaynara Santana Rabelo, Stella Melgaço, Fabiana Pereira Coelho, Daniele Maia Bila, and Elisabeth Ritter

Abstract Throughout the productive life of an oil field there is usually a simultaneous production of gas, oil, water, and impurities. This formation water which composes the crude oil presents high levels of dissolved salts, being on average three times superior to those of seawater, whose salinity is 35 g L^{-1} . In this perspective, crude oil contaminated soil presents great influence of the salinity requiring studies to determine its compartment, bringing clarity to the interaction between the soil, oil, and salt and the process involved in soil remediation. The soil was sampled in an area of oil extraction on land in the state of Sergipe, northeast of Brazil. For this purpose, stable oil-in-water emulsions were prepared from a heavy oil sample and a light oil sample. The aqueous phase of the emulsions was distributed with different salinities: 0 L^{-1} to 150 g L^{-1} sodium chloride. All the emulsions were prepared at $80 \text{ }^\circ\text{C}$ and rotation speed (Turrax) of 16,000 or 22,000 rpm for 15–20 min. The batch test was used for the determination of soil-contaminant interaction parameters. The assay was performed during the 24 h period in Erlenmeyers of 250 ml containing a 1:10 ratio of soil:emulsions. Chloride, sodium, and electrical conductivity were measured. As a result, it was observed that high contents of NaCl results in desorption of Chloride for sorption tests with saline solution and emulsions. Sorption Tests appointed to higher sorption of sodium on Emulsion Tests (light oil > heavy oil). Three isotherm models were tested therefore none of them could fit the sorption process observed.

Keywords Soil contamination · Crude oil · Salinity · Batch test

T. S. Rabelo (✉) · S. Melgaço · E. Ritter
Universidade do Estado do Rio de Janeiro, Rio de Janeiro, Brazil
e-mail: rabelo.thay@gmail.com

F. P. Coelho · D. M. Bila
Instituto SENAI de Tecnologia Ambiental, Rio de Janeiro, Brazil

1 Introduction

Crude oil is a complex mixture composed primarily of n-alkanes, aromatic hydrocarbons, asphaltenes, resins, non-hydrocarbon compounds, such as polar fractions with nitrogen, sulfur, and oxygen heteroatoms, forming water and impurities. Although undoubtedly the most important resource in modern history, soil contamination by oil has become a critical issue as a result of releases during exploration, production, maintenance, transportation, storage, and accidents, generating a series of impacts on the environment and posing a substantial threat to human resources and health [1].

Brazil is one of the world's oil producers, being exploited both onshore and offshore. Despite the higher production of offshore reserves, there are currently 192 onshore exploration blocks under concession in Brazil, of which 75% are in the Northeast Region. According to the National Petroleum Agency (ANP), in 2016, the production of oil and natural gas land reached the level of 300 thousand barrels of oil per day.

Onshore exploration is based on the use of large areas for the exploration of crude oil. [2] and [3] have demonstrated the relevance of studies in contaminated soils since the accidental oil spill is common in the oil industry. There are several sources of contamination of the soil in an onshore exploration. It is possible to highlight possible tank leaks, problems in production wells and rupture of pipelines transporting oil (primary post-processing), water produced and/or crude oil (composed of the emulsion of produced water and petroleum before the primary processing).

This produced water is the main by-product of the exploration and production industry, if presented in contents ranging from 50% to approximately 100% of the crude oil extracted depending on the reservoir characteristics and its [4]. The composition of the production water is variable, but generally presents dissolved oils, chemicals, solids, dissolved gases, metals, and a high content of dissolved salts that can vary from 28 to 300 g. L⁻¹ according to the literature [5:8].

When considering the Brazilian tropical soils that usually have a high content of clay minerals, the remediation of these areas presents a great challenge. This type of soil hinders the biodegradation process, mainly by the interaction of the hydrocarbons (HC) with the clay particles.

Recent studies have focused on this problem and point out that salinity negatively affects soil microbial biomass and, consequently, reduces crude oil degradation, however, does not yet provide solutions to the matter [2, 9].

Thus, the oil sector needs to address the issue of areas contaminated by crude oil in clayey soils with a high degree of salinity resulting from the oil exploration process. In this context, soils contaminated by crude oil are strongly influenced by salinity and studies are necessary, which bring clarity to the oil–soil interaction and the processes involved in the remediation of these areas.

Table 1 Soil characterization

Fraction	Result
% Gravel	0.37
% Sand	42.43
% Silt	21.86
% Clay	35.34
Moisture (%)	3.08

2 Materials and Methods

2.1 Soil Characterization

The soil sample was collected in the municipality of Carmópolis, in the State of Sergipe, Northeastern Brazil, in a region close to the terrestrial petroleum fields but with no possibility of contamination. Table 1 presents the granulometry characterization.

For the sorption test, the soil was air-dried and subsequently squeezed and sieved in a 2 mm sieve.

2.2 Preparation of Emulsions

Two oils donated from the Collection of the Laboratory of Colloidal Systems of the Research Institute of Tiradentes University in Sergipe—Brasil were used for the preparation of emulsions. The heavy oil is of terrestrial origin from a field located in the state of Sergipe. The light oil is of maritime origin from a field located in the state of Rio de Janeiro.

For the preparation of emulsions, a pretest was performed where the emulsions with the two different oils and BSW were considered. For all pretests were adopted the salinity of 150 g/L, the usual concentration of produced water on northeast fields. To prepare the emulsions, a Turrax type homogenizer was used for shearing and dispersion of the oil phase. All the emulsions were prepared at 80 °C (water bath) and rotation speed of 22,000 rpm for 20 min.

2.3 Batch Tests

The batch test was used for the determination of soil-contaminant interaction parameters according to EPA/530/SW-87/00-F [10]. The method of constant soil: solution was adopted. The test was performed over the 24-h period in Erlenmeyers containing a 1:10 ratio of soil:emulsions.

A stock emulsion with 0.5% oil and 150 g/L NaCl was prepared. From this emulsion the dilutions were made in the following concentrations: 100, 50, 25, 12.5, and 6.25%.

After 24 h, the contents of the Erlenmeyers were centrifuged for 5 min at 2200 rpm. For the samples where that time was insufficient the contents were centrifuged for 15 min at 2200 rpm. The intermediate aliquot was then piped to perform the chemical analyses (Fig. 1).

Chloride analysis was performed by the titration method (APHA, 2012, 4500-Cl-B). For the sodium analysis, acidic digestion was performed in microwaves followed by reading in Atomic Absorption Spectrometer (Bruker-AAS240). Conductivity analysis (DIGINED-DM31) was used for conductivity analysis. The matrix emulsion was evaluated for the concentration of oils and greases prior to the sorption test (Standard Methods – 5520 D).

Fig. 1 Batch Test Steps. A- Erlenmeyers with Solo-Emulsion under agitation; B- Samples after centrifugation. C- Example of the phases generated after centrifugation

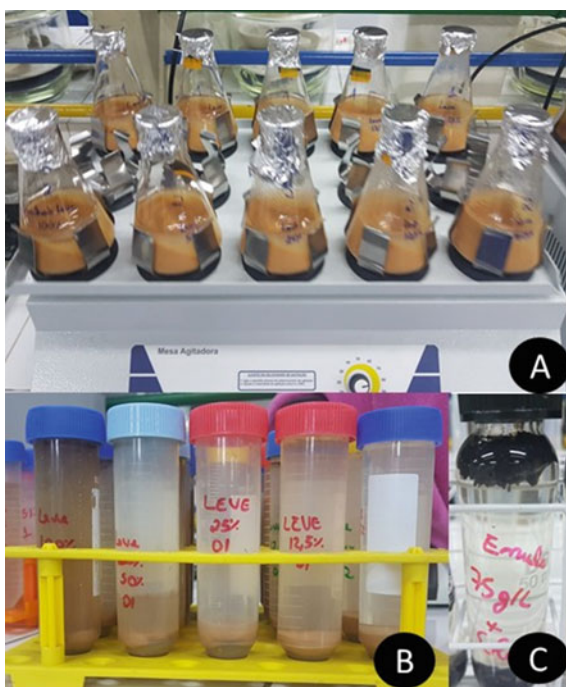


Table 2 Emulsion Tests

Emulsion	Oil type	%Oil	NaCl (g. L ⁻¹)	Qualitative evaluation
01	Heavy	10	150	The oil became too attached to the wall of the Erlenmeyer because no additive was used. When transferred, it presented large bubbles that soon turned into a layer of free oil supernatant
02	Light	5	150	As with the 10% test, the oil phase showed strong adhesion to the Erlenmeyer wall. On transfer it had medium bubbles which soon turned into a layer of free oil supernatant. After 2 h the phases were completely separated
03	Light	0,5	150	Although still present some adhesion to the Erlenmeyer glass and to the Turrax, bedding of adhesion was thinner and did not form free supernatant phase. Transfer was possible without destabilizing the emulsion
04	Heavy	0,5	150	Although more dense and with greater tendency to adhesion to glass, it presented similar results to light oil

3 Results

3.1 Preparation of Emulsions

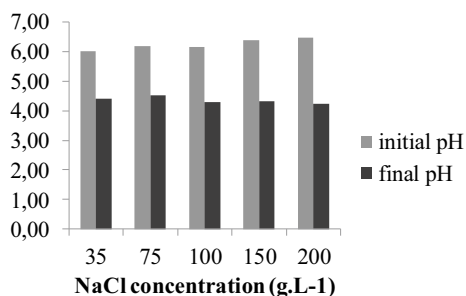
The first stage was the emulsion test. Due to the high salinity the emulsions of oil and water produced are not very stable. Even at the time of exploitation, primary processing uses mostly physical processes of separation [4]. In this way, mimicking the reservoir/holding conditions is a challenge there as it is not possible to have the same pressure and temperature conditions. One of the alternatives would be the use of additives [11], but this could influence the adsorption of the elements and therefore was not adopted. In this work, tests were conducted to evaluate the quality of these emulsions. Table 2 presents a summary of the trials. Emulsions with compositions of water produced above 90%, compatible with characteristics of a mature field, were evaluated.

After these tests, concentration of 0,5% of crude oil was adopted for the batch tests with emulsions described in this paper.

3.2 Batch Test—Saline Solution

Soil and saline analyses were performed for comparison purposes. For this tests, saline solutions were prepared in the following concentrations 0 g.L⁻¹; 35 g.L⁻¹; 75 g L⁻¹; 100 g L⁻¹, 150 g L⁻¹, and 200 g.L⁻¹ of sodium chloride. The batch test

Fig. 2 pH values before and after batch test



followed the same method as the emulsions and pH, Conductivity, Chloride, and Sodium were evaluated.

There wasn't observed any significant difference on conductivity values. This is probably due to no sorption of chlorides and very low sorption of sodium. Samples presented a reduction of pH values after contact with soil (Fig. 2). Samples of saline solution had a pH of 6, and after contact with acid soil, the pH values decreased to 4.

Sorption of chloride by soil is presented in Fig. 3. The results showed no sorption of chloride or desorption in some points. This anion, especially in acidic environments, is considered conservative because it does not react with the materials analyzed [12].

Sodium sorption by soil is presented in Fig. 4. The best fit was Freundlich isotherm model with R^2 value of 0.97. [13] found similar results, but instead of low values of sorbed concentration of sodium, they found a noticeable desorption. It can be explained because high salinity promotes a competition for sorption sites of the solid phase which could result in desorption of Na [14].

As in the saline test, the reduction of the pH was observed in all the sorption tests, but no variation was observed in relation to the oil type or the salinity concentration, reinforcing the theory that this reduction occurred due to the characteristics of the soil (Fig. 5). The conductivity values also remained constant (same magnitude) for

Fig. 3 Chloride Curve for Saline Solution

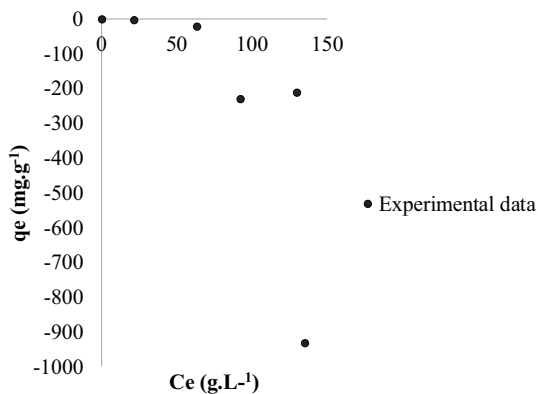


Fig. 4 Sodium curve saline solution

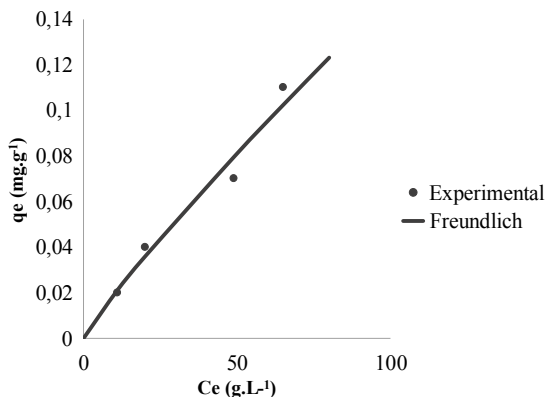
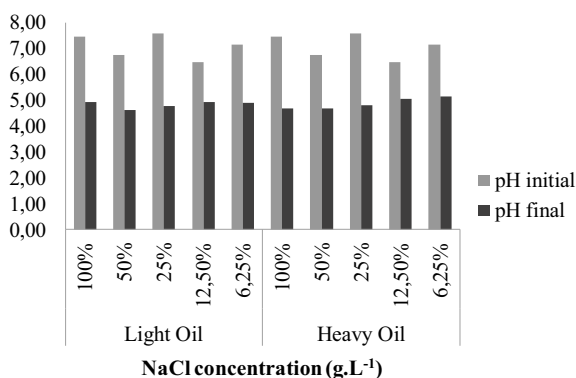


Fig. 5 Reduction of pH throughout the sorption test



each concentration of saline solution regardless of the type of oil that made up the emulsion.

As in the saline test, the results of emulsion showed low sorption of chloride or desorption in some points (Fig. 6).

Differently from the saline solution, where a sodium sorption was observed directly proportional to the concentration of the saline solution, the sodium sorption in the emulsion tests presented two different behaviors depending on the theoretical concentration of NaCl (Fig. 7). For the diluted samples a tendency of sodium desorption was observed, suggesting a possible influence of the presence of the oil.

It was observed a higher sorption of Na⁺ on samples with high concentration of chlorides. That may be explained by an increase in the exchangeable Na when there is high dissolved salt content [15]. The sorption of 100% emulsions was in the same magnitude as that observed in the sorption test using only the saline solution, indicating that for high salinity the oil presents less influence on sodium sorption processes.

As described in the emulsion test, the oil has a tendency to stick to the wall of the Erlenmeyer where the emulsion is produced. As a result, oil and grease tests were

Fig. 6 Chloride curve emulsion

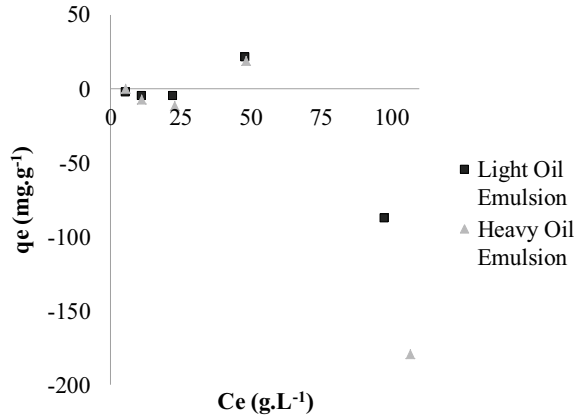
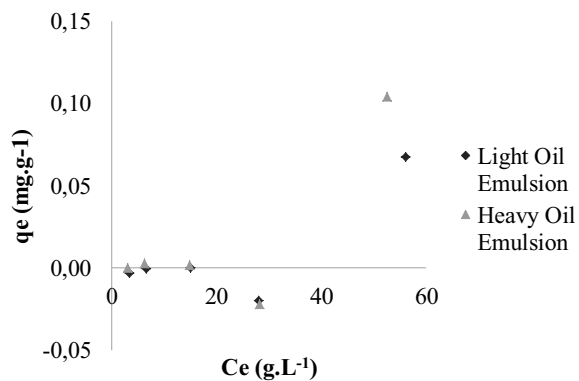


Fig. 7 Sodium curve emulsion



performed on 100% emulsions. The results of oils and greases for light and heavy oil emulsions were respectively 0.7426 gqL and 0.2525 g/L. This result corroborates that observed in the sorption of 100% emulsions where the light emulsion (higher concentration of oils and greases) presented a lower sorption of sodium.

For better understanding of the data, three isotherm models were tested: Linear, Langmuir, and Freundlich. None of the models presented significant R2 for the emulsion sodium data per soil.

4 Conclusions

The soil study with crude oil (water and oil emulsion) is complex, mainly when water produced with high salinity is considered. The results showed a chloride desorption for saline solution assays and emulsions. For the sodium, a low sorption was observed being directly proportional to the case of the saline solution. For the emulsion tests,

a complex behavior for the sodium was observed which needs to be more detailed through new sorption tests with different concentrations of oil and column tests. In addition, it is suggested that oils and greases concentration analyses would be observed in all the dilutions.

References

1. LIU, Y. et al. Isolation and characterization of crude-oil-degrading bacteria from oil-water mixture in Dagang oilfield, China. *Chinese Journal of Chemical Engineering*. 25, 1838–1846, 2017
2. Cai B, Ma J, Yan G, Dai X, Li M, Guo S (2016) Comparison of phytoremediation, bioaugmentation and natural attenuation for remediating saline soil contaminated by heavy crude oil. *Biochem Eng J* 112:170–177
3. EBADI, A.; KHOSHKHOLGH SIMA, N. A.; OLAMAE, M.; HASHEMI, M.; GHORBANI NASRABADI, R. Effective bioremediation of a petroleum-polluted saline soil by a surfactant-producing *Pseudomonas aeruginosa* consortium. *Journal of Advanced Research*, v. 8, n. 6, p. 627–633, 2017
4. THOMAS, José Eduardo. Fundamentos de engenharia de Petróleo. 2º Ed. Rio de Janeiro: Interciência, PETROBRÁS, 2004
5. Aizenshtat Z, Miloslavski I, Aschengrau D, Oren A (1999) Hypersaline depositional environments and their relation to oil generation. In: Oren A (ed) *Microbiology and Biogeochemistry of Hypersaline Environments*. CRC Press, Boca Raton, pp 89–108
6. FERNANDES JUNIOR, W. E. Projeto e operação em escala semi – industrial de um equipamento para o tratamento de águas produzidas na indústria do petróleo utilizando nova tecnologia: Misturador – Decantador à inversão de fases (MDIF). Tese (Doutorado) - Departamento de Engenharia Química, Universidade Federal do Rio Grande do Norte. Natal, 2006
7. CAMPOS, J. C.; BORGES, R. M. H.; OLIVEIRA FILHO, A. M.; NOBREGA, R.; SANT’ANNA, G. L. Oilfield wastewater treatment by combined microfiltration and biological processes. *Water Research*, v. 36, n. 1, p. 95–104, 2002
8. Weschenfelder SE, Louvise AMT, Borges CP, Meabe E, Izquierdo J, Campos JC (2015) Evaluation of ceramic membranes for oilfield produced water treatment aiming reinjection in offshore units. *J Petrol Sci Eng* 131:51–57
9. GAO, Y. et al. Effects of salinization and crude oil contamination on soil bacterial community structure in the Yellow River Delta region, China. *Applied Soil Ecology*, Vol. 86, p (165–173), 2015
10. USEPA. (United States Environmental Protection Agency) - Batch-type procedures for
11. estimating soil adsorption of chemicals. Report, 1992
12. TANUDJAJA, H. J.; TARABARAB, V. V.; FANEC, A. G.; CHEWA, J. W. Effect of cross-flow velocity, oil concentration and salinity on the critical flux of an oil-in-water emulsion in microfiltration. 530. 11–19. *Journal of Membrane Science*, 2017
13. SANTOS, L. V.; POLIANOV, H.; ALAMINO, R; C. J.; SILVA, V. H. G. The Sorption of Chloride and Potassium in Tropical Soils. *Geosciences Institute Anuary*. v. 29, p. 101–121, 2006
14. RITTER, Elisabeth. Efeito da salinidade na difusão e sorção de alguns íons inorgânicos em um solo argiloso saturado. Tese (Doutorado). COPPE. Engenharia Civil. Universidade Federal do Rio de Janeiro. Rio de Janeiro, 1998
15. DU LAING, G; RINKLEBE, J.; VANDECASTEELE, B.; MEERS, E.; TACK, F. M. G. Trace metal behaviour in estuarine and riverine floodplain soils and sediments: A review. Vol 407, Issue 13, pp. 3972–3985. *Science of The Total Environment*, 2009

16. FERREL, R. E. & BROOKS, R. A. The selective adsorption of sodium by clay minerals in lakes Pontchartrain and Maurepas, Louisiana. Vol. 19, pp. 75–81. *Clays and Clay Minerals*, 1971

Photochemical Oxidation of Complex Organic Contaminants in Water



Santiago Urréjola, Claudio Cameselle, Susana Gouveia, and Mercedes Pardo

Abstract Various complex organic pollutants resist conventional wastewater treatments. Thus, it is not possible to assure that water and wastewater treatment plants achieve the adequate removal of such organic contaminants, increasing the risk for human health and ecosystems. In this work, we have studied the capacity of the photochemical treatment for the degradation of complex organic pollutants in water. Selected dyes and pesticides were tested for their possible degradation by UV-C light. All the tested compounds were decomposed by the UV-C. The dyes malachite green and indigo carmine were completely degraded in 17 h whereas the tested pesticides (thiamethoxam, pyriproxifen, difenoconazol, and phosmet) were only partially degraded in 8 h. A detailed study with thiamethoxam proved that the UV-C light was able to decompose the molecule in just 15–30 min, and then the degradation products were oxidized with the UV light but at a much slower rate. The chemical oxygen demand showed no or minor removal of organic matter in water, proving that the photochemical oxidation was not able to mineralize the organic compounds.

Keywords UV light · Photochemical oxidation · Contaminated water

1 Introduction

The synthesis and use of many complex organic molecules are creating an environmental problem due to the release of these compounds into the environment. These complex organics include dyes, pesticides, and other xenobiotic compounds. These molecules tend to accumulate in the tissues of living organisms with the subsequent toxic effects and health problems. These organic compounds affect also the health

S. Urréjola (✉) · M. Pardo
University Center of Defense at the Naval Military School, 36920 Marín, Spain
e-mail: urrejola@tud.uvigo.es

C. Cameselle · S. Gouveia
BiotecnIA. Chemical Engineering, University of Vigo, 36310 Vigo, Spain

of humans when they are exposed to such contaminants through water and food. Furthermore, conventional treatment technologies for water and wastewater are not able to degrade and remove such contaminants. Thus, it is necessary to implement new treatment technologies that can remove such complex compounds from wastewaters, thus protecting the environment and ecosystems from the slow but continuous release of recalcitrant contaminants [1, 2].

The photochemical oxidation technology has been proposed as a new sustainable technology for the degradation and removal of complex organic contaminants in water. The photochemical process consists in the exposure of the water to an ultraviolet (UV) light source [3]. The UV light is able to kill or deactivate microorganisms, but it is also able to degrade a wide range of organic compounds. This is an environmentally friendly technology because it does not use chemical reagents and does not generate residual sludge.

The aim and objective of this study is to test the capability of the UV-C light to degrade some selected organic compounds of environmental concern. The organic compounds tested include common pesticides used in agriculture (thiamethoxam, pyriproxifen, difenoconazol, and phosmet) and dyes (malquite green and indigo carmine) used in the industry. The objective of this work is the assessment of the photochemical degradation as a practical technology to be used for the removal of recalcitrant organic contaminants in wastewater and residual effluents.

2 Materials and Methods

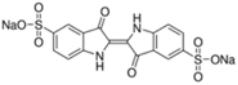
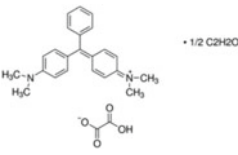
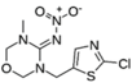
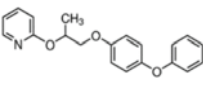
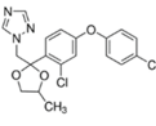
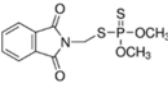
2.1 Organic Compounds

Six complex organic compounds have been used in this study: two dyes (malachite green and indigo carmine), and four pesticides (thiamethoxam, pyriproxifen, difenoconazol and phosmet). The dyes were purchased from Sigma-Aldrich as pure reactants. The pesticides were obtained from commercial pesticides in the market for general use in agriculture. Table 1 lists the organic compounds, their chemical formula and chemical structure, the concentration used in the photochemical studies, and the wavelength used to monitor their concentration in water with a spectrophotometer. The concentrations of organics in this study were selected based on their solubility and their expected concentrations in residual effluents and wastewaters.

2.2 Experimental Setup

All tests were performed in a beaker with 200 mL of the solution of the organic compound to be tested. The solution was continuously homogenized with a magnetic stirrer. The beaker was made of quartz to allow the UV-C radiation to reach the

Table 1 Selected organic compounds for the photochemical treatment

Organic compound	Concentration (mg/L)	Absorbance UV-Vis (nm)	Chemical structure
Indigo carmine C ₁₆ H ₈ N ₂ Na ₂ O ₈ S ₂ CAS 860-22-0	50	611	
Malachite green oxalate salt C ₂₃ H ₂₅ N ₂ ·C ₂ H ₂ O ₄ ·0.5C ₂ H ₂ O ₄ CAS 2437-29-8	8.5	620	
Thiamethoxam C ₈ H ₁₀ ClN ₅ O ₃ S CAS 153719-23-4	25	249	
Pyriproxifen C ₂₀ H ₁₉ NO ₃ CAS 95737-68-1	0.19	254	
Difenoconazol C ₁₉ H ₁₇ Cl ₂ N ₃ O ₃ CAS 119446-68-3	0.38	220	
Phosmet C ₁₁ H ₁₂ NO ₄ PS ₂ CAS 732-11-6	10	224	

solution from any direction. The UV-C source was an 11 W tube installed in the upper lid of a closed box. The distance from the UV-C lamp to the surface of the liquid was 10 cm. A hole in the upper lid of the box allowed for sampling of the solution in the beaker.

2.3 Analysis

The concentration of the organic compound was followed taking periodic samples during the photochemical treatment. The concentration of the organic compound was determined at the peak of maximum absorbance in a UV-Vis spectrophotometer. Table 1 shows the wavelength used for the measurement of each organic compound. Dyes were measured in the visible spectrum (611–620 nm) and pesticides were measured in the UV range spectrum (220–254 nm). HPLC (Agilent, model 1260 infinity II) was used to determine the concentration of thiamethoxam. The analysis

conditions are as follows: eluent: 60% of phosphoric acid 0.1% in water, 20% of acetonitrile and 20% methanol; flow: 1.2 mL/min; separation column: Poroshell 120; temperature: 25 °C; and detector: diode array at 249 nm. Chemical oxygen demand was analyzed with the PrimeLab 1.0 Multitest photometer.

3 Results and Discussion

3.1 Dye Degradation

Figure 1 shows the concentration profile of the six organic compounds along the photochemical degradation tests. The dyes were completely degraded in 17 h as it can be seen in the concentration profile of Fig. 1, in the spectra of Fig. 2, and in the coloration of the dye samples in Fig. 3. The dye spectra in Fig. 2 show the disappearance of the peaks in the visible range but not the peaks in the UV range. This confirms the destruction of the chromophoric group in the photochemical treatment but not the total mineralization of the molecule. This result is confirmed with the COD removal in Table 2. The dyes molecules are decomposed in smaller molecules but the total amount of organic carbon measured as COD remains the same.

The pesticides showed different behavior. The extension of the pesticide degradation was lower than that of dyes. The degradation of pesticides in Fig. 1 only progresses at a significant rate during 1 or 2 h, and then the degradation rate is much slower. In about 8 h, the degradation of the pesticides ranges from 42% for phosmet and 82% for difenoconazol. The spectra in Fig. 2 confirm the limited degradation of the pesticides.

A detailed study of the degradation of thiamethoxam using HPLC to follow its concentration showed very promising results for the photochemical technology (Fig. 4). UV-C light was able to decompose the thiamethoxam molecule. 99.5% of thiamethoxam was removed in 15 min, and in 1 h, thiamethoxam was not detected

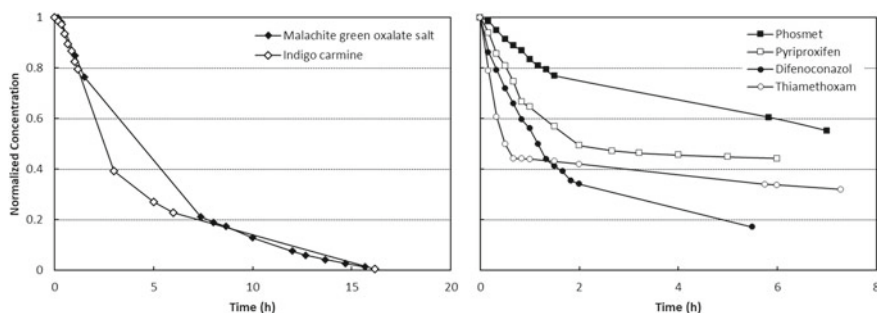


Fig. 1 Photochemical degradation of dyes and pesticides

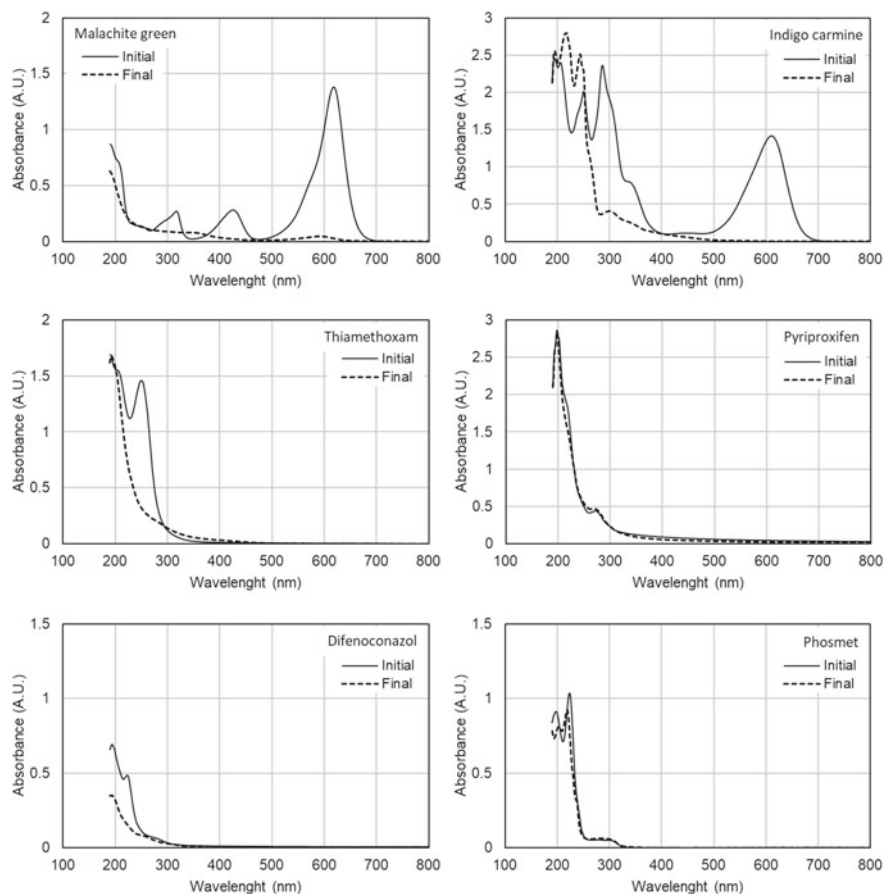


Fig. 2 UV-V is spectra of dyes and pesticides after the photochemical degradation

in the chromatogram (Fig. 4). The HPLC chromatograms also showed the appearance of other peaks that corresponded to the decomposition products. Those peaks also decreased along the time, confirming that the photochemical treatment was able to oxidize thiamethoxam and its degradation products. The COD removal (59%) also proved a partial mineralization of the thiamethoxam with the photochemical treatment.

4 Conclusions

The photochemical treatment with UV-C light is able to degrade a wide variety of complex organic compounds in water. The degradation products can also be degraded

Fig. 3 Indigo carmine and malachite green before and after the photochemical treatment

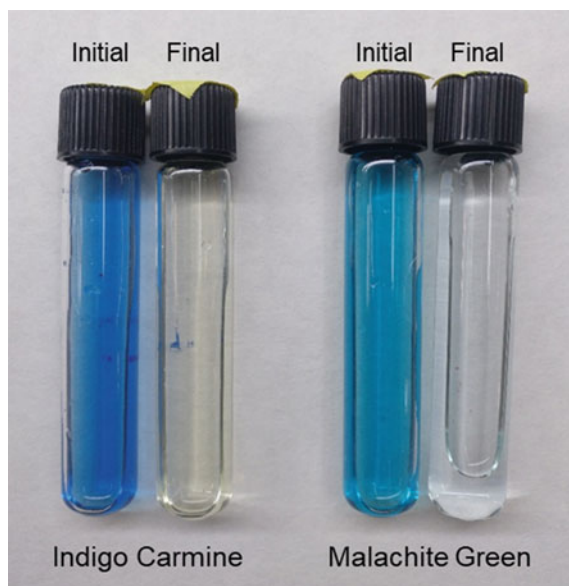


Table 2 Chemical Oxygen Demand (COD) removal in the photochemical treatment

Organic compound	Initial COD (mg/L)	Final COD (mg/L)	COD removal (%)
Indigo carmine	46.8	46.4	0
Malachite green oxalate salt	10.6	10.5	0
Thiamethoxam	52.4	21.5	59
Pyriproxifen	141.4	118.1	16
Difenoconazol	18.6	13.0	30
Phosmet	30.8	24.9	19

by the UV-C light resulting in a net removal of COD from the water. More research is necessary to assess the capabilities of the photochemical treatment in water. The research has to focus on the complete mineralization of the organics.

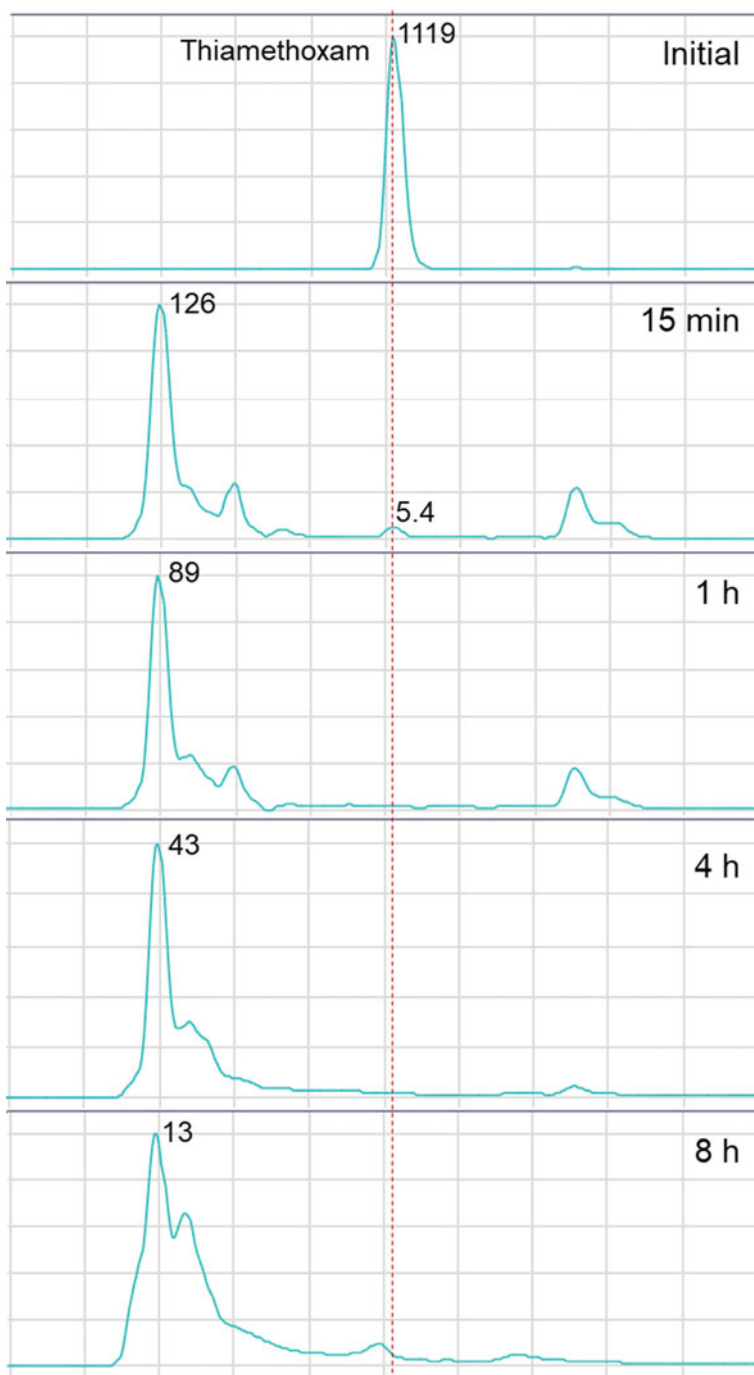


Fig. 4 Thiamethoxam chromatograms during the photochemical degradation

References

1. Comninellis C, Kapalka A, Malato S, Parsons SA, Poulios I, Mantzavinos D (2008) Advanced oxidation processes for water treatment: advances and trends for R&D. *J Chem Technol Biotechnol: Int Res Process, Environ Clean Technol* 83(6):769–776
2. Deng Y, Zhao R (2015) Advanced oxidation processes (AOPs) in wastewater treatment. *Current Pollut Rep* 1(3):167–176
3. Reddy PVL, Kim KH (2015) A review of photochemical approaches for the treatment of a wide range of pesticides. *J Hazard Mater* 285:325–335

A Zero Emissions Landfill: Turning Myth to Reality



Jyoti K. Chetri and Krishna R. Reddy

Abstract The ever increasing population has been the root cause for the outburst of solid wastes. Dumping wastes in a pit or an open area had been in practice ever since the advent of civilization. With the growing awareness about the health risks associated with the open dumping of the wastes, landfills gained eminence. Landfills have been modified from simple dumping to the engineered landfills with the liners. Initially, the major concern of a landfill was the pervasive odor which affected the lives of dwellers around the landfill area. As the gases such as methane (CH_4) and carbon dioxide (CO_2) got recognized as the major contributors of global climate change, the landfill emissions became more critical. Currently, landfills are considered to be the third largest source of CH_4 emissions in the United States (US). Various efforts have been made to control the landfill emissions such as providing low permeability landfill covers, installing gas extraction systems, and the biocovers. Landfills used to be considered as a liability due to the emissions and the odor. However, with the gas collection and recovery systems installed, the landfills have been able to generate revenue as well as lower the carbon footprint by converting extracted gas to energy. Modern engineered landfills with the engineered covers and gas extraction systems are able to keep the emissions to the minimum level, however there are fugitive emissions emanating from the landfills and contributing to the global climate change. Recently, in an attempt to capture those fugitive emissions and render landfills emissions free, an alternative landfill cover called biogeochemical cover concept was introduced. The biogeochemical cover aims to remove CO_2 , hydrogen sulfide (H_2S), and CH_4 . This paper discusses the progressive transformation of landfills into zero emissions landfills.

Keywords Landfills · Landfill cover · Biochar · Steel slag · Landfill gas extraction

J. K. Chetri (✉) · K. R. Reddy
University of Illinois at Chicago, Chicago, IL 60607, USA
e-mail: jkc4@uic.edu

© Springer Nature Switzerland AG 2020
K. R. Reddy et al. (eds.), *Sustainable Environmental Geotechnics*, Lecture Notes
in Civil Engineering 89, https://doi.org/10.1007/978-3-030-51350-4_26

243

1 Introduction

The world has been dealing with the problems of waste disposal since the advent of the civilization. Wastes including household waste, human and animal excreta, etc. were thrown on the streets in the cities of Europe and the US until the late 1800 [1]. Outbreak of many infectious diseases such as cholera was linked to the poor sanitation conditions [2]. Until the mid of nineteenth century, waste disposal was very rampant mainly by dumping or burning [3]. In the late 1900s, with the realization that the disposal of the wastes on the streets causes health issues, cities started garbage collection and disposal systems to collect and dispose the wastes from the cities to far away open dumps, incinerators, or at sea [1].

The first step toward modern landfilling started in California in 1935 with throwing of the waste into a pit and covering it with soil periodically [1]. Solid Waste Disposal Act was passed by Congress in 1965, which devised the framework for states to manage the disposal of wastes from different sources [4]. After the formation of Environmental Protection Agency (EPA) in 1970, Congress passed the Resource Conservation and Recovery Act (RCRA) in 1976. RCRA regulates the waste management program in order to protect human health and environment.

With the growing awareness on the adverse health effects caused by the releases or emissions from the wastes, landfills have changed over the time from just an open dump to the modern engineered landfills. The modern engineered landfills are provided with well-designed liner as well as cover systems which can intercept the leachates from entering the subsurface and emissions from leaving the landfill and contaminate the surrounding environment.

Municipal solid waste (MSW) landfills generate large amount of gases as a result of aerobic and anaerobic decomposition of the wastes. The landfill gas (LFG) mainly comprises of CH_4 and CO_2 . CH_4 and CO_2 are highly potent greenhouse gases (GHG) and major contributors for global warming. LFG comprise of trace amount of other gases such as H_2S and non methane organic compounds (NMOCs) which contribute to degradation of local air quality.

This paper highlights the progressive development made in the field of landfills for capturing landfill emissions and making landfills emissions free. In the past, emissions free landfills were considered to be a myth as one could always sense that pungent smell of garbage while passing by a landfill. However, with the technological advancement and researches, landfills are becoming more sophisticated and marching toward the path of emissions free landfills.

2 Landfill Gas Management

Everyday huge amount of wastes is generated which needs disposal. Figure 1 shows the amount of waste generated by some countries in 2012 and the projected waste generation in the year 2025. The amount of waste generated is projected to be

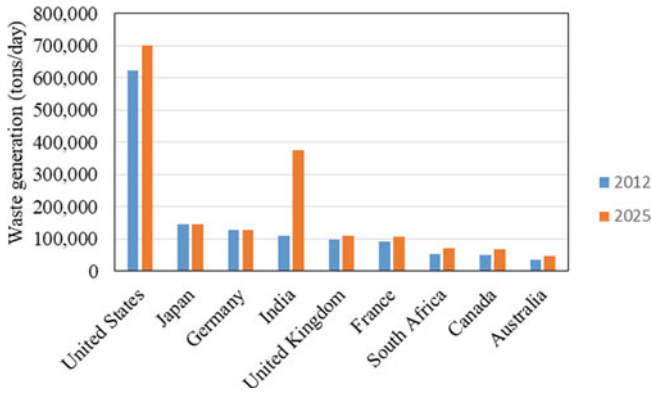


Fig. 1 Waste generated by the countries in the year 2012 and projected waste generation in the year 2025 [5]

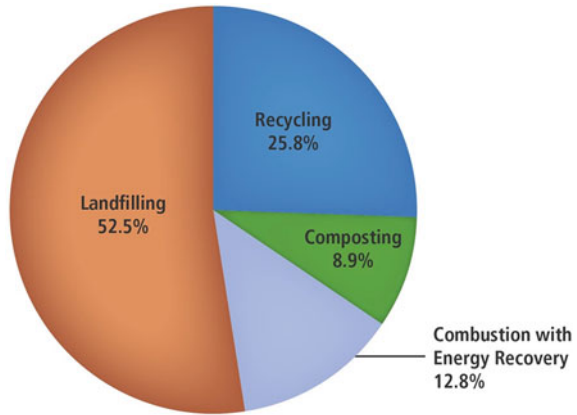
increasing in the coming years. There are various ways to manage the waste which include reuse and recycling, energy recovery, and treatment and disposal, which involves landfilling. Although landfilling is the least preferred choice in the waste management hierarchy (Fig. 2), most of the wastes are diverted to the landfills. In the US, 52.5% of the total MSW generated goes to landfill (Fig. 3).

MSW in the landfill undergoes series of decomposition processes generating various gases such as CH₄, CO₂, H₂S, NMOCs, etc. Around 300 cubic feet per minute (cfm) of LFG is produced by one million tons of MSW, and it continues to



Fig. 2 Waste management hierarchy [6]

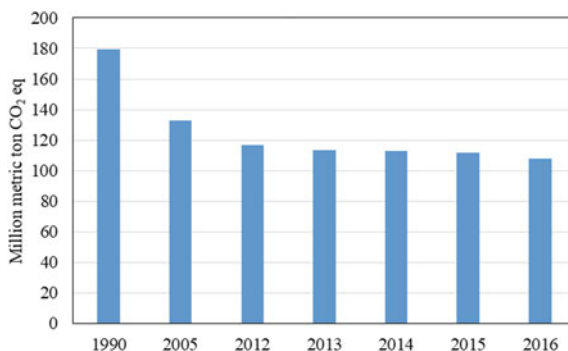
Fig. 3 MSW management in the USA [6]



generate LFG for 20 to 30 years of landfilling [7]. LFG if released to the atmosphere, can cause several health issues as well as environmental hazards. To protect the environment and humans from adverse effects of landfill emissions, every country has some statutes for LFG management in the landfills. In the USA, RCRA regulates the LFG from MSW landfills under 40 CFR Part 258 [8]. RCRA requires every owner/operators of MSW landfills to ensure that the concentration of CH_4 generated by the landfill does not exceed 25% of the lower explosion limit for CH_4 in facility structures.

Engineered landfills are usually provided with gas collection systems which can be active and passive collection systems. The collected LFG is either flared or used for energy recovery. The presence of CH_4 in a significant proportion makes the LFG of high energy value with a heating value of 500 British thermal units (BTU) per standard cubic foot (scf) [7]. With the advancement in the technology and growing concerns of resource scarcity, LFG has found use in various applications. LFG recovery from landfill, on one hand reduces the risks of environmental pollution as well as human health hazards and on the other hand provides an opportunity to the landfill operators to generate revenue by converting LFG to energy. In addition, energy generation from LFG offsets the burden on the natural resources for meeting energy demand. High calorific value of LFG makes it suitable for various applications, however direct use and electricity generation are the two prime uses of the LFG [9]. Conversion of LFG to pipeline quality gas is an emerging technology in the field of LFG to energy projects [9]. LFG to energy projects have proven to be a game changer in controlling landfill emissions. In the USA alone, there are 623 operational LFG energy projects [10]. Figure 4 shows the trend of CH_4 emissions from the year 1990 to 2016. As the LFG to energy technologies are gaining prominence, the CH_4 emissions from the landfills are on decreasing trend. However, there is still significant amount of CH_4 emitted into the atmosphere. Even with the LFG recovery system installed in the landfill, it is difficult to recover all of the LFG generated in the landfill due to the permeability of the wastes, inefficiencies, and the timing of the installation of the

Fig. 4 Trend of CH₄ emissions from landfills over the years [13]



LFG recovery system [11]. Around 60–90% of the landfill CH₄ is estimated to be captured by the active LFG recovery system [12].

While significant portion of landfill emissions is captured by LFG recovery system, there are still some fugitive emissions emanating from the MSW landfills which are enough to degrade the air quality. Similarly, the LFG recovery systems might not prove effective during the low gas generation phase of the landfill or in older landfills as the LFG extraction in such cases become highly cost intensive. Hence, the emissions which cannot be captured by the LFG recovery system tend to diffuse out to the atmosphere. A lot of researches have been conducted in the past and is being conducted currently to mitigate those fugitive emissions from the landfills. Various alternative covers have been developed and are being developed to capture and extenuate the fugitive emissions from MSW landfills.

2.1 Alternative Landfill Covers

Many researchers have focused on mitigating landfill CH₄ emissions as CH₄ is a more potent GHG than CO₂. Landfill cover soils are known to have the potential to convert CH₄ to CO₂ by the CH₄ oxidizing bacteria which are naturally present in the cover soil [14, 15]. Researchers have explored alternative cover materials to enhance the microbial CH₄ oxidation in landfill cover to mitigate fugitive CH₄ emissions. Biocovers have been one of the most studied alternative covers and have shown the promising potential to enhance CH₄ oxidation. Biocovers comprise of organics rich materials such as compost, sewage sludge, peat, etc. individually in a separate layer or amendment to the soil [16]. Biocovers with organic amendments appear to be an attractive alternative for mitigating fugitive CH₄ emissions, however they suffer from some limitations such as self-degradation of the materials resulting into production of CH₄ thereby increasing CH₄ emissions from landfill.

Another bio-based cover system is biochar-amended soil cover, which has shown promising CH₄ oxidation potential. Biochar is a highly porous organic material, produced by thermochemical transformation of biomass under various conditions

[17]. High internal porosity and recalcitrant nature of biochar favors its use in landfill cover soil amendment to enhance the microbial CH_4 oxidation. Biochar-amended cover soil has shown promising potential to enhance microbial CH_4 oxidation by providing greater internal surface area for methanotrophs to reside as well as improving water retention capacity of amended soil thereby protecting formation of desiccation fissures and cracks in the cover [18, 19].

Some studies explored alternative covers for attenuating H_2S emissions from landfills. Study by Raga et al. [20] showed activated carbon membranes to be effective in adsorbing H_2S emanating from the landfills. In another study [21], waste biocover soil was tested as an alternative cover material for H_2S removal from the landfill and the results showed high adsorption removal capacity in waste biocover soil. Plaza et al. [22] studied various materials such as sandy soil, sandy soil amended with lime, clayey soil and concrete as alternative cover material for attenuating H_2S from construction and demolition waste landfill. Sandy soil amended with lime and fine concrete were found to be effective in limiting H_2S emissions.

Although several studies have explored and developed alternative cover systems that can attenuate emissions of CH_4 and H_2S , none of the studies focuses on mitigation of CO_2 which comprises 50% (v/v) of LFG and is a major contributor of global greenhouse warming. Another unanswered question is can these alternative covers mitigate the major gases, mainly CO_2 , CH_4 , and H_2S simultaneously? Can the biological and geochemical processes be coupled to mitigate all the fugitive landfill emissions and render landfills emissions free? One such attempt is being made by Reddy et al. [23] by introducing biogeochemical cover which uses biochar-amended soil and steel slag as alternative cover materials to remove CH_4 , CO_2 , and H_2S simultaneously.

2.2 *Biogeochemical Cover*

Biogeochemical cover concept was introduced by Reddy et al. [23], which aims to couple the biogeochemical processes by using biochar amended soil and steel slag for simultaneous removal of fugitive CH_4 , CO_2 , and H_2S emanating from MSW landfills. Biochar amended soil can mitigate CH_4 by oxidizing CH_4 with the help of methanotrophs. On the other hand, steel slag, which is a byproduct of steel making process, can sequester CO_2 as well as H_2S by the series of chemical reactions with various oxides present in the slag. Figure 5 shows the schematic of the biogeochemical cover applied in unison with gas extraction well. Since the radius of influence of gas extraction wells is limited, there is always a chance of some emissions escaping the cover. Biogeochemical cover will effectively capture those fugitive emissions. The steel slag holds the capacity of sequestering H_2S emissions as shown in Fig. 5, which implies that the biogeochemical cover can attenuate the landfill odor. Studies by Reddy et al. [24, 25] have shown significant CO_2 removal potential in steel slag under landfill conditions. The research group is engaged in further exploring the

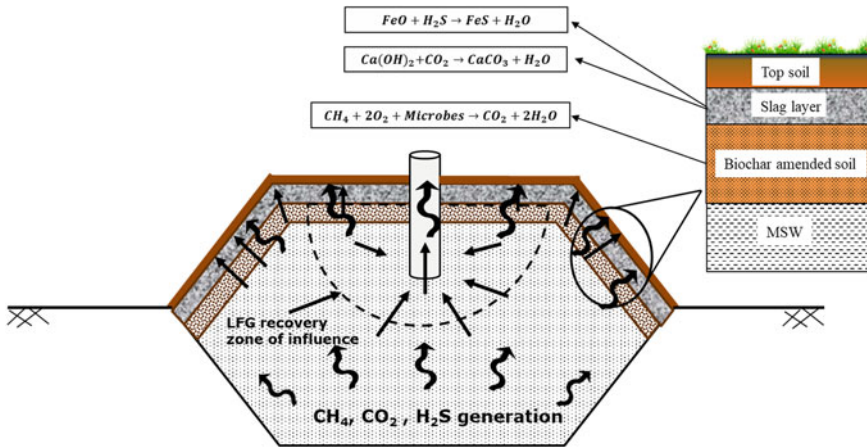


Fig. 5 Schematic of biogeochemical cover concept

coupled behavior of biochar-amended soil and slag under dynamic meteorological conditions which may prevail in the landfill.

Biogeochemical cover could be an environmentally as well as economically viable alternative for landfill cover as it has the potential to remove major GHGs, odor as well as opportunity for the use of industrial byproduct which is otherwise stockpiled in the steel industries that affects the atmosphere and aesthetics. Odor is one of the biggest challenges of landfill operators as they continuously get grievances from the nearby communities about the pungent smell. Biogeochemical cover possesses the capacity to deal with the odor forming compound (mainly H₂S). Successful application of biogeochemical cover in landfills will be a step toward “zero emissions landfills.” Further study of feasibility of biogeochemical cover under dynamic environmental conditions is under study.

3 Conclusion

Over the years, disposal of waste has progressed from mere open dumping to landfilling. Although landfilling has been through great transformations in the recent years in terms of engineered designs and stringent regulations for environmental protection, they are still viewed as liability due to the fugitive emissions emanating from the landfills. With the advancement in technologies and growing awareness about LFG as energy source, more and more landfills are operating LFG to energy projects. LFG to energy projects are not only capturing LFG and reducing environmental hazards but also generating revenue and offsetting the burden on natural resources for meeting energy demand. Almost every engineered landfills are provided with

LFG recovery system, which has been proven successful in keeping the LFG emissions low. However, the provision of LFG recovery system does not always ensure 100 percent removal of LFG due to various reasons such as limited radius of influence of gas collection wells, variable permeability of the waste, low gas production in the waste and lower efficiency of the LFG recovery system. Therefore, some emissions tend to make their way to the atmosphere affecting the air quality and human health. Various studies have explored and studied alternate cover materials to tackle these fugitive emissions such as biocovers for mitigating CH₄, waste biocover soil for H₂S removal etc. One such alternative cover is biogeochemical cover which possesses the potential to remove CH₄, CO₂, and H₂S simultaneously from the landfill. Successful application of biogeochemical cover could render landfills emissions free which was just a hypothesis until today. Biogeochemical cover could not only reduce the global climate change problem but also enhance the quality of life of people residing around the landfills.

References

1. National Solid Waste Management Association. (NSWMA) (2008) Modern landfills: a far cry from the past. Washington, DC
2. Wilson DG (1976) A brief history of solid-waste management. *Int J Environ Stud* 9(2):123–129
3. Wilson DC (2007) Development drivers for waste management. *Waste Manage Res* 25(3):198–207
4. Horinko ML (2002) 25 years of RCRA: building our past to protect our future. Office of Solid Waste and Emergency Response. EPA-K-02-027, US Environmental Protection Agency, Washington
5. Hoornweg D, Bhada-Tata P (2012) What a waste: a global review of solid waste management. World Bank, Washington, DC. Available at: <https://openknowledge.worldbank.org/handle/10986/17388>
6. United States Environmental Protection Agency (USEPA) (2018) National overview: facts and figures on materials, wastes and recycling. Available at: <https://www.epa.gov/facts-and-figures-about-materials-waste-and-recycling/national-overview-facts-and-figures-materials>
7. Landfill Methane Outreach Program (LMOP) (2017) LFG energy project development handbook. United States Environmental Protection Agency. Available at: <https://www.epa.gov/lmop/landfill-gas-energy-project-development-handbook>
8. Sharma HD, Reddy KR (2004) Geoenvironmental engineering: site remediation, waste containment, and emerging waste management technologies. Wiley, New York
9. United States Environmental Protection Agency (USEPA) (2012) International best practices guide for landfill gas energy projects. Global methane initiative. Available at: https://www.globalmethane.org/documents/toolsres_lfg_ibpgcomplete.pdf
10. Landfill Methane Outreach Program (LMOP) (2018) Landfill gas energy project data and landfill technical data. Available at: <https://www.epa.gov/lmop/landfill-gas-energy-project-data-and-landfill-technical-data> (Accessed 02 Sept 2019)
11. Solid Waste Association of North America (SWANA) (2007) Landfill gas collection system efficiencies. SWANA Applied Research Foundation Landfill Gas Project Group
12. Landfill Methane Outreach Program (LMOP) (2018a) Benefits of Landfill Gas Energy Projects. Available at: <https://www.epa.gov/lmop/benefits-landfill-gas-energy-projects> (Accessed on 22 Sept 2019)

13. United States Environmental Protection Agency (USEPA) (2018b) Inventory of U.S. greenhouse gas emissions and sinks 1990–2016. EPA 430-R-18-003. Available at: https://www.epa.gov/sites/production/files/2018-01/documents/2018_complete_report.pdf
14. Scheutz C, Mosbæk H, Kjeldsen P (2004) Attenuation of methane and volatile organic compounds in landfill soil covers. *J Environ Qual* 33(1):61–71
15. Cao Y, Staszewska E (2011) Methane emission mitigation from landfill by microbial oxidation in landfill cover. In: International conference on environmental and agriculture engineering IPCBEE, vol 15, p 57
16. Sadasivam BY, Reddy KR (2014) Landfill methane oxidation in soil and bio-based cover systems: a review. *Rev Environ Sci Bio/Technol* 13(1):79–107
17. Xie T, Sadasivam BY, Reddy KR, Wang C, Spokas K (2015) Review of the effects of biochar amendment on soil properties and carbon sequestration. *J Hazard Toxic Radioact Waste* 20(1):04015013
18. Yargicoglu EN, Reddy KR (2017) Biochar-amended soil cover for microbial methane oxidation: Effect of biochar amendment ratio and cover profile. *J Geotech Geoenviron Eng* 144(3):04017123
19. Yargicoglu EN, Reddy KR (2017) Microbial abundance and activity in biochar-amended landfill cover soils: Evidence from large-scale column and field experiments. *J Environ Eng* 143(9):04017058
20. Raga R, Pivato A, Lavagnolo MC, Megido L, Cossu R (2018) Methane oxidation and attenuation of sulphur compounds in landfill top cover systems: lab-scale tests. *J Environ Sci* 65:317–326
21. He R, Xia FF, Bai Y, Wang J, Shen DS (2012) Mechanism of H₂S removal during landfill stabilization in waste biocover soil, an alternative landfill cover. *J Hazard Mater* 217:67–75
22. Plaza C, Xu Q, Townsend T, Bitton G, Booth M (2007) Evaluation of alternative landfill cover soils for attenuating hydrogen sulfide from construction and demolition (C&D) debris landfills. *J Environ Manage* 84(3):314–322
23. Reddy KR, Grubb DG, Kumar G (2018) Innovative biogeochemical soil cover to mitigate landfill gas emissions. In: Proceedings of the international conference on protection and restoration of the environment XIV. Thessaloniki, Greece
24. Reddy KR, Gopakumar A, Rai RK, Kumar G, Chetri JK, Grubb DG (2019) Effect of basic oxygen furnace slag particle size on sequestration of carbon dioxide from landfill gas. *Waste Manage Res*. <https://doi.org/10.1177/0734242X18823948>
25. Reddy KR, Chetri JK, Kumar G, Grubb DG (2019) Effect of basic oxygen furnace slag type on carbon dioxide sequestration from landfill gas emissions. *Waste Manag* 85:425–436

Treatment of Diethyl Phthalate from Municipal Solidwaste Open Dumpsite Through Ozone-Based Advanced Oxidation Process



S. Mohan and D. Gokul

Abstract A high content of organic matter especially the refractory organic matter, ammonia, heavy metals and toxic compounds in the leachate from open municipal solid waste dumping makes the treatment of leachate from open dumps more complex. Leachate generation is a major problem for solid waste landfills and causes significant impact on surface water, groundwater and soil. Leachate sample was collected from open dumpsite for Chennai city during the pre-monsoon period. Due to its non-segregation in nature, it has non-homogeneous chemical composition as well as concentration it is essential to treat the leachate before letting out into drains which ultimately reaches the water bodies. In this paper, synthetic leachate was prepared in accordance with the characteristics of the dumpsite leachate and removal of Diethyl Phthalate (DEP) through Ozone-Based Advanced Oxidation Process (AOP) was investigated and reported. AOP plays a significant role in leachate treatment techniques due to its capability of rapid breakdown of DEP which are resistant to conventional biological or Physico-chemical treatment. Semi-batch studies with $O_3, O_3 + H_2O_2$ were demonstrated and the control parameters are optimized for the leachate treatment. $O_3, O_3 + H_2O_2$ process was performed in the natural pH range and initial experiments were carried out with semi-batch ozone only. The addition of different concentrations of H_2O_2 leads to increase in pollutant removal and the results are discussed. Various influencing parameters that govern the efficiency of AOP are evaluated and reported. The influence of pH, COD, heavy metals, UVA and intermediate products on the performance of AOP was also studied and efficiency of the process was determined. It is found that Peroxone-based AOP process is an efficient and viable treatment technique for the treatment of leachate from open dumping site of municipal solid waste.

Keywords Plastic wastes · Solid waste dumpsite · Leachate · Advanced oxidation process · Peroxone · Intermediate products

S. Mohan (✉) · D. Gokul
Indian Institute of Technology Madras, Chennai, India
e-mail: smohan@iitm.ac.in

1 Introduction

Waste is the most visible environmental problem among many in many Indian cities. India has also been experiencing rapid urban growth since the late 1980s in terms of increasing population, changing consumption patterns, economic development, changing income, urbanization and industrialization result in increased generation of solid waste and a diversification of the types of the solid waste generated. Increased waste generation creates more environmental problems in this area, as many cities are not able to manage wastes due to institutional, financial, technical, regulatory, knowledge and public participation shortcomings [1]. The consequence is environmental degradation, caused by inadequate disposal of waste. The impact of disposed waste is composed of: (i) the contamination of surface and groundwater through leachate; (ii) soil contamination through direct waste contact or leachate; (iii) spreading of diseases by different vectors like birds, insects and rodents; (iv) odour in landfills. Although Indian government has formulated policies for environmental protection, these policies have been implemented only in very few cities. In most of the huge cities and rural areas, solid waste open dumpsite is the most commonly used method of solid waste disposal. According to Seadon [2], waste cannot responsibly be dumped without due concern and preparation, because not only is it unsightly, unhygienic and potentially disastrous to our environment, it also requires the allocation of space and incurs costs related to the consequences of the waste disposal. Moreover, suitable landfill sites are becoming more difficult to find as urban areas expand. Also, individuals are not willing to accept the implementation of a new landfill site near them because of concerns about smell, litter, pollution, pests and the reduction in the value of their homes. There are large costs involved in providing conveniently located and environmentally responsible landfill facilities.

According to a study published in science journal in the year 2010, around 8 million tonnes of plastic wastes were dumped into the oceans globally. Plastic littering and mismanaged plastic waste systems are prime causes of this. India ranks 12th in mismanaging 0.60 million tonnes of plastic waste per year [3]. As estimated, the cumulative amount of plastic waste will more than double in the next decade due to the absence of any improvement to waste management systems in the 192 coastal countries. However, 50% improvement in waste disposal in the 20 top-ranked countries will lead to a reduction in mismanaged waste by 41% by 2025. Plastics are synthetic resinous substances that can be moulded with the help of heat or pressure [4]. There are two main classes of plastics:

- Thermosetting—plastics that can only be heated and be moulded once. If re heated they cannot soften.
- Thermoplastics—plastics that are moulded by heating and can be remoulded if heated again.

According to Esakku et al. [5], the solid waste composition of Chennai is given in Figs. 1 and 2 represents different usages of plastics produced globally.

Fig. 1 Solid waste composition in Chennai

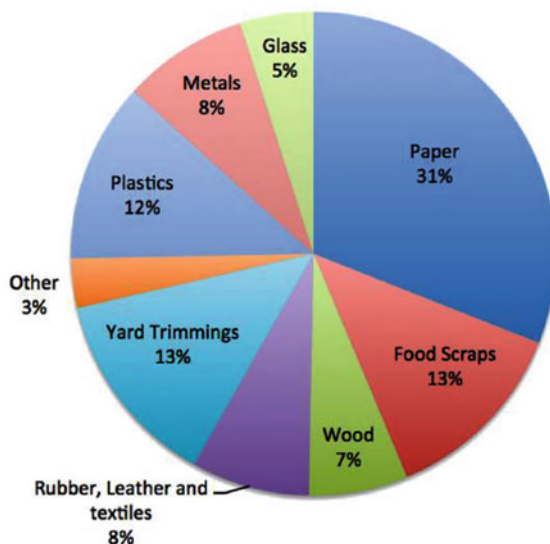
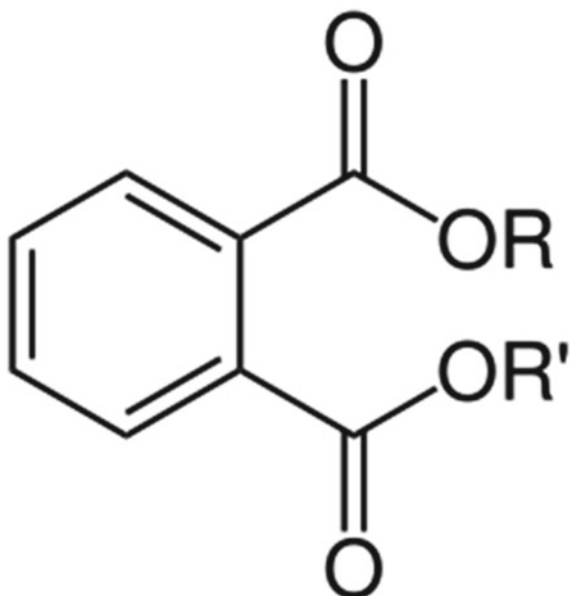


Fig. 2 General structure of phthalates



Phthalates/Phthalate esters are mainly used as plasticizers to increase its flexibility, transparency, durability and longevity. Phthalates are essentially an additive to products, usually as a solvent used to dissolve and carry fragrances in cosmetic and personal care products. Phthalates are not firmly attached to plastic molecules, thus they easily migrate to the surface of the products and leached out. In 2011

according to USEPA, ~8.5 Million Tonnes of plasticizers are produced globally out of which 70% (~6 Million Tonnes) are phthalates (CEH: Plasticizers (Report). IHS Markit. July 2015. Retrieved 2017-04-07.) About 25 types of phthalates are commonly produced worldwide for the plastic industry. Four environmental toxic phthalates were reported:

- Diethyl phthalate (DEP)
- Dibutyl phthalate (DBP)
- Dimethyl phthalate (DMP)
- Diethylhexyl phthalate (DEHP)

DEP is the most commonly found phthalate in water/wastewater due to its high solubility followed by DEHP. The general structure of phthalates/phthalic esters is shown in Fig. 2.

Due to its common presence in plastics, majority of the people are exposed to phthalates. Three phthalates such as Diethyl phthalate, Dimethyl phthalate and Diethyl phthalate are endocrine disruptors in the human reproductive systems; resulting in a change in the hormone. Degradation of plastic wastes results in leaching of phthalates finally ends up in surface water and groundwater. DEP and DMP are highly volatile and thus found in higher concentrations in the environment [6]. Advanced Oxidation Process (AOP) is an array of Physico-chemical processes [7] used to oxidize/mineralize organic pollutants in water/wastewater by the accelerated production of hydroxyl free radical ($\bullet\text{OH}$) [8–10]. There are different types of AOP classification which is shown in Fig. 3 [11–13].

2 Materials and Methods

Relevant data were collected from government sources and various news articles, journal papers, etc. Synthetic leachate was prepared in correlation with the characteristics matching with the solid waste open dumpsite located at Perungudi through leachate sampling at different time periods and the maximum concentration of each parameter are used for preparation of synthetic leachate [14]. All chemicals and reagents were purchased in analytical grade from Sigma Aldrich company for our research purposes.

3 Results and Discussion

According to a survey conducted in Chennai city, Plastic trash comes from a variety of sources and is exacerbated by multiple factors such as restaurants, roadside eateries and bars are among the largest consumer of plastics. Every day around 3 lakhs single-use plastic cups are sold at 300 bars attached to the government which is a concerning factor. Around 10 tonnes of plastics used by 20,000 roadside eateries every day and

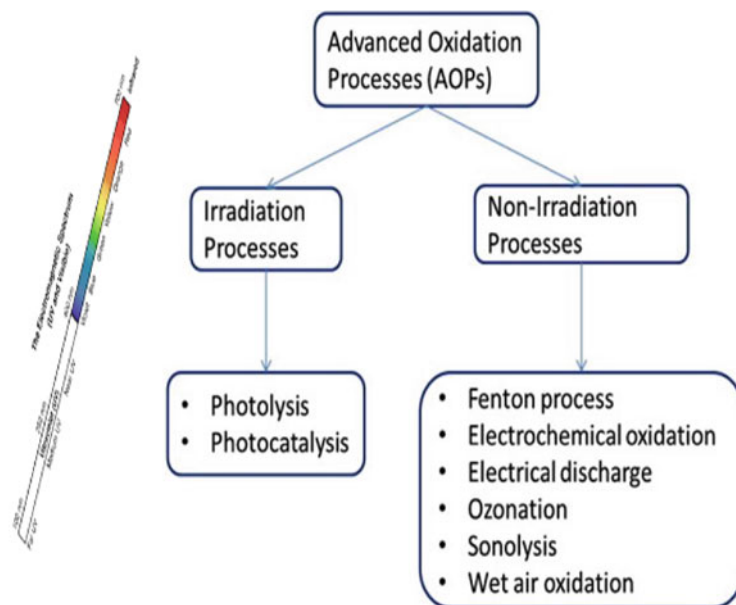


Fig. 3 AOP classification

around 3 lakhs water pouches are sold every day in Chennai. Around 4000 licensed restaurants generate around 5250 kg of plastics daily including packaging of foods and other usages.

Ozone-based advanced oxidation process is used for treatment of phthalates in wastewater/leachate before discharging into land. The characteristics of the synthetic wastewater are given in Table 1.

Table 1 Synthetic leachate characteristics

Parameters	Concentration (mg/L)
COD	10500
BOD	650
DEP	10
Chloride	2500
Zinc	2
Copper	1.5
Manganese	10
Nickel	0.5
Sulphate	5
Total chromium	1.5
Lead	5

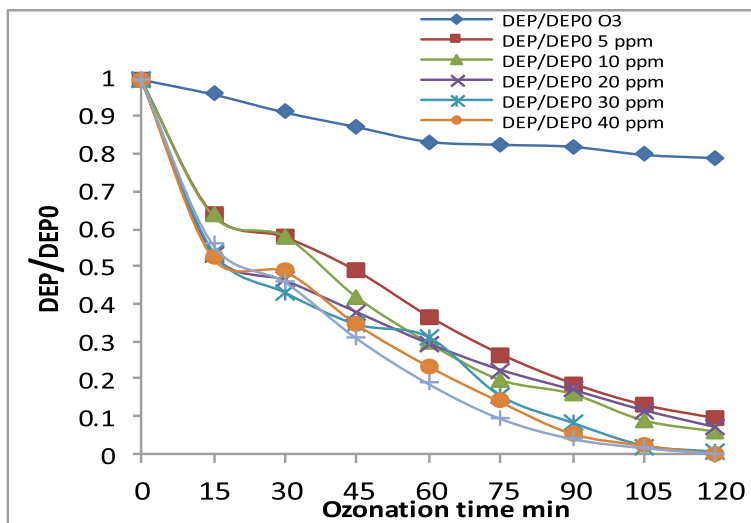


Fig. 4 Degradation of DEP in ozone and peroxone process

Diethyl phthalate (10 mg/L) was used as a model compound for phthalate representation and spiked into the wastewater. Semi-batch ozone system was used for the treatment of DEP and various concentrations of H_2O_2 (5, 10, 20, 30, 40 and 50 mg/L) [15] were added into the ozone system to study the removal of DEP and formation/degradation of the intermediate products. AOP experiments were carried out for 2 h and for each 15 min sampling was done to study the efficiency and optimization of the experiments. Degradation of DEP in various O_3 and $\text{O}_3/\text{H}_2\text{O}_2$ experiments was shown in Fig. 4.

From Fig. 4, DEP removal with ozonation results around 25% efficiency which is very less. To increase the removal efficiency of DEP various concentrations of H_2O_2 such as 5, 10, 20, 30, 40 and 50 mg/L were added in the semi-batch ozone system which results in around 99% of DEP removal optimized to $\text{O}_3/40$ mg/L of H_2O_2 .

4 Conclusion

This work has shown the performance of O_3 alone and O_3 combined with H_2O_2 concentrations for degradation of DEP from wastewater. $\text{O}_3 + 40$ mg/L of H_2O_2 found to degrade 99.9% of DEP which is considered as optimum treatment condition. Also, for this optimized condition, COD removal was achieved higher than the other H_2O_2 concentrations. Plastic pollution impacts the environment in all means knowingly or unknowingly in the form of phthalates which leach out to the wastewater/water by different means. We need to initiate various research innovative things

carved from plastic wastes dumped in the environment. Plastic recycling schools should be created to have a positive impact on the society and environment.

References

1. Pires A, Martinho G, Chang NB (2011) Solid waste management in European countries: a review of system analysis techniques. *J Environ Manag* 92:1033–1050
2. Seadon JK (2010) Sustainable waste management systems. *J Cleaner Prod* 18:1639–1651
3. Al-Salem SM, Lettieri P, Baeyens J (2009) Recycling and recovery routes of plastic solid waste (PSW): a review. *Waste Manag* 29(99):2625–2643
4. Kumar SM, Mudliar SN, Reddy KMK, Chakrabarti T (2004) Production of biodegradable plastics from activated sludge generated from a food processing industrial wastewater treatment plant. *Biores Technol* 95:327–330
5. Esakku S, Selvam A, Palanivelu K, Nagendran R, Joseph K (2006) Leachate quality of municipal solid waste dumpsites at Chennai, India. *Asian J Water Environ Pollut* 3:69–76
6. Rudel RA, Perovich LJ (2009) Endocrine disrupting chemicals in indoor and outdoor air. *Atmos Environ* 43(1):170–181
7. Pignatello JJ, Oliveros E, MacKay A (2006) Advanced oxidation processes for organic contaminant destruction based on the fenton reaction and related chemistry. *J Environ Sci Technol* 36:1–7
8. Tizaoui C, Bouselmi L, Mansouri L, Ghrabi A (2007) Landfill leachate treatment with ozone and ozone/hydrogen peroxide systems. *J Hazard Mater* 140:316–324
9. Abbas AA, Ping GJLZ, Ya PY, Al-Rekabi WS (2009), Review on landfill leachate treatments. *Am J Appl Sci* 6(4):672–684
10. Lopez A, Pagano M, Volpe A, Di Pinto A, (2004) Fenton's pre-treatment of mature landfill leachate. *Chemosphere* 54:1000–1005
11. Umar M, Aziz HA, Yusoff MS (2013) Trend in the use of Fenton, electro-Fenton and photo-Fenton for the treatment of landfill leachate. *J Waste Manag* 30:2113–2121
12. Sanjay M, Amit D, Mukherjee SN (2013) Applications of adsorption process for treatment of landfill leachate. *J Environ Res Develop* 8(2):1–7
13. Trujillo D, Font X, Sanchez A (2006) Use of Fenton reaction for the treatment of leachate from composting of different wastes. *J Hazard Mater B138*:201–204
14. Mohan S, Mamane H, Avisar D, Gozlan I, Kaplan A, Dayalan G (2019) Treatment of diethyl phthalate leached from plastic products in municipal solid waste using an ozone-based advanced oxidation process. *Mater* 12(24):4119
15. Wu JJ, Wu CC, Hong WN, Chang CC (2004) Treatment of landfill leachate by ozone-based advanced oxidation processes. *Chemosphere* 54:997–1003
16. Ngoc UN, Schnitzer H (2009) Sustainable solutions for solid waste management in Southeast Asian countries. *Waste Manag* 29:1982–1995
17. <http://www.grida.no/resources/6925>

Static and Dynamic Leaching Studies on Coal Gangue



Mohammed Ashfaq , M. Heera Lal , and Arif Ali Baig Moghal 

Abstract In the present study, an attempt has been made to determine the leachability of selected trace metals like As, Cr, Co, Se, Ni, Cu, Zn, Cd, Pb and Mn from coal gangue sourced from an underground and open cast mining area(s) of Bhupalpally Coalfields of Telangana State, India. A standard laboratory leaching test (dynamic in nature) developed for combustion residues has been adopted to study the leachability of these trace elements as a function of liquid to solid ratio and pH. A series of static column leaching tests were also conducted to investigate the leachability of these selected heavy metal ions simulating field conditions. The column tests revealed that heavy metals from coal gangue exhibit greater mobility particularly under acidic conditions. Further, relatively higher concentrations were leached for both static and dynamic leaching conditions at low pH levels and is attributed to the difference in solubility product values of respective metal ion complexes. Among the targeted metal ions, with a metal extraction of 30% and 65%, respectively, As and Se showed highest mobility from both static and dynamic leaching tests.

Keywords Coal gangue · Trace metal elements · Leaching

1 Introduction

Mining is a primary activity in obtaining minerals and fossil fuels that produce enormous amounts of waste, which is a continuous source of contamination posing a threat to the surrounding environment [1]. In India, coal is the fundamental source of fuel for the production of commercial energy. Coal mining is often associated with the generation of huge volumes of wastes at various stages of its extraction and waste generated during the mineral processing phase is popularly known as ‘coal gangue’.

Of the total mining waste, coal gangue alone accounts to 20–40% and it is characterised by its diversity in grain size and petrographic composition [1–4]. Among the industrial solid wastes, coal gangue is one of the largest and most harmful wastes

M. Ashfaq · M. Heera Lal · A. A. B. Moghal (✉)
Department of Civil Engineering, National Institute of Technology Warangal, Warangal 506004,
Telangana, India
e-mail: baig@nitw.ac.in

generated from the coal production process [5]. Currently, coal gangue is loosely stockpiled at the mining sites and annual accumulative stockpiles of coal gangue in India are to an extent of 550 million tonnes [6]. The disposal of such a large amount of coal gangue induces many environmental and ecological issues like the contamination of soil and underground water bodies.

Coal gangue is used extensively as a raw material in thermal power plants to effectively leverage its calorific value. Though, such utilisation measures of reducing the amount of coal gangue can yield immediate economic benefits but can give rise to serious environmental implications. Exploring avenues for sustainable recycling of coal gangue for economic and environmental concerns is a pressing task for geotechnical and environmental engineers [5].

The significant factor which limits the bulk utilisation of many novel geomaterials is the leaching phenomenon of trace elements into the ground surface. Trace elements due to their cumulative nature and inability to decompose in natural processes pose a special concern [7]. Leaching has proven to be one of the primary pathways for trace elements entry into the ecosystem and studies focused on the leaching behaviour of trace elements from coal gangue are relatively sparse [8]. Compared to coal, coal gangue has shown higher trace element concentrations and subsequently, the emission behaviour of coal gangue trace elements will be in contrast to that of coal [9]. Thus, understanding the type and extent of trace element mobilisation in coal gangue becomes extremely pivotal.

In this context, the present work intends to analyse the leaching phenomenon of trace elements from coal gangue from a sustainability perspective. Based on the review of the literature, As, Cr, Co, Se, Ni, Cu, Zn, Cd, Pb and Mn are the trace metal elements selected for the current study. An attempt has been made to study the effect of testing methodology on the leaching behaviour of trace elements by adopting static and dynamic leaching methods. The effect of liquid to solid ratio on the leaching phenomenon of trace metal elements from coal gangue has also been studied.

2 Materials and Methodology

Coal gangue was procured from Kakatiya Coal mines, Bhupalpally, Telangana. The sourced samples were immediately sealed in plastic bags to prevent contamination. These samples were air-dried and crushed prior to passing through a 2 mm mesh sieve to homogenise them for the subsequent analysis. The powdered coal gangue samples were dried in a temperature-controlled oven at 100 °C for 24 h to remove moisture. Later the content was stored in air-tight polyethylene containers. The samples were sealed for 30 days to reach radioactive equilibrium.

The coal gangue samples were digested using an acid mixture (HCl: HNO₃) in the ratio of 3:1 in accordance with the procedure described in USEPA (3050B) [11]. After digestion, the concentrations of toxic elements in coal gangue were determined by inductively coupled plasma atomic emission spectroscopy (ICP-AES). The shake

Table 1 Physical properties of coal gangue

Properties	Values
Specific gravity	2.57
Grain size distribution	11
Coarse fraction (%)	89
Fine fraction (%)	
Atterberg limits	28
Liquid limit (%)	NP
Plastic limit (%)	NP
Plasticity Index (%)	
Compaction characteristics	17.6
Optimum moisture content (%)	21
Maximum dry density (kN/m ³)	
pH	7.24
Carbon content (%)	3.5

extraction of solids as detailed in ASTM D3987-85 [12] was carried out for dynamic leaching analysis. In this method, a varying liquid to solid ratio of 5–100 has been used and agitated at a rate of 29 rpm for a period of 18 h at a controlled temperature of 27 °C.

Column apparatus setup described in ASTM D4874-95 [13] has been used for static leaching study. The coal gangue sample was moved into a fixed glass column of 30 mm internal diameter and having a length of 60 cm. The column setup was packed at the top of the sample for uniform dispersion of the solution. The physical properties and chemical composition of the coal gangue are presented in Tables 1 and 2, respectively. And, the particle grain size distribution curve of coal gangue is shown in Fig. 1. It was observed from the grain size distribution curve that no substantial amount of sample passed through the sieve sizes smaller than 0.2 mm mesh sieve.

Table 2 Chemical composition of coal gangue

Constituents	Values (%)
Silica (SiO ₂)	52.70
Alumina (Al ₂ O ₃)	22.60
Ferric (Fe ₂ O ₃)	6.37
Calcium (CaO)	2.45
Magnesium (MgO)	1.22
Titanium (TiO ₂)	0.98
Potassium (K ₂ O)	2.48
Sulfur (SO ₃)	0.43
Sodium (Na ₂ O)	0.65
Loss on ignition	12.65

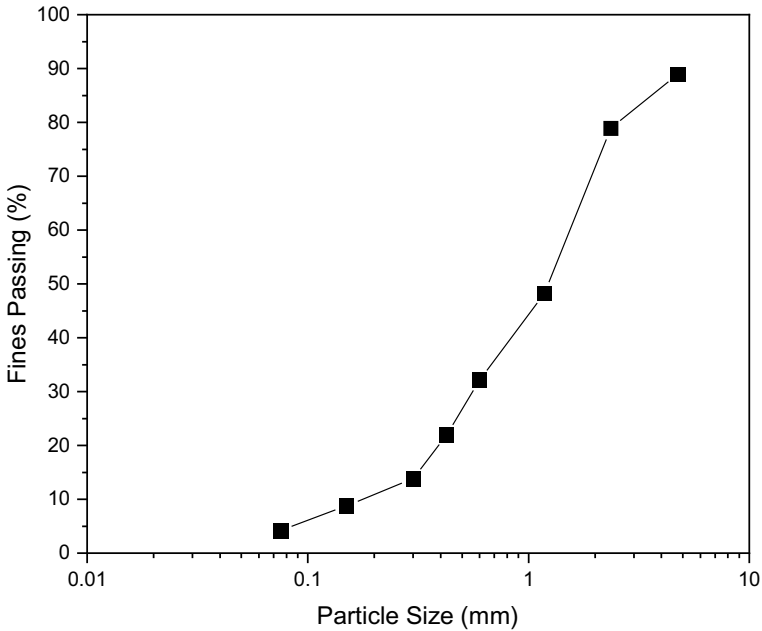


Fig. 1 Grain size distribution curve of pulverised coal gangue

3 Results and Discussion

3.1 pH of Coal Gangue

The pH of the coal gangue sample was determined using a digital pH metre as detailed in ASTM 4972-13 [14]. The pH was established corresponding to varying liquid to solid (L/S) ratio of 5–100 of deionised double distilled water and coal gangue. From the pH results presented in Fig. 2, it is evident that coal gangue is mostly acidic in nature and the acidity of the sample keeps increasing with L/S ratio up to 80. The highest variation and transition towards the acidic nature from neutral pH was observed at L/S ratio of 20. The continuous decrease in pH with increasing L/S ratio is attributed to an increase in the attack on mineral phases of trace elements by hydrogen ions. Similar observations have been made by Sivapullaiah and Baig [15].

3.2 Static and Dynamic Leaching of Coal Gangue

The cumulative concentration of selected trace metal elements with varying L/S ratio is presented in Fig. 3 and it can be inferred that the leaching phenomenon is complex and distinct to each trace metal element. The variation of cumulative concentration

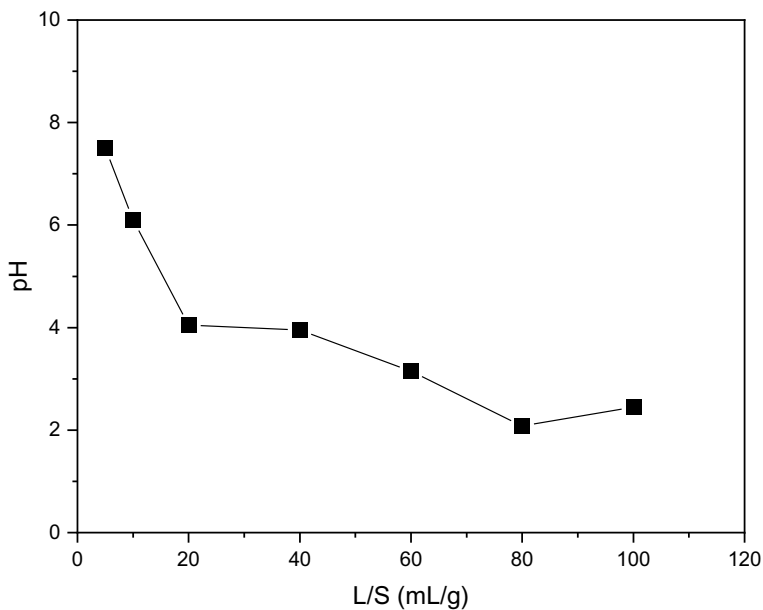


Fig. 2 pH versus L/S ratio of coal gangue

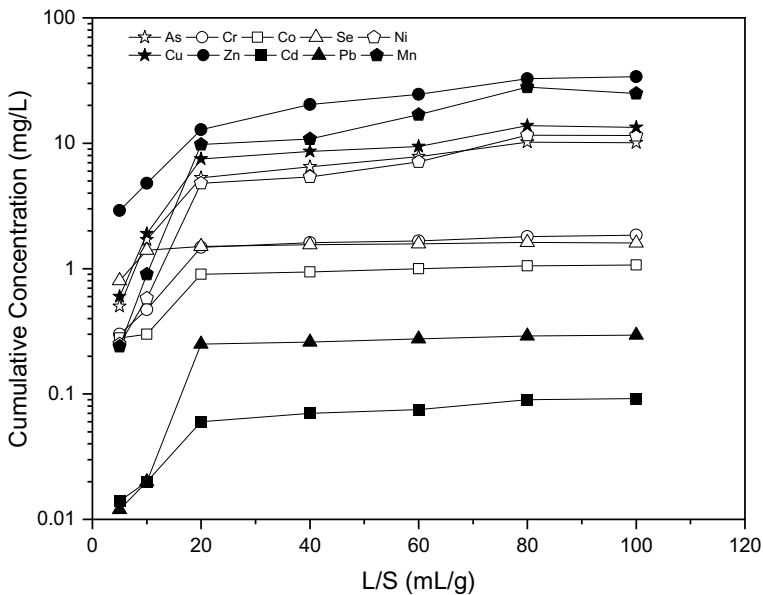


Fig. 3 Cumulative concentration(s) of trace metal elements versus L/S ratio

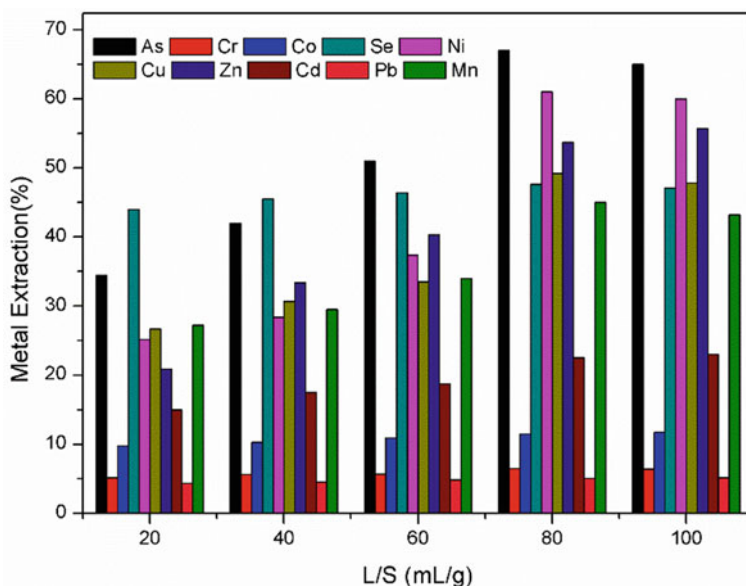


Fig. 4 Metal extraction (%) rates of trace elements from coal gangue with different L/S ratio

of selected trace metal elements at any L/S ratio is observed to be in the following order: Zn > Mn > Cu > Ni > As > Cr > Se > Co > Pb > Cd. The variation in the cumulative concentration of trace elements with the L/S ratio is may be due to the variations in pH with the L/S ratio.

The metal extraction % (ME) of selected trace elements with varying L/S ratio is presented in Fig. 4. At any L/S ratio, ME of selected trace metal elements was found to be in the order of As > Ni > Zn > Cu > Se > Mn > Cd > Co > Cr > Pb. The oxyanionic elements like As, Cr and pH-sensitive elements like Ni, Cu and Mn exhibited greater leaching under acidic medium with increasing L/S ratio. Whereas, Zn and Se have shown amphoteric leaching phenomenon in both acidic and neutral media. The trace metal elements Pb, Cd and Co have shown a relatively lower amount of extraction even at higher L/S ratio.

To simulate static leaching condition which is usually the case in open cast mines, column studies were performed. A comparison of ME from coal gangue for static leaching and dynamic leaching test was performed at L/S ratio of 20 and the results are presented in Fig. 5. From the results, an inconsistent leaching pattern was observed for both the leaching methods. It was observed that the order of ME is the same for both the tests, but the quantity of ME was relatively higher in static leaching method.

The higher leaching time and greater sample amount in static leaching test are the possible influencing factors for relatively greater mobility of metals [16]. Thus, from this study, it can be concluded that the selected trace metal elements have shown the tendency to leach from the coal gangue. The results obtained are in coherence with the previous studies [8, 16, 17].

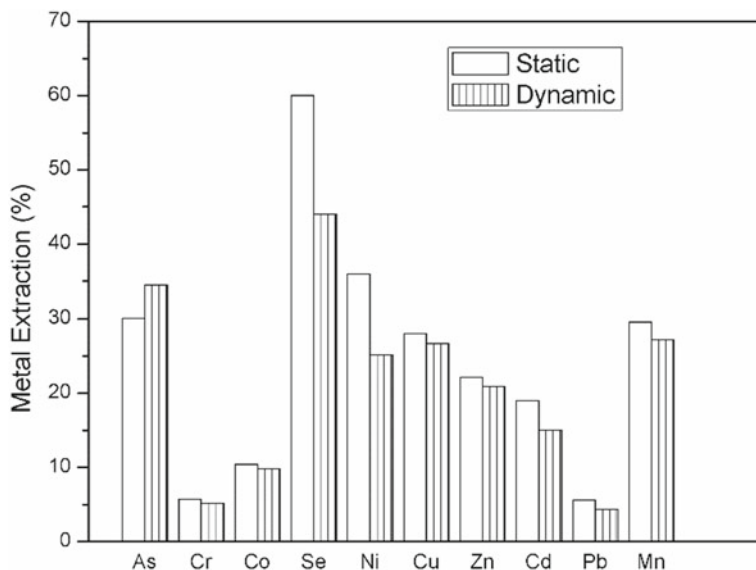


Fig. 5 Metal extraction (%) rates of trace elements from coal gangue through static and dynamic leaching tests at a fixed L/S ratio of 20

3.3 Leaching Mechanism of Selected Trace Metal Elements from Coal Gangue

Arsenic (As) In the current study, As exhibited very high mobility ME of 30%. Being oxyanionic in nature, leaching phenomenon of arsenic is characterised by its pH sensitivity particularly in the acidic medium as it impedes the ability of arsenate to react with other trace elements in forming precipitates [18, 19].

Chromium (Cr (III)) Chromium in bituminous coal is mostly in the trivalent state Cr (III) which is relatively insoluble compared to Cr (VI). Owing to its feebly lower solubility, it remains in insoluble form in the coal gangue matrix.

Cobalt (Co) Though the concentrations of Co in coal gangue are found to be higher, except at L/S of 20, it has largely remained immobile. The greater affinity of Co towards the iron and Fe-bearing species contributes to its poor leaching even under acidic conditions.

Selenium (Se) Coal gangue is highly enriched with Se and among the selected trace metal elements, it exhibited the highest mobility with a ME of 65%. Se usually exists as Selenate in oxidised coal or is bound to Fe oxides. Under both these modes, Se is bound weakly to its respective oxides enabling its easy release [22–24].

Nickel (Ni) The release characteristics of Ni are known to be pH-sensitive and the results from this study reconfirm this fact. The leaching phenomenon of Ni is observed to be similar to Se and As.

Copper (Cu) Cu is observed to leach in a greater degree throughout the range of pH and a rate of mobility was particularly higher in acidic conditions. The Cu ions are not controlled by the dissolution of minerals but are dependent on adsorption [18]. The lack of carbonates and oxy-hydroxides, which resist the mobility of Cu by chemisorption might be the detrimental factor in the higher mobility of copper [20].

Zinc (Zn) The Zn is widely regarded as a mobile element and it is often out-competed by other cations like Pb and Cu adsorption sites [25, 26]. Zn is controlled by its ability to form complexes with organic ligands [27]. In the present study, Zn has shown mobility over a wide range of pH reconfirming its amphoteric nature as observed by Van der Sloot [28].

Cadmium (Cd) The high solubility potential in aquatic conditions makes Cd the element of highest concern for the environment. However, compared to other trace elements, coal gangue is short in Cd concentrations. In addition to this, Cd forms Otavite [CdCO_3], a relatively insoluble mineral, which further minimises its leaching [18]. In the present study, Cd exhibited relatively lower mobilisation rates compared to other trace elements (Figs. 4 and 5). Though cadmium has shown considerable mobility in acidic medium, the concentration of it is still nominally.

Lead (Pb) Though the concentration of Pb in coal gangue is relatively higher compared to other trace elements, it remains immobile even in acidic medium. This immobility of Pb is attributed to its mineral form, i.e. pyromorphite which is formed due to precipitation of phosphate-based minerals, which is stable and resists hydronium ion interference in acidic medium [20, 29–32].

Manganese (Mn) From the results, the pH-sensitive leaching behaviour of Mn is observed and mobility of Mn increases with the decrease in pH. The lack of oxy-hydroxides and carbonates, which resist the mobility of Mn by chemisorption could have contributed to the higher mobility of Mn.

4 Conclusions

In the present study, the static and dynamic leaching behaviour of trace metal elements from coal gangue was analysed under varying pH conditions and liquid to solid ratio. The following conclusions are drawn:

- With an increase in L/S ratio, the pH value of the coal gangue leachate exhibited consistent decrease. The transition from alkaline to acidic medium occurred at a L/S ratio of 20.
- The order of variations of cumulative concentrations of selected trace metal elements at any L/S ratio is observed to be: Zn > Mn > Cu > Ni > As > Cr > Se > Co > Pb > Cd.
- At a given L/S ratio, metal extraction (%) of selected trace metal elements was found to be in the order: As > Ni > Zn > Cu > Se > Mn > Cd > Co > Cr > Pb. The study further revealed that this order remained unchanged with increase in L/S ratio.

- The oxyanionic elements like As, Cr and other pH-sensitive elements like Ni, Cu and Mn exhibited greater leaching rates under acidic medium particularly with an increase in L/S ratio.
- Zn and Se exhibited amphoteric leaching behaviour under neutral and acidic ranges.
- Elements Pb, Cd and Co have shown relatively lower extraction rates with increase in L/S ratio.

References

1. Karaca O, Cameselle C, Reddy KR (2016) Electrokinetic removal of heavy metals from mine tailings and acid Lake sediments from can basin, turkey. In: GSP 273. ASCE, Chicago, pp 225–234
2. Plewa F, Mysiek Z (2001) Industrial waste management in underground mining technologies. In: ICEE. Gliwice
3. Keefer RF, Sajwan K (1993) Trace element in coal and coal combustion residues. Advances in Trace Substances. Research. Florida: Lewis Publishers
4. Jablonska B, Kityk AV, Busch M, Huber P (2017) The structural and surface properties of natural and modified coal gangue. *J Environ Manage* 190:80–90
5. Wu H, Wen Q, Hu L, Gong M, Tang Z (2017) Feasibility study on the application of coal gangue as landfill liner material. *Waste Manag* 63:161–171
6. Ministry of Coal: Annual Report. Available online: <https://coal.nic.in/content/annual-report-2017>
7. Chuncai Z, Guijian L, Dun W, Ting F, Ruwei W, Xiang F (2014) Mobility behaviour and environmental implications of trace elements associated with coal gangue: a case study at the Huainan Coalfield in China. *Chemosphere* 95:193–199
8. Yang L, Song J, Bai X, Song B, Wang R, Zhou T, Jia J, Pu H (2016) Leaching behavior and potential environmental effects of trace elements in coal gangue of an open-cast coal mine Area, Inner Mongolia. China. *Minerals* 6(50):1–18
9. Zhang YY, Nakano J, Liu LL, Wang XD, Zhang ZT (2015) Trace element partitioning behaviour of coal gangue-fired CFB plant: experimental and equilibrium calculation. *Environ Sci Pollut Res* 22:15469–15478
10. Moghal AAB, Shamrani MAA, Zahid WM (2015) Heavy metal desorption studies on the artificially contaminated Al-Qatif soil. *Int J Geomate* 8(2):1323–1327
11. U.S. EPA.3050B (1996) Acid Digestion of Sediments, Sludges, and Soils, Revision 2. Washington, DC
12. ASTM D3987 (2016) Standard practice for shake extraction of solid waste with water. ASTM international, West Conshohocken, PA
13. ASTM D4874 (2016) Standard test method for leaching solid material in a column apparatus. ASTM international, West Conshohocken, PA
14. ASTM D4972 (2012) Standard test method for pH of soil. ASTM international, West Conshohocken, PA
15. Sivapullaiah PV, Baig MAA (2010) Leachability of trace elements from two stabilized low lime Indian fly ashes. *Environ Earth Sci* 61(8):1734–1735
16. Guo S (2017) Trace elements in coal gangue: a review. In: Contributions to mineralization, Ali Ismail Al-Juboury, Intech Open, vol 6, pp 127–144
17. Ashfaq M, Heera LM, Moghal AAB (2018) Characterization of heavy metals from coal gangue. In: Indian geotechnical conference. Bangalore

18. Komonweera K, Cetin B, Aydilek A, Benson CH, Edil TB (2015) Geochemical analysis of leached elements from fly ash stabilized soils. *J Geotech Geoenviron Eng* 141(5):1–14
19. Izquierdo M, Querol X (2012) Leaching behaviour of elements from coal combustion fly ash: An overview. *Int J Coal Geol* 94:54–66
20. Kumpiene J, Langerkvist A, Maurice A (2008) Stabilization of As, Cr, Cu, Pb and Zn in soil using amendments—a review. *Waste Manag* 28:215–225
21. Huggins FE, Huffman GP (2004) How do lithophile elements occur in organic association in bituminous coals? *Int J Coal Geol* 58:193–204
22. Riley KW, French DH, Lambropoulos NA, Farrell OP, Wood RA, Huggins FE (2007) Origin and occurrence of selenium in some Australian coals. *Int J Coal Geol* 72(2):72–80
23. Shah P, Strezov V, Prince K, Nelson PF (2008) Speciation of As, Cr, Se and Hg under coal fired power station conditions. *Fuel* 87(10–11):1859–1869
24. Yudovich YE, Ketris MP (2005) Arsenic in coal: a review. *Int J Coal Geol* 61(3–4):141–196
25. Xinde C, Lena QM, Dean RR, Chip SA (2004) Mechanisms of lead, copper, and zinc retention by phosphate rock. *Environ Pollut* 131(3):435–444
26. Kiikkilä O (2003) Heavy-metal pollution and remediation of forest soil around the Harjavalta Cu–Ni smelter, in SW Finland. *Silva Fennica* 37(3):399–415
27. Kiekens L (1995) Heavy metals in soils. Zink. In: Alloway BJ (ed) 2nd ed. Blackie Academic & Professional, Glasgow, UK
28. Van der Sloot HA (1990) Leaching behaviour of waste and stabilized waste materials. Characterization for environmental assessment purposes. *Waste Manag Res* 8:215–228
29. Cornelis G, Poppe S, Van Gerven T, Van den Broeck E, Ceulemans M, Vandecasteele C (2008) Geochemical modelling of arsenic and selenium leaching in alkaline water treatment sludge from the production of non-ferrous metals. *J Hazard Mater* 159(2–3):271–279
30. Sivapullaiah PV, Moghal AAB (2011) Gypsum treated fly ash as a liner for waste disposal facilities. *Waste Manag* 31:359–369
31. Moghal AAB (2013) Geotechnical and physico-chemical characterization of low lime fly ashes. *Adv Mater Sci Eng* 1–11:674306
32. Moghal AAB (2017) A state-of-the-art review on the role of fly ashes in geotechnical and geo-environmental applications. *J Mater Civil Eng* 29(8):04017072

Sustainability of Vertical Barriers for Environmental Containment



Jeffrey C. Evans, Daniel G. Ruffing, Krishna R. Reddy, Girish Kumar, and Jyoti K. Chetri

Abstract Vertical barriers have long been used to control groundwater flow and subsurface contaminant migration from contaminated land sites. Commonly employed vertical barrier types available to owners and designers include those constructed using slurry trenching techniques such as soil-bentonite (SB), and cement-bentonite with slag (slag-CB), in situ soil mixed walls (SMW), as well as driven barriers such as sheet piles. The selection of the appropriate vertical barrier technique depended upon site geology, cost, and regulatory requirements with no consideration of the global environmental impact of the type of vertical barrier chosen in terms of sustainable engineering. In this paper, the sustainability of four commonly deployed vertical barrier techniques is discussed. Using the case study method, the paper evaluates a previously completed project where an SB slurry wall was constructed. Evaluations are described for an environmental sustainability assessment (based on the materials, fuels, and equipment used; transport distances for personnel travel and materials/equipment transport), an economic sustainability assessment (based on the direct and indirect costs), and a social sustainability assessment (based on a survey taken by stakeholders/professionals/experts). The paper closes with findings, conclusions, and recommendations regarding the sustainability of vertical barriers.

Keywords Vertical barrier · Sustainability · Soil-bentonite · Slag-cement-bentonite · Soil mixing · Sheet piles

J. C. Evans (✉)
Bucknell University, Lewisburg, PA 17837, USA
e-mail: evans@bucknell.edu

D. G. Ruffing
Geo-Solutions, LLC, New Kensington, PA 1506, USA

K. R. Reddy · G. Kumar · J. K. Chetri
University of Illinois at Chicago, Chicago, IL 60607, USA

1 Introduction

The United States Congress has declared sustainability as national policy committing “to create and maintain conditions under which humans and nature can exist in productive harmony, that permit fulfilling the social, economic and other requirements of present and future generations” (The National Environmental Policy Act of 1969). For environmental remediation projects, sustainability is an important consideration in the selection of remediation approaches or even a comparison of sub-approaches, e.g., vertical barrier walls. This paper provides a summary of a comparison of the sustainability of four common vertical barrier installation methods in terms of their relative environmental, economic, and social sustainability. Although this study is limited in scope, especially due to the relatively small size of the case study project, the methods presented may be used to assess the sustainability of larger vertical barriers or vertical barriers vs. alternate remediation methods.

2 Vertical Barriers

The four cutoff wall (i.e., vertical barrier) installation methods that were chosen for evaluation in this paper are commonly used techniques for slowing the flow of groundwater or the migration of subsurface contaminants. A planned companion paper will address other available installation methods and sub-variations of these methods.

2.1 *Method 1: Soil-Bentonite Slurry Trenches*

The terms slurry trench and slurry cutoff wall are widely recognized to refer to the installation of nonstructural walls using long, continuous slurry supported excavations [1]. The slurry trench installation method refers to construction practices that utilize an engineered fluid, generally consisting of some mixture of clay and water, to hold open the sidewalls of an excavation, thereby permitting the excavation of deep and narrow trenches without the need for other conventional excavation support systems. Slurry trench cutoff walls have been employed at thousands of sites across the United States and internationally in a variety of applications, including at waste sites to contain contaminated groundwater, at “clean” sites to dewater excavations, and at dams, levees, and similar structures to improve stability. Most slurry trenches are excavated with excavators which can be modified to dig up to 30 m deep and deeper depths are possible with clamshell excavators.

In the installation of soil-bentonite (SB) slurry trench cutoff walls, the trench is excavated under slurry followed by a distinct backfilling step wherein the slurry is displaced by a mixture of soil and slurry. This is sometimes referred to as a two-step

or two-stage slurry trench installation. SB cutoff walls are the most common type of nonstructural slurry trench. These walls were sporadically used in the United States between the 1940s and 1970s after which their use became commonplace. Thousands of these walls have been constructed for a number of purposes.

SB backfill may be blended using a variety of equipment, but the most common and convenient method is to mix batches of backfill alongside the slurry trench using small excavators and/or dozers. The resultant mix looks like wet concrete (i.e., low to moderate slump) and is normally placed in the trench with an excavator. The mixture is placed in a semi-fluid state which allows it to flow into the trench and displace the trench slurry. Once the backfill operation is complete, the SB backfill consolidates slightly, ultimately behaving like a soft clayey soil. The most important property of the SB backfill is low permeability. Typically, SB backfill has a permeability in the range of 10^{-6} to 10^{-8} cm/s. Environmental projects often require a permeability less than 1×10^{-7} cm/s, but a levee or dewatering project may require a permeability less than 1×10^{-6} cm/s. Either value is achievable with the right mix of materials. SB backfill has low strength and will remain soft (in the range of 0 to 15 kPa) for the life of the barrier, but this is nearly always sufficient to maintain a vertical cut through the wall for subsequent installation of utilities and other light structures. The most important variables in a SB mix design are bentonite content and grain size distribution. In general, SB backfill performs well when exposed to pure phase contaminants or impacted groundwater due largely to the fact that most of the matrix is composed of inert soil particles [2].

2.2 Method 2: Self-hardening Slurry Trenches, e.g., Cement-Bentonite or Slag-Cement-Bentonite

Cement-Bentonite (CB) slurry trenches represent a smaller and more specialized type of slurry trench installation method used in the US since the early 1970s. In Europe and many other international locales, CB walls are the more common barrier wall choice. In this method, the wall is excavated through a slurry that typically consists of water, bentonite, cement, and granulated ground blast furnace slag cement. The trench slurry hardens in place, normally overnight. The hardened CB slurry serves as the final barrier wall. CB installations do not require a separate backfilling operation, and it's for this reason that this technique is sometimes referred to as one-step or one-phase slurry trench construction.

CB walls are excavated using hydraulic excavators and/or clamshell excavation equipment, the same equipment used for other slurry trench installations. At the slurry plant, cement, or some other setting agent, is added to the bentonite slurry. The viscosity of the mixed slurry is designed to be in the fluid range during the excavation process. The slurry is then pumped from the mix plant to the excavation. Once the excavation is completed to full depth, the bottom is cleaned, and the process moves

on. The slurry stays in the trench and is allowed to set. Typical CB slurry will attain a butter-like consistency overnight and a clay-like consistency after fully hardening.

The properties of interest for most CB slurry walls are strength and permeability. CB slurry has relatively high water content, and because of this, there are more water-filled voids than in a SB backfill. Despite the higher void ratio, typical permeability values are similar to SB backfills, generally less than 1×10^{-7} cm/s after a month of curing. Without the addition of slag, permeability values are one to two orders of magnitude higher. CB can take months to fully harden, and long-term tests have shown CB permeability gradually decreases (improves) over long time scales, measured in years. CB material generally attains 75% of its ultimate strength after 28–56 days of curing and close to 100% after 90 days of curing. The addition of blast furnace slag typically results in a higher strength, lower permeability material, but it takes much longer to achieve the final properties with properties shown to improve out to 6 months and beyond [3]. Chemical compatibility is also an important factor when designing containment systems for impacted groundwater. CB is particularly well-suited to resisting certain oils and petroleum products, and thus, it is often preferred on sites with heavily contaminated groundwater.

2.3 Method 3: Soil Mixed Walls

The term soil mixing loosely refers to any construction approach used to mix soils with or without a reagent additive. In the fields of geotechnical and environmental construction, the term often refers to methods of soil mixing performed in situ for the addition of a cementitious reagent, most commonly Portland cement. The concept for soil mixing originated in the US, but much of the early technological development took place in Europe and Japan until the technology was reintroduced into the US market in the 1980s [4]. There are many equipment configurations and processes that can be used for the successful completion of soil mixing, but the goal is almost always the efficient creation of a soil-reagent mixture with improved properties relative to the soils alone. Independent of the approach, soil mixing equipment typically includes some sort of cutting component (an auger or wheel), mixing paddles, and grout ports through which a fluid grout is pumped through a hollow shaft and out the grout ports. The fluid (which usually contains additives) acts as an aid to drilling and is mixed into the soil column creating the soil-reagent mixture. The term deep soil mixing (DSM) often refers to the use of multi-auger soil mixing rigs that can be used to install linear elements, e.g., cutoff walls. DSM auger configurations are specific to each contractor, but typically include 3 or 4 relatively small (~1 m) diameter augers spaced evenly apart. Another method of soil mixing for the installation of linear elements is chain trenching (Evans and Garbin 2009). This type of soil mixing is completed using essentially a large chainsaw mounted on a tracked chassis.

Soil mixing is often a preferred cutoff wall installation method on highly contaminated sites due to the limited handling of the contaminated soils, the high strengths (350 to 1400 kPa unconfined compressive strength UCS) and low permeability (~5

$\times 10^{-7}$ cm/s) values that are achievable, and because the method is less susceptible to variations in surface topography and soil consistency.

2.4 Method 4: Sheet Pile Walls

Sheet pile in the context of vertical barriers generally refers to methods of driving, vibrating, or placing interlocked individual components of “sheet” material into the ground for the purpose of constructing a barrier. In most cases, the “sheet” material used is steel, but HDPE and vinyl can be used as well. The individual sheet piles often have a “Z” or “W” shaped cross-section in order to give the sheet pile enough rigidity to withstand the driving forces. Various interlock configurations are available, but all are designed to promote continuity between the individual components for the construction of a continuous barrier. Sheet pile barriers are regularly used in temporary applications in which the sheet piles can be retrieved at the end of the project for reuse elsewhere or in applications where the wall is expected to withstand substantial stresses, e.g., seawalls. Conventional sheet piling installations are generally limited to 40’ unless sheet piles are welded together to install deeper walls. Steel is the sheet pile material of choice for the case study sustainability evaluation.

2.5 Case Study

A SB cutoff wall having a length of 200 m, a width of 0.8 m, and an average depth of 7 m was constructed on a site near the Bucknell University campus during the summer of 2016 as part of an NSF-funded research project. The subsurface stratigraphy as determined prior to construction is depicted in Fig. 1. The original design included stripping of topsoil, and backfill made of the excavated silty sands, sands, and gravels

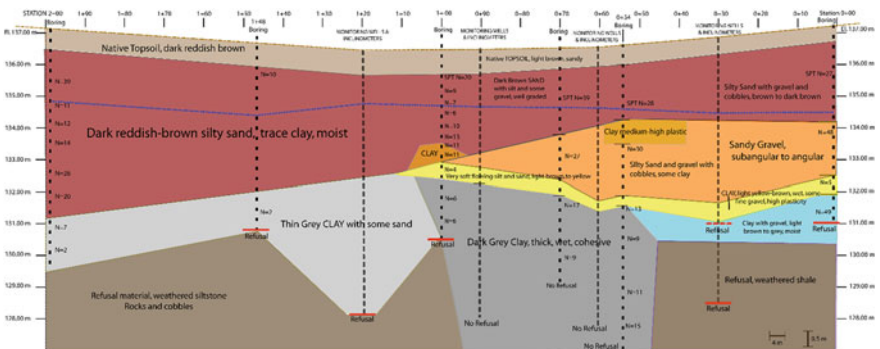


Fig. 1 Subsurface profile along the cutoff wall alignment based upon preconstruction investigations

and underlying clays. These inferred subsurface conditions are assumed the same for each of the four alternative vertical barrier methods assessed for this sustainability assessment case study.

2.6 Sustainability Assessment

In this study, sustainability assessment of the four vertical barrier alternatives (soil-bentonite wall (SB), cement-bentonite wall with slag (CB), in situ soil mixed wall (SM), and sheet pile wall (SP)) was performed using the triple bottom line sustainability framework [5–7]. It consists of environmental sustainability assessment, economic sustainability assessment, and social sustainability assessment.

Environmental Analysis. The schematic in Fig. 2 shows the primary work phases for each barrier wall type and the inputs and outputs assessed for each in terms of environmental sustainability. The life cycle assessment (LCA) was conducted in SimaPro v8.5.2 software using the inventory data for each of the life cycle stages involved in each of vertical barrier methods [8, 9]. The scope of the LCA was limited to the construction stage only so the use and maintenance and end-of-life stages were not included. The functional unit used for the LCA was a 200 m long, 7 m deep,

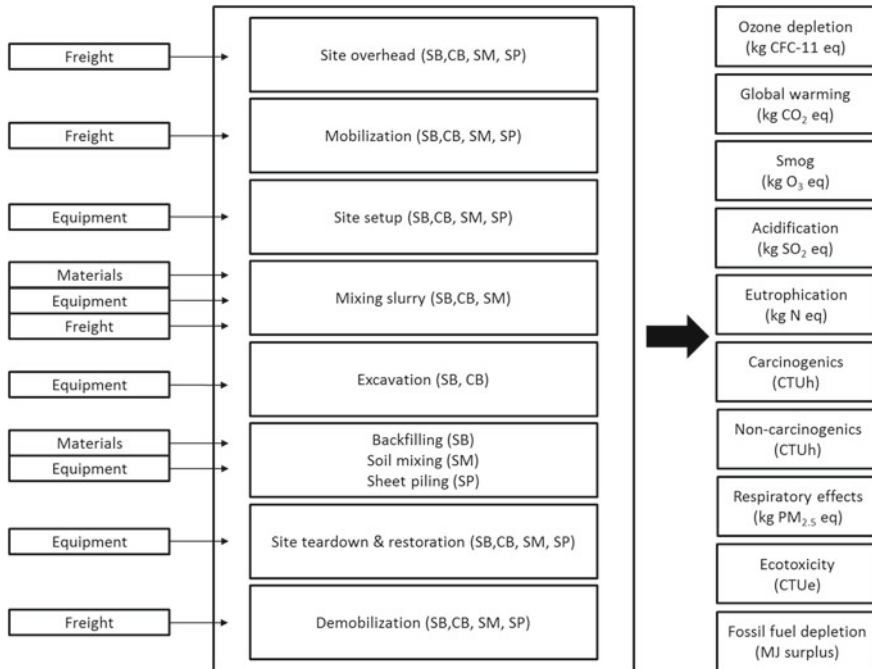


Fig. 2 Phases of construction, system boundary, inputs and outputs for life cycle assessment

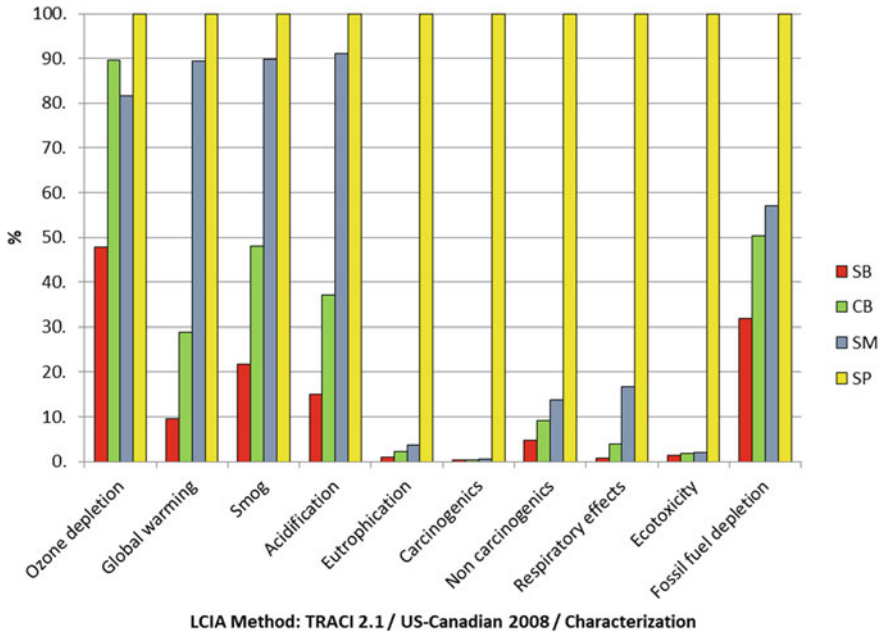


Fig. 3 Environmental impacts of the four vertical barrier systems across the midpoint impact categories of TRACI 2.1 LCIA method

and 0.3 m wide vertical barrier, i.e., the entire case study wall, including the specific geographic location.

The Tool for the Reduction and Assessment of Chemical and other environmental Impacts (TRACI) version 2.1 US–Canadian 2008 life cycle impact assessment (LCIA) method [10] was used for the environmental impact assessment. Using these methods, Fig. 3 shows the environmental impacts from the LCA of the four vertical barrier systems across all the impact categories of TRACI v2.1 LCIA method. Figure 4 shows the results of the LCA with the freight distances limited to ten miles to determine if the reduction in freight distances influenced the results.

Economic Analysis. Figure 5 shows the direct and indirect costs associated with each of the four vertical barrier types. The direct cost accounted for the costs of freight/transport, labor, materials, and equipment/machinery used in the construction of the vertical barrier system. The indirect costs were based on the carbon emissions during the design and implementation and were calculated using the social cost of carbon (SCC) established by United States Environmental Protection Agency [11].

Social Analysis. Social sustainability [12] is a subjective field which makes it difficult to quantify the social impacts of any activity. However, a few approaches, such as Social Sustainability Evaluation Matrix (SSEM), have been developed to quantify the social impacts of an activity [13]. In this study, the functional and social impacts of each vertical barrier option were assessed by conducting an online survey among professionals familiar with these barrier systems. Questions for the survey

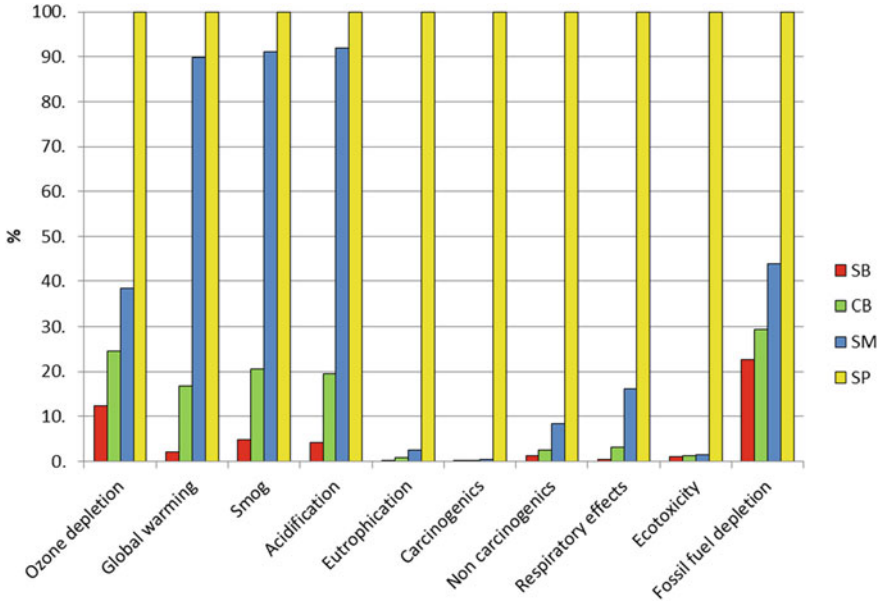


Fig. 4 Environmental impacts of the four vertical barrier systems across the midpoint impact categories of TRACI 2.1 LCIA method with freight distances limited to ten miles

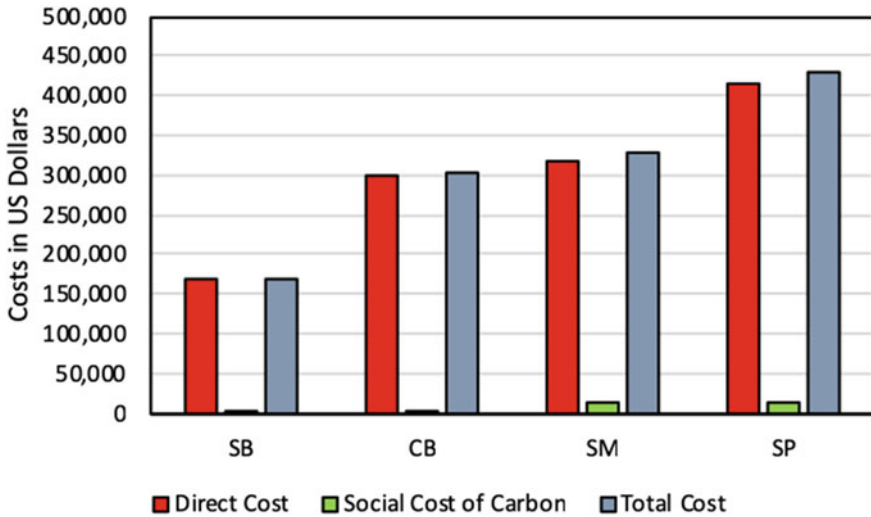


Fig. 5 The direct, social cost of carbon, and total costs of the four vertical barrier systems

were structured to provide indicators of the social impact of each of the vertical barrier options on aspects at the functional, individual, community, economic, and environmental levels.

The survey results were analyzed and scores ranging from 1 to 4 (1 represents the best, preferred, or most positive impact case and 4 represents the worst, least preferred, or least positive impact case) were assigned to each indicator under each category. The survey was performed using a Google survey with the indicators as shown in Table 1. Respondents included mainly contractors, designers, researchers, and students with various years of experience in the field of vertical barriers. In total, 20 responses were received among which 12 were from contractors/designers/researchers with more than 10 years of experience, 3 were

Table 1 Social sustainability assessment of the barriers based on the relative preference of the respondents

Category	Indicator description	Scores based on the survey			
		SB	CB	SM	SP
Functional Indicators	Relative preference of barrier type (by industry)	12	27	28	40
	Relative level of research and development involved for barrier type	24	27	29	32
	Relative ease of design (e.g. specialty designs)	18	30	34	25
	Relative ease of construction (e.g. equipment, skilled labor, no. of laborers, specialty construction technique)	20	34	35	24
	Relative duration of construction	16	23	36	31
	Relative ease of maintenance and repair	21	29	27	34
	Relative flexibility ⁷ to change design during construction for changed site conditions	21	22	28	36
	Relative level of noise pollution	19	19	30	46
Socio-Individual (workers, residents)	Relative exposure to dust and contaminants (if applicable)	35	34	25	17
	Relative risk of accidents (safety during construction)	20	22	24	41
	Relative opportunities for skill development	26	20	20	31
	Relative employment opportunities for locals	27	29	35	27

(continued)

Table 1 (continued)

Category	Indicator description	Scores based on the survey			
		SB	CB	SM	SP
Sodo-Commmtty	Relative traffic congestion during construction	26	27	29	26
	Relative involvement of community organizations in the project	32	33	30	26
	Relative improvement in quality of life	22	25	27	29
	Relative use of local materials	21	30	26	36
Socio-Economical	Relative impact of the project on the local economic growth	28	31	28	32
	Relative impact on properly value increase	32	32	29	25
	Relative potential for beneficial land use	32	27	22	24
	Relative impact on surrounding local water resources	19	22	23	24
Socio-Environmental	Relative air emissions (air pollutants) during construction	26	23	24	29
	Relative impact on land and agriculture	30	24	22	21
	Relative use of renewable resources	30	32	30	34
	Total Score	989	1055	1087	1151

Note Lowest score = most preferred/best, highest score = least preferred/worst

from contractors/designers with 5–10 years of experience, 3 were from contractors/designers with 1–5 years of experience and 2 were from students/researchers with less than one year of experience. The total score obtained for each barrier alternative under each category is also summarized in Table 1.

The sustainability index was calculated for each alternative following the Spanish Integrated Value Model for Sustainability Assessment (MIVES) methodology as explained in Reddy et al. [7]. The MIVES methodology assists with normalizing the scores obtained from the survey in the range of 0 to 1 which makes the comparison more transparent. The larger the number, the greater the sustainability. Table 2 shows the sustainability index values obtained by the barriers under each category and this information, along with overall social sustainability index, is also presented graphically in Fig. 6.

Discussions. A review of Fig. 3 indicates that the SB and the SP vertical barrier systems have the least and the highest negative environmental impacts, respectively, across their life cycle (from raw materials acquisition to end of construction). The

Table 2 Social sustainability index for the alternative vertical barriers

Category	SB	CB	SM	SP
Functional	0.12	0.08	0.05	0.04
Socio-individual	0.15	0.15	0.14	0.09
Socio-community	0.12	0.10	0.08	0.11
Socio-economic	0.09	0.10	0.13	0.09
Socio-environmental	0.12	0.11	0.14	0.11

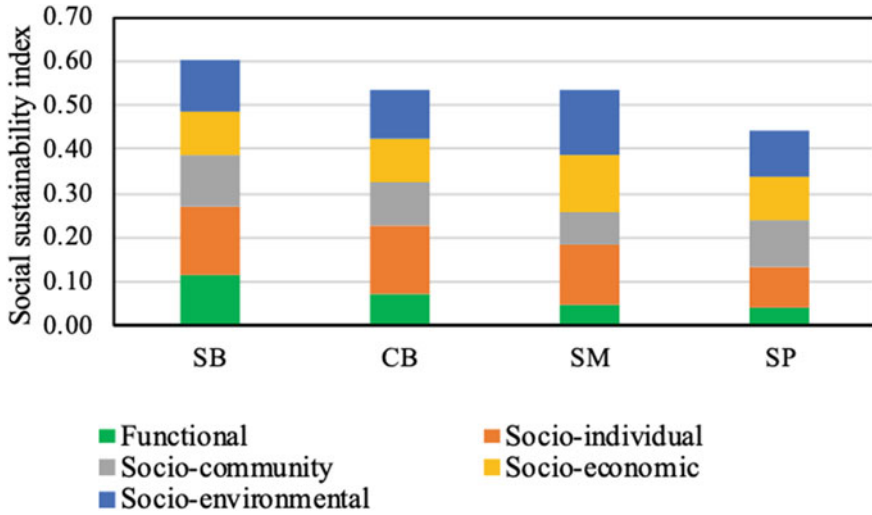


Fig. 6 Comparison of social sustainability of alternative vertical barriers

high negative environmental impacts of the SP wall mainly derived from the manufacture of the steel that was used, fuel used by the equipment to drive the piles, and the impacts from the transportation of the materials and equipment to the site. In the CB and SM cases, most of the environmental impacts were due to the manufacture of the Portland cement, the transportation of the materials and equipment to the site, and the use of fuel for the equipment for mixing the slurry. The conclusions are drawn from Fig. 3 do not change with a review of the information in Fig. 4 which shows the environmental impacts from the transport distance limited analysis as there is no significant difference in the outcome compared to the actual case. Thus, the SB wall can be regarded as the most environmentally sustainable vertical barrier system evaluated for the case study project.

In Fig. 5, the magnitude of the indirect cost is not as high as the direct cost because the carbon emissions across the life cycle of the case study barrier were limited due to the small size of the project. Based on the direct and indirect costs, the SB and SP cases were the most economical and least economical options, respectively. Even

if the indirect costs are not considered, the SB option is still the most cost-effective option among the four alternatives.

As shown in Table 2, the SB wall obtained the highest social sustainability index values under most of the categories except for socio-economic and socio-environmental, which means the SB vertical barrier is the most socially preferred choice. As shown in Fig. 6, the SB wall also received the highest total social sustainability index meaning it is the most preferred choice socially. Since social sustainability is subjective to the relative preference of stakeholders, this conclusion could vary with an increased number of respondents.

3 Conclusions and Future Study

The sustainability assessment performed for this paper was limited in size and scope and the conclusions are relevant only in the context of the inherent biases for the case study project. However, the general conclusion that the SB barrier wall type is the most sustainable method among the four methods evaluated makes sense in the context of the simplicity of this method in terms of relative offsite material consumption and onsite material reuse.

For future sustainability assessments of vertical barriers, the economic sustainability analysis could include other indirect costs, e.g., the cost of other emissions, or a cost–benefit analysis could also be performed for a thorough investigation of the economic sustainability of the different barrier systems. In that case, the indirect costs would sometimes far exceed the direct costs. However, in this study the indirect costs are limited to the SCC only. SCC is essentially an estimate of the monetized damages associated with an incremental increase in carbon emissions in a given year. The SCC integrates different climatic processes, economic growth, and interactions between the climate and the global economy to reflect the climatic impacts in terms of economic damages/costs. Although this does not account for all the economic and social issues associated with a vertical barrier, it does help in evaluating the broader long-term consequences of the different vertical barrier systems and thereby on the decision-making of the most appropriate vertical barrier system to be used. A multi-criteria decision analysis could also be performed to integrate environmental, economic and social impacts, and derive an overall sustainability index.

Acknowledgments The authors gratefully acknowledge the support of the National Science Foundation (Award# 1463198) that enabled the construction of the SB cutoff wall used as a basis for this sustainability analysis.

References

1. Evans JC (1993) Vertical Cutoff Walls, Chap. 17. In: Daniel DE (ed) Geotechnical practice for waste disposal. Chapman and Hall
2. Ruffing DG, Evans JC, Coughenour N (2018) Soil-Bentonite Slurry trench cutoff wall longevity. In: International foundations congress and equipment expo, pp 214–223
3. Opdyke SM, Evans JC (2005) Slag-cement-Bentonite Slurry Walls. *ASCE J. Geotech Geoenviron Eng* 131(6):673–681
4. Evans JC, Garbin EJ (2009) The TRD Method for In Situ Mixed Vertical Barriers. In: Proceedings of the U.S.-China workshop on ground improvement technologies GSP188, pp 271–280
5. Reddy KR, Kumar G (2019) Application of triple bottom line sustainability framework to select remediation method at industrial contaminated site. In: Proceedings of GeoCongress, ASCE, Reston, VA
6. Reddy KR, Adams JA (2015) Sustainable remediation of contaminated sites. Momentum Press, New York
7. Reddy KR, Chetri JK, Kiser K (2018) Quantitative sustainability assessment of various remediation alternatives for contaminated lake sediments: case study. *Sustain J Record* 11(6):307–321. (<https://doi.org/10.1089/sus.2018.0021>)
8. Pré (2018) SimaPro 8.5 LCA software. Amersfoort, The Netherlands
9. International Standardization Organization (ISO) (2006) Environmental management –life cycle assessment –principles and framework ISO 14040
10. Bare JC (2002) TRACI. *J Ind Ecol* 6(3-4):49–78
11. USEPA (2017) The Social Cost of Carbon. https://19january2017snapshot.epa.gov/climatechange/social-cost-carbon_.html. (Accessed 29 Jan 2018)
12. U.S.C. §4321 et seq (1969) <http://www.businessdictionary.com/definition/social-sustainability.html>
13. Reddy KR, Sadasivam BY, Adams JA (2014) Sustainability evaluation matrix (SSEM) to quantify social aspects of sustainable remediation. In: ICSI 2014: creating infrastructure for a sustainable world, ASCE, pp 831–841

A Study on the Behavior of Pond Ash in Unsaturated Conditions Through WRCC



Sanjay Kumar Singh and Janmeet Singh

Abstract Pond ash is a residue obtained from the combustion of pulverized coal in Thermal power plants. Out of the total production of pond ash, only a small quantity of ash is utilized and the remaining unutilized pond ash is deposited as a waste material covering several hectares of land. Usefulness of coal (Pond) ash has been explored in various geotechnical and geoenvironmental practices like the construction of ash dyke, road and railway embankment, landfill liners, etc. which requires detailed knowledge of geotechnical and unsaturated behavior of pond ash. The understanding of the engineering behavior of unsaturated soil is totally dependent on the water retention characteristic curve (WRCC) which is a graphical relationship between volumetric water content and soil suction. In this paper, the geotechnical characterization and water retention characteristic curves of pond ash have been studied. WRCC has been drawn experimentally using Fredlund device based upon the pressure plate technique for wetting and drying cycles, both. Further, an investigation was carried out to study WRCC hysteresis of Pond ash. There exists considerable hysteresis in drying and wetting curves of pond ash samples which indicates a significant difference in behavior between drying and wetting phases. The different WRCC models were used to fit the experimental WRCC data. The measured WRCC match satisfactorily with predicted WRCC using Fredlund and Xing equation whereas there is an upward shift in the WRCC curve derived using Van Genuchten equation as compared to experimental WRCC. Since the direct measurement of unsaturated hydraulic conductivity is difficult to obtain in engineering practices, the unsaturated hydraulic conductivity function is predicted using measured WRCC as the input parameter using SEEP/W software. The behavior of pond ash was also compared with the results obtained for natural sand as a reference material.

Keywords Water Retention Characteristic Curve (WRCC) · Pond ash · Unsaturated behavior · Fredlund and Xing model · Van Genuchten model

S. K. Singh (✉) · J. Singh
Civil Engineering Department, Punjab Engineering College (Deemed to Be University),
Chandigarh 160012, India
e-mail: sksingh@pec.ac.in

1 Introduction

In India, the major source of power generation is from thermal power stations which are the backbone of power capacity addition. The coal used in the country is of low grade having an ash content of 30–45% [1]. The coal ash produced from the combustion of coal requires a vast area of land for its safe disposal. The small proportion of coal ash is utilized and the remaining 40–50% of total production is mixed with water in the ratio of 1:10 and that slurry is disposed of in an ash pond. In the process of their disposal, the coarser particles settle near the inflow point as they are heavier and the finer ash particles move with the flow and settle at the far end near the outlet point of an ash pond. Pond ash has found various applications in the field of geotechnical and geoenvironmental engineering. Use of Coal ash conserves scarce natural resources on one hand and saves the precious land which is otherwise occupied by ash pond and many environmental issues related to the deposited ash. To encourage the use of pond ash, the geotechnical and unsaturated behavior of pond ash is required to be ascertained so that it can be used in place of natural sand. Currently, pond ash has been successfully used as a filling material in road and rail embankments, in dams, in low lying lands and dumping yards, and in a majority of these practices the unsaturated behavior of pond ash prevails.

There are various materials present in the geotechnical field whose characteristics are not consistent with the theory of saturated soil mechanics. The existence of different fluid phases causes the occurrence of unsaturated behavior which is not in line with the concepts and principles of classical engineering practice. Soil material near the ground surface where the level of the water table is beneath the ground surface has negative pore-water pressures resulting in the possible reduction in the degree of saturation. It is difficult to understand the behavior of compacted soils within the framework of classical soil mechanics. The direct practice of unsaturated soil at the highest level involves measurement of soil suction in the unsaturated phase which is relatively time consuming and complex to perform as compared to the test for saturated soil. Other approaches for the implementation of unsaturated soil theories in practice have been suggested wherein the water retention characteristic curve (WRCC) is used along with saturated soil parameters to estimate unsaturated soil properties [2]. The measurement of the WRCC has risen among all other constitutive relations as the necessary parameter required in the field of unsaturated soil mechanics. WRCC have various applications in the geotechnical field related to natural slopes that are subjected to environmental change, in the process of mounding below contaminant retention ponds, in the Stability of deep Vertical or Near-Vertical Excavations, Bearing strength for Shallow Foundations, and Road and Railroad Structures. The present paper deals with the study of the unsaturated behavior of pond ash through WRCC.

2 Materials

The pond ash used was collected from an ash pond situated on the bank of river Satluj in Ropar (India). The representative ash pond sample was collected from the outflow point approximately at a distance of 450 m from ash dyke. The collection point (RP-O) is marked in Fig. 1. The natural sand used in the study was collected from the Beas river.

2.1 Geotechnical Characterization

The specific gravity of the sample is determined as per the procedures mentioned in IS 2720: Part 3 [3]. The specific gravity of pond ash comes out to be 2.13 whereas the value for natural sand is 2.67. The value of the specific gravity of the ash sample is lower than that of sand. The reason for this is pond ash consists of hollow particles or cenosphere from which air cannot be removed. The particle size distribution of pond ash and sand is found as per the method outlined in IS 2720: Part 4 [4]. The grain size distribution of the portion of ash particles which retained on 0.075 mm sieve was determined through sieve analysis. The remaining material which is finer than 0.075 mm was collected and a hydrometer test was conducted. The grain size distribution of ash provides considerable details about its properties and behavior. The ash sample is in the range of silt size containing 90% silt-sized particles. Pond ash sample used in the study is nonplastic and is classified as ML as per IS 1498: 1970. As per classification, the sample of sand is poorly graded and denoted as SP. To measure the MDD and OMC of pond ash, the standard proctor test was conducted as described in IS 2720: Part 7 [5]. The maximum dry unit weight (MDD) and optimum moisture content (OMC) of pond ash sample are 10.67 kN/m^3 and 35.5%, respectively. Further, the maximum density γ_{\max} and minimum density γ_{\min} of sand have been determined using the vibratory table and is found to be 16.45 kN/m^3 and



Fig. 1 Satellite image of Ropar ash pond

13.72 kN/m³, respectively. The permeability coefficient of pond ash and sand was determined as per the method prescribed in IS 2720: Part 17 [6]. The pond ash sample was prepared at 95% MDD and natural sand was prepared at 70% relative density which represents the dense state of samples [7, 8]. The values of the permeability coefficient for pond ash and sand are shown in Table 1. The value of coefficient of permeability of pond ash is in the range of sand and silt. The value of permeability of pond ash is greater than 10⁻⁹ m/s and hence could not be used as a barrier material independently. However, with the addition of bentonite, the value of permeability could be reduced in order to be used as a barrier material [9, 10]. The loss on ignition (LOI) test was performed as per IS 1917: Part 1 [11]. Loss on ignition shows the presence of unburnt carbon in pond ash. In this study, the pond ash was first oven-dried and the temperature of the muffle furnace was increased incrementally till the furnace temperature reaches 1000 °C. The LOI value of the pond ash is 6.25%. This value indicates the presence of low unburnt carbon which shows that the spontaneous heating of pond ash is minimal. Therefore, the pond ash which is a waste material could be used in bulk as a filling material in the construction of embankments without any concern of overheating.

The Morphological characteristics signify the physical description of ash particles and sand which was carried out using a scanning electron microscope (SEM) technique. The SEM of pond ash and sand was carried out for magnification ($\times 100$) and is shown in Fig. 2a, b. It is observed from Fig. 2a that there is a presence of irregular shaped particles containing complex pore structures in the pond ash sample. Larger ash particle is a combination of smaller ones which contains intraparticle voids. The SEM of sand as observed in Fig. 2b indicates that there are no intraparticle voids.

Table 1 Basic properties of soil

Test	Pond ash	Sand
Specific Gravity, G_s	2.13	2.67
Sand (%)	7.40	98.20
Silt (%)	90.40	1.80
Clay (%)	2.20	0.00
D_{10} (mm)	0.016	0.121
D_{60} (mm)	0.030	0.261
Coefficient of uniformity (C_u)	1.87	2.15
Coefficient of curvature (C_c)	0.92	1.32
Maximum dry unit weight (MDD) (kN/m ³)	10.67	–
Optimum moisture content (OMC) (%)	35.50	–
Relative density Test	–	γ_{max} –16.45 kN/m ³
		γ_{min} –13.72 kN/m ³
Coefficient of permeability (m/s)	Dense - 9.1 E-07	Dense - 5.1 E-05
LOI value (%)	6.25	–

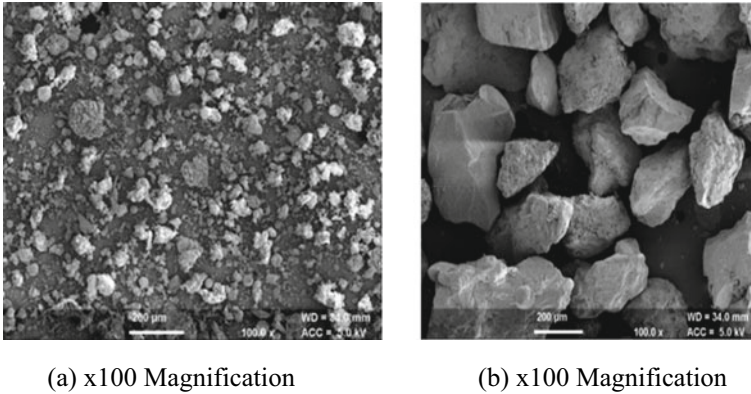


Fig. 2 a and b SEM micrographs of pond ash and sand at $\times 100$ magnification

3 Experimental Methods

The study of geotechnical characteristics result in the index properties and permeability coefficient of pond ash being in the range of silt and sand. Therefore, pond ash could be used in various geotechnical applications as a filling material and in most of these applications, the material is compacted to OMC where the unsaturated behavior of the material prevails. In unsaturated soil, the behavior of soil is dependent upon the negative pore pressure. Thus, it is necessary to understand the unsaturated behavior of pond ash and for which the water retention characteristic curve is needed to be studied. In the present study, Fredlund SWCC device which is a pressure plate device was used to determine the water retention characteristic curve (WRCC) experimentally. Figure 3 shows the actual picture of the instrument used in this study. The sample was compacted in a laboratory at 95% MDD and put into the rings to determine WRCC for the dense state [12].

4 Results and Discussions

4.1 Drying Water Retention Characteristic Curve

The drying stage represents the removal of water from the sample while increasing the matric suction which was determined using a Fredlund SWCC device. The experimental data of matric suction (Ψ) and volumetric water content (θ_w) for pond ash for drying is shown in Fig. 4. It has been observed from the test data that the sample gets nearly desaturated at the application of pressure of 400 kPa. The air entry value (AEV) and residual suction (Ψ_r) were determined by the graphical method [12] and its value is found to be 30 kPa.



Fig. 3 Fredlund SWC-150 device

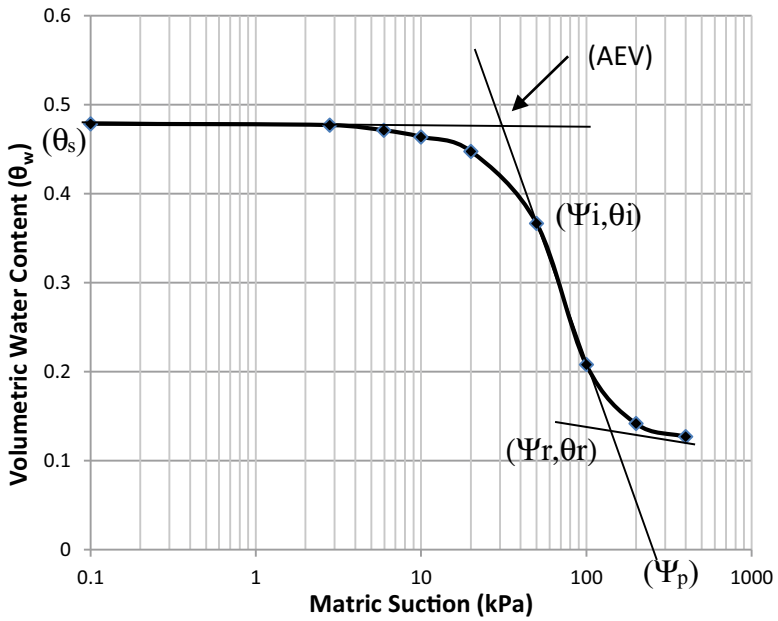


Fig. 4 Drying water retention characteristic curve

4.2 Modeling of Experimental Data

The experimental data obtained was the best fit using the equation proposed by Fredlund and Xing (FX) [13], Van Genuchten (VG) [14] and the estimation method. The Fredlund and Xing method (FX) is a closed-form type solution which is used to develop the volumetric water content function for all ranges of negative pressures ranging between zero and minus one million kPa based on the soil fit parameters (a, n, m).

The governing equation of the FX is as follows:

$$\theta = \theta_s \left[\frac{1}{\ln \left[e + \left(\frac{\psi}{a} \right)^n \right]} \right]^m \tag{1}$$

where

- θ the volumetric water content,
- θ_s the saturated volumetric water content,
- a, n, m soil fit parameters,
- ψ soil suction

The fitting parameters a, n, m were used to predict the WRCC of the sample using GeoStudio software SEEP/W version 2012. Table 2 shows the value of fitting parameters. The results obtained experimentally from Fredlund SWC-150 device are up to a certain limit. As the matric suction reaches beyond that limit, the values of volumetric water content can be numerically predicted through different models using SEEP/W. It is observed from Fig. 5 that the FX equation fitted well with the measured data for the pond ash sample.

Van Genuchten (VG) proposed a four-parameter equation which is a closed-form type solution that can be used for predicting the volumetric water content function. The governing equation is as follows:

Table 2 Parameters for drying WRCC

WRCC model	Description	Pond ash
Fredlund and Xing	Saturated volumetric water content (θ_s)	0.478
	Residual volumetric water content (θ_r)	0.136
	Residual matric suction Ψ_r	120
	Air entry value (kPa)	30
	Volumetric water content at inflection point (θ_i)	0.368
	a (kPa)	50
	n	1.632
	m	0.9616
	s	2.374×10^{-3}

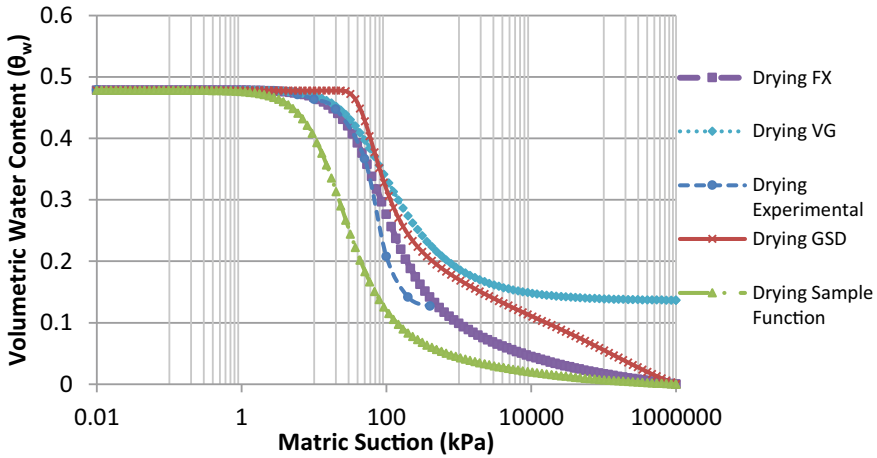


Fig. 5 Measured and Predicted Drying WRCC using different methods

$$\theta = \theta_r + \frac{\theta_s - \theta_r}{\left[1 + \left(\frac{\psi}{a}\right)^n\right]^m} \tag{2}$$

where

- θ the volumetric water content,
- θ_r the residual water content,
- θ_s the saturated volumetric water content,
- ψ soil suction,
- a, n, m curve fitting parameters

The terminology of the a, n and m parameters used in Van Genuchten (VG) equation is similar to that of Fredlund and Xing. The soil fit parameters a and n are used to best-fit the Van Genuchten (VG) equation. It is observed from Fig. 5 that the VG equation fitted well with the measured data for soil suction up to 100 kPa. After 100 kPa, the WRCC curve derived from the VG function shifts upward as compared to measured WRCC. The water retention characteristic curve can also be estimated using SEEP/W which also provides several typical water content functions for different types of soils. From the geotechnical characterization of the sample, it is observed that pond ash sample lies in the range of Silt. Therefore, the Silt sample function was selected to predict the WRCC. These functions are provided as a means to set up some test models quickly, change functions easily and decide how sensitive the results are to function shape. In the estimation method, the WRCC of pond ash sample was also predicted using grain size parameters (D_{10} , D_{60}), consistency limits and saturated water content in SEEP/W. The measured and predicted WRCC are shown in Fig. 5.

It is observed from Fig. 5 that the FX method closely relates to the experimental result. The WRCC curve predicted from the VG method closely fits up to 100 kPa,

after that there is variation in the VG result as compared to experimental results. The estimation method using grain size and sample function shows a wide variation in WRCC as compared to the experimental curve. It is significant to understand the variation between experimental and analytical models. There are certain limits of experimental equipments up to which the soil suction can be induced in the sample. The soil of low permeability requires high matric suction to reach up to the residual water content. Hence, it is required to understand the relation between experimental and analytical models. Therefore, the calculated a , n and m parameters can be used to produce the WRCC curve up to 10^6 by fitting these parameters in FX, VG and the estimation method. In the present study, it is observed from Fig. 5 that the FX method closely fits well with the experimental results, therefore, this method is the best fit to predict WRCC of pond ash materials.

4.3 Hysteresis of Water Retention Characteristics Curve

Hysteresis in the WRCC signifies the behavior of soil in the unsaturated phase in all climate types. Yang [15] observed that the total hysteresis is quantified by calculating the total area between the drying and wetting WRCC. It is observed from Fig. 6 that there is considerable hysteresis between drying and wetting of pond ash. Thus, it is necessary to consider WRCC of pond ash for all climate types. During wetting larger pores control the water movement while on draining processes the smaller

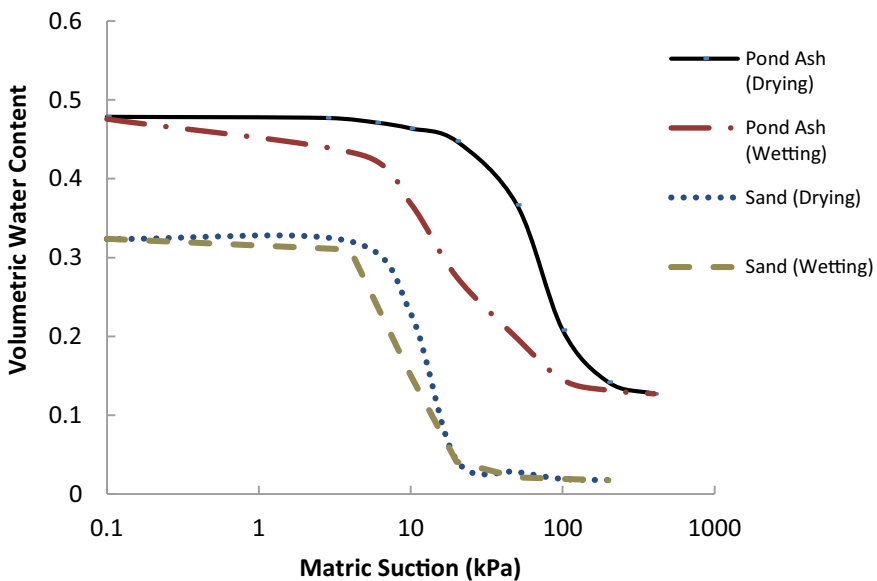


Fig. 6 Hysteresis of WRCC of pond ash

pores control the flow. It is also observed from Fig. 6 that the sand shows little hysteresis. This means sand behaves similarly in all climate types and has identical properties during drying and wetting.

4.4 Unsaturated Hydraulic Conductivity

Unsaturated hydraulic conductivity is an important soil property which affects the rate at which water percolates through the soil. The direct measurement of unsaturated hydraulic conductivity using experimentation is a complex phenomenon as it is time consuming and expensive. The alternative is to predict the unsaturated hydraulic conductivity using estimation methods. There are various estimation techniques which are acceptable to geotechnical engineering that can be used for the determination of unsaturated hydraulic conductivity function. One of the approaches for the implementation of unsaturated soil theories in practice is the determination of the water retention characteristic curve and using it along with saturated hydraulic conductivity [16]. These estimation procedures find the indirect way for determination and the application of unsaturated soil mechanics in geotechnical engineering practices.

In this study, the unsaturated hydraulic conductivity was determined using the SEEP/W 2012 software by inserting the value of the saturated coefficient of permeability and WRCC obtained using the Fredlund and Xing (FX) model and Van Genuchten (VG) model. The WRCC obtained for both the models differs at the high suction range and hence there exists a variation in predicted unsaturated hydraulic conductivity for Fredlund and Xing model and Van Genuchten model. Figure 7 shows the variation of unsaturated hydraulic conductivity with matric suction for pond ash. It is observed from Fig. 7 that the sample is nearly saturated close to zero suction. The saturated hydraulic conductivity at this stage of the sample is $9.1 \text{ E-}07 \text{ m/s}$. As matric suction in the sample is increased, the air starts entering the pores and the hydraulic conductivity goes on decreasing. It is significant to note from the figure that as the matric suction reaches the air entry value, i.e. 30 kPa; air starts entering the pore of samples progressively which is indicated by the steep increase in matric suction (Ψ) and the corresponding decrease in hydraulic conductivity. Further, as the sample gets nearly desaturated, the pores get totally filled with air which resists the movement of water through the pores and hydraulic conductivity becomes negligible. Also, it is found that there is a significant variation in hydraulic conductivity predicted from the Fredlund and Xing model and Van Genuchten model for matric suction greater than 10^4 kPa .

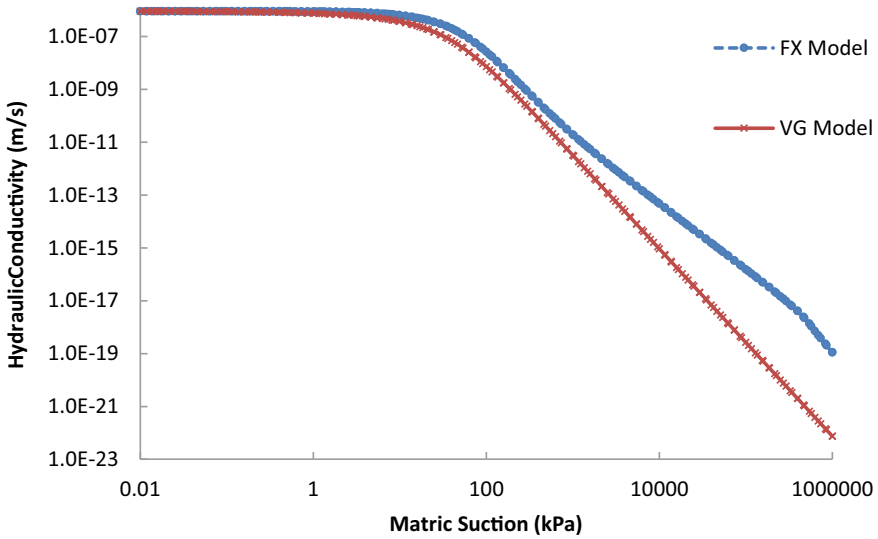


Fig. 7 Variation of Unsaturated hydraulic conductivity with matric suction

5 Conclusions

In this study, the detailed investigation of geotechnical characterization and unsaturated behavior of Pond ash was carried out. The experimental data of WRCC obtained were best-fitted using the Fredlund and Xing equation, Van Genuchten equation and the estimation method. The following conclusions can be drawn based on the study.

- The particle size distribution of pond ash indicates that particles are mostly in silt range.
- The value of the specific gravity of natural sand is higher than that of pond ash
- Loss on ignition value of the ash sample is low and thus, bulk use of pond ash as a filling material can be done with no risk of self-heating.
- Particles of pond ash are of irregular shapes with complex pore structures. The coefficient of permeability for the ash sample is lesser than that of natural sand.
- The measured WRCC matches satisfactorily with the predicted WRCC using the Fredlund and Xing equation whereas there is an upward shift in the WRCC curve derived using the Van Genuchten equation as compared to experimental WRCC.
- There is considerable hysteresis in the drying and wetting curve of the pond ash sample which indicates a pronounced difference in behavior between the wetting and drying phases.
- There is a significant variation in hydraulic conductivity predicted from the Fredlund and Xing model and Van Genuchten model for matric suction greater than 10^4 kPa.

It can be concluded that there is a significant variation in drying and wetting curves for pond ash which makes it necessary to study WRCC so that it can be effectively used in all climate types. Moreover, there are various applications which arise the need to study the unsaturated behavior of soil. The study also concluded that the prediction of the water retention characteristic curve using different models may have variation in results and may require careful evaluation.

References

1. Central Electricity Authority (2016) Fly ash generation at coal/lignite based thermal power stations and its utilization in the country. New Delhi, India
2. Fredlund DG, Rahardjo H (1993) Soil mechanics for unsaturated soils. Wiley, New York
3. IS 2720 Part 3 (1980) Methods of test for soils—determination of specific gravity. Bureau of Indian Standards, New Delhi
4. IS 2720 Part 4 (1985) Methods of test for soils—grain size analysis. Bureau of Indian Standards, New Delhi
5. IS 2720 Part 7 (1980) Methods of test for soils—determination of water content-dry density relation using light compaction. Bureau of Indian Standards, New Delhi
6. IS 2720 Part 17 (1986) Laboratory determination of permeability. Bureau of Indian Standards, New Delhi
7. Jakka RS, Ramana GV, Datta M (2010) Shear strength characteristics of loose and compacted pond ash. *Geotech Geol Eng* 28:763–778
8. Jakka RS, Datta M, Ramana GV (2010) Liquefaction behavior of loose and compacted pond ash. *Soil Dyn Earthq Eng* 30(7):580–590
9. Sobti J, Singh SK (2017) Hydraulic conductivity and compressibility characteristics of bentonite enriched soils as a barrier material for landfill. *Innovat Infrastruct Solut* 2(12):1–13
10. Sobti J, Singh SK (2017) Investigation of hydraulic conductivity and matric suction in sand–bentonite–coal ash mixes. *Indian Geotech J* 47(4):542–558
11. IS 1917 Part 1 (1991) Chemical analysis of quartzite and high silica sand—determination of loss on ignition. Bureau of Indian Standards, New Delhi
12. Singh J, Singh SK (2018) Geotechnical characterization and WRCC for spatially varied pond ash within an ash pond. *Indian Geotech J* 1–11
13. Fredlund DG, Xing A (1994) Equations for the soil-water characteristic curve. *Can Geotech J* 21:533–546
14. Van Ganuchten MT (1980) A closed-form equation for predicting the hydraulic conductivity of unsaturated soils. *Soil Sci Soc Am J* 44:892–898
15. Yang H, Rahardjo H, Leong EC et al (2004) Factors affecting drying and wetting soil water characteristic curves of sandy soils. *Can Geotech J* 41(5):908–920
16. Fredlund DG, Rahardjo H, Fredlund MD (2012) Unsaturated soil mechanics in engineering practice. Wiley, New York

Utilization of Bagasse Ash in the Compacted Clay Liner



**Dharmil Baldev, Apurv Kumar, Sutesh Tiwari, M. Muthukumar,
and Sanjay Kumar Shukla**

Abstract Landfills are highly engineered waste containment systems, designed to minimize the impact of waste on the environment. In modern landfills, the waste is contained by liner and cover systems. Due to the scarcity of natural clay, the commercially available bentonite is often used in the construction of liners. The bentonite layer generally shrinks during the summer, and therefore, severe cracks are formed; thus, it fails to control the migration of leachate. In the past, various additives have been used to stabilize bentonite. In recent years, studies have been focused on using reactive materials as additives so that they can stabilize bentonite, and also, it can adsorb the heavy metals from the leachates. The sugar industry produces fly ash, known as the bagasse ash, which causes a disposal problem. This bagasse ash is found to be a good absorbent material. Hence, a study was carried out to assess the stabilization of compacted clay liner blended with bagasse ash. Several tests, including consistency limits and hydraulic conductivity tests, have been performed by blending different contents of bagasse ash. From the test results and their analysis, it is observed that 40% of bagasse ash can be mixed with bentonite so that the essential requirements of the liner are maintained.

Keywords Clay liner · Bagasse ash · Contamination

1 Introduction

The greatest threat to groundwater posed by landfills is the infiltration of leachate through the geo-mass underlying the liner. The barrier layers in the liner system

D. Baldev · A. Kumar · S. Tiwari · M. Muthukumar (✉) · S. K. Shukla
School of Civil Engineering, Vellore Institute of Technology (VIT), Vellore 632014, Tamil Nadu,
India
e-mail: mmuthukumar@vit.ac.in

S. K. Shukla
Discipline of Civil and Environmental Engineering, School of Engineering, Edith Cowan
University, Perth, Australia

Fiji National University, Suva, Fiji

are used to prevent the flow of leachate out of the landfill. Highly impervious soils are commonly used for the construction of landfill liners [1]. Due to the paucity of impervious soils available in many parts of the world, commercially available bentonite is often used. Bentonite is a clay mineral composed of mainly montmorillonite mineral, which undergoes large volume changes and loses its effectiveness due to the formation of desiccation cracks. The leachate migrates through the desiccation cracks at a higher rate than the surrounding soil matrix. Hence several research attempts were made to arrest the formation of desiccation cracks. One of the popular improvement techniques uses a sand–bentonite mixture [1]. In this technique, 20% of bentonite is mixed with sand to arrest the formation of desiccation cracks and reduce hydraulic conductivity. Stern and Shackelford [2] observed that the hydraulic conductivity of sand–bentonite mixtures increased dramatically upon permeation of chemical solutions. Shackelford et al. [3] observed a similar type of problem in the case of geosynthetic clay liner (GCL) also. In recent years, researchers have focused on using the wastes/by-products generated from various industries to avoid disposal problems. Deng and Tikalsky [4] studied the geotechnical and leaching properties of waste foundry sand mixed, cement and fly ash with bentonite. The study indicates that the leaching of toxicity is reduced. Fly ash obtained from the combustion of coals was also used to stabilize the liners [5]. The incorporation of fly ash with soil reduces the hydraulic conductivity by filling the pores between the soil particles [5].

Sugar cane is one of the important agricultural product in India. Sugar cane industries generate fly ash which is known as the bagasse ash, which causes problems to human health and the environment [6]. Bagasse ash contains activated carbon and is fibrous in nature; it is found to be a good adsorbent material. Column studies on bagasse ash found that nearly 90/95% of copper and zinc are adsorbed by the bagasse ash. In the present work, an investigation was done to assess that the bagasse ash–bentonite mixture is suitable in place of sand–bentonite mixtures. For this analysis, the hydraulic conductivity tests were conducted in a laboratory on bagasse ash–bentonite mixture with different compositions to obtain the optimum blend with least hydraulic conductivity.

2 Experimental Investigation

Sodium bentonite was used for the present study. The scanning electron microscopy (SEM) images and EDX analysis were also performed to investigate the microstructural changes. The free swell index of the bentonite was found to be 177% which is considered to be of high swelling nature. Bagasse ash was collected from Thiruvallam Sugar Mill, located in Vellore District, Tamil Nadu, India. SEM analysis was performed and is reported in Fig. 1. The EDX analysis was also carried out and the chemical composition and is presented in Table 1. From the EDX analysis, it is observed that the bagasse ash contains a high percentage of carbon. The bagasse ash also contains sodium, magnesium, calcium and chloride ions. Various studies such as liquid limit, plastic limit, proctor compaction, permeability adsorption and leachate

Fig. 1 SEM image of bagasse ash

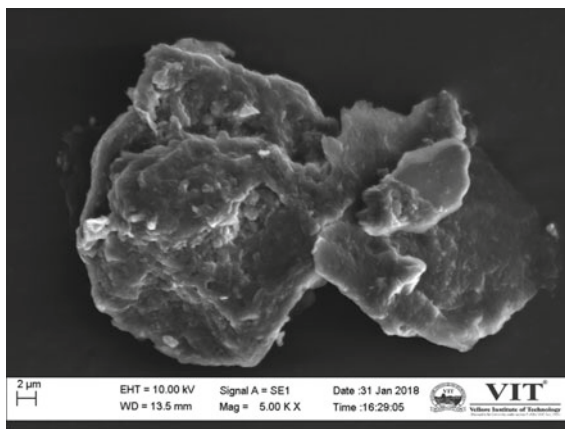


Table 1 Chemical composition of bagasse ash

Element	Weight (%)	Atomic (%)
C	56.15	65.99
O	32.99	29.11
Na	0.86	0.53
Mg	0.72	0.42
Al	1.00	0.52
Si	1.97	0.99
S	1.89	0.83
Cl	1.16	0.46
Ca	3.25	1.15

studies were conducted on bentonite blended with different percentages of bagasse ash. The bagasse ash content was varied as 5, 10, 15, 20, 30 and 40%. In this paper, the results of liquid limit, plastic limit, proctor compaction test and permeability studies are reported.

3 Results and Discussion

The liquid limit of the bentonite is found to be 151.5%, which indicates that bentonite is highly plastic according to the unified soil classification system (USCS). By increasing the bagasse ash content, the liquid limit tends to decrease (Fig. 2). For 5% of ash content, the liquid limit is 143%; for 10%, 15%, 20%, 30% and 40% of ash content, the liquid limits were 154%, 148%, 129%, 118% and 114%, respectively. It is observed that there is not much noticeable change in the plastic limit with an increase in the ash content of up to 20% in the mixture. By adding the ash for more

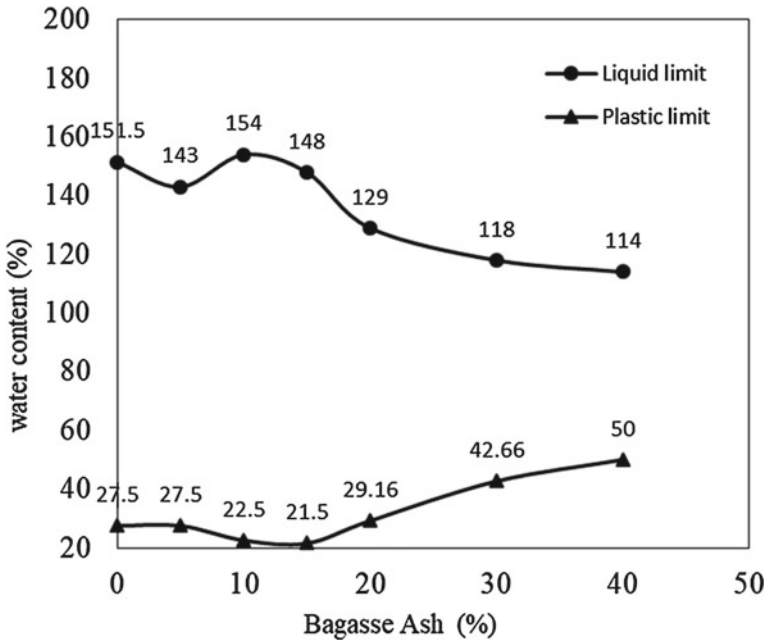


Fig. 2 Variation of liquid limit and plastic limit with ash content

than 20%, the plastic limit increases significantly by up to 50%. As the ash content increases, the bentonite–bagasse ash mixture loses its plasticity. This attribute is due to the presence of calcium ions present in the bagasse ash. The calcium ions react with the silica and alumina ions, resulting in reducing the plasticity characteristics of the soil.

In Fig. 3, we can observe that there is an increment in the optimum moisture content with an increase in the ash content in the ash–bentonite mixture, which is due to the good water-absorbing capacity of bagasse ash, whereas the dry density decreases with an increase in the ash content. Bagasse ash has a specific gravity of 1.42, whereas the bentonite has a specific gravity of 2.79. Due to the significant difference in specific gravities, there is a decrement in the density.

Hydraulic conductivity is the most important factor which governs the design of landfill liners. Hence, as per IS 2720, the permeability test was conducted and the observation of permeability was monitored for 7–10 days until a steady state is reached. It was observed that permeability values of all the various combinations such as 5, 10, 15, 20, 30 and 40% were in the order of 10^{-9} m/s. For designing the clay liner, it is necessary for a mixture to have the permeability in the order of 10^{-9} m/s. Here, in Fig. 4, it can be seen that the hydraulic conductivity is in the order of 10^{-9} m/s for an ash content 40%.

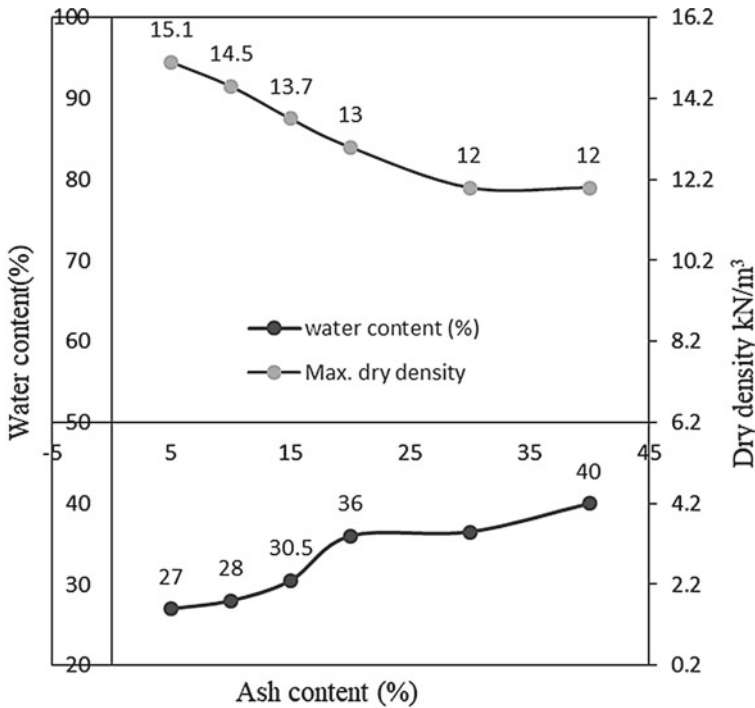


Fig. 3 Variation of optimum moisture content and dry density for different ash content

4 Conclusions

Based on the test results presented here, the following conclusions are made:

- (1) The plasticity index of the soil tends to decrease with an increase in the bagasse ash content. The plasticity index of the soil is found to decrease from 121 to 64%, when the ash content was increased from 0 to 40%.
- (2) The optimum moisture content increases with an increase in the ash content in the ash–bentonite mixture which is due to the good water-absorbing capacity of bagasse ash, whereas the dry unit weight decreases with an increase in the ash content. The maximum dry unit weight for 40% ash content is found to be 12 kN m³.
- (3) The hydraulic conductivity tends to increase with an increase in the ash content of up to 15%. Beyond 15%, hydraulic conductivity is found to increase. The hydraulic conductivity is in the order of 10⁻⁹ m/s for an ash content of 40%, thereafter the hydraulic conductivity tends to be more than 10⁻⁹ m/s.

In view of the essential requirement of the clay liner, it is concluded that 40% of bagasse ash can be added to bentonite.

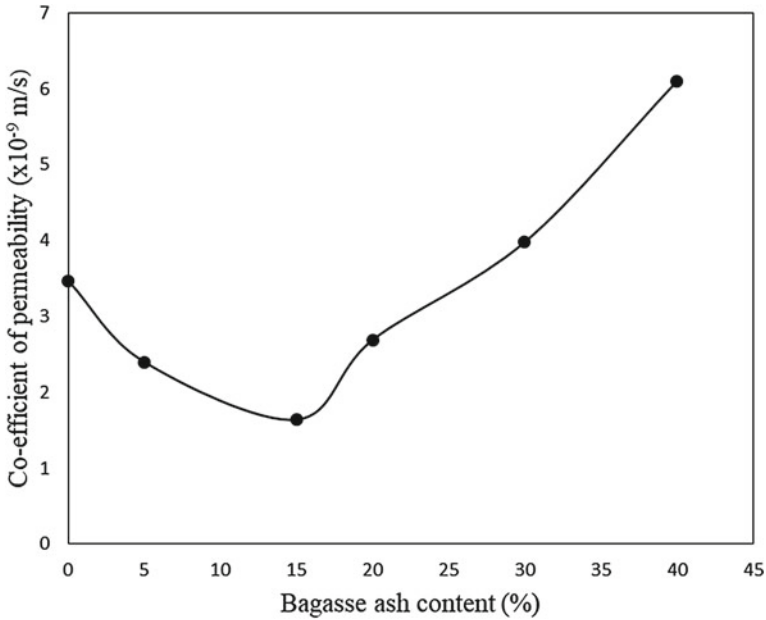


Fig. 4 Variation of coefficient of permeability for varying ash content

References

1. Al-Rawas AA, Mohamedzein YEA, Al-Shabibi AS, Al-Katheiri S (2006) Sand-attapulgitic clay mixtures as a landfill liner. *Geotech Geol Eng* 24(5):1365–1383
2. Stern RT, Shackelford CD (1998) Permeation of sand-processed clay mixtures with calcium chloride solutions. *J Geotech Geoenviron Eng* 124(3):231–241
3. Shackelford CD, Benson CH, Katsumi T, Edil TB, Lin L (2000) Evaluating the hydraulic conductivity of GCLs permeated with non-standard liquids. *Geo-text Geomembranes* 18(2–4):133–161
4. Deng A, Tikalsky PJ (2008) Geotechnical and leaching properties of flowable fill incorporating waste foundry sand. *Waste Manag* 28(11):2161–2170
5. Amadi AA (2011) Hydraulic conductivity tests for evaluating compatibility of lateritic soil-fly ash mixtures with municipal waste leachate. *Geotech Geol Eng* 29(3):259–265
6. Gupta VK, Ali I (2000) Utilisation of bagasse fly ash (a sugar industry waste) for the removal of copper and zinc from wastewater. *Sep Purif Technol* 18(2):131–140

Shear Behaviour of Geosynthetic Clay Liner (GCL) Interfacing with Manufactured Sand



Anjali G. Pillai and Gali Madhavi Latha

Abstract In view of the problems of sand extraction and its harmful impact on coastal erosion, research now focusses on viable alternatives. Manufactured sand (Msand) has become an admissible alternative to be used in concrete instead of river sand. In countries like India, sand mining is illegal, considering the adverse effects it can cause to river basins. Replacement of river sand with Msand as a suitable subgrade or capping material in landfills needs to be investigated. When Geosynthetic Clay Liners (GCL) are used on sloping grounds, interface friction between GCL and the base soil becomes important to ensure bonding and arrest slippage issues. While the interface shear characteristics of natural sand with GCLs are well established in the literature, not many studies are reported on the interface characteristics of GCLs and Msand. This study is an approach towards understanding the interface shear strength parameters of GCLs with manufactured sand and compare them against those of river sand under identical loading conditions. To avoid the effects of morphology, identical gradation of both the sands is used in the tests. This gradation is arithmetic average of grain sizes of both the sands, which is achieved by tweaking with the proportions of different sized grains. Chemical analysis of both the sands is carried out for comparison using X-ray diffraction. A GCL with bentonite sandwiched between a woven geotextile on one side and nonwoven geotextile on the other side is used in the tests. Interfacing surface is a nonwoven geotextile in all the tests. Interface shear tests are carried out on river Sand-GCL and Msand-GCL interfaces to obtain adhesion and interface friction angle of both these interfaces. Further, damage assessment of GCL surface due to interaction with these two different types of sands is carried out using Optical Microscopy and image analysis. Results from these studies provided clear directions towards the replacement of river sand with Msand in landfills in terms of interface friction characteristics and the comparative surficial changes in GCLs with the indentation of sand particles, which can give confidence about sand replacement.

Keywords Interface shear strength · Manufactured sand · Shape analysis of sand

A. G. Pillai (✉) · G. M. Latha
Department of Civil Engineering, Indian Institute of Science, Bangalore, India
e-mail: anjali.gpillai9221@gmail.com

1 Introduction

The Geosynthetic Clay Liners (GCL) are prefabricated geocomposites which offer high performance as hydraulic barriers compared to the conventional compacted clay liners (CCL). They are the vital components of the baseliner and capping of an engineered landfill. Hence, a careful assessment of the interface and internal shear strength of GCL is requisite. The interface and internal shear strength of geosynthetics are studied with shear tests and the assessment of their strength is analysed with peak and residual values [1]. Significant insight into the interface shear strength of GCL with the geomembrane as the interfacing material have been provided by numerous studies [2]. However, the strength assessment of GCL with soil as the base material have not been explored in detail. The studies related to GCL and residual soil has been able to ascertain the effect of subgrade on internal erosion of the GCL [3]. The bonding between the GCL and the base material is correlated to frictional characteristics associated with the morphology of the interacting particles. This plays a crucial role in the slope stability of a landfill facility. From the recent studies, sand has been identified as an appropriate base material for establishing the required frictional characteristics [4, 5, 6]. The frictional resistance offered by the sand is attributed to the size and shape parameters. It contributes to the interface shear strength development when interfaced with geosynthetics [7]. The identification and differentiation of shape and size parameters have been innovatively done with image analysis that quantifies the change in the shape and size among particles [8].

In recent times, the waste generation has seen an exponential increase leading to the construction of new landfill units. Owing to the shortage of suitable land and appropriate subgrade, huge quantities of sand is required to form an appropriate base material. In countries like India, the sand extraction rates have escalated to alarming rates leading to several adverse impacts. Instream sand mining causes destruction of riparian habitats through large shifts in channel morphology. It causes bed degradation, lowered water tables and channel instability. Further, the channel incisions caused by mining can undermine bridge piers and expose buried pipelines and other structures.

Thus, the compulsion and the need to replace the river sand has led to the use of manufactured sand (Msand). Msand is produced by crushing of hard granite, and India has a reserve of 37,426 m³ of granite. Recent years have seen the substitution of river sand with Msand in the manufacturing process of concrete. The durability and strength assessment of such concrete blocks have been studied and proven.

The present work focusses on the attempt to replace the river sand with Msand as a base material of in placement of GCL by assessing their interface shear strength characteristics when tested with the modified Direct Shear test setup. The preliminary investigations focus on the gradation and the chemical composition of river sand and Msand. The qualitative damage assessment of the interfacing surface with the scanning electron microscopic (SEM) technique asserts the notion of replacement.

Table 1 Specifications of GCL (Macline GCL W)

<i>Geotextile characteristics</i>	
Basal layer	Nonwoven geotextile
Upper layer	Woven geotextile
Polymer	Polypropylene
<i>Bentonite characteristics</i>	
Type	Sodium bentonite
Specific weight (g/cm ³)	2.60
Melting point (°C)	1340
Montmorillonite content (%)	>70
Water absorption (%)	>650
Free swelling capacity (ml/2 g)	>24
<i>Composite characteristics</i>	
Mass per unit (g/m ²)	4300
Nominal thickness (mm)	6.0
Permeability (m/s)	5×10^{-11}
Tensile strength (longitudinal) (kN/m)	11.5
Elongation (longitudinal) (%)	<20
Static puncture resistance (CBR)	2.2

2 Material Specifications

2.1 Geosynthetic Clay Liner

The Geosynthetic Clay Liner (GCL) used in the study consisted of bentonite encapsulated between a nonwoven geotextile as a basal layer and woven geotextile as the upper layer, needle punched together for maximum performance. It is a factory product in the name of Macline GCL W and supplied by Macaferri Environment Solutions Pvt Ltd. The specifications pertaining to the GCL is listed in Table 1.

2.2 Base Materials—River Sand and Msand

The preliminary investigations on the base materials; river sand and Msand were done to acquire information on the morphological and compositional aspects. The plot of the gradation curve for river sand and Msand is shown in Fig. 1. The individual plots categorise the river sand as medium to fine grained sand and Msand as medium-grained sand. Based on the IS Code of Soil classification, the river sand is classified as SP and the Msand as SW. To simulate identical test conditions the gradation was tweaked to the average gradation of the two test materials and is shown as a

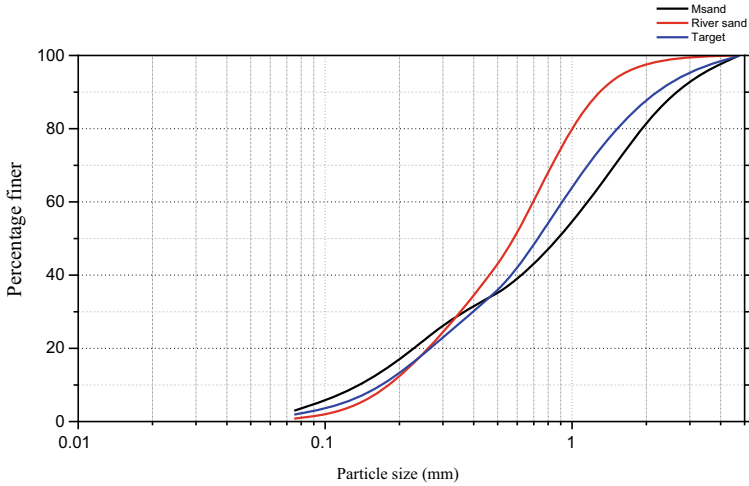


Fig. 1 The gradation of Msand (blue), River sand (orange) and the target gradation (grey)

target in Fig. 1. The specific gravity was 2.56 and 2.69 for the Msand and river sand, respectively. To understand the chemical adaptability, the X-ray Diffraction was performed on both samples. The plots are shown in Fig. 2 which highlights the chemical composition of both in terms of silica, alumina and calcium oxides.

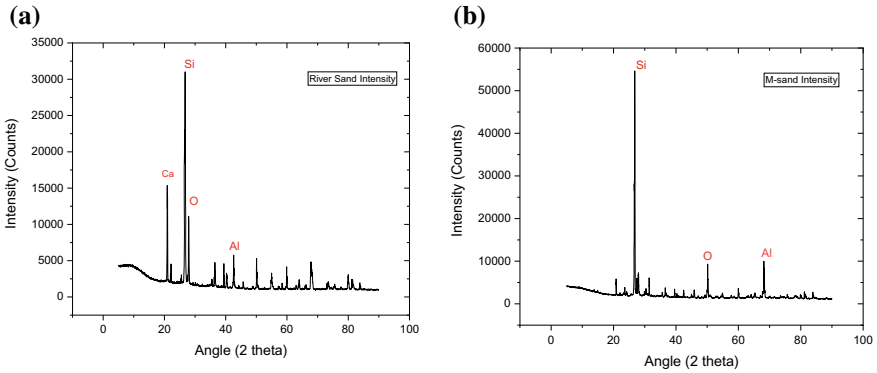


Fig. 2 a The plot of XRD analysis of river sand. **b** The plot of XRD analysis of Msand

3 Test Setup

The specimen dimensions were distinctly marked out on the roll of GCL and were accurately cut out with Angle Grinder. It ensured sharp edges of the specimen which was unattainable with other cutting tools as the fibres were being pulled out as shown in Fig. 3. The Fig. 4(a) and (b) shows the cutout specimens.

The target gradation of the soil sample was sieved out from both; river sand and Msand as shown in Fig. 5. The first phase of interface shear testing was carried out under normal stresses of 31.23, 61.01 and 100.67 kPa for air-dried samples. The second phase of testing was conducted on samples with the normal stress of



Fig. 3 The edge of the GCL and its close-up view



Fig. 4 a The specimen dimension drawn b the cutout specimens



Fig. 5 Msand (left) and River sand (right)

100.67 kPa and moisture content of 12 and 25%. The lower and higher bound of moisture content was fixed based on the literature studies of natural moisture content in sand. The shearing was done for a maximum horizontal displacement of 15 mm and shearing rate of 0.625 mm/min.

The analysis of the test results gives an insight into the variation of shear strength parameters with the variation in subgrade samples, as well as the alteration of the moisture conditions of subgrade.

4 Results and Discussions

The analysis provides an insight into the variation of interface shear strength developed between the GCL and the subgrade materials. Further, the change in moisture conditions pertaining to the subgrade highlights the changes in the interface shear strength due to the high suction of the bentonite within the GCL. The following sections give a detailed analysis of the results obtained.

4.1 Variation of Shear Stress with a Change in the Subgrade

The plot Fig. 6a–c shows the variation of shear strength with an increase in the horizontal displacement for normal loading stresses of 31.23, 61.01 and 100.67 kPa. All the plots show a distinct increase in the shear strength for Msand (MS) when compared to river sand (RS) after a displacement of 2 mm as depicted in Fig. 7.

From the plots, it is evident in the lower normal stress conditions the peak shear stress is attained in RS and is 39.67 kPa and 54.44 kPa for normal stress of 31.23 kPa and 61.01 kPa, respectively. The shear stress plot for MS shows a steep slope after 6 mm of displacement with a maximum shear stress of 54.79 kPa and 75.13 kPa for 15 mm of displacement. However, for higher normal stress of 100.67 kPa, the shear stress plot does not show a peak for RS, and the maximum shear stress developed is 100.68 kPa and 83.22 kPa for MS and RS, respectively.

The variation in the development of interface shear stress within the same subgrade under varying normal stress can be seen clearly in the combined plot as shown in Figs. 8 and 9.

4.2 Variation of Interface Shear Strength Parameter with Subgrade

The development of shear strength is dependent on the normal stresses applied to the subgrade. Since the subgrade has low fines content, the cohesion intercept (c)

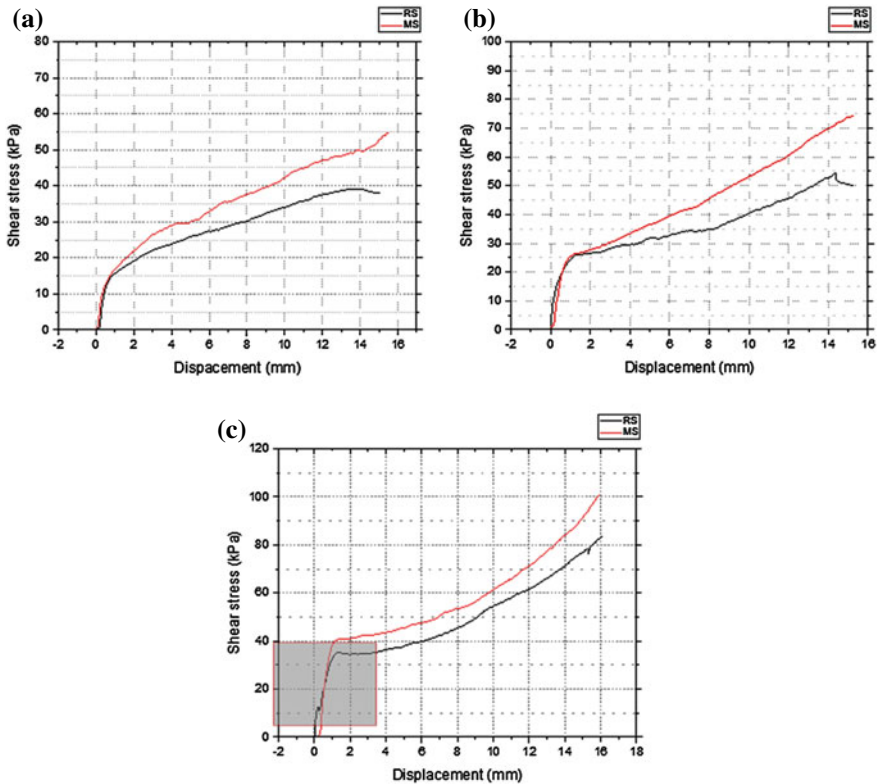


Fig. 6 **a** Shear stress versus displacement for normal stress of 31.23 kPa. **b** Shear stress versus displacement for normal stress of 61.01 kPa. **c** Shear stress versus Displacement for normal stress of 100.67 kPa

is negligible. The angle of interface friction (Φ) is evaluated purely as a function of shear stresses and normal stresses exercised on the subgrade. Figures 10 and 11 shows the variation of interface friction developed with an increase in displacement.

The interface shear strength parameter, Φ , shows a significant increase with the change in subgrade from RS to MS. The Φ varies from 51.36° to 60.31° with a shift in subgrade material from RS to MS, while the normal stress remains identical at 31.23 kPa. From Fig. 10, it is seen that Φ attains a peak value at 14.5 mm of displacement in RS, while it shows an increasing trend in MS. The trend in RS corresponds to the observation made in earlier studies for sand subgrade where peak strength is attained at 2–10 mm of displacement. However, with an increase in normal stress conditions, the plot of Φ shows an increasing trend in both RS and MS as shown in Fig. 11.

The research studies on the interface shear strength of GCL with the residual soil proved that sand is the best possible subgrade material to be used is liner facilities with GCL. The comparative analysis of river sand and manufactured sand (Msand) as

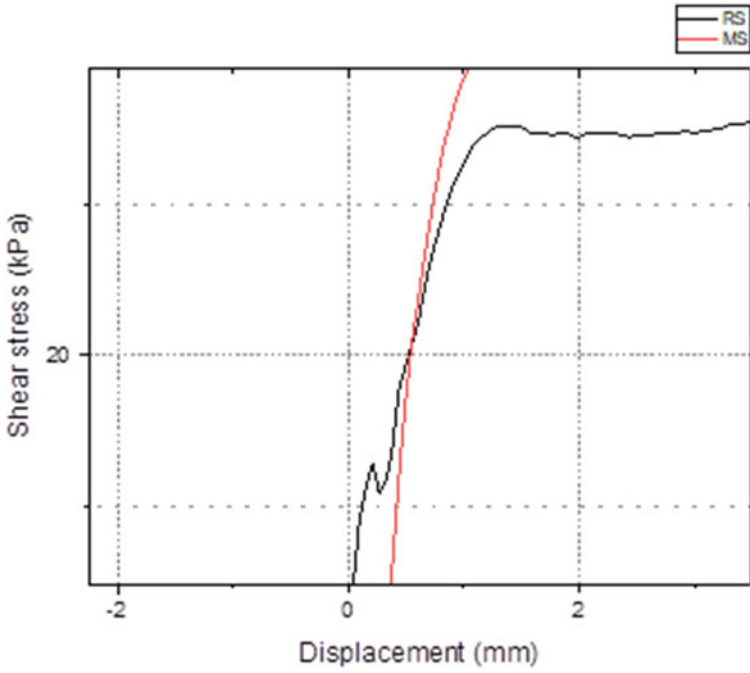


Fig. 7 Enlarged view of the shear stress transition

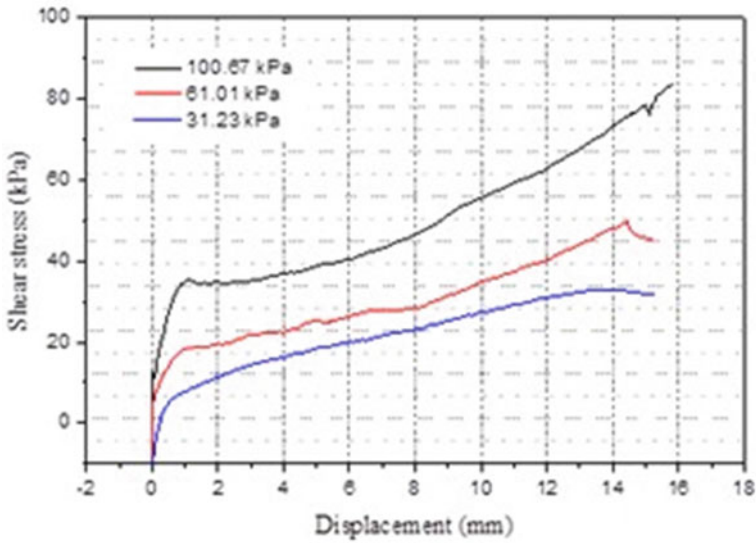


Fig. 8 The variation of shear stress under normal stresses for RS

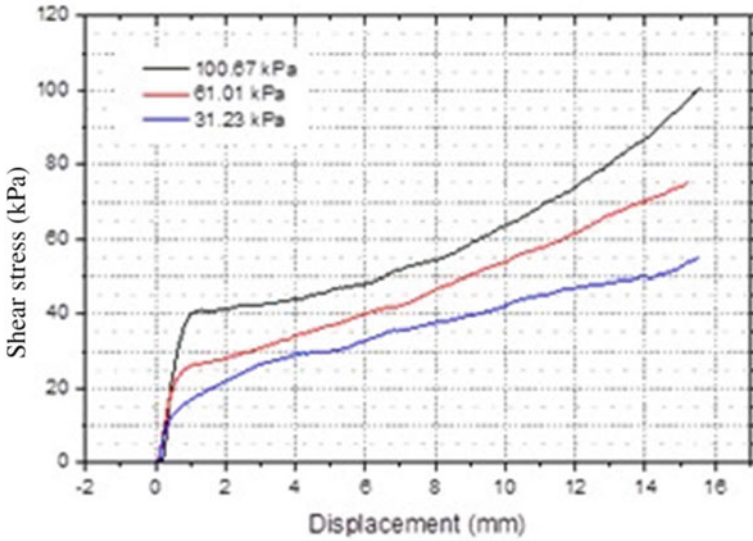


Fig. 9 The variation of shear stress under normal stresses for MS

subgrade material of GCL, shows an increase in interface shear strength parameter, Φ , for Msand. The increase is significantly higher for lower normal loading conditions as seen from the plot in Fig. 12.

$$\Phi_{MS} = 1.2 \text{ (Normal stress } < 100 \text{ kPa)}$$

$$\Phi_{MS} = 1.15 \text{ (Normal stress } > 100 \text{ kPa)}$$

The plot in Fig. 13 further gives an insight into the failure envelope developed in RS and MS. The failure conditions developed in RS for a combination of normal and shear stresses are still safe in MS. It further provides an insight into the use of Msand as a suitable subgrade material in liner facilities of GCL-Soil type.

4.3 Hydration of GCL from Subgrade Moisture Conditions

Hydration of GCL is a parameter that is often underestimated in interface studies. The hydration of GCL can take place in the following circumstances

- (a) through the punctured hole in geomembrane which enables hydration though contained liquid in liners where the interface is between GCL-Geomembrane.
- (b) through suction from subgrade material.

The following analysis enables us to view the variation in interface shear strength of GCL due to the changes in subgrade moisture conditions. It is evident that the

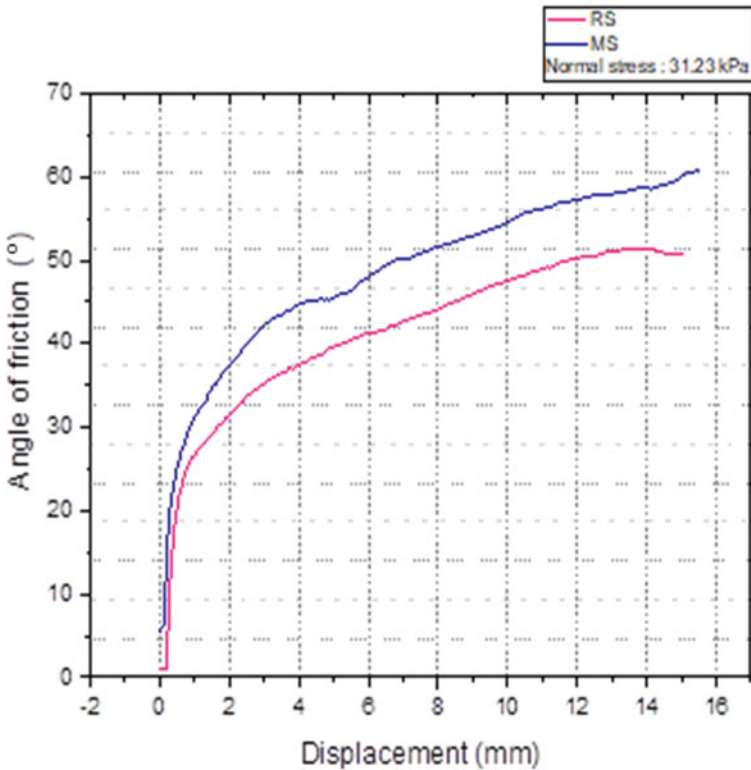


Fig. 10 Angle of friction versus displacement for normal stress of 31.23 kPa

increase in normal loading conditions results in the development of higher shear stresses and lowering of shear strength parameter Φ as seen in Fig. 13. To understand the reduction of interface shear strength with suction from subgrade, the moisture conditions were varied from 12 to 25% for subgrade material.

The normal loading was maintained at 100.67 kPa, while the moisture content was varied for RS and MS. The plot in Fig. 14, indicates the variation in shear stress for RS subgrade. The increase in moisture content significantly reduces the shear stress development at the interface. This is mainly attributed to the lubrication provided by the water in the interface. The presence of water results in lubrication of the soil particles, consequently in reduced frictional force between the individual particles as indicated by plots in Figs. 15 and 16.

The variation in shear strength parameter, Φ , with an increase in the moisture content of subgrade indicates that the reduction in RS and MS subgrade are almost equivalent, with the reduction being slightly higher in RS subgrade as seen from Fig. 17.

$$\Phi_{\text{wet}} = 0.78 \Phi_{\text{dry}} \text{ (For MS subgrade, water content 12 – 25\%)}$$

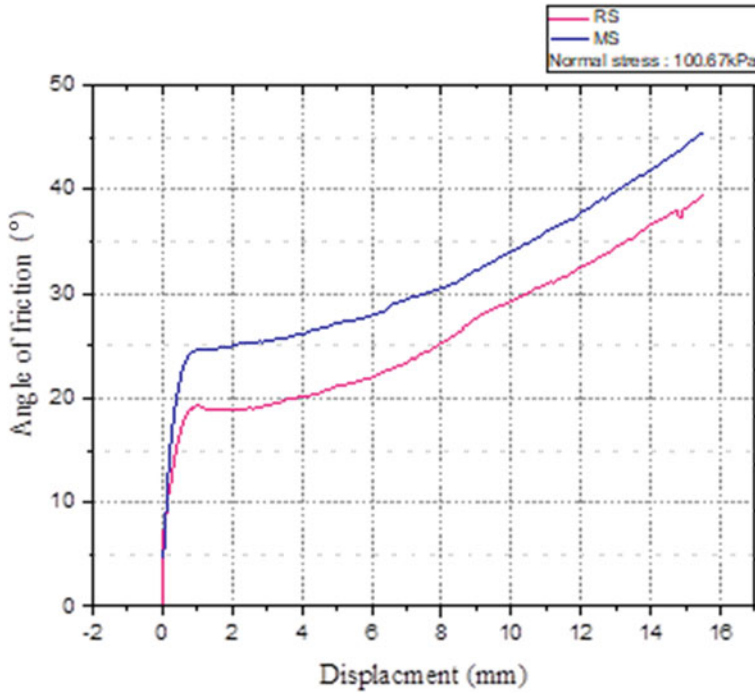


Fig. 11 Angle of friction versus displacement for normal stress of 100.67 kPa

$$\Phi_{wet} = 0.74 \Phi_{dry} \text{ (For RS subgrade, water content 12 – 25\%)}$$

The free swell conditions developed in the GCL results in enough pressure conditions that can cause the fibre to pullout of needle punched reinforcements. However, GCLs which are hydrated from suction through hydraulic contact with adjacent soil will exhibit reinforced strength when sufficient confining stress is applied during hydration. The swell pressure developed in GCL for these subgrades (RS and MS) causes a maximum reduction in shear strength between 0 and 12% moisture conditions, whereas it is almost negligible beyond that. The pullout of fibres in needle punched GCL further causes entanglement that results in adhesion of soil particles on to the shearing surface of GCL reducing the frictional force. Figure 18 shows the difference in adhesion of particles on the shearing face of GCL in dry and wet subgrade conditions.

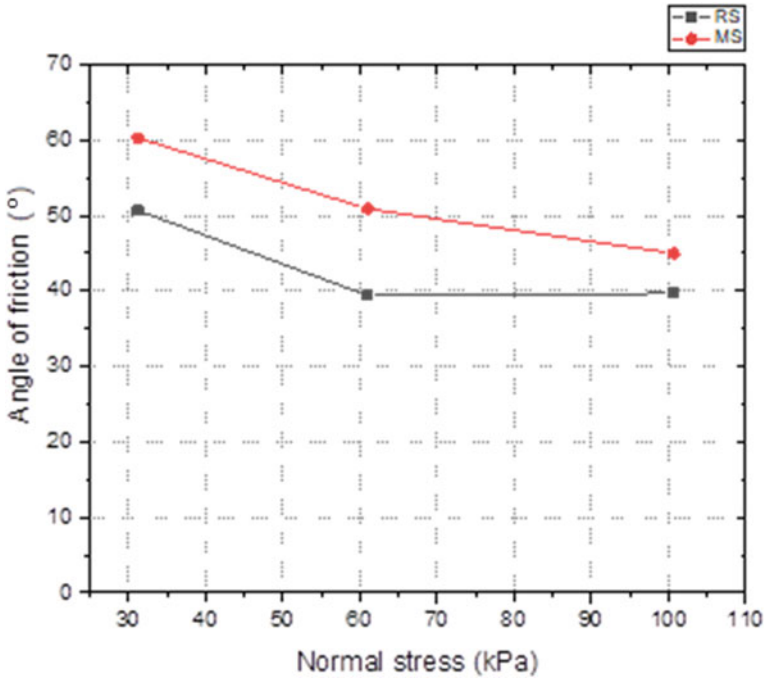


Fig. 12 Angle of friction versus normal stresses

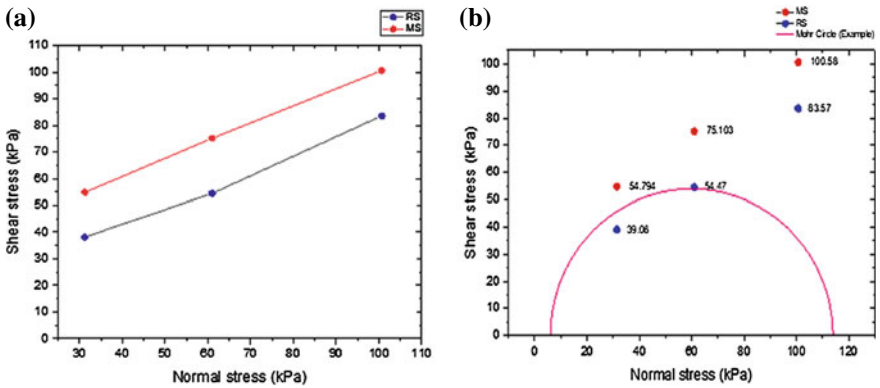


Fig. 13 a Shear stress versus normal stress b Mohr circle

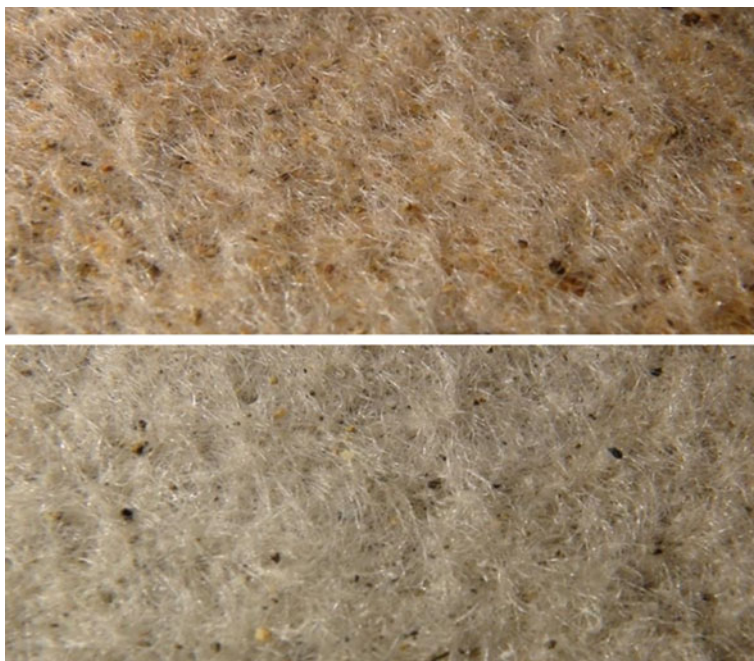


Fig. 14 The tested specimens with RS subgrade (top) and with MS subgrade (bottom)

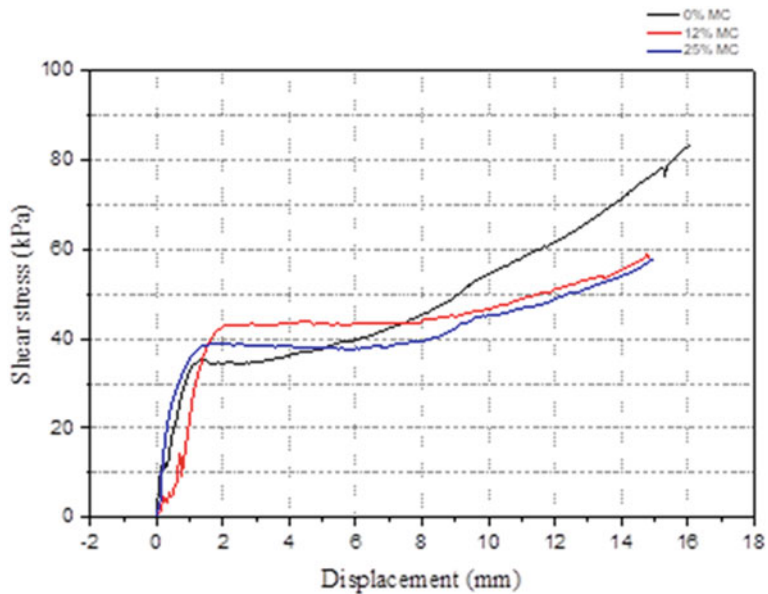


Fig. 15 Shear stress versus displacement for RS subgrade

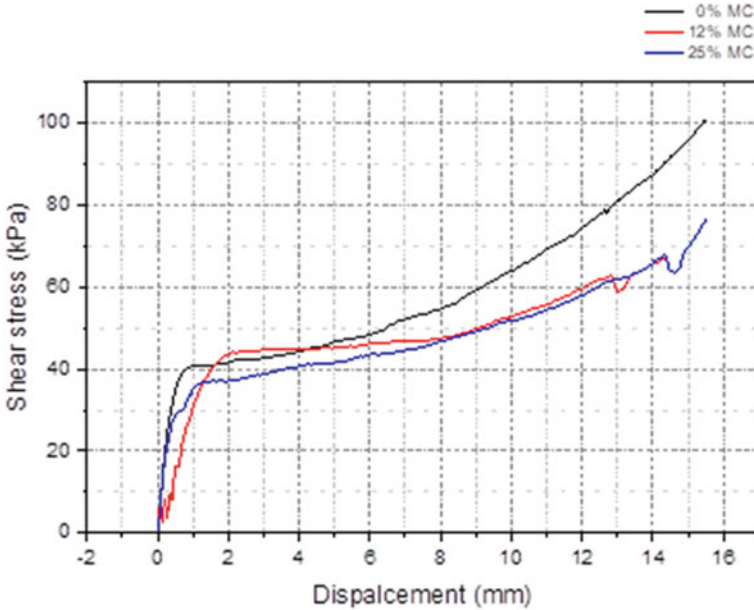


Fig. 16 Shear stress versus displacement for MS subgrade

5 Image Analysis

Image analysis is an extensively used method for characterization of materials based on grey levels of SEM or Optical microscopic images. In our study, the morphological characterization of the sand particles is done through optical microscopic images and image analysis in MATLAB. Further, the image analysis is used for quantification of the changes to the shearing interface of GCL which provides an insight into the variation of shear strength due to changes in hydration levels of subgrade.

5.1 Shape Analysis of Sand Particles

Particle shape is an important parameter which is recognised to play a vital role in shear behaviour of granular material. Sphericity, roundness, roughness and texture are the commonly used descriptors for particle shape. Since the gradation is maintained at target gradation for this study, the variation in shear strength at the interface for

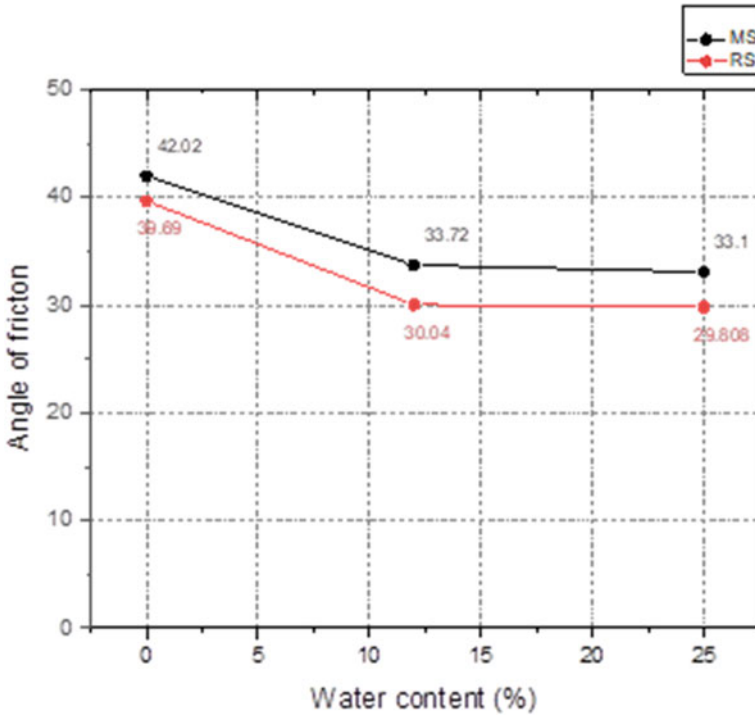


Fig. 17 Variation of friction angle with water content

the subgrades are attributed to the difference in their particle shape. An attempt to quantify those parameters is done with image analysis for specific size ranges.

Image acquisition and Image segmentation

Images of particles were captured using Nikon eclipse 80i optical microscope and the Q-Imaging Micropublisher imaging system was used to capture the images at 20x magnification. The captured images were converted to greyscale and the segmentation of particles was done using MATLAB as shown in Fig. 19.

Image analysis

The image was analysed for convexity, elongation, circularity, aspect ratio to quantify the particle shape. Convexity measures the roughness and elongation measures the particle symmetry. The result of the analysis is tabulated in Table 2.

The results indicate that the particles of MS subgrade are more elongated and less circular providing greater surface area than the particles of RS subgrade which indicates that the shear surface area occupied by MS is statistically greater than RS particles. The convexity is an indication of the surface roughness of the particles (smoother the particle more will be the convexity). The values of convexity show that the MS particles are rougher than the RS particles providing more frictional force on the shear interface.



Fig. 18 a Sand-fibre adhesion in dry RS (left) and 25% water content RS (right). b Sand-fibre adhesion in dry MS (left) and 25% water content MS (right)

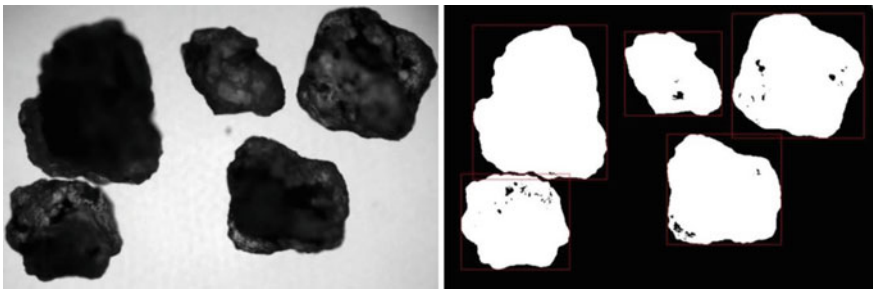


Fig. 19 Greyscale image (left) and segmented image (right) of particles

5.2 Assessment of Changes in Shearing Interface of Tested GCL

The shearing interface of GCL (nonwoven side) with the sand particles was analysed for the changes in the coverage of the area occupied by sand when sheared during

Table 2 Particle shape parameters

Size–1.18 mm	Aspect ratio	Circularity	Convexity	Elongation
RS	0.8509	0.7192	0.9125	0.1491
MS	0.7145	0.7123	0.9077	0.2855
Size–0.6 mm				
RS	0.8420	0.8020	0.8927	0.158
MS	0.8166	0.7823	0.9075	0.183
Sizez–0.3 mm				
RS	0.8213	0.8910	0.9229	0.1787
MS	0.7439	0.7260	0.8791	0.2561

the test. The images of tested specimens were captured by Sony HDR-XR550 and analysed in MATLAB.

Image Analysis

The images were analysed to obtain the difference between the untested GCL specimen and the tested GCL. The segmentation allowed the identification of sand particles within the tested specimen as shown in Fig. 20.

The results of the analysis on both RS and MS trapped specimens are shown in Table 3. It clearly shows the reduction in the shearing area of RS tested specimens as compared to MS tested specimens, when tested in dry state, is almost similar. However, the hydration of subgrade results in a significant reduction in the shearing area in RS tested specimen when compared to MS tested specimen. The voids in nonwoven geotextile are more compared to woven side, and the swelling pressure developed in GCL on the hydration of bentonite results in pullout failure of needle punched fibres resulting in the entanglement of fibres. Thus, the particles get trapped in the voids and entangled fibres during shearing. Since the RS particles are comparatively less rough and rounder, it consequently gets trapped more. Effectively, the interface friction angle Φ can be related to the area occupied by sand particles of both subgrades as shown in Fig. 21.

6 Conclusion

Large-scale interface direct shear tests on river sand (RS) and manufactured sand (MS) interfacing with GCL showed that MS-GCL interface shows higher shear stress than RS-GCL interface, the superiority in performance becoming more evident at higher displacement levels. Typically, the shear stress transition was observed beyond 3 mm of displacement under unsaturated conditions. The reason for the better performance of MS-GCL is due to the shape features of MS, as established through particle shape analysis of both the sands. Microscopic images taken from particles of different size ranges from both MS and RS showed MS particles in all the tested size ranges have

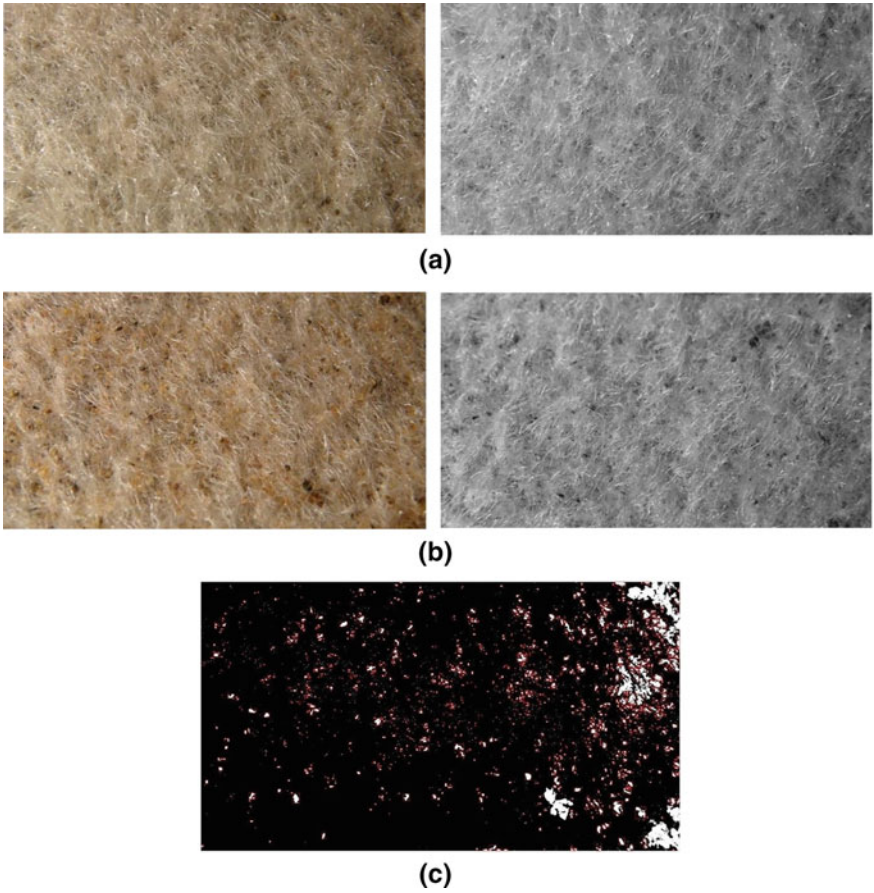


Fig. 20 a Original untested GCL and greyscale GCL b Tested GCL and Greyscale GCL c Identified sand particles marked in red boxes

Table 3 Analysis of area occupied by sand particles

Moisture content (%)	RS coverage area (%)	MS coverage area (%)
0	3.44	2.29
12	33.13	14.3
25	35.55	20.8

lower convexity values, owing to which they exhibit higher roughness, consequently, higher frictional resistance. The particles are more elongated and asymmetrical in MS when compared to river sand which is attributed to the natural weathering and erosion of particles.

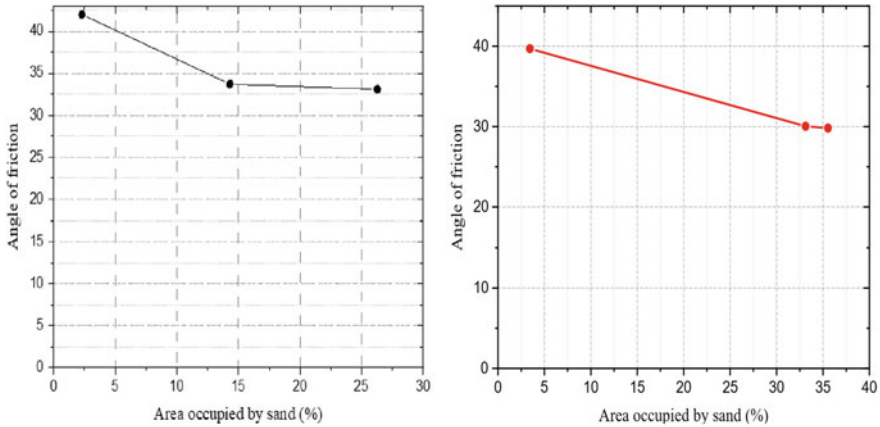


Fig. 21 Plot of angle of friction versus area Msand (left) River sand (right)

Further, the study also involved the assessment of the changes in the shearing surface of the GCL when tested with RS and MS. Images of GCL surface before and after the shear test showed that particle entrapment into the voids of the nonwoven geotextile is higher in RS, resulting in progressively less geotextile area available for shearing in case of RS. With the hydration of subgrade material, the entrapment increased due to pullout of needle punched fibres from GCL resulting in the swelling of granular bentonite within the GCL. The entrapment of MS particles was less, in both unsaturated and hydrated conditions, when compared to RS particles.

The study concludes that the manufactured sand fulfils the criteria of suitable subgrade material to be used with GCL in liner facilities. The performance of manufactured sand is significantly better as indicated by the test results. In areas where the shortage of river sand is acute, manufactured sand can be used as a viable material for liners along with GCL.

References

1. Marr WA (2001) Interface and internal shear testing procedures to obtain peak and residual values. In: Proceedings of 15th GRI conference: hot topics in geosynthetics II, pp 1–28
2. Zanzinger H (2016) Contribution to the long-term shear strength of a needle punched GCL. *Int J Geosynth Gr Eng* (2):8
3. Rowe KR (2018) Geosynthetic clay liners: perceptions and misconceptions. In: Proceedings of international conference on geosynthetics
4. Rowe KR, Orsini C (2003) Effect of GCL and subgrade type on internal erosion in GCLs under high gradients. *Geotext Geomembranes* 21(1):1–24
5. Zaini M, Kasa A, Nayan K (2012) Interface shear strength of Geosynthetic Clay Liner (GCL) and residual soil. *Int J Adv Sci Eng Inf Technol* 43–45
6. Li Y (2013) Effects of particle shape and size distribution on the shear strength behaviour of composite soils. *Bull Eng Geol Environ* 72(3):371–381

7. Afzali-Nejad A, Lashkari A, Shourijeh PT (2017) Influence of particle shape on the shear strength and dilation of sand-woven geotextile interfaces. *Geotext Geomembranes* 45(1):54–66
8. Sochan A, Zieliński P, Bieganowski A (2015) Selection of shape parameters that differentiate sand grains, based on the automatic analysis of two-dimensional images. *Sediment Geol* (327):14–20

Impact on Bentonite Due to the Presence of Various Concentrations of Lead and Copper Solutions



Saswati Ray, Anil Kumar Mishra, and Ajay S. Kalamdhad

Abstract Heavy metals are directly introduced to the environment, groundwater and waterways by means of several industrial activities. Migration of metal from the landfill to the surrounding environment is a serious environmental issue worldwide. A liner is a low permeable material used in the waste disposal sites to prevent the migration of toxic pollutants to contaminate the surrounding atmosphere and groundwater resources. Compacted bentonite is used as a liner material because of its high sorption capacity, low hydraulic conductivity and high swelling capacity. The presence of chemicals in the leachate can shrink the thickness of the diffuse double layer (DDL) and may reduce the effectiveness of the liner by reducing its swelling capacity and increasing hydraulic conductivity. Therefore, in the present study, high swelling bentonite is analysed on the change in their behaviour due to the presence of copper (Cu^{2+}) and lead (Pb^{2+}) solutions. One of the essential behaviours of bentonite is consolidation, which is necessary for investigating the settlement analysis of the liner. The study was conducted to determine the impact of lead (Pb^{2+}) and copper (Cu^{2+}) solutions of different concentrations, on the consolidation behaviour of bentonite. In the existence of lead (Pb^{2+}) and copper (Cu^{2+}) of concentrations of 0, 500 and 1000 mg/L, various consolidation parameters, such as compression index (C_c), coefficient of consolidation (c_v), volume change (m_v) and time, are required for the completion of 90% of consolidation (t_{90}), which were studied. Result shows that c_v increases with an increase in concentration of the heavy metal, whereas C_c , m_v and t_{90} of the bentonite decrease. The study also indicates that the rate of consolidation of the bentonite increases in the presence of copper and lead. The results of this study may deliver a general idea for estimating the liner performance in the presence of different kinds of toxic chemicals existing in the leachate.

Keywords Bentonite · Swelling · Hydraulic conductivity · Consolidation · Heavy metal

S. Ray (✉) · A. K. Mishra · A. S. Kalamdhad
Department of Civil Engineering, Indian Institute of Technology, Guwahati, India
e-mail: r.saswati@iitg.ernet.in

1 Introduction

The exponential increment of various industrial activities has caused severe metal pollution of the ecosystem. Heavy metals directly introducing into the soil, waterways and surrounding environment may enter into the food chain of human being and can cause severe health issues like DNA alteration (mutagenesis), cellular damage and several chronic diseases if consumed beyond permissible limits [1–4].

Mostly, leachate produced inside the landfills from various wastes is the possible source of metal pollution and is the biggest threat to the groundwater supplies and surrounding environment. Therefore, to prevent the metal pollution, a liner is provided at the bottom of the landfills to stop the percolation of leachates. Bentonite is used in garbage disposal site as a barrier material due to high cation exchange capacity, pollutant adsorption capacity, high specific surface area and low hydraulic conductivity. For the discarding of radioactive as well as municipal solid waste, bentonite is used as a buffer and liner material in the waste disposal sites due to its high sorption capacity and low permeability [5, 6]. In long term, liner properties may alter because of the existence of the various harmful chemicals inside landfills that consecutively reduce its efficiency. Various investigators have examined the consequence of various heavy metal ions on the alteration in the properties of bentonite. Lo et al. [7] conducted various tests to study the relocation of Cd, Zn and Pb in bentonite–soil admixture and saturated sand and found that the permeability of the bentonite–soil admixture was lower in comparison of the compacted sand when infused with different heavy metals. Ouhadi et al. [8] examined the consolidation properties of soil in the existence of Pb^{2+} and Zn^{2+} at various pHs and concluded that the microstructural alteration in the bentonite soil occurs at high metal concentration and low pH. They also found that osmotic phenomenon governs the rheological performance of the bentonite soil. Nakano et al. [9] studied the sorption and hydraulic conductivity behaviour of four different bentonites and observed that U.S. bentonite shows lower hydraulic conductivity value as compared to Japanese bentonites because of high swelling capacity and montmorillonite mineral content. They also concluded that carbonate plays a major role in precipitation of lead on to the bentonite in the form of $PbCO_3$. Du et al. [10] conducted various experiments to determine the effect of different levels of Pb^{2+} concentration on bentonite and observed that the compression index, pH and Atterberg limit of the bentonite clay reduced with the rise in metal ion concentration.

Since the type of metal and concentrations can influence the consolidation parameters of bentonite, hence, it is very important to investigate the variation in the behaviour of bentonite clay in the existence of different levels of the heavy metal solution. The present investigation emphasises on the effect of various concentrations of lead and copper on the change in consolidation parameters, for example, coefficient of consolidation (c_v), coefficient of volume change (m_v), time required to achieve 90% of the consolidation (t_{90}) and compression index (C_c) of bentonite clay. The study will be helpful for design engineers for designing a liner system.

Table 1 Composition of bentonite

Property	Bentonite
Liquid limit (%)	480.0
Plasticity index	440
Free swelling (ml/2 g)	32.5
Clay content (%)	66
Cation exchange capacity (CEC) (meq/100 g)	40.2
Specific surface area (SSA) (m ² /g)	396.3
Optimum moisture content (OMC) (%)	33.00
Maximum dry density (MDD) (gm/cc)	1.31

2 Materials and Methods

2.1 Bentonite

In the present study, the bentonite used was procured from Barmer district, Rajasthan, India. The composition of the bentonite is given in Table 1. According to ASTM D4318 [11] and ASTM D5890 [12], Atterbergs limit and free swelling capacity of the bentonite were analysed. By hydrometer analysis, the grain size distribution of the bentonite was analysed by following ASTM D422 [13].

Procedure described by Chapman and Pratt [14, 15] was followed to determine the cation exchange capacity (CEC) and type of exchangeable cations of the bentonite. Specific surface area (SSA) of the bentonite was determined by following Ethylene Glycol Monoethyl Ether (EGME) method [16]. By following ASTM D698 [17], the compaction parameter of the bentonite was examined.

2.2 Permeant Liquid

In the present investigation, the metals used were comprised of Pb²⁺ and Cu²⁺. To examine the effect of various concentrations on the change in consolidation, behaviours of bentonite these metal solutions were selected. Different concentrations of lead and copper, i.e. 500 and 1000 mg/L, were prepared by dissolving the powdered salts (Copper nitrate and lead nitrate in deionized (DI) water. DI water was used as a reference solution in the present study. From the literature, it has been observed from the past works that maximum level of metal ion in the municipal solid waste leachate is 1000 mg/L [18]. Hence, in this investigation, the highest concentration of 1000 mg/L has been used.

2.3 Determination of Consolidation Characteristics

As per ASTM D2435 [19], consolidation test was performed to determine the consolidation parameters of bentonite. Soil was mixed with deionized (DI) water to bring the initial water content corresponding to its optimum moisture content, and then the soil sample was placed for 24 h in the moisture-controlled desiccator to achieve equilibrium. Inside the oedometer ring, the soil sample was then statically compacted to its MDD to make a sample of 15 mm thickness and 60 mm diameter having an initial void ratio of 1.07. In the loading frame, the setup was then kept inside the consolidation cell and then infused in DI water, Pb^{2+} and Cu^{2+} solutions of various concentrations and was permitted to swell. The void ratio was found to be increased to 1.77, 1.59 and 1.52 for DI water, 500 and 1000 mg/l of Pb^{2+} solution and 1.41 and 1.36 for 500 and 1000 mg/l of Cu^{2+} solution, respectively, after the completion of the swelling.

The sample was consolidated after the swelling ends with the load increment ratio one up to a maximum vertical pressure 784.5 kPa started from 4.9 kPa. The change in thickness of the sample was measured by mean of the dial gauge for each load increment. With each of the load increments, the variation in the void ratio triggered was computed as

$$\Delta e = \frac{\Delta H(1 + e_0)}{H} \quad (1)$$

where ΔH is the change in the thickness of soil sample; H is the initial thickness of the soil sample due to; e_0 is the initial void ratio; and Δe is the change in void ratio.

Taylor square-root-of-time method [20] was applied at each load increment, and a time–settlement graph was plotted, and then the coefficient of consolidation (c_v) was determined.

$$c_v = \frac{D^2 T_v}{t_{90}} \quad (2)$$

where t_{90} is the time required to achieve 90% of consolidation; T_v is the time factor (For 90% of consolidation = 0.848).

The coefficient of volume change (m_v) was computed for each increment in pressure as in Eq. (3)

$$m_v = -\frac{\Delta e}{\Delta \sigma(1 + e_0)} \quad (3)$$

where $\Delta \sigma$ is the change in pressure.

The compressibility behaviour of the soil can be specified by compression index (C_c) of a soil and was determined as the slope of the straight-line portion of the void ratio–pressure ($e - \log P$) curve as

$$C_c = \frac{e_i - e_j}{\log \frac{p_i}{p_j}} \tag{4}$$

where e_i and e_j are the void ratios corresponding to the consolidation pressures of p_i and p_j at i th and j th steps of loading, respectively.

3 Results and Discussion

3.1 Coefficient of Volume Change (M_v)

The plot in Fig. 1 depicts the relationship between coefficient of volume change (m_v) and the vertical consolidation pressures at various concentrations of Pb^{2+} and Cu^{2+} . The plot depicts that the m_v value of the bentonite clay primarily rises and then reduced. The reason is at lower vertical pressure; initially, the void ratio was high. However, a higher reduction in void ratio occurs with the increase in consolidation pressure resulting in a higher m_v value. Though after attaining the peak value with the further rise is consolidation pressure, the m_v value declined. The plot also demonstrates that the m_v value reduced with the increase in Pb^{2+} and Cu^{2+} concentrations. This reason is for DI water the diffuse double-layer thickness is large. Therefore, a higher compression occurs due to the application of vertical load, in turn, resulting in a higher m_v value. However, in the presence of different concentrations of metal ions the thickness of diffuse, double layer gets reduced.

Fig. 1 Coefficient of volume change and consolidation pressures of Bentonite at various Pb^{2+} and Cu^{2+} concentration

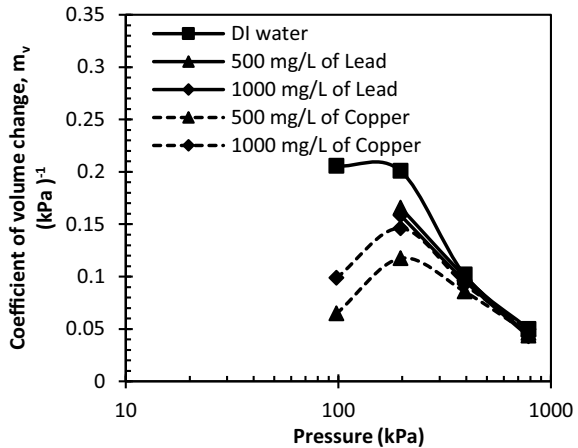
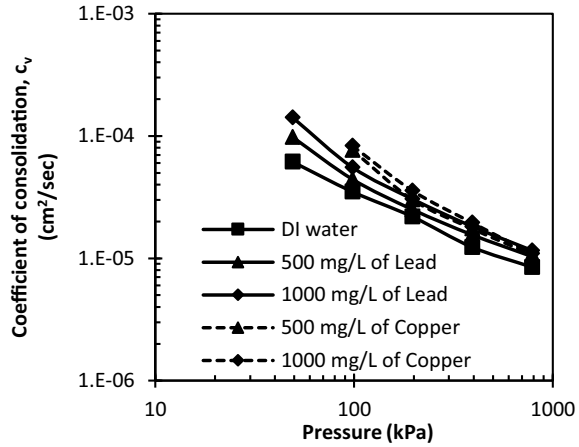


Fig. 2 Coefficient of consolidation and consolidation pressures of Bentonite at various Pb^{2+} and Cu^{2+} concentration



3.2 Coefficient of Consolidation (C_v)

Figure 2 explains that the c_v values declined with the rise in vertical pressure. This implies that with the increment of vertical consolidation pressure the degree of consolidation rises because of the presence of the Pb^{2+} and Cu^{2+} ions in the pore fluid. A rapid settlement of liner material in the waste containment system occurs with the interaction of the metal ions present in the leachate [21]. Robinson and Allam [22] found a similar kind of trend for montmorillonite soil; however, an opposite trend was observed by Mishra et al. [23] for sand–bentonite mixtures. For this opposite trend, mechanical aspects that govern the compressibility behaviour of bentonite–sand mixtures are mostly responsible [21]. However, for bentonite clay due to the physicochemical factors, a range of attractive and repulsive forces is generated which governs the compressibility behaviour [22].

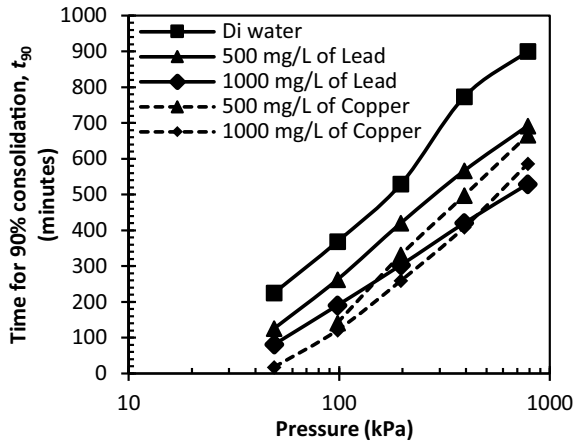
3.3 Coefficient of Consolidation (C_v)

The plot in Fig. 2 depicts the relationship between coefficient of consolidation (c_v) and consolidation pressures. The plot illustrates that with the rise in Pb^{2+} and Cu^{2+} concentrations the c_v value reduces which implies faster consolidation rate when the sample is infused with different metal concentrations.

The repulsive forces among the clay particles reduce with the rise in the concentrations of Pb^{2+} and Cu^{2+} causing decrease in DDL thickness. Consequently, consolidation of the soil sample undergoes more rapidly which results in decline in the c_v value.

Figure 2 demonstrates that, for bentonite soil infused in DI water, the c_v value declines from 6.15×10^{-5} to 8.47×10^{-6} cm^2/s with the increase in pressure from

Fig. 3 Time for 90% of consolidation and pressure of bentonite at various Pb^{2+} and Cu^{2+} concentrations



19.6 to 784.5 kPa. However, for soil infused with 1000 mg/L of Pb^{2+} solutions, the c_v reduced from 1.4×10^{-4} to 1.16×10^{-5} cm^2/s .

3.4 Time to Complete 90% of Consolidation (T_{90})

The plot in Fig. 3 depicts the relationship between pressure and time for 90% of settlement (t_{90}). The plot illustrates that with the rise in Pb^{2+} and Cu^{2+} concentrations t_{90} for the bentonite declines.

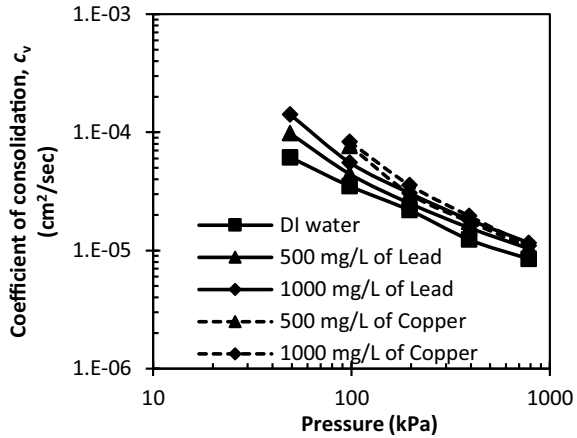
As the c_v value rises with the rise in the concentration of heavy metal, the time essential to attain a desired degree of consolidation reduces causing a decline in t_{90} .

On the contrary, the plot in Fig. 3 also demonstrates that with the rise in vertical pressure t_{90} increases. The reason is due to the increase in the vertical pressure; the clay plates come to a nearer distance as a result of which the repulsion among clay plates rises, which avoids any further movement of the clay plates and consequences in a decline in the c_v and rise in t_{90} . Figure 3 reveals that, for bentonite soil infused in DI water, the t_{90} value rises from 225.0 min to 900.0 min with the increase in pressure from 19.6 to 784.5 kPa. However, for soil infused with 500 mg/L of Pb^{2+} solutions, the t_{90} increased from 125.44 to 691.69 min. Similarly, for 1000 mg/L, the t_{90} rises from 81.0 to 529.0 min.

3.5 Compression Index (C_c)

The plot between C_c and various metal concentrations in Fig. 4 shows that with the rise in Pb^{2+} and Cu^{2+} concentrations from 0 (DI water) to 1000 mg/L, the C_c value declined from 0.79 to 0.62 (21.52%) and 0.79 to 0.65 (17.72%), respectively. The

Fig. 4 Compression index of bentonite at different concentrations of Pb^{2+} and Cu^{2+} solutions



plot in Fig. 4 depicts the relationship between C_c and various metal concentrations. The plot illustrates that with the increase in the concentrations of Pb^{2+} and Cu^{2+} from 0 (DI water) to 1000 mg/L the C_c decreased from 0.64 to 0.58 (10.38%) and 0.64 to 0.54 (15.62%), respectively. The reason is that the clay particles come nearer and turn out to be aggregated with the rise in Pb^{2+} and Cu^{2+} concentrations. As a consequence, the DDL thickness reduces, hence, resisting settlement and triggering the decline in C_c value.

4 Conclusions

The present investigation aimed to study the change in behaviour of bentonite soil in the presence of various concentrations of Pb^{2+} and Cu^{2+} . The study revealed that the consolidation parameters (C_c , m_v , c_v and t_{90}) of bentonite could be influenced by several factors such as composition of bentonite, type and concentration of heavy metal. The results indicate that with the rise in the concentrations of Pb^{2+} and Cu^{2+} , the void ratio declines. Similarly, the plot suggests that C_c value of the bentonite decreased with the rise in metal concentration. It was also depicted from the graph that m_v decreased with the rise in the concentrations of Pb^{2+} and Cu^{2+} . The reason is because of the implementation of vertical load in the presence of different heavy metal concentrations, consequences in the decrease in compressibility of bentonite, which in turn influence the m_v value. The investigation revealed that the c_v value increased with the increase in Pb^{2+} and Cu^{2+} concentrations. The study also indicates that the value of t_{90} increased with the increase in vertical consolidation pressure.

References

1. Ernst WHO: Mine vegetation in Europe. Heavy metal tolerance in plants: evolutionary aspects. In: Shaw AJ (ed) CRC, BocaRaton (1990), pp 21–51
2. Ernst WHO: Decontamination or consolidation of metalcontaminated soils by biological means. Heavy metals: problems and solutions. In: Salomons W, Forstner U, Mader P (eds) Springer, Berlin (1995), pp 141–149
3. Wang S, Shi X (2001) Molecular mechanisms of metal toxicity and carcinogenesis. *Mol Cell Biochem* 222:3–9 [PubMed: 11678608]
4. Beyersmann D, Hartwig A (2008) Carcinogenic metal compounds: recent insight into molecular and cellular mechanisms. *Arch Toxicol* 82(8):493–512 [PubMed: 18496671]
5. Dutta J, Mishra AK (2016) Consolidation behaviour of bentonite in the presence of salt solution. *Appl Clay Sci* 120:61–69
6. Khan SA, Riaz-ur-Rehman, Khan MA (1955b) Sorption of strontium on bentonite. *Waste Manage* 15(8):641–650. [https://doi.org/10.1016/0956-053X\(96\)00049-9](https://doi.org/10.1016/0956-053X(96)00049-9)
7. Lo I, Luk A, Yang X (2004) Migration of heavy metals in saturated sand and bentonite/soil admixture. *J Environ Eng* 130:906–909. Special Issue: Waste Containment Barrier Materials (2004)
8. Ouhadi VR, Yong RN, Sedighi M (2006) Influence of heavy metal contaminants at variable pH regimes on rheological behaviour of bentonite. *Appl Clay Sci* 32:217–231
9. Nakano A, Li LY, Ohtsubo M, Mishra AK (2008) Lead retention mechanisms and hydraulic conductivity studies of various bentonites for geoenvironment applications. *Environ Technol* 29:505–514
10. Du YJ, Fan RD, Reddy KR, Liu SY, Yang YL (2015) Impacts of presence of lead contamination in clayey soil–calcium bentonite cutoff wall backfills. *Appl Clay Sci* 108:111–122
11. ASTM (2000) Standard test methods for liquid limit, plastic limit, and plasticity index of soils. D 4318. American Society for Testing and Materials, Philadelphia
12. ASTM (2001) Standard test method for swell index of clay mineral component of geosynthetic clay liners. D 5890. American Society for Testing and Materials, Philadelphia
13. ASTM (2002) Standard test method for particle-size analysis of soils. D 422-63. American Society for Testing and Materials, Philadelphia
14. Chapman HD (1965) Cation exchange capacity. *Methods of soil analysis, part 2 chemical and microbiological properties*. 2nd edn. Soil Science Society of America, Madison, pp 891–895
15. Pratt PF (1965) Sodium, methods of soil analysis, part 2 chemical and microbiological properties, 2nd edn. Soil Science Society of America, Madison, pp 1031–1034
16. Cerato AB, Lutenegeger AJ (2002) Determination of surface area of fine-grained soils by the ethylene glycol monoethyl ether (EGME) method. *Geotech Test J* 25:1–7
17. ASTM D698 (2012) Standard Test Methods for Laboratory Compaction Characteristics of Soil Using Standard Effort. American Society for Testing and Materials, Philadelphia
18. Prudent P, Domeizel M, Massiani C (1996) Chemical sequential extraction as a decision-making tool: application to municipal solid waste and its individual constituents. *Sci Total Environ* 178:55–61
19. ASTM (1996) Standard test method for one-dimensional consolidation properties of soils. D 2435. American Society for Testing and Materials, Philadelphia
20. Taylor DW (1948) *Fundamentals of soil mechanics*. Wiley, New York
21. Ouhadi VR, Sedighi M (2003) Variation of experimental results of oedometer testing due to the changes of pore fluid. In: *Deformation characteristics of geomaterials*. Taylor & Francis, New York, pp 299–304
22. Robinson RG, Allam MM (1998) Effect of clay mineralogy on coefficient of consolidation. *Clays Clay Miner* 46(5):596–600
23. Mishra AK, Ohtsubo M, Li LY, Higashi T (2010) Influence of the bentonite on the consolidation behaviour of soil bentonite mixtures. *Carbonates Evaporites* 25(1):43–49

Seismic Response of Bentonite Enhanced Soils to be Used as Fabricated Liner in Engineered Landfills



Jaskiran Sobti and Sanjay Kumar Singh

Abstract Earthquakes are one of the most severe natural disasters that are responsible for significant damage to structures causing vertical settlements, lateral spreads and tipping of buildings. Solid waste landfills can also be seriously affected by seismic activity. In landfills, liners of low permeability material are used to arrest the leachate. If the landfills are located in regions of high seismicity, the fabricated liners may be susceptible to damage. Generally, cohesionless soils are considered to be vulnerable to damage caused by earthquakes. Also, evidence of sandy soils with a substantial amount of fines being prone to liquefaction is available in the literature. If cracks develop in the liner, the whole purpose of engineered landfill gets defeated and all the investment incurred towards the landfill would go in vain. This paper aims at understanding the behaviour of landfill liner systems subjected to static and dynamic loading with emphasis laid on ascertaining the effect of adding plastic fines (bentonite) to the cyclic resistance of liquefiable sands and coal ash. The stress-controlled undrained cyclic triaxial tests were carried out at a frequency of 1 Hz and initial effective confining pressure of 150 kPa on soil specimens with 70 mm diameter and 140 mm height. It was observed that pore water pressure generated in sand-bentonite mixes with 10% bentonite is high and slowed down thereafter upon an increase in bentonite content up to 20% in the soil mix resulting in the increased cyclic resistance. The number of cycles required for initial liquefaction were quite less in coal ash, as compared to clean sand. It was found that coal ash is more susceptible to liquefy in comparison to sand.

Keywords Sand · Bentonite · Coal ash · Seismic response · Landfill liner

J. Sobti (✉)

Department of Civil Engineering, Guru Nanak Dev University, Amritsar, India
e-mail: sobti.kiran@gmail.com

S. K. Singh

Department of Civil Engineering, Punjab Engineering College (Deemed to be University), Chandigarh, India
e-mail: sksingh99_99@yahoo.com

© Springer Nature Switzerland AG 2020

K. R. Reddy et al. (eds.), *Sustainable Environmental Geotechnics*, Lecture Notes in Civil Engineering 89, https://doi.org/10.1007/978-3-030-51350-4_34

333

1 Introduction

It has been witnessed from the past case histories that large earthquake-induced ground deformations can cause serious damage to various civil engineering structures subjected to undrained cyclic loading conditions. Cyclic loading of significant amplitude leads to the generation of excess pore water pressure and decreases the stiffness and strength of the soil [1]. The pore water pressure developed is relatively incompressible and its magnitude increases with the duration of cyclic loading and at times dissipates after the ground shaking has ended. Solid waste landfills can also be seriously affected by seismic activity. The tension developed during an earthquake can lead to stretching or tearing of the liner material. There may also be a risk of development of cracks on top of the landfill and disruption of the gas collection systems. From the geotechnical engineering point of view, the stability analysis of waste repositories under both static and dynamic loads is necessary keeping in mind the theories of soil dynamics.

A peep into the past shows incidences of damage caused to the landfills due to earthquakes, affirming the fact to ensure the liquefaction resistance of soil liner. The massive earthquake that struck in Northridge, California, on January 17, 1994, with a 6.7 magnitude on the Richter scale led to shaking in several landfills [2]. The Chiquita Canyon landfill experienced a mass movement of waste material against a lined slope. At the Operating Industries Inc. (OII) landfill, California in Monterey Park California, 43 km from the earthquake source zone, a significant crack developed on a bench on the north slope of the landfill [2]. Even though these case histories revealed that significant financial and human losses did not occur, they exhibited a need to lay emphasis on the due understanding of the geotechnical aspects of lining systems under seismic loading conditions.

The presence of fines does not rule out the possibility of failure due to liquefaction. A majority of studies have shown that the presence of plastic fines tend to increase the liquefaction resistance of soil. Various researchers [3, 4], have analysed that an increase in the plastic fines up to 10–15% led initially to a loss of strength, but with an increased amount, the rate of strength loss decreased. Seed et al. [5] concluded that if a soil has a clay content greater than 20% it will not liquefy. El Mohtar et al. [6] evaluated the mechanical properties of bentonite-treated sand and observed that the effect of the bentonite addition is to increase the number of loading cycles for a given cyclic stress ratio to which a sand specimen under undrained cyclic triaxial conditions may be subjected before reaching liquefaction.

In this study, liner and cover material were fabricated using local soil (sand) and waste material (coal ash) with bentonite as an admixture keeping in mind the statutory requirement of hydraulic conductivity for the barrier material as $<10^{-9}$ m/s. In order to study the seismic response of the locally available sand and coal ash for use as a liner material, stress-controlled cyclic tests were performed by adding varying percentages of bentonite to the soil mix aiming to understand the failure mechanisms of landfill liner systems and pore pressure generation in soils subjected to earthquake loading, with emphasis laid on the cyclic triaxial testing of the fabricated liner systems

of landfills ascertaining the effect of the addition of plastic fines (bentonite) and nonplastic fines (coal ash) to the cyclic resistance of highly liquefiable sands. In literature, the assessment of the seismic response of liner materials used in landfills has not been reported, though it is essential for landfills located in high seismic zones.

2 Materials Used

The possible deficient soils in meeting the criteria of hydraulic conductivity being $<10^{-9}$ m/s which may be locally available sand, coal ash (which is treated as a waste material) were chosen in this study with bentonite as an admixture. The grain size distributions of the sand, coal ash and bentonite as per IS 2720 (Part 4)—1985 [7], are shown in Fig. 1. The index properties of the materials used in the present study including the specific gravity, plasticity characteristics, etc. are reported in Table 1 [8].

Fig. 1 Grain size distribution curves

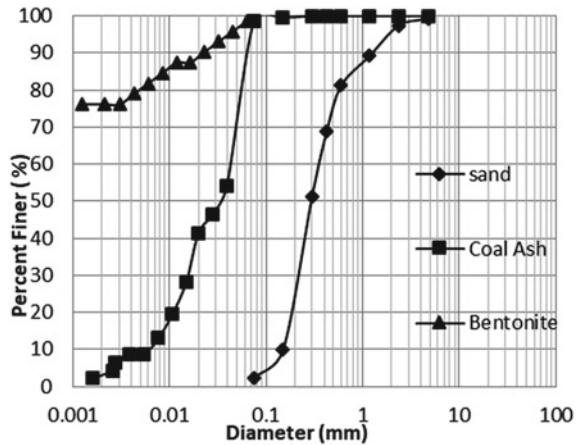


Table 1 Index properties of materials used

Property	Standard specification	Sand	Bentonite	Coal ash
Specific gravity, G	IS: 2720 (Part 3) [11]	2.66	2.82	2.17
Liquid limit, LL (%)	IS: 2720 (Part 5) [12]	NonPlastic	363	NonPlastic
Plastic limit, PL (%)	IS: 2720 (Part 5) [12]	NonPlastic	65.2	NonPlastic
Plasticity index, PI (%)	IS: 2720 (Part 5) [12]	NonPlastic	297.8	NonPlastic
Maximum Void Ratio, e_{max}	IS: 2720 (Part 14) [13]	0.91	–	–
Minimum Void Ratio, e_{min}	IS: 2720 (Part 14) [13]	0.32	–	–
Unified soil classification system	IS 1498: 1970 (Reaffirmed 1987)	SP	CH	ML

2.1 Sand

The sand investigated in this study was local fine sand, which is typical to that used in local construction. The uniformity and curvature coefficients for this sand were $C_u = 2.82$ and $C_c = 1.21$, respectively. It was classified as poorly graded sand or 'SP' as per IS 1498: 1970 (Reaffirmed 2007) [9]. The hydraulic conductivity of sand was found out experimentally as 1.75×10^{-5} m/s at 80% of relative density with e_{\max} and e_{\min} being 0.91 and 0.32, respectively, classifying it as deficient in meeting the mandatory requirement of hydraulic conductivity $<10^{-9}$ m/s, to serve as a barrier material.

2.2 Coal Ash

The coal ash used in this study was obtained from ash pond of Ropar Thermal Plant, Punjab. The ash may be categorized as Class 'F' type according to the ASTM 618 [10] specification for class 'F' fly ash. As per the Unified Classification System, the coal ash may be classified as equivalent to a low plastic silt or 'ML' type soil.

2.3 Bentonite

The bentonite used in this study was sodium bentonite obtained from a local supplier. The results of the chemical analysis show that the bentonite consists mainly of silicates 54%, with 16% aluminates. The mineralogical composition of bentonite using the X-ray diffraction technique indicated the percentage of montmorillonite in the bentonite used in the study as 81.8% and the percentage of calcite as 18.2%.

2.4 Sample Preparation

The samples used in the experimental programme were prepared by first dry mixing of materials, i.e. sand and/or ash and bentonite, and then water was added to the mix in definite proportions. Normal tap water was added to the mixtures to obtain the desired water contents. The specimens for conducting various tests like hydraulic conductivity, direct shear test, triaxial test, etc. have been prepared at a moisture content 2% wet of optimum and at the corresponding dry density obtained from the standard Proctor test, simulating the field conditions as the barrier materials in the landfill construction are placed at the wet of optimum. For the hydraulic conductivity tests, the sample was weighed in predefined proportions and compacted in the standard oedometer moulds itself measuring 60 mm in diameter and 20 mm

thick at maximum dry density. During sample preparation for hydraulic conductivity tests, as well as for other tests, a sufficient period (24 h) as curing time was adopted to homogenize the mix and allow the bentonite to swell and absorb moisture in the sample mix prepared prior to testing.

3 Testing Procedure

The soil testing programme consisted of the hydraulic conductivity studies, static and cyclic triaxial tests in addition to the evaluation of the index properties of the soil mixes. Permeability tests were conducted in compliance with ASTM D 5084-10 [14], as shown in Fig. 2. The testing apparatus for triaxial test consists of a servo-controlled automated loading unit with a triaxial cell and a pneumatic control panel for creating confining and back pressures to be applied to the soil specimens measuring 70 mm in diameter and 140 mm in height. The internal friction angle, cohesion intercept and Mohr-Coulomb failure envelopes were obtained for the soil specimens tested by unconsolidated undrained tests. For the cyclic triaxial test in compliance with ASTM D 5311 [15], as shown in Fig. 3, after the preparation of the soil sample, it was saturated and consolidated to the desired level. Then, a cyclic load of 40 kg was applied at a confining pressure of 250 kPa to the sample keeping the frequency constant at 1 Hz. The amplitude of the cyclic stress level was designated by the cyclic stress ratio (*CSR*) which was fixed at 0.346. The evaluation of pore pressure generated during cyclic loading was done by plotting data in terms of excess pore pressure ratio against the number of cycles. The applied load of 40 kg, i.e. 1.04 kg/cm^2 corresponds to a typical height of 7–8 m of landfill. Generally, the height of landfill goes up to



Fig. 2 a Sample under preparation b Flexible wall permeability test apparatus

Fig. 3 Triaxial test in progress



20 m. But, since the occurrence of liquefaction generally does not take place beyond 10–12 m, therefore, the pressure of 1.04 kg/cm² has been considered in the study.

4 Results and Discussion

Various geotechnical properties of the soil specimens were evaluated and enumerated in Table 2. It can be observed that the liquid limit and plastic limit values increase as the bentonite content in the mix increases because of increased plasticity. In coal ash-bentonite mixes, a very less maximum dry density (*MDD*) was achieved due to ash being a lightweight material, while the optimum moisture content (*OMC*) was high at 32%, in contrast to sand-bentonite mixes. It can be clearly realized that

Table 2 Geotechnical properties of bentonite enhanced soil mixes

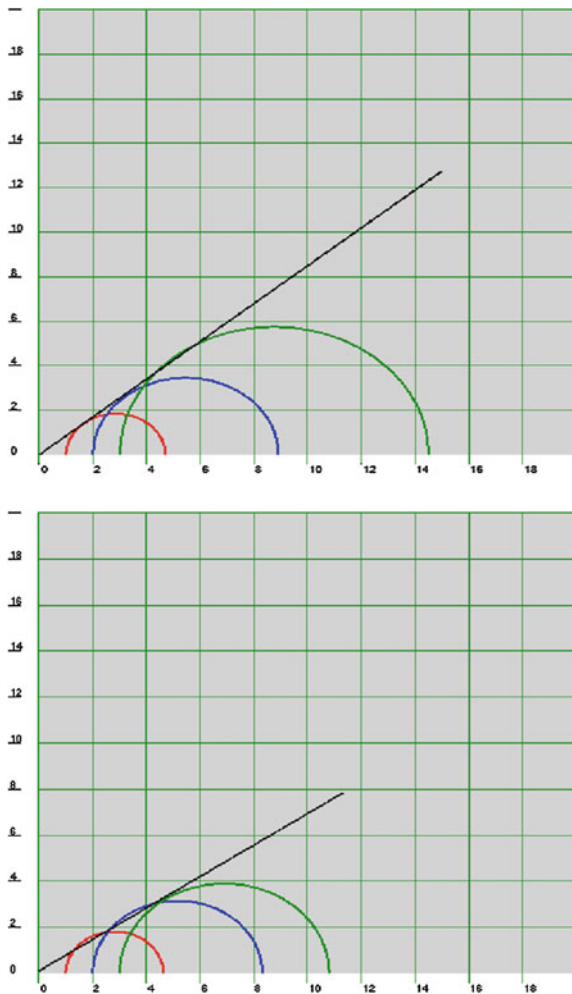
Soil Mix	LL	PL	PI	OMC	γ_d (kN/m ³)	G	k (m/s)
90S + 10B	33.80	17.42	16.38	15.32	17.54	2.67	2.74E-10
100S	NP	NP	NP	–	–	2.66	1.75E-05
80S + 20B	53	27.40	25.60	15.60	17.44	2.69	1.55E-10
80S + 10B + 10F	35	25.40	9.60	15.39	17.35	2.63	5.16E-10
90F + 10B	59	45	14	41.50	10.39	2.60	9.88E-11
100F	NP	NP	NP	32	10.60	2.17	2.70E-06
80F + 20B	80.10	30	50.10	30.73	11.96	2.68	6.01E-11
80F + 10B + 10S	43.5	20.8	22.7	25	13	2.29	5.02E-11

Note S stands for sand, F for coal ash, B for bentonite and the figure preceding the symbol used is the percentage added as a dry % weight of the material. For, e.g. 90S + 10B stands for a mix with 90% sand, 10% bentonite and 0% coal ash

hydraulic conductivity decreases with increasing bentonite content. Soil mixes with higher plasticity possessed lower hydraulic conductivity values at any stress level as compared to a soil which was less plastic.

Static triaxial tests were performed with three normal stresses of 1, 2 and 3 kg/cm² for sand and coal ash at 2% wet of *OMC* for establishing the Mohr-Coulomb failure envelopes and the strength parameters, i.e. angle of internal friction and cohesion. It was observed from the test results that the maximum shear strength increases linearly with normal stresses for the soil specimens tested. Figure 4 show the shear strength parameters for sand and coal ash, respectively. The values of cohesion and friction angle for sand and coal ash were found to be 0.0 kg/cm² (0 kPa), 40.4° and 0.11 kg/cm² (11 kPa), 34.4°, respectively.

Fig. 4 Mohr-Coulomb Plot, Shear Stress (kg/cm²) vs Normal Stress (kg/cm²) for sand and coal ash



4.1 Effect of Bentonite on Excess Pore Pressure Ratio Versus Number of Cycles

The generation of excess pore pressure under undrained loading condition is a mark of all liquefaction phenomena. The relative incompressibility of the pore water makes the rapid compaction of the sand difficult. Due to increase in pore water pressure during cyclic loading, the effective stress on the soil and hence the shear strength decreases and eventually reach to zero, the soil being unable to support the load from the structure.

The work undertaken seems to increase the understanding of the mechanisms responsible for the response of excess pore pressure in sands with the addition of plastic and nonplastic fines. It examines the effects of the presence of bentonite, which is a highly plastic clay and coal ash, which is nonplastic on the initiation of excess pore pressure during cyclic loading from stress-controlled undrained cyclic triaxial tests. Figure 5a compares the response of clean sand and the effect of the addition of 10 and 20% bentonite to sand and subjected to cyclic loading. During undrained cyclic loading, the presence of bentonite affects the magnitude of the pore pressure during all stages of the test. The pore pressure generated for the 10% bentonite mix (90S + 10B) was greater than clean sand, the excess pore pressure ratio reached unity in 72 cycles.

This implies that the initial liquefaction was triggered earlier in case of 90S + 10B as compared to sand, in which the number of cycles for initial liquefaction were 80. However, the rate of pore pressure generation slows down thereafter, resulting in the increased cyclic resistance of the soil mix upon an increase in bentonite content up to 20% in the soil mix. This increased bentonite content reduces the rate of pore pressure generation during cyclic loading, allowing the soil to sustain a more significant effective stress loss prior to the acceleration of excess pore pressure generation.

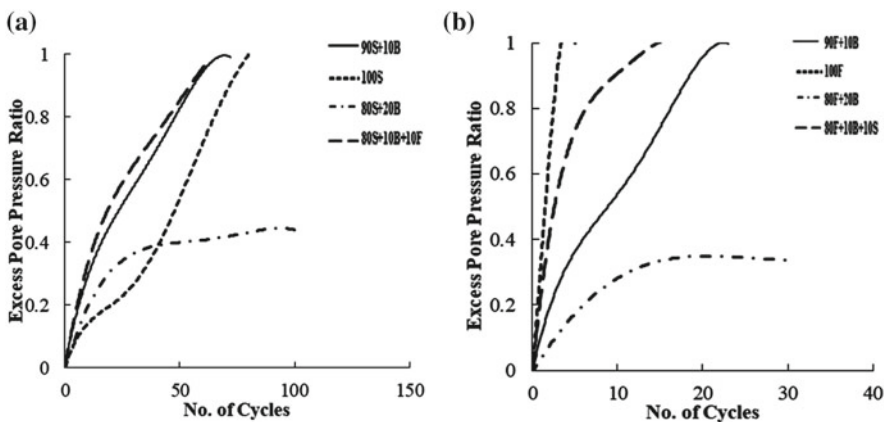


Fig. 5 Effect of bentonite on excess pore pressure ratio versus number of cycles for a sand b Coal ash

Thus, these effects contribute to a dramatic increase in the liquefaction resistance of the sand upon addition of bentonite content up to 20%. It is anticipated that the observed changes in behaviour are due to the swelling of the bentonite inside the sand pore space and the formation of a thixotropic pore fluid of concentrated bentonite suspension.

Figure 5b depicts the excess pore pressure ratio variation of coal ash and coal ash-bentonite mixes and the effect of the addition of sand to coal ash-bentonite with the number of cycles to liquefaction. It was observed that in coal ash, there was a rapid increase in the development of pore pressure and the onset of liquefaction occurred merely in 5 cycles. Upon addition of 10% bentonite to coal ash, a definite increase in cyclic resistance was observed. The pore pressure built up reduces drastically upon addition of bentonite to coal ash up to 20% signifying an increased liquefaction resistance of the soil specimens.

4.2 Effect of Plasticity of Soil on Cyclic Resistance

The initiation of liquefaction is defined as either when excess pore pressure is equal to effective confining pressure or when the double amplitude axial strain of 5% is reached. The liquefaction resistance of soil mixes is represented by the number of cycles required to initiate the liquefaction. Figure 6 depicts the number of cycles required to trigger initial liquefaction. The effect of increasing plasticity of soil with the increasing percentage of bentonite added to the soil mixes can be visualized. In case of sand-bentonite mixes, upon addition of bentonite to sand, the pore pressure gets built up rapidly in less number of cycles. Beyond a certain percentage of bentonite addition, the generation of pore pressure decreases due to increased cyclic resistance. This trend is clearly illustrated in Fig. 5 in which excess pore pressure generated for

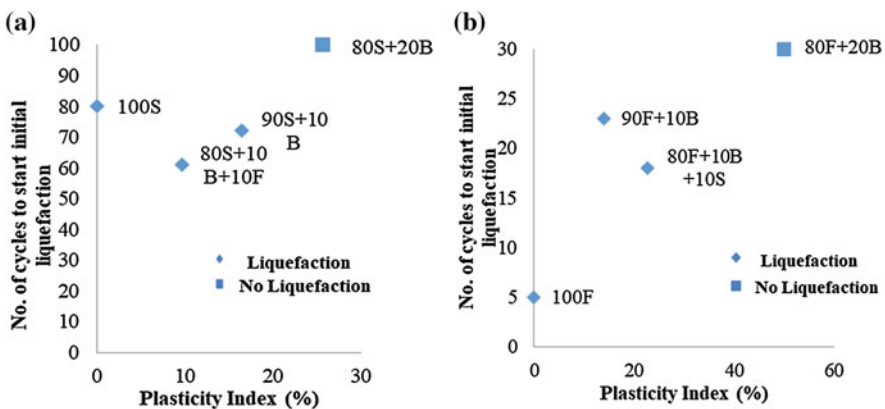


Fig. 6 Effect of bentonite on number of cycles to trigger initial liquefaction for a sand b coal ash

90S + 10B shows a lesser resistance to liquefaction due to an abrupt increase in excess pore pressure, even greater than that for sands. But, when the percentage of bentonite is increased to 20%, the soil mix becomes highly liquefaction resistant. This implies that the behaviour of the specimen becomes more ductile by increasing the bentonite content. The reason for this behaviour can be attributed to the fact that as the clay content increases, contact between sand particles decrease and the dominant phase of specimen changes from sand to bentonite.

The effect of the addition of bentonite to coal ash can be seen in Fig. 6b. The coal ash specimen, which is nonplastic, is subjected to initial liquefaction quite early at 5 cycles. But, when 10% bentonite is added to coal ash, the plasticity index increases to 14 as in 90F + 10B, the number of cycles to initial liquefaction increase to 23. When the plasticity index is increased further increased to 50, upon addition of 20% bentonite, the mix becomes highly resistant and does not liquefy.

Thus, it can be foreseen from the experimental results obtained from the stress-controlled cyclic triaxial tests conducted to assess the liquefaction resistance with the addition of bentonite and coal ash to sand, that upon addition of 10% bentonite addition to sand, the liquefaction resistance decreases. On further increasing the percentage of bentonite up to 20%, the strength and resistance to liquefaction increases manifold. Hence, while confirming an optimum mix for use as a barrier material, a higher percentage of 15–20% bentonite is recommended on account of the seismic response of bentonite enriched soils. While considering the typical coal ash-bentonite or sand-bentonite-coal ash category of mixes, it can be witnessed that addition of bentonite up to 20% to coal ash increases the cyclic resistance of the soil specimens. For maximum utilization of waste material, the fabricated soil mix (80F + 20B) is highly recommended on account of seismic response, in regions prone to seismic action for use as a barrier material.

5 Conclusions

Following conclusions may be drawn from the study conducted on the seismic response of fabricated soil liners:

- Seismic stability of barrier material for landfills fabricated by mixing bentonite in sand/coal ash is required to be studied for the landfills situated in high seismic zones.
- At 10% bentonite addition to sand, an increase in excess pore pressure was observed as compared to sand. With a bentonite content of 20%, the strength and resistance to liquefaction increased manifold. Hence, while confirming an optimum mix for use as a barrier material, a percentage of 15–20% bentonite to sand is recommended on account of seismic response of bentonite enriched soils, keeping in view the high swelling characteristics of sand-bentonite. While considering the typical coal ash-bentonite or sand-bentonite-coal ash category of mixes,

it can be witnessed that addition of bentonite up to 20% to coal ash increases the liquefaction resistance of the soil specimens.

- For maximum utilization of waste material, the fabricated soil mix 80F + 20B is highly recommended on account of seismic response, in regions prone to seismic action for use as a barrier material.
- Coal ash is more susceptible to liquefy in comparison to sand.

References

1. Ishihara K (1993) Liquefaction and flow failure during earthquakes. *Geotechnique* 43(3):351–415
2. Augello AJ, Matasovic N, Bray JD, Kavazanjian E, Seed RB (1995) Evaluation of solid waste landfill performance during the Northridge earthquake. *Geotech Special Publ ASCE* 54:17–50
3. Abedi M, Yasrobi SS (2010) Effect of plastic fines on the instability of sand. *Soil Dyn Earthq Engg* 30:61–67
4. Dey AK, Gandhi SR (2008) Evaluation of liquefaction potential of pond ash. In: *Proceedings of 2nd international conference on geotechnical engineering for disaster mitigation and rehabilitation*. Springer, Science Press, Berlin, Beijing, pp 315–320
5. Seed HB, Idriss IM, Arango I (1983) Evaluation of liquefaction potential using field performance data. *J Geotech Eng ASCE* 109(3):458–482
6. El Mohtar CS, Santagata M, Bobet A, Drnevich V, Johnston C (2008) Effect of plastic fines on the small strain stiffness of sand. In: *Proceedings of 4th international symposium on deformation characteristics of geomaterials (IS-Atlanta)*, Amsterdam, Netherlands, vol 1, pp 245–251
7. IS: 2720 (Part 4) (1985) *Methods of test for soils: Part 4, Grain size analysis (second revision)*, Bureau of Indian Standards, New Delhi
8. Sobti J, Singh SK (2017) Investigation of hydraulic conductivity and matric suction in Sand–Bentonite–Coal Ash mixes. *Indian Geotech J* 47(4):542–558
9. IS: 1498 (1970) *Indian standard classification and identification of soils for general engineering purposes*, Bureau of Indian Standards, New Delhi
10. ASTM C 618-12. *Standard specification for coal fly ash and raw or calcined natural pozzolana for use in concrete*. American Society for Testing and Materials, West Conshohocken, PA
11. IS: 2720 (Part 3/Set 2) (1980) *Methods of test for soils: Part 3 Determination of specific gravity, Section 2 Fine, medium and coarse grained soils (first revision)*, Bureau of Indian Standards, New Delhi
12. IS: 2720 (Part 5) (1985) *Methods of test for soils: Part 5, Determination of liquid and plastic limit (second revision)*, Bureau of Indian Standards, New Delhi
13. IS: 2720-Part 14 (1983) *Methods of test for soils: Determination of density index (relative density) of cohesionless soils (second revision)*, Bureau of Indian Standards, New Delhi
14. ASTM D 5084-03 *Standard test methods for measurement of hydraulic conductivity of saturated porous materials using a flexible wall permeameter*, American Society for Testing and Materials, West Conshocken, PA
15. ASTM D 5311-92 (Reapproved 1996) *Standard test method for load controlled cyclic triaxial strength of soil*, Annual book of American Society for Testing and Materials (ASTM) standards, 04

Interpretation of Hydraulic Conductivity of Bentonites Based on Sedimentation Characteristics



Esra Dikişçi, El Hassen Abd Moulana, and A. Hakan Ören

Abstract This study suggests a new test method for the interpretation of hydraulic conductivity of GCLs. The proposed methodology is sedimentation test which can be applied after swell index test by vigorously shaking the graduated cylinder. The study basically shows that the bentonites may have the same swell index values, but different hydraulic conductivities. Therefore, swell index may not be a suitable test method for the interpretation of hydraulic conductivity. However, bentonites have different sedimentation characteristics which can be correlated well with the hydraulic conductivity. For example, bentonites serving accumulation type of settling (AS) may have greater hydraulic conductivity than the bentonites serving mixed or flocculated type of settling (i.e., MS and FS).

Keywords Swell index · Sedimentation test · Hydraulic conductivity

1 Introduction

The resulted leakage from waste repositories leads to pollution of the environment therefore several studies focused on how to solve this problem. One of the proposed solutions to handle the contamination problems is enclosing the waste in a specific place then isolated from the environment by using bentonitic barriers. Bentonite is significant constituent of geosynthetic clay liners (GCLs) and sand–bentonite mixtures (SBMs). GCLs are used in solid waste landfills, mining enterprises, tunnels, and many other areas to isolate the contaminants from the environment. The main advantage of bentonite is its low hydraulic conductivity ($\leq 2.0 \times 10^{-11}$ m/s).

The test duration required for the hydraulic conductivity tests in the laboratory is quite long. Therefore, researchers have focused on to establish some relationships to predict the hydraulic conductivity from some properties of bentonite such as swell index, consistency limits, smectite content, cation exchange capacity, etc. [1–6]. However, among these tests, the most known is swell index which is a mandatory

E. Dikişçi · E. H. A. Moulana · A. Hakan Ören (✉)
Dokuz Eylül University, Buca-Izmir, Turkey
e-mail: ali.oren@deu.edu.tr

test under quality control and assurance requirements. Despite its advantages, the swell index test has some limitations where (i) air bubbles may remain between swollen particles, (ii) the interface between bentonite surface may not be flat and thus, swell volume may not be read exactly, (iii) some factors may not be easily controlled during the test such as rapid settling of swollen bentonite from the water surface during 0.1 g of bentonite adding, insufficient time (i.e., 10 min) for the swell of bentonite particles after pouring. As an alternative, settling behavior of bentonite can also give some information about the hydraulic conductivity of bentonites. Simply, once the swell index test is conducted on the bentonite, the swollen sample after 24 h can be vigorously shaken and then allowed free settling in the graduated cylinder.

The settling behavior may be different depending on the solid/liquid ratio, clay mineralogy, and pore medium chemistry (solution type, concentration, and pH). Imai (1980) collected the sedimentation behaviors of soils under four categories depending on the water content (or solid/liquid ratio (S/L)): (i) Dispersed free settling (observed at low S/L), (ii) flocculated-free settling (observed at medium S/L), (iii) zone settling (consist of flocculation, settling and consolidation stages and observed at high S/L), and (iv) consolidation settling (observed at very high S/L). Sridharan and Prakash [7] examined the sedimentation behavior depending on clay mineralogy under the name of dispersed free settling and flocculated-free settling by reducing the behaviors into two which have distinct characteristics from those proposed by Imai [8]. Kaya et al. [9] have suggested another type of settling as “mixed settling” in which the heavier particles settle immediately, and remaining particles have form flocs (or aggregates) to serve flocculation settling. This type of settling can be seen in the study of Sridharan and Prakash [7] as well.

The aim of this study is to show the efficiency of an alternative test method, sedimentation test, over swell index test while interpreting the hydraulic conductivity of geosynthetic clay liners (GCLs) to water. To do this, an observational relationship between the hydraulic conductivity of bentonites and sedimentation characteristics was established.

2 Materials and Methods

2.1 Materials

A total of eight bentonites were used in this study three of which had been taken from GCLs manufactured by the local producer, and the rest had been gathered from the companies that are available in the local market in Turkey. Some bentonites were rich in sodium; some of polymer-treated and some were in their natural state and not subjected to any treatment. These bentonites were oven-dried at 105 °C. After drying, they were grinded in a mortar and passed through No 200 sieve (<0.075 mm). Then, all samples were kept in plastic bags until testing. Swell index and sedimentation tests were conducted in 100 mL graduated cylinders using deionized water (DIW).

2.2 Methods

Swell index was conducted in accordance with ASTM:D5890-11 [10]. The graduated cylinder tests were initially filled with water until 90 mL level. Then, 0.1 g of bentonite was weighed and poured in the cylinder within 30 s. After 10 min of waiting for bentonite swell, another 0.1 for all samples were poured. After 24 h of hydration, the swell index value of bentonite was recorded.

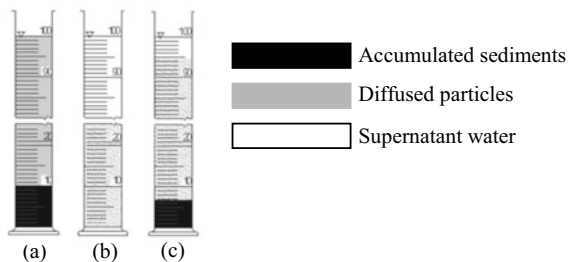
The sedimentation tests were conducted immediately after swell index value had been recorded. The cylinder was vigorously shaken until it was ensured that there were no bentonite particles remained at the bottom of the cylinder. Once it was ensured, the shaking was continued a few more minutes. The suspension formed by shaking was allowed to settle, and sedimentation behavior was examined with time. Sedimentation volumes were recorded at the end of 1, 2, 5, 10, 15, 30, 60, 120, 240, 480, and 1440 min (sometimes with extended reading times). Since the swelling index experiments were repeated three times, the sedimentation tests were performed three times for each bentonite as well.

Hydraulic conductivity tests had been run on artificially prepared (AP) and original GCLs which were reported elsewhere [3, 11]. Artificial GCLs had been prepared by placing bentonite between non-woven and woven geotextiles without needle-punching. The hydraulic conductivities of bentonites had been measured by permeating deionized water and using flexible wall permeameters. Other testing details can be found in [3, 11].

3 Results and Discussions

The sedimentation characteristics of bentonites were categorized into three different regimes. In the first type of settling, the particles settled down quickly and accumulated at the bottom of the graduated cylinder. Since accumulation was in upward direction, the sediment volume of the particles increased with time. Accumulated layer was followed by diffused particle layer in the graduated cylinder. This type of settling is called accumulation sedimentation (AS) and is shown in Fig. 1a. The other type of settling was in the flocculated form (Fig. 1b). That is, when settling

Fig. 1 Different sedimentation behaviors of bentonites: (a) Accumulation sedimentation (AS), (b) mixed sedimentation (MS), and (c) flocculation sedimentation (FS)



was begun, the particles immediately formed aggregates and flocculated structure start to settle down together. Thus, the sediment volume decreased with time. This type of settling is called flocculation sedimentation (FS). The third type of settling was in between AS and FS (Fig. 1c) and is called mixed sedimentation (MS) where the settling was in the form of accumulation initially and then turned to flocculation with time. All these forms of sedimentation characteristics and sharp interface should be seen between any type of sediments and diffused particles or clear (supernatant) water.

The typical sedimentation curves of the bentonites are shown in Fig. 2 as a function of time. As shown in Fig. 2a, the accumulated thickness of the sediments increases with time. In Fig. 2b, however, the sediment thickness (or volume) decreases with time. Generally, it is expected to have larger sediment volumes for FS than for

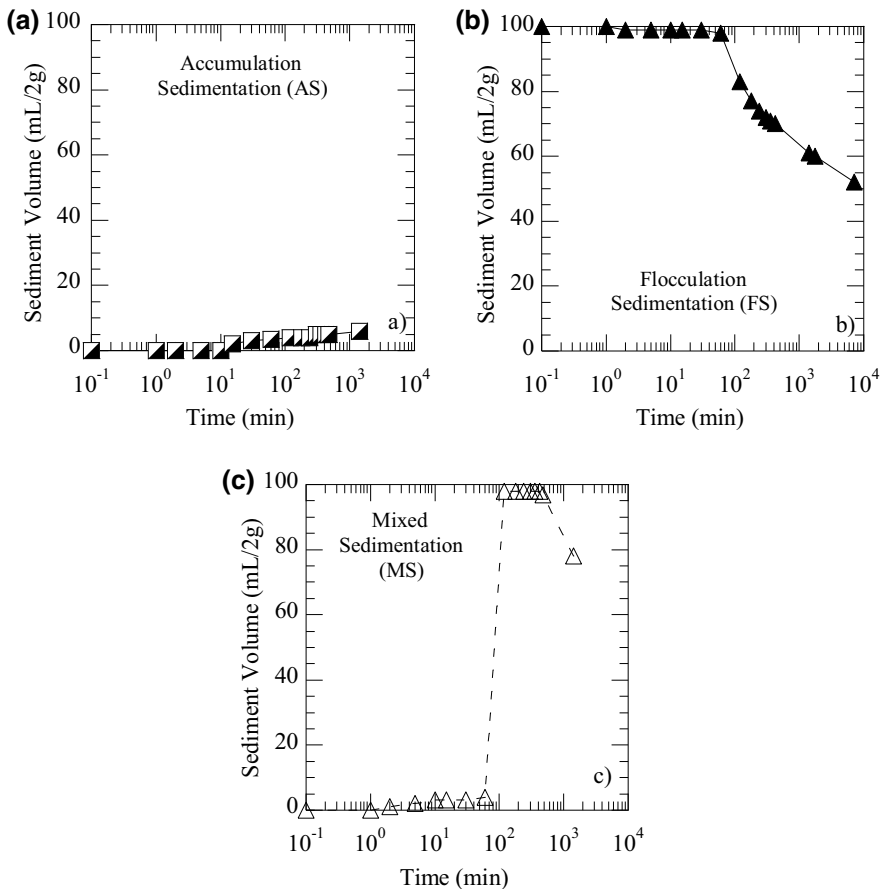


Fig. 2 Sedimentation behavior of bentonites as a function of time: (a) Accumulation sedimentation (AS), (b) mixed sedimentation (MS), and (c) flocculation sedimentation (FS)

Table 1 Swell index and sedimentation behavior

Bentonite	Swell index	Category level	Sedimentation behavior	Hydraulic conductivity (m/s)
B-1	15	1	AS	–
B-2	17		MS	6.1×10^{-12}
B-3	21	2	AS	5.8×10^{-11}
B-4	21		AS	3.8×10^{-11}
B-5	21		AS	3.2×10^{-11}
B-6	24	3	MS	5.2×10^{-12}
B-7	25		AS	8.1×10^{-12}
B-8	26		FS	5.9×10^{-12}

AS. Mixed sedimentation shown in Fig. 2c is the combination of accumulation and flocculation sedimentation. The sedimentation thickness first increases from bottom of the cylinder, and then the interface between accumulated sediments and diffused particles disappears and flocs start to settle down.

The swell indices and the sedimentation characteristics of bentonites are presented in Table 1. Based on similar swell index values, bentonites can be categorized into three groups. In the first group, bentonite had an average of 16 mL/2 g swell index value. In the second and third groups, the average swell indices were 21 and 25 mL/2 g, respectively. As given in Table 1, the same swell index might have either the same or different sedimentation behaviors. Although B-3, B-4, and B-5 had swell index of 21 mL/2 g, the sedimentation characteristics were in accumulation type. In contrast, B-6, B-7, and B-8 had an average of 25 mL/2 g swell index. However, the settling type of these bentonites was totally different from each other. The same conclusion can be drawn between B-1 and B-2 as well (Table 1).

The hydraulic conductivities of GCLs are preferably well correlated with swell index of bentonites. Table 1 summarizes the hydraulic conductivity of GCLs to DIW. From Table 1, it can be seen that the bentonites with the same swell index may have different hydraulic conductivities. In each category, the difference between the hydraulic conductivities of bentonites is 1.8 at most. One can argue that this difference may not be so important and can be acceptable. However, except Category 2, the sedimentation characteristics were different from each category, indicating that sedimentation behavior may be more effective than swell index while interpreting the hydraulic conductivity.

To show the efficiency of sedimentation test over swell index test, hydraulic conductivity of GCLs is plotted as a function of swell index category (Fig. 3a) and sedimentation behavior (Fig. 3b). Since sedimentation characteristics of bentonites were different from each other, the relationship was established by considering sediment behavior rather than sediment volumes. Because different settling regimes have different sediment volumes. Therefore, giving the tendency with a quantitative correlation is avoided. The interpretation of sedimentation characteristics depends on visual observations. Thus, this kind of relationship is defined as “observational”.

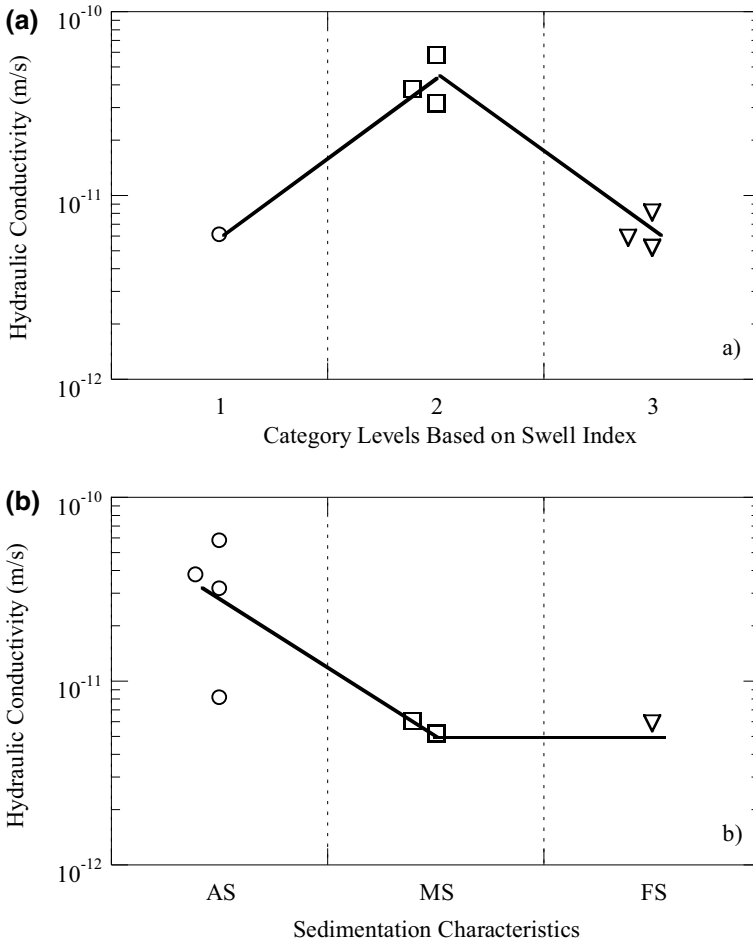


Fig. 3 Observational relationship between: (a) swell index category and hydraulic conductivity and (b) sedimentation characteristics and hydraulic conductivity

To make better comparison, the relationship between swell index and hydraulic conductivity is given in terms of category level.

Based on these relationships, Fig. 3a shows that correlation between the swell index and hydraulic conductivity is poor, whereas correlation between sediment behavior and hydraulic conductivity is good. In Fig. 3a, the hydraulic conductivity increased when category level increased from 1 to 2. Then, it decreased ~ 7 times (from 4.2×10^{-11} m/s to 6.4×10^{-12} m/s) at Category 3. If the hydraulic conductivity is interpreted with sedimentation characteristics, it can be seen that the hydraulic conductivity was high in the case of AS, whereas it was low when settling regime turned to MS or FS (Fig. 4).

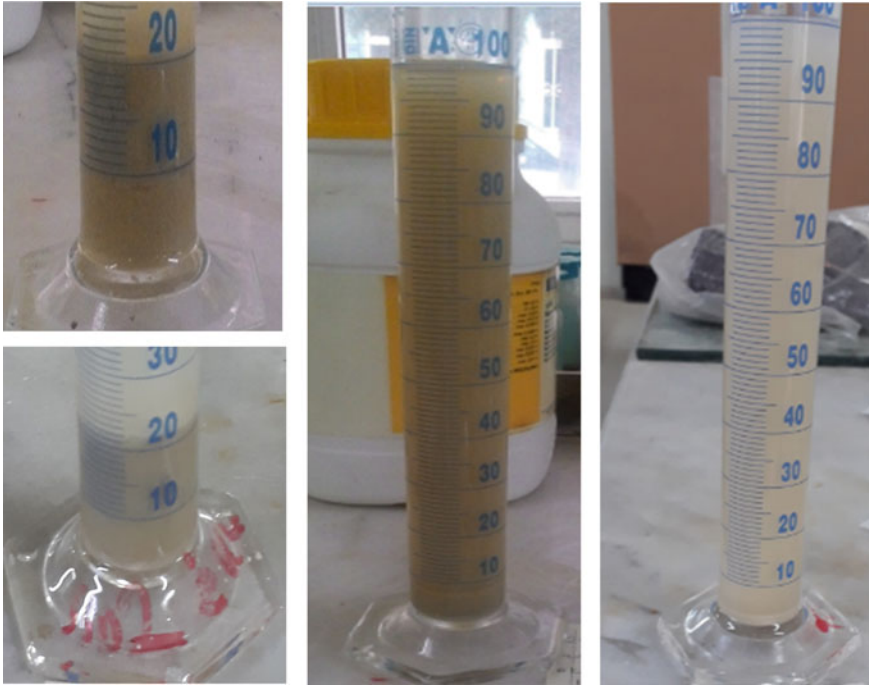


Fig. 4 Swell index of: (a) B-3 and (b) B-5. Despite accumulation type of settling, the columns or the solid to liquid ratio (S/L) of the accumulated and diffused particle zones of B-3 (c) and B-5 (d) are different

Table 1 presents that the Category 2 had similar settling regimes. Although these bentonites serve AS type of settling, neither accumulated nor diffused particles zones were the same. In other words, the accumulated sediment volumes and the diffused particle volumes of bentonite were different from each other. An example is given for B-3 and B-5 which had the same swell index and settling characteristics, whereas different accumulated sediment volumes and solid-to-liquid ratio (S/L) in diffused particle zones. This indicates that although sedimentation characteristics were defined as AS, there were still major differences in the volumes of accumulated or diffused zones of bentonites. Thus, sedimentation-based interpretation needs further improvement.

4 Summary and Conclusions

This study basically shows the superiority of sedimentation tests over the swell index tests while interpretation of hydraulic conductivity of GCLs. The interpretation was made with the sedimentation characteristics of bentonites. After swell index tests,

the samples were shaken vigorously and allowed settling. The methodology is quite simple and has some advantages with respect to swell index tests.

Bentonites served different settling regimes, namely, accumulation, flocculation, and mixed (AS, FS, and MS). To make better comparison with sedimentation characteristics, swell index was categorized into three levels such as Category 1 represents the average swell index of 16 mL/2 g, and Category 2 and Category 3 cover an average swell index of 21 and 25 mL/2 g. When these observational parameters were related to hydraulic conductivity results, it was seen that sedimentation characteristics correspond well with the hydraulic conductivity when compared to swell index categories.

References

1. Mishra AK, Ohtsubo M, Li L, Higashi T (2011) Controlling factors of the swelling of various bentonites and their correlations with the hydraulic conductivity of soil-bentonite mixtures. *Appl Clay Sci* 52:78–84. <https://doi.org/10.1016/j.clay.2011.01.033>
2. Lee J-M, Shackelford CD, Benson CH et al (2005) Correlating index properties and hydraulic conductivity of geosynthetic clay liners. *J Geotech Geoenviron Eng* 131:1319–1329. [https://doi.org/10.1061/\(ASCE\)1090-0241\(2005\)131:11\(1319\)](https://doi.org/10.1061/(ASCE)1090-0241(2005)131:11(1319))
3. Ören AH, Yükselen Aksoy Y, Önal O, Demirkıran H (2018) Correlating the hydraulic conductivities of GCLs with some properties of bentonites. *Geomech Eng* 5:1091–1100
4. Jo HY, Katsumi T, Benson CH, Edil TB (2001) Hydraulic conductivity and swelling of nonprehydrated GCLs permeated with single-species salt solutions. *J Geotech Geoenviron Eng* 127(7):557–567
5. Katsumi T, Ishimori H, Onikata M, Fukagawa R (2008) Long-term barrier performance of modified bentonite materials against sodium and calcium permeant solutions. *Geotext Geomembranes* 26:14–30. <https://doi.org/10.1016/j.geotextmem.2007.04.003>
6. Kolstad DC, Benson CH, Edil TB (2004) Hydraulic conductivity and swell of nonprehydrated geosynthetic clay liners permeated with multispecies inorganic solutions. *J Geotech Geoenviron Eng* 130:1236–1249. [https://doi.org/10.1061/\(ASCE\)1090-0241\(2004\)130](https://doi.org/10.1061/(ASCE)1090-0241(2004)130)
7. Sridharan A, Prakash K (2001) Settling behaviour and clay mineralogy. *Soils Found* 41:105–109
8. Imai G (1980) Settling behaviour of clay suspension. *Soils Found* 20:61–77. <https://doi.org/10.1248/cpb.37.3229>
9. Kaya A, Ören AH, Yükselen Y (2006) Settling of kaolinite in different aqueous environment. *Mar Georesour Geotechnol* 24:203–218
10. ASTM:D5890-11 (2011) Standard test method for swell index of clay mineral component of geosynthetic clay liners. In: ASTM international, West Conshohocken, PA, USA. pp 7–9
11. Ören AH, Akar RÇ (2017) Swelling and hydraulic conductivity of bentonites permeated with landfill leachates. *Appl Clay Sci* 142:81–89. <https://doi.org/10.1016/j.clay.2016.09.029>

Effect of Organic Matter on Index Swell Properties of a Conventional and Bentonite–Polymer GCL



Christian Wireko and Tarek Abichou

Abstract Like inorganic salts, organic matter is also a major component of leachate from municipal solid waste (MSW) landfills. This study uses humic substances (HS) to investigate the influence of organic matter on the swell index (SI) and liquid limit (LL), a conventional sodium bentonite (Na–B), and a dry mixture of Na–B and proprietary polymer (B–P), extracted from commercially available geosynthetic clay liners (GCLs). The SI and LL tests were performed using 5–200 mM NaCl and CaCl₂ solutions prepared either with or without 100 mg/L HS. Adding 100 mg/L HS to the NaCl solutions resulted in an increase in SI of Na–B for Na⁺ concentration ≥ 20 mM. However, with the Ca²⁺ solutions adding HS caused a slight decrease in SI of Na–B at low Ca²⁺ concentrations (≤ 20 mM) but had no effects on the SI of Na–B at Ca²⁺ concentrations ≥ 50 mM. On the other hand, the SI of B–P with Na⁺ solutions containing HS was consistently lower than with the pure NaCl solutions. But like the Na–B, HS had no effect on the SI observed for B–P with the Ca²⁺ solutions. Within the range of Na⁺ and Ca²⁺ concentrations used in this study, the addition of 100 mg/L HS did had no significant influence on the LL of Na–B. At similar Na⁺ and Ca²⁺ concentrations, LL of B–P with solution containing HS was significantly higher than with the pure salt solution. Hydraulic conductivity testing of the GCLs is currently ongoing using test solutions of interest selected based on the results of the SI and LL tests.

Keywords Bentonite–polymer · Geosynthetic clay liners · Humic substances

1 Introduction

Geosynthetic Clay Liners (GCLs) consist of a thin layer of sodium bentonite (Na–B) bonded between two geotextiles or glued to a geomembrane and are widely used as hydraulic barrier in waste containment facilities [1]. When they do not contain a geomembrane, the hydraulic conductivity of GCLs is controlled by the Na–B [1].

C. Wireko (✉) · T. Abichou

Department of Civil and Environmental Engineering, Florida A&M University-Florida State University College of Engineering, 2525 Pottsdamer Street, Tallahassee, FA 32310, USA
e-mail: ckw17b@my.fsu.edu

© Springer Nature Switzerland AG 2020

K. R. Reddy et al. (eds.), *Sustainable Environmental Geotechnics*, Lecture Notes in Civil Engineering 89, https://doi.org/10.1007/978-3-030-51350-4_36

353

Na–B contains high montmorillonite content with Na^+ – as the dominant interlayer cation and undergoes osmotic swelling with hydrated [2, 3]. Swelling reduces pore spaces in the bentonite fabric and increases the travel path of free water; thus, Na–B has low hydraulic conductivity to deionized (DI) water ($\sim 10^{-9}$ cm/s) [4, 5].

A significant number of studies have been conducted on GCL using inorganic salt solutions or real leachate. These studies show that aggressive liquids, with high ionic strength and/or consisting predominately of polyvalent cations, can inhibit osmotic swelling of Na–B, thus causing unacceptable increase in hydraulic conductivity ($> 1 \times 10^{-5}$ cm/s) [4, 6–14]. Efforts to improve the chemical compatibility of Na–B to aggressive liquids have led to the development of several amended bentonites, including bentonite modified at a nanoscale by intercalating organic molecules [15] or polymers [16–18] into the interlayer spaces of the montmorillonite particles, and bentonite modified by dry mixing with polymers [19–22].

Municipal solid waste (MSW) landfill leachate, including landfills where MSW and MSW incineration fly and bottom ash are co-disposed, contain organic matter in varying concentrations depending on factors such as type of waste composition, age of landfill, etc. [23–25]. Humic substances make up a large portion of organic matter in landfill leachate and become even more dominant as a landfill mature [23, 26–30]. Han et al. [31] evaluated the hydraulic conductivity of a Na–B GCL using solutions of humic and fulvic acids extracted from leachates of a 6-month-old and a 10-year-old MSW landfill and found that the hydraulic conductivities were similar to DI water ($\sim 10^{-9}$ cm/s). Suggesting organic matter alone did not have any significant impact on the hydraulic conductivity of GCLs. However, the effect of organic matter has on the hydraulic properties of GCLs has not been investigated in the presence of inorganic salts.

In this study, a series of swell index and liquid limit tests were conducted on bentonite extracted from a conventional GCL (granular Na–B) and a bentonite–polymer (B–P) GCL (dry blend of granular Na–B and proprietary polymer) using aqueous Na^+ and Ca^{2+} salt solutions of various concentrations prepared either with or without organic matter to assess the impact organic matter has on index hydraulic properties of GCLs.

2 Background

2.1 Nature of Humic Substances

Humic substances (HS) are the most abundant naturally occurring organic matter in both terrestrial and aquatic environments and are formed from partially degraded or microbially modified organic materials [32]. HS are heterogenous in terms of elemental composition, chemical functionality, and structural conformation, and have large number functional groups, with the most dominant and reactive ones being carboxylic ($-\text{COOH}$) and phenolic ($-\text{OH}$) groups [33]. In slight acidic-to-basic

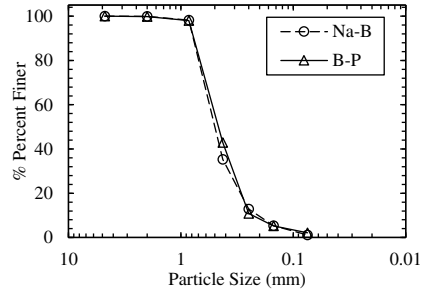
aqueous solutions ($\text{pH} > 6$), the $-\text{COOH}$, $-\text{OH}$ groups, and other acidic groups' functional dissociates into $-\text{COO}^-$ and $-\text{O}^-$, thus behaving more like a polyanionic electrolyte [33, 34]. These ionized functional groups repel each other causing the HS to take up a more spread or stretched out conformation in the solution [34]. Multivalent cations such as Ca^{2+} , Fe^{3+} , and Al^{3+} have an affinity to these ionized functional groups and can form complexes with HS, and thus HS also contribute to cation exchange capacity (CEC) [35] and pore solution pH [33] of soil systems. The ability of HS to form complexes with multivalent cations in a solution can also cause HS molecules to aggregate and potentially precipitate out of solutions [36–38].

2.2 Mechanism of Interaction Between Humic Substances and Montmorillonite

Factors such as electrolyte species, solution ionic strength, and pH influence the mode and degree of interaction between HS and montmorillonite in a montmorillonite–electrolyte–HS aqueous system [34]. In a solution of pH greater than 6, HS are polyanionic, and thus adsorption of HS by the negatively charged montmorillonite particles is hindered due to electrostatic repulsion [34]. However, exchangeable cations at the basal surfaces of montmorillonite can enhance HS adsorption by bridging exchange sites at the mineral surface and the anionic functional groups of the HS either directly (referred to as “cation-bridging”) or indirectly through water molecules in the outer hydration shells of the cations (referred to as “water-bridging”) [34, 39, 40]. Polyvalent exchangeable cations are, however, required for any significant adsorption of HS to take place via cation-bridging or water-bridging [34, 41–43]. In an experimental study, Preston and Riley [43] and Feng et al. [39] showed that the amount of HS adsorbed on Na-montmorillonite particles in the presence of Ca^{2+} was significantly greater than observed for Na^+ .

Moreover, as the ionic strength of the medium increases, there is considerable charge neutralization or screening of the anionic functional groups of the HS, as well as compression of the DDL of both the functional groups and the montmorillonite particles [39, 44]. This promotes proximity between the anion groups of the HS and the montmorillonite mineral surfaces, thus inducing the attraction due to van der Waals interactions. Thus, sorption of HS on montmorillonite increases with the ionic strength of the bulk solution [39, 45]. In the presence of Na^+ and Ca^{2+} electrolyte with the same ionic strengths, however, Ca^{2+} will cause relatively greater adsorption of HS on the montmorillonite particles [45]. Functional groups of the HS can also infiltrate edges the montmorillonite mineral and exchange for terminal hydroxyl or water molecules in the octahedral units in a process known as ligand exchange [34]. However, HS adsorption on montmorillonite mineral through ligand exchange is less favorable due to its relatively small edge surface area [34, 46].

Fig. 1 Granule size distribution of the air-dried bentonite extracted from the GCLs used in this study



3 Materials and Methods

3.1 Bentonites

Index tests were performed on bentonite extracted from two commercially available GCLs: One contained conventional granular Na-B, and the other contained dry mixture of granular Na-B and proprietary polymer (B-P), both encapsulated between a nonwoven geotextile and a scrim-nonwoven geotextile bonded together by needle-punched fibers. Both GCLs were obtained from the same manufacturer. The granule size distributions of both GCLs were obtained through mechanical sieve analysis of the extracted and air-dried bentonite following ASTM C136/C136M as shown in Fig. 1. The polymer loading (content) of the B-P was estimated to be 4.4% (by mass) via loss on ignition (LOI) in accordance with ASTM D7348, following the procedure described by Scalia et al. [47].

3.2 Liquids

Inorganic salt solutions of varying concentrations were prepared either with or without humic substances (HS). The HS was a technical grade (<90% purity) powdered sodium humate (Sigma-Aldrich). The average carbon content of the HS was estimated to be 45.5% (by mass) based on total organic carbon (TOC) measurements of different HS concentrations. The pure inorganic salt solutions were prepared by dissolving reagent grade chloride salts in Type II DI water. Inorganic salt solutions containing HS were prepared by dissolving the HS and salts in Type II DI water, in that respective order. The concentration of HS was fixed at 100 mg/L for this study because the HS did not totally dissolve in water at concentrations greater than 100 mg/L. The solutions were homogenized by shaken rigorously every time before use. The ionic strength of solutions used in study ranged from 0.01 M to 0.7 M, and the pH ranged from 6.4 to 8.3. Measured chemical properties of the solutions used in this study are summarized in Table 1.

Table 1 Chemical characteristics of liquids used in study

Type of solution	Target solute concentration (mM)	Measured solute concentration (mM) ^a		Measured pH	Measured electrical conductivity (mS/cm) ^b
		Sodium (Na ⁺)	Calcium (Ca ²⁺)		
DI water	N/A	ND	0.01	6.98	0.01
NaCl	5	8.42	0.04	6.94	0.62
	10	19.83	0.07	6.80	1.22
	20	23.97	0.05	6.69	2.41
	50	106.57	0.05	6.96	5.13
	100	137.02	0.04	6.76	9.96
	200	210.09	0.02	6.48	19.04
CaCl ₂	5	0.13	5.00	6.68	1.16
	10	0.02	8.00	6.52	1.93
	20	0.13	10.40	6.45	4.04
	50	0.03	53.00	6.64	10.77
	100	0.04	84.50	6.10	24.96
	200	0.08	173.00	6.35	44.37
Na-HS ^c	5	5.14	0.10	6.36	0.63
	10	9.13	0.12	8.25	1.20
	20	18.49	0.15	8.26	1.86
	50	47.02	0.07	8.18	4.97
	100	89.17	0.08	8.08	9.52
	200	187.04	0.11	8.07	18.38
Ca ^d -HS	5	0.00	2.40	6.81	1.31
	10	0.00	4.70	6.73	2.59
	20	0.10	10.00	6.58	4.17
	50	0.10	23.90	6.33	10.07
	100	0.80	45.30	6.38	18.75
	200	0.10	107.80	6.36	35.60

Note N/A = Not applicable, ND = Not detectable, HS = Humic substances

^aConcentration average of 10 samples

^bMeasured at 20 °C

^cContains 100 mg/L of HS

^dMeasured in the supernatant solution

3.3 Swell Index Tests

Swell index (SI) tests were performed on the Na-B GCL in accordance with the procedure stipulated in the ASTM D5890 using the test solutions. SI tests on B-P GCL were performed analogous to the ASTM D5890 but using the sample as

retrieved from the GCL without subjecting it to any kind of grinding and sieving, because grinding and sieving were found to alter the composition of B–P samples in a different study. All SI tests were performed in triplicates, in a controlled laboratory environment.

3.4 Liquid Limit Tests

Liquid limit (LL) tests were conducted on the GCLs with the permeant solutions following the methods described in ASTM D4318. Four trials were performed for each test solution by repeatedly remixing and adding the test solution to produce successive numbers of blow counts between 15 and 35. Each liquid limit test was repeated twice.

4 Results and Discussions

4.1 Swell Index

Effect of HS in varying concentrations of Na⁺. Results of the SI tests performed using the pure NaCl solutions and the NaCl solutions containing 100 mg/L HS (Na–HS) are shown in Fig. 2a for Na⁺ concentrations ranging from 0 mM (DI water) to 200 mM.

Similar to what Jo et al. [11] observed for Na–B, SI of the Na–B in the NaCl solutions decreased gradually as the concentration of Na⁺ increased. The decrease in SI seen here can be attributed to the movement of interlayer water molecules into

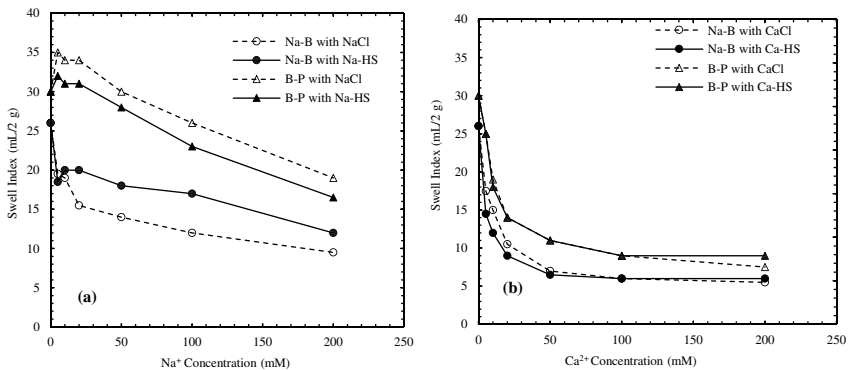


Fig. 2 Swell index (SI) of the Na–B and B–P with: **a** NaCl solutions with and without humic substances (HS), and **b** CaCl₂ solutions with and without HS

the bulk solution to equilibrate the elevated Na^+ concentrations [33, 48]. With the Na–HS solutions, SI of Na–B was almost the same as with the NaCl solutions at low concentrations of Na^+ (<20 mM). However, at Na^+ concentrations ≥ 20 mM, the Na–B swelled relatively greater in the solutions containing HS. This increase in swelling may be as a result of the slight decrease in electrical conductivity of the NaCl solutions when HS was added (see Table 1). Anionic functional groups of the HS attract the positive Na ions, therefore reducing the overall electrical conductivity of the solutions.

A trend opposite to that of Na–B was observed for the B–P GCL. With pure NaCl solution, SI of B–P initially increased to 35 mL/2 g and then did not change much until the Na^+ concentration was 50 mM where SI dropped back to 30 mL/2 g (same as DI water). This increase in swell volume of modified bentonites in low concentration monovalent salt solutions has also been observed in other studies [49, 50]. SI of B–P then decreased almost linearly as the concentrations of Na^+ increased above 50 mM. SI of B–P with the Na–HS solutions evolved in a manner similar to that of the NaCl solutions. However, SI of B–P with the Na–HS solutions was on the average 3 mL/2 g lower than SI in the pure NaCl solutions. The observed decrease in swelling for B–P with the Na–HS solutions may be due to complex bentonite–polymer–HS interactions.

Effect of HS in varying concentrations of Ca^{2+} . SI test result for Na–B and B–P with CaCl_2 and Ca–HS solutions is plotted in Fig. 2b versus 0 mM (DI water)–200 mM Ca^{2+} concentrations.

With the CaCl_2 solutions, SI of Na–B decreased as Ca^{2+} concentration increased, as was observed with the NaCl solutions; however, the drop in SI is more rapidly here. This is consistent with the DDL theory [51–54]. The swell indices of Na–B with >20 mM CaCl_2 solutions were similar to SI usually reported for Ca bentonite (Ca–B) (i.e., SI < 15 mL/2 g) [11, 13, 55, 56]. The result here indicates that full transformation of Na–B into Ca–B occurred when it was hydrated with CaCl_2 having concentrations >20 mM. The drop in SI was even more rapid with the addition of HS, with the transformation of Na–B into Ca–B occurring at 10 mM Ca^{2+} . This could be due to the HS promoting the bringing of individual montmorillonite particles in the presence of the polyvalent Ca^{2+} ions.

Similarly, SI of B–P reduced sharply with increasing CaCl_2 concentration (from 30 mL/2 g with DI water to 7.5 mL/2 g). A similar trend in SI evolution with CaCl_2 concentration has been observed for other modified bentonites [47, 49, 50]. No discernible difference was observed in the swell indices of B–P with the CaCl_2 solutions and the Ca–HS solutions.

4.2 Liquid Limit

Effect of HS in varying concentrations of Na^+ . Figure 3a shows results of the LL test performed on the GCLs using NaCl solutions with and without HS. With the NaCl solutions, LL of Na–B gradually decreased from approximately 415–160 as the

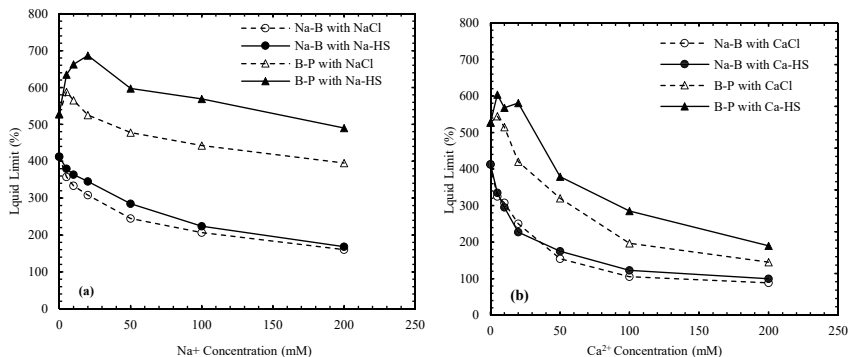


Fig. 3 Liquid limit (LL) of the Na-B and B-P with: **a** NaCl solutions with and without humic substances (HS), and **b** CaCl₂ solutions with and without HS

concentration of Na⁺ increased. LL of Na-B with the Na-HS solutions was comparable to LL with the pure NaCl solutions over the entire range of Na⁺ concentrations used in study.

The evolution of the LL of B-P with the NaCl solutions with and without HS was different. With the pure NaCl solutions, LL of the B-P slightly increased to 588 at 5 mM Na⁺ concentration (from 525 with DI water), and then dropped gradually to 220 with 200 mM NaCl solution. When HS was added to the solution, LL of B-P continued to increase with Na⁺ concentrations at low concentrations (from 5 mM to 20 mM). But at Na⁺ concentrations >20 mM, the LL of B-P began to drop. However, LL with the Na-HS solutions did not drop lower than LL with DI water until the Na⁺ concentration was >100 mM. At 200 mM Na⁺ concentration, the LL of B-P with the Na-HS solution was over 1.25 times higher than with pure NaCl solution. The relatively high LL measured with the Na-HS solutions for B-P can be attributed to the decreased in electrical conductivity observed for the Na-HS solutions as explained before.

Effect of HS in varying concentrations of Ca²⁺. Results of the LL test with the pure CaCl₂ and Ca-HS solutions are shown in Fig. 3b for both GCLs. For the Na-B, the LL obtained with the CaCl₂ and Ca-HS solutions were comparable and decreased as Ca²⁺ concentration increased. The LL results for Na-B with the CaCl₂ solutions are consistent with other LL results reported for Na-B with CaCl₂ solutions [13, 57, 58]. The LL of Na-B with the solutions containing Ca²⁺ concentration >100 mM was similar to LL reported for Ca-B in DI water (<150%) [58].

In the case of the B-P, LL with the CaCl₂ solutions (at 5 and 10 mM) were initially comparable to DI water (525) but dropped rapidly as the Ca²⁺ concentrations increased to 145 (at 200 mM). With the Ca-HS solutions, however, at low concentrations of Ca²⁺ (<20 mM) LL of B-P was greater than with DI water. At higher Ca²⁺ concentrations (>20 mM), however, a rapid decreased in LL was observed. Nevertheless, in the presence of HS, the LL of B-P was consistently higher than in the pure CaCl₂ solutions. This increase in LL may be also attributed to relatively lower

electrical conductivity of the Ca–HS solutions and complex bentonite–polymer–HS interactions.

In general, the evolution of the LL for both Na–B and B–P was different from that of the SI. This may be due to the relatively high ratio of liquid volume to solids volume required for the SI test as compared to the LL test. This suggests relatively high exposure of the solids to the test solutions in the SI tests as compared to the LL test.

5 Summary and Conclusions

The influence of organic matter on the swelling and liquid limit of bentonite extracted from two commercial GCLs, one containing Na–B GCL and the other containing a dry mixture of Na–B and proprietary polymer (B–P), was investigated using Na^+ and Ca^{2+} aqueous salt solutions of varying concentrations (5–200 mM) prepared either with or without 100 mg/L humic substances (HS).

SI of Na–B was higher with the NaCl solutions containing HS than the SI with the pure NaCl solutions at Na^+ concentrations ≥ 20 mM. This suggests that in a sodium-rich leachate the presence of HS may enhance the hydraulic compatibility of the Na–B GCL. Compared to the pure CaCl_2 solutions, swell indices of Na–B were slightly lower with solutions containing HS at Ca^{2+} concentrations ≤ 20 mM. However, the swell indices of Na–B were comparable at Ca^{2+} concentrations ≥ 50 mM. For B–P, SI with the NaCl solutions containing HS was consistently lower than those without HS. However, the presence of HS had no effect on the swelling of B–P in the Ca^{2+} solutions.

Results of the LL tests showed that within the range of concentration of Na^+ and Ca^{2+} solutions used in this study the addition of 100 mg/L HS had no significant influence on the LL of Na–B. However, LL of B–P was significantly higher with the salt solutions (both Na^+ and Ca^{2+}) containing HS than with salt solutions without HS. Based on the results of the SI and LL tests, hydraulic conductivity testing of the GCLs using selected test solutions with and without HS are currently ongoing

References

1. Koerner RM (2012) *Designing with geosynthetics*, vol 1, 5 ed. Pearson Prentice Hall, Upper Saddle River, New Jersey 07458
2. Norrish K (1954) The swelling of montmorillonite. *Discuss Faraday Soc* 18:120–134
3. Grim RE, Guven N (1978) Bentonites: geology, mineralogy, properties, and uses. In: *Developments in sedimentology*, vol 24. Elsevier, Amsterdam, The Netherlands, p 256
4. Shackelford CD et al (2000) Evaluating the hydraulic conductivity of GCLs permeated with non-standard liquids. *Geotext Geomembr* 18(2–4):133–161
5. Petrov RJ, Rowe RK, Quigley RM (1997) Selected factors influencing GCL hydraulic conductivity. *J Geotech Geoenviron Eng* 123(8):683–695

6. Petrov RJ, Rowe RK (1997) Geosynthetic clay liner (GCL)-chemical compatibility by hydraulic conductivity testing and factors impacting its performance. *Can Geotech J* 34(6):863–885
7. Katsumi T et al (2001) Chemical compatibility of modified bentonite permeated with inorganic chemical solutions. In: *Geoenvironmental impact management*, Edinburgh
8. Bradshaw SL, Benson CH (2014) Effect of municipal solid waste leachate on hydraulic conductivity and exchange complex of geosynthetic clay liners. *J Geotech Geoenviron Eng* 140(4)
9. Bradshaw SL, Benson CH, Rauen TL (2016) Hydraulic conductivity of geosynthetic clay liners to recirculated municipal solid waste leachates. *J Geotech Geoenviron Eng* 142(2)
10. Jo HY et al (2005) Long-term hydraulic conductivity of a geosynthetic clay liner permeated with inorganic salt solutions. *J Geotech Geoenviron Eng* 131(4):405–417
11. Jo HY et al (2001) Hydraulic conductivity and swelling of nonprehydrated GCLs permeated with single-species salt solutions. *J Geotech Geoenviron Eng* 127(7):557–567
12. Kolstad DC, Benson CH, Edil TB (2004) Hydraulic conductivity and swell of nonprehydrated geosynthetic clay liners permeated with multispecies inorganic solutions. *J Geotech Geoenviron Eng* 130(12):1236–1249
13. Lee J-M et al (2005) Correlating index properties and hydraulic conductivity of geosynthetic clay liners. *J Geotech Geoenviron Eng* 131(11):1319–1329
14. Jo HY, Benson CH, Edil TB (2004) Hydraulic conductivity and cation exchange in non-prehydrated and prehydrated bentonite permeated with weak inorganic salt solutions. *Clays Clay Miner* 52(6):661–679
15. Onikata M, Kondo M, Kamon M (1996) Development and characterization of a multiswellable bentonite. In: Kamon M (ed) *Environmental geotechnics*, vol 1, pp 587–590
16. Di Emidio G, Van Impe W, Mazzieri F (2010) A polymer enhanced clay for impermeable geosynthetic clay liners. In: *6th International congress on environmental geotechnics (6ICEG)*. Tata McGraw Hill Education
17. Trauger R, Darlington J (2000) Next-generation geosynthetic clay liners for improved durability and performance. In: *Proceedings of the 14th GRI conference*. Geosynthetic Institute
18. Scalia J et al (2011) Geosynthetic clay liners containing bentonite polymer nanocomposite. In: *Geo-Frontiers 2011: advances in geotechnical engineering*, pp 2001–2009
19. Tian K, Benson CH, Likos WJ (2016) Hydraulic conductivity of geosynthetic clay liners to low-level radioactive waste leachate. *J Geotech Geoenviron Eng* 142(8):04016037
20. Salihoglu H et al (2016) Hydraulic conductivity of bentonite-polymer geosynthetic clay liners in coal combustion product leachates. In: *Geo-Chicago 2016*, pp 438–447
21. Tian K, Benson CH (2017) Chemical compatibility of geosynthetic clay liners to aggressive bauxite liquor. In: *Proceedings of 35th international ICSOBA conference 2017*, Hamburg, Germany
22. Tian K, Benson CH, Likos WJ (2017) Effect of an anion ratio on the hydraulic conductivity of a bentonite-polymer geosynthetic clay liner. In: *Geotechnical frontiers 2017*, pp 180–189
23. Christensen TH, Kjeldsen P (1989) Basic biochemical processes in landfills. In: Christensen TH, Cossu R, Stegmann R (eds) *Sanitary landfilling: process, technology, environmental impact*. Academic Press, New York, pp 29–49
24. Kjeldsen P et al (2002) Present and long-term composition of MSW landfill leachate: a review. *Crit Rev Environ Sci Technol* 32(4):297–336
25. Moody CM, Townsend TG (2017) A comparison of landfill leachates based on waste composition. *Waste Manag* 63:267–274
26. Kang KH, Shin HS, Park H (2002) Characterization of humic substances present in landfill leachates with different landfill ages and its implications. *Water Res* 36(16):4023–4032
27. Renou S et al (2008) Landfill leachate treatment: review and opportunity. *J Hazard Mater* 150(3):468–493
28. Liu Z et al (2015) Characterization of dissolved organic matter in landfill leachate during the combined treatment process of air stripping, Fenton SBR and coagulation. *Waste Manag* 41:111–118

29. Harmsen J (1983) Identification of organic-compounds in leachate from a waste tip. *Water Res* 17(6):699–705
30. Artiolafortuny J, Fuller WH (1982) Humic substances in landfill leachates: I. Humic acid extraction and identification. *J Environ Qual* 11(4):663–669
31. Han YS et al (2009) Characterization of humic substances in landfill leachate and impact on the hydraulic conductivity of geosynthetic clay liners. *Waste Manag Res* 27(3):233–41
32. Aiken G et al (1985) An introduction to humic substances in soil, sediment, and water. In: *Humic substances in soil, sediment, and water: geochemistry, isolation, and characterization*. Wiley, New York
33. Sposito G (2008) *The chemistry of soils*, 2nd ed. Oxford University Press, Oxford
34. Theng BKG (2012) *Formation and properties of clay-polymer complexes*, vol 4. Elsevier
35. Stevenson F (1985) Geochemistry of soil humic substances, in *Humic substances in soil, sediment, and water: geochemistry, isolation, and characterization*. Wiley, New York, pp 13–52
36. Baalousha M, Motelica-Heino M, Le Coustumer P (2006) Conformation and size of humic substances: effects of major cation concentration and type, pH, salinity, and residence time. *Colloids Surf Physicochem Eng Aspects* 272(1–2):48–55
37. Kloster N et al (2013) Aggregation kinetics of humic acids in the presence of calcium ions. *Colloids Surf Physicochem Eng Aspects* 427:76–82
38. Chilom G, Bruns AS, Rice JA (2009) Aggregation of humic acid in solution: contributions of different fractions. *Org Geochem* 40(4):455–460
39. Feng XJ, Simpson AJ, Simpson MJ (2005) Chemical and mineralogical controls on humic acid sorption to clay mineral surfaces. *Org Geochem* 36(11):1553–1566
40. Majzik A, Tombacz E (2007) Interaction between humic acid and montmorillonite in the presence of calcium ions I. Interfacial and aqueous phase equilibria: adsorption and complexation. *Organ Geochem* 38(8):1319–1329
41. Shevchenko SM, Bailey GW, Akim LG (1999) The conformational dynamics of humic polyanions in model organic and organo-mineral aggregates. *J Mol Struct-Theochem* 460(1–3):179–190
42. Evans LT, Russell EW (1959) The adsorption of humic and fulvic acids by clays. *J Soil Sci* 10(1):119–132
43. Preston MR, Riley JP (1982) The interactions of humic compounds with electrolytes and three clay minerals under simulated estuarine conditions. *Estuar Coast Shelf Sci* 14:567–576
44. Tombác E et al (1988) Effect of electrolyte concentration on the interaction of humic acid and humate with montmorillonite. *Appl Clay Sci* 3:31–52
45. Arnarson TS, Keil RG (2000) Mechanisms of pore water organic matter adsorption to montmorillonite. Elsevier, Netherlands. p 309
46. Kahle M, Kleber M, Jahn R (2004) Retention of dissolved organic matter by phyllosilicate and soil clay fractions in relation to mineral properties. *Org Geochem* 35(3):269–276
47. Scalia J et al (2014) Long-term hydraulic conductivity of a bentonite-polymer composite permeated with aggressive inorganic solutions. *J Geotech Geoenviron Eng* 140(3)
48. Norrish K, Quirk JP (1954) Crystalline swelling of montmorillonite—use of electrolytes to control swelling. *Nature* 173(4397):255–256
49. Di Emidio G (2010) Hydraulic and chemico-osmotic performance of polymer treated clays. Ghent University
50. Katsumi T et al (2008) Long-term barrier performance of modified bentonite materials against sodium and calcium permeant solutions. *Geotext Geomembr* 26(1):14–30
51. McBride MB (1994) *Environmental chemistry of soils*. Oxford University Press, New York, vii + 406 pp
52. Sposito G (1981) *The thermodynamics of soil solutions*. Oxford University Press, Oxford, 223 pp
53. Mitchell JK (1993) *Fundamentals of soil behavior*, 2 ed. Wiley, New York, xiii + 437 pp
54. Olphen HV (1977) *An introduction to clay colloid chemistry, for clay technologists, geologists, and soil scientists*. Wiley-Interscience, 318 pp
55. Lee JO et al (2012) Swelling pressures of compacted Ca-bentonite. *Eng Geol* 129–130:20–26

56. Egloffstein TA (2001) Natural bentonites—influence of the ion exchange and partial desiccation on permeability and self-healing capacity of bentonites used in GCLs. *Geotext Geomembr* 19(7):427–444
57. Bouazza A, Jefferis S, Vangpaisal T (2007) Investigation of the effects and degree of calcium exchange on the Atterberg limits and swelling of geosynthetic clay liners when subjected to wet–dry cycles. *Geotext Geomembr* 25(3):170–185
58. Gleason MH, Daniel DE, Eykholt GR (1997) Calcium and sodium bentonite for hydraulic containment applications. *J Geotech Geoenviron Eng* 123(5):438–445

Chemical Compatibility of Slurry Trench Cutoff Wall Backfills Comprised of SHMP-Amended Ca-Bentonites in Lead-Contaminated Solutions: Hydraulic Conductivity Assessment



Yu-Ling Yang, Yan-Jun Du, Krishna R. Reddy, and Ri-Dong Fan

Abstract Sodium bentonite is the major type of bentonite used for soil–bentonite slurry trench cutoff wall construction. However, application of low swelling calcium bentonite (Ca-bentonite) is extremely meaningful for countries where high-quality sodium bentonite is scarce, while Ca-bentonite is plentiful. This study presented investigation of hydraulic conductivity of soil–bentonite backfill containing sodium hexametaphosphate (SHMP)-amended Ca-bentonite in lead nitrate solution with Pb concentration of 4.8 mM (1000 mg/L). Duplicate flexible-wall hydraulic conductivity tests were conducted using tap water first and followed by the lead nitrate solution. The volume, pH, and electrical conductivity of the inflow and outflow liquids were monitored, and Pb concentrations in the outflow liquid were measured. The variation in hydraulic conductivity with the pore volume of flow of permeant liquid was assessed. The results show that the hydraulic conductivity maintained a value lower than 10^{-9} m/s in either tap water or Pb solution. The Pb solution had insignificant adverse effects on hydraulic performance of the backfill containing amended bentonite during the tested period.

Keywords Slurry wall · Bentonite · Hydraulic conductivity · Amendment · Contaminated solution

Y.-L. Yang · Y.-J. Du (✉)

Jiangsu Key Laboratory of Urban Underground Engineering & Environmental Safety, Institute of Geotechnical Engineering, Southeast University, Nanjing 211189, China
e-mail: duyanjun@seu.edu.cn

K. R. Reddy

Department of Civil & Materials Engineering, University of Illinois at Chicago, Chicago, IL 60607, USA

R.-D. Fan

School of Materials Science and Engineering, Southeast University, Nanjing 210096, China

© Springer Nature Switzerland AG 2020

K. R. Reddy et al. (eds.), *Sustainable Environmental Geotechnics*, Lecture Notes in Civil Engineering 89, https://doi.org/10.1007/978-3-030-51350-4_37

365

1 Introduction

Soil–bentonite (SB) slurry trench cutoff walls are widely used in the U.S. and Canada as in situ engineering barrier to control migration of the contaminated groundwater [1, 2]. Traditionally, procedures for SB wall construction include excavating a vertical trench with width of approximately 0.6–1.5 m, and pumping bentonite–water slurry into the trench simultaneously; preparing backfill mixture beside the trench; and finally replacing the slurry within the trench by the backfill mixture. The backfill composes of excavated in situ spoils or appropriate imported soils, sodium bentonite (Na-bentonite)–water slurry, and dry Na-bentonite, if needed. Hydraulic conductivity, which is commonly accepted as not higher than 1×10^{-9} m/s, is one of the key mechanisms controlling containment performance of the walls [3].

It should be aware that for countries such as China and India where resource of high-quality Na-bentonite is scarce, commonly available calcium bentonite (Ca-bentonite) is considered to be an alternate material for use. However, Ca-bentonite is known to possess lower swelling capacity than the Na-bentonite, and its direct employment into backfill may cause unacceptable higher hydraulic conductivity. Thus, proper modification is needed for the Ca-bentonite before its use. Sodium hexametaphosphate (SHMP), one of the polyphosphate dispersants, has been manifested to be positive amendment for enhancing workability of Ca-bentonite/water slurry and decreasing hydraulic conductivity of the sand/Ca-bentonite backfills in tap water permeated condition [4–7]. However, hydraulic conductivity of the backfill containing SHMP-amended Ca-bentonite subjected to contaminated solution has not been investigated so far.

Based on the abovementioned considerations, this study describes the results of tests performed to assess the hydraulic conductivity of backfill containing sand and SHMP-amended Ca-bentonite in either tap water or Pb solution with solute concentration of 4.8 mM (1000 mg/L). Duplicate samples were tested using flexible-wall hydraulic conductivity permeameters. The obtained results will yield useful insight into evaluating hydraulic performances of slurry trench cutoff walls containing amended bentonite as interim barrier to contain groundwater plume impacted by Pb. This study belongs to the category of environmental geotechnology.

2 Materials and Methods

2.1 Solid Materials

Clean sand and powered SHMP-amended Ca-bentonite were used to prepare the backfill mixture. The sand, named Three River Sand, was obtained from a quarry in Beloit, Wisconsin, USA. The raw Ca-bentonite, with the brand name of Panther Creek 200, was supplied by the CETCO (Colloid Environmental Technologies Co.,

Hoffman Estates, IL), and the SHMP used was obtained from Humboldt Manufacturing Co., Elgin, IL. The SHMP-amended Ca-bentonite was prepared by blending the raw bentonite into pre-prepared SHMP-distilled water solution with SHMP concentration of 10 g/L. The soil-to-water ratio of the slurry is approximately 1:2 (g/mL), and the resulting optimum SHMP-to-bentonite ratio is 2% (dry weight basis), as per Yang et al. [5, 6]. The slurry is then cured for 24 h, oven-dried, milled, and screened (using 0.075 mm standard sieve), and the resulting SHMP-amended Ca-bentonite was stored in a sealed plastic container for further use.

2.2 Permeated Liquids

Both clean tap water and Pb solution were used as permeated liquid in this study. The Pb solution was prepared by dissolving 1.5 g of lead nitrate into 1 L distilled water to create an expected Pb concentration of 4.8 mM (1000 mg/L). The pH and electrical conductivities of the Pb solution were measured to be 4.86 and 1,130 $\mu\text{S}/\text{cm}$, respectively, and the actual Pb concentration was determined as 873.6 mg/L.

2.3 Backfill Preparation

By using a high-speed blender, the bentonite–water slurry was prepared by mixing the SHMP-amended Ca-bentonite with tap water in a bentonite content of 20% as recommended by Yang et al. [5]. After hydrated for 24 h, the slurry possessed Marsh viscosity and density of 39 s and 1.15 g/cm³, respectively, and the filtrate loss volume and pH of 22.6 mL and 6.8, respectively. A model SB backfill was prepared by mixing clean sand and SHMP-amended Ca-bentonite in sand-to-bentonite ratio of 8:2 (by dry weight). The slurry was then added into the model backfill until a slump height (ASTM C143 [8]) corresponding to 125 mm in a standard slump cone was achieved, as suggested by Evans [9]. During the slump test, appropriate additional amount of sand was added along with the slurry to ensure an optimum-amended Ca-bentonite content of 20% (by dry weight) in the backfill as recommended by Yang et al. [6]. The moisture content of the finally backfill at the target slump was 30.0%.

2.4 Hydraulic Conductivity Tests

Duplicate hydraulic conductivity tests on backfill specimens were conducted in flexible-wall permeameters using tap water as permeant in accordance with the falling headwater-rising tailwater method (method C) in ASTM D5084 [10]. A rigid acrylic cylinder as described in Malusis et al. [11] was used during the specimen preparing, setting up, and consolidating periods.

The specimens were subjected to back-pressure saturation prior to permeation. An average effective stress of 34.5 kPa and a hydraulic gradient less than 30 were used in the permeation process. Tap water was used as the permeated solution first to create a baseline hydraulic conductivity until the following termination criteria were achieved: (1) the ratio of inflow to outflow rate was between 0.75 and 1.25; and (2) the hydraulic conductivity was steady, e.g., four or more consecutive hydraulic conductivity measurements were within 25% of their mean and no distinct upward or downward trend in hydraulic conductivity versus time curve was observed. Then, the test was continued by replacing the tap water with Pb solution as the permeant until the end of the test. The volume, pH, electrical conductivity, and Pb concentration in the outflow liquid were monitored during the tested period.

3 Results and Discussion

Figure 1 presents the measured hydraulic conductivity versus volumetric flow ratio of the duplicate specimens, i.e., specimen-1 and specimen-2. The elapsed time for tap water and Pb solution permeation were 53 days and 39 days in specimen-1, and 59 days and 34 days in specimen-2, respectively. It can be seen from Fig. 1 that the hydraulic conductivity of the specimen permeated with both tap water and Pb solution are lower than the commonly used limited value of 10^{-9} m/s for soil-bentonite slurry wall. The average hydraulic conductivity of the last four consecutive data points in tap water is 1.90×10^{-10} m/s and 3.04×10^{-10} m/s for specimen-1 and specimen-2, respectively. The average hydraulic conductivities of Pb solution permeation scenario are 1.66×10^{-10} m/s and 1.63×10^{-10} m/s for the duplicate specimens, respectively. This indicates that, during the tested period, insignificant variation in hydraulic conductivity of the specimens is resulted from changing the permeant liquid form tap water to Pb solution.

Fig. 1 Hydraulic conductivities of the sand/SHMP-amended Ca-bentonite backfill specimens

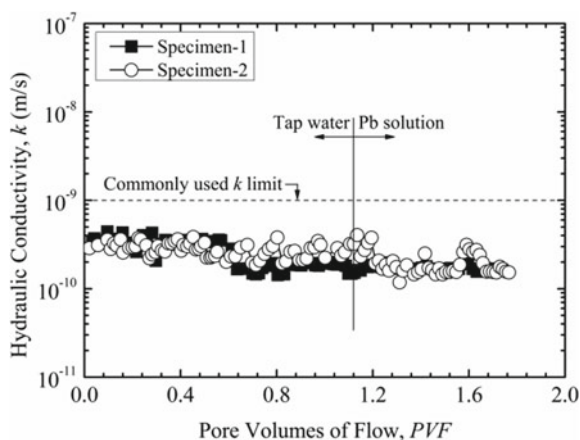


Fig. 2 Volumetric ratio between outflow and inflow during the hydraulic conductivity tests

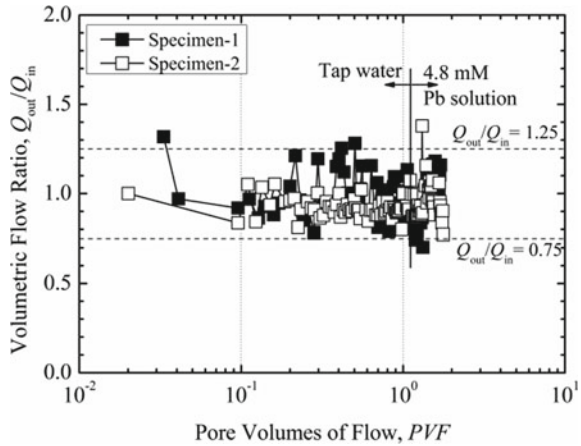


Figure 2 shows the ratio of outflow to inflow (Q_{out}/Q_{in}) of the tested specimens as a function of PVF . It is observed that Q_{out}/Q_{in} values fall on a range of 0.75–1.25, indicating hydraulic equilibrium is achieved during the hydraulic conductivity measured period. Figure 3 illustrates the pH and electrical conductivity (EC) equilibrium status of the specimens as PVF increases. The pH ratio between outflow and inflow liquids (pH_{out}/pH_{in}) is found above the range of 0.9 to 1.1 as regulated in ASTM D7100 to evaluate chemical compatibility of soils. Similar finding is observed in the ratio of electrical conductivity in outflow to that in inflow (EC_{out}/EC_{in}) and ratio of Pb concentration in outflow and inflow (which is not shown in this study).

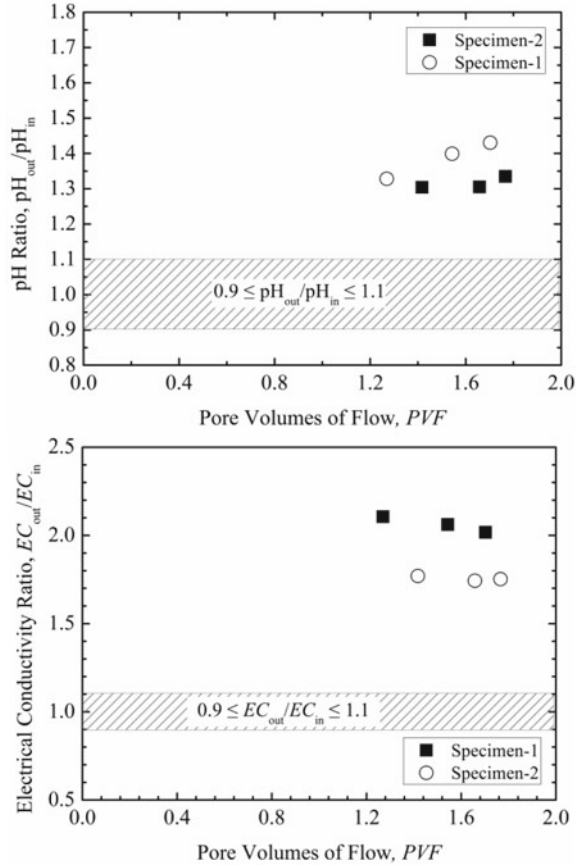
Thus, results obtained from this study represent only short-term hydraulic performance of the tested specimens. Longer testing period is needed to evaluate long-term compatibility behavior of the backfill permeated with Pb solution.

4 Conclusions

This study evaluated the hydraulic conductivity of soil–bentonite backfill composed of sand and sodium hexametaphosphate (SHMP)-amended Ca-bentonite in sand-to-bentonite ratio of 8:2. Duplicate flexible-wall hydraulic conductivity tests were conducted using tap water and 4.8 mM Pb solution as permeant liquid.

The duplicate specimens exhibit similar hydraulic conductivities in this study. As the tested liquid changed from tap water to Pb solution, hydraulic conductivity of the specimen-1 varies from 1.90×10^{-10} m/s to 1.66×10^{-10} m/s, while that of the specimen-2 changes from 3.04×10^{-10} m/s to 1.63×10^{-10} m/s. Insignificant variation in hydraulic conductivity of the specimens is resulted from Pb solution.

Fig. 3 pH and electrical conductivity equilibrium statuses of outflow and inflow during the hydraulic conductivity tests



However, pH and electrical conductivity status in the outflow and inflow implies that the chemical equilibrium was not achieved at the end of experiments. Extend testing period is needed to evaluate long-term containment performance of the backfill containing SHMP-amended Ca-bentonite to the Pb solution.

Acknowledgments Financial support for this project is provided by National Key Research and Development Programme (Grant Nos. 2018YFC1803100, 2018YFC1802300 and 2019YFC1806000), Primary Research & Development Plan of Jiangsu Province (Grant No. BE2017715), and National Natural Science Foundation of China (Grant Nos. 41877248 and 41907248). The authors thank CETCO for providing the bentonites used in this study. The first author acknowledges the China Scholarship Council, which made it possible to undertake this research at the University of Illinois at Chicago.

References

1. D'Appolonia DJ (1980) Soil-bentonite slurry trench cutoffs. *J Geotech Eng Div* 106(4):399–417
2. Sharma HD, Reddy KR (2004) *Geoenvironmental engineering: Site remediation, waste containment, and emerging waste management technologies*. Wiley, Hoboken
3. Evans JC (1994) Hydraulic conductivity of vertical cutoff walls. In: *Hydraulic conductivity and waste contaminant transport in soil*. In: Daniel DE, Trautwein SJ (eds) ASTM STP 1142. ASTM, West Conshohocken, PA, pp 79–93
4. Du YJ, Yang YL, Fan RD, Wang F (2016) Effects of phosphate dispersants on the liquid limit, sediment volume and apparent viscosity of clayey soil/calcium-bentonite slurry wall backfills. *KSCE J Civ Eng* 20(2):670–678
5. Yang YL, Du YJ, Reddy KR, Fan RD (2017) Phosphate-amended sand/Ca-bentonite mixtures as slurry trench wall backfills: assessment of workability, compressibility and hydraulic conductivity. *Appl Clay Sci* 142:120–127
6. Yang YL, Reddy K, Du YJ, Fan RD (2018) Short-term hydraulic conductivity and consolidation properties of soil-bentonite backfills exposed to CCR-impacted groundwater. *J Geotech Geoenviron Eng* 144(6):04018025
7. Zhang T, Yang YL, Liu SY (2020) Application of biomass by-product lignin stabilized soils as sustainable Geomaterials: A review. *Sci Total Environ*:138830
8. ASTM (2012) Standard test methods for slump of hydraulic-cement concrete I. C143/C143M, West Conshohocken, PA
9. Evans JC (1993) Vertical cutoff walls. In: DE Daniel (ed) *Geotechnical practice for waste disposal*. Chapman & Hall, London, pp 430–454
10. ASTM (2010) Standard test methods for measurement of hydraulic conductivity of saturated porous materials using a flexible wall permeameter. D5084, West Conshohocken, PA
11. Malusis MA, Barben EJ, Evans JC (2009) Hydraulic conductivity and compressibility of soil-bentonite backfill amended with activated carbon. *J Geotech Geoenviron Eng* 135(5):664–672

Mechanical, Hydraulic, and Chemical Behavior of Steel Slag-Amended Loessical Silt–Bentonite Liners



Franco M. Francisca, Clara A. Mozejko, and Daniel A. Glatstein

Abstract Liners are engineered layers of low hydraulic conductivity designed to isolate solid, semisolid, or liquid wastes from the environment. Most common materials for liners construction are natural soils amended with bentonite to achieve the low hydraulic conductivity specified by current regulations. This work evaluates the potential reuse of steel slag to improve the performance of landfill liners. We evaluate the effect of adding slag to soil on its mechanical and reactive properties when compacted. Used soil is a loessical silt from the center of Argentina which is frequently used for the construction of bottom liners. The effect of slag content and curing time on the unconfined compression strength of slag–silt mixtures is assessed. Obtained values are incorporated in contaminant transport models to evaluate the transport of metal ions present in leachate through landfill barriers. Results show that the retention of metal ions within a compacted barrier amended with steel slag is mainly associated with the increase of the pH of the barrier material.

Keywords Coupled phenomena · Reactive barrier · BOF slag

1 Introduction

During the steel production, raw iron, coke, and limestone are combined, and impurities from steel are separated. These impurities are called “Steel Slag” (SS) which presents vitreous characteristics and potentially cementitious properties. This solid waste generated during the steel production can be classified according to the type of steel, such as carbon steel slag or stainless steel slag, or according to the manufacturing process as basic oxygen furnace (BOF) slag, electric arc, refining and blast furnace, or foundry residue.

F. M. Francisca (✉) · C. A. Mozejko · D. A. Glatstein
Universidad Nacional de Córdoba, X5016CGA Córdoba, Argentina
e-mail: franco.francisca@unc.edu.ar

Instituto de Estudios Avanzados en Ingeniería y Tecnología (IDIT, CONICET-UNC), X5016CGA Córdoba, Argentina

Nowadays, there exists a growing interest in environmental topics and new approaches are being sought in order to minimize the production of industrial waste. Likewise, there exists a tendency to achieve reutilization of wastes within various production processes [1]. The main steel producer in Argentina is “Ternium-Siderar”, which produces 230,000 tons of hot laminate steel per month, generating 45,000 tons of BOF slag which is not reused within the production process and is partially sold to the cement industry.

The reuse of the remaining fraction of BOF slag is a challenging issue. In the last few years, research on possible re-uses of SS has been addressed, and several industries identified it as a replacement for raw materials [2]. Many applications that have been found are due to the fact that SS is compatible with multiple applications by their chemical composition and their low risk of environmental contamination. Some examples include the replacement of fine aggregates in concrete production [3–5], as fine aggregate in asphalt or pavements [6–9], as additive in Portland cement production [10, 11], or as raw material in other processes [12–14]. Currently, knowledge about behavior of SS as stabilizing agent in soils is recent and stimulating [15–19]. Other authors began to develop different approaches in which SS is used as component of permeable reactive barriers, as materials for landfill closures or as reactive material itself, for remediation in metal-contaminated sites [20, 21].

Pozzolanic reactions take place when the material contains fine particles, siliceous compounds, water, and a high pH environment [22, 23]. This phenomenon may develop when loessical soils are mixed with BOF slag at proper environmental conditions [24]. Needed conditions include the presence of amorphous silica and clay particles (siliceous compounds of soil fraction) and iron and calcium oxides (activators provided by the slag).

The objective of this research is to study the behavior of BOF slag analyzing its quality as stabilizer of compacted loessical soil liners. The main motivation is determining the effect of time on the shear strength of the compacted loessical silt mixed with the BOF slag. Finally, we also evaluate the expected behavior of this reactive material to improve the retention of heavy metals when used as bottom liner in landfills.

2 Materials and Methods

2.1 Used Materials

BOF slag used in this study is generated by the “Ternium–Siderar” group in Argentina. Main constituents of the BOF slag are silica, alumina, and magnesia in about 95% of its composition, and minor components include manganese, iron, sulfur compounds, and free lime. Due to its appearance, BOF slag can be classified as poorly graduated sand with low content of a fine fraction [SP]. Particle shape is subangular to subrounded.

Table 1 Main physical properties of tested materials

Property	Loessical silt	Steel slag
Specific gravity	2.64	3.16
Particles < 0.075 mm (%)	57.04	4.39
Particles < 0.002 mm (%)	42.96	2.88
Liquid limit LL (%)	24.70	–
Plastic limit LP (%)	19.02	–
Coefficient of uniformity Cu	4.88	6.84
Coefficient of curvature Cc	0.42	0.22

The silt used is a loessical sediment from Córdoba, Argentina. This sediment was collected from an open pit at the campus of Universidad Nacional de Córdoba. This geomaterial covers over 600,000 km² in the North and center of Argentina and is frequently mixed with bentonite and used for the construction of landfill liners.

The main physical properties of the BOF slag and loessical silt are summarized in Table 1.

2.2 Test Procedures

Unconfined compressive strength (UCS) tests were conducted on BOF slag-amended soil samples by following ASTM D2166 standard. After drying materials, specimens with 0 and 20% slag were compacted in a cell 50 mm in diameter and 100 mm in height using standard Proctor energy (ASTM D 4254-00). Four samples were prepared and stored in the humid chamber for different curing periods. At 0, 7, 28, and 56 days, the samples were tested to determine the unconfined compression strength UCS.

Following the UCS tests, the pH and electrical conductivity of the samples were measured. Luxan's method [25] was followed for electrical conductivity measurements. This method measures the changes in electrical conductivity that occurs after the addition of 5 g of solid material (soil, slag, or mixture of both materials) in 200 mL of a calcium hydroxide saturated solution. This is an indirect method to categorize materials based on their pozzolanic activity by means of a pozzolanicity index (PzI). The PzI is defined as the difference between the initial electrical conductivity of the solution when the solid material is added to the liquid and the electrical conductivity 2 min after. If PzI < 0.4 mS/cm the material is classified as non-pozzolanic, PzI between 0.4 and 1.2 mS/cm corresponds to intermediate pozzolanicity and PzI > 1.2 mS/cm are expected for high pozzolanicity materials [25].

In addition, pH was measured in a suspension of distilled water with 5 g of slag under stirring at 40 °C at 1-min intervals for 15 min in order to verify the existence of appropriate basic conditions to favor pozzolanic reactions.

2.3 Numerical Modeling

The current work considers percolation through a compacted clay liner (CCL), and also through a composite barrier made of a CCL and a geomembrane (CCL + GM). A 1D advection–dispersion equation (ADE) with retardation was solved by means of finite differences [26]:

$$\frac{\delta C}{\delta t} = \frac{D_L}{R} \frac{\delta^2 C}{\delta x^2} - \frac{v}{R} \frac{\delta C}{\delta x} \quad (1)$$

where v = average seepage velocity, C = contaminant concentration, D_L = longitudinal hydrodynamic dispersion coefficient, and R = retardation factor. The average seepage velocity can be obtained from the Darcy's law and soil porosity (n) as follows:

$$v = \frac{1}{n} ki \quad (2)$$

where k = hydraulic conductivity (adopted as 10^{-9} m/s as the required value in most common regulations for landfill liners), i = hydraulic gradient, and n = effective porosity. For CCL + GM barrier, the permeation is conducted through holes (defects) on the barrier, and therefore flux was computed as [27]:

$$v = \frac{Q_h}{A_w * n_d} \quad (3)$$

where A_w = wet area under each imperfection, n_d = defects number on the geomembrane (adopted as 6.54 m²/ha [28]), and Q_h = volumetric flow that is computed as follows [27]:

$$Q_h = n_d C_{q10} \left[1 + 0.1 \left(\frac{H_w}{t_s} \right)^{0.95} \right] a^{0.1} H_w^{0.9} H_b^{0.74} \quad (4)$$

where C_{q10} = contact quality factor between the CCL and GM, H_w = leachate height, H_b = CCL thickness, and a = defect area. Typically, n_d is considered as 5 defects/ha, and a equal to 290 mm² [27, 29, 30].

The peculiarity of this work lies on the metal removal mechanisms that are characteristic of the SS and on the reactive barrier configuration. Analyzed remediation mechanisms include precipitation and sorption, both highly dependent on pH. In particular, the alkalinity of its chemical components confers the slag a high acid neutralization capacity (ANC), which increases the solution pH and promotes the precipitation of metal ions.

Numerical tests were carried out to determine the influence of the barrier thickness and height of leachate accumulated above the liner for Compacted Clay Liner (CCL)

and Composite CCL with Geomembrane (CCL + GM). The barrier thickness (H_b) was adopted as 0.6 and 1.0 m as in most international standards. The leachate height above the liner (H_w) was 0.3 m (as current regulations) and 0.6 m assuming a poor leachate management system.

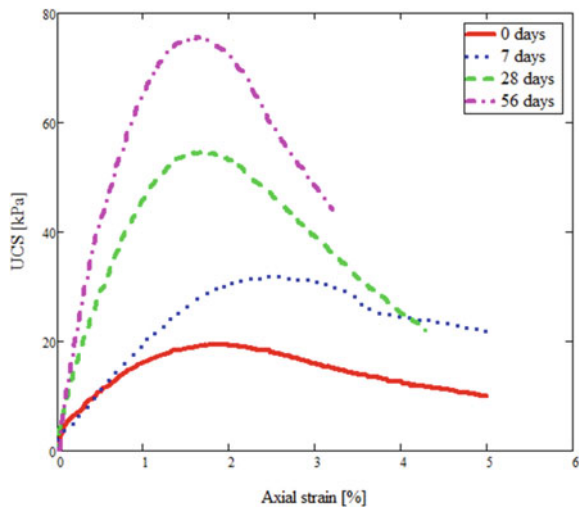
Permeation for each condition was analyzed to determine the time required for the center of mass of the metal to break through the barrier that occurs when $C/C_0 = 0.5$. Retention of metal cations within the barrier either by sorption or precipitation emerges as retardation in their transport. This is considered in this work by incorporating a retardation factor in the ADE (Eq. 1). When analyzing sorption, bentonite retardation factor was considered as $R = 10$, and as incorporating this mineral in 10% of the barrier mass to reduce its hydraulic conductivity, the “mix” retardation factor becomes $R = 1.1$. In the case of precipitation, the acid neutralization capacity (ANC) of the slag was considered as 100, which is analogous to retardation for the removal mechanism considered here. As 20% of the slag is used in the barrier, the mix factor is $R = 20$.

3 Obtained Results

3.1 Mechanical Properties of Soil–Slag Mixtures

Figure 1 shows the UCS of the silt–slag mixture after different curing periods. The UCS raises from 19 kPa for the sample tested immediately after compaction to 76 kPa at 56 days of curing period. Because both moisture and weight of the specimens had

Fig. 1 Influence of curing time on the UCS of compacted slag–silt mixtures



negligible variations during curing, the observed increases in UCS are attributed to the cementation promoted by pozzolanic reactions.

The observed increases in soil stiffness can also be attributed to the natural cementation that occurs due to the interaction between BOF slag and the vitreous fraction of loessical soil through pozzolanic reactions.

For each curing period, the pH and electrical conductivity of the soil–slag mixture were measured as described above. The initial pH of distilled water was 7 and grew up to 12.2 after the addition of BOD slag particles. Then, steel slag develops an environment that favors pozzolanic reactions within the specimens.

After the UCS tests, the electrical conductivity of the silt–slag mixtures was measured over time. All samples showed a significant decrease in electrical conductivity within the first 2 min. The silt–slag mixture showed a $PzI = 1.23$ the day the mixture is prepared indicating a very good level of pozzolanic activity [25]. Then, it decreases to 0.92 for 56 days of curing time (medium values are expected for 7 and 28 days of curing time). The decrease of PzI with the curing time indicates a lower reaction capacity due to the partial development of pozzolanic chemical reactions over time.

3.2 Retention of Metals Within Environmental Barriers

During permeation of leachate through landfill liners, different chemical reactions may affect the displacement of metals when the barrier contains reactive materials. Common chemical reactions that may develop include adsorption and precipitation. If that happens, the displacement of some chemical compounds is delayed. This effect was evaluated by means of numerical models by solving the ADE with retardation for the displacement of metals through CCL and CCL + GM.

Figure 2 shows the influence of the permeation time on the pH of the liquid inside the pores and relative concentration (C/C_0) of metals in solution. The pH starts to slowly decrease from the initial value ($pH = 12.2$) due to the reaction between the barrier material and leachate with a lower pH. This decrease in pH is almost negligible at short times and starts to become significant when the acid neutralization capacity of the soil–slag mixtures is reached. At this point, a sudden reduction in the pH is observed reaching values that lower the solubilization pH for most of the metals. At this point, all precipitated ions dissolve and flow through the barrier that releases a contaminant peak. After these peaks pass through the barrier, a steady state condition is expected when a lower equilibrium pH is reached.

Figure 2 also shows that as the hydraulic head (H_w) decreases the contact time between the fluid and the reactive material increases extending the percolation time. This trend highlights the importance of keeping a low level of leachate above bottom liners in landfills. At the same time, that promotes a higher pH for a longer period, which turns into a greater metal accumulation due to the larger volume of leachate permeated (Fig. 1). For this reason, once the pH reaches the solubilization value, the contaminant peak released at the end of the barrier becomes higher.

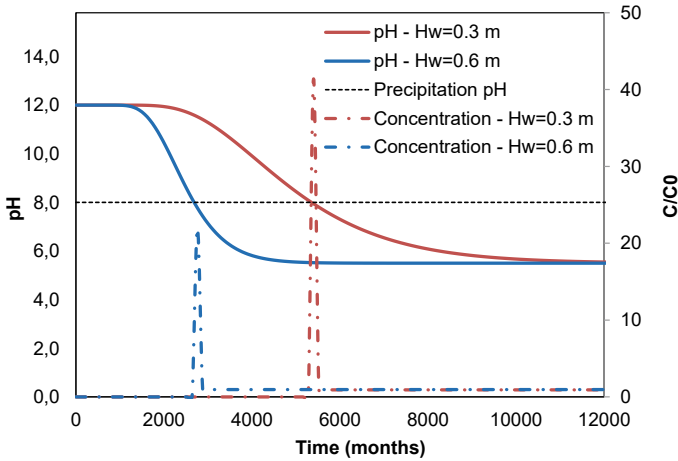


Fig. 2 Influence of time on pH and relative concentration of metal ions

Table 2 Percolation time of metals for landfill liners permeated with leachate

Barrier properties			Percolation time (months)	
Barrier	k (m/s)	Hb (m)	Advection + Dispersion + Sorption ($R = 1.1$)	Advection + Dispersion + Precipitation ($R = 20$)
CCL	10^{-9}	0.6	60	1266
		1.0	120	2464
CCL + GM	10^{-9}	0.6	167	3845
		1.0	316	6973

Table 2 shows the “safety time” or time required for the metal ions to percolate through the barrier for CCL and CCL + GM. According to these results and considering the retention of heavy metals, amending a liner with slag may allow reducing the barrier height and having safer barriers against possible undesirable scenarios as increases in leachate head, or increases in hydraulic conductivity (e.g., due to poor compaction conditions). It is important to emphasize that the effect of adding the slag on the percolation time of metal ions was one order of magnitude more significant than the effect of adding a geomembrane. Also, largest percolation times are also expected for the case of composite liners (CCL + GM) when precipitation is favored by adding BOF slag to the barrier. Obtained results may help in designing safer environmental barriers to isolate/sequestrate metal ions.

4 Conclusions

This work evaluates the advantages of using BOF slag for soil stabilization and to prevent metal ions displacement when used as construction material for landfill liners.

The pH of water or leachate increases when in contact with BOF slags. The high resulting pH and acid neutralization capacity of BOF slag significantly affect the mechanical and chemical behaviors of landfill liners. The high pH promotes chemical reactions with amorphous silica and clay fraction of loessical silt favoring environmental conditions to develop pozzolanic reactions. Under this condition, iron and calcium oxides present in the slag react with the amorphous silica and clay particles of the loessical silt. The pozzolanic activity of this material could be demonstrated by means of the PzI and macroscopically emerges as higher expected UCS for the soil–slag mixture over time.

The increase of pH also promotes precipitation of metal ions within soil pores. Precipitation of most heavy metals during mass transport produces retardation in their displacement. The ADE with retardation was solved to evaluate the transport of ions in two simulated landfill liners (a CCL and a CCL + GM). The increase of pH due to the presence of slag within the barrier promotes ion precipitation. However, the pH starts to decrease during permeation due to the lower pH of leachate. Once the ANC is reached, the pH suddenly decreases to values lower than the pH of solubilization and a high concentration contaminant pulse is released.

Percolation time for metal ions significantly increases when BOF slag is added to the CCL and CCL + GM barriers. This can be used for the design of safer barriers due to the higher expected permeation time needed for the contaminant to pass through the barrier.

Acknowledgments This work was supported by CONICET, ANPCyT (PICT-2014-3101), and SECyT-UNC.

References

1. van Oss, Hendrik G (2003) Slag-iron and steel. US geological survey minerals yearbook 1
2. Akinmusuru JO (1991) Potential beneficial uses of steel slag wastes for civil engineering purposes. *Resour Conserv Recycl* 5(1):73–80
3. Maslehuddin M, Sharif A, Shameem M, Ibrahim M, Barry MS (2003) Comparison of properties of steel slag and crushed limestone aggregate concretes. *Constr Build Mater* 17(2):105–115
4. Anastasiou E, Georgiadis FK, Stefanidou M (2014) Utilization of fine recycled aggregates in concrete with fly ash and steel slag. *Constr Build Mater* 50:154–161
5. Ding, Y-C, Cheng TW, Liu PC, Lee WH (2017) Study on the treatment of BOF slag to replace fine aggregate in concrete. *Constr Build Mater* 46:644–651
6. Xue Y, Wu S, Hou H, Zha J (2006) Experimental investigation of basic oxygen furnace slag used as aggregate in asphalt mixture. *J Hazard Mater* 138(2):261–268
7. Ferreira VJ, Sáez De Guinoa Vilaplana A, García Armingol T, Aranda Uson A, Lausín González C, López Sabirón AM, Ferreira G (2016) Evaluation of the steel slag incorporation

- as coarse aggregate for road construction: technical requirements and environmental impact assessment. *J Clean Prod* 130: 175–186
8. Chen, J-S, Wei S-H (2016) Engineering properties and performance of asphalt mixtures incorporating steel slag. *Constr Build Mater* 128:148–153
 9. Kambole C, Paige-Green P, Kupolati WK, Ndambuki JM, Adeboje AO (2017) Basic oxygen furnace slag for road pavements: A review of material characteristics and performance for effective utilisation in- southern Africa. *Constr Build Mater* 148:618–631
 10. Reddy SA, Pradhan RK, Chandra S (2006) Utilization of basic oxygen furnace (BOF) slag in the production of a hydraulic cement binder. *Int. J. Miner Process* 79:98–105
 11. Carvalho SZ, Vernilli F, Almeida B, Demarco M, Silva SN (2017) The recycling effect of BOF slag in the Portland cement properties. *Resour Conserv Recycl* 127:216–220
 12. Tsakiridis PE, Papadimitriou GD, Tsvilis S, Koroneos C (2008) Utilization of steel slag for portland cement clinker production. *J Hazard Mater* 152:805–811
 13. Ozturk BZ, Gultekin EE (2015) Preparation of ceramic wall tiling derived from blast furnace slag. *Ceram Int* 41:12020–12026
 14. Ding L, Ning W, Wang Q, Shi D, Luo L (2015) Preparation and characterization of glass-ceramic foams from blast furnace slag and waste glass. *Mater Lett* 141:327–329
 15. Manso JM, Ortega-López V, Polanco JA, Setién J (2013) The use of ladle furnace slag in soil stabilization. *Constr Build Mater* 40:126–134
 16. Sharma KA, Sivapullaiah PV (2016) Ground granulated blast furnace slag amended fly ash as an expensive soil stabilizer. *Soils Found* 56(2):205–212
 17. Yildirim IZ, Prezzi M (2015) Geotechnical properties of fresh and aged basic oxygen furnace steel slag. *J Mater Civ Eng* 27(12)
 18. Shalabi FI, Asi IM, Qasraei HY (2017) Effect of by-product steel slag on the engineering properties of clays soils. *J King Saud Univ-Eng Sci* 29:394–399
 19. Yi Y, Gu L, Liu S, Jin F (2016) Magnesia reactivity on activating efficacy for ground granulated blast furnace slag for soft clay stabilization. *Appl Clay Sci* 126:57–62
 20. Park SJ, Kang K, Lee CG, Choi JW (2018) Remediation of metal contaminated marine sediments using active capping with limestone, steel slag, and activated carbon: a laboratory experiment. *Environ Technol* 1–13
 21. Abichou T, Benson CH, Edil TB (2002) Foundry green sands as hydraulic barriers: field study. *J Geotech Geoenviron Eng* 128(3):206–215
 22. Adami A, Rinaldi VA (2017) The influence of amorphous silica on the aging of remolded loessial soil. *Soils Found* 57:315–326
 23. Muhmood L, Vitta S, Venkateswaran D (2009) Cementitious and pozzolanic behavior of electric arc furnace steel slags. *Cem Concr Res* 39:102–109
 24. Mozejko C, Francisca FM Caracterización mecánica de los suelos loéssicos de Córdoba estabilizados con escorias siderúrgicas. In: 24th “Congreso Argentino de Mecánica de Suelos e Ingeniería Geotécnica” Salta, Argentina (2018)
 25. Luxan MP, Madruga F, Saavedra F (1989) *Cem Concr Res* 19:63–68
 26. Fetter CW Contaminant hydrogeology, vol 458, 2a edn. Prentice Hall, Upper Saddle River (1999)
 27. Giroud JP (1997) Equation for calculating the rate of liquid migration through composite liners due to geomembrane defects. *Geosynth Int* 4(3–4):335–348
 28. Glatstein DA, Montoro MA, Carro Pérez ME, Francisca FM (2017) Hydraulic, chemical and biological coupling on heavy metals transport through landfills liners. *J Solid Waste Technol Manag* 43(3):261–269(9)
 29. Giroud JP, Bonaparte R (1989) Leakage through liners constructed with geomembranes. Part I. Geomembrane liners. *Geotext Geomembr* 8(2): 27–67
 30. Touze-Foltz N, Barroso M (2006) Empirical equations for calculating the rate of liquid flow through GCL-geomembrane composite liners. *Geosynth Int* 13(2):73–82

Finite Element Analysis and Simulation Test Research of Deformation of Anti-Seepage Wall in Landfill



Guozhong Dai, Jia Zhu, Guicai Shi, and Shujin Li

Abstract As the most effective way for municipal solid waste disposal in the world, the anti-seepage treatment of sanitary landfill is one of the important factors to be considered in landfill site selection and construction. In the case of no natural water barrier at the bottom of landfill, the landfill site needs to be taken anti-seepage treatment to prevent landfill leachate from contaminating the surrounding soil and groundwater. At present, the vertical anti-seepage wall constructed with bentonite as the main material is the most common method of the landfill seepage control system. The working environment of anti-seepage wall in landfill site is very complicated. The anti-seepage wall not only bears the gravity produced by landfill and the earth's pressure caused by surrounding soil, but also interacts with the outer covering soil. Therefore, the research on the deformation and stress distribution of the anti-seepage wall in practical applications is of great significance for the design and construction of landfills.

Keywords Anti-seepage wall · Finite element analysis · Simulation experiment

1 Introduction

At present, the treatment of domestic garbage is mainly carried out by landfill [1]. In the process of accumulating domestic garbage, a large amount of highly polluted leachate is produced [2, 3]. Groundwater pollution incidents in a large number of landfills indicate that leachate is the most important source of pollution for groundwater [4, 5]. Therefore, the construction of a safe and reliable anti-seepage system is very important for landfills. The seepage control system of landfill generally includes the ground bottom anti-seepage lining system and vertical anti-seepage system [6]. Compared with the horizontal anti-seepage system is not repairable, occupies a large space and high cost, vertical anti-seepage wall has a broad application prospect with low cost, less investment, and easy to repair. The setting of vertical anti-seepage wall

G. Dai (✉) · J. Zhu · G. Shi · S. Li
School of Civil Engineering & Architecture, Changzhou Institute of Technology, Changzhou,
People's Republic of China
e-mail: daigz@czu.cn

around the landfill can effectively prevent the migration of landfill leachate to the surrounding soil and water [7, 8].

The vertical anti-seepage wall of the landfill does not need to bear a large vertical load, but it will have a large horizontal displacement. Therefore, the vertical anti-seepage wall needs to have a similar deformation modulus to the surrounding soil [9]. This requires that the vertical anti-seepage wall of the landfill site has strong strain coordination ability with the surrounding soil. However, the elastic modulus of the commonly used concrete anti-seepage wall is $(2-3) \times 10^4$ MPa. When the foundation is subjected to compressive deformation caused by the upper load, the top of the concrete anti-seepage wall will bear much more load than the upper soil column. At the same time, the two sides of the wall will also bear a lot of friction, which will cause the stress of the wall to crack over the strength of the concrete design in engineering application, and even damage the wall. In comparison, plastic concrete is a flexible material prepared by replacing most of the cement in ordinary concrete with blending materials such as bentonite and clay. It has the characteristics of low elastic modulus, large ultimate deformation, and small elastic ratio. It can significantly reduce the stress concentration or tensile stress at the joint of the wall bottom and prevent cracks from developing, so it can effectively prevent the migration of pollutants in the soil [10].

The development of cement–bentonite anti-seepage slurry has been relatively mature [11]. The difference in the ratio of cement and bentonite will lead to the difference of anti-seepage effect of cement–bentonite slurry. In the experiment, the cement–bentonite slurry with different ratios is prepared. The permeability coefficient of water as a permeate is 10^{-6} – 10^{-7} cm/s. On the basis of previous formulation development, a new type of anti-seepage grout material was prepared by using polyvinyl alcohol modified bentonite. In order to study the law of displacement and deformation in the actual use process, a solid model of anti-seepage wall of landfill was established based on the soil conditions of the actual landfill. The model data and finite element analysis data were compared to verify the applicability of the new polyvinyl alcohol modified anti-seepage material.

2 Slurry Formulation and Performance

In the previous study, sodium bentonite, cement, and fly ash were used as the main materials, and polypropylene fibers were added at the same time. Study on the permeability and adsorption properties of the slurry. This kind of slurry meets the retardation of pollutants in the garbage dump to a certain extent. The sodium-based bentonite in the slurry has better adsorption and removal effects on the cationic surfactant, but the adsorption removal effect on the anionic surfactant and the non-ionic surfactant is not satisfactory [12]. Moreover, because the surface of natural bentonite particles is hydrophilic and the amount of hydrophobic organic matter adsorbed is not high, the modification of sodium-based bentonite is considered. Polyvinyl alcohol is used as a modifier to modify bentonite, and ordinary Portland cement, ordinary

secondary fly ash, sodium carbonate, and polycarboxylic acid water-reducing agent are added in a certain proportion. The slurry formula is optimized by orthogonal experimental method. The slurry formulation is 20% cement, 22% bentonite, 0.2% polyvinyl alcohol, 0.03% water reducer, 18% fly ash, and 0.5% sodium carbonate.

The related properties of slurry were tested by experiments. The permeability coefficient of the slurry is 1.86×10^{-8} cm/s. The blocking rate of COD_{Cr}, BOD₅, NH₄-N, TP, and SS was more than 85%, and the blocking rate of heavy metal ions (such as Hg and Pb) was more than 99%. The unconfined compressive strength is 1.5 MPa, and the axial ultimate strain is 6.42%.

The reason why polyvinyl alcohol is used as modifier is that the surface of bentonite particles is dense and high viscosity film after modification by polyvinyl alcohol. Due to the dispersion and suspension of bentonite, the particles are evenly distributed, the cohesion between them is greater, the structure compactness is improved, and the adsorption retardation is enhanced [13]. At the same time, the particles in the slurry are wrapped by polyvinyl alcohol to form fine superabsorbent particles on the surface to improve their impermeability. Polyvinyl alcohol can promote the progress of cement hydration reaction [14]. The organic polymer polyvinyl alcohol contains a large amount of alcohol hydroxyl reactive groups, which can interact with cement hydration products and change the formation site and morphology of hydration products. The filling effect of the product can make the sample more compact.

3 Solid Model and Finite Element Model

3.1 Solid Model

The model side plate is made of 3 mm steel plate. Due to the influence of the nature of the foundation, the bottom is made of 10-mm-thick steel plate to simulate the rigid foundation. The net space is 360 cm long, 320 cm wide, and 200 cm high. The model is made in blocks and unified in assembly. The parts are connected by bolts. The anti-seepage wall is grouted by layers. After each layer is poured, the surface is roughened, and then the next layer is poured. Finally, the anti-seepage wall is regularly watered and maintained after the grouting of all the slurries. After the completion of the maintenance, the surrounding soil is piled up. The anti-seepage wall is 25 cm wide and 200 cm high, and the thickness of surrounding soil is 150 cm. Clay and sandy soil are used in the landfill. In order to prevent the model board from uplifting outward due to soil filling, wooden strips are used around the model. The model completion diagram is shown in Fig. 1.

Fig. 1 Model completion diagram



3.2 Finite Element Model

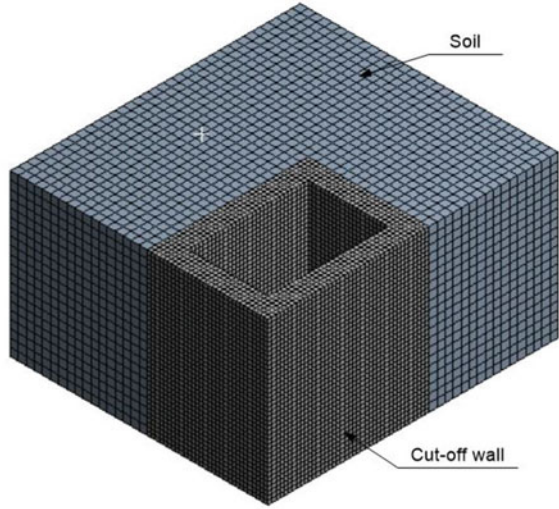
Considering that the unconfined compressive strength of the slurry consolidation used in the anti-seepage wall of the landfill is in the range of 0.5–0.5 MPa in 28 days, which is far greater than its tensile strength and expands when it is sheared, the Drucker–Prager (DP) plastic model is suitable for numerical analysis of stress and deformation of the anti-seepage wall and surrounding soil. Drucker–Prager (DP) plastic model takes into account the volume expansion due to yield but does not consider the effect of temperature change. It is suitable for granular (friction) materials, such as concrete, rock, and soil [15]. The yield criterion for Drucker–Prager materials is

$$F = 3\beta\sigma_m + \left[\frac{1}{2}\{s\}[M]\{s\} \right]^{\frac{1}{2}} - \sigma_y$$

where σ_m is the hydrostatic pressure, β is the material constant, s is the bias stress, M is the material constant matrix, σ_y is the yield strength, and $\{s\}^T$ is the transposed matrix of $\{s\}$.

The finite element meshing of the indoor model is shown in Fig. 2. Quadrilateral element is used for all materials, and mesh refinement is carried out for the anti-seepage wall. The boundary conditions are as follows: the vertical computational boundary around is horizontal constraint, the bottom is fixed constraint, and the other boundary conditions are free boundary.

Fig. 2 Division of the model grid

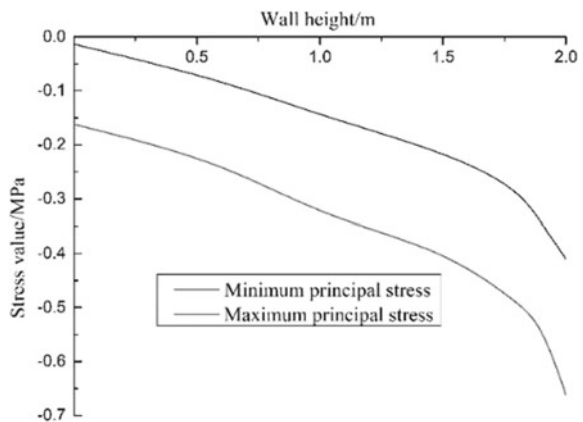


4 Analysis of Calculation Results

4.1 Stress Analysis

The variation trend of the maximum principal stress and the minimum principal stress of the anti-seepage wall is shown in Fig. 3. After calculation and analysis, the variation trend of the maximum principal stress along the wall height (calculated from the elevation of the wall bottom) decreases gradually, and a turning point appears at the wall height of 1.8 m. The variation trend of the minimum principal stress along the wall height is the same as that of the maximum principal stress, and the stress value increases at the wall height of 1.8 m. The maximum principal stress is

Fig. 3 The trend of principal stress



located at the bottom of the wall, and its value is 0.168 MPa. The maximum stress value is far less than the ultimate value of the unconfined compressive strength of the wall, which fully meets the stress requirements. The magnitude and distribution of the earth's pressure on the side of the wall mainly depend on the deformation of the wall, the layout, and construction procedure of the anti-seepage wall. For the flexible anti-seepage wall with lower elastic modulus, it can further coordinate the deformation of the wall and reduce the phenomenon of stress concentration.

4.2 Stress Analysis

The overall displacement calculation cloud chart of anti-seepage wall is shown in Fig. 4. Comparing the model calculation data with the measured data, the results are shown in Fig. 5. The figure shows that the horizontal displacement of the anti-seepage wall increases with the increase of height when the bottom is fixed, and the maximum horizontal displacement measured is 3.36 mm. The displacement increase ratio is linearly proportional to the wall height. This is because the sand wall is deposited on the anti-seepage wall to make the earth's pressure distribution more uniform.

Fig. 4 Cloud chart of total displacement

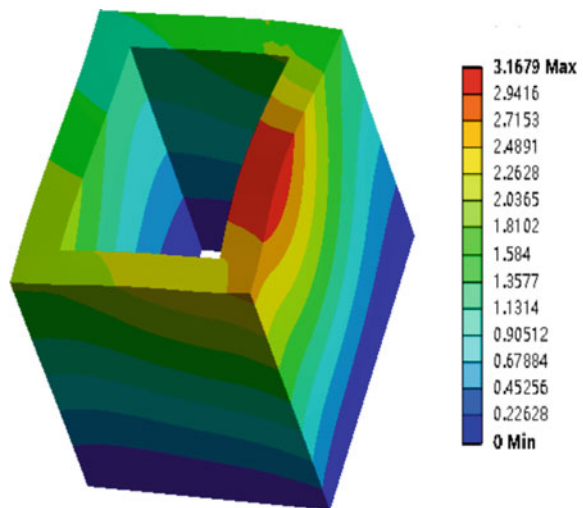
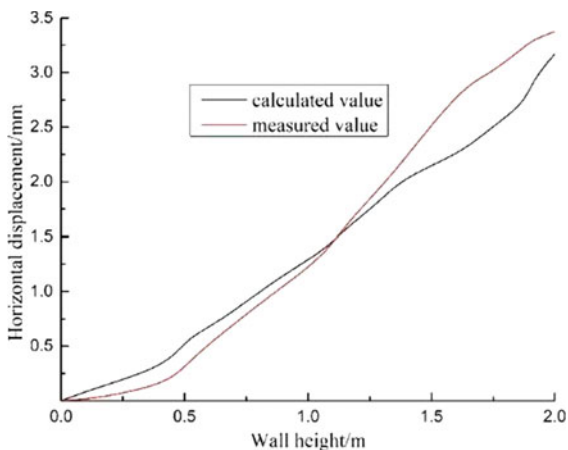


Fig. 5 Horizontal displacement



5 Conclusion

1. The horizontal displacement of the polyvinyl alcohol modified bentonite anti-seepage wall increases linearly with the increase of the wall height. The ultimate strain value of the wall is much smaller than the maximum strain limit of the slurry, which enhances the safety of anti-seepage wall.
2. The stress of the anti-seepage wall decreases gradually from the bottom to the top of the wall, and no tensile stress is detected in the wall. The elastic modulus of the wall is close to that of the surrounding soil, which can reduce the occurrence of wall cracks and prolong the service life of the wall in practical use.

Acknowledgments The paper is supported by the National Natural Science Foundation of China (Grant No. 51678083)

References

1. Samadder SR, Prabhakar R, Khan D, Kishan D, Chauhan MS (2017) Analysis of the contaminants released from municipal solid waste landfill site: a case study. *Sci Total Environ* 580:593–601
2. NaveenBP, Mahapatra DM, Sitharam TG, Sivapullaiah PV, Ramachandra TV Physico-chemical and biological characterization of urban municipal landfill leachate *Environ Pollut* 220(A):1–12
3. MounirAR, Mahdi S, Clark P (2015) Contemporary environmental issues of landfill leachate: assessment and remedies. *Crit Rev Environ Sci Technol* 45(5):472–590
4. RenouS, Givaudan JG, Poulain S, Dirassouyan F, Moulin P (2008) Landfill leachate treatment: review and opportunity. *J Hazard Mater* 150(3):468–493
5. Clarke BO, Anumol T, Barlaz M, Snyder SA (2015) Investigating landfill leachate as a source of trace organic pollutants. *Chemosphere* 127:269–275

6. Dai GZ, Shi GC, Wu XF, Wang Y (2011) Preparation and basic performance of anti-seepage slurry for domestic waste landfill site. *Adv Mater Res* 250–253:2302–2306
7. Ghosh P, Thakur IS, Kaushik A (2017) Bioassays for toxicological risk assessment of landfill leachate: a review. *Ecotoxicol Environ Saf* 141:259–270
8. Adamcová D, Vaverková MD, Barton S, Havlíček Z, Břoušková E (2016) Soil contamination in landfills: a case study of a landfill in Czech Republic. *Solid Earth* 7(7):2927–2952
9. Sivakumar S, Begum NA, Premalatha PV (2018) Numerical study on deformation of diaphragm cut off walls under seepage forces in permeable soils. *Comput Geotech* 102:155–163
10. Dai GZ, Zhu J, Shi GC, Sheng YM, Li SJ (2017) Analysis of the properties and anti-seepage mechanism of PBFC slurry in landfill. *Struct Durab Health Monit* 11(2):169–190
11. Yang Y, Cui Z, Li X, Dou H (2016) Development and materials characteristics of fly ash- slag-based grout for use in sulfate-rich environments. *Clean Technol Environ Policy* 18(3):949–956
12. Toor M, Jin B, Dai S, Vimonses V (2015) Activating natural bentonite as a cost-effective adsorbent for removal of Congo-red in wastewater. *J Ind Eng Chem* 21(1):653–661
13. Dai G, Zhu J, Shi G (2018) Analysis on the basic properties of PBFC antiseepage slurry in landfill. *Appl Ecol Environ Res* 16(6):7657–7667
14. Singh NB, Rai S (2001) Effect of polyvinyl alcohol on the hydration of cement with rice husk ash. *Cem Concr Res* 31(2):239–243
15. Zhang Y, Bernhardt M, Biscontin G, Rong L, Lytton RL (2015) A generalized Drucker–Prager viscoplastic yield surface model for asphalt concrete. *Mater Struct* 48(11):3585–3601

Predicting Gaseous Emissions and Leachate Production in Landfills Using Neural Model



Sunayana and Arvind Kumar

Abstract The solid waste management problems in developing countries like India are increasing at a fast pace because of heterogeneous nature of waste used in any remedial solution. This is so because India has not been able to impart segregation efficiently in its waste management logistic. Therefore, the only disposal method that is widely practiced to dispose solid waste is sanitary landfills. Landfills receiving such a huge quantum of waste need to be monitored and studied rigorously as they produce gaseous emissions and leachate. The dispersion or dissolution of these two phases of emissions is polluting the environment and affecting the public health and also the planet health. Therefore, to study the possible scenarios arising in the future from landfill, they are to be fragmented for each imparting factor. The artificial neural networks in this regard can be used to develop an integrated predictive model that can account for all the toxic compounds coming in the form of gas and liquid. This study combines all possible factors affecting landfill working from previous studies and presents a conceptual neural model with variables defined to be included for developing an efficient prediction model.

Keywords Landfill · Neural network · Leachate and gaseous emissions

1 Introduction

In India, the disposal method for municipal solid waste (MSW) that is widely followed by several municipal corporations across country is landfill. The construction and maintenance of landfills in country which houses the second largest population on planet are difficult and also less efficient. Owing to less efficient waste management system, the quantum of waste going to landfills should be checked so

Sunayana (✉)
CSIR-NEERI, Mumbai, India
e-mail: sunayana@neeri.res.in

A. Kumar
CE Department, NIT, Jalandhar, India
e-mail: agnihotriak@nitj.ac.in

as to evaluate the logistic steps of waste management such as reduce, reuse, and recycle. 90% of waste collected in India goes to landfill or remains on land in unacceptable manner posing threat to human health and natural environment [1, 2]. The waste going to landfill therefore has household, construction, and demolition waste and treated bio-medical wastes [3]. Therefore, it is evident that commingled waste going to the landfills in the country poses serious threat to natural survival elements like water and air if left unmanaged. In such a scenario, the by-products of landfill be it leachate or gaseous emissions (CH_4 and CO_2) need to be monitored and managed regularly. For better solid waste management, landfills are classified under various classes based on the type of waste (hazardous waste, designated waste, and MSW) received by the landfills [4] but categorical data in Indian context is missing.

India because of its location experiences winter, summer, monsoon, and post-monsoon period classified as per international standard [5]. The climatic factors like air temperature, precipitation (rain or melted snow), and relative humidity having a close relationship on leachate production [6] suggest the need to monitor leachate in different climatic seasons also. There are several methods available for quantification of leachate flow rates and peak hours or hours like water balance method (WBM) [7], flow investigation of leachate [8], or US EPA's HELP model [9]. On the other hand, the production of landfill gases such as CH_4 and CO_2 with some traces of NH_3 and H_2S is a temperature- and time-dependent process along with C/N ratio in the waste [10]. The complex process of leachate and gaseous production for landfills requires such models which can simultaneously predict leachate and gaseous produce arising from landfill under different conditions. For such scenarios, artificial intelligence-based neural models can be used to predict the by-products generating through particular landfill.

Artificial Neural Networks (ANNs) have been used for advance understanding of anaerobic digestion and hence prediction of biogas [11], prediction of NH_3 and H_2S using ANN in anaerobic digestion [12], and prediction of methane in landfill gas using ANN for field-scale landfill reactors [13]. With few studies, it has been understood that there are very few studies which use ANN-based models to assess the behavior of landfills. There are no studies available which use all the landfill-related parameters to predict leachate and gaseous emissions simultaneously. Therefore, this study proposes a conceptual neural model to predict leachate and gaseous emissions simultaneously.

2 Brief about ANN

The Artificial Neural Networks (ANNs) are basically the adoption of working of human brain. The capability of functioning of human brain in executing various tasks in human life derives the structure artificially in solving and understanding real-life problems. The brain network is captured in ANN in terms of architecture which is optimized to solve a problem. The design of ANN requires the input (input layer), the hidden neurons (hidden layer), and the output (Output layer) as shown in

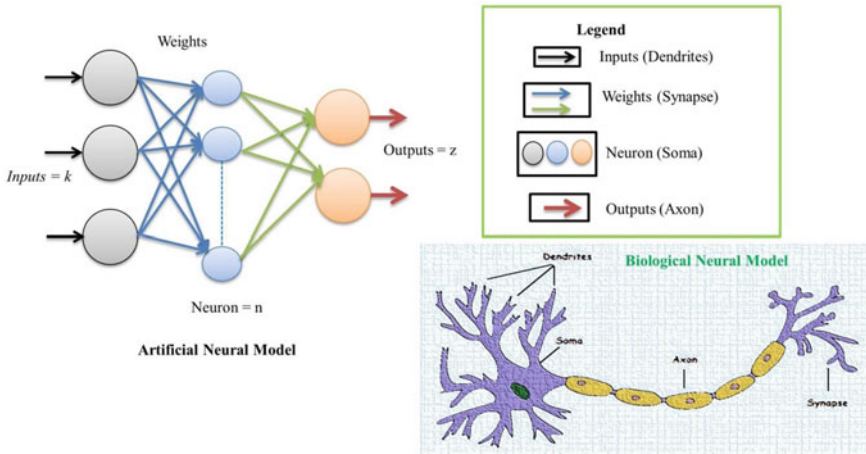


Fig. 1 Comparison of biological neural model with artificial neural model

Fig. 1. The design of these types of models is basically a data-driven process and provides a continuous function type with certain accuracy too [14]. These models are used when the complex relationships in any process or phenomenon are not known or not well understood. The three layers classified here can have n number of elements in an individual layer depending upon the problem. Once the combinations of input and output are fixed, the ANN architecture is optimized by changing and fixing the neurons in hidden layer as it is purely a hit and trial process, while some thumb rules can be followed. Once the architecture is fixed, the final topology of neural model needs to be trained and tested for problem-solving. The architecture which is to be trained can be feed-forwarded or feedback for deciding the flow of connections in the architecture. The feedback and feed-forward type of both neural models can be used while designing the neural model. The training is done by using various algorithms which had been developed for neural model training and depending upon the type of problem it could be supervised or unsupervised. The trained model can be tested and used for prediction, pattern recognition, classification, clustering, and simulation depending upon task identified during the training phase.

3 Methodology

In this study, feed-forward backpropagated neural network model has been suggested for predicting gaseous emissions and leachate production using neural model. As mentioned earlier, for landfills both the types of effluents are important to be monitored and studied. The monitoring will also give relationships among various factors which affect the production and rate of emissions. For making neural model for

gaseous emission and leachate production prediction from landfills, inputs required are shown in Table 1.

The inputs are chosen, those affect the quantity of leachate and gaseous production. Further, for evaluating landfill performance and characteristics leachate parameters like BOD, COD, TOC, NH_3 , SO_4^{2-} , and chlorides can be measured and by using factor analysis these may or may not be included in developing neural models.

The outputs for neural model are given in Table 2.

The model proposes to predict the amount of leachate production and emissions in gaseous form from landfills by using all the input parameters. For evaluating the composition of gases, N_2 by volume and other gases like NH_3 , Mercaptans, etc. can be evaluated. The data matrix required for the neural model development should have sufficient data points to train and test the model, and then it can be used for

Table 1 Input parameters for neural model

Type	Parameters	Unit
Solid waste-related	Quantity of waste dumped per day (W_1)	(tons/day)
	Temperature (T_w)	(°C)
	Field Capacity (FC)	Fraction of water in the waste based on dry weight of the waste
	C/N ratio	
Meteorological parameters [6]	Month (m)	[1–12]
	Temperature (T_m)	(°C)
	Pressure (P)	(mbar)
	Cloudiness (C)	Scale in oktas (0–9)
	Relative Humidity (RH)	(%)
	Precipitation (P_m)	(mm)
	Maximum temperature ($T_{m(max)}$)	(°C)
	Minimum temperature ($T_{m(min)}$)	(°C)
Leachate-related parameters	Leachate recirculation volume (LRV)	m^3/day

Table 2 Output parameters for neural model

Type	Parameters	Unit
Leachate-related parameters	Quantity of leachate produced per day or flow rate (Q_1)	(m^3/day)
Gaseous emissions	CH_4 (by volume)	(% by vol.)
	CO_2 (by volume)	(% by vol.)

predicting the simultaneous concentration of gases and leachate. The architecture for the proposed neural model is shown in Fig. 2. The inputs presented in Fig. 2 can be reduced or increased while preparing the model with field data. The number of inputs and outputs is fixed but the number of neurons in hidden layer needs to be optimized for every problem as it is purely trial-and-error-based process. The connections (i.e., weights) are adjusted in the training process, and the final optimized architecture will have fixed connections later. There are several adjustments that are done for training purposes like minimum gradient, training time (max.), performance (min.), validation instances increasing, and number of training epochs (iterations).

The inputs chosen for landfill emissions here are a mix of measurable and derived variables for any landfill. The relation of parameters in input layer affects the quantum of emissions shown in output layer, and thus this model if used will predict the concentrations for any condition existing in a landfill. These models are helpful in assessing the performance of landfill and monitoring the changes along with the identification of factors.

The selection of input and output parameters is based on basic understanding of the problem. Some statistical options like factor analysis by the use of principal component analysis can be adopted for the selection of major inputs out of many

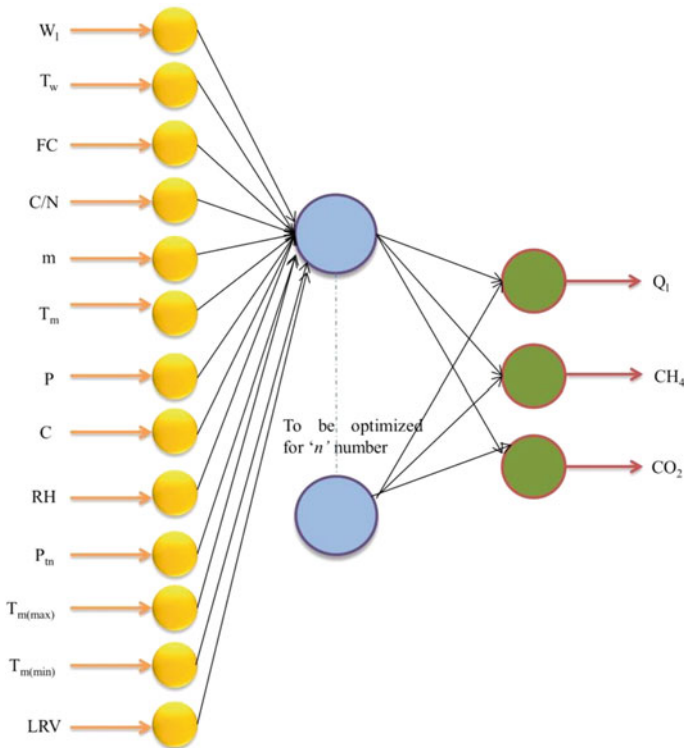


Fig. 2 Proposed ANN for predicting emissions (leachate and gaseous)

redundant inputs. The comparison of results obtained from model with tested values can be done by using three statistical parameters: root mean square error (RMSE), percent volume error (%VE), and coefficient of correlation (r). The following equations can be used to calculate the statistical parameters for performance evaluation of trained neural models during training and testing phases.

$$RMSE = \left[\frac{\sum_{i=1}^N (\text{Value}_{\text{observed}} - \text{Value}_{\text{predicted}})^2}{n} \right]^{1/2} \quad (1)$$

$$\%VE = \frac{\sum_{i=1}^n \left| \frac{\text{Value}_{\text{observed}} - \text{Value}_{\text{predicted}}}{\text{Value}_{\text{observed}}} \right|}{n} \quad (2)$$

$$r = \frac{\sum_{i=1}^n (\text{Value}_{\text{predicted}} - \overline{\text{Value}_{\text{predicted}}})(\text{Value}_{\text{observed}} - \overline{\text{Value}_{\text{observed}}})}{\sqrt{\sum_{i=1}^n (\text{Value}_{\text{predicted}} - \overline{\text{Value}_{\text{predicted}}})^2} \sqrt{\sum_{i=1}^n (\text{Value}_{\text{observed}} - \overline{\text{Value}_{\text{observed}}})^2}} \quad (3)$$

4 Discussion

The proposed neural model suggested for predicting leachate and gaseous emissions from landfills incorporates all the parameters which affect the production of quantity of leachate produced, percentage of methane, and carbon dioxide produced. The neural models are easy to relate various parameters which affect the result without actually knowing the explicit relation of each of them. The selection and deletion of parameters are easy in neural model compared to any mathematical model. The sensitivity analysis of results expresses the effect of individual parameter on output and thus helps to identify the most sensitive parameter. The neural model is once developed for any time period of landfill stage to predict the emissions.

5 Conclusions

The proposed neural model if supplied with proper data can predict the emissions from landfill. This type of model has not been developed before and used for prediction in the case of landfills. The proposed model if used will also ascertain the possibility of successful neural model application in this field also. The suggested model is a multilayer perceptron and can be optimized for more hidden layers in the architecture.

References

1. National Environmental Engineering Research Institute, NEERI (2010) Air quality assessment, emissions inventory and source apportionment studies. Central Pollution Control Board (CPCB), Mumbai, New Delhi
2. Kumar S, Bhattacharya JK, Vaidya AN, Chakrabarti T, Devotta S, Akolkar AB (2009) Assessment of the status of municipal solid waste management in metro cities, state capitals, class I cities, and class II towns in India: An insight. *Waste Manag* 29:883–895
3. <https://www.indiawaterportal.org/topics/solid-waste>. Accessed 01 Feb 2019
4. Tchobanoglous G, Kreith F (2002) Handbook of solid waste management, 2nd edn. Mc Graw Hill Companies, USA
5. https://en.wikipedia.org/wiki/Climate_of_India. Accessed 01 Feb 2019
6. Karaca F, Ozkaya B (2006) NN-LEAP: a neural network-based model for controlling leachate flow-rate in a municipal solid waste landfill site. *Environ Model Softw* 21:1190–1197
7. Fenn DG, Hanley KJ, DeGare TV (1975) Use of the water balance method for predicting leachate generation from solid waste disposal sites. U.S. Environmental Protection Agency, EPA/530/SW-168, Washington, DC
8. Khanbilvardi RM, Ahmed S, Gleason PL (1995) Flow investigation for landfill leachate (FILL). *J Environ Eng* 121(1):45–57
9. Schroeder PR, Dozier TS, Zappi PA, McEmce BM, Sjostrom JW, Peyton RL (1994) The hydrologic evaluation of landfill performance (HELP) model: engineering documentation for version 3. EPA/600/R-94/1686. U.S. Environmental Protection Agency Office of Research and Development, Washington, DC
10. Qdais HA, Hani KB, Shatnawi N (2010) Modeling and optimization of biogas production from a waste digester using artificial neural network and genetic algorithm. *Resour Conserv Recycl* 54:359–363
11. Holubar P, Zani L, Hager M, Froschl W, Radak Z, Braun R (2002) Advanced controlling of anaerobic digestion by means of hierarchical neural networks. *Water Resour* 36:2582–2588
12. Strik D, Domnanovich A, Zani L, Braun R, Holubar P (2005) Prediction of trace compounds in biogas from anaerobic digestion using the MATLAB neural network toolbox. *Environ Model Softw* 20:803–810
13. Ozkaya B, Demir A, Bilgili M (2007) Neural network prediction model for the methane fraction in biogas from field-scale landfill bioreactors. *Environ Model Softw* 22(6):815–822
14. Araghinejad S (2014) Data-driven modeling: using MATLAB® in water resources and environmental engineering. *Water Sci Technol Libr* 67:139–194